

**Leveraging an Allenic Pauson-Khand Reaction to Synthesize 6,12-Guaianolide Analogs
with a Tunable α -Methylene- γ -lactam Electrophile**

by

Paul A. Jackson

B.S. Chemistry, California University of Pennsylvania, 2011

B.A. Philosophy, California University of Pennsylvania, 2011

Submitted to the Graduate Faculty of the
Kenneth P. Dietrich School of Arts and Sciences in partial fulfillment
of the requirements for the degree of
Doctor of Philosophy

University of Pittsburgh

2017

UNIVERSITY OF PITTSBURGH

Kenneth P. Dietrich School of Arts and Sciences

This dissertation was presented

by

Paul A. Jackson

It was defended on

May 03, 2017

and approved by

W. Seth Horne, Associate Professor, Department of Chemistry

Craig S. Wilcox, Professor, Department of Chemistry

Thomas E. Smithgall, Professor, Department of Microbiology and Molecular Genetics

Dissertation Advisor: Kay M. Brummond, Professor, Department of Chemistry

University of Pittsburgh

2017

Leveraging an Allenic Pauson-Khand Reaction to Synthesize 6,12-Guaianolide Analogs

with a Tunable α -Methylene- γ -lactam Electrophile

Paul A. Jackson, PhD

University of Pittsburgh, 2017

Copyright © by Paul A. Jackson

2017

**Leveraging an Allenic Pauson-Khand Reaction to Synthesize 6,12-Guaianolide Analogs
with a Tunable α -Methylene- γ -lactam Electrophile**

Paul A. Jackson, PhD

University of Pittsburgh, 2017

Unsaturated amides have emerged as invaluable electrophilic motifs as evidenced by the recent FDA approval of acrylamide-containing drugs, afatinib, ibrutinib, and osimertinib, as treatments for lung and blood cancers. These Michael acceptors represent a class of irreversible, targeted covalent inhibitors that selectively react with a cysteine in the active site of a specific protein. Inspired by these successful drugs, 6,12-guaianolide isosteres equipped with electronically tunable α -methylene- γ -lactams are envisioned as compounds with great potential for exhibiting desired biological activities. The guaianolide family was selected for study because it exhibits an exciting range of biological activities including inhibition of the NF- κ B pathway. However, the indiscriminate reactivity of the α -methylene- γ -lactone embedded in many of these natural products raises many concerns. Towards this end, guaianolide isosteres have been prepared using an allenic Pauson-Khand reaction of α -methylene- γ -lactam tethered allene-ynes affording rapid access to the [5,7,5]-ring system characteristic of this class of compounds. In turn, these products are equipped with an unsaturated amide whose electrophilic reactivity is modulated by varying substituents at the lactam nitrogen. The allenic Pauson-Khand precursors were prepared using an allylboration/lactamization reaction to afford the alkynyl functionalized α -methylene- γ -lactam, a heretofore unprecedented transformation utilizing α -imino alkynes. Substituents on the sterically encumbered lactam nitrogen were introduced using Buchwald-Hartwig cross-coupling conditions.

Finally, the chemical reactivity of the 6,12-guaianolide isosteres towards biothiols was measured qualitatively and their activity as inhibitors of the NF- κ B signaling pathway was demonstrated. The use of allenyl acetates in the allenic Pauson-Khand reaction with α -methylene- γ -lactam tethers was examined to synthesize lactam-containing guaianolide analogs with an α -acyloxy cyclopentenone.

TABLE OF CONTENTS

1.0	THIOL REACTIVITY AND BIOLOGICAL ACTIVITY OF ACRYLAMIDES, α-METHYLENE-γ-LACTONES, AND α-METHYLENE-γ-LACTAMS.....	1
1.1	TARGETED COVALENT INHIBITION IN DRUG DESIGN.....	4
1.2	THIOL REACTIVITY AND BIOLOGICAL ACTIVITY OF α-METHYLENE-γ-LACTONES, α-METHYLENE-γ-LACTAMS, MACROCYCLIC α-METHYLENE LACTAMS, AND ACRYLAMIDES.....	14
1.2.1	Comparison of the Biological Activities of Isosteric α-Methylene-γ-lactams and α-Methylene-γ-lactones.....	16
1.2.2	Thiol Reactivity of α-Methylene-γ-lactones.....	19
1.2.3	Thiol Reactivity of α-Methylene-γ-lactams.....	23
1.2.4	Thiol Reactivity and Biological Activity of Macrocyclic α-Methylene Lactams.....	24
1.2.5	Thiol Reactivity of Acrylamides.....	26
1.3	ISOSTERIC REPLACEMENT OF LACTONES WITH LACTAMS IN NATURAL PRODUCTS: BIOLOGICAL STABILITY, ACTIVITY, AND THIOL REACTIVITY.....	33
1.4	CONCLUSION.....	41
2.0	METHODS OF α-METHYLENE-γ-LACTAM SYNTHESIS.....	44
2.1	INTRODUCTION.....	44

2.2	SYNTHESIS OF α -METHYLENE- γ -LACTAMS USING MORITA-BAYLIS-HILLMAN REACTIONS.....	46
2.3	SYNTHESIS OF α -METHYLENE- γ -LACTAMS FROM ALLYLMETAL REAGENTS (DERIVED FROM ALLYLBROMIDES) OR ALLYLBORONATES.....	49
2.4	USE OF DIALKOXYPHORPHORYL REAGENTS TO INSTALL THE α -METHYLENE MOIETY.....	53
2.5	INSTALLATION OF THE α -METHYLENE MOIETY ON AN α -UNSUBSTITUTED- γ -LACTAM VIA THE LACTAM ENOLATE.....	54
2.6	CONCLUSION.....	55
3.0	PREPARATION OF LACTAM ANALOGS OF 6,12-GUAIANOLIDES.....	57
3.1	INTRODUCTION.....	57
3.1.1	Synthetic Strategies to Access 6,12-Guaianolides.....	58
3.1.2	Pauson-Khand Reactions with Amide or Lactam Tethers.....	64
3.1.3	Retrosynthetic Design of α -Methylene- γ -lactam Guaianolide Analogs.....	68
3.2	FEASIBILITY OF ALLENIC PAUSON-KHAND APPROACH TO α -METHYLENE- γ -LACTAM CONTAINING GUAIANOLIDE ISOSTERES.....	70
3.3	TRANSITION STATE ANALYSIS FOR LACTAMIZATION REACTION.....	79

3.4	EXPANDING THE SCOPE OF THE ALLENIC PAUSON-KHAND APPROACH TO α-METHYLENE-γ-LACTAM CONTAINING GUAIANOLIDE ISOSTERES.....	85
3.4.1	Feasibility of Secondary Amides in the APKR.....	86
3.4.2	Synthesis of α-Methylene-γ-lactams Containing a Silyl-substituted Alkyne.....	89
3.4.3	Optimization of Allene Formation from Propargyl Pivalates using Stryker's Reagent.....	92
3.4.4	Allene Formation using Stryker's Reagent with Cis-substituted Lactams.....	106
3.4.5	Investigation of Alternative Reactions for 1,1-Disubstituted Allene Formation.....	108
3.4.6	Modification of the Lactam Nitrogen of Allene-yne.....	120
3.4.7	Modifications to the Alkyne Terminus.....	127
3.5	ALLENIC PAUSON-KHAND REACTION OF α-METHYLENE-γ-LACTAM TETHERED ALLENE-YNES.....	133
3.6	ASSIGNMENT OF RELATIVE STEREOCHEMISTRY OF α-METHYL-γ-LACTAMS BY CALCULATION AND NMR ANALYSIS.....	139
3.7	APKR WITH CIS-FUSED, LACTAM-TETHERED ALLENE-YNE SUBSTRATES.....	143
3.8	ANALYSIS OF ^{13}C AND ^1H NMR DATA FOR ESTIMATING THE ELECTROPHILICITY OF α-METHYLENE-γ-LACTAM GUAIANOLIDE ANALOGS.....	145

3.9	THIOL REACTIVITY OF α-METHYLENE-γ-LACTAMS.....	147
3.9.1	Rate of Glutathione (GSH) Addition to an α-Methylene-γ-lactam: Rate Constant and Half-life.....	150
3.10	BIOLOGICAL ACTIVITY OF α-METHYLENE-γ-LACTAM GUAIANOLIDE ISOSTERES: CYTOTOXICITY AND NF-κB PATHWAY INHIBITION.....	155
3.10.1	Introduction to the NF-κB Pathway.....	155
3.10.2	Inhibition of the NF-κB Pathway by α-Methylene-γ-lactam Guaianolide Analogs.....	158
4.0	ALLENYL ACETATES IN THE ALLENIC PAUSON-KHAND REACTION WITH α-METHYLENE-γ-LACTAM-TETHERED ALLENE-YNES AND AN UNEXPECTED [2 + 2] CYCLOADDITION PRODUCT.....	164
4.1	INTRODUCTION.....	164
4.2	PREPARATION OF ALLENYL ACETATES FROM PROPARGYL ALCOHOLS.....	167
4.3	APKR OF ALLENYL ACETATES WITH N-ACETYL α-METHYLENE-γ- LACTAM TETHER.....	168
4.4	PROPOSED MECHANISM FOR THE [2 + 2] CYCLOADDITION.....	170
4.5	OPTIMIZATION OF CONDITIONS TO SELECTIVELY OBTAIN THE APKR PRODUCT OR THE [2 + 2] CYCLOADDITION PRODUCT FROM ALLENYL ACETATES WITH AN α-METHYLENE-γ-LACTAM TETHER.....	175

4.6	DESIGN AND SYNTHESIS OF LESS-ELECTRON DEFICIENT α-METHYLENE-γ-LACTAMS FOR ALLENIC PAUSON-KHAND REACTIONS USING ALLENYL ACETATES.....	178
4.7	STRUCTURE CONFIRMATION OF THE [2 + 2] CYCLOADDITION PRODUCT BY 2D NMR ANALYSIS.....	180
4.8	CONCLUSION.....	184
APPENDIX A EXPERIMENTAL PROCEDURES AND COMPOUND CHARACTERIZATION DATA.....		
		186
APPENDIX B ^1H AND ^{13}C NMR SPECTRA.....		
		288
BIBLIOGRAPHY.....		
		435

LIST OF TABLES

Table 1.1. Comparison of cytotoxicity of γ -substituted α -methylene- γ -lactams and lactones.....	17
Table 1.2. Cytotoxicity of β -aryl- γ -alkyl- α -methylene- γ -lactams, lactones, and isoxazilidinones.....	18
Table 1.3. Kinetic competition experiments between acrylamides and GSH.....	29
Table 1.4. Half-lives for the reaction of various acrylamides with GSH.....	32
Table 3.1. Reaction optimization for formation of 1,1-disubstituted allenes.....	104
Table 3.2. Formation of allenes from cis-substituted lactams.....	108
Table 3.3. APKR with trans-substituted α -methylene- γ -lactam tethered allene-ynes.....	136
Table 3.4. ^1H NMR Calculations Compared to Experimental Data for 3.193	142
Table 3.5. ^1H NMR Calculations Compared to Experimental Data for 3.195	143
Table 3.6. ^{13}C and ^1H NMR data for α -methylene- γ -lactam guaianolide analogs.....	147
Table 3.7. Gradient of 0.1% formic acid in MeCN (B) to 0.1% formic acid in H ₂ O (A).....	154
Table 4.1. APKR or [2 + 2] cycloaddition with allenyl acetates.....	179
Table 4.2. NMR Data for [2 + 2] cycloaddition product 4.44	185

LIST OF FIGURES

Figure 1.1. Recently approved, irreversible covalent drugs containing acrylamides.....	2
Figure 1.2. Guaianolide natural products and model for tunable α -methylene- γ -lactam analogs..	3
Figure 1.3. HCV protease inhibitors.....	8
Figure 1.4. Reversible and irreversible EGFR inhibitors.....	10
Figure 1.5. FGFR inhibitors.....	11
Figure 1.6. Btk inhibitors.....	12
Figure 1.7. Pan JNK 1/2/3 inhibitors.....	13
Figure 1.8. Natural products with α -methylene- γ -lactones or α -methylene- γ -lactams.....	16
Figure 1.9. α -Methylene- γ -lactam inhibitors of homoserine transacetylase (HTA).....	19
Figure 1.10. Example of a microcystin.....	25
Figure 1.11. Epothilone B and lactam analog ixabepilone.....	34
Figure 1.12. Artemisinin and lactam analogs.....	34
Figure 1.13. Sarcophine and γ -lactam analogs.....	35
Figure 1.14. Macrospheptide natural products and lactam analogs.....	36
Figure 1.15. Salicylihalamide A and A26771B with lactam analogs.....	37
Figure 1.16. Natural product resorcylic acid lactones tunable lactam analog.....	39
Figure 1.17. Parthenolide and lactam analog.....	39
Figure 2.1. Summary of methods to form α -methylene or α -alkylidene- γ -lactams.....	46
Figure 3.1. Examples of 6,12-guaianolides that contain an α -methylene- γ -lactones.....	57
Figure 3.2. Crystal structure of tricycle 3.116 , showing the trans lactam.....	136
Figure 3.3: Depletion of acrylamide 3.208 (A) or tricycle 3.187 (B) over time.	153

Figure 3.4. Summary of NF- κ B pathway with major points of inhibition.....	156
Figure 3.5. Synthetic guaianolide analogs and natural product parthenolide with remaining NF- κ B activity following treatment of cells with inhibitor.....	159
Figure 3.6. Graph of NF- κ B activity relative to induced levels for α -methylene- γ -lactams.....	161
Figure 3.7. Graph of cell viability relative to nontreated cells for α -methylene- γ -lactams.....	162
Figure 3.8. Plot of NF- κ B activity and cellular toxicity for α -methylene- γ -lactams.....	164
Figure 4.1. Oxidation level of naturally occurring 6,12-guaiainolides.....	166
Figure 4.2: Crystal structure of [2 + 2] cycloaddition product from lactone.....	171
Figure 4.3. COSY and HMBC correlations of structure of [2 + 2] cycloaddition product.....	186

LIST OF SCHEMES

Scheme 1.1. α -Methylene- γ -lactones that react with cysteamine in ^1H NMR assay.....	20
Scheme 1.2. Cysteine adduct formation with α -methylene- γ -lactone natural products.....	21
Scheme 1.3. Chemoselectivity of glutathione and cysteine addition to helenalin.....	22
Scheme 1.4. Thiol adduct formation with α -methylene- γ -lactams and oxindoles.....	24
Scheme 1.5. Rakicidin A and analog: a 1,6-addition product with methyl thioglycolate.....	26
Scheme 1.6. Relative rates of GSH addition to <i>N</i> -arylacrylamides.	30
Scheme 1.7. Thiol additions to synthetic strigolactone and strigolactam.....	41
Scheme 2.1. α -Methylene- γ -lactams as synthetic intermediates.....	45
Scheme 2.2. Intramolecular Morita-Baylis-Hillman reactions to form α -methylene- γ -lactams...47	
Scheme 2.3. Synthesis of α -methylene- γ -lactams using Morita-Baylis-Hillman adducts.....	48
Scheme 2.4. Allylzinc addition to an imine to form α -methylene- γ -lactams.....	49
Scheme 2.5. Indium promoted addition to imines and cyclization.....	50
Scheme 2.6. Enantioselective synthesis of α -methylene- γ -lactams with chiral sulfinyl imines...51	
Scheme 2.7. 3-Component reaction of allylboronates, aldehydes, and ammonium hydroxide...52	
Scheme 2.8. Enantioselective lactamization with chiral allylboronates and imines.....	52
Scheme 2.9. Synthesis of α -methylene- γ -lactams with dialkoxyphosphoryl reagents.....	53
Scheme 2.10. Installation of an α -methylene moiety from the enolate of γ -lactams.....	55
Scheme 3.1. Semisynthesis of arglabin from parthenolide.....	59
Scheme 3.2. Methods to form 5,7-ring system in the total syntheses of guaianolides.....	61
Scheme 3.3. Synthesis of guaianolide analogs using an APKR.....	63
Scheme 3.4. APKR to prepare precursor to ingenol and phorbol.....	63

Scheme 3.5. Pauson-Khand reactions with lactam and amide tethers.....	65
Scheme 3.6. APKR with tertiary amide tethers.....	66
Scheme 3.7. Rhodium catalyzed allenic Alder-ene reactions with secondary amides.....	67
Scheme 3.8. Mechanism of allenic alder-ene and allenic Pauson-Khand reactions.....	67
Scheme 3.9. Retrosynthesis of α -methylene- γ -lactam guaianolide analog.....	70
Scheme 3.10. Synthesis of 2-alkoxycarbonyl allylboronate.....	71
Scheme 3.11. Formation of allylboronate via vinyl aluminum intermediates.....	74
Scheme 3.12. Activation of DIBALH with CuMe.....	74
Scheme 3.13. Synthesis of chloromethyl pinacolboronate.....	75
Scheme 3.14. Three-component reaction to form α -methylene- γ -lactams.....	76
Scheme 3.15. Synthesis of 3-phenyl propynal.....	76
Scheme 3.16. Feasibility of allenic cyclocarbonylation approach to guaianolide analogs.....	79
Scheme 3.17. Chair transition states for diastereospecific α -methylene- γ -lactam formation.....	80
Scheme 3.18. Boat transition states for diastereospecific α -methylene- γ -lactam formation.....	81
Scheme 3.19. Possible transition states for <i>Z</i> -allylboronate addition to primary aldimines.....	83
Scheme 3.20. Possible transition states for <i>E</i> -allylboronate addition to primary aldimines.....	85
Scheme 3.21. Feasibility of secondary amides in the APKR.....	88
Scheme 3.22. Synthesis of α -methylene- γ -lactams using silyl-substituted propynals.....	90
Scheme 3.23. Synthesis of 1,1-disubstituted allenes with <i>N</i> -unsubstituted lactams.....	92
Scheme 3.24. Formation of 1,1-disubstituted allenes using Stryker's reagent.....	94
Scheme 3.25. Proposed mechanism for allene formation with Stryker's reagent.....	106
Scheme 3.26. Feasibility of <i>N</i> -silyl protection.....	110
Scheme 3.27. <i>N</i> -silyl α -methylene- γ -lactams in the formation of 1,1-disubstituted allenes.....	111

Scheme 3.28. Alternative strategies to access 1,1-disubstituted allenes.....	112
Scheme 3.29. Attempt at deoxyallenylation of tertiary, alkyl propargyl alcohol.....	113
Scheme 3.30. Petasis allenylation.....	115
Scheme 3.31. Propargyl carbonate formation and Tsuji reduction attempts.....	116
Scheme 3.32. Attempts to formylate tertiary, propargyl alcohol.....	117
Scheme 3.33. Propargyl carbonate formation and Tsuji reduction on model substrate.....	119
Scheme 3.34. Formylation of model substrate and decarboxylative hydrogenolysis.....	120
Scheme 3.35. Copper catalyzed amidation of aryl halides.....	122
Scheme 3.36. Proposed mechanism for copper catalyzed N-arylation (Buchwald).....	124
Scheme 3.37. N-Arylation of lactams with potassium carbonate as a base.....	125
Scheme 3.38. N-Arylation of lactam-tethered allene-ynes.....	126
Scheme 3.39. Nucleophilic addition of lactams to electrophiles.....	128
Scheme 3.40. Modification of alkyne substituents.....	130
Scheme 3.41. Alkyne methylation with tertiary amide.....	131
Scheme 3.42. Alkyne methylation at low temperatures with model substrate.....	133
Scheme 3.43 Removal of TIPS substituent from cis lactams to generate terminal alkynes.....	134
Scheme 3.44. APKR with trans-substituted α -methylene- γ -lactam tethered allene-ynes.....	137
Scheme 3.45. APKR with α -methyl lactams.....	139
Scheme 3.46. N-Acylation of tricyclic APKR products.....	140
Scheme 3.47. APKR of mixtures of α -methylene and α -methyl- γ -lactams.....	144
Scheme 3.48. ^1H NMR monitoring of cysteamine addition to an α -methylene- γ -lactam.....	148
Scheme 3.49. Thiol additions to α -methylene- γ -lactams.....	149
Scheme 3.50. Conditions to measure the rate of GSH addition to acrylamides.....	151

Scheme 3.51. Reaction of helenalin or analog with Cys38 of p65.....	157
Scheme 4.1. Formation of allenyl acetate and APKR to form α -acetoxy cyclopentenone.....	167
Scheme 4.2. Retrosynthesis of lactam guaianolide analog with α -acetoxy cyclopentenone.....	168
Scheme 4.3. Synthesis of allenyl acetates.....	169
Scheme 4.4. APKR of allenyl acetate and alkyne tethered by an α -methylene- γ -lactam.....	170
Scheme 4.5. APKR of allenyl acetate and alkyne tethered by an α -methylene- γ -lactone.....	170
Scheme 4.6. Proposed mechanisms for cyclobutane formation.....	172
Scheme 4.7. Regioselectivity in thermal [2 + 2] cycloadditions of alkenes and allenes.....	174
Scheme 4.8. Enantioselective, Lewis acid catalyzed [2 + 2] cycloaddition.....	175
Scheme 4.9. Gold-catalyzed [2 + 2] cycloaddition of allenes and alkenes.....	175
Scheme 4.10. Catalytic cycle for gold-catalyzed [2 + 2] cycloaddition.....	176
Scheme 4.11. Formation allenyl pivalates with <i>N</i> -unsubstituted or <i>N</i> -methyl lactams.....	181
Scheme 4.12. APKR of allenyl pivalate with <i>N</i> -unsubstituted lactam tether.....	182

LIST OF EQUATIONS

Equation 1.1 Covalent inhibition of an enzyme.....	7
Equation 3.1. Rate equation for GSH addition to acrylamides (or α -methylene lactams).....	151
Equation 3.2. Calculation of half-life from pseudo-first order rate constants.....	152

1.0 THIOL REACTIVITY AND BIOLOGICAL ACTIVITY OF ACRYLAMIDES, α -METHYLENE- γ -LACTONES, AND α -METHYLENE- γ -LACTAMS

Portions of this chapter are adapted with permission from: Jackson, P. A.; Widen, J. C.; Harki, D. A.; Brummond, K. M. Covalent Modifiers: A Chemical Perspective on the Reactivity of α,β -Unsaturated Carbonyls with Thiols via Hetero-Michael Addition Reactions. *J. Med. Chem.* **2017**, *60*, 839-885 ©2017 American Chemical Society

Acrylamides are an emerging motif in drug discovery because of the recent FDA approval of afatinib (**1.1**), ibrutinib (**1.2**), and osimertinib (**1.3**) as treatments for non-small cell lung cancer (**1.1**, **1.3**) and various blood cancers (**1.2**, Figure 1).¹⁻⁴ These drugs are irreversible inhibitors of the epidermal growth factor receptor (**1.1**, **1.3**) or Bruton's tyrosine kinase (**1.2**), and they gain selectivity over other kinases by forming covalent bonds to unique cysteine residues in these enzymes.⁵⁻⁸ The success of acrylamides for targeting discreet cysteine residues in a number of kinases and the HCV protease has resulted in a renewed interest in covalent drugs.⁹⁻¹⁷ Acyclic acrylamides generally have limited reactivity with thiols because they are only weakly electrophilic, which limits nonspecific interactions with off-target proteins and endogenous thiols like glutathione; the positioning of the electrophile near a cysteine residue of a target protein through noncovalent interactions promotes covalent bond formation.¹⁸⁻¹⁹ Inspired by this emerging area and an interest in synthetic access to biologically relevant guaianolide analogs, we

hypothesized that α -methylene- γ -lactams could serve as tunable isosteres of α -methylene- γ -lactones by modifications to the lactam nitrogen.

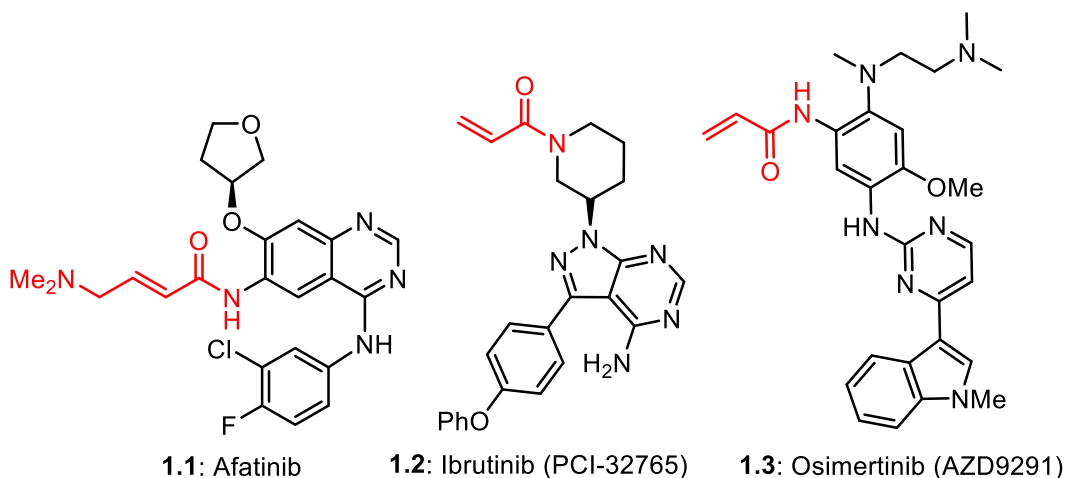


Figure 1.1. Recently approved, irreversible covalent drugs containing acrylamides.

This thesis describes the synthesis of guaianolide analogs containing an isosteric replacement of the α -methylene- γ -lactone Michael acceptor with an α -methylene- γ -lactam. Guaianolides possess a range of biological properties, and they contain an electrophilic α -methylene- γ -lactone which is often important for the observed bioactivity; examples of guaianolides include arglabin (**1.4**), eupatochinilide VI (**1.5**), moxartenolide (**1.6**), and chinensiolide B (**1.7**, Figure 1.2).²⁰⁻²⁴ However, the α -methylene- γ -lactone is also attributed to the toxicity of these compounds. By changing the nitrogen substituent of α -methylene- γ -lactam guaianolide analogs (e.g. **1.8**), the rate of hetero-Michael addition of thiols as well as the biological activity can be significantly affected due to the change in electrophilic reactivity of acrylamides and α -methylene- γ -lactams when electronically diverse nitrogen substituents are installed. Guaianolides have been shown to inhibit the NF- κ B (nuclear factor κ B) pathway by forming a

covalent bond between the α -methylene- γ -lactone and a sulfhydryl group of the p65 protein. Inhibition of the NF- κ B pathway promotes apoptosis and is frequently overactive in many cancers and inflammatory diseases making it a desirable drug target.²⁵⁻²⁷

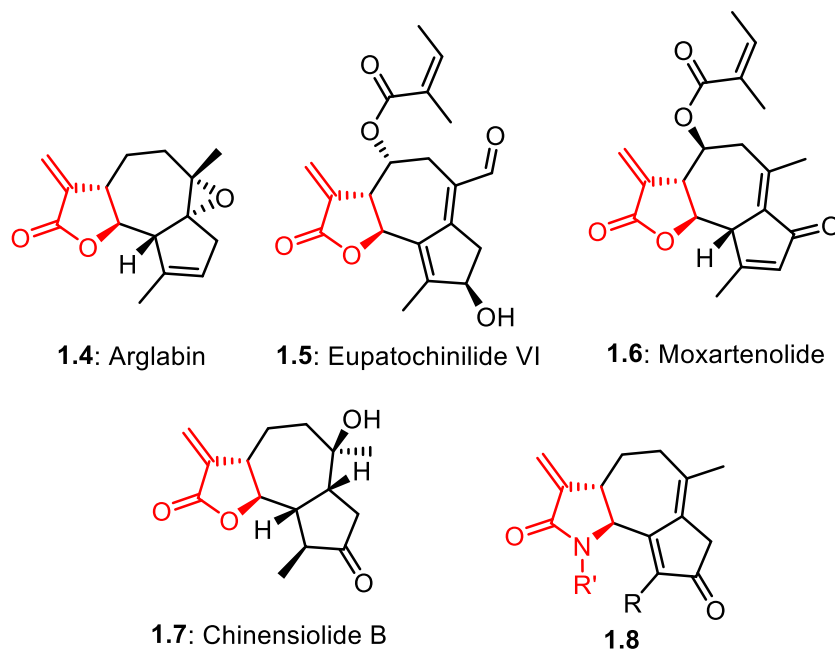


Figure 1.2. Guaianolide natural products and a model for tunable α -methylene- γ -lactam analogs.

To put this work in context, an introduction to covalent modifiers and examples of targeted covalent inhibition with acrylamides is presented. The hetero-Michael addition of thiols to α,β -unsaturated amides or lactams is compared to that of α -methylene- γ -lactones. Previous studies on the isosteric replacement of lactones with lactams are presented, as well as the tunability of α,β -unsaturated amide or lactam Michael acceptors. Methods for the synthesis of α -methylene- γ -lactams are reviewed before the synthesis of novel α -methylene- γ -lactam guaianolide analogs, which are accessible in 10-12 synthetic operations from commercially available starting materials, is discussed.

1.1 TARGETED COVALENT INHIBITION IN DRUG DESIGN

Covalent modifiers are an important class of compounds that, despite numerous successful examples, are typically avoided in target-directed drug discovery efforts.¹⁵ Protein reactive drugs inhibit protein function by forming covalent bonds with nucleophilic amino acids in proteins, in contrast with noncovalent drugs, which inhibit protein function by intermolecular interactions, and DNA reactive drugs that form covalent adducts with DNA bases. Covalent drugs are prevalent in the pharmaceutical industry, with at least 42 protein reactive covalent drugs being approved by the FDA as of 2011.¹⁶ Covalent drugs can bond to proteins or DNA via different mechanisms including acylation, alkylation, metal/metalloid binding, disulfide bond formation, hemiacetal formation, Michael addition, and the Pinner reaction.¹⁵ Of the approved covalent drugs, 14 are known to react with cysteine residues, and only five have been shown to undergo Michael addition (gemcitabine, floxuridine, afatanib (**1.1**), ibrutinib (**1.2**), and osimertinib (**1.3**)). One reason covalent drugs have been avoided in drug design is their potential for off-target reactivity that can lead to toxicity or an immune response,¹⁶ even though there has not been a systematic study demonstrating that covalent modifiers can lead to idiosyncratic effects.²⁸ However, covalent inhibitors containing weak electrophiles that require a significant noncovalent interaction for covalent bond formation to occur (i.e. quiescent irreversible inhibitors), should be distinguished from strongly electrophilic compounds that bind to many accessible nucleophilic residues on a variety of proteins.¹⁶ Weakly

electrophilic compounds bearing some noncovalent target affinity are more easily developed into biologically useful agents due to their enhanced predictability with respect to target binding.¹⁶

The majority of covalent drugs were discovered through screening of natural product or synthetic compound libraries and were demonstrated to have covalent mechanisms of action after FDA approval; the most conspicuous examples being aspirin and β -lactam antibiotics.¹⁶ More recently, covalent drugs have gained popularity by virtue of their ability to modulate difficult molecular targets.¹⁶ For example, selective kinase inhibitors that form covalent adducts to rare cysteine residues located in the active sites of kinases have been reported. Kinases are notoriously difficult to target with high selectivity using noncovalent inhibitors due to sequence conservation and the similarity of the ATP (adenosine triphosphate) binding pocket among the more than 500 human kinases.¹⁷ Covalent inhibition has also been used to target shallow binding pockets in HCV protease²⁹ and is being investigated for targeting protein-protein interactions.³⁰⁻³³ Thus, covalent drugs offer an approach to expanding the druggable landscape of biological molecules.

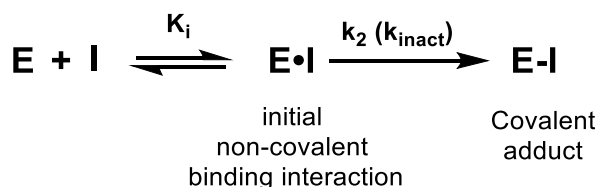
Covalent drugs can function as reversible and irreversible inhibitors of proteins. Irreversible inhibitors have been classified as covalent modifiers that undergo a reverse reaction slower than the rate of protein synthesis, while reversible covalent inhibitors undergo the reverse reaction faster than the rate of protein synthesis.¹⁶ Drugs that function as irreversible inhibitors have several advantages over ones that operate through noncovalent interactions alone. These include selectivity for specific proteins in the same family by targeting non-conserved residues in a binding site, small infrequent dosing due to a shutdown of protein function until that protein is resynthesized, and higher binding affinities. Covalent drugs have been shown to overcome drug resistance as seen with irreversible epidermal growth factor receptor (EGFR) inhibitors¹⁸⁻¹⁹ and hepatitis C viral (HCV) protease inhibitors.⁹ Mutations can cause drug resistance by changing the

shape of the active site and lowering the binding affinity by reducing noncovalent interactions (increasing k_i), but a covalent mechanism of inhibition may avoid this resistance mechanism.¹⁶ If the amino acid that is to be covalently modified is itself mutated, it is possible that a drug can still act as a noncovalent inhibitor.

Alternatively, rapidly reversible covalent inhibitors bind and release proteins like noncovalent inhibitors, but covalent bond formation provides a stronger binding affinity than most noncovalent interactions such as hydrogen bonding, van der Waals forces, π -stacking, and hydrophobic effects.²⁸ When compared to noncovalent inhibitors, reversible covalent inhibitors can have longer residence times and afford increased selectivity by forming covalent bonds to uniquely positioned amino acids. For example, one strategy for increasing the selectivity of an inhibitor involves the attachment of a Michael acceptor to a noncovalent inhibitor at a site that will be proximal to a cysteine when bound to a protein; targeting cysteine residues in this way is known as targeted covalent inhibition.¹⁶ Bioinformatics has shown that 211 kinases contain a cysteine in the ATP binding pocket in the active conformation which is distributed over 27 distinct positions.³⁴ For the inactive kinase conformations, which have extended binding pockets, 16 additional cysteine positions in 193 kinases were identified. However, only a few of these positions have been exploited for targeted covalent inhibition.³⁴

Targeted covalent modifiers initially form a noncovalent complex with a target protein through noncovalent interactions. This is followed by covalent bond formation with a nucleophilic amino acid as depicted by Equation 1.1. The initial binding specificity, k_i , can be improved by optimizing the noncovalent interactions between a small-molecule inhibitor and its protein target, similar to noncovalent drugs. The k_{inact} (k_2) is the rate at which the covalent modification occurs and is typically optimized by placing an electrophilic moiety in close proximity to a nucleophile

in the binding site. Alternatively, increasing the reactivity of the electrophilic moiety can increase the rate of covalent bond formation to a target protein. The potency and selectivity of covalent drugs can be measured by the specificity constant, which is equal to k_{inact}/k_i , and is considered a more reliable measure of potency for irreversible inhibitors than IC_{50} (half maximal inhibitory concentration) values.^{16, 35-37} This is because irreversible, covalent inhibitors display time-dependent inhibition which is not accounted for in typical IC_{50} assays. IC_{50} measurements are commonly used for the characterization of irreversible inhibitors in biochemical assays with an associated time (i.e. IC_{50} for target inhibition after treatment with an inhibitor for 0.5 h) and, more appropriately, in cellular assays where the activity of the irreversible inhibitor is dependent on multiple factors such as cellular uptake, compound stability, and target inhibition.



Equation 1.1 Covalent inhibition of an enzyme.

As targeted covalent modification has been validated as an approach to drug development, a number of acrylamide-containing covalent inhibitors have displayed promising biological activity. In addition to the approved drugs afatinib (**1**), ibrutinib (**2**), and osimertinib (**3**), there have been a number of other acrylamide compounds that have shown potential as drugs and biological probes.

Telaprevir (**1.9**) is a reversible covalent modifier that treats hepatitis C virus (HCV) by targeting a catalytic serine in the HCV protease. This serine is common across many viral and

human proteases (Ser139 in HCV protease); a reversible covalent bond occurs by forming a hemiacetal between the hydroxyl group of serine and the ketoamide functionality of telaprevir.²⁹ The utility of telaprevir (**1.9**) inspired the development of irreversible HCV protease inhibitors **1.10** and **1.11** which included an acrylamide motif on a structurally related scaffold (Figure 1.3).⁹ Inhibitors **1.10** and **1.11** were designed to target Cys159, a unique amino acid to HCV protease identified using structural bioinformatics.⁹ In a fixed time point enzymatic assay, compounds **1.10** and **1.11** with a Michael acceptor were potent inhibitors of HCV protease ($IC_{50} = 4$ and 2 nM for **1.10** and **1.11**, respectively) while compound **1.12** which lacks the acrylamide group, showed only weak inhibition of HCV protease ($IC_{50} = 1147$ nM).⁹ A targeted covalent inhibition mechanism for compounds **1.10** and **1.11** was supported by mutation of Cys159 to serine, which resulted in a reduction in potency of **1.10** and **1.11**, whereas **1.12** maintained a similar potency compared to the non-mutated protein. Co-crystallization of inhibitor **1.10** with HCV protease confirmed a covalent C–S bond between Cys159 and the acrylamide group.⁹

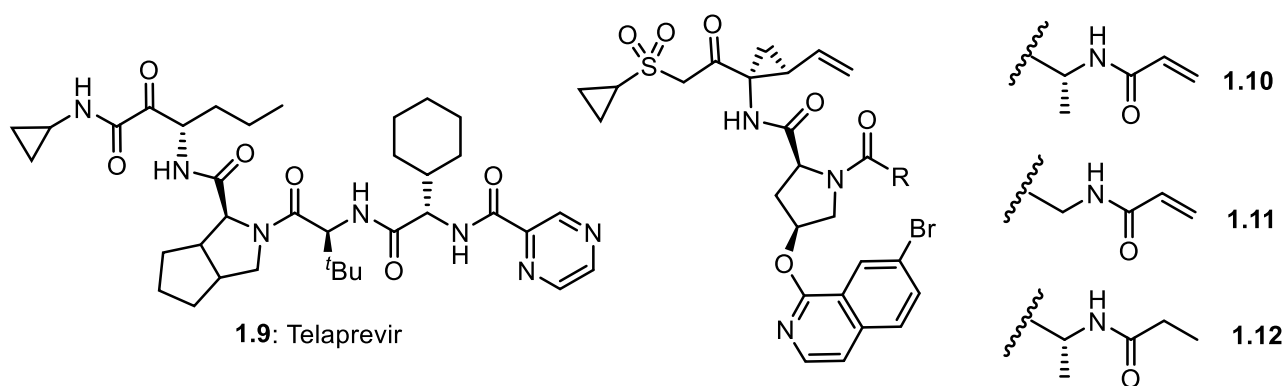


Figure 1.3. HCV protease inhibitors.

Gefitinib (**1.13**) is a small molecule inhibitor that targets mutated forms of EGFR in cancer cells. After FDA approval in 2003, it was discovered that EGFRs acquire resistance through

specific mutations within the binding pocket; nearly half of the patients had a T790M single point mutation responsible for resistance to therapy.⁶ To combat this acquired resistance, structural modifications were made to gefitinib (**1.13**) that included replacement of the 3-morpholino propyl group with a 4-dimethylaminobutenamide to produce afatinib (**1.1**), a compound designed to undergo a hetero-Michael addition with Cys797 in the active site of EGFR (Figure 1.4). Indeed, this second-generation EGFR inhibitor afatinib (**1.1**) was active at the nanomolar level against lung cancer cells containing this mutation.⁵⁻⁶ X-ray crystallography and in situ labeling followed by LC-MS/MS analysis confirmed a covalent bond between afatinib (**1.1**) and Cys797.¹⁰ Despite FDA approval, afatinib (**1.1**) was somewhat toxic and required large dosages due to low efficacy. It has been postulated that this toxicity is due to inhibition of wild-type EGFR and that the low efficacy was a result of diminished noncovalent binding of **1.1** to T790M EGFR.³⁸ Third-generation EGFR inhibitors osimertinib (**1.3**) and rociletinib (**1.14**) were developed to selectively target T790M-mutated EGFR over wild-type EGFR.³⁹ Osimertinib (**1.3**, AZD9291, Tagrisso) is an irreversible, mutant-selective EGFR inhibitor, developed by AstraZeneca, which was approved in November 2015 for treatment of non-small cell lung cancer for patients with the T790M mutation of EGFR; osimertinib (**1.3**) has an IC₅₀ value of 12 nM for EGFR with the L858R/T790M mutation and an IC₅₀ value of 480 nM for wild-type EGFR.^{2, 8} Rociletinib (**1.14**, CO-1686, AVL-301) is another mutant selective covalent inhibitor of L858R/T790M EGFR, currently in clinical trials, with a k_i of 21.5 nM against this mutation and a k_i of 303.3 nM against wild type EGFR (Figure 1.4).⁴⁰⁻⁴¹ Recently, mutation of Cys797 to serine has been discovered as a mutation that imparts resistance to these covalent modifiers **1.1**, **1.3**, **1.13**, **1.14**, as the less nucleophilic serine fails to form a covalent bond with the acrylamide Michael acceptors.⁴²

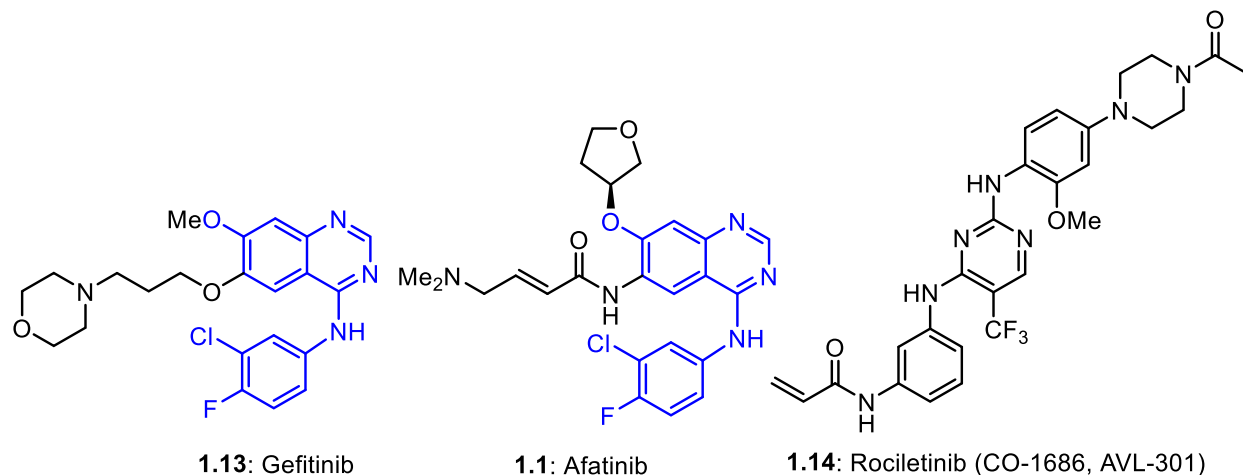


Figure 1.4. Reversible and irreversible EGFR inhibitors.

Fibroblast growth factor receptors (FGFR1-4) and Bruton's tyrosine kinase (Btk) are tyrosine kinases related to EGFR and which are also susceptible to irreversible, covalent inhibition. Inhibitors of these enzymes were designed using a similar targeted covalent inhibition strategy to that described above. Noncovalent FGFR inhibitor PD173074 (**1.15**) led to the design of FIIN-1 (**1.16**) possessing an acrylamide group that reacts with Cys486 in the ATP binding pocket of FGFR1 to form a hetero-Michael adduct (Figure 1.5).¹¹ Reduction of the acrylamide double bond of **1.16** resulted in a 24-fold decrease in activity for blocking proliferation and survival of FGFR1-transformed Ba/F3 cells (EC_{50} , 14 nM vs 340 nM) and a 100-fold decrease in activity against FGFR3-transformed Ba/F3 cells (EC_{50} , 10 nM vs 1040 nM), demonstrating the importance of the Michael acceptor for effective inhibition.¹¹

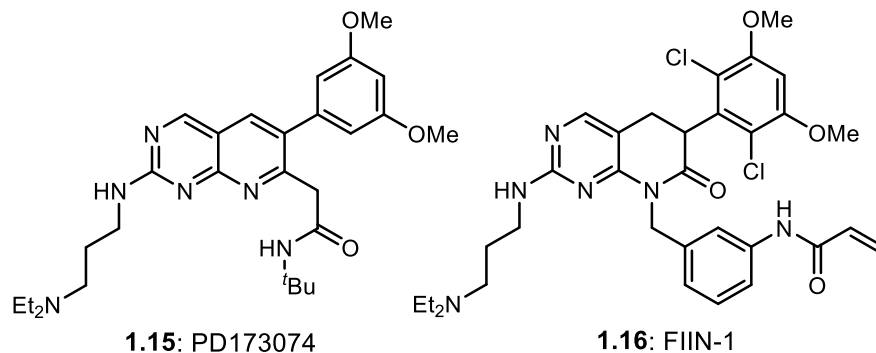


Figure 1.5. FGFR inhibitors.

The Btk noncovalent inhibitor PCI-29732 (**1.17**) was used in the design of targeted covalent inhibitor ibrutinib (**1.2**, PCI-32765), which shows a 500-fold increase in selectivity for Btk over related kinases Lck/Yes-related novel tyrosine kinase (Lyn) and spleen tyrosine kinase (Syk) in Ramos cells; PCI-29732 (**1.17**) showed only a 4-fold selectivity for Btk in the same assay (Figure 1.6).¹² This increased selectivity is a result of covalent bond formation between the acrylamide group of ibrutinib (**1.2**) and Cys481 in the ATP-binding pocket of Btk.⁷ Ibrutinib (**1.2**) favors inhibition of kinases containing a cysteine or serine at position 481 with >100-fold selectivity, inhibiting only a few kinases, Btk, Blk (B lymphocyte kinase), and Bmx (bone marrow tyrosine kinase gene in chromosome x, also called Etk), with subnanomolar potencies due similarities in their binding sites.⁷ Lou et al. propose that amino acids larger than cysteine or serine at the position equivalent to Cys481 of Btk clash with the pyrazolidine ring, leading to increased selectivity over kinases lacking a cysteine or serine at this position, but there is no evidence of serine undergoing covalent bond formation to **1.2**.⁷ Ibrutinib (**1.2**) was approved by the FDA in 2013 for the treatment of mantle cell lymphoma and in 2014 for the treatment of chronic lymphocytic leukemia; it is predicted to reach peak annual sales of \$5 billion a year and is currently in clinical trials for the treatment of other types of cancers.^{3-4, 43} Spebrutinib (**1.18**, AVL-292, CC-

292) is similar in structure to ibrutinib (**1.2**) and is an irreversible Btk inhibitor under investigation for the treatment of chronic lymphocytic leukemia as well as rheumatoid arthritis and multiple myeloma (Figure 1.6).⁴⁴⁻⁴⁵ The recent approvals of several covalent drugs utilizing an acrylamide motif have led to the development of acrylamide-containing, irreversible inhibitors for a number of protein targets which are difficult to target noncovalently due to similarities with other proteins. By utilizing rare cysteine residues in the active sites of various proteins, target selectivity can be achieved. Identification of unique cysteine residues in kinases through analysis of available crystal structures, sequencing information, and proteomics methods have identified 404 kinases with cysteines in the active site. These cysteines are located at 43 distinct positions (27 positions for active conformations in 211 kinases and 16 positions for inactive conformations in 193 kinases), indicating potential for the development of selective, covalent kinase inhibitors.^{34, 46-47}

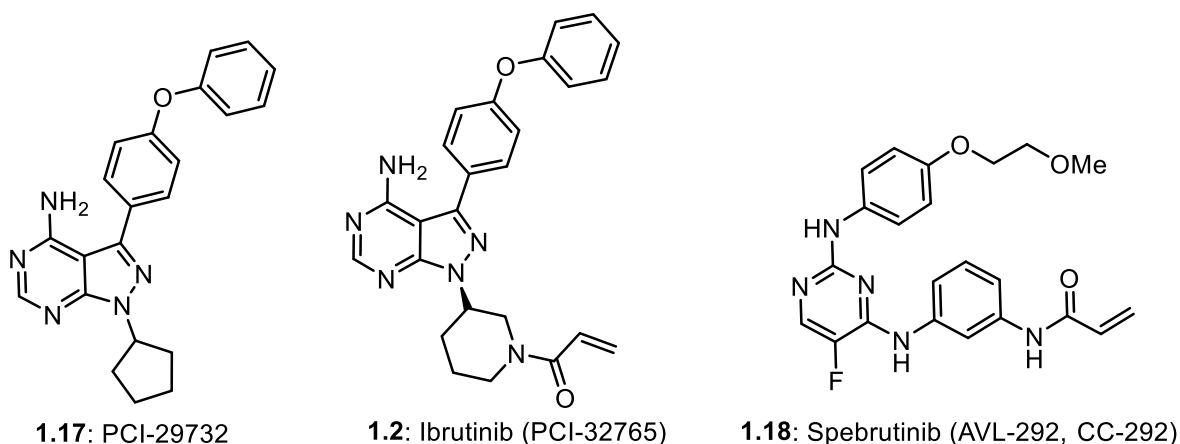


Figure 1.6. Btk inhibitors.

Screening of covalent inhibitors for kinase inhibitions led to the development of pan JNK (c-jun NH₂-terminal kinase) inhibitors **1.19-1.21** (Figure 1.7).¹³ JNK-IN-11 (**1.19**), the most potent inhibitor tested with IC₅₀ values of 0.5-1.3 nM for inhibition of JNK1/2/3, also showed significant

inhibition against several other kinases. However, JNK-IN-8 (**1.20**) showed excellent selectivity for JNK1/2/3 over other kinases with only a small decrease in activity (IC_{50} of 1-18.7 nM for inhibition of JNK1/2/3). Incorporation of an acrylamide motif was necessary for in vivo potency and selectivity for JNK1/2/3 in a panel of 200 kinases using a fixed time point enzymatic assay; without this group, the activity of each inhibitor was reduced 100-fold.¹³ Covalent kinase inhibitors for Bmx and cyclin dependent kinase 7 (CDK7) have also been developed using this strategy.⁴⁸⁻⁴⁹

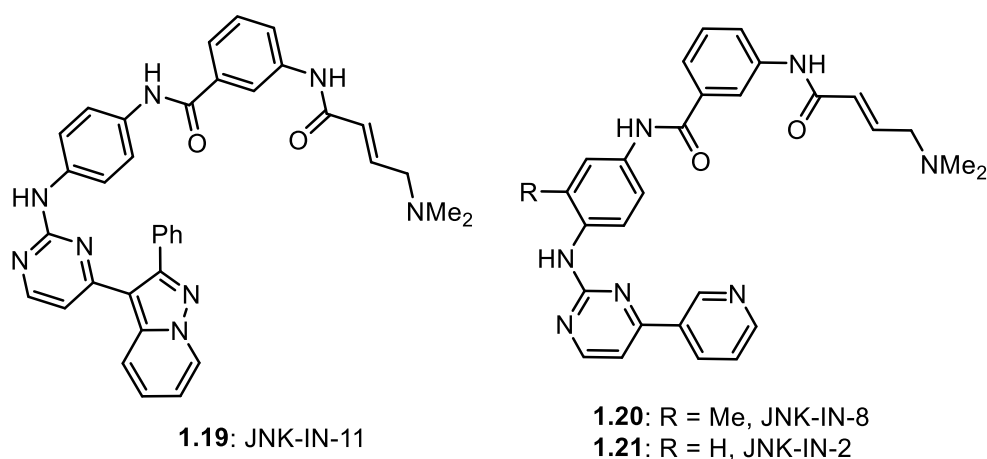


Figure 1.7. Pan JNK 1/2/3 inhibitors.

Gaining specificity to a target protein through targeted covalent inhibition has been demonstrated as a successful strategy in the examples presented above. An acrylamide group is often used as the Michael acceptor in these approaches because it is weakly electrophilic, limiting an off-target reactivity. An alternative strategy to incorporating weakly electrophilic groups at key locations in an inhibitor is the inclusion of strong electrophiles that form rapidly reversible covalent bonds in a non-biological environment, such as cyanoacrylamides.⁵⁰ The additional electron-withdrawing cyano group increases the reaction kinetics of the thiol addition, but in turn decreases the equilibrium constant, possibly by decreasing the pK_a of the α -proton on the Michael

adduct.⁵¹ Designing inhibitors with sufficient noncovalent affinity to place the acrylamide near an a cysteine residue in a binding pocket is required for covalent bond formation to occur, thus minimizing side reactions with other cellular thiols, such as GSH and solvent-exposed cysteines on other proteins.^{16, 28, 52} Several reviews have been published on the development and use of irreversible kinase inhibitors.^{17, 46, 52-55} The development and approval of several acrylamide-containing targeted covalent modifiers demonstrate that this is a valid strategy for drug development. In order to develop new targeted covalent modifiers, the thiol reactivity of other electrophiles needs to be better understood.

1.2. BIOLOGICAL ACTIVITY AND THIOL REACTIVITY OF α -METHYLENE- γ -LACTONES, α -METHYLENE- γ -LACTAMS, MACROCYCLIC α -METHYLENE LACTAMS, AND ACRYLAMIDES

The biological activity and thiol reactivity of various α -methylene- γ -lactones, α -methylene- γ -lactams, macrocyclic α -methylene lactams, and acrylamides are presented for comparison of these different structures. As not a lot of information is available for direct comparison of these various electrophiles, the bioactivity and thiol reactivity is presented in various ways depending on the availability; this includes rate data for thiol addition, yields of thiol addition reactions, evidence for protein adduct formation, and toxicity of isosteric α -methylene-lactones and lactams. Sesquiterpene lactones are a major class of natural products and several reviews have covered the biological importance and therapeutic potential of α -methylene- γ -lactone-containing compounds.⁵⁶⁻⁵⁸ α -Methylene- γ -lactones react with biologically relevant thiols such as cysteine

and glutathione (GSH) via a hetero-Michael addition reaction to form thiol adducts both in a flask and in biologically relevant systems.⁵⁹⁻⁶²

Examples of sesquiterpene lactone natural products containing an α -methylene- γ -lactone for which thiol reactivity data is available include melampomagnolide B (**1.22**), parthenolide (**1.23**), costunolide (**1.24**), anhydroverlatorin (**1.25**), and verlatorin (**1.26**, Figure 1.8).⁶³⁻⁶⁷ The α -methylene- γ -lactone is responsible for the many of the observed biological activities of sesquiterpene lactones, as reduction of the exocyclic methylene generally eliminates biological activity, with a few exceptions.^{22-24, 68} α -Methylene- γ -lactams are much less common in natural products, and their biological activity and thiol reactivity are not as well studied as their lactone counterparts.⁶⁹ However, α -methylene- γ -lactams are generally categorized as less toxic than the isosteric lactones. Lactams such as pukeleimide (**1.27**), anatin (**1.28**), gelegamine (**1.29**), and bisavenanthramide B-6 (**1.30**) are some of the only natural products known that possess α -methylene or α -alkylidene moieties on small rings. (Figure 1.8).^{69 70} Macrocyclic α -methylene-lactams such as the microcystins and rakicidin A have been shown to react with thiols and are also discussed in this section.

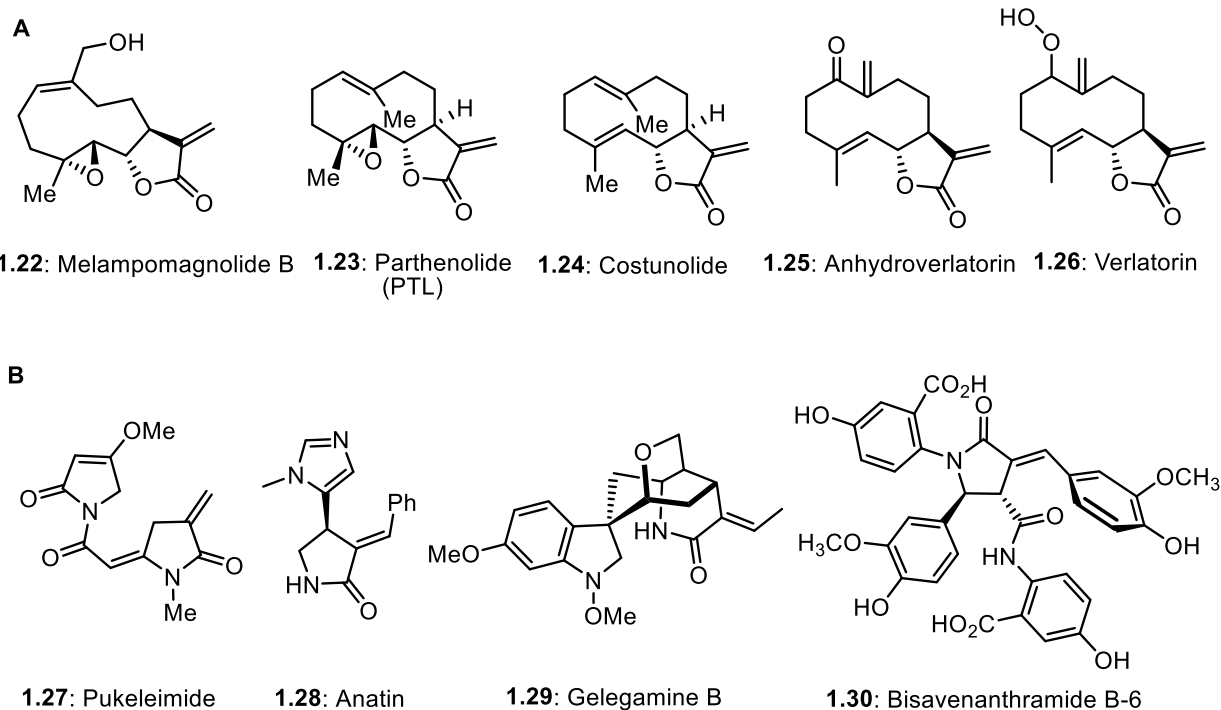


Figure 1.8. Natural products with α -methylene- γ -lactones (A) or α -methylene- γ -lactams (B).

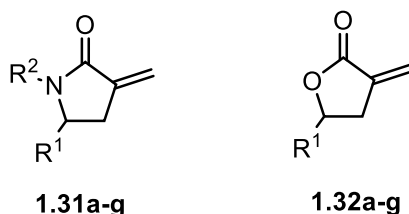
1.2.1. Comparison of the Biological Activities of Isosteric α -Methylene- γ -lactams and α -Methylene- γ -lactones

The biological activities of synthetic, small molecule α -methylene- γ -lactams have been compared to the corresponding lactones when small libraries of these compounds were prepared. A recent review highlights the biological activity of natural product α -methylene- γ -lactones and lactams.⁷¹ In most cases the lactam is less active than the lactone, but few studies have examined the effects of changing the nitrogen substituent, instead focusing on the substituents at the β and γ -positions of the lactones and lactams, while the nitrogen remained unsubstituted or methylated. Additionally, the reduced toxicity observed for α -methylene- γ -lactams compared to isosteric α -methylene- γ -

lactones could be beneficial in cases where the bioactivity for a particular target or pathway is maintained.

Table 1.1 compares the cytotoxicity of isosteric α -methylene- γ -lactams and lactones with various γ -substituents.⁷²⁻⁷³ The cytotoxicity of α -methylene- γ -lactones ranges from 1.3-32.5 μ M in the mouse lymphocytic leukemia cell line L-1210, while the corresponding lactams range from 20.0 to >100 μ M. The L-1210 cell line is the only one where a lactam is more cytotoxic than the lactone, although **1.31a** and **1.32a** are fairly close in cytotoxicity (entries 1-2). The human leukemia cell lines (HL-60 and NALM-6) show a much greater difference in cytotoxicity between the α -methylene- γ -lactones (IC₅₀ = 20-100 μ M) and the isosteric lactams (IC₅₀ = 83-989 μ M, Table 1.1).

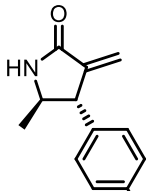
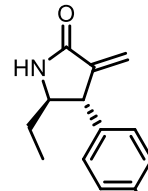
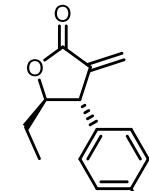
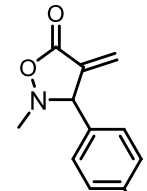
Table 1.1. Comparison of cytotoxicity of γ -substituted α -methylene- γ -lactams and lactones.



Entry	Compound	R ¹	R ²	Cytotoxicity (IC ₅₀ , μ M)		
				L-1210	HL-60	NALM-6
1	1.31a	Me	H	20.0	640	658
2	1.32a	Me	-	32.5	77.4	41.0
3	1.31b	Et	H	>100	894	387
4	1.32b	Et	-	6.0	39.5	51.6
5	1.31c	n-pentyl	H	59.0	397	82.7
6	1.32c	n-pentyl	-	20.0	99.4	23.6
7	1.31d	Bn	H	93.0	490	420
8	1.32d	Bn	-	15.5	42.7	5.4
9	1.31e	CH ₂ -3,4-OMeC ₆ H ₃	H	79.0	402	507
10	1.32e	CH ₂ -3,4-OMeC ₆ H ₃	-	4.3	46.3	6.0
11	1.31f	Ph	Me	>50	989	553
12	1.32f	Ph	-	1.4	36.9	9.1
13	1.31g	4-BrC ₆ H ₄	Me	>50	220	141
14	1.32g	4-BrC ₆ H ₄	-	1.3	20.3	85.3

Table 1.2 compares the cytotoxicities of β , γ -substituted α -methylene- γ -lactams **1.33-1.34** to the structurally similar lactone **1.35** and isoxazolidinone **1.36**.⁷⁴⁻⁷⁶ As above, the α -methylene- γ -lactams **1.33-1.34** are significantly less toxic than the lactone **1.35** and isoxazolidinone **1.36**, which each show similar cytotoxicity values in the 3 cell lines tested. Surprisingly, the γ -ethyl lactam **1.34** is 5-8 fold more cytotoxic than the γ -methyl substituted lactam **1.33**, suggesting that thiol reactivity is not the only factor that influences the cytotoxicity of these compounds, but molecular recognition or lipophilicity may play a role.

Table 1.2. Cytotoxicity of β -aryl- γ -alkyl substituted α -methylene- γ -lactams, lactones, and isoxazolidinones.

Compound	Cell line	Cytotoxicity (IC ₅₀ , μ M)			
					
		1.33 Br	1.34 Br	1.35 Br	1.36 Br
	L-1210	-	43	1.6	0.7
	HL-60	516	66	1.2	5.1
	NALM-6	434	81	0.6	4.6

Hall and coworkers synthesized a library of α -methylene and α -arylidene- γ -lactones and lactams which were screened for inhibition of homoserine transacetylase (HTA).⁷⁷ HTA is an essential enzyme involved in the biosynthesis of methionine, which is found in fungi, gram positive and some gram negative bacteria, but not in more complex eukaryotes; it is a potential target for new antibiotics. Out of 111 compounds screened, ten hits were obtained and five hits were confirmed upon further testing. IC₅₀ values were obtained for two α -methylene- γ -lactams **1.37** and **1.38** which inhibited HTA with IC₅₀ values of 144 and 140 μ M, respectively (Figure 1.9).

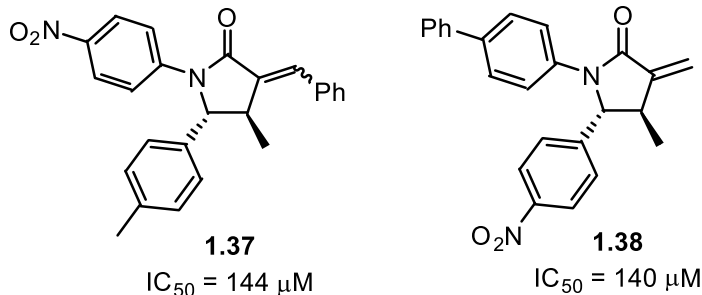


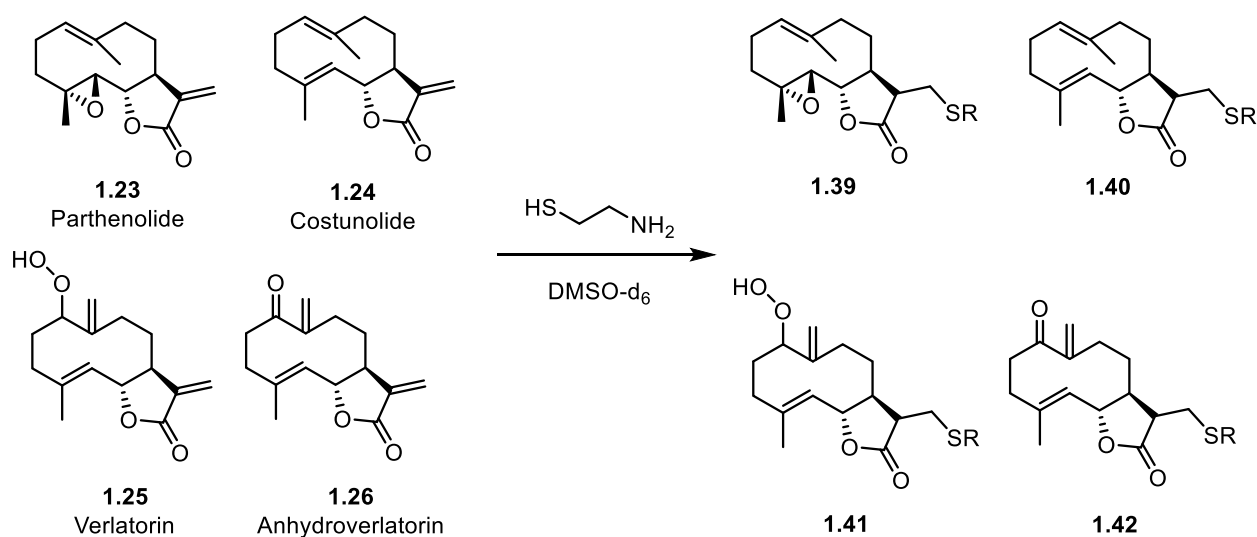
Figure 1.9. α -Methylene- γ -lactam inhibitors of homoserine transacetylase (HTA).

α -Methylene- γ -lactams are generally less toxic than isosteric α -methylene- γ -lactones, although the reasons for this are unclear from the data available. One possibility is the reduced electrophilic reactivity of α -methylene- γ -lactams compared to α -methylene- γ -lactones.

1.2.2. Thiol Reactivity of α -Methylene- γ -lactones

Thiol adduct formation can be used to predict the potential of α -methylene- γ -lactones to form covalent adducts to cysteine residues in proteins. Rapid formation of thiol adducts can indicate that an electrophile will react indiscriminately with solvent exposed cysteine residues. Parthenolide (**1.23**), costunolide (**1.24**), verlatorin (**1.25**), and anhydroverlatorin (**1.26**) were all confirmed to react with cysteamine in DMSO- d_6 , a ^1H NMR method that measured the disappearance of the α -methylene peaks of the lactone.⁷⁸ Costunolide (**1.24**), possessing an α -methylene-lactone was used as a benchmark for measuring conjugate addition, as thiol addition to **1.24** has been documented.⁷⁹⁻⁸⁰ Unactivated thiols dodecanethiol or *N*-acetyl-cysteamine did not react with costunolide (**1.24**) in 24 h with toluene, chloroform, MeCN, MeOH, or DMSO solvents.⁷⁸ Cysteamine is an activated thiol due to the free amine which can act as a base for

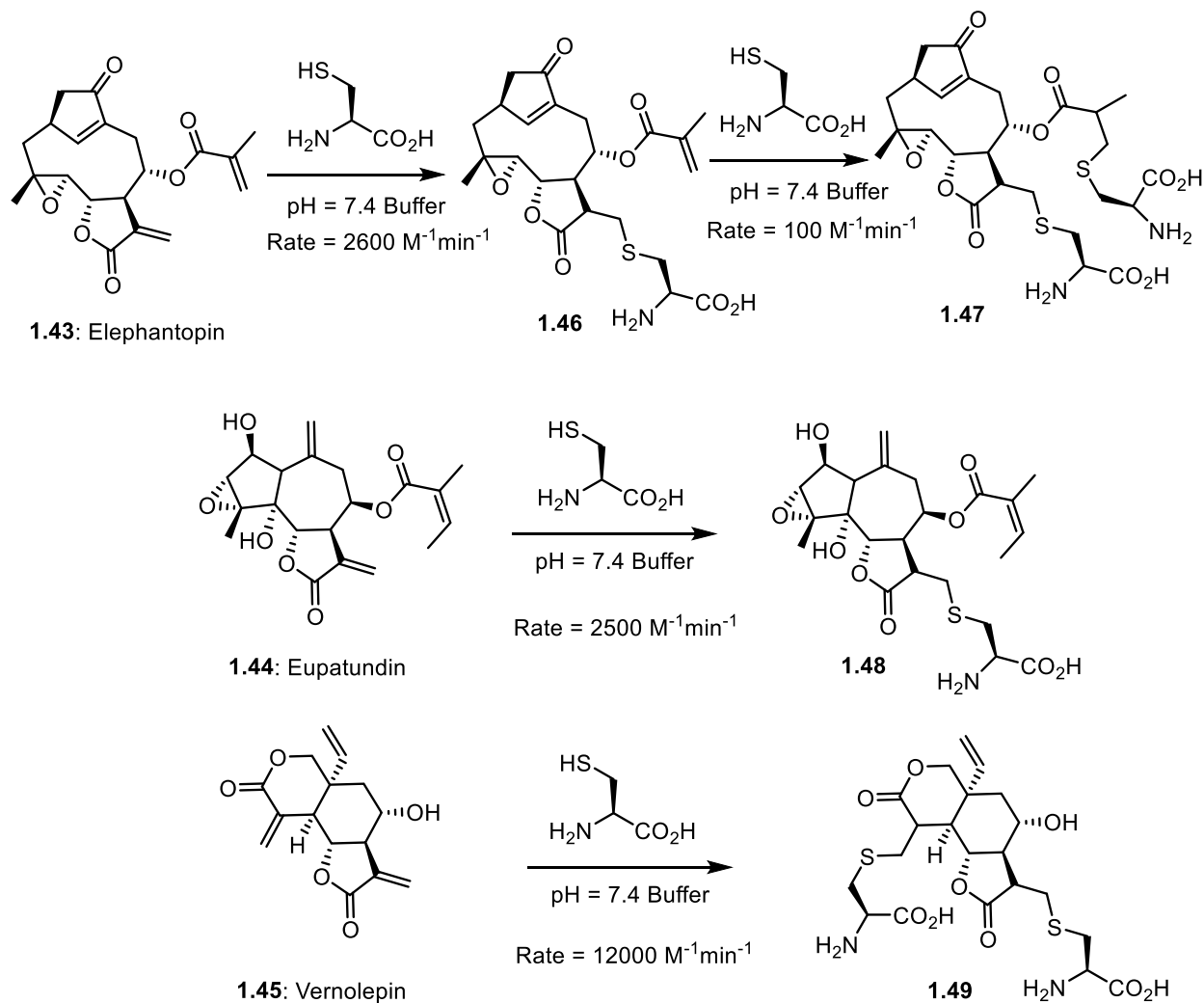
deprotonating the thiol or a hydrogen bond donor to activate the carbonyl of the α -methylene- γ -lactone towards conjugate addition. Hetero-Michael addition of cysteamine to **1.24** occurred slowly in methanol or acetonitrile and instantaneously in DMSO. Using this data Michael acceptors were classified as reactive or nonreactive based on whether they formed adducts with cysteamine. The reactive compounds were further classified as reversible or irreversible based upon the reversibility of the hetero-Michael addition upon 10-fold dilution with CDCl_3 . This method also demonstrated the selectivity of cysteamine for thiol addition with Michael acceptors as no reaction with the peroxide of **1.25** or the epoxide of **1.26** was detected.



Scheme 1.1. α -Methylene- γ -lactones that react with cysteamine in ^1H NMR assay.

The reactivity of three α -methylene- γ -lactone-containing natural products, elephantopin (**1.43**), eupatundin, (**1.44**), and vernolepin (**1.45**) with endogenous nucleophiles, such as lysine and cysteine, was measured in a kinetic study by Kupchan et al. in aqueous phosphate buffer (pH = 7.4, Scheme 1.2).⁵⁹ The reaction with lysine formed less than 25% of an adduct after 6 d at rt, while cysteine reacted with the α -methylene- γ -lactone moiety of these compounds to form thiol

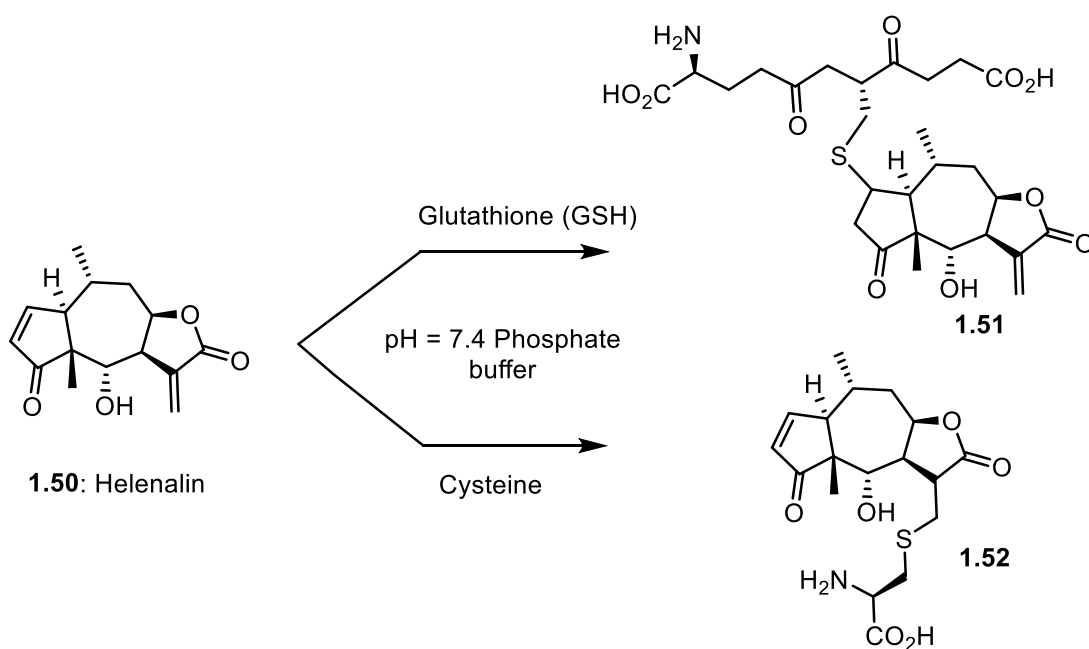
adducts within minutes. The second order rate constant for addition of cysteine to the exocyclic α -methylene- γ -lactone of elephantopin (**1.43**) was $2600 \text{ M}^{-1}\text{min}^{-1}$ while addition to the acyclic methacrylate of **1.46** to form **1.47** was about 26 times slower with a rate constant of $100 \text{ M}^{-1}\text{min}^{-1}$. The rate constant for cysteine addition to eupatundin (**1.44**) was $2500 \text{ M}^{-1}\text{min}^{-1}$, while vernolepin (**1.45**) reacted the fastest with cysteine with a rate constant of $12000 \text{ M}^{-1}\text{min}^{-1}$.



Scheme 1.2. Cysteine adduct formation with α -methylene- γ -lactone natural products.

Helenalin (**1.50**) is a natural product containing a cyclopentenone and an exocyclic α -methylene- γ -lactone, which reacts with biological thiols cysteine and glutathione (GSH). Characterization of the thiol adducts of helenalin (**1.51-1.52**) by NMR showed that GSH addition

preferentially occurred at the cyclopentenone, while cysteine addition occurred at the α -methylene- γ -lactone when a single equivalent of thiol was added (Scheme 1.3).⁶¹ When excess glutathione or cysteine was reacted with helenalin (**1.50**), addition to both Michael acceptors was observed. The rate of glutathione addition to the cyclopentenone was found to be about 10-fold faster than the rate of glutathione addition to the α -methylene- γ -lactone ($0.08 \text{ M}^{-1}\text{min}^{-1}$ compared to $0.008 \text{ M}^{-1}\text{min}^{-1}$). Cysteine addition to helenalin (**1.50**) added to the α -methylene- γ -lactone in less than 5 min, while requiring approximately 17 hours to completely react with the cyclopentenone. The rate of glutathione addition to related pseudoguaianolide compounds showed a dependency on the pH, where the rate increased at a more basic pH, as would be expected.⁶²



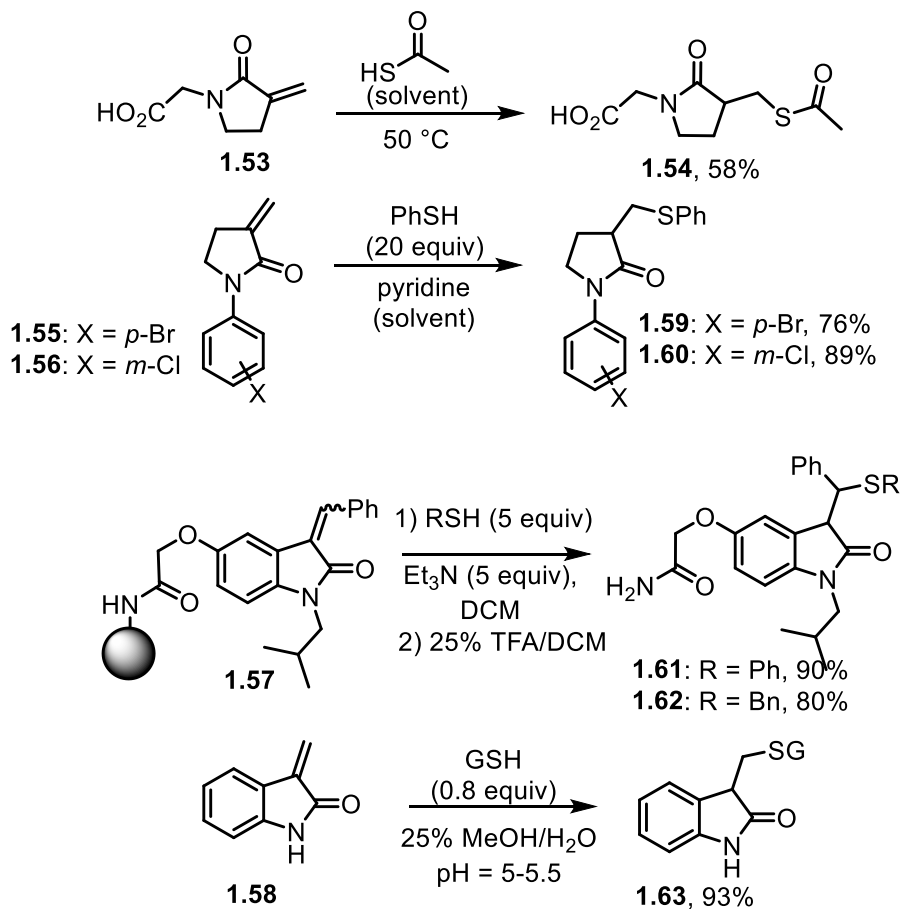
Scheme 1.3. Chemoselectivity of glutathione and cysteine addition to helenalin.

The thiol reactivity of α -methylene- γ -lactones has been demonstrated for a variety of complex natural products, and the rates of thiol addition have been compared to other Michael acceptors such as enones or α,β -unsaturated esters. The rate of thiol addition was sensitive to the

pH of a solution as well as the structure of the thiol used. Although the thiol reactivity of α -methylene- γ -lactones has been studied, little is known about the isosteric α -methylene- γ -lactams.

1.2.3. Thiol Reactivity of α -Methylene- γ -lactams

The thiol reactivity of α -methylene- γ -lactams or 3-methylenepyrrolidin-2-ones is not well documented, especially compared the reactivity of α -methylene- γ -lactones. In general, α -methylene lactams are less reactive towards thiols than the corresponding lactones and formation of the thiol adducts usually requires more forcing conditions.⁸¹⁻⁸⁵ For example, α -methylene- γ -lactam **1.53** required thioacetic acid solvent and heating to 50 °C to obtain adduct **1.54** in 58% yield;⁸⁵ for lactams **1.55**, **1.56**, and oxindole **1.57**, thiols were used in excess, and base additives were needed to effect thiol addition in good yields (Scheme 1.4).⁸¹⁻⁸² For oxindole **1.58**, thiol addition occurred with an acidic pH between 5 and 5.5 to give adduct **1.63** in 93% yield (based on GSH).⁸³



Scheme 1.4. Thiol adduct formation with α -methylene- γ -lactams and oxindoles.

Although α -methylene- γ -lactams are less susceptible to thiol addition than the isosteric α -methylene- γ -lactones, it is clear from the limited available data that more work is needed to better understand the thiol reactivity of α -methylene- γ -lactams.

1.2.4. Thiol Reactivity and Biological Activity of Macrocyclic α -Methylene Lactams

Although α -methylene- γ -lactams are relatively uncommon in natural products, macrocyclic α -methylene lactams are present in natural products such as the microcystins and rakicidin A. The

thiol reactivity and biological activity of macrocyclic α -methylene lactams are presented in this section to provide insight into the thiol reactivity of α -methylene- γ -lactams.

Microcystins are heptapeptides containing a dehydroalanine moiety, one member from this class of compounds, **1.64**, is depicted in Figure 1.10. Microcystins have been reported to form covalent bonds with noncatalytic cysteine residues in serine/threonine phosphatases (PP1 and PP2A).⁸⁶ Moreover, GSH and cysteine have both been shown to add to the exocyclic double bond of the unsaturated amide of microcystins; these thiol adducts were tested and showed an approximate 8-fold reduction in LD₅₀ values compared to unconjugated microcystins in mice.⁸⁷ Mutation studies involving the conversion of Cys273 to alanine resulted in the inability of microcystin LR **1.64** to form a covalent adduct, but the inhibition of C273A mutant PP1 by **1.64** was not significantly affected, suggesting that there is considerable noncovalent affinity of microcystin LR **1.64** for PP1. Covalent targeting by macrocycle **1.64** was further confirmed by a co-crystal structure of the compound covalently bound to Cys273 of PP1.⁸⁸⁻⁸⁹

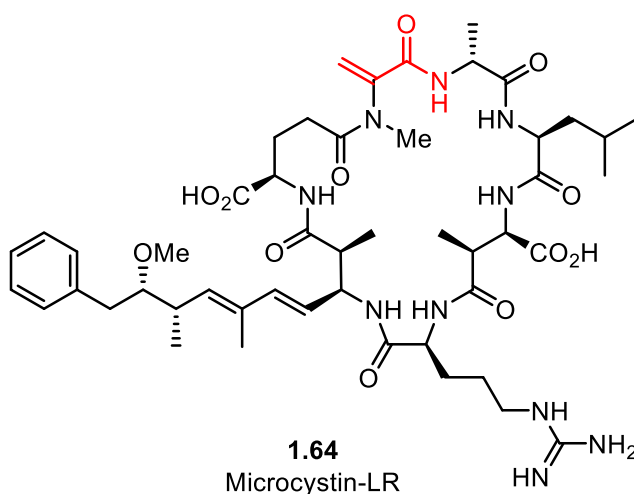
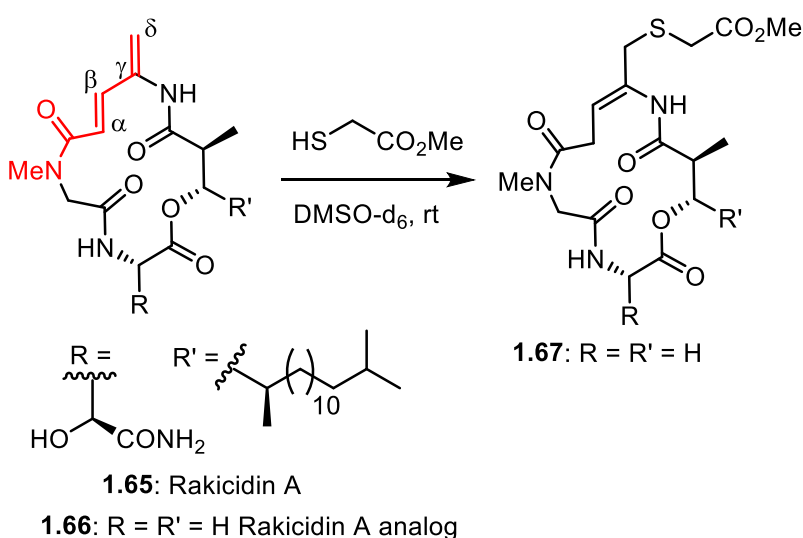


Figure 1.10. Example of a microcystin.

Rakicidin A (**1.65**) shows cytotoxicity against some cancer cell lines and contains a 4-amido-2,4-pentadienoate moiety that is critical for bioactivity (Scheme 1.5). An analog of Rakicidin A **1.66** was prepared and shown to form adduct **1.67** with methyl thioglycolate through 1,6-addition.⁹⁰ When monitoring the reaction by ¹H NMR, a different thiol adduct was the major product detected after 24 h, but this compound could not be isolated and only adduct **1.67** was detected after a longer reaction time of 72 h. The initial adduct formed was proposed to arise from thiol addition to the γ carbon, which could occur via 1,4-addition of methyl thioglycolate to the acyl-imine tautomer of Rakicidin A analog **1.66**.



Scheme 1.5. Rakicidin A and analog: a 1,6-addition product with methyl thioglycolate.

Thiol adduct formation to macrocyclic α -methylene lactams occurs with both small molecule thiols as well as cysteines in proteins. Although microcystin LR showed covalent bond formation to Cys273 in a co-crystal structure, the inhibition of a C273A mutant of PP1 by microcystin LR was only minimally affected, suggesting that noncovalent binding between the macrocycle and PP1 promotes covalent bond formation.

1.2.5. Thiol Reactivity of Acrylamides

The thiol reactivity of acrylamides has been studied due to their incorporation into targeted covalent modifiers as discussed in section 1.1. Examples that show the various effects of the nitrogen substituent and substituents at the α and/or β -positions of acrylamides are presented in this section. It is hypothesized that α -methylene- γ -lactams should display similar reactivities to acrylamides. Generally, acrylamides are weakly electrophilic and relatively unreactive towards thiols. These acyclic α,β -unsaturated amides are similar in electrophilic reactivity to α -methylene- γ -lactams. However, there are exceptions and these include the placement of an additional electron withdrawing group at the α position of the acrylamide.⁵⁰ The relative thiol reactivities of acrylamides possessing different substituents were compared in a competition assay with a limiting amount of GSH.¹⁸⁻¹⁹ Two acrylamides (2.5 mM of each) were reacted with GSH (1.25 mM) in a THF-H₂O-MeOH mixture at rt for 20-24 h and the amount of adduct formation was calculated by integration of HPLC peaks. These conditions were chosen to give low conversion to GSH adducts so that the ratios of GSH adducts formed would reflect kinetic control. The Lewis basic aminomethylene group of **1.69** afforded more of the GSH adduct relative to acrylamide **1.68** (entry 1, Table 1.3A). β -Morpholinomethylene **1.77** afforded less of a GSH adduct than an *N,N*-dimethylaminomethylene **1.69** (entry 2). Competition experiments between acrylamide **1.69** and propynamide **1.71** showed the acrylamide to be more reactive towards GSH (entry 3). Methyl substituted propynamide **1.73** is more reactive than β -methyl acrylamide **1.72** (entry 4).¹⁸⁻¹⁹ However, acrylamide **1.68** is more reactive than a methyl substituted propynamide **1.73** (entry 5). The morpholinomethylene group at the α position of the acrylamide **1.74** is more reactive than β -morpholinomethylene acrylamide **1.70** (entry 6).¹⁸⁻¹⁹ Comparison of *cis* **1.75** and *trans* **1.72** β -

methyl substituted acrylamides shows no difference in reactivity as equal amounts of each GSH adduct was formed (entry 7). Isomerization of cis acrylamide **1.75** to the trans isomer under the reaction conditions is possible. For unreactive samples, excess base (diisopropylamine or triethylamine) was added to the reaction mixture to promote GSH adduct formation (entries 4, 5, and 7, Table 1). Utilizing a different heterocyclic scaffold, β -methyl substituted acrylamide **1.76** showed no reactivity with glutathione whereas **1.77** possessing a *N,N*-dimethylmethanamine at the β position showed increased reactivity (entry 1, Table 1.3B). The authors initially proposed that under aqueous conditions, the dimethylamino group would exist primarily in its protonated form, which would lead to an increase in the electrophilicity of the Michael acceptor through induction. However, this hypothesis was revised because inhibitor **1.78** bearing a trimethylmethanium ion did not react with GSH, therefore it was proposed that an intramolecular base catalysis is operating to increase the reactivity of GSH (entries 2 and 3).¹⁸⁻¹⁹

Table 1.3. Kinetic competition experiments between acrylamides and GSH.

A

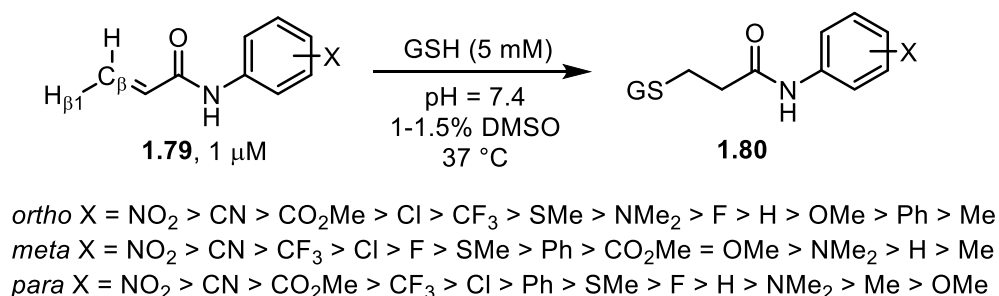
B

Entry	R (A)	R (B)	% ^a	
			Conversion	
			A	B
1			2	23
2			17	0
3			33	8
4			8 ^b	42 ^b
5			36 ^c	6 ^c
6			41	0
7			8 ^b	8 ^b

a) Two inhibitors (2.5 mM each) were allowed to react with a limiting quantity of GSH (1.25 mM), 20-24 h, rt; *b*) 12 equiv diisopropylethylamine were added; *c*) 1000 equiv triethylamine were added

Recently, scientists at Amgen examined the GSH reactivity of a series of arylacrylamides with the structure of **1.79** (Scheme 1.6).⁹¹ In their study, 34 *N*-arylacrylamides were incubated with a large excess of GSH at 37 °C in buffer (pH = 7.4) containing 1-1.5% DMSO. The progress of the reactions was monitored by LC-MS. The consumption of the acrylamide was determined by MS (using the total ion current) where the ratio of acrylamide to internal standard decreased over time.⁹² The relative rates of GSH addition to *N*-arylacrylamides are arranged in decreasing order in Scheme 1.6 and range from $2.03 \times 10^{-3} \text{ min}^{-1}$ ($t_{1/2} = 343 \text{ min}$) for the slowest reacting *p*-

methoxyphenyl acrylamide to $115 \times 10^{-3} \text{ min}^{-1}$ ($t_{1/2} = 6 \text{ min}$) for the fastest reacting *o*-nitrophenyl acrylamide. Substitution of the aryl ring of *N*-arylacrylamides at the *ortho* and *para* positions impacted the reaction rate more than substituents at the *meta* position.⁹¹ Additionally, some substituents had different effects depending on their position on the ring. For example, the methyl ester increased the rate of thiol addition when it was at the *ortho* or *para* positions due to resonance. However, when the methyl ester was in the *meta* position, this ester had the same effect as a methoxy group. These rates showed correlation to the chemical shifts of $H_{\beta 1}$ and C_{β} , as well as calculated kinetic reaction barriers, where downfield chemical shifts corresponded to increased rates of GSH addition.

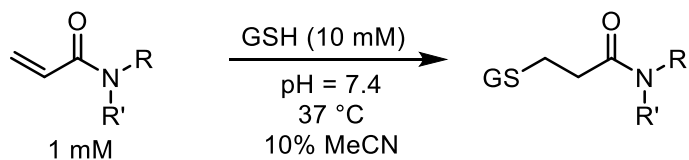


Scheme 1.6. Relative rates of GSH addition to *N*-arylacrylamides.

Similarly, scientists at Pfizer studied a more diverse set of acrylamides substituted with *N*-aryl, *N*-alkyl, and/or substituents at the α or β position of the double bond (Table 1.4).⁹³ The acrylamide was incubated with 10 equivalents of GSH in buffer (pH = 7.4) containing 10% acetonitrile at 37 °C using either LC-MS or ^1H NMR to measure the consumption of the acrylamide. The researchers found that the rate of GSH addition using 10% dimethylacetamide in buffer (pH of 7.4) was slower than the rate measured using 10% acetonitrile as the cosolvent for five samples tested.⁹³ This is just one example of how experimental conditions can influence the

rates of reactions, making direct comparisons between different studies difficult. The most reactive acrylamides **1.81-1.85** had no substitution at the α or β carbon and were *N*-substituted with aryl or heteroaryl groups (entries 1-5, Table 1.4). Substitution of the β carbon with a trifluoromethyl group **1.86** increased reactivity relative to the unsubstituted acrylamide **1.89** (compare entries 6 and 9). Alkyl substitution at the α or β carbons greatly reduced reactivity, but some reactivity was regained with certain β -aminomethyl substituents (compare entries 12 and 14 to entries 15-21).⁹³ The half-lives of three nonreactive acrylamides **1.95-1.97** were measured at a higher temperature (60 °C); the half-life of cyclobutene containing acrylamide **1.95** decreased to 20 h (versus > 60 h at 37 °C), while α -methyl acrylamide **1.96** and cyclopentene containing acrylamide **1.97** were still nonreactive (entries 15-17).

The thiol reactivity of acrylamides can be tuned by changing the substituents on the nitrogen atom of the acrylamide or by changing the α or β substituents of the alkene. For example, *N*-aryl acrylamides react with thiols faster than *N*-alkyl acrylamides; electron-donating aryl groups on the nitrogen slow the hetero-Michael addition reaction of thiols relative to electron-withdrawing aryl groups as one might expect. Alkyl substituents at the α or β position of α,β -unsaturated amides slow thiol adduct formation, but β -aminomethylene substituents increase the rate of thiol addition relative to alkyl substitution.

Table 1.4. Half-lives for the reaction of various acrylamides with GSH.

<u>Reactive $t_{1/2} < 8$ h</u>			<u>Mildly Reactive $t_{1/2} = 15 - 41$ h</u>			<u>Non-Reactive $t_{1/2} > 60$ h</u>		
Entry	Acrylamide	$t_{1/2}$ (h) ^a	Entry	Acrylamide	$t_{1/2}$ (h) ^a	Entry	Acrylamide	$t_{1/2}$ (h) ^a
1		0.13	8		15	15		> 60 /20 ^b
2		0.44	9		17	16		> 60 /58 ^b
3		0.88	10		25	17		> 60 / >60 ^b
4		1.6	11		27	18		> 60
5		3.5	12		28	19		> 60
6		4.0	13		33	20		> 60
7		8.0	14		41	21		> 60

b) Half-lives ($t_{1/2}$) of acrylamides (1 mM) when reacted with GSH (10 mM) at pH = 7.4 at 37 °C with 10% MeCN. *b*) $t_{1/2}$ measured at 60 °C.⁹³

Another method for tuning the reactivity of Michael acceptors is by placing two electron-withdrawing groups at the α -position, which generates Michael acceptors that easily undergo the reverse Michael reaction to regenerate the original Michael acceptor. Covalent inhibitors that form reversible, covalent adducts could offer advantages over irreversible inhibitors because they can have similar effects on the selectivity and potency with less potential for off-target side effects.⁹⁴ Taunton's lab has demonstrated the tunability of acrylonitrile Michael acceptors by changing the

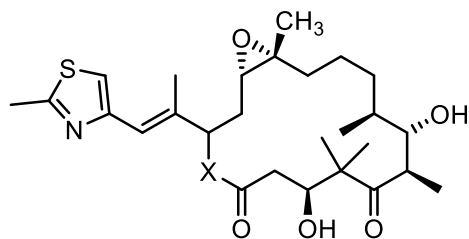
α -substituent to various electron withdrawing substituents and showed that thiol addition to the acrylonitriles was highly sensitive to the strength of the electron withdrawing α -substituent.^{50-51, 94}

The tunable electrophilicity of acrylamides by changing the nitrogen substituent to electronically diverse substituents have been demonstrated. α -Methylene- γ -lactams should be similarly tunable through modifications to the lactam nitrogen.

1.3. ISOSTERIC REPLACEMENT OF LACTONES WITH LACTAMS IN NATURAL PRODUCTS: BIOLOGICAL STABILITY, ACTIVITY, AND THIOL REACTIVITY

Macrocyclic lactams are more stable to hydrolysis and esterase cleavage than the corresponding lactones. This has led to the preparation of various lactam analogs (or aza-analogs) of lactone natural products.⁹⁵⁻⁹⁸ Generally, these lactam analogs have been prepared to increase the biological stability of compounds, but in a few cases electrophilic Michael acceptors (such as enones) have been replaced by less electrophilic unsaturated amides. This section contains natural product, macrocyclic lactones for which lactam analogs have been prepared. Additionally, the replacement of electrophilic enones and lactones with less reactive, unsaturated amides and comparisons of thiol reactivity are presented.

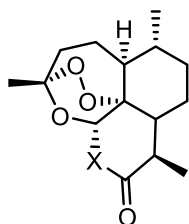
The most notable example of lactone to lactam replacement in macrocycles is the lactam analog of epothilone B **1.102** (ixabepilone, **1.103**), which was synthesized at Bristol-Myers Squibb. Ixabepilone (**1.103**) was nearly as cytotoxic as the parent compound with an IC₅₀ value of 3.6 nM while the lactone natural product **1.102** had an IC₅₀ of 0.42 nM. Ixabepilone (**1.103**) was more stable to esterase cleavage and was approved by the FDA in 2007 for the treatment of breast cancer (Figure 1.11).⁹⁹⁻¹⁰⁰



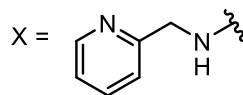
1.102: X = O, Epothilone B
1.103: X = NH, Ixabepilone

Figure 1.11. Epothilone B and lactam analog ixabepilone.

Lactam analogs of artemisinin (**1.104**) were prepared and showed similar activity for inhibition of a chloroquine resistant strain of *Plasmodium falciparum* (the parasite that causes malaria), however, compounds **1.107** and **1.108** were 9-fold and 22-fold more potent than artemisinin (**1.104**) for inhibition of *P. falciparum*.⁹⁷



1.104: X = O, Artemisinin
1.105: X = NH
1.106: X = N-allyl
1.107: X = N-isobutyl
1.108: X = NBn

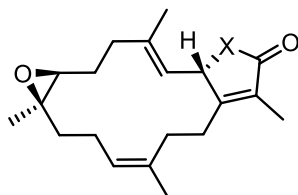


1.109

Figure 1.12. Artemisinin and lactam analogs.

Sarcophine (**1.110**) displays anticancer and antidepressant activities, but the lactam analogs **1.111-1.112** did not show significant cytotoxicity in several cell lines. Sarcophine (**1.110**) and the lactam analogs **1.111-1.112** all showed weak antimalarial activity (the highest activity was an IC₅₀

of 529-4100 ng/mL compared to artemisinin (**1.104**) which has an IC₅₀ of 13 ng/mL against *Plasmodium falciparum*).¹⁰¹



- 1.110:** X = O, Sarcophine
- 1.111:** X = NBn
- 1.112:** X = NEt

Figure 1.13. Sarcophine and γ -lactam analogs.

Macrosphelides (**1.113-1.114**) are a class of macrocyclic lactones that are under investigation as anticancer drug leads (Figure 1.14).¹⁰² The lactam analogs of the macrosphelides varied in their ability to induce apoptosis, with *N*-unsubstituted lactam **1.116** having no activity, while the activity of the *N*-phenyl lactam **1.117** was comparable to that of lactone **1.115**.¹⁰³ *N*-benzyl lactam **1.118** was the most active compound tested (about 2-fold more active than lactone **1.115**), inducing early apoptosis in 43% of human lymphoma cells (U937) at a 10 μ M concentration.

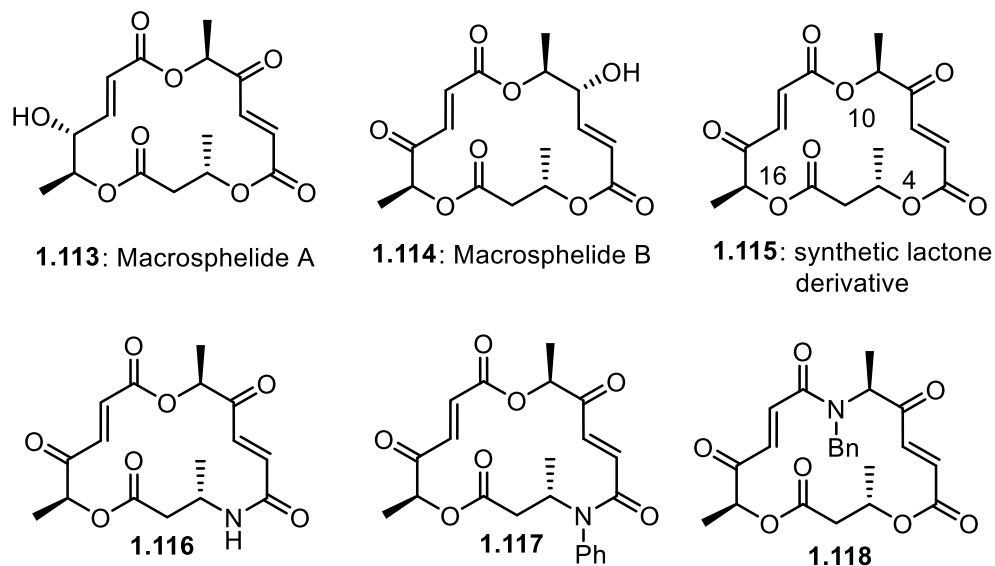
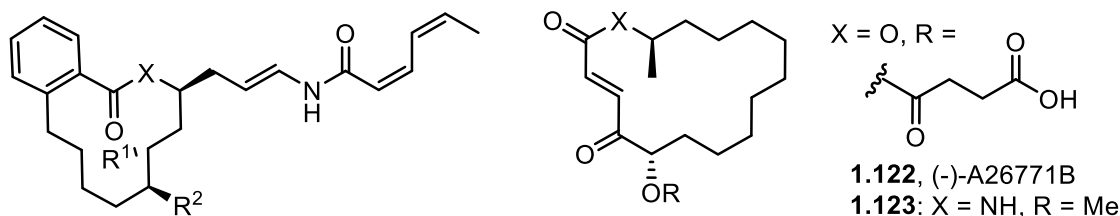


Figure 1.14. Macrosp helide natural products and lactam analogs.

Salicylhalamide A (**1.119**) is an antitumor compound that inhibits mammalian vacuolar-type (H^+)-ATPase inhibitor containing a 12-membered macrolide (Figure 1.15).⁹⁸ Lactam analog **1.121** showed growth inhibition of 5-cancer cell lines with IC_{50} values from 117-506 nm. Similarly, a lactam analog of natural product (-)-A26771B (**1.122**) shows moderate antibiotic activity and improved pharmacokinetic properties, such as maintaining antibacterial activity when human serum was added to the culture media.¹⁰⁴ The minimum inhibitory concentration (MIC) for lactone **1.122** was 2-16 $\mu\text{g/mL}$ while lactam **1.123** was 5-10-fold more active against most strains of bacteria and even showed activity against 2 strains that were not inhibited by the natural product **1.122**.



- 1.119:** X = O, R¹ = OH, R² = Me, Salicylihalamide A
1.120: X = O, R¹ = R² = H
1.121: X = NH, R¹ = R² = H, aza-Salicylihalamide A

- 1.122,** (-)-A26771B
1.123: X = NH, R = Me

Figure 1.15. Salicylihalamide A and A26771B with lactam analogs.

Lactam analogs of other natural products that were prepared in order to increase the metabolic stability and/or improve the biological activity compared to the isosteric lactones include (-)-galiellalactone, brefeldin C, and a number of gangliosides represented by GD3 lactam, but biological data for these lactams was not reported.^{95, 105-106} In addition to hydrolytic stability, amides or lactams have been incorporated into natural products to reduce the electrophilic reactivity of enones or α -methylene- γ -lactones.

Resorcylic acid lactones (RALs), such as hypothemycin (**1.124**), are a family of benzannulated macrolides with a 12- or 14-member macrolactone and many contain a *cis*-enone. RALs have demonstrated numerous biological properties including antifungal, antibiotic, antitumor, and antiviral activities by inhibiting heat shock protein 90 (HSP90), mitogen activated protein kinases (MAPKs), herpes simplex virus 1 (HSV1) and the NF- κ B pathway (Figure 1.16).¹⁰⁷⁻¹⁰⁹ The *cis*-enone functionality of many RALs leads to irreversible inhibition of a subset of kinases by hetero-Michael addition of a conserved cysteine located in the ATP binding pocket; studies with hypothemycin (**1.124**) have shown ATP-competitive, time-dependent inhibition of these kinases.¹¹⁰⁻¹¹¹ The k_{inact}/K_i of hypothemycin (**1.124**) ranges from 160-120,000 M⁻¹s⁻¹ for various kinases and reacts much slower with small molecule thiols β -mercaptoethanol and

glutathione displaying second order rate constants (k_2) of 3.6 and 6.6 $M^{-1}s^{-1}$, respectively, thus showing that reactions with kinase targets are faster than the reaction with free thiols.¹¹¹

The related enone natural product LL-Z1640-2 (**1.126**) forms adducts with dithiothreitol (DTT).¹¹² The design of lactam analogs of resorcylic acid lactones, which are known to react with thiols, by replacing an enone in the 14-membered ring with an α,β -unsaturated amide demonstrated the tunability of this functionality.¹¹³ The enone natural product L-783,277 (**1.125**) and the isosteric lactam with *N*-acetyl (**1.128**) substitution both form thiol adducts with cysteamine in DMSO- d_6 , as monitored by 1H NMR, and they show similar inhibition of mitogen-activated protein kinase interacting kinase 1 and 2 (MNK1/2) in enzymatic assays. The IC_{50} of enone **1.125** was 0.33 μM for inhibition of MNK1 and 0.061 μM for inhibition of MNK2, while the *N*-acetyl lactam **1.128** inhibited MNK1 and 2 with IC_{50} values of 1.3 and 8.9 μM , respectively. The *N*-unsubstituted lactam **1.127** failed to react with thiols and showed weak inhibition of MNK1 ($IC_{50} > 50 \mu M$) and MNK2 ($IC_{50} = 41.7 \mu M$).¹¹³ The growth inhibition of MDAMB435s breast cancer cells was also similar for natural product **1.125** ($GI_{50} = 7.5 \mu M$) and the corresponding *N*-acetyl lactam **1.128** ($GI_{50} = 8.5 \mu M$).

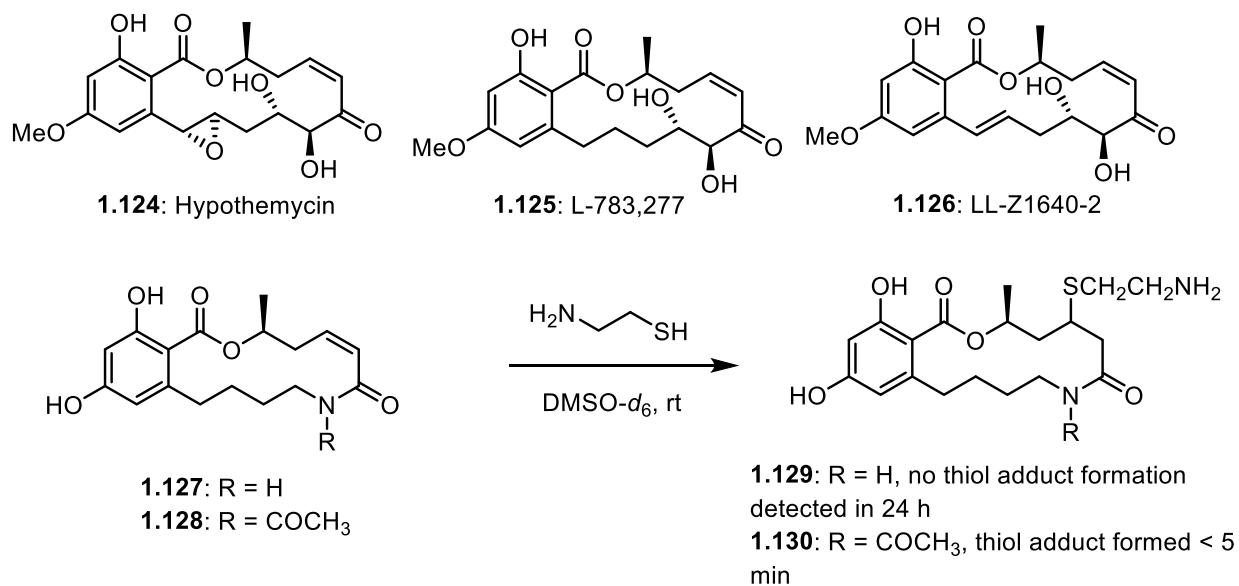
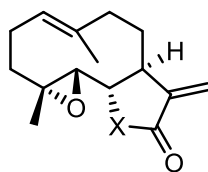


Figure 1.16. Natural product resorcylic acid lactones tunable lactam analog.

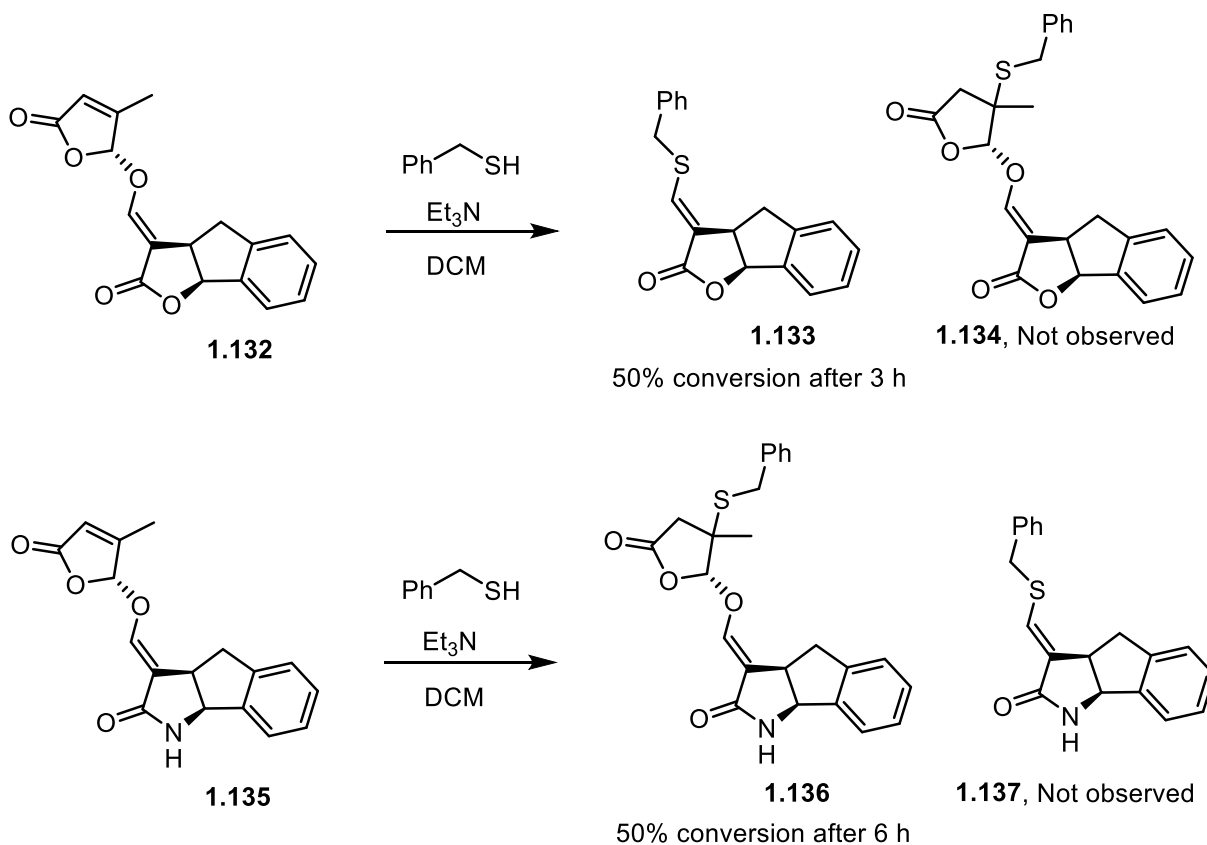
Although the replacement of macrocyclic lactones in natural products with lactams to increase their stability to hydrolysis is a known strategy, the replacement of lactone Michael acceptors is less common, and replacement of an α -methylene- γ -lactone with an α -methylene- γ -lactam is even more rare. One example of this replacement is a lactam-containing parthenolide analog **1.131**, which had no anticancer activity, despite parthenolide (**1.23**) being cytotoxic to cancer cells in the low micromolar range when tested in 6 different cancer cell lines (Figure 1.17).¹¹⁴



1.23: X = O, parthenolide
 IC₅₀ = 2.1-5.0 μ M
1.131: X = NH, lactam analog
 IC₅₀ > 50 μ M

Figure 1.17. Parthenolide and lactam analog.

Strigolactones are phytohormones with potential activity as seed germination stimulators and plant growth regulators. Synthetic strigolactone GR-24 (**1.132**) is commonly employed in plant studies (Scheme 1.7).¹¹⁵ Lactone **1.132** reacts with benzyl thiol preferably at the α -methylene- γ -lactone to form **1.133** in 50% conversion after 3 h; **1.134**, arising from addition of benzyl thiol to the butenolide ring, was not observed. Lactam analog **1.135** showed the opposite regiochemistry when reacted under identical conditions with benzyl thiol.¹¹⁵ In this case, only addition of benzyl thiol to the butenolide ring to form **1.136** was observed, highlighting the reduced electrophilicity of α -methylene- γ -lactams compared to α -methylene- γ -lactones. Lactam **1.135** was more potent for induction of seed germination than lactone **1.132** (a dose of 0.0001 mg/L of **1.135** gave a 92.6% germination while the same dose of **1.132** gave only a 24.6 germination). Additionally, seed germination was impacted by the stereochemistry of the vinyl ether group, where a lactam with the opposite stereochemistry of **1.135** at the vinyl ether was completely inactive at all concentrations tested.



Scheme 1.7. Thiol additions to synthetic strigolactone and strigolactam.

The isosteric replacement of lactones with lactams has been demonstrated to improve hydrolytic stability of macrocycles and reduce the electrophilic reactivity of α -methylene- γ -lactones.

1.4. CONCLUSION

The recent approval of several covalent drugs and the success of targeted covalent inhibitors for enhancing the ligand binding selectivity for structurally related proteins, increasing the binding affinity for proteins with shallow binding sites, and the ability to overcome drug resistance has led

to a renewed interest in covalent drug design. When considering α,β -unsaturated carbonyls in the design of covalent inhibitors, it is important to understand the factors that govern their ability to form adducts with thiols, especially under biologically relevant conditions (pH = 6-8). Thiol adduct formation is one of the major pathways for covalent inhibition of proteins and is also a major pathway for covalent inhibitor deactivation when adducts are formed with free cellular thiols such as GSH. The ability to tune the electrophilicity of α,β -unsaturated carbonyls through careful selection of the type of carbonyl and selective modifications to the surrounding structure plays an important role in the future of covalent inhibitor design in order to maximize selectivity and efficacy for a desired protein. The factors that govern the reversibility of thiol adduct formation is another important consideration, since rapidly reversible covalent bonds offer a strong interaction that complements the typical noncovalent interactions used in the design of reversible inhibitors. To summarize, the rate of thiol addition to α,β -unsaturated carbonyls, under biologically relevant conditions, decreases in the order of enals > enones > α,β -unsaturated esters > acrylamides > α,β -unsaturated carboxylic acids.¹¹⁶ However, substituents at the α or β positions of a Michael acceptor can greatly influence the rate of thiol addition. Electron donating groups such as alkyl or electron rich aryl groups at the α or β position significantly reduce the rate of thiol addition relative to unsubstituted Michael acceptors. Electron withdrawing groups at the α position increase the rate of hetero-Michael addition, but also make the resulting adducts more prone to the reverse Michael reaction.

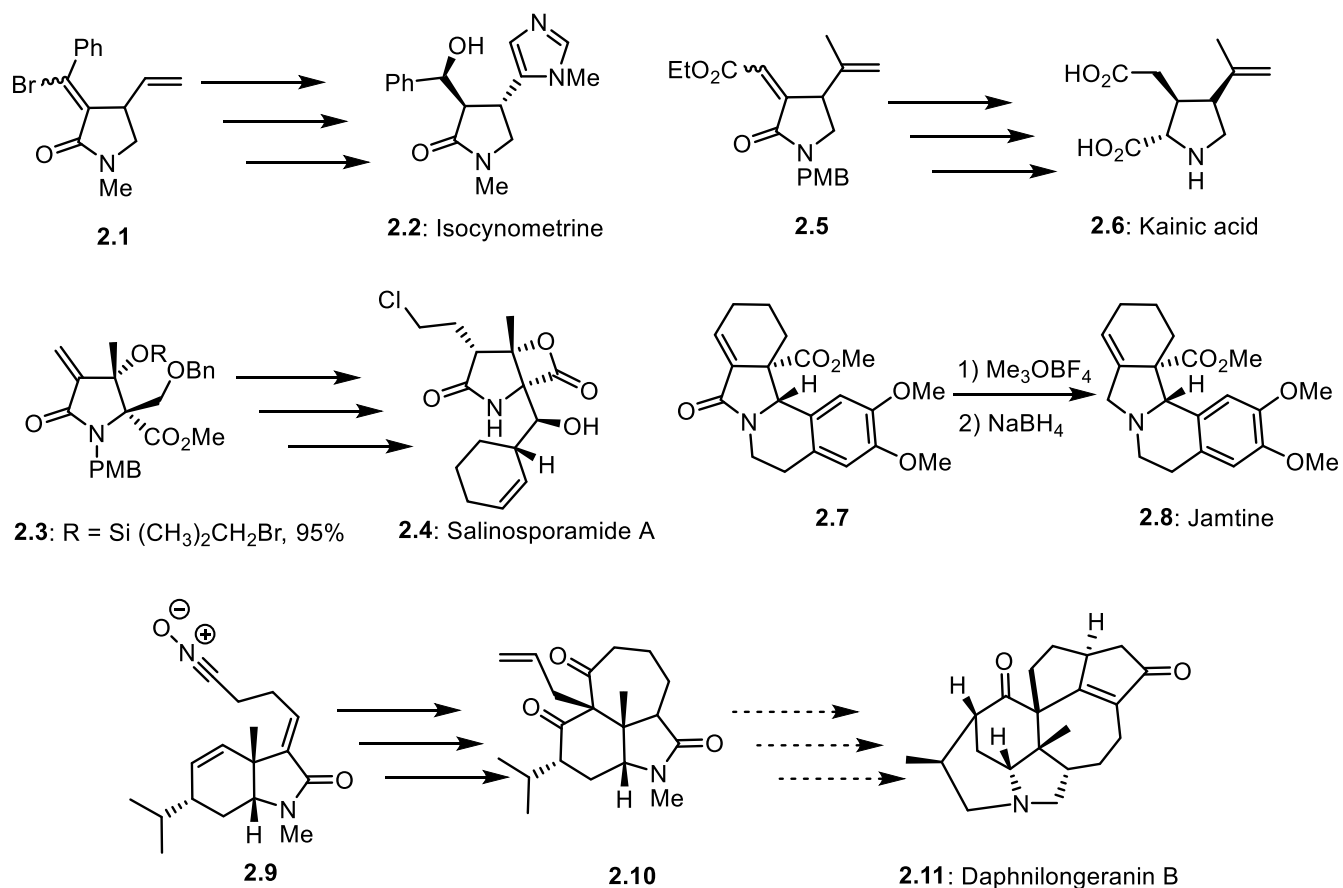
The reduction in thiol reactivity of α -methylene- γ -lactams compared to isosteric lactones is generally accompanied by a reduction in toxicity. However, in some cases, the bioactivity for a specific target or pathway is maintained by lactam isosteres of lactones. The tunability of the electrophilic reactivity of acrylamides and the increased stability of lactams compared to lactones

in biological systems led to the hypothesis that α -methylene- γ -lactams could serve as tunable isosteres for α -methylene- γ -lactones in guaianolide natural products. These lactams would have tunable electrophilicity by changing the substituent on the lactam nitrogen. Guaianolides are a large class of sesquiterpene lactones possessing a range of biological properties; many guaianolides contain an electrophilic α -methylene- γ -lactone which is often important for the observed bioactivity.²⁰⁻²⁴ Our lab has previously shown that the allenic Pauson-Khand reaction of allene-ynes tethered by an α -methylene- γ -lactone can form the [5,7,5]-fused ring system of guaianolides.¹¹⁷⁻¹¹⁸ Thus, methods to synthesize α -methylene- γ -lactams in order to prepare lactam-containing guaianolide analogs were examined.

2.0. METHODS OF α -METHYLENE- γ -LACTAM SYNTHESIS

2.1. INTRODUCTION

α -Methylene- γ -lactams are uncommon in natural products and bioactive compounds, but they have been used as synthetic intermediates towards γ -lactam-containing natural products and pyrrolidine-containing alkaloids. Some notable examples include the synthesis of isocynometrine (**2.2**) from **2.1**,¹¹⁹ salinosporamide (**2.4**) from **2.3**,¹²⁰ kainic acid (**2.6**) from **2.5**,¹²¹ jamtine (**2.8**) from **2.7**,¹²² and the tricyclic core **2.10** of daphnilongeranin B (**2.11**) from **2.9** (Scheme 2.1).¹²³ The use of α -methylene- γ -lactams as synthetic intermediates towards natural products and a growing interest in their biological activity has led to the development of various synthetic methods to access this structure.



Scheme 2.1. α -Methylene- γ -lactams as synthetic intermediates.

There are a number of methods to synthesize α -methylene- γ -lactams such as: a) intramolecular Baylis-Hillman reactions (section. 2.2), b) the addition of nitro compounds to Baylis Hillman alcohols, acetates, or allylbromides followed by reduction of the nitro group to an amine and subsequent cyclization (section 2.2), c) addition of allyl metal reagents (formed by the insertion of a metal into an allyl bromine bond) that react with imines (section 2.3), d) reaction of allylboronates with imines (section 2.3), e) reactions of α -dialkoxyphosphoryl lactams with aldehydes (section 2.4), f) conversion of α -unsubstituted- γ -lactams to the α -methylene- γ -lactams (section 2.5), g) radical cyclizations and other reactions (section 2.6). A 2011 review by Janecki and coworkers summarizes methods to access α -methylene and α -alkylidene lactams and lactones;

the major methods to synthesize α -methylene- γ -lactams are summarized in Scheme 2.1, and the advantages and disadvantages to each of these methods is discussed in this chapter.⁶⁹

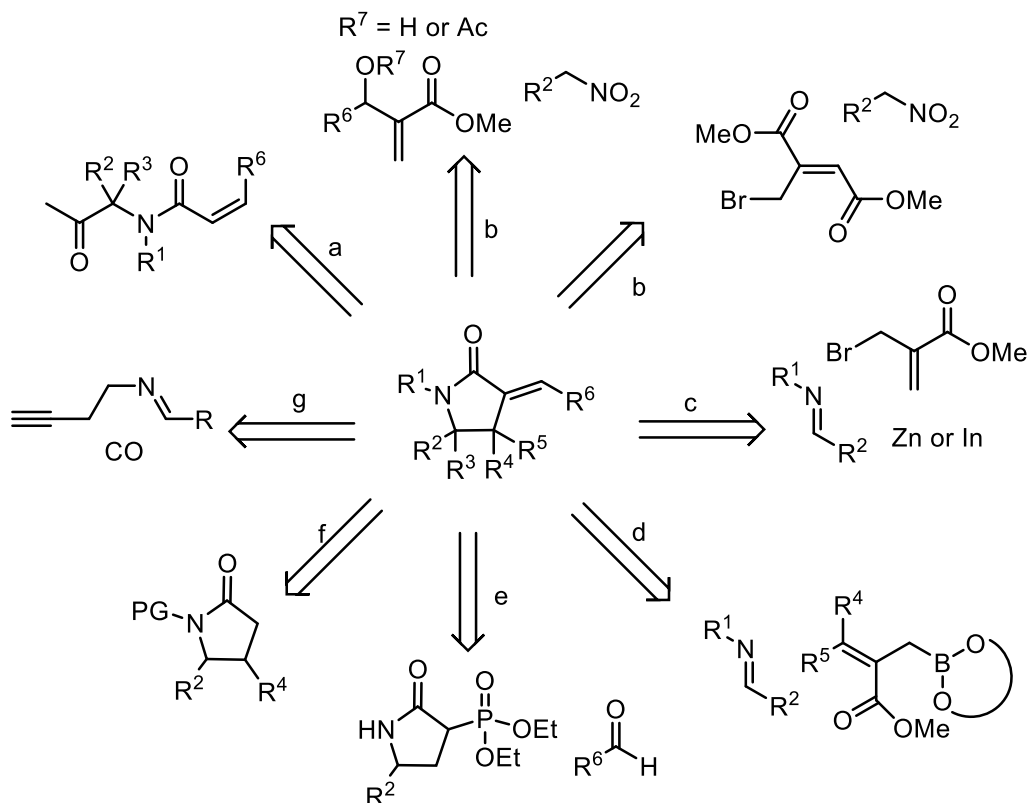
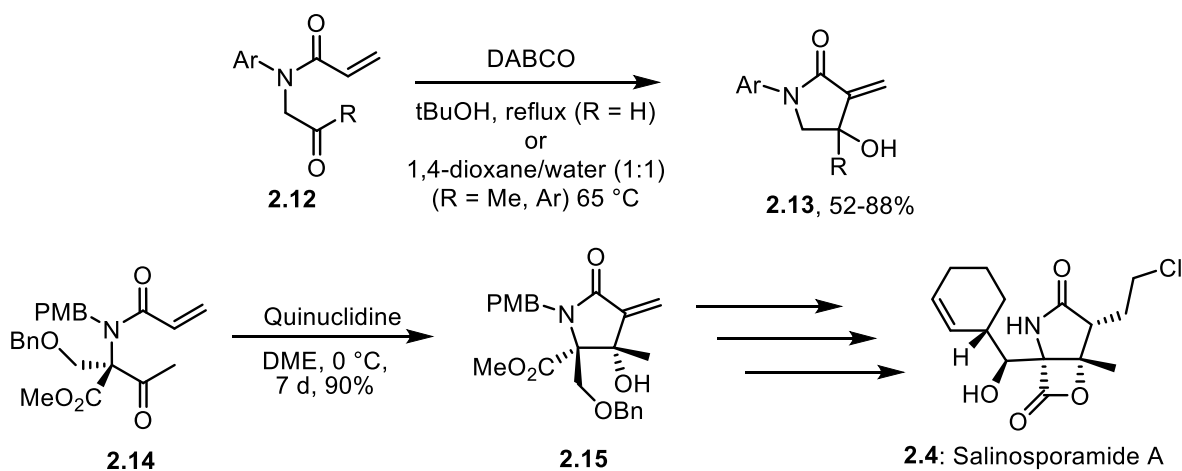


Figure 2.1. Summary of methods to form α -methylene or α -alkylidene- γ -lactams.

2.2. SYNTHESIS OF α -METHYLENE- γ -LACTAMS USING MORITA-BAYLIS-HILLMAN REACTIONS

Intramolecular Morita-Baylis-Hillman reactions of β -oxoacrylamides with aldehydes or ketones are one method for the synthesis of α -methylene- γ -lactams. For example, the reaction of **2.12** produces lactam **2.13** in 52-88% yield (Scheme 2.2).¹²⁴⁻¹²⁵ Corey and coworkers have shown this method to be applicable to functionally dense precursors by the conversion of **2.14** to **2.15** in 90%

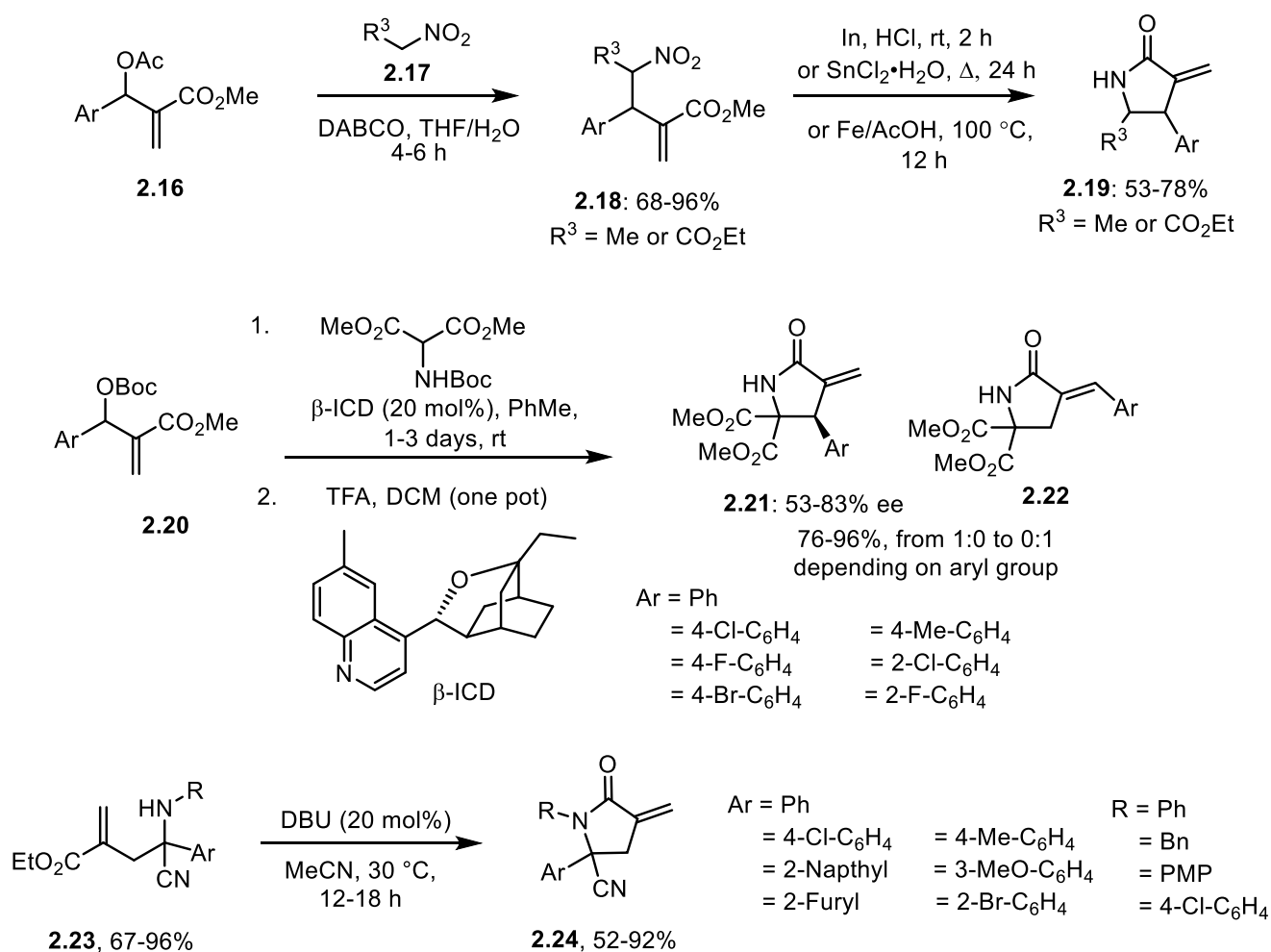
yield which was ultimately transformed into salinosporamide A (**2.4**).¹²⁰ The advantages of this method are the mild conditions to perform the Baylis-Hillman cyclization and the diastereoselectivity achievable with chiral bases (although this can be substrate dependent). The disadvantages are the long reaction times required and the potentially difficult synthesis of β -oxoacrylamides with the desired functionality.



Scheme 2.2. Intramolecular Morita-Baylis-Hillman reactions to form α -methylene- γ -lactams.

A related method for the synthesis of α -methylene- γ -lactams is the intermolecular Morita-Baylis-Hillman reaction with nitro compounds or α -diester amides followed by cyclization of the resulting adducts. Nucleophilic addition of acetate **2.16** to nitro compound **2.17** gives adduct **2.18**; reduction of the nitro compound and cyclization gives α -methylene- γ -lactams **2.19** in 53-78% yields (Scheme 2.3).¹²⁶⁻¹²⁷ Alternatively, carbonate protected diethylamino malonate can be added to the Baylis-Hillman adduct **2.20** which cyclizes following removal of the tert-butoxy carbonyl (Boc) group to afford lactams **2.21** or **2.22** in various ratios and yields ranging from 76-96% depending on the aryl substituent; DABCO favors α -methylene- γ -lactams **2.21** in good yields but without stereoselectivity while DIPEA favors formation of arylidene lactams **2.22** in good

yields.¹²⁸ Another synthesis that uses Baylis-Hillman adducts is a multicomponent reaction to form α -amino nitriles such as **2.23**. α -Amino nitriles such as **2.23** were converted to α -methylene- γ -lactams such as **2.24** with a nitrile at the γ -position in 52-92% using catalytic DBU.¹²⁹



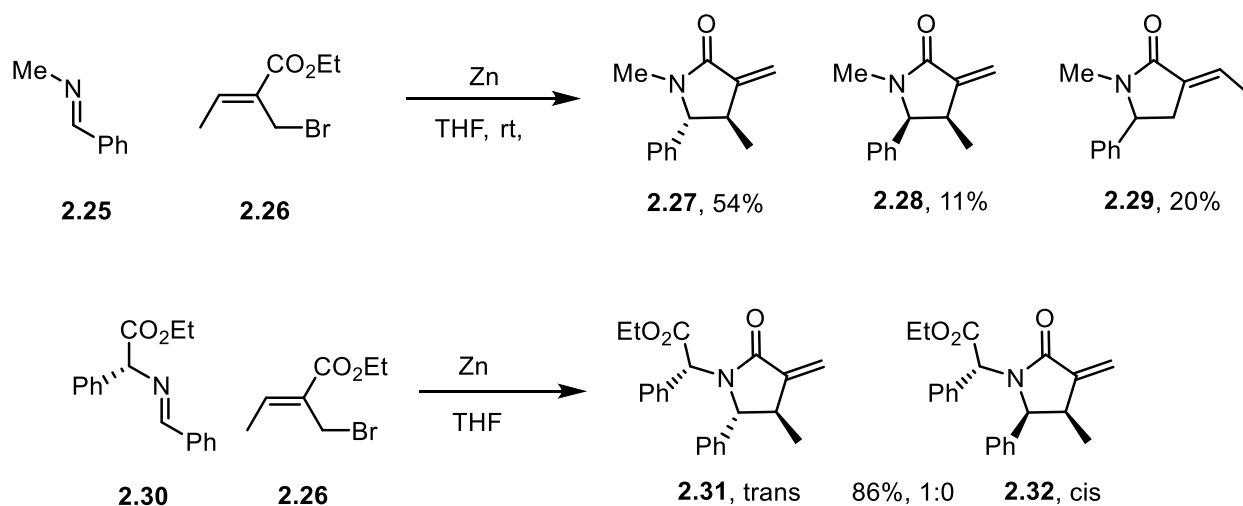
Scheme 2.3. Synthesis of α -methylene- γ -lactams using Morita-Baylis-Hillman adducts.

The advantage of these methods is the modular installation of substituents at the β - and γ -positions of the lactam, but in all examples an aryl group is installed at one of these positions which

limits the substrate scope. Additionally, reduction of the nitro group can require harsh conditions, while amides result in selectivity problems.

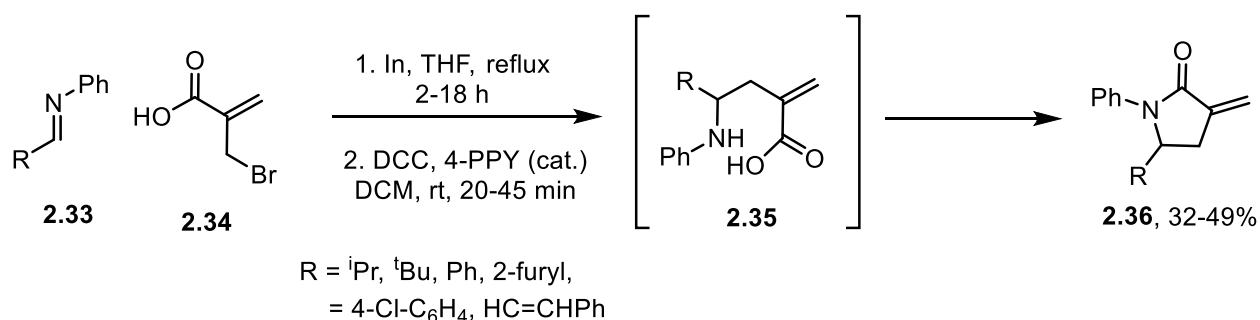
2.3. SYNTHESIS OF α -METHYLENE- γ -LACTAMS FROM ALLYLMETAL REAGENTS (DERIVED FROM ALLYLBROMIDES) OR ALLYLBORONATES

The reaction of allylbromides with indium or zinc forms allylmethyl reagents that when reacted with imines form α -methylene- γ -lactams. These reactions generally require substituted imines that result in *N*-substituted α -methylene- γ -lactams, and they often give alkylidene lactams resulting from a byproduct.¹³⁰⁻¹³² For example, *N*-methyl imine **2.25** reacts with an allylzinc reagent formed from allylbromide **2.26** to give lactams **2.27-2.29** in a 85% overall yield and 5:1:2 ratio of **2.27:2.28:2.29** (Scheme 2.4).¹³² When chiral imine **2.30** was reacted with the same allylzinc reagent, complete selectivity for the *trans* lactam afforded **2.31** in 86% yield.



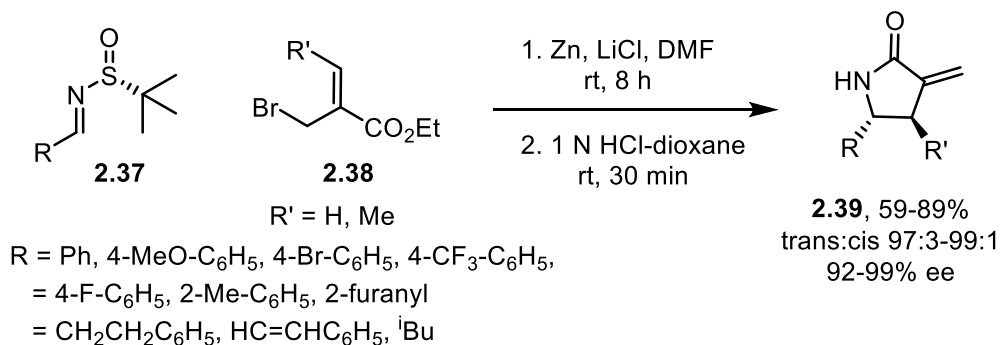
Scheme 2.4. Allylzinc addition to an imine to form α -methylene- γ -lactams.

In addition to zinc, indium has been reacted with imines **2.33** and bromomethyl acrylic acid (**2.34**) to afford γ -amino acids **2.35** that were cyclized with dicyclohexyl carbodiimide (DCC) and 4-pyrrolidinopyridine (4-PPY) to form γ -substituted α -methylene- γ -lactams **2.36** in yields of 32-49% over 2 steps (Scheme 2.5).¹³³ This reaction resulted in lower yields than the allylmetal reagents derived from zinc, but carboxylic acids could be used in place of esters.



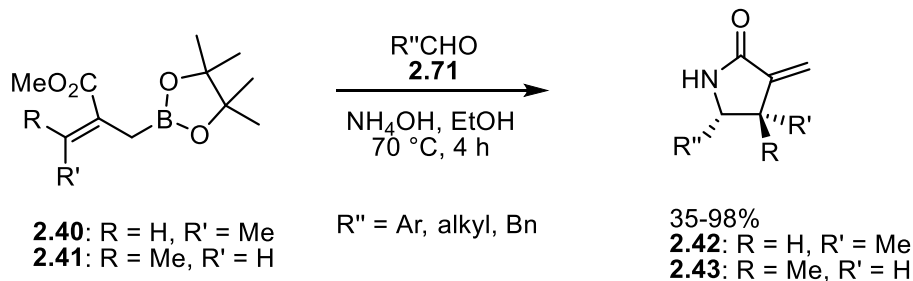
Scheme 2.5. Indium promoted addition to imines and cyclization.

Chiral sulfinyl imines **2.37** react with alkoxy carbonyl allylbromides **2.38** to give α -methylene- γ -lactams **2.39** with good yields (51-89%), diastereoselectivities (97:3 to 99:1 trans:cis), and enantioselectivities (92-98% ee, Scheme 2.8).¹³⁴⁻¹³⁵ The sulfinyl group was removed with HCl in dioxane to give *N*-unsubstituted lactams **2.39**. The diastereo- and enantioselectivities of these reactions is impressive and the tolerance of aryl, alkyl, and alkenyl substituents on the sulfinyl imine is useful. However, only relatively simple allyl bromides were employed, and it was anticipated that additional functionality such as an allene or a functional group that could be converted to an allene would not tolerate these conditions.

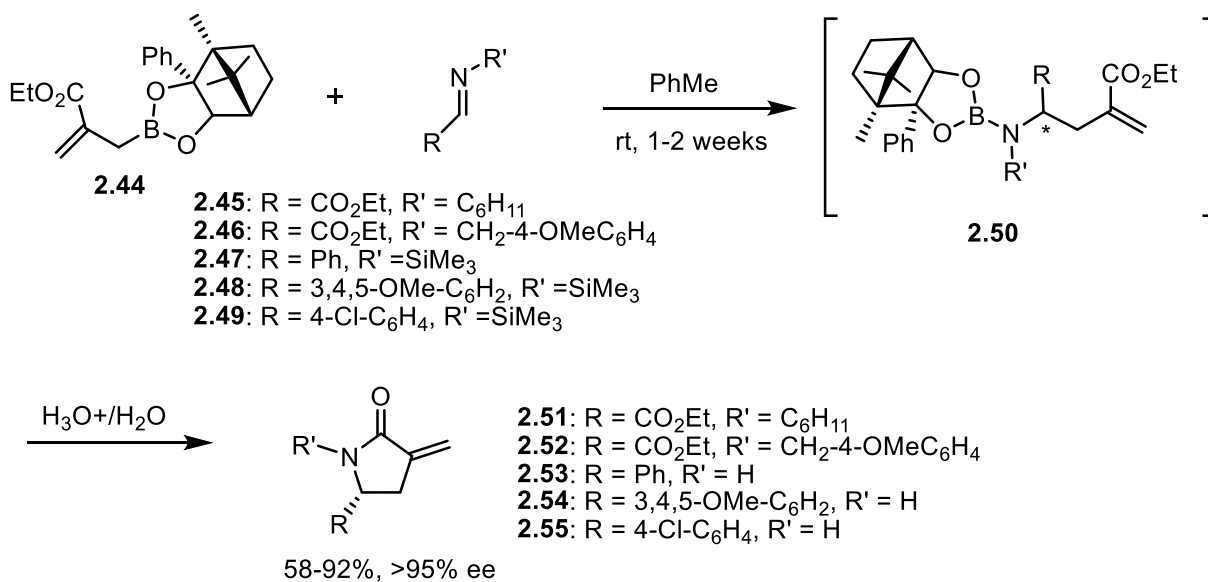


Scheme 2.6. Enantioselective synthesis of α -methylene- γ -lactams with chiral sulfinyl imines.

A convenient procedure using 2-alkoxycarbonyl allylboronates for the synthesis of α -methylene- γ -lactams is the 3-component reaction reported by Hall and coworkers.¹³⁶ In this case, E-allylboronates **2.40** reacted with in-situ formed imines to give cis-lactams **2.42** selectively while Z-allylboronates **2.41** provided trans-lactams **2.43** selectively (Scheme 2.7). Most aryl aldehydes provided the α -methylene- γ -lactams in moderate to good yields (> 60%). However, a benzyl and alkyl aldehyde gave lower yields of 35 and 39% which was attributed to enamine formation under the basic conditions. Chiral allylboronates such as **2.44** react with imines to form α -methylene- γ -lactams stereoselectively.¹³⁷ In these cases, chiral allylboronate **2.44**, prepared from the achiral pinacolboronate, reacted slowly (1-2 weeks) with activated imines **2.45-2.49** to give α -methylene- γ -lactams **2.51-2.55** in moderate to good yields (58-92%) and enantioselectivities greater than 95% after acidic work-up (Scheme 2.8). Alkyl and benzyl imines **2.45-2.46** required additional stirring with toluene sulfonic acid to effect lactamization, but silyl imines **2.47-2.49** provided lactams **2.54-2.55** directly.



Scheme 2.7. 3-Component reaction between allylboronate, aldehyde, and ammonia.

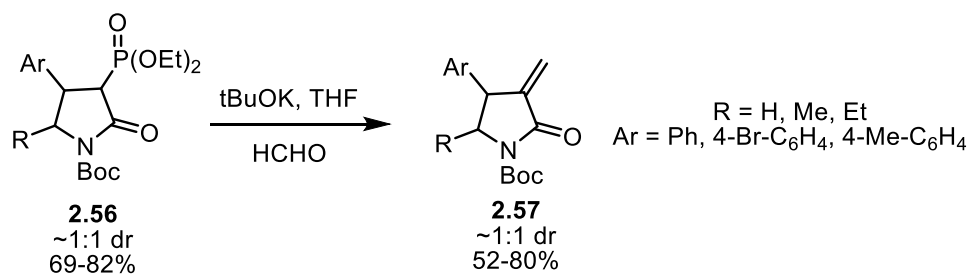


Scheme 2.8. Enantioselective lactamization with chiral allylboronates and imines.

The advantages of α -methylene- γ -lactam formation from allylboronates is the broad substrate scope and the ability to enact lactamization enantioselectively with chiral boronates. This method was selected to form α -methylene- γ -lactams with the required functionality to synthesize guaianolide analogs since similar allylboronates have been utilized in our lab for the synthesis of guaianolides containing an α -methylene- γ -lactone ring.¹¹⁷⁻¹¹⁸ We also envisioned that once the feasibility of this allylboronate approach was demonstrated, this method would allow the enantioselective synthesis of lactam-containing guaianolide analogs.

2.4. USE OF DIALKOXYPHOSPHORYL REAGENTS TO INSTALL THE α -METHYLENE MOIETY

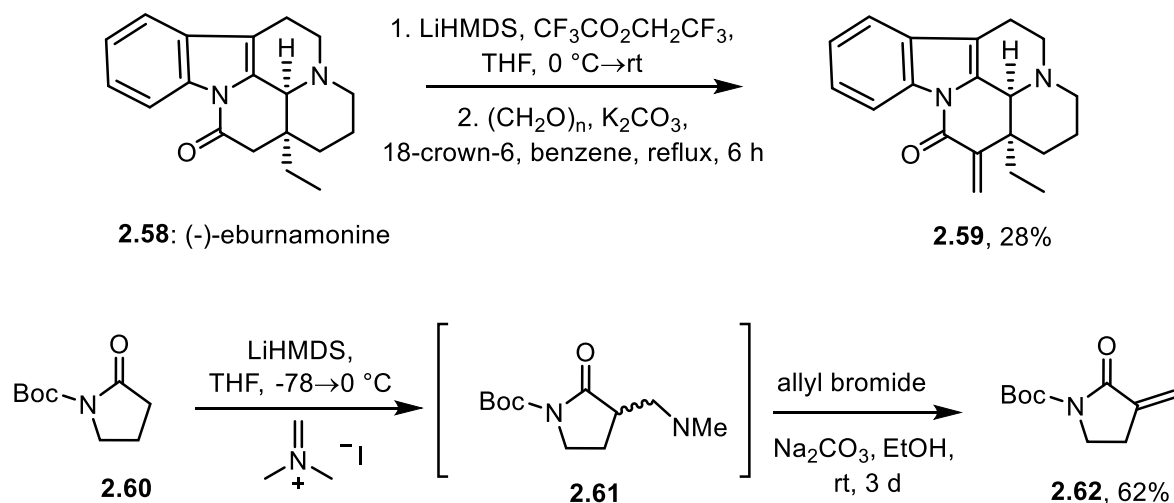
A different approach to α -methylene- γ -lactams is through the installation of the α -methylene group after cyclization. One method to accomplish this is through the synthesis of α -dialkoxyphosphoryl lactams which can be converted to the α -methylene- γ -lactam with base and formaldehyde.^{74, 76, 138} One advantage to this method is the ability to form α -alkylidene lactams using various aldehydes in addition to α -methylene lactams formed using formaldehyde, but a drawback to this method is the number of steps involved in the synthesis, including reduction of a nitro group to an amine and protection/deprotection of the lactam nitrogen. An example of this strategy is the conversion of dialkoxyphosphoryl lactam **2.56** to α -methylene- γ -lactam **2.57** in 52-80% yield using a Horner-Wadsworth-Emmons reaction with formaldehyde (Scheme 2.9). The poor diastereoselectivity for cyclization to the lactam is another drawback of this method.



Scheme 2.9. Synthesis of α -methylene- γ -lactams from dialkoxyphosphoryl reagents.

2.5. INSTALLATION OF THE α -METHYLENE MOIETY ON AN α -UNSUBSTITUTED- γ -LACTAM VIA THE LACTAM ENOLATE

The α -methylene group can be installed by amide α -enolate formation, addition to an electrophile, followed by elimination. Thus, γ -lactams unsubstituted at the α -position can be converted to α -methylene- γ -lactams, but tertiary amides and strongly basic conditions are required. The conversion of (-)-eburnamonine (**2.58**) from a δ -lactam to α -methylene- δ -lactam **2.59** proceeded in 28% yield and is one of the few examples with a functionalized starting material; this strategy has been applied to a number of other acyclic ketones, lactones, and lactams with yields ranging from 59-98% in less sterically congested systems (Scheme 2.10).¹³⁹ The use of Eschenmoser's salt to add α -methylene substituents to ketones and lactones is common, but not many examples have been reported for the α -methylenation of lactams.¹⁴⁰ In one example, *N*-Boc lactam **2.60** is converted to α -methylene lactam **2.62** in 67% yield over 2-steps.¹⁴¹ The advantage of this method is a late stage introduction of the potentially reactive Michael acceptor, but most examples of this methodology involve relatively unfunctionalized lactams and the yields are only moderate.¹⁴²⁻¹⁴³



Scheme 2.10. Installation of an α -methylene moiety from the enolate of γ -lactams.

2.6. CONCLUSION

Radical cyclizations, Wittig olefinations, and intramolecular, palladium-catalyzed cyclizations of acrylamides and alkenes are three other methods used to form α -methylene- γ -lactams.^{119, 144-146} The major strategies for the synthesis of α -methylene- γ -lactams involve Morita-Baylis-Hillman reactions, Wittig-type reactions of dialkoxyphosphoryl reagents or addition/elimination procedures to install the α -methylene subunit, and allylmetal or allylboronate reactions with imines. The major advantage of reactions with allylzinc and allylboronate reagents is the ability to enact enantioselective formation of α -methylene- γ -lactams through the use of chiral imines or chiral allylboronates. Our lab has previously demonstrated the utility of allylboronate reactions with aldehydes for the preparation of α -methylene- γ -lactone-tethered allene-ynes which were transformed into guaianolides via an allenic Pauson-Khand reaction.¹¹⁷⁻¹¹⁸ Thus, it was proposed

that allylboronates with the required functionality could be prepared and reacted with imines instead of aldehydes to synthesize α -methylene- γ -lactam-containing guaianolide analogs.

3.0. PREPARATION OF LACTAM ANALOGS OF 6,12-GUAIANOLIDES

3.1. INTRODUCTION

Inspired by the ability to tune the electrophilic reactivity of acrylamides towards biothiols and by the incorporation of an acrylamide motif into three recently FDA-approved targeted covalent modifiers **1.1-1.3**, replacing the α -methylene- γ -lactone of the 6,12-guaianolide structure with an α -methylene- γ -lactam was proposed as a method to reduce the indiscriminate reactivity and increase the relevance of this bioactivity-rich class of sesquiterpene lactones in the drug discovery process. Lactam isosteres are known to be more stable to esterase hydrolysis than the corresponding lactones,^{95, 97-99, 101, 103-104, 147} but few examples of α -methylene- γ -lactone replacement with an α -methylene- γ -lactam have been reported, as discussed in section 1.3.^{96, 114} As naturally occurring α -methylene- γ -lactams are rare, and comparisons of isosteric α -methylene- γ -lactones and lactams reveal the latter to be considerably less toxic, it was hypothesized that α -methylene- γ -lactam isosteres of 6,12-guaianolides would result in less toxic compounds that would maintain similar bioactivities to their lactone counterparts.^{69, 71}

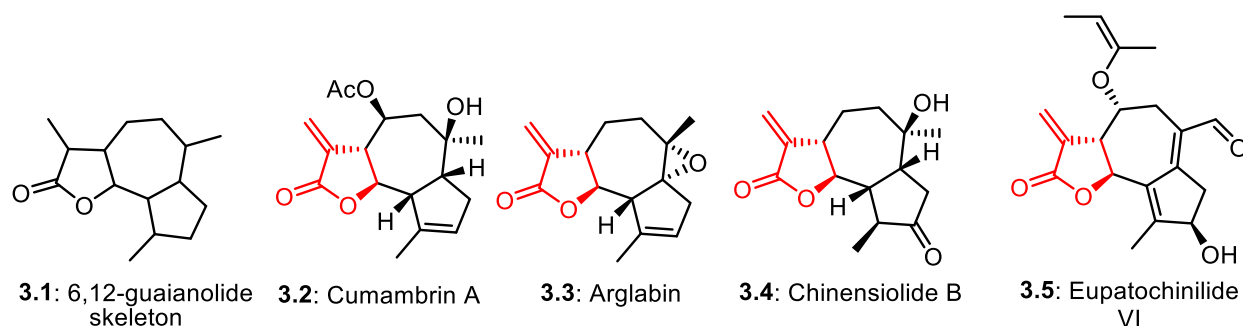


Figure 3.1. Examples of 6,12-guaianolides that contain an α -methylene- γ -lactones.

The 6,12-guaianolides represent a class of natural products possessing an angular [5,7,5]-fused ring system where one of the five-membered rings is a γ -lactone (Figure 3.1).²¹ This compound class is replete with functionality, which is likely an evolutionary response to enhance the compounds' selectivity for specific protein targets.²⁰ Another well recognized structural feature of many guaianolides is the methylene group adjacent to the lactone carbonyl, a motif that is present in 3% of all natural products.²² This moiety can covalently modify proteins, which is one source of bioactivity associated with compounds possessing it, but the reactivity of the α -methylene- γ -lactone is also blamed for its cytotoxicity. α,β -Unsaturated carbonyl-containing compounds are often removed from screening libraries due to their perceived indiscriminate reactivity.¹⁴⁸⁻¹⁵⁰ However, the recent interest in targeted covalent inhibitors demonstrates that a better understanding of the mechanisms of action of natural products containing reactive functionality is needed.

Certain guaianolides, such as cumambrin A (**3.2**), have been shown to inhibit the p50/p65 transcription factor heterodimer from binding to DNA, the most downstream process in the NF- κ B signaling pathway, by forming a covalent bond between the α -methylene- γ -lactone and the sulfhydryl group (Cys-38) of the p65 protein (Figure 3.1).²⁵ Inhibition of the NF- κ B (nuclear factor κ B) pathway promotes apoptosis and is frequently overactive in cancer and inflammatory diseases.²⁶⁻²⁷ Thus, it represents a desirable drug target (the NF- κ B pathway is discussed in more detail in Section 3.11).

3.1.1. Synthetic Strategies to Access 6,12-Guaianolides

Naturally occurring, 6,12-guaianolides possess a preponderance of oxygen-containing groups, multiple stereogenic carbons, and conformationally mobile five- and seven-membered rings that make stereochemistry difficult to control.²⁰⁻²¹ The challenges of synthesizing these compounds and their analogs cannot be overstated.^{22, 151} Some common strategies to access the 6,12-guaianolides are discussed below. In these strategies, the lactone moiety is generally installed at a late stage in the synthesis due to its reactivity.

Semisynthesis from abundant and/or commercially available natural products, such as parthenolide (**3.6**) or α -santonin (**3.9**), is one method that has been used to synthesize some 6,12-guaianolides. For example, parthenolide (**3.6**) was converted to micheliolide (**3.7**) in 90% yield using toluene sulfonic acid (Scheme 3.1).¹⁵² This could be further modified with *m*CPBA and Martin's sulfurane to generate arglabin (**3.3**); a water soluble dimethylamino adduct of arglabin was in clinical trials for cancer treatment.



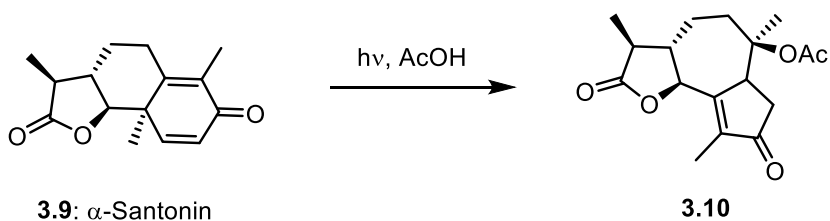
Scheme 3.1. Semisynthesis of arglabin from parthenolide.

Another semisynthesis procedure uses α -santonin (**3.9**), which affords the [5,7,5] ring system **3.10** of 6,12-guaianolides after UV irradiation under acidic conditions (Scheme 3.2). Examples of guaianolides that have been synthesized by this method in less than 5 synthetic steps

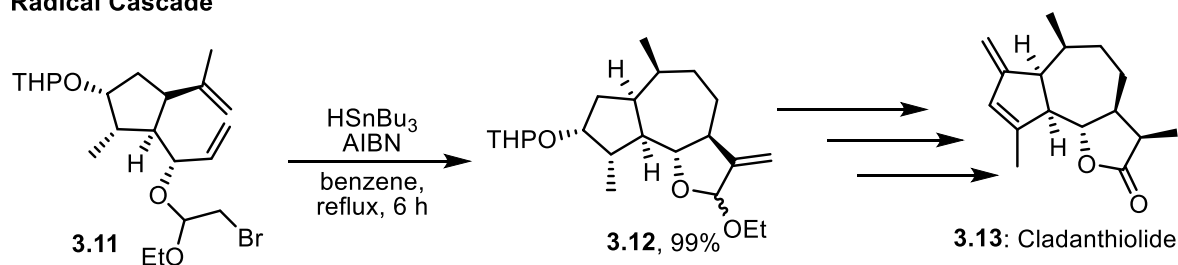
include achillin,¹⁵³ estafiatin,¹⁵⁴ and compressanolide.¹⁵⁵ In 2017, Baran and coworkers published an 11-step synthesis of thapsigargin, where irradiation of a more functionalized cross-conjugated cyclohexenone provided the 5,7-fused ring system of thapsigargin.

Other total syntheses of 6,12-guaianolides have used radical cascades, ring closing metathesis, and ring expansion to access the 5,7-hydroazulene core of guaianolides, with further functionalization to install the γ -lactone. Examples include the radical cascade of highly functionalized cyclopentane **3.11** to provide [5,7,5]-ring system **3.12** in 99% yield, which afforded cladanthiolide (**3.13**) upon further modification (Scheme 3.2).¹⁵⁶ Ring closing metathesis of functionalized cyclopentane **3.14** provided 5,7-ring system **3.15** in 88% yield, which was used in a 42-step total synthesis of thapsigargin (**3.16**).¹⁵⁷ Ring expansion of perhydroazulene **3.17** provided the 5,7-fused ring system **3.18** in 74% yield, which was then transformed into estafiatin (**3.19**).¹⁵⁸ [2 + 2] Cycloaddition of cycloheptatriene **3.20** and ring expansion provided the 5,7-ring system **3.22** in 52% yield over 3 steps; several more steps provided 6,12-guaianolide **3.23**.¹⁵⁹ These methods have primarily been used in target-directed syntheses of one specific natural product and are not easily adapted to the synthesis of analogs. Additionally, the ring expansion methods have only been performed on substrates with limited functionality.

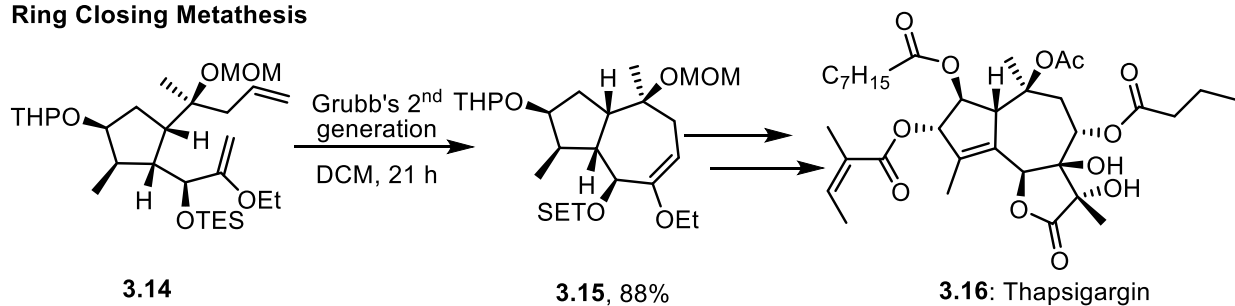
Photochemical Rearrangement



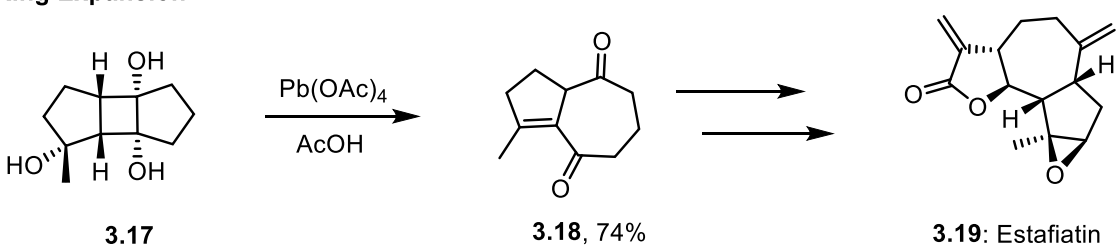
Radical Cascade



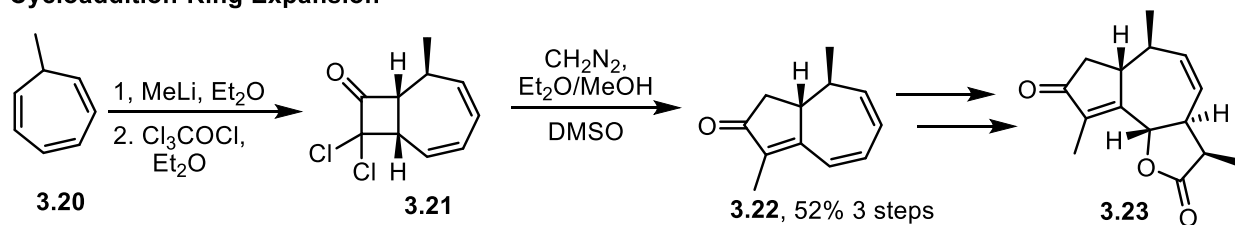
Ring Closing Metathesis



Ring Expansion

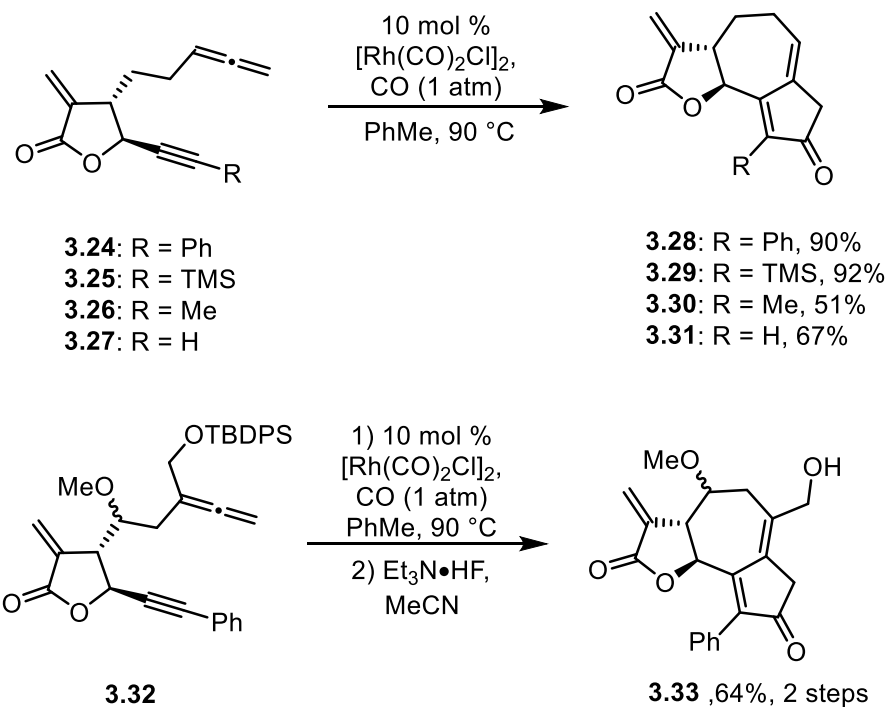


Cycloaddition-Ring Expansion

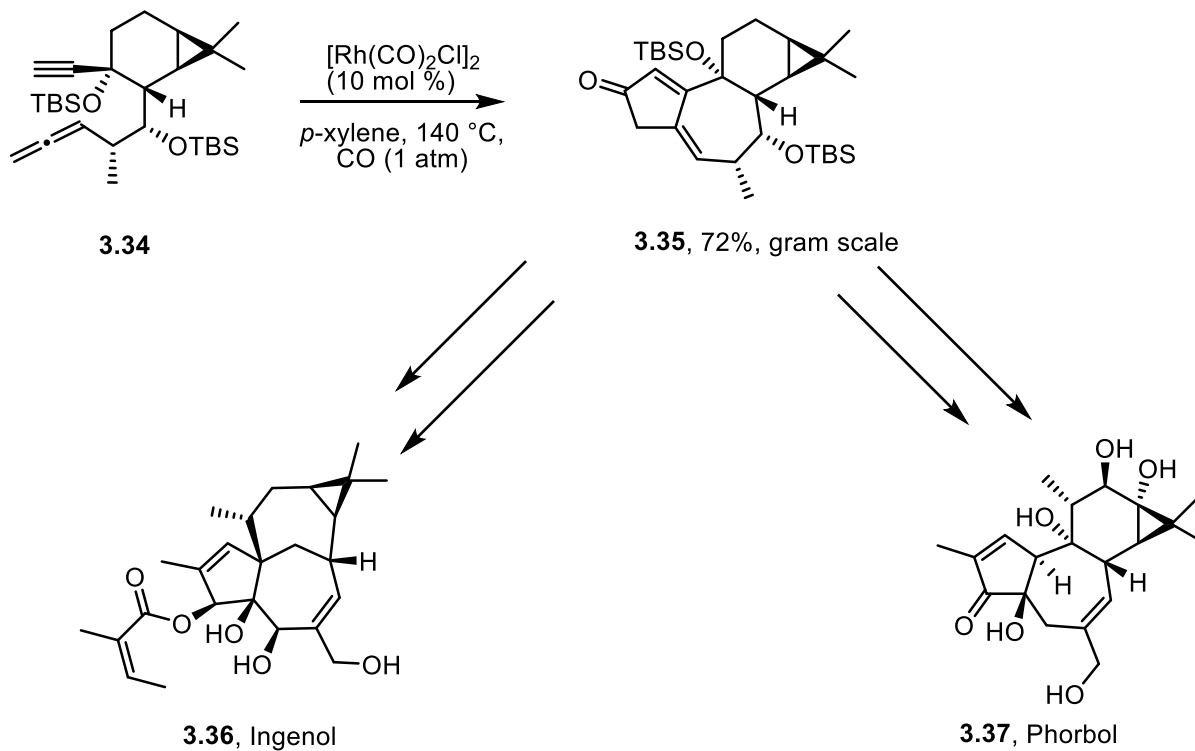


Scheme 3.2. Methods to form 5,7-ring system in the total syntheses of guaianolides.

The synthetic utility of the allenic Pauson–Khand reaction (APKR) for preparation of the structurally complex framework of 6,12-guaianolides has been demonstrated by our group in the past. This strategy involved an early introduction of the α -methylene- γ -lactone motif into the cyclization precursor showcasing the functional group compatibility and mild reaction conditions used for the APKR process.¹¹⁷⁻¹¹⁸ In these cases, monosubstituted allenes **3.24-3.25** underwent the APKR with aryl and silyl substituted alkynes to provide [5,7,5]-ring system **3.28-3.29** in good yields above 90%, while a methyl-substituted and terminal alkyne **3.26-3.27** gave 51 and 67% yields of APKR products **3.30-3.31** (Scheme 3.3). More oxygenated allene-yne **3.32**, containing a disubstituted allene, provided guaianolide analog **3.33** in 64% yield after the APKR and *tert*-butyldiphenylsilyl (TBDPS) removal. Others have shown the extraordinary utility of the APKR for accessing molecularly complex 5,7-ring systems. Notably, Baran has used the APKR of allene-yne **3.34** to access **3.35** in multigram quantities; this common intermediate was used in the step-economical syntheses of both (+)-ingenol **3.36** and (+)-phorbol **3.37** (Scheme 3.4).¹⁶⁰⁻¹⁶² The advantages of the APKR include broad substrate compatibility and rapid access to the 5,7,5-ring system of guaianolides which allows the preparation of various analogs. One disadvantage is that the allene can be difficult to install in some cases. Additionally, lower yields of the APKR were observed for substrates with terminal or methyl substituted alkynes and for 1,1-disubstituted allenes, although this was recently solved by our lab using high dilution conditions.¹⁶³



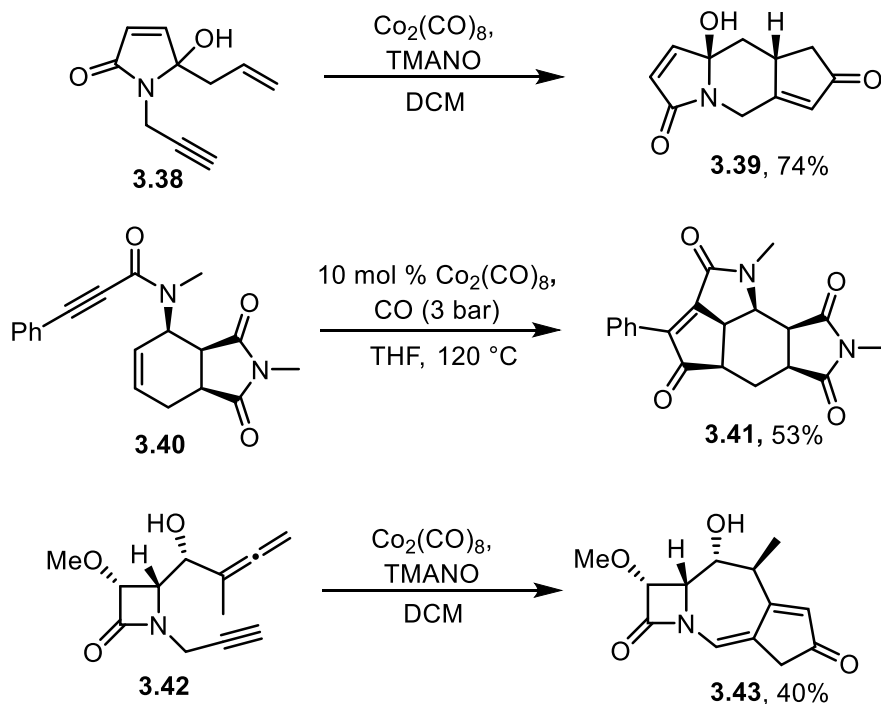
Scheme 3.3. Synthesis of guaianolide analogs using an APKR.



Scheme 3.4. APKR to prepare precursor to ingenol and phorbol.

3.1.2. Pauson-Khand Reactions with Amide or Lactam Tethers

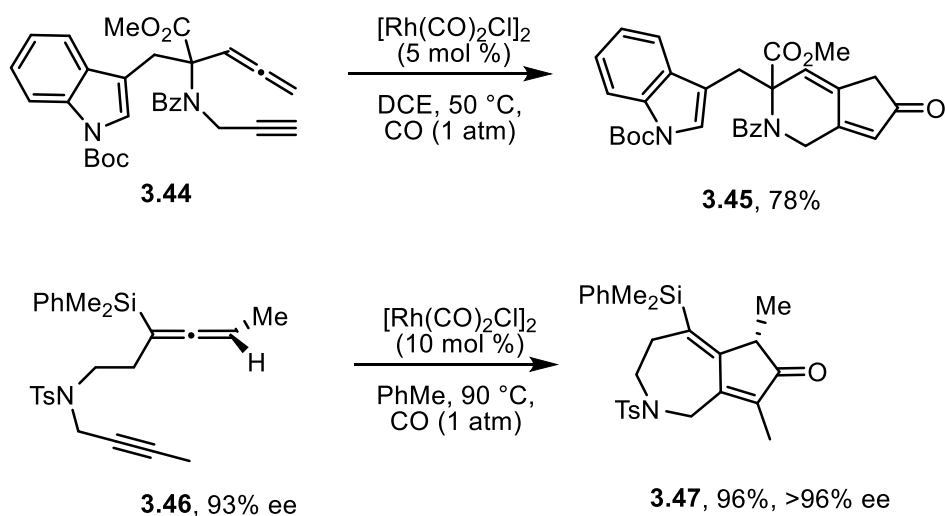
The utility and functional group compatibility of the allenic Pauson-Khand reaction led to the hypothesis that an APKR of an α -methylene- γ -lactam tethered allene-yne would be a viable route to guaianolide analogs containing an α -methylene- γ -lactam in place of the naturally occurring α -methylene- γ -lactone. Pauson-Khand reactions mediated or catalyzed by dicobalt octacarbonyl have been performed using amide and lactam tethers, including an APKR to form a 7-membered ring. In one example, ene-yne **3.38** with an unsaturated γ -lactam tether provided [5,6,5]-fused ring system **3.39** in 74% yield using stoichiometric dicobalt octacarbonyl (Scheme 3.5).¹⁶⁴ Ene-yne **3.40** with an amide tether, provided tetracycle **3.41** in 54% yield under cobalt catalyzed conditions.¹⁶⁵ Amide rotation likely led to the need for the high temperature in this reaction Cobalt-mediated APKR of allene-yne **3.42**, tethered by a β -lactam, provided [4,7,5]-fused tricycle **3.43** in 40% yield after isomerization of the alkene.¹⁶⁶ Although lactams and amides have been used in the Pauson-Khand reaction and APKR, only tertiary amides and cobalt mediated or catalyzed reactions have been reported to the best of my knowledge.



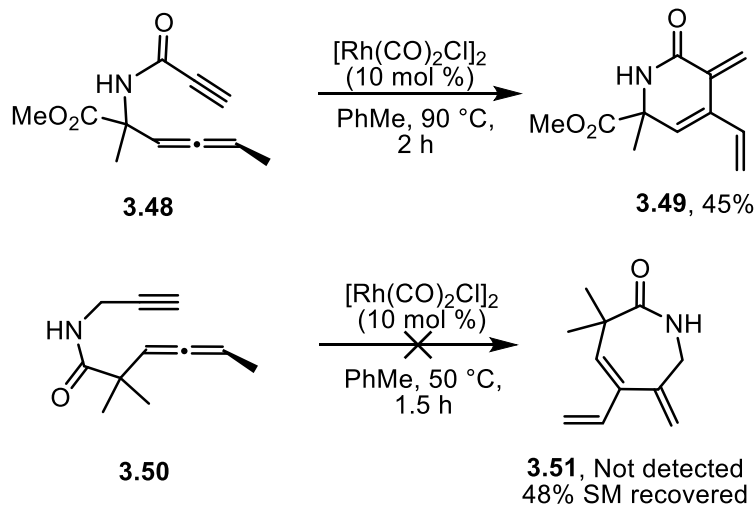
Scheme 3.5. Pauson-Khand reactions with lactam and amide tethers.

Our group has demonstrated that tertiary benzamide or sulfonamide tethered allene-yne undergo the rhodium catalyzed APKR in good yields. Benzamide **3.44** provides fused bicycle **3.45** in 78% yield (Scheme 3.6).¹⁶⁷ Sulfonamide **3.46** provides fused 5,7-ring system **3.47** in 96% yield with complete transfer of chirality from the enantiomerically enriched allene.¹⁶⁸ To my knowledge, there are no examples of a rhodium-catalyzed, Pauson-Khand reaction with α -methylene- γ -lactam tethers. Indeed, most examples of Pauson-Khand or APKRs with cobalt or rhodium involve tertiary amides. In the allenic alder-ene reaction of secondary amide **3.48**, 6-membered rings such as **3.49** could be formed, albeit at higher temperatures and longer reaction times than the corresponding benzamides; 7-membered rings were not formed when secondary amide **3.50** was used in this reaction, despite the successful formation of a 7-membered ring with the corresponding benzamide (Scheme 3.10).¹⁶⁹ This could indicate a potential problem in the APKR with secondary amides as

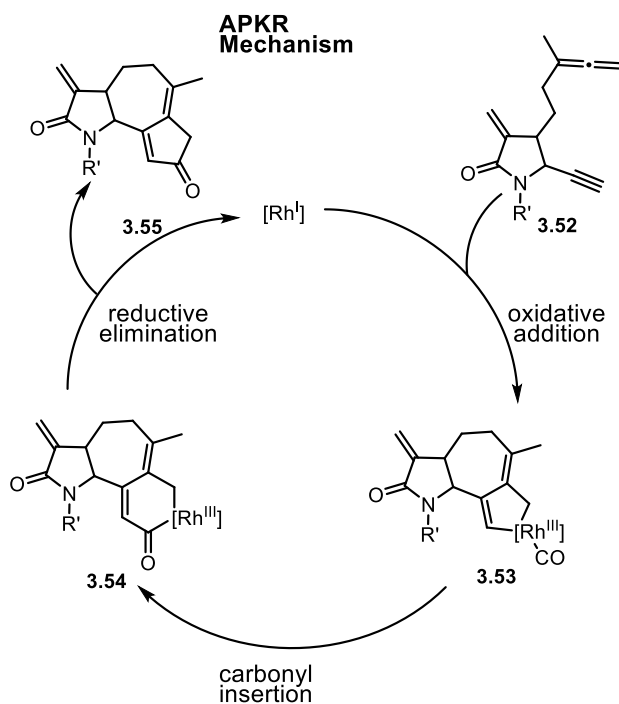
rhodium biscarbonyl chloride dimer is used as the catalyst in both reactions, although under the carbon monoxide atmosphere in APKR, the rhodium will coordinate to an additional molecule of CO, thus changing the active catalyst. Additionally, it is possible that the secondary amide of **3.50** requires higher temperatures to form the required conformation for cyclization. The mechanisms for both the allenic alder-ene reaction and the APKR involve formation of a 5-member rhodium metallacycle **3.53** as a result of oxidative addition of the rhodium catalyst (Scheme 3.8). In the case of the allenic alder-ene reaction, the rhodium metallacycle undergoes β -hydride elimination followed by reductive elimination to give the product and regenerate the Rh(I) catalyst. In the APKR, rhodium metallacycle **3.53** undergoes carbonyl insertion to give **3.54**, followed by reductive elimination to afford **3.55** and regenerate the catalyst.



Scheme 3.6. APKR with tertiary amide tethers.



Scheme 3.7. Rhodium catalyzed allenic Alder-ene reactions with secondary amides.



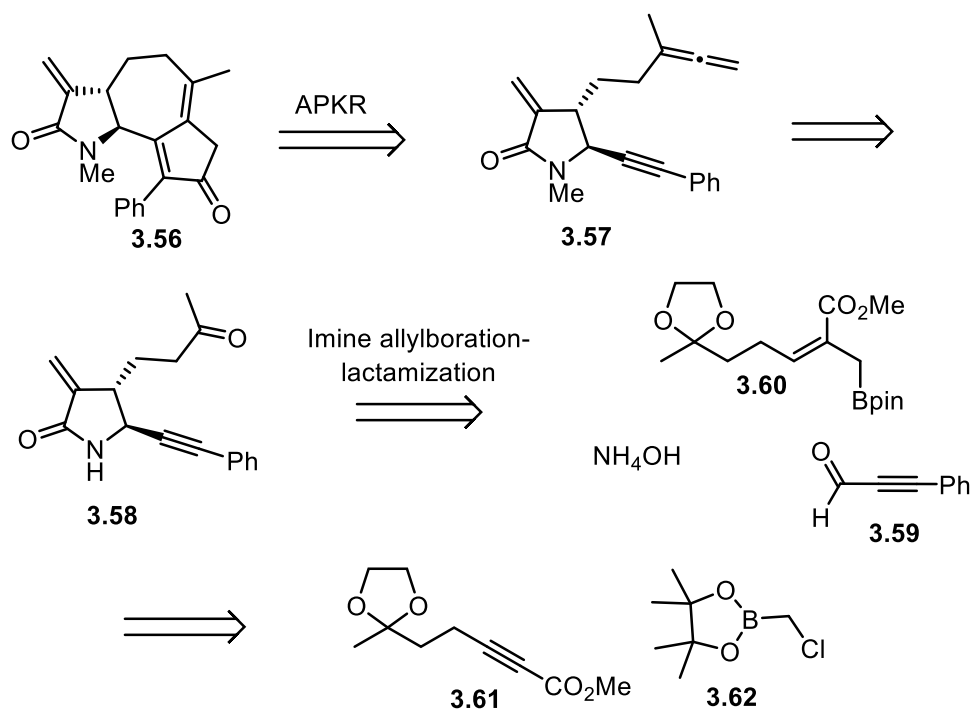
Scheme 3.8. Mechanism of allenic Pauson-Khand reaction.

3.1.3. Retrosynthetic Design of α -Methylene- γ -lactam Guaianolide Analogs

Based on the success of α -methylene- γ -lactone-tethered allene-ynes in the APKR and precedent for amides or lactams in PK reactions, it was hypothesized that lactam guaianolide isosteres such as **3.56**, could be prepared using an APKR and an early introduction of the α -methylene- γ -lactam. To test this hypothesis, compound **3.56** was envisioned as an initial target with an *N*-methyl group to protect the lactam and render the α -methylene group less reactive (Scheme 3.9). In turn, the C-4 phenyl group serves to lower the volatility of precursors in the early stages of the synthetic sequence and to provide a compound that could be benchmarked against similar α -methylene- γ -lactones in terms of chemical reactivity, NF- κ B pathway inhibition, and cellular toxicity. Working retrosynthetically, it was predicted that the tricyclic ring system of **3.56** could be obtained from allene-yne **3.57** using the APKR. It was anticipated that the rate of the formal cycloaddition reaction would be slower than the corresponding lactone derivative because of the developing A^{1,3} interaction between the *N*-methyl group of the lactam and phenyl groups, an interaction not present in the lactone-containing systems, but it was predicted that this steric hindrance should not prevent the APKR from occurring.

The allenyl group of **3.57** should be available from methyl ketone **3.58**, using a 3-step reaction sequence involving Grignard addition of ethynyl magnesium bromide, acetylation of the tertiary alcohol, and a formal S_N2' hydride addition with triphenylphosphine copper hydride hexamer to form the allene.¹⁷⁰ Triphenylphosphine copper hydride hexamer (Stryker's reagent) is commonly used for conjugate reductions of α,β -unsaturated ketones and aldehydes.¹⁷¹ Indeed, the α -methylene unit of similar α -methylene- γ -lactones was reduced to a methyl substituent when Stryker's reagent was used to form the allene, thus requiring protection of the α -methylene via

Michael addition of an amine that was eliminated after allene formation to regenerate the α -methylene- γ -lactone (Dr. François Grillet, unpublished data). It was hypothesized that the lower electrophilicity of α -methylene- γ -lactams would lower the propensity for α -methylene reduction in these systems relative to methylene- γ -lactones; conjugate reductions of α,β -unsaturated aldehydes, ketones, esters, and lactones, have been reported, but not amides or lactams.¹⁷¹ Finally, it was proposed that α -methylene- γ -lactam **3.58** could be formed using a 3-component reaction between propynal **3.59**, ammonium hydroxide, and allylboronate **3.60** (Scheme 3.11).¹³⁶ Alkynals have not been used previously in this 3-component reaction for the preparation of α -methylene- γ -lactams; only aryl and alkyl aldehydes were reported. The requisite allylboronate **3.60** could be prepared from known alkynoate **3.61** using diisobutylaluminum hydride (DIBALH) and chloromethylpinacol boronate **3.62** as has been demonstrated by our lab and others to prepare similar allylboronates.^{117-118, 136-137, 172} The stereochemistry of the allylboronate controls the stereochemistry of lactam **3.58**, with the *Z*-isomer providing the *trans* lactam and the *E*-isomer providing the *cis* lactam (not shown). Thus, this route has the potential to provide access to both *cis* and *trans* lactam isomers. We also envisioned that this strategy could be employed to generate *N*-unsubstituted lactams, which could be modified at a late stage in the synthesis to introduce electronically diverse substituents on the lactam nitrogen through substitution or amide-aryl halide coupling reactions. Thus, this synthetic approach would provide a method to tune the electrophilicity of the α -methylene- γ -lactam Michael acceptor.¹⁷³

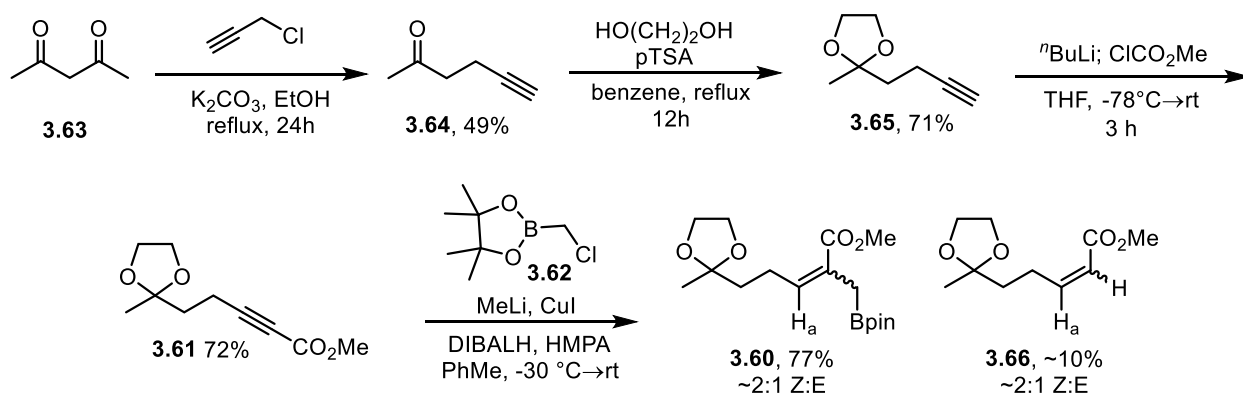


Scheme 3.9. Retrosynthetic analysis of α -methylene- γ -lactam guaianolide analog.

3.2. FEASIBILITY OF ALLENIC PAUSON-KHAND APPROACH TO α -METHYLENE- γ -LACTAM CONTAINING GUAIANOLIDE ISOSTERES

The synthesis of APKR precursor **3.57** began with the preparation of alkynoate **3.61** in 3 steps from 2,4-pentanedione (**3.63**) in multi-gram quantities. Alkylation of 2,4-pentanedione was achieved by refluxing **3.63** with propargyl chloride and potassium carbonate in ethanol for 24 h (Scheme 3.10). This afforded ketone **3.64** in 49% yield through loss of ethyl acetate. Ketone **3.64** was purified by filtration to remove potassium carbonate, concentration by simple distillation at atmospheric pressure, and vacuum distillation at 45 mmHg and 90 °C; the spectral data matched that reported in the literature.¹⁷⁴ Ketone **3.64** was protected as the ketal by treatment with ethylene glycol and catalytic *para*-toluene sulfonic acid (*p*TSA) in refluxing benzene to provide ketal **3.65**

in 71% yield after aqueous work up, concentration by simple distillation at atmospheric pressure, and vacuum distillation at 30 mmHg and 120 °C. The purified ketal **3.65** contained about 10% benzene based on integration of the ¹H NMR resonance for benzene at 7.19 ppm and the terminal alkyne resonance at 1.87 ppm.¹⁷⁵ Ketal **3.65** was treated with *n*-butyllithium at -78 °C to form the lithium acetylide which was reacted with methyl chloroformate for 3 h at rt to afford alkynoate **3.61** in 72% isolated yield after purification by column chromatography.¹⁷⁶



Scheme 3.10. Synthesis of 2-alkoxycarbonyl allylboronate.

Alkynoate **3.61** was treated with with DIBALH and chloromethyl pinacolboronate using the procedure first reported by Vilieras et al., and previously utilized by our group in the synthesis of α -methylene- γ -lactones, to afford allylboronate **3.60** in 77% yield along with 10% of alkene byproduct **3.66**, arising from the quench of the intermediate vinyl aluminum species with a hydrogen source (Scheme 3.12).^{117-118, 137} Difficulties were encountered during this reactions, but we ultimately settled on the following optimized process. This reaction was performed using catalytic quantities of both copper iodide and methyl lithium (10 mol%) which were stirred at -30 °C for 20 min; hexamethylphosphoramide (HMPA), toluene, and DIBALH (1 M solution in

hexanes or toluene) were added and stirred for 2 h at -30 °C. A solution of alkynoate **3.61** in toluene was then added to the DIBALH solution and this was allowed to warm to -20 °C for 5 h. Chloromethyl pinacolboronate **3.62** dissolved in toluene was added to the alkynoate solution and the reaction was allowed to warm to rt. After 16 h at rt, the reaction was quenched by dropwise addition of 1 N HCl after dilution with diethyl ether, followed by sequential washing of the organic layer with small portions of 1 N HCl, saturated aqueous ammonium bicarbonate, water, and brine. Removal of the solvent by rotary evaporation followed by filtration of the crude residue through a plug of silica gel gave allylboronate **3.60** in yields ranging from 40-90%. This reaction was performed over 10 times and the yields were typically 60-80% with 10-20% of alkene byproduct **3.66**, which had the same Z:E ratio as the allylboronate. Additionally, this reaction was performed on 2-3 g of alkynoate **3.61** with minimal changes in yield or byproduct formation.

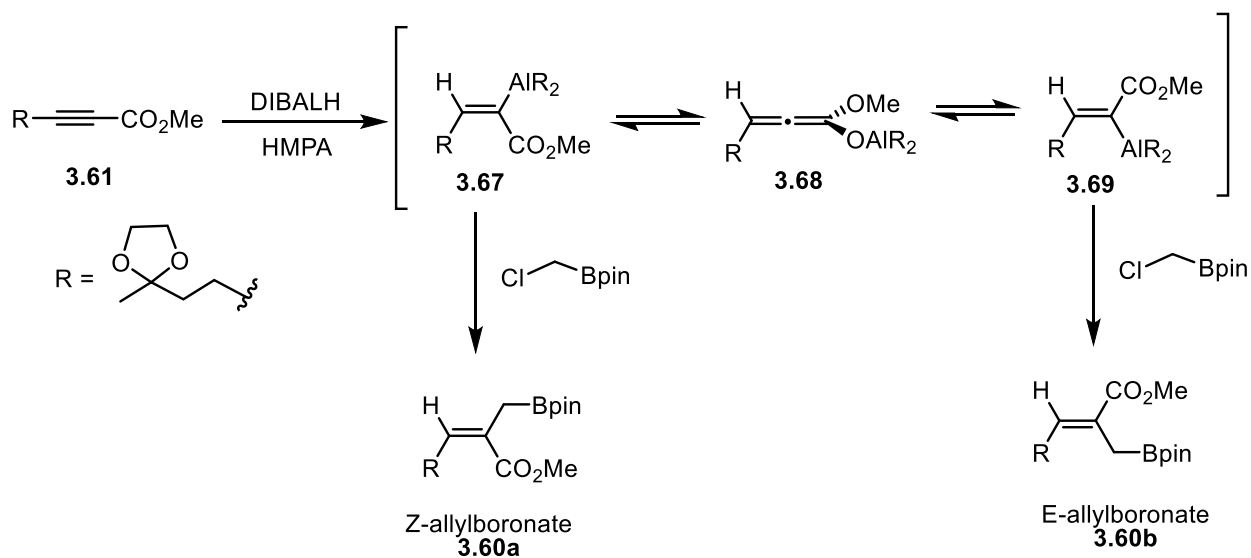
Allylboronate **3.60** was obtained as a mixture of isomers in a ratio between 2 and 3 to 1 (Z:E). The ratio was determined by integration of the ¹H NMR resonances at 5.92 ppm (Z) and 6.71 ppm (E) corresponding to H_a of **3.60** (Scheme 3.10). The Z and E isomers were identified by analogy to similar allylboronates formed under the same conditions which reported the E-isomer as having a chemical shift further downfield than the Z-isomer.^{117, 136-137} The ratio of allylboronate **3.60** to alkene **3.66** was determined by the integration of allylboronate proton H_a to the β proton of the unsaturated alkenes which appeared as a doublet of triplets at 6.98 ppm (E) and 6.26 ppm (Z). The E and Z isomers were inseparable by flash chromatography. The alkene byproduct **3.66** could be separated from allylboronate **3.60** by chromatography, but allylboronate **3.60** was unstable when exposed to silica gel for extended periods of time, resulting in decreased yields (20-40%). Therefore, the mixture of products was filtered through a plug of silica gel and the allylboronate isomers and alkene byproducts were taken onto the next synthetic step as a mixture.

As long as the allylboronate contained less than 20% of the alkene byproduct, the yield of the following lactamization reaction was not affected. If larger amounts of the alkene byproduct were taken on to the lactamization reaction, it resulted in lower yields and made the lactam difficult to purify due to the presence of other byproducts.

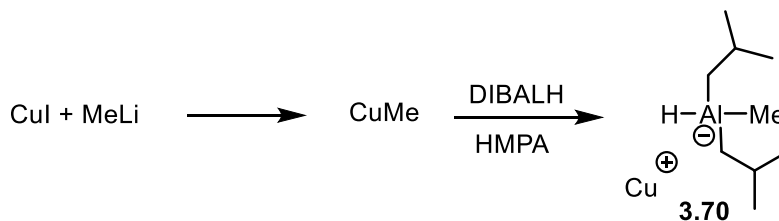
In order to obtain optimal yields and minimal byproduct formation for this reaction, chloromethyl pinacolboronate needed to be freshly distilled, even though no change in the ^1H NMR of this compound was detected upon storage. The toluene was also freshly distilled from calcium hydride, while the HMPA was distilled over calcium hydride with reduced pressure and then stored over 4 Å molecular sieves. It was important to know the exact concentration of DIBALH; in many cases where significant amounts (>20%) of the alkene byproducts were obtained, the DIBALH concentration was between 0.6 and 0.8 M, not 1 M as the bottle stated (determined by titration with *p*-anisaldehyde using Hoye's no D NMR procedure).¹⁷⁷ This led to incomplete formation of the allylboronate. However, if excess DIBALH was used, reduction of the ester to the alcohol was observed as a minor byproduct.

Formation of allylboronates from alkynoates can be performed without catalytic copper iodide and methyl lithium, but these reactions require longer reaction times.^{118, 178} The mechanism for this reaction in the absence of copper iodide and methyl lithium involves a 1,4-conjugate addition of DIBALH to alkynoate **3.61** to form vinyl aluminum intermediate **3.67**, which can isomerize via allene **3.68** to vinyl aluminum **3.69**.¹⁷⁹ These two vinyl aluminum species are trapped with chloromethyl pinacolboronate to give *Z*-allylboronate **3.60a** and *E*-allylboronate **3.60b** as a mixture of *Z* and *E* isomers (Scheme 3.11). Copper iodide and methyl lithium form methyl copper which can activate the DIBALH by formation of a negatively charged aluminum

species such as **3.70** that then undergoes conjugate reduction to a vinyl aluminum species, but this mechanism has not been elucidated (Scheme 3.12).¹⁸⁰



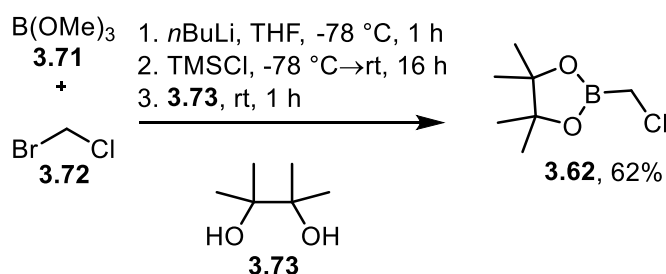
Scheme 3.11. Formation of allylboronate via vinyl aluminum intermediates.



Scheme 3.12. Activation of DIBALH with CuMe.

Chloromethyl pinacolboronate **3.62** was prepared as previously described.¹⁸¹ A mixture of trimethyl borate (**3.71**) and bromochloromethane (**3.72**) in THF was treated with *n*-butyllithium at $-78\text{ }^{\circ}\text{C}$ and stirred for 1 h at this temperature (Scheme 3.13). Trimethylsilylchloride (TMSCl) was added at $-78\text{ }^{\circ}\text{C}$ and the reaction was allowed to warm to rt with stirring, then allowed to stand overnight (16 h) without stirring. Pinacol (**3.73**) was added at rt, and the reaction was stirred for 1 h, then partitioned between water and ether (1:1). Concentration of the organic layer after drying over magnesium sulfate gave the crude residue which was purified by fractional distillation at 12

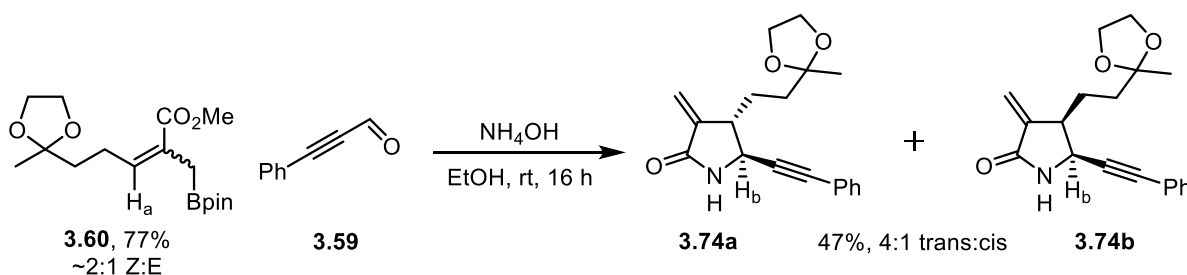
mmHg and 90-110 °C to afford pure chloromethyl pinacolboronate **3.62**. In addition to small amounts of THF and ether that were not removed by rotary evaporation, the major impurity of the crude residue was bromobutane which distilled at 12 mmHg and 45-60 °C.



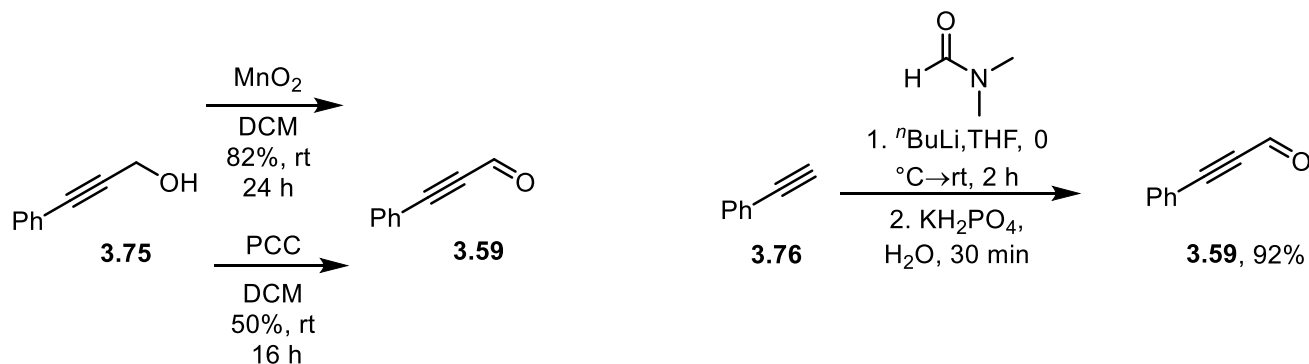
Scheme 3.13. Synthesis of chloromethyl pinacolboronate.

In order to test if propynals were viable substrates for the 3-component lactamization reaction, phenyl propynal and aqueous ammonia were stirred together in ethanol for 30 minutes, then an ethanol solution of allylboronate **3.60** (2:1 Z:E) was added and the reaction was stirred for 16 h to provide lactams **3.74a** and **3.74b** in 47% combined yield, and as a 4:1 trans (**3.74a**) to cis (**3.74b**) isomeric mixture (Scheme 3.14). The lactams could be identified by new methylene resonances in the ^1H NMR spectrum at 6.10 and 5.40 ppm for **3.74a** and **3.74b**. Broad amide singlet resonances appeared between 6-7 ppm for the lactams **3.74a,b**, and these chemical shifts changed depending on the concentration of the lactam in the NMR sample. The cis and trans methylene and amide signals were indistinguishable for trans and cis isomers **3.74a,b**. However, the isomers could be distinguished by the chemical shift of the resonance for the hydrogen attached to the γ -carbon of the lactam ring, labeled H_b in Scheme 3.15, which appeared as a doublet at 4.2 ppm for trans lactam **3.74a** and as a doublet at 4.7 ppm for the cis lactam **3.74b**; integration of these doublets indicated a trans:cis ratio of about 4:1. This three component reaction was originally

reported by Hall and Elford for aryl or alkyl aldehydes and 2-alkoxycarbonyl allylboronates at 70 °C to afford α -methylene- γ -lactams after 4 h (see Section 2.2).^{77, 136} Propynals are also viable substrates in this reaction and propynals do not need to be heated for a reaction to occur.^{77, 136} Indeed, initial attempts to perform this reaction at 70 °C led to significant decomposition of the starting materials and only small amounts (<20%) of the lactam products were isolated. Additionally, attempts to perform this reaction with less basic ammonium acetate in place of ammonium hydroxide did not lead to any product formation.



Scheme 3.14. Three-component reaction to form α -methylene- γ -lactams.



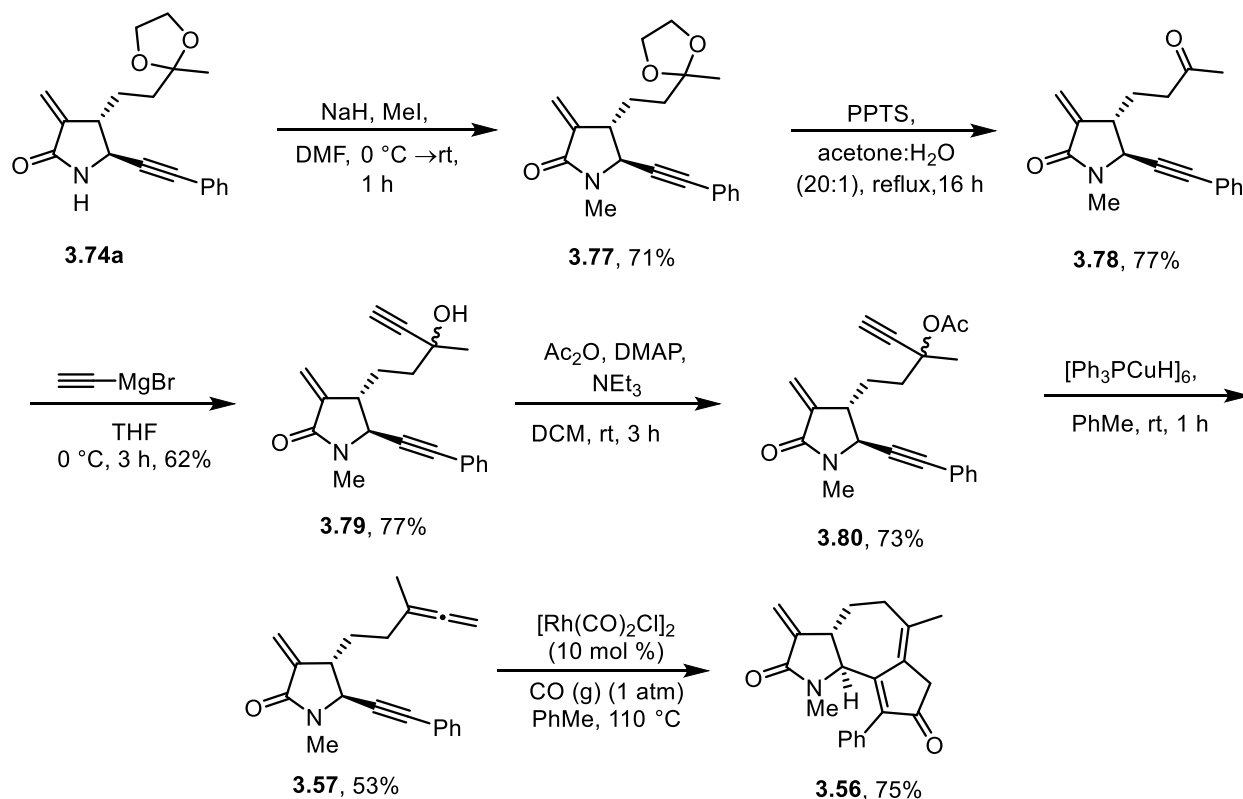
Scheme 3.15. Synthesis of 3-phenyl propynal.

3-Phenyl propynal **3.59** was prepared using 3 different methods. Oxidation of 3-phenyl propargyl alcohol **3.75** with pyridinium chlorochromate (PCC) gave only 50% of the desired aldehyde **3.59**, and the toxicity of PCC made this route unappealing (Scheme 3.15). Oxidation of

alcohol **3.75** with manganese dioxide (MnO_2) provided 3-phenyl propynal **3.59** in 82% yield when MnO_2 was prepared from potassium permanganate and manganese sulfate, but 5-10 equivalents of MnO_2 were required for complete oxidation of alcohol **3.75**.¹⁸² Attempts to oxidize **3.75** with commercially available MnO_2 failed to go to completion even when a large excess (20 equiv) of MnO_2 was employed. The fastest, highest yielding, and most economical formation of propynals was achieved using the Bouveault aldehyde synthesis where the lithium acetylide of phenyl acetylene **3.76** was treated with dimethylformamide followed by an aqueous work-up with monobasic potassium phosphate to form propynal **3.59** in 92% yield.¹⁸³

With a successful method to synthesize α -methylene- γ -lactams containing an alkyne substituent at the γ -position, efforts to install an allene were pursued. Towards this end, trans-lactam **3.74a** was isolated and the lactam nitrogen was blocked by treatment with sodium hydride and methyl iodide to provide *N*-methyl lactam **3.77** in 71% yield. The ketal of **3.77** was hydrolyzed by refluxing with pyridinium *para*-toluenesulfonate (PPTS) in a 20:1 acetone to water solvent which afforded ketone **3.78** in 77% yield (Scheme 3.16). Ketone **3.78** was identified by the appearance of a new carbonyl resonance in the ^{13}C NMR at 207.1 ppm and a downfield shift of the methyl singlet resonance from 1.33 to 2.17 ppm. Treatment of ketone **3.78** with ethynyl magnesium bromide at 0 °C in THF for 3 h provided tertiary propargyl alcohol **3.79** in 77% yield as a 1:1 mixture of alcohol diastereomers. The diastereomers were apparent in the ^{13}C NMR spectrum which showed a 1:1 ratio of peaks for most carbons. The hydroxyl group of **3.79** was transformed into an acetoxy group by treatment with acetic anhydride, dimethylaminopyridine, and triethylamine in DCM for 3 h, affording **3.80** in 73% yield. Acetate **3.80** was identified by a new singlet resonance at 2.03 ppm that integrated for three hydrogens in the ^1H NMR and a new carbonyl resonance at 169.4 ppm of the ^{13}C NMR. Acetate **3.80** was converted to APKR precursor

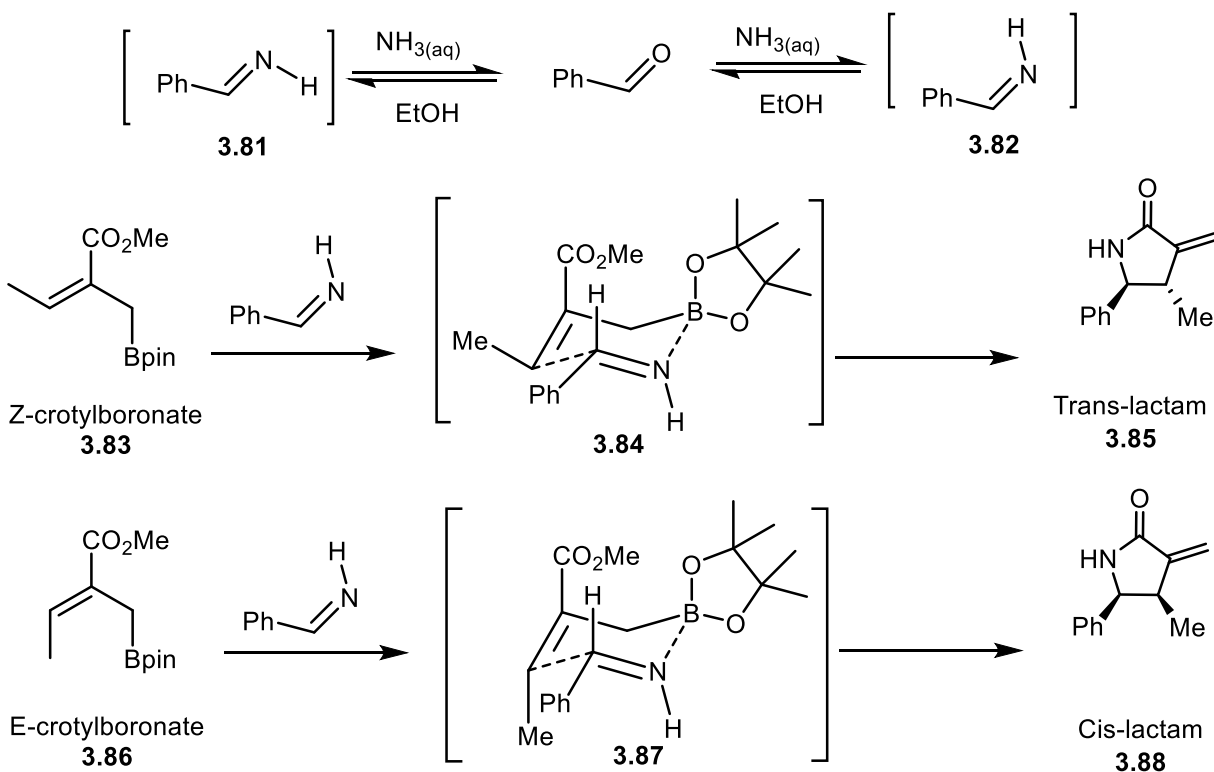
3.57 via a formal S_N2' hydride addition using triphenylphosphine copper hydride hexamer (Stryker's reagent) in 53% yield. To our delight, the α -methylene group was unaffected by Stryker's reagent, as was predicted for weakly electrophilic α -methylene- γ -lactams. Allene-yne **3.57** was identified by the terminal allene resonance which appeared as a multiplet at 4.66-4.64 ppm in the ^1H NMR and new resonances in the ^{13}C NMR at 201.2, 97.7, and 75.2 corresponding to the central allene carbon, the terminal allene carbon, and the internal allene carbon, respectively. The APKR was performed by dropwise addition of a toluene solution of allene-yne **3.57** to a dilute solution of rhodium(I) biscarbonyl chloride dimer (10 mol%) in toluene over 1 h at 110 °C under a carbon monoxide atmosphere.¹⁶³ After addition of the allene-yne **3.57** was complete, the reaction was heated for an additional 30 min to afford the desired [5,7,5]-fused tricycle **3.56** in 75% yield, thus demonstrating that the proposed route to access guaianolide analogs with a lactam replacing a lactone was achievable. These slow addition conditions have been shown to improve the yield of the APKR for methyl substituted allenes and alkynes due to a more dilute solution of rhodium catalyst and allene-yne.¹⁶³ This was the first reported APKR with an α -methylene- γ -lactam tether.



Scheme 3.16. Feasibility of allenic cyclocarbonylation approach to guaianolide analogs.

3.3. TRANSITION STATE ANALYSIS FOR LACTAMIZATION REACTION

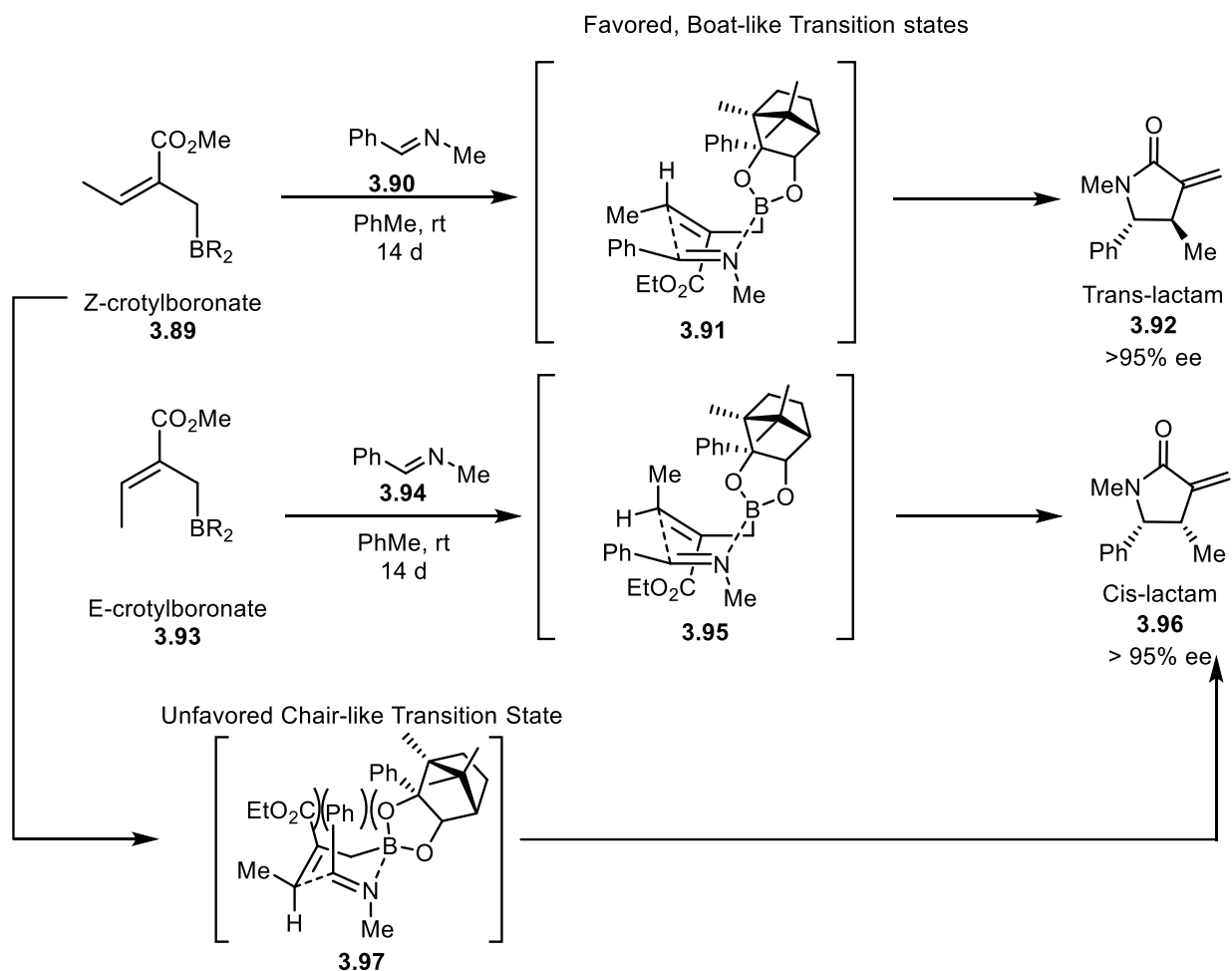
Hall and Elford reported complete diastereospecificity for conversion of pure *Z*-crotylboronate **3.83** to trans α -methylene- γ -lactam **3.85** and pure *E*-crotylboronate **3.86** to cis α -methylene- γ -lactam **3.88**; they proposed a chair-like transition state **3.84** with the primary aldimine substituent in a pseudoequatorial position trans to the boronate to account for this diastereospecificity (Scheme 3.17).¹³⁶ These transition states are formed from the *Z* imine **3.82**, which is in equilibrium with the *E* imine **3.81** under the aqueous conditions employed.



Scheme 3.17. Proposed transition states for diastereospecific α -methylene- γ -lactam formation from crotylboronates and primary aldimines.

Alternatively, boat-like transition states were proposed by Villieras and coworkers for their chiral allylboronates containing a chiral boronate in place of the pinacolborane and their reaction with secondary aldimines; they proposed that imines such as **3.90** would form in the E conformation due to the nitrogen substituent and would not equilibrate under their conditions (Scheme 3.18).¹³⁷ In this case, a chair-like transition state (**3.97**) for Z-crotylboronate **3.89** would be unfavored due to 1,3-diaxial interactions, and indeed the Z-crotylboronate **3.89** was converted to the trans lactam **3.92**. A boat-like transition state **3.91** or **3.95** was proposed to account for the observed diastereospecificity in these cases, however, it has recently been demonstrated that allylboroxines catalyze the E/Z isomerization of imines.¹⁸⁴ Thus, if boronates behave similar to the

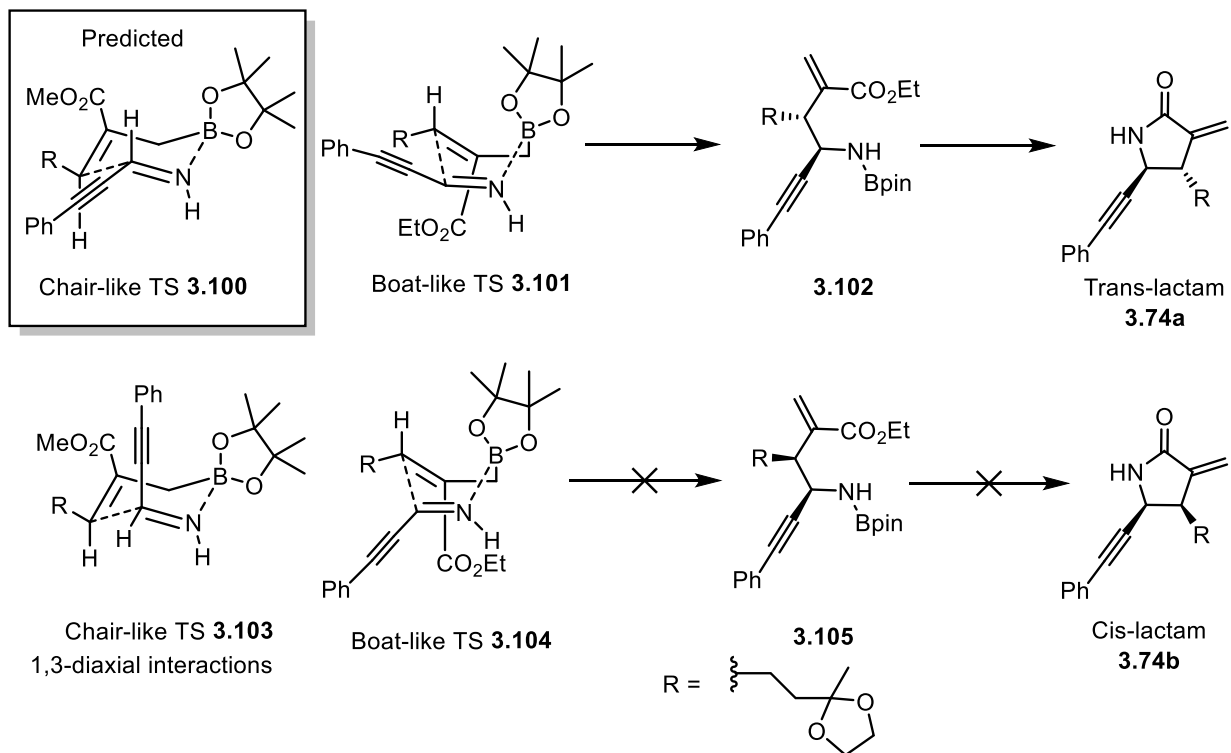
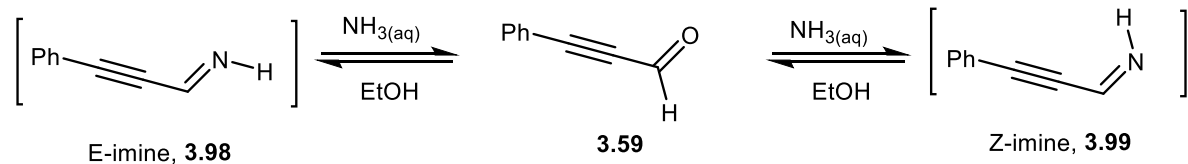
boroxines, isomerization of the imines would allow chair-like transition states that involve the Z imine as discussed above.



Scheme 3.18. Proposed transition states for diastereospecific α -methylene- γ -lactam formation from chiral crotylboronates and secondary aldimines.

It is proposed that Z-allylboronate **3.60a** goes through chair-like transition state **3.100** to give trans lactam **3.74a**, similar to the transition states proposed by Hall and Elford (Scheme 3.19). Under conditions that utilize aqueous ammonia, the imine exists in equilibrium with the aldehyde **3.59** and both E and Z imine isomers **3.98** and **3.99**, therefore, the Z-imine can form chair-like

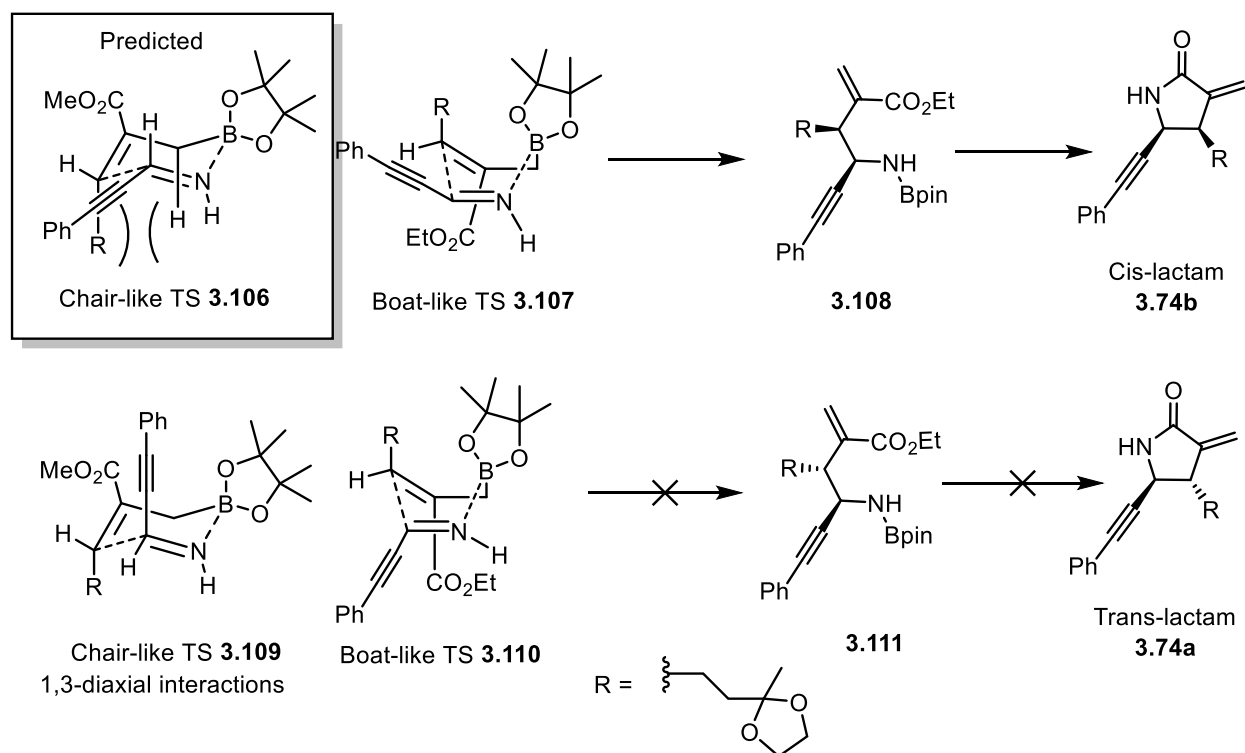
transition state **3.100** where the alkyne is trans to the boronate. A boat-like transition state **3.101**, which is formed from the E imine **3.98** and places the alkyne substituent on the same face as the boronate, can also be drawn for conversion of the Z-allylboronate to the trans lactam **3.74a**. For Z-allylboronate **3.60a** to be converted to a cis lactam, it would need to go through the unfavorable chair-like transition state **3.103** with 1,3-diaxial interactions between the alkyne and the ester, as well as 1,3-diaxial interactions between alkyne and the boronate. Boat-like transition state **3.104** formed from the Z-imine **3.99** would also provide the cis lactam **3.74b**. There does not appear to be much difference between the boat-like transition states **3.101** and **3.104**, so if these substrates went through a boat-like transition state, it is unlikely that **3.101** would be favored over **3.104** and diastereospecific reactions would not be observed.



Scheme 3.19. Possible transition states for Z-allylboronate addition to primary aldimines.

The conversion of E-allylboronate **3.60b** to cis lactam **3.74b** likely goes through the chair-like transition state **3.106** for the reasons described above (Scheme 3.20). Chair-like transition state **3.106** is less favorable than transition state **3.100** because the alkyl group is in the pseudo-axial position leading to a 1,3-diaxial interaction with a methylene hydrogen. Boat-like transition state **3.107** can also be drawn to account for the conversion of E-allylboronate to cis lactam **3.74b**, but this transition state includes an unfavorable flagpole interaction between the alkyl substituent and the boronate. Since the transition states for the E-allylboronate are less-favorable than those drawn

for the Z-allylboronate, a slower conversion to cis lactam **3.74b** is likely and decomposition of the E-allylboronate could occur during the lactam forming reaction. This would explain the change in ratio of Z:E allylboronate (2:1) when converting the mixture to trans and cis lactams (4:1) and is the most likely explanation based on the complete diastereospecificity reported for similar systems.^{136-137, 185} This change in ratio was also reported by our lab for the triflic acid promoted conversion of similar allylboronates to lactones.¹¹⁷ The larger alkyl substituent (R) in our systems has a bigger impact in the transition state than the smaller methyl groups described above. An alternative possibility, is that the E-allylboronate could go through a different, transition state such as transition states **3.109** or **3.110** to give the trans lactam **3.74a**. In this case transition state **3.110** still contains an unfavorable flagpole interactions, but transition state **3.109** is reasonable because the alkyne in these systems is less bulky than a phenyl substituent, which was reported by Hall or Vilieras in the previous examples (See Schemes 3.17 and 3.18). Thus, enrichment of the trans lactam by formation from both the Z and E allylboronates is possible, although cis lactam formation from E allylboronate is likely favored.



Scheme 3.20. Possible transition states for E-allyboronate addition to primary aldimines.

3.4. EXPANDING THE SCOPE OF THE ALLENIC PAUSON-KHAND APPROACH TO α -METHYLENE- γ -LACTAM CONTAINING GUAIANOLIDE ISOSTERES

With a successful APKR in hand, efforts to expand the scope of this strategy for the preparation of other lactam-containing guaianolide analogs were pursued. Modifications of the lactam nitrogen at a late stage in the synthesis, by substitution reactions with electrophiles or coupling reactions with aryl halides, would provide a general synthetic route to lactam containing guaianolide analogs with various nitrogen substituents. In turn, these nitrogen substituents could be used to tune the electrophilicity of the α -methylene- γ -lactam Michael acceptor. Additionally, the scope of alkynes tolerated in the cyclocarbonylation strategy were explored. Towards this end, a silyl substituted propynal was hypothesized as a starting material which would afford silyl-substituted alkynes;

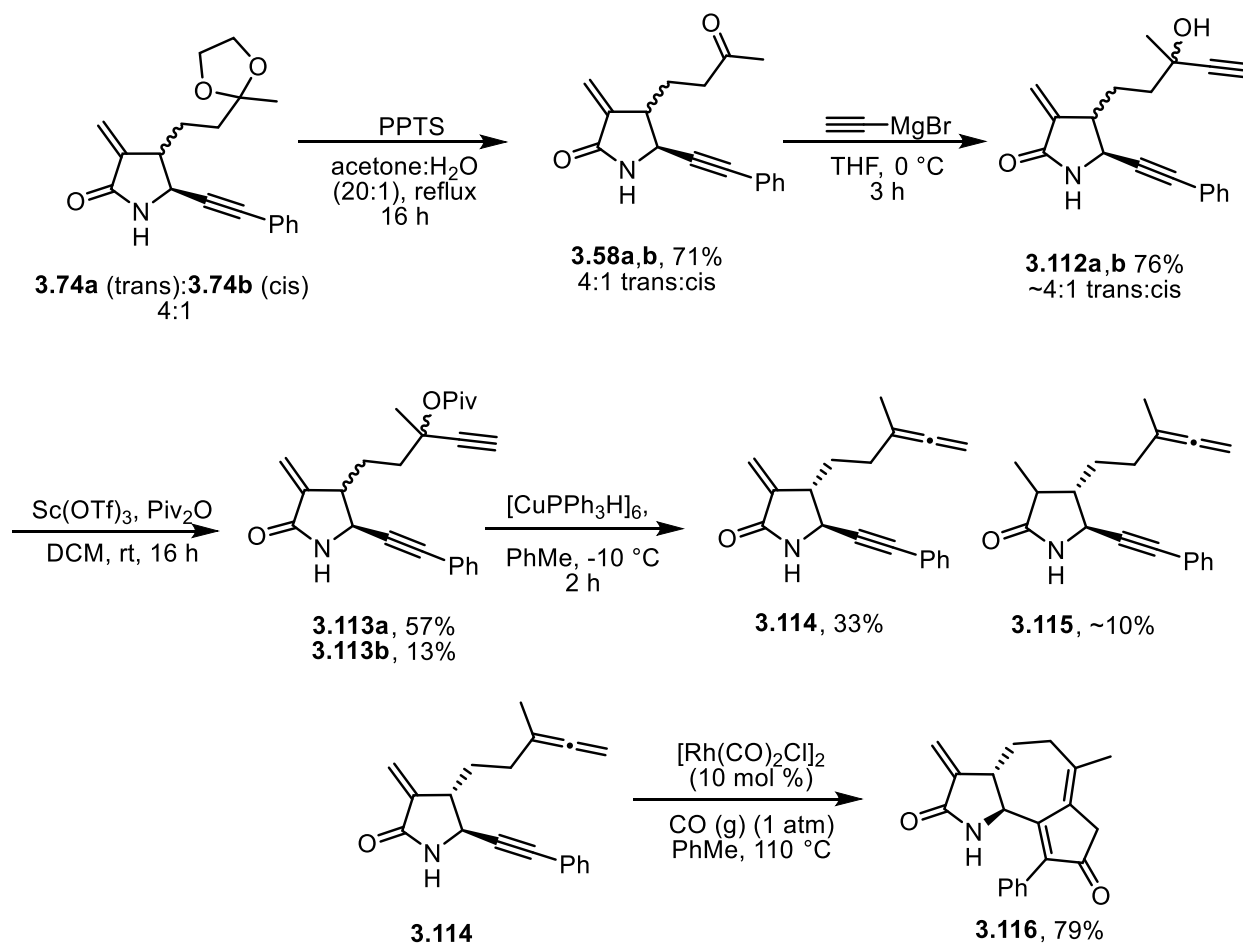
these could be modified at a late stage by removal of the silyl group, providing terminal alkynes that could be further modified through substitution or coupling reactions.

3.4.1. Feasibility of Secondary Amides in the APKR

First, the feasibility of secondary amides in the APKR was examined by synthesizing an allene-yne with an α -methylene- γ -lactam tether containing a secondary amide. This was accomplished by a synthetic protocol analogous to the synthesis of *N*-methyl lactam **3.56** described above. A 4:1 mixture of ketals **3.74a** (trans) and **3.74b** (cis) lactams were hydrolyzed with PPTS in acetone and water (20:1) at reflux for 16 h to afford ketones **3.58a,b** in 71% as a 4:1 mixture of trans (**3.58a**) and cis (**3.58b**) isomers (Scheme 3.21). Ketones **3.58a,b** were identified by the disappearance of the ketal multiplet at 3.98-3.89 ppm in **3.74**. The trans and cis lactam isomers of **3.58a,b** could be separated by silica gel column chromatography or taken on to the next step as a mixture without impacting the yield, as evidenced by the similar yields obtained when the isolated trans lactam **3.58a** was carried through the synthesis compared to the yields below, where mixtures of the trans and cis lactams were used. Additionally, the ratio of trans to cis lactams did not change throughout the synthesis. In most cases, the lactams were taken on as a mixture, and only separated for characterization purposes, since they were more easily separable at later stage in the synthesis.

Ketones **3.58a,b** were reacted with ethynyl magnesium bromide (4 equiv) in THF at 0 °C for 3 h, followed by quenching with saturated ammonium chloride and stirring vigorously for 15-30 min before extraction into ether. This provided propargyl alcohols **3.112a,b** in 76% yield, as a 1:1 mixture of alcohol diastereomers (Scheme 3.21). For the cis lactams, alkyne singlet resonances were observed at 2.36 and 2.38 for both diastereomers of **3.112b**. The trans lactam diastereomers

of **3.112a** were indistinguishable by ^1H NMR, although the ^{13}C NMR showed two diastereomers as two peaks with nearly the same chemical shift (< 0.2 ppm difference). The hydroxyl group of **3.112a,b** was chemoselectively modified by stirring with pivalic anhydride and substoichiometric scandium triflate (0.4 equiv) to give pivalates **3.113a,b** in 70% combined yield. When acetylation was attempted using acetic anhydride, DMAP, and triethylamine the nitrogen was also acetylated (these products are discussed in Chapter 4). As with the propargyl alcohol **3.112a**, the diastereomers of trans lactam **3.113a** were only distinguishable by ^{13}C NMR, but the diastereomers of cis pivalate **3.113b** could be distinguished in the ^1H NMR spectrum by two singlet resonances for the terminal alkyne at 2.42 and 2.36. Pivalates **3.113a** (trans) and **3.113b** (cis) were separated by column chromatography, and the isolated yields of **3.113a** (57%) and **3.113b** (13%) reflected the ratio of the starting material determined by ^1H NMR.



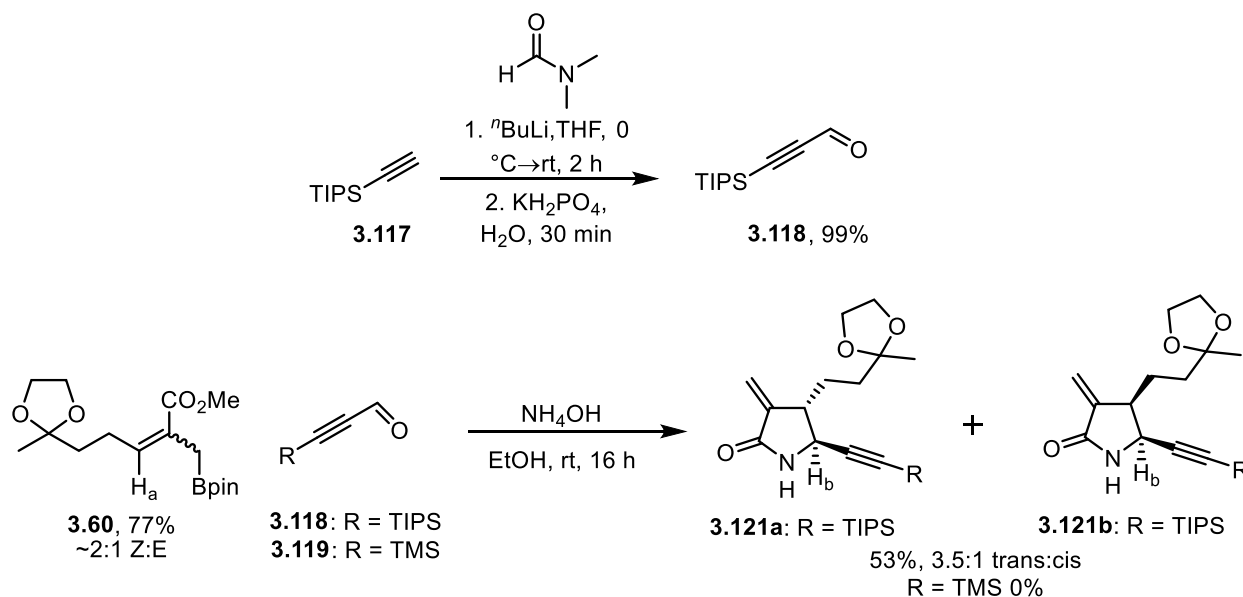
Scheme 3.21. Feasibility of secondary amides in the APKR.

Propargyl pivalate **3.113a** was converted to allene-yne **3.114** in 33% yield when reacted with Stryker's reagent. This low yield is in part due to a competing reduction of the α -methylene group providing **3.115**, and is discussed in further detail in Section 3.4.3 on the optimization of this allene forming reaction. The reaction of cis pivalate **3.113b** with Stryker's reagent is also discussed later in section 3.4.4. Allene-yne **3.114** was subjected to the APKR conditions utilizing slow addition of the allene-yne to rhodium biscarbonyl chloride dimer (110 mol%) in toluene to provide [5,7,5]-fused tricyclic **3.116** in 79% yield. This demonstrated that secondary amides were tolerated in the APKR. This also represents the first APKR with a secondary amide. Thus, it was

envisioned that the lactam nitrogen could be modified at a late stage in the synthetic sequence to modulate the electrophilic reactivity of the α -methylene- γ -lactam.

3.4.2. Synthesis of α -Methylene- γ -lactams Containing a Silyl-substituted Alkyne

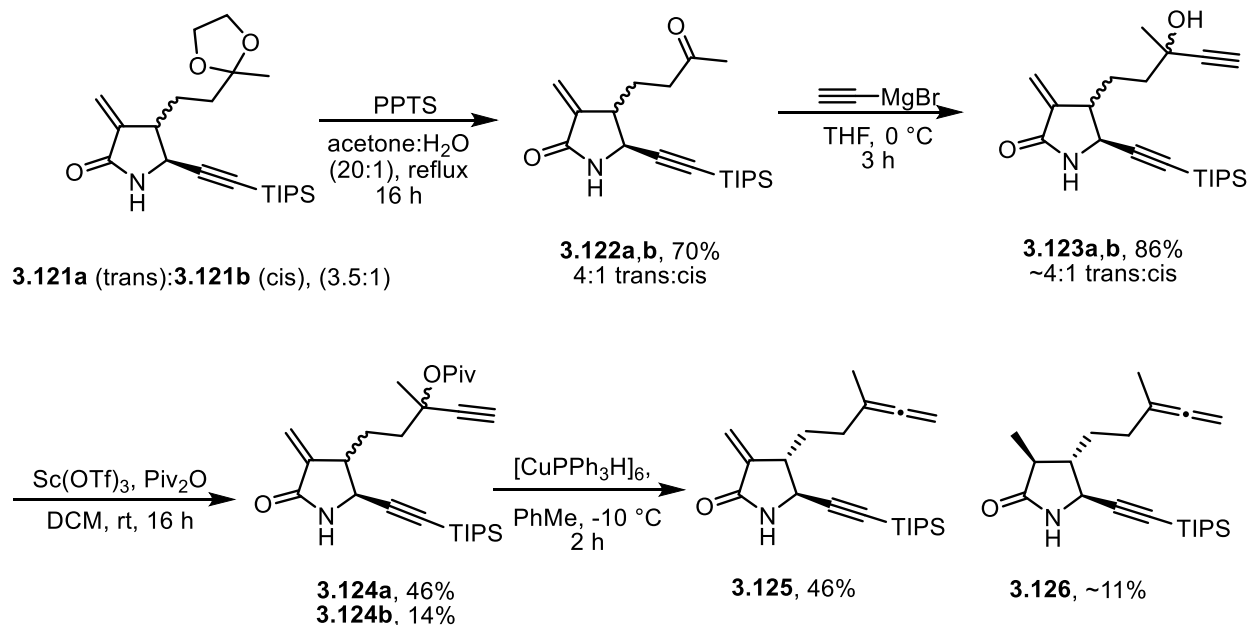
In order to make late stage modifications to the terminus of the alkyne, the feasibility of silyl-substituted propynals in the 3-component lactamization reaction was tested. Triisopropylsilyl (TIPS) propynal **3.118** was prepared by reacting the lithium acetylide of triisopropylsilylacetylene **3.117** with DMF followed by acidic work-up with monobasic potassium phosphate to provide propynal **3.118** in nearly quantitative yields (Scheme 3.22).¹⁸³ Propynal **3.118** was reacted with allylboronate **3.60** in ethanol and ammonium hydroxide to afford lactams **3.121a** (trans) and **3.121b** (cis) in a 53% yield and a 3.5:1 trans (**3.121a**) to cis (**3.121b**) ratio, as determined by integration of the resonances for H_b at 4.2 ppm for the trans isomer and 4.7 ppm for the cis isomer. These lactams **3.121a,b** containing a TIPS-substituted alkyne were subjected to the same synthetic sequence as lactams **3.74a,b** with a phenyl-substituted alkyne and the reactions proceeded in similar yields. Trimethylsilyl (TMS) propynal **3.119** was subjected to the lactamization reaction, but the TMS group was unstable to the strongly basic conditions, and none of the desired lactam was obtained.



Scheme 3.22. Synthesis of α -methylene- γ -lactams using silyl-substituted propynals.

The ketals were hydrolyzed by refluxing lactams **3.121a,b** in an acetone/water (20:1) solvent containing PPTS to give ketones **3.122a,b** in 70% yield, with a 4:1 trans:cis isomeric ratio (Scheme 3.23). As with the phenyl substituted alkyne examples, little change in the ratio of trans:cis isomers was observed going from ketal **3.121a,b** to ketone **3.122a,b**, where the ratio was determined by the same ^1H NMR signals as ketals **3.121a,b** at 4.2 and 4.7 ppm. Ketones **3.122a,b** were used to synthesize the desired allenes in three synthetic steps. Reaction of ketones **3.122a,b** with ethynyl magnesium bromide in THF for 3 h at 0 $^\circ\text{C}$ afforded propargyl alcohols **3.123a,b** in 86% yield, each as a 1:1 mixture of propargyl alcohol diastereomers. The trans lactam diastereomers of **3.123a** were indistinguishable by ^1H NMR, although the ^{13}C NMR showed two equimolar diastereomers as two peaks for most carbons. Cis propargyl alcohol **3.123b** diastereomers displayed two distinct alkyne resonances at 2.44 and 2.42 ppm, and two doublets were visible for the hydrogen on the γ -carbon of the lactam at 4.49 for **3.123b**. The hydroxyl groups of **3.123a,b** were transformed into pivalates **3.124a,b** in 60% combined yield by stirring

with pivalic anhydride and substoichiometric scandium triflate (0.4 equiv). Pivalates **3.124a** and **3.124b** were separated by column chromatography to give 46% of **3.124a** and 14% of **3.124b**. These were taken on as single isomers for the remainder of the synthesis. Pivalate **3.124a** was identified by a new carbonyl carbon at 177 ppm in the ^{13}C NMR spectrum and a singlet integrating for nine hydrogens at 1.1 ppm in the ^1H NMR spectrum. As with the propargyl alcohol **3.123a**, the diastereomers of trans lactam **3.124a** were only distinguishable by ^{13}C NMR, but the diastereomers of cis pivalate **3.124b** could be distinguished in the ^1H NMR spectrum by two singlet resonances for the terminal alkyne at 2.52 and 2.51. The ^{13}C NMR also showed two nearly equivalent peaks for most carbons which differed by less than 0.2 ppm. The isolated yields of **3.124a** and **3.124b** reflected the ratios of the starting material determined by ^1H NMR. Pivalate **3.124a** was reacted with Stryker's reagent to provide allene-yne **3.125** in 46% yield, along with 11% of **3.126**, an overreduction product resulting from reduction of the α -methylene group to a methyl group. The stereochemistry of the lactam methyl group on **3.126** was assigned by comparison of experimental ^1H NMR coupling constants to calculated coupling constants *vide infra* (Section 3.6) Conditions for the synthesis of allenes from propargylic carboxylates using Stryker's reagent were examined before further modifications to the alkyne terminus or lactam nitrogen were pursued.



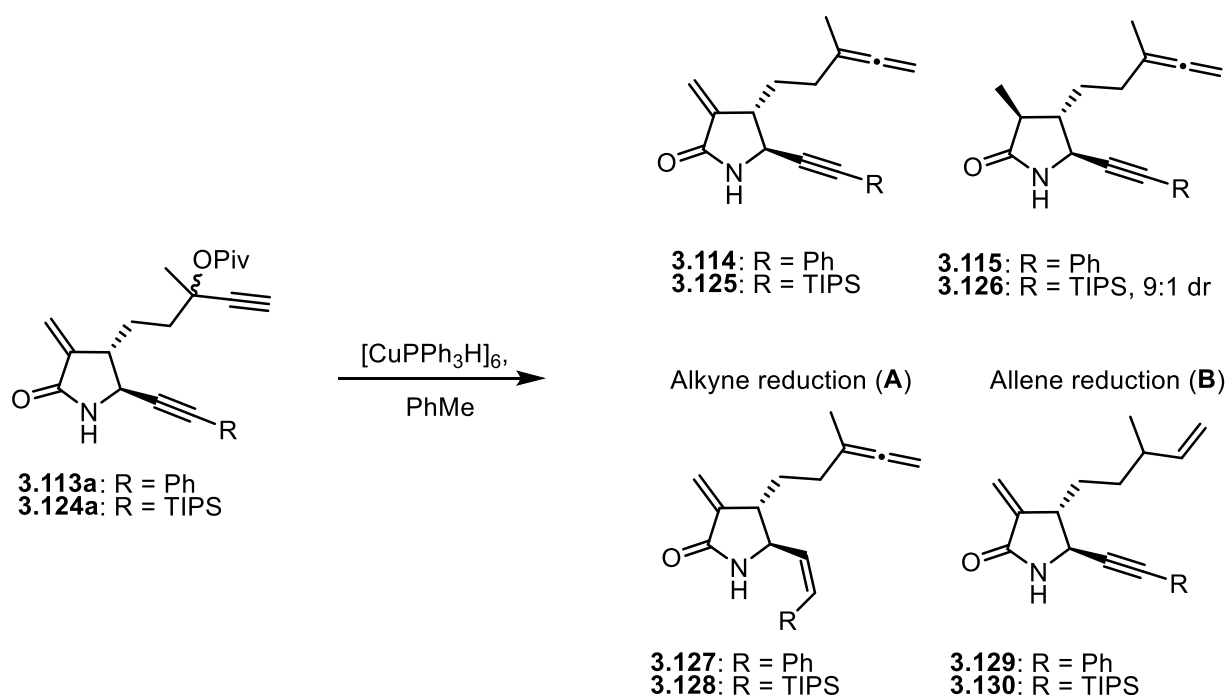
Scheme 3.23. Synthesis of 1,1-disubstituted allenes with *N*-unsubstituted lactams.

3.4.3. Optimization of Allene Formation from Propargyl Pivalates using Stryker's Reagent

Because the copper hydride was reacting with the α -methylene group of the lactam, efforts to increase the chemoselectivity and the yield for the transformation of propargyl pivalates to allenes ensued. Optimization studies involved changing the reaction temperature, equiv of Stryker's reagent, reaction time, quench and work-up methods, scale, and source of Stryker's reagent. Propargyl pivalates **3.113a** or **3.124a** were converted to 1,1-disubstituted allenes **3.114** or **3.125** in 28-89% yields via a formal S_N2' reaction with triphenylphosphine copper hydride hexamer (Stryker's reagent), and these allenes were identified by new resonances in the ^1H NMR corresponding to the hydrogens on the allene terminus at 4.6 ppm for **3.114** and **3.125**. This reaction was typically performed by addition of Stryker's reagent (0.9 equiv, weighed in a glovebox) to a solution of propargyl pivalate **3.113a** or **3.124a** in degassed (by bubbling nitrogen

through solution for 10 min), wet toluene (containing 2 equiv water relative to propargyl pivalate) at rt and stirring for 0.5-5 h with a concentration of 0.04 M. The reaction was quenched either by addition of saturated ammonium chloride solution to the reaction mixture followed by dilution with diethyl ether or by pouring the reaction mixture into a biphasic, 1:1 mixture of saturated ammonium chloride and diethyl ether. In most cases the reaction mixture was stirred for 30 min with the ammonium chloride to facilitate precipitation of triphenylphosphine and triphenylphosphine oxide byproducts. Two work up procedures were utilized. The first involved filtration of both the organic and aqueous layers through Celite, separation of these layers, and extraction of the aqueous layer (3x) with diethyl ether. The second involved separation of the organic and aqueous layers, extraction of the aqueous layer with diethyl ether (3x), then filtration of the combined organic layers through Celite. The first work up procedure helped reduce the formation of emulsions during extraction. Addition of water (2-20 equiv) to reductions using Stryker's reagent has been shown to increase the reaction rate and decrease the formation of side products, presumably by rapidly quenching the intermediate copper species formed during the reaction, and it was observed that addition of water reduced the reaction time from 3-4 h to 0.5-1 h when the reaction was conducted at rt (Table 3.1, compare entries 4 and 7).¹⁸⁶⁻¹⁸⁷ A few minor side products were observed in most cases with this reaction. These byproducts are the result of the reduction of the α -methylene moiety to provide methyl lactams **3.115** or **3.126** due to a conjugate reduction reaction (Scheme 3.24). These was identified by a disappearance of the α -methylene hydrogen resonances from the ¹H NMR spectrum and the appearance of a methyl doublet at 1.0 ppm. The two other common side products are believed to be reduction of the internal alkyne or the allene based upon ¹H NMR resonances. A doublet at 6.64 ppm ($J = 11.4$ Hz) for H_b and doublet of doublets at 5.55 ppm ($J = 11.4, 9.7$ Hz) for H_a is consistent with the reduction

of the internal alkyne to cis alkene (**A**) **3.127** or **3.128**; reductions of alkynes to cis alkenes with Stryker's reagent have been reported.¹⁸⁸ Two multiplets at 5.05-4.91 and 5.78-5.61 ppm are likely due to the reduction of the allene to a terminal alkene (**B**) **3.129** or **3.130**, but these minor byproducts were isolated but were not pure enough for full characterization. The product ratios presented in Table 3.1 were determined by integration of the ¹H NMR resonances of product mixtures after column chromatography.



Scheme 3.24. Formation of 1,1-disubstituted allenes using Stryker's reagent.

The procedure employed for this reaction varied slightly among entries. In entry 1, a solution of pivalate **3.113a** in toluene (0.05 M) was added to a solution of Stryker's reagent in dry toluene (0.1 M) at rt all at once and stirred for 4 h. This reaction was quenched by addition of saturated, aqueous ammonium chloride solution to the reaction mixture, dilution with ether, and filtration through Celite. The layers were separated and the organic layer was washed with brine,

dried over magnesium sulfate, filtered, concentrated, and purified by silica gel flash column chromatography. This reaction gave a 53% overall yield and a 90:10 ratio of desired allene **3.114** to α -methylene reduction product **3.115** and only trace amounts of other byproducts (entry 1). For entry 2, the same procedure was followed, except that the concentration was increased to 0.06 M and the vial was evacuated and filled with nitrogen three times after addition of all reagents, which likely increased the concentration further in this small-scale reaction. Entry 2 provided a 61% overall yield with a 72:6:22 ratio of desired allene **3.114** to α -methylene reduction product **3.115** to alkyne reduction **3.127**, where the increased concentration likely lead to an increase in alkyne reduction product **3.127** (entry 2). For entry 3, Stryker's reagent was added directly to a solution of pivalate **3.113a** in toluene (0.04 M); when ammonium chloride was added, it was stirred vigorously for 5 min before diluting with ether (a blue aqueous layer was observed) and the remainder of the work up was performed as described for entries 1-2. This provided a good overall yield of 89%, with a ratio of 75:11:14 of desired allene **3.114** to α -methylene reduction product **3.115** to alkyne reduction **3.127** (entry 3). For entry 4, pivalate **3.124a** (0.04 M, with a TIPS-substituted alkyne instead of the Ph alkyne in entries 1-3) was added to a solution of Stryker's reagent (0.1 M), analogous to entries 1-2. An aliquot of the reaction mixture showed that the reaction was complete after 2.5 h by ^1H NMR, but it was left to stir for a total of 4.5 h. To quench this reaction, saturated ammonium chloride was added to the reaction and this was stirred 15 minutes open to air, then diluted with ether and the layers separated providing an overall yield of 47% with an 85:15 ratio of desired allene **3.125** to allene reduction product **3.130** (entry 4). The large triisopropyl silyl substituent on the internal alkyne may have prevented reduction of this alkyne by the bulky Stryker's reagent, instead leading to the allene reduction byproduct **3.130** that was observed in only trace amounts for entries 1-3.

In entry 5, water was added to the pivalate **3.113a** solution (0.04 M in toluene containing 0.01 mL of water) because water has been reported to speed up reactions with Stryker's reagent.¹⁷¹ An aliquot of the reaction after 1 h showed the disappearance of the terminal alkyne resonance of the starting material by ¹H NMR, so the reaction was quenched and an overall yield of 43% with a 65:10:25 ratio of desired product **3.114** to α -methylene reduction product **3.115** to alkyne reduction **3.127** was obtained (entry 5). Thus, water sped up the rate of allene formation, but it also led to an increase in the alkyne reduction product **3.127** (entry 5). For entry 6, *N*-methyl substituted lactam **3.91** was used to see if a more electron-rich α -methylene- γ -lactam would be less susceptible to reduction. An aliquot showed consumption of the starting material after 30 min, again demonstrating the increase in the rate of reaction with the addition of water. This *N*-methyl lactam **3.91** gave a good overall yield of 70% and showed only trace amounts of α -methylene reduction product (75:trace:25 desired product **3.65** to α -methylene reduction product to alkyne and allene reduction, entry 6). This is attributed to the reduced electrophilicity of the α -methylene when an electron-donating alkyl group was attached to the lactam nitrogen. For entry 7, the temperature was reduced to 0 °C to slow the reduction of the α -methylene moiety. Performing the reaction at 0 °C resulted in only trace amounts of the undesired byproducts **3.126**, **3.128**, and **3.130** being isolated when propargyl pivalate **3.124a** was reacted with Stryker's reagent providing an overall yield of 64% (entry 7). The reaction conditions from entry 7 were repeated for entry 8 with pivalate **3.113a** and the desired allene **3.114** was obtained in 52% yield with only trace amounts of byproducts. Entries 9-10 were performed under the same conditions as entries 7-8 except a different bottle of Stryker's reagent from Sigma-Aldrich was used. Entry 9 gave a lower yield possibly due to the small scale, but entry 10 gave the same yield as entry 8 (52%), with only trace amounts of α -methylene reduction and other side-products detected.

Entry 11 was performed using the same procedures as entries 7-10 except that a new bottle of Stryker's reagent purchased from Acros was used and the reaction was quenched after 1 h because an aliquot after 45 min showed consumption of the starting material by ^1H NMR. This resulted in a good overall yield (73%) but a large amount of the α -methylene reduction product **3.126** was obtained (60:40 desired allene **3.125** to α -methylene reduction product **3.126**). This led us to try a lower temperature of $-10\text{ }^\circ\text{C}$ and to decrease the amount of Stryker's reagent from 1 equiv to 0.8 equiv in entry 12. The reaction was monitored by quenching aliquots of the reaction mixture, extraction into ether, concentrating, and obtaining a ^1H NMR spectrum. This reaction appeared nearly complete after 90 min (3:1 prod:SM). After column purification, the overall yield was 66% with a 63:25:12 ratio of desired allene **3.125**, α -methylene reduction product **3.126**, and SM (**3.124a**) with only trace amounts of other byproducts detected. From this it was concluded that the Stryker's reagent from Acros was more active than that from Sigma Aldrich, but due to the increase in yields, attempts to optimize allene formation with Stryker's reagent from Acros were pursued. In entry 13, the temperature was lowered to $-20\text{ }^\circ\text{C}$, 0.9 equiv of Stryker's was used. We sought to find an optimal temperature that would allow for allene formation but not for α -methylene reduction. This resulted in a slightly lower overall yield of 58% with a 4:1 ratio of desired allene **3.125** to α -methylene reduction **3.126**, but no SM was recovered and only trace amounts of alkyne or allene reduction products **3.128** and **3.130** were observed under these conditions (entry 13). Although the allene with a TIPS alkyne (**3.125**) was separable from overreduction product **3.126**, the allene with a phenyl alkyne (**3.114**) was inseparable from **3.115**, so further decreasing the amount of overreduction product was desired.

For entry 14, the temperature was lowered to $-78\text{ }^\circ\text{C}$ and the rest of the procedure was the same as in entry 13. This eliminated the formation of overreduction product **3.126** and gave a good

overall yield of 71%, but a nearly 1:1 ratio of desired product to recovered starting material was obtained (entry 14). For entry 15, the reaction was kept at -78 °C for 3.5 h instead of 1.5 h as in entry 14. An aliquot of the reaction mixture taken after 2 h showed a nearly complete reaction with a 5:1 ratio of product **3.114** to starting material **3.113a**. However, when the reaction was quenched after 3.5 h, a 67:26 ratio of starting material **3.113a** to product **3.114** was obtained along with 7% of the α -methylene reduction product **3.115** (entry 15). This could be due to the reaction not being quenched immediately upon addition of saturated ammonium chloride, or due to the warming of the small aliquot upon removal from the reaction mixture. It appears that the allene formation and conjugate reduction reactions have similar energetic barriers, although an intermediate temperature (between -20 and -78 °C) was not tested. Additionally, Stryker's reagent is only partially soluble in toluene, so very low temperatures could be inhibited by poor solubility of the triphenylphosphine copper hydride hexamer. For entry 16, water was not added to the reaction in an effort to prevent the reduction of the α -methylene moiety. The reaction was stirred at -78 °C for 20 min, then -30 °C for 30 min, then -10 °C for 30 min, then 0 °C for 150 min. Aliquots of the reaction mixture showed a 10:1 ratio of starting material **3.124a** to product **3.125** by ^1H NMR after stirring at -78 °C with no α -methylene reduction detected and this ratio remained the same as the reaction was warmed slowly to 0 °C for 30 min. After stirring for an additional hour at 0 °C, an aliquot of the reaction mixture showed a 2:2:1 mixture of desired product **3.125** to α -methylene reduction **3.126** to starting material **3.124a**. The reaction was quenched after a total of 4 h as described for entries 12-15 and a 60% overall yield was obtained with the same ratio of products as the second aliquot (2:2:1, entry 16). This suggested that water was not contributing to the reduction of the α -methylene moiety, but the absence of water significantly slowed the rate of the reaction, especially at lower temperatures.

Due to the increased amount of α -methylene reduction products **3.115/3.116** obtained when using Stryker's reagent purchased from Acros (entries 11-16), a new bottle of Stryker's from Sigma-Aldrich was purchased and used in entry 17. For entry 17, the conditions from entries 8-10 were repeated using the same amount of Stryker's reagent (1 equiv) and the same concentration of pivalate (0.04 M). This provided a 53% overall yield with a ratio of 52:7:10:12:19 of the desired product **3.114** to α -methylene reduction product **3.115** to starting material **3.113a** to allene reduction **3.129** to an unidentified byproduct (entry 17). Due to the variability in product ratios when using different sources of Stryker's reagent, it was synthesized from copper (II) acetate, triphenylphosphine, and diphenylsilane according to the method reported by Lee and Yun.¹⁸⁹ This synthetic Stryker's reagent was used in entry 18 providing a 40% overall yield with a 69:6:12:13 ratio of desired allene **3.114** to α -methylene reduction product **3.115** to byproducts **3.127** and **3.129** and a new byproduct. This previously unencountered byproduct was isolated by column chromatography and appeared to be allene formation due to the allene resonance at 4.6 ppm. Reduction of the α -methylene was also apparent in this byproduct due to disappearance of the resonances at 6.11 and 5.41 ppm in the ¹H NMR corresponding to the hydrogens on the α -methylene group and the appearance of a methyl doublet at 1.2 ppm. Reduction of the lactam carbonyl to an alcohol is proposed due to a disappearance of the carbonyl carbon at 169 ppm and a new peak at 67 ppm of the ¹³C NMR. The resonances for the other hydrogens on the lactam were shifted upfield considerably from 4.3 and 3.0 ppm in the α -methylene reduction product **3.115** to 2.5 and 2.0 ppm in this byproduct.

In entry 19, 0.9 equiv of Stryker's reagent from Aldrich was used at a reaction temperature of -10 °C for 2 h. This provided an overall yield of 70% and a ratio of 70:16:14 of desired product **3.114**, α -methylene reduction product **3.115**, and allene reduction product **3.129** (entry 19). Entry

20 utilized the same conditions as entry 19 but was quenched by pouring the reaction into 0 °C saturated ammonium chloride as in entries 12-18. This reaction gave a lower overall yield (31%) than most entries, but it provided the best ratio of desired product **3.114** to α -methylene reduction product **3.115** to allene reduction product **3.129** of 80:10:10 (entry 20). In entry 21, the same procedure as entries 19-20 was followed, except that 0 °C saturated ammonium chloride was added to the reaction for the quench. In this case, a 56% overall yield was obtained with a 90:10 ratio of desired allene **3.114** to α -methylene reduction product **3.115** and only trace amounts of the allene reduction product **3.129** was observed (entry 21). Entry 22 followed the same procedure as entries 20-21, except for the work-up, which involved filtration through Celite after stirring the reaction with ammonium chloride, but before extracting with ether (the same work-up as in entries 4-18). This provided an overall yield of 38% with a 94:6 ratio of desired allene **3.114** to α -methylene reduction product **3.115** with no starting material and only trace amounts of other byproducts. In entry 23, the reaction with rt saturated ammonium chloride, and it was stirred 2 h instead of the normal 30 min. A new bottle of Stryker's reagent from Aldrich was also used in entry 23. The longer quenching time may have led to the low yield of 28%. The ratio of products was 84:8:8 of the desired allene **3.114** to the α -methylene reduction product **3.115** to alkyne reduction product **3.127** (entry 23). Entry 24 followed the same procedure as entry 19, and the difference from entries 20-23 was that rt saturated ammonium chloride was added to the reaction during the quench. In this case, a good overall yield of 78% was obtained with a 77:23 ratio of desired allene **3.125** to α -methylene reduction product **3.126**. For entry 25 the same conditions from entry 24 were employed on a larger scale (440 mg compared to 220 mg). This provided an overall yield of 49% with a 72:19:9 ratio of the desired allene **3.125** to α -methylene reduction product **3.126** to starting material **3.124a**. The larger scale of this entry may account for the reduction in overall yield when

compared to entry 24, however, the yield of this reaction was somewhat variable, with an average yield of $55 \pm 15\%$.

Initially, these reactions were quenched by addition of rt, saturated ammonium chloride solution to the reaction. The biphasic mixture was stirred open to the atmosphere for 20-30 minutes causing triphenylphosphine oxide byproducts to precipitate from the mixture. In other cases, the reaction was quenched by addition of 0 °C ammonium chloride solution and pouring the reaction mixture into a 0 °C mixture of ammonium chloride and ether. The work-up was also performed two different ways: filtration through Celite prior to extraction or filtration through Celite after extraction. These alternate quenching and work-up protocols made little difference in the yield of the reaction or the ratio of desired allenes to α -methylene reduction products although the variability in the yield and product ratios made a conclusion difficult. Thus, to test the effect of quenching and work-up procedure on the yield and ratio of products, a single reaction was divided into two equal portions and the two major quenching and work-up procedures were performed in entry 26. For this reaction, the typical reaction conditions were employed (0.04 M, -10 °C, 2 equiv water), but before quenching 1 equiv of mesitylene was added as an internal standard. Then, half of the reaction mixture was removed via syringe and added to 0 °C ammonium chloride solution (quench procedure E). Room temperature ammonium chloride was added to the remainder of the reaction mixture (still in ice bath at 0 °C, quench procedure D), and the two solutions were stirred for 30 minutes open to the atmosphere. After 30 minutes, the first half of the reaction mixture (quench E) was diluted with ether and filtered through Celite; the aqueous layer was extracted with ether (2 x 25 mL), the combined organic layers were dried over magnesium sulfate, and this was gravity filtered, concentrated, and a ^1H NMR was obtained. Meanwhile, the second half of the reaction mixture (quench D) was diluted with ether, the layers separated, the aqueous layer

extracted with ether (2 x 25 mL), the combined organic layers dried over magnesium sulfate, then filtered through Celite, concentrated, and a ^1H NMR obtained. The amount of crude product after concentration was nearly the same (203 mg for the first method, 197 mg for the second method) and the NMRs showed about the same ratio of products to mesitylene (~1:3). There were still triphenylphosphine byproducts in these crude products, and the ratio of product to mesitylene was determined by integration of the allene resonance at 4.6 ppm and mesitylene CH_3 resonance at 2.3 ppm. After column chromatography, a 61% overall yield was obtained with a 67:9:24 ratio of desired allene **3.125** to α -methylene reduction product **3.126** to starting material **3.124a** (entry 26).

To summarize the results presented in Table 3.1, the order of addition of reagents made little difference in the yield or ratio of products (compare entries 1 and 4). The addition of water (2 equiv) to the reaction sped up product formation 2-3 fold but did not significantly affect the ratio of desired allene **3.114/3.125** to other byproducts **3.127-3.130** (compare entries 2 and 5). Lowering the reaction temperature from rt to 0 °C provided the desired allenes **3.114** or **3.125** in moderate yields with minimal formation of undesired byproducts (compare entry 4 to 7 and entry 5 to 8). However, significant differences in product ratios were obtained using different sources of Stryker's reagent under similar conditions (compare entry 7 to 11 and 10 to 18). It should be noted that the source of Stryker's reagent was visibly different, with the older bottles from Aldrich (90%, entries 1-10, stored in glovebox for about 2 years) having a dark, brick red color; the bottles from Acros (97%, entries 11-16) and the synthetic Stryker's reagent had a bright red, almost orange color; and the new bottles from Aldrich (90%, entries 17, 19-25) were brown with only a slight red tint. Reducing the reaction temperature to -10 or -20 °C helped reduce byproduct formation compared to reactions ran at 0 °C (compare entries 11 and 13). Further reducing the reaction temperature to -78 °C resulted in longer reaction times that did not prevent the formation of α -

methylene reduction product **3.115/3.126** and starting material was recovered (compare entry 13 to 14, 15 and 16). Additionally, removing water from the reaction and allowing to warm slowly from -78 °C to 0 °C did not prevent the overreduction product **3.126** from forming. The amount of Stryker's reagent could be reduced from 1 to 0.9 equiv but lowering the amount to 0.8 equiv resulted in the recovery of starting material and similar amounts of byproducts compared to 0.9 equiv (compare entries 11-13). α -Methylene- γ -lactam **3.113a** with a phenyl substituted alkyne gave increased amounts of alkyne reduction product **3.127** with less α -methylene reduction **3.115**, while substrates with a TIPS alkyne gave increased amounts of α -methylene reduction **3.126** and less alkyne reduction **3.128** (compare entry 18 to 24). This could be due to the bulkiness of the TIPS substituent or the electron donating ability of the silyl group, both of which would decrease the reactivity of the internal alkyne towards reduction by Stryker's reagent. Finally, allene **3.125**, with a TIPS substituent on the alkyne, could be separated from the reduced product **3.126** by column chromatography. However, separation of allene **3.114** from the reduced product **3.115** was not achieved with column chromatography, therefore **3.114** and **3.115** were taken on to the next synthetic step as a mixture.

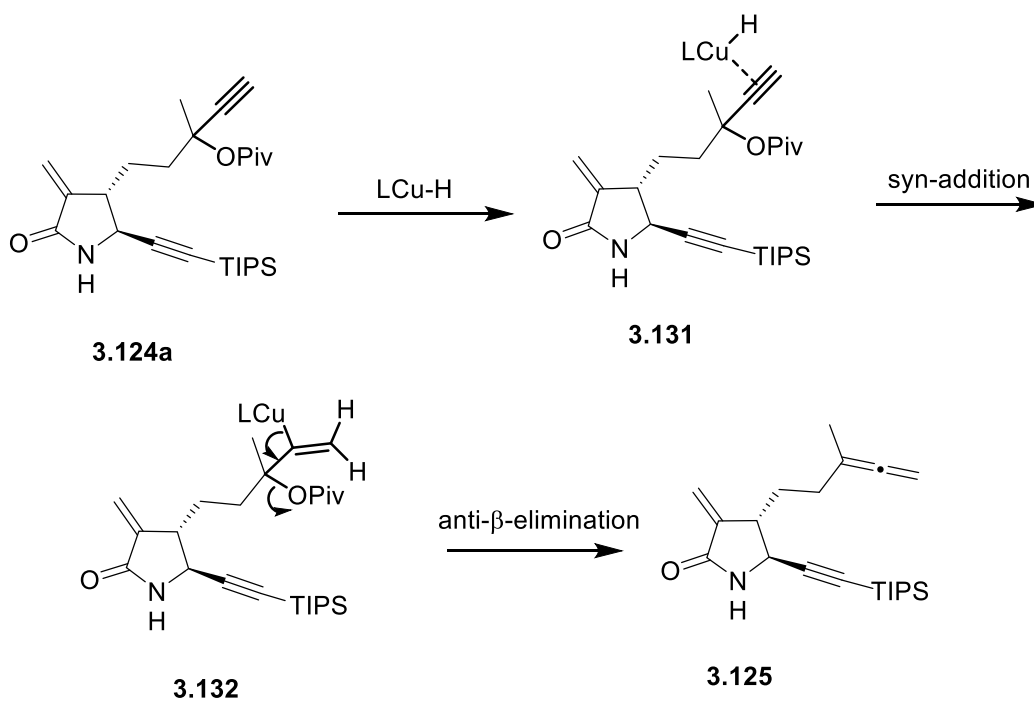
Table 3.1. Reaction optimization for formation of 1,1-disubstituted allenes.

Entry	Notebook Page	SM	Source Stryker's	Equiv Stryker's/ Solvent Conc (M)	Temp (°C)	Time (h)	Total yield (%)	Desired (3.114/3.125): overreduction (3.115/3.126):SM :byproducts (A,B)	Scale of Lactam	Quench	Work-up
1	6-166	3.113a	Aldrich-1 ^a	1 (0.04)	rt	4 ^b	53	90:10:0:trace	20 mg	D	H
2	6-172	3.113a	Aldrich-1 ^a	1 (0.06)	rt	3 ^b	61	72:6:0:22A	19 mg	D	H
3	6-194	3.113a	Aldrich-1	1 (0.04)	rt	4 ^b	89	75:11:0:14A	140 mg	D	H
4	7-74	3.124a	Aldrich-1 ^a	1 (0.04)	rt	4.5 ^b	47	85:0:0:15B	60 mg	D	I
5	7-82	3.113a	Aldrich-1	1 (0.04)	rt	1.5	43	65:10:0:25A	107 mg	D	I
6	7-134	3.91	Aldrich-1	1 (0.04)	rt	1	70	75:trace:0:25A/B	80 mg	G	I
7	7-164	3.124a	Aldrich-1	1 (0.04)	0	1.5	64	100:trace:0:trace	110 mg	D	I
8	7-186	3.113a	Aldrich-1	1 (0.04)	0	2	52	100:trace:0:trace	145 mg	D	I
9	7-198	3.113a	Aldrich-2	1 (0.04)	0	1.5	35	100:trace:0:0	24 mg	D	I
10	7-209	3.113a	Aldrich-2	1 (0.04)	0	1.5	52	100:trace:0:trace	145 mg	D	I
11	8-52	3.124a	Acros-1	1 (0.04)	0	1	73	60:40:0:trace	110 mg	D	I
12	8-54	3.124a	Acros-1	0.8 (0.04)	-10	2	66	63:25:12:trace	110 mg	E	I
13	8-62	3.124a	Acros-1	0.9 (0.04)	-20	2	58	80:20:0:trace	110 mg	E	I
14	8-64	3.124a	Acros-1	0.9 (0.04)	-78	1.5	71	52:0:48:trace	110 mg	E	I
15	8-80	3.113a	Acros-1	0.9 (0.03)	-78	3.5	44	26:7:67:trace	110 mg	E	I
16	8-86	3.124a	Acros-2	0.9 (0.03)	-78 ^c	4 ^b	60	42:38:19:trace	110 mg	E	I
17	8-98	3.113a	Aldrich-3	1 (0.04)	0	2	53	52:7:10:12A:19J	110 mg	E	I
18	8-110	3.113a	Synthetic	1 (0.04)	0	2	40	69:6:0:12A/B:13K	110 mg	E	I
19	8-202	3.113a	Aldrich-3	0.9 (0.04)	-10	2	70	70:16:0:14B	110 mg	D	H
20	9-28	3.113a	Aldrich-3	0.9 (0.04)	-10	1.5	31	80:10:0:10B	122 mg	E	H
21	9-34	3.113a	Aldrich-3	0.9 (0.04)	-10	1.5	56	90:10:0:trace	122 mg	F	H
22	9-42	3.113a	Aldrich-3	0.9 (0.04)	-10	2	38	94:6:0:trace	122 mg	F	I
23	9-52	3.113a	Aldrich-4	0.9 (0.04)	-10	2	28	84:8:0:8A	122 mg	G	H
24	9-86	3.124a	Aldrich-4	0.9 (0.04)	-10	2	78	77:23:0:trace	220 mg	D	I
25	9-102	3.124a	Aldrich-4	0.9 (0.04)	-10	2	49	72:19:9:trace	440 mg	D	H
26	9-108	3.124a	Aldrich-4	0.9 (0.04)	-10	2	61	67:9:24:trace	250 mg	E/D	H/I

a) propargyl pivalate added to solution of Stryker's; b) no water added to reaction; c) kept at -78 °C for 1 h, then slowly warmed to -20 over 1 h, then to -10 for 1 h, then to 0 °C for 1 h; d) rt saturated NH₄Cl added to reaction at reaction temperature, diluted with ether, and stirred 30 min open to air while allowing to warm to rt; e) reaction poured into 0 °C biphasic mixture of saturated NH₄Cl and diethyl ether and stirred 30 min open to air at rt; f) 0 °C saturated ammonium chloride was added to the reaction; g) stirred 2 h open to air after addition of rt saturated ammonium chloride; h) filtration through Celite after quench but before extraction; i) extraction into ether then filtration of combined organic layers through Celite; j) unidentified byproduct; k) carbonyl reduction byproduct

Toluene and benzene are the most common solvents employed in reactions with Stryker's reagent, but it has been reported that THF can reduce the reaction time for conjugate reduction reactions of α -methylene- γ -lactones and unsaturated esters.¹⁹⁰ This reaction was not attempted because it was predicted that THF would increase the amount of undesired α -methylene reduction products **1.115** and **1.126** by increasing the rate of conjugate reduction. However, the increased solubility of Stryker's reagent in THF compared to aromatic solvents could allow for the reaction to be performed at lower temperatures which may facilitate selective allene formation over conjugate reduction. Conditions that utilized Stryker's reagent or related copper hydride reagents with different ligands (e.g. P(O^{*i*}Pr)₃, Me₂PPh) and silanes as hydrogen donors under catalytic conditions were also not attempted, since these conditions were optimized for conjugate reduction or carbonyl reduction.^{171, 191} Catalytic copper hydride reductions utilizing Xantphos or N-heterocyclic carbene ligands and hydrosilane hydrogen donors have been reported for propargylic carbonates, but these conditions were only reported to form 1,3-disubstituted and 1,1,3-trisubstituted allenes as no terminal alkyne starting materials were reported.¹⁹²⁻¹⁹³ The mechanisms proposed in these studies involved syn-addition of copper hydride across the alkyne, followed by anti- β -elimination of the carbonate, and finally regeneration of the copper hydride catalyst through transmetallation with a silane. Based on these studies, it is expected that the mechanism for allene formation with Stryker's reagent involves a similar pathway. Thus, formation of π complex **3.131**

between the alkyne and copper hydride reagent followed by syn-addition of copper hydride across the alkyne bond to form **3.132**. Finally, anti-β-elimination of pivalate **3.132** provides the desired allene **3.125** (Scheme 3.25).

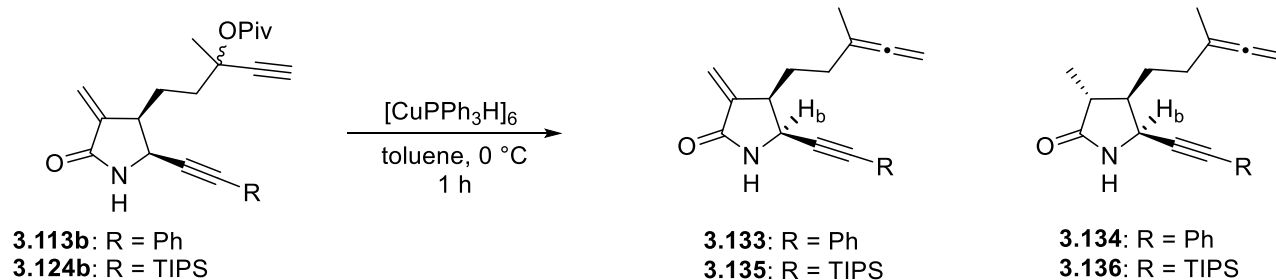


Scheme 3.25. Proposed mechanism for allene formation with Stryker's reagent.

3.4.4. Allene Formation using Stryker's Reagent with Cis-substituted Lactams

Cis-substituted lactams **3.113b** and **3.124b** were more susceptible to conjugate reduction than trans-substituted lactams discussed above. Treatment of cis-substituted lactams with Stryker's reagent provided allenes **3.133** or **3.135** in low overall yields of 25-52% and various ratios of the desired allenes **3.133** or **3.135** to **3.134** or **3.136** where the α -methylene was reduced to a methyl group; unfortunately, these compounds were inseparable by column chromatography (Table 3.2).

These reactions were conducted by adding Stryker's reagent to a degassed solution of propargyl pivalate in wet toluene (2 equiv water) and quenched by addition of saturated ammonium chloride to the reaction mixture. For **3.124b**, the desired allene **3.135** was obtained as the major product in ratios of 10:1 (**3.135:3.136**) with a 52% overall yield along with 16% recovered starting material (Table 3.2, entry 1). In a separate experiment using a bottle of Stryker's reagent from Acros, the desired allene **3.135** was obtained in a 2.5:1 ratio with the reduced product **3.136** and a 25% combined yield (entry 2). For pivalate **3.113b**, the desired allene **3.133** was obtained as the minor isomer in a ratio of 1:2 with overreduction product **3.134** and a 36% overall yield in one case (entry 4). Using the same conditions with a different bottle of Stryker's reagent from Acros provided only the overreduced α -methyl lactam **3.134** in 34% yield (entry 3). The reduced compounds **3.134** and **3.136** could be identified by absence of the two α -methylene hydrogen resonances and an appearance of a methyl doublet at 1.2 ppm in the ^1H NMR. The ratio of desired allene **3.133** or **3.135** to reduced compounds **3.134** and **3.136** was determined by integration of H_b on the γ -carbon of the lactam which was shifted upfield by 0.2 ppm for the reduced compounds **3.134** and **3.136**. These reduced compounds appeared to be single diastereomers based upon the ^1H NMR, and the stereochemistry of the methyl group was determined by comparison to calculated values after the allenic Pauson-Khand reaction (*vide infra*). Since the cis lactams were the minor isomer, only small amounts of cis pivalates **3.113b** and **3.124b** were available to optimize conditions for the allene formation. As the desired allene-ynes and the over-reduction products were inseparable by column chromatography, they were taken on to the next synthetic step as a mixture, except in the single instance where only the over-reduction product was obtained.

Table 3.2. Formation of allenes from cis-substituted lactams.

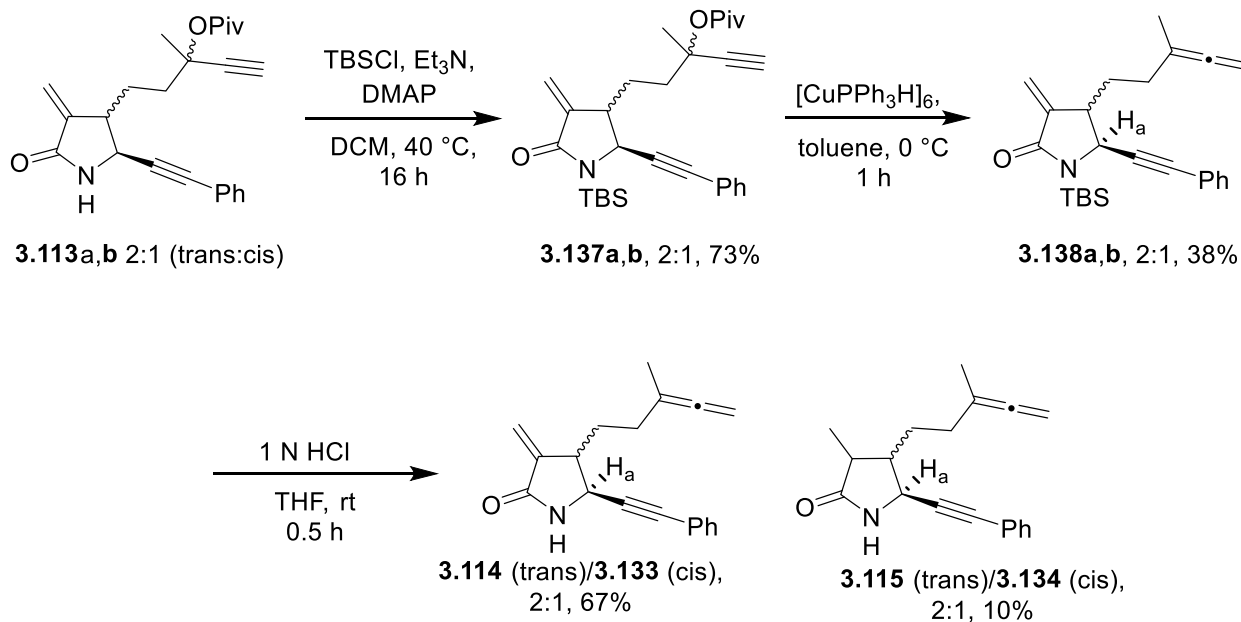
Entry	Notebook Page	R	Source	Temp (° C)	Time (h)	Total Yield (%)	Ratio
			Stryker's				
1	7-156	TIPS	Aldrich-1	0	2	52 ^a	10:1 (3.135:3.136)
2	8-40	TIPS	Acros-1	0	1	25	2.5:1 (3.135:3.136)
3	7-192	Ph	Aldrich-2	0	1.5	36	0:1 (3.133:3.134)
4	8-46	Ph	Acros-1	0	1	34	1:2 (3.133:3.134)

a) 16% recovered starting material

3.4.5. Investigation of Alternative Reactions for 1,1-Disubstituted Allene Formation

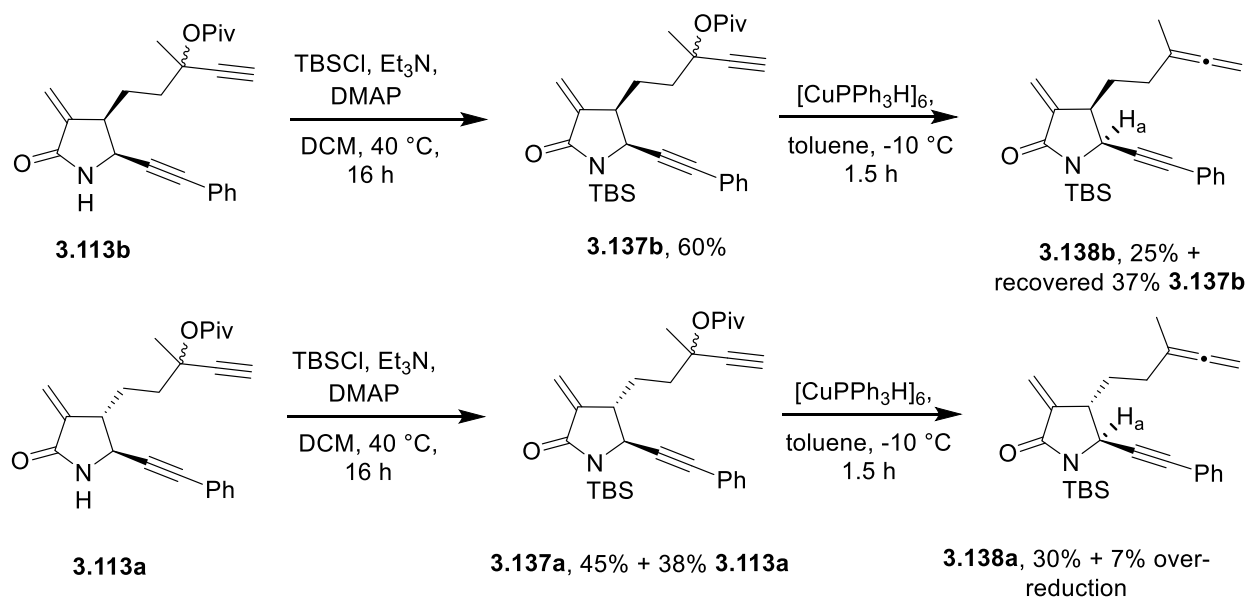
Due to the problems of overreduction in the allene formation reactions using Stryker's reagent, especially with cis-substituted lactams, it was proposed that protection of the lactam nitrogen with an electron donating silyl-substituent would reduce the electrophilicity of the α -methylene- γ -lactam and thus prevent the reduction of this moiety. This was based partially on the success with *N*-methyl lactam **3.91**, which provided an improved yield of the desired allene **3.65** and only trace amounts of α -methylene reduction even at rt (Table 3.1, entry 6). Silyl-protected lactams have been used to prevent reaction of *N*-unsubstituted lactams, and they are reportedly stable to chromatographic purification as well as lithium bases such as *n*BuLi and LDA; similarly, *N*-silyl

indoles are stable to chromatographic purification but unstable to storage.¹⁹⁴⁻¹⁹⁵ To test this hypothesis, **3.113a,b** (2:1) was reacted with *tert*-butyldimethylsilyl chloride (TBS, 10 equiv), triethylamine (15 equiv), and dimethylaminopyridine (10 mol%) in refluxing DCM to afford TBS protected lactam **3.137a,b** in 73% yield as a 2:1 mixture of *trans* and *cis* isomers (Scheme 3.26). Lactam **3.137a,b** was identified by disappearance of the amide hydrogen resonance in the ¹H NMR as well as a new singlet resonance at 1.03 ppm that integrated for 9 hydrogens and 2 singlet resonances at 0.41 and 0.39 ppm that integrated for 3 hydrogens each, corresponding to the silyl protecting group. Reaction of *N*-silyl lactam **3.137a,b** with Stryker's reagent (0.9 equiv) provided allenes **3.138a,b** in 38% overall yield as a 10:1 ratio of **3.138a,b** to the overreduction product as determined by ¹H NMR integration of H_a. Additionally, 6% of the desilylated lactams **3.114** and **3.133** were isolated after chromatographic purification. Removal of the silyl protecting group was achieved by stirring **3.138a,b** in THF with 1 N HCl for 0.5 h, affording desilylated lactams **3.114** (*trans*)/**3.133** (*cis*) in 67% with a small amount of over-reduction products **3.115** (*trans*)/**3.134** (*cis*).



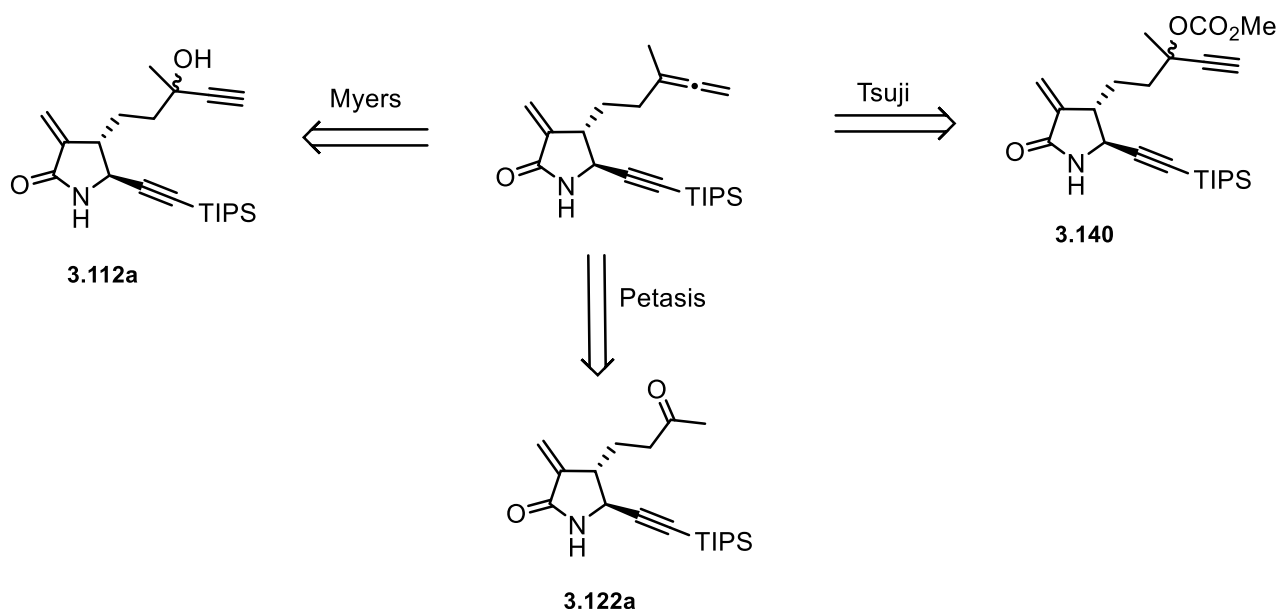
Scheme 3.26. Feasibility of *N*-silyl protection.

As the *cis*-substituted lactams were more prone to overreduction than the *trans*-substituted lactams this silyl-protection strategy was tested with pure *cis* lactam **3.113b**. The reaction of **3.113b** with *tert*-butyldimethylsilyl chloride provided *N*-silyl lactam **3.137b** in 60% yield (Scheme 3.27). Reaction of **3.137b** with Stryker's reagent for 1.5 h at -10 °C provided allene **3.138b** in 25% yield, with no overreduction product as determined by crude ¹H NMR; 37% of the starting material was also recovered. Protection of the *trans*-lactam **3.113a** as the *N*-silyl lactam **3.137a** occurred in 45% yield, with 38% of the starting material recovered. *N*-Silyl lactam **3.137a** provided allene **3.138a** in 30% yield with a 7% yield of the over-reduction product. Although the methylene moiety of the *N*-silyl lactams appeared slightly less vulnerable to conjugate reduction by Stryker's reagent, the low to moderate yields obtained for silyl protection and deprotection, stability of the silyl group, low yields for the allene formation, and our inability to prevent reduction of the α -methylene- γ -lactam led us to consider alternative strategies for the formation of 1,1-disubstituted allenes from a ketone moiety.



Scheme 3.27. Use of *N*-silyl α -methylene- γ -lactams in the formation of 1,1-disubstituted allenes.

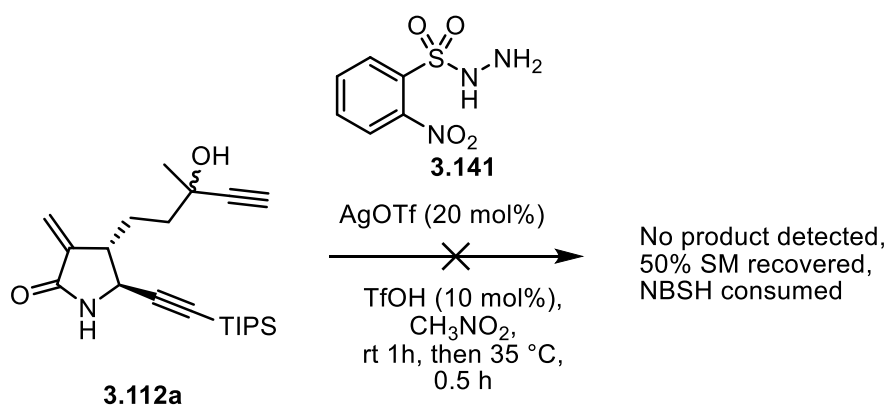
Several alternative strategies to form 1,1-disubstituted allenes from a ketone moiety were examined and tested on our lactam substrate (Scheme 3.28). The first was a modification to Myers's deoxyallenylation that displaces the propargyl alcohol of **3.112a** with nitrobenzenesulfonyl hydrazide followed by loss of nitrogen gas and toluene sulfinic acid to give allenes.¹⁹⁶⁻¹⁹⁷ Another strategy we examined was the Petasis allenylation, which converts the ketone of **3.122a** directly to the allene using a divinyl dicyclopentadienyl titanium reagent.¹⁹⁸ The final strategy examined was the Tsuji reduction, which converts a propargyl carbonate or formate to the allene under palladium catalyzed conditions.¹⁹⁹⁻²⁰¹



Scheme 3.28. Alternative strategies to access 1,1-disubstituted allenes.

The exploration of alternative allene formation conditions began by attempting a recently reported Lewis and Brønsted acid catalyzed reductive deoxyallenylation of propargyl alcohols using 2-nitrobenzenesulfonylhydrazide (NBSH), which provided mono-, 1,1-di, and 1,1,3-trisubstituted allenes in yields of 42-89%.¹⁹⁷ This reaction is complementary to previously reported allene formations using NBSH by Myers, which were applicable to primary and secondary

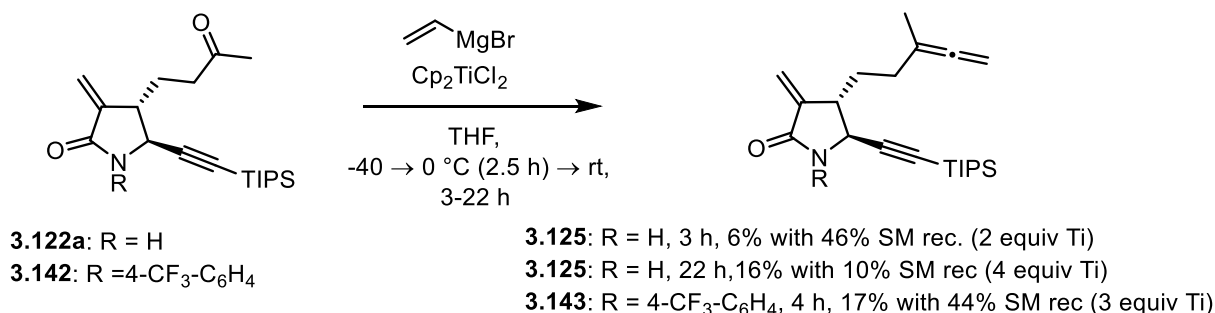
propargyl alcohols as Mitsunobu conditions were used to displace the alcohol, providing intermediate. Upon warming of the intermediate hydrazide to rt, spontaneous loss of nitrogen and *p*-toluenesulfinic acid occur to generate monosubstituted and 1,3-disubstituted allenes in yields of 51-91%.¹⁹⁶ The Lewis and Brønsted acid catalyzed conditions were applicable to secondary and tertiary alcohols, although, in the formation of 1,1-disubstituted allenes, all of the reported substrates were benzylic, tertiary alcohols. Despite this observation, propargyl alcohol **3.112a** was submitted to the reported conditions by dissolving **3.112a** in nitromethane, followed by addition of NBSH (**3.141**), silver triflate, and triflic acid in that order (Scheme 3.29). The reaction was stirred at rt for 1 h, but no reaction was observed by TLC, so it was heated to 35 °C for 30 min. The reaction still showed starting material, but several new spots were observed, and the NBSH had been consumed. After quenching with saturated ammonium bicarbonate solution, extraction with Et₂O, and chromatographic purification, 50% of the starting material was recovered and the other compounds observed by TLC appeared to be byproducts of NBSH such as sulfinic acid. Since no formation of the desired allene was detected, and because only benzylic alcohols were reported in the literature, this transformation was not pursued further.



Scheme 3.29. Attempt at deoxyallenylation of tertiary, alkyl propargyl alcohol.

The Petasis allenylation is a transformation that converts a ketone or aldehyde directly into an allene via a titanocene alkenylidene intermediate.¹⁹⁸ The titanocene is formed by treating bis(cyclopentadienyl) titanium(IV) dichloride (Cp₂TiCl₂) with 2 equiv of an alkenyl Grignard reagent which reacts with carbonyls to form allenes in a single pot. Petasis reported yields of 77-88% for this reaction with propynals and aryl aldehydes, 72 and 81% for a vinyl and aryl ketone, respectively, and 40% for a cyclohexanone derivative.¹⁹⁸ This reaction was performed according to the literature procedure, which involved dropwise addition of vinyl magnesium bromide (4 equiv) to a -40 °C solution of Cp₂TiCl₂ (2 equiv) in THF, slow warming of this solution to 0 °C over 2.5 h, addition of ketone **3.122a** (1 equiv) dissolved in THF, and allowing this to warm to rt (Scheme 3.30). The reaction was monitored by TLC but did not reach completion after 3 h. After purification, only 6% of the desired allene **3.125** was isolated, along with 46% of recovered starting material. A longer reaction time (22 h) and increased amount of titanium reagent (4 equiv) gave a slightly higher yield of 16%, but only 10% of the starting material was recovered. This reaction was then performed with ketone **3.149**, containing an *N*-aryl lactam, because it was proposed that the secondary amide could be reacting or coordinating to the titanium reagent. The intermediate titanium species are reported to be minimally stable and unable to be isolated.¹⁹⁸ Additionally, only a minimal increase in yield was observed upon longer reaction times with the secondary amide **3.122a**, thus this reaction was quenched after 4 h, despite the observation of starting material by TLC; 17% of desired allene **3.150** was isolated and 44% of the starting material **3.149** was recovered. A previous post-doc in our lab, Dr. Bo Wen, had attempted this reaction on a similarly structured lactone (Ph substituted alkyne instead of TIPS) and obtained similarly low yields of 10-20%.²⁰² Considering these results and that Petasis had obtained only a moderate yield of 40% for

a dialkyl ketone, other methods for allene formation were explored. In the synthesis of (\pm)-bakuchiol, allenylation of a simple dialkyl ketone under these conditions provided the allene in only a 4% yield, while conditions reported by Tsuji provided the allene in 65% yield from a propargyl carbonate.²⁰³

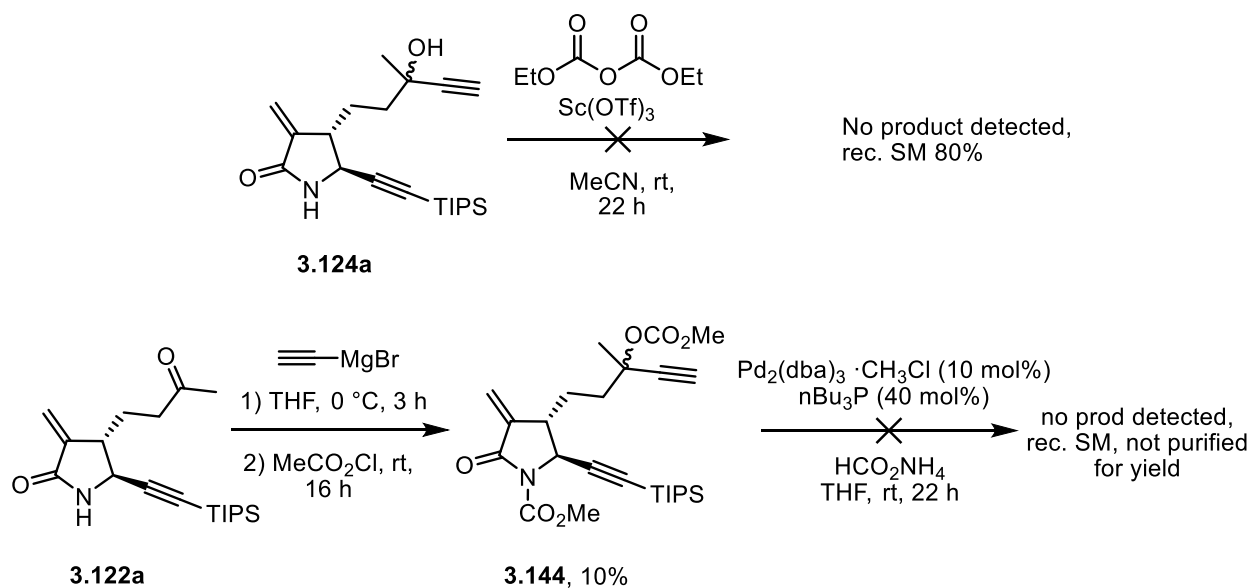


Scheme 3.30. Petasis allenylation.

The next method attempted for the formation of 1,1-disubstituted allenes was the palladium catalyzed hydrogenolysis of propargyl carbonates or formates, first reported by Tsuji.¹⁹⁹⁻²⁰¹ Secondary and tertiary propargyl carbonates with alkyl or aryl substituents were treated with tris(dibenzylideneacetone)dipalladium(0)-chloroform adduct, *n*-butylphosphine (2:1 ligand: Pd), and ammonium formate to provide allenes in yields of 66-87% (Scheme 3.31). Additionally, propargyl formates underwent a similar reaction without addition of ammonium carbonate. Tsuji's conditions were only applied to terminal alkynes. More recently, Sawamura et al. reported that propargyl formates treated with palladium(II) acetylacetonate and diphenylphosphinoethane (1:1) provided 1,3-di or 1,1,3-trisubstituted allenes in good yields of 83-99%.²⁰⁴

In order to test the Tsuji reduction, we set out to make propargyl carbonates using the same conditions applied to formation of propargyl pivalates discussed above. Other conditions to form carbonates, such as deprotonation and reaction with methyl chloroformate or quenching of a

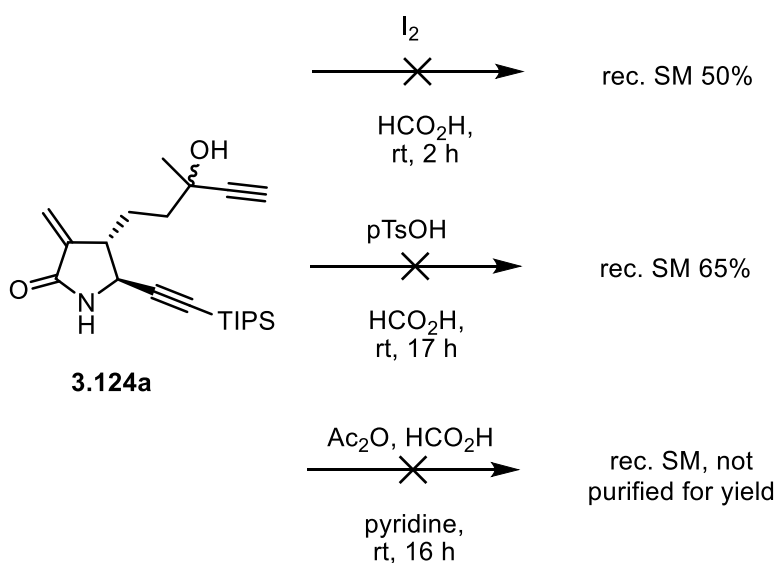
Grignard reaction with methyl chloroformate were expected to react with the lactam nitrogen. Treatment of propargyl alcohol **3.124a** with scandium(III) triflate and diethyl dicarbonate failed to provide carbonate any product, and only starting material (80%) was recovered after 22 h (Scheme 3.31). Carbonate **3.144** was prepared by quenching the Grignard reaction of ketone **3.122a** and ethynyl magnesium bromide with methyl chloroformate. The ester on the lactam nitrogen could be removed under basic conditions.^{199, 203} As expected, these conditions provided carbonate **3.144**, where the nitrogen and oxygen atoms both reacted. However, the product **3.144** was obtained in only a 10% yield. Upon submission of carbonate **3.144** to the Tsuji reduction conditions, no product was obtained, and only starting material was detected in the crude ¹H NMR spectrum.



Scheme 3.31. Propargyl carbonate formation and Tsuji reduction attempts.

An *N*-formyl group is removed under milder conditions than an *N*-ester moiety (sodium carbonate²⁰⁵ vs sodium methoxide).²⁰⁶ Thus, we sought to prepare propargyl formates from

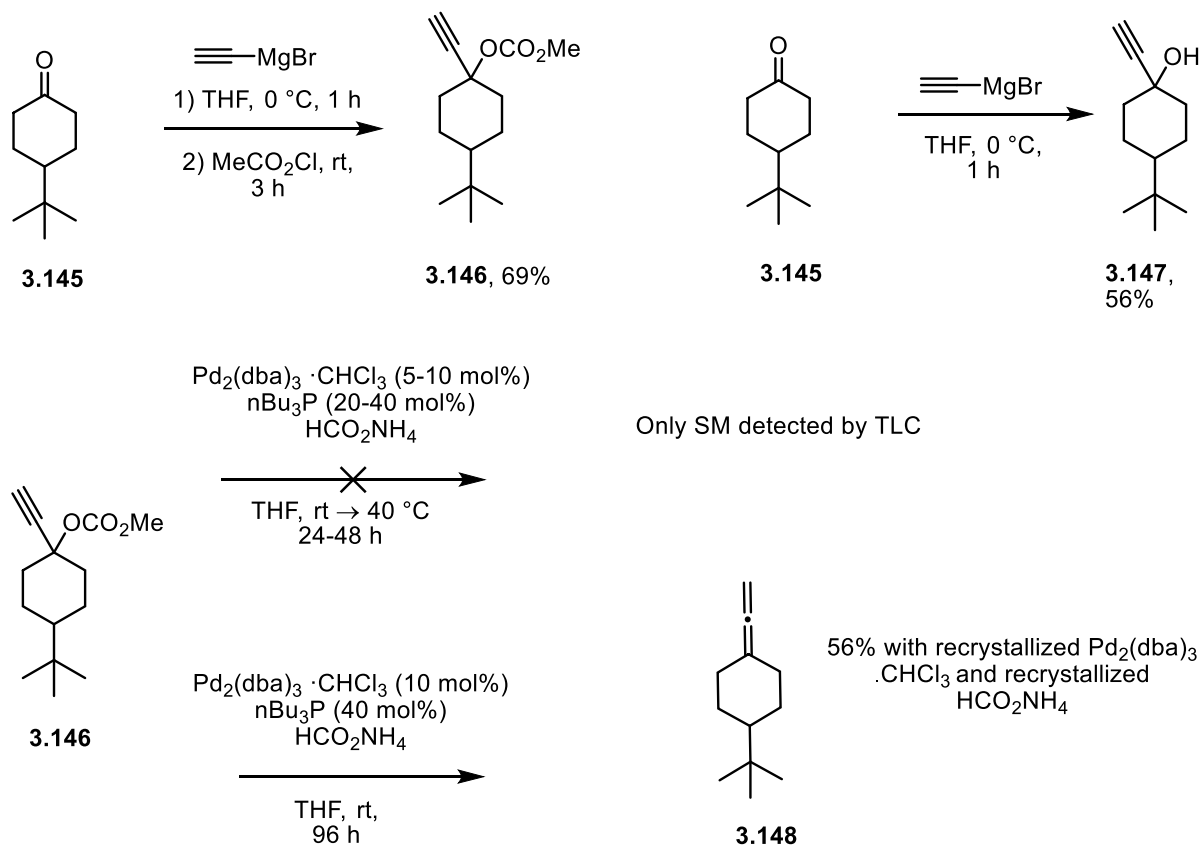
propargyl alcohols under several reported conditions. It was expected that formylation of the lactam nitrogen in addition to formylation of the propargyl alcohol would occur, but the *N*-formyl group could be easily removed with sodium carbonate under mild conditions. Attempts to formylate tertiary propargyl alcohol **3.124a** with iodine in neat formic acid,²⁰⁷ *para*-toluenesulfonic acid in neat formic acid,²⁰⁸ or acetic anhydride and formic acid in pyridine²⁰⁰ all failed to formylate either the hydroxyl group or the lactam nitrogen. Tertiary formates are reported to be unstable (Scheme 3.32).²⁰¹



Scheme 3.32. Attempts to formylate tertiary, propargyl alcohol.

After these failed attempts to form allenes, the formylation and Tsuji reduction conditions were tested on a model substrate **3.146** to determine if the lactam was the problem in these reactions. Addition of ethynyl magnesium bromide to 3-*tert*-butyl cyclohexanone (**3.145**) in THF at 0 °C provided the intermediate alkoxide (Scheme 3.33). TLC indicated consumption of the starting material in 1 h, so methyl chloroformate was added and the reaction was allowed to warm to rt for 3 h to afford propargyl carbonate **3.146** in 69% yield after aqueous work-up and

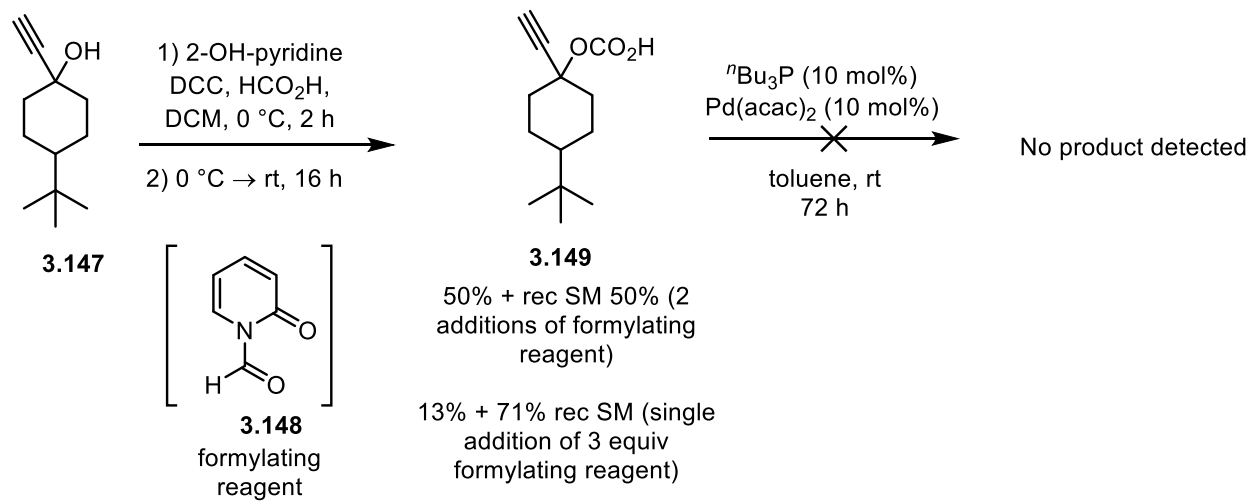
chromatographic purification. Similarly, cyclohexanone **3.145** was treated with ethynyl magnesium bromide and quenched with saturated ammonium chloride to provide propargyl alcohol **3.147** in 56% yield. Propargyl carbonate **3.146** was subjected to the Tsuji reduction conditions described above, but this reaction provided none of the expected allene, despite a cyclohexyl propargyl carbonate being reported to undergo allene formation in 66% yield by Tsuji. The palladium catalyst was purified according to the method reported by Ananikov, who also reported that commercially available tris(dibenzylideneacetone)dipalladium(0) commonly contained significant amounts (up to 40%) of palladium nanoparticles.²⁰⁹ The simple purification procedure involved dissolving tris(dibenzylideneacetone)dipalladium(0) in excess chloroform, filtering off the insoluble impurities, concentrating, dissolving in a minimal amount of chloroform, adding acetone (4:1 with CHCl₃), and cooling to -20 °C overnight in the freezer. The purified tris(dibenzylideneacetone)dipalladium(0) was filtered, washed with acetone, and dried under vacuum. When propargyl carbonate **3.146** was subjected to the Tsuji reduction conditions using the purified palladium catalyst, 56% of the expected allene was obtained. However, this reaction required 4 d at rt to reach completion, so propargyl formates were pursued to obtain allene 1,1-disubstituted allenes in a higher yield and shorter reaction time.



Scheme 3.33. Propargyl carbonate formation and Tsuji reduction on model substrate.

In order to formylate tertiary, propargyl alcohol **3.147**, a 4th set of formylation conditions were tested, using 2-hydroxy pyridine with dicyclohexylcarbodiimide (DCC) and formic acid to generate *N*-formyl pyridone **3.148**, which is the active formylating reagent (Scheme 3.34).^{204, 210} Propargyl alcohol **3.147** was added to a premixed solution of 2-hydroxy pyridine, DCC, and formic acid in DCM at 0 °C and the resulting mixture was allowed to warm to rt for 16 h. TLC indicated that starting material was still present, therefore, additional 2-hydroxy pyridine, DCC, and formic acid were mixed at 0 °C and added to the solution which was then allowed to stir for an additional 24 h (40 h total rxn time). This reaction still failed to go to completion, but after purification, 50% of the desired formate **3.149** was obtained; 50% of the starting material **3.147** was also recovered. This reaction was repeated with 3 equivalents of formylating reagents (2-hydroxy pyridine, DCC,

formic acid) to provide only 13% of formate **3.149** with 71% recovered starting material after 16 h. Formylation with *para*-toluene sulfonic acid and formic acid also failed to give formate **3.149**. Allene formation using formate **3.149** under the conditions reported by Sawamura et al. failed to provide any detectable product by TLC after 3 d at rt.



Scheme 3.34. Formylation of model substrate and attempted decarboxylative hydrogenolysis.

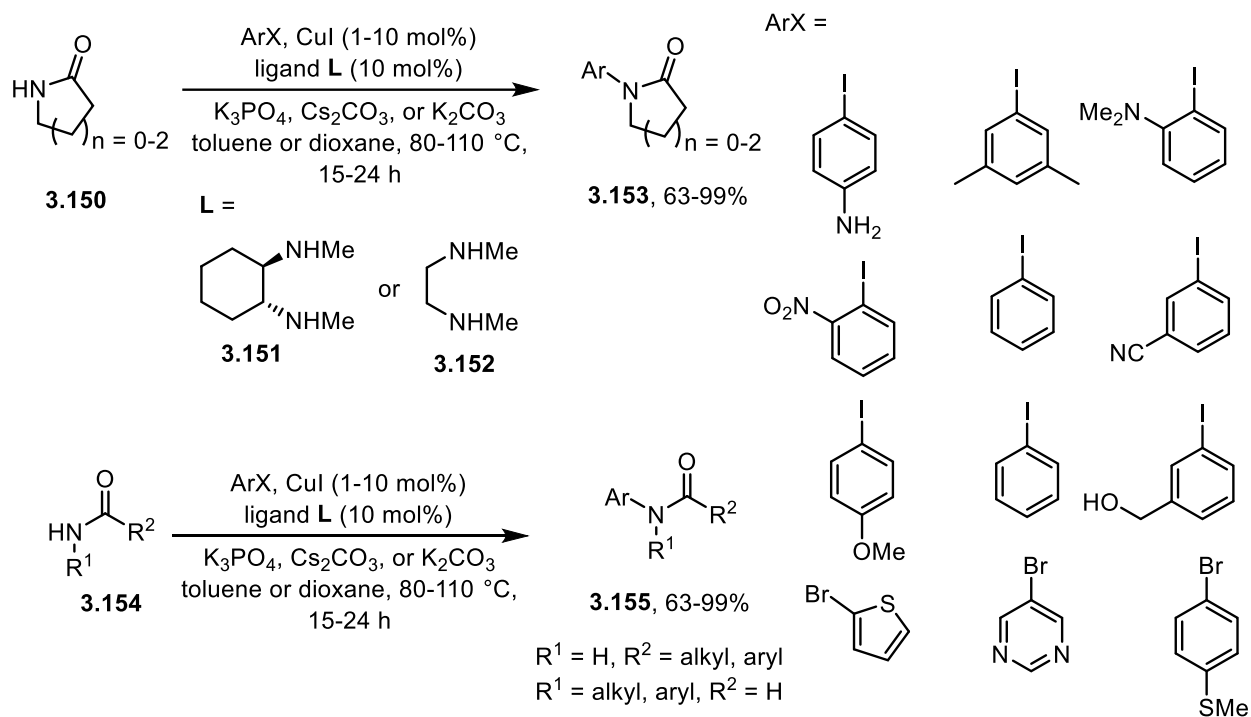
Based on the lower yield obtained for allene formation in model systems **3.146** and the difficulty in forming tertiary propargyl formates or carbonates, especially with the lactam substrates, these conditions were not further pursued. Thus, allene formation from propargyl pivalates was performed with Stryker's reagent, despite the moderate yields and chemoselectivity of this reaction.

3.4.6. Modification of the Lactam Nitrogen of Allene-yne

The aryl substituent of *N*-aryl acrylamides has been shown to influence the rate of glutathione addition to acrylamides, with electron withdrawing substituents increasing the rate and electron donating substituents decreasing the rate (see Chapter 1).^{91,93} It was proposed that coupling an aryl halide to the lactam nitrogen using either copper or palladium catalyzed conditions developed by Buchwald and coworkers would provide *N*-aryl and *N*-heteroaryl α -methylene- γ -lactams.^{173, 211} Additionally, it was proposed that modifying the lactam nitrogen with electronically different aryl groups would provide a method of systematically changing the electrophilicity of the Michael acceptor by changing the electron withdrawing strength of the aryl substituent.^{50-51, 94} Functionalization of the lactam nitrogen after the APKR has obvious advantages when considering the preparation of the widest array of analogs. However, the secondary amide of lactam-tethered allene-yne was modified to investigate both the scope of the allenic Pauson-Khand reaction and the effects of the nitrogen substituent on the electrophilicity of the α -methylene- γ -lactam Michael acceptor.

Buchwald's copper catalyzed amide arylation has been shown to form *N*-aryl amides and lactams from 4, 5, and 6 membered lactams **3.150**, primary alkyl or aryl amides, and secondary alkyl or aryl formamides **3.154** in good yields of 63-99% (Scheme 3.35). These conditions use copper iodide (1-10 mol%) as the copper(I) source; 1,2-diamine ligands **3.151** or **3.152** (2:1 copper:ligand ratio); aryl and heteroaryl iodides or bromides; potassium phosphate, cesium carbonate, or potassium carbonate as a base; and toluene or 1,4-dioxane as the solvent at 80-110 °C for 15-24 h. These conditions proved general and tolerant of various functional groups, but were problematic for sterically hindered, secondary alkyl amides; they have also not been shown

to arylate α -methylene- γ -lactams or substituted γ -lactams such as β,δ -substituted α -methylene- γ -lactam **3.114**.

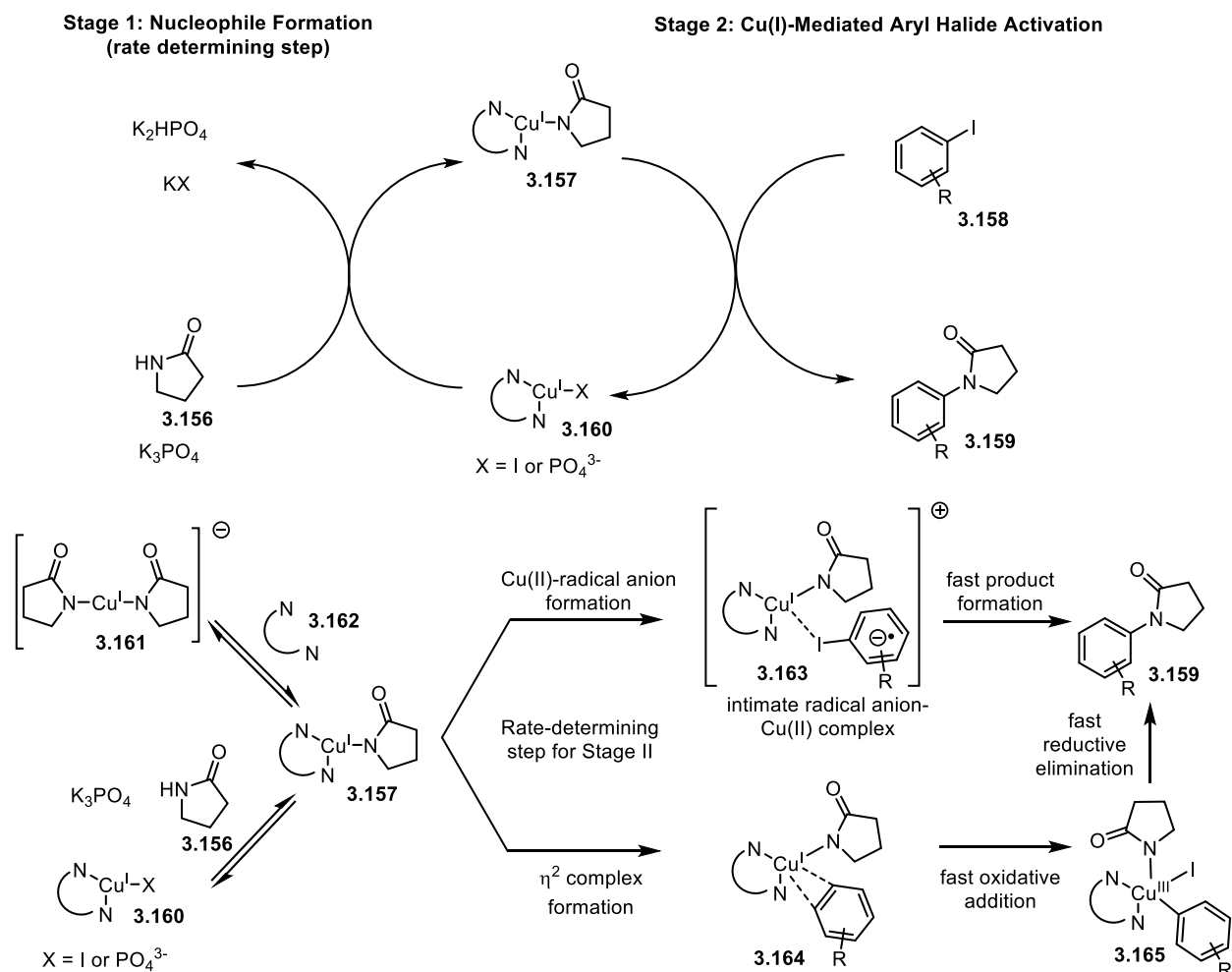


Scheme 3.35. Copper catalyzed amidation of aryl halides.

Mechanistic studies on the copper-catalyzed arylation of amides by Buchwald and others have shown that N-arylation reactions go through a 2-stage process involving nucleophile formation in the first stage followed by copper mediated aryl-halide activation (Scheme 3.36). Furthermore, these studies have shown that a copper(I)-nucleophile complex must form prior to aryl halide activation.²¹² Based on the observation that high concentrations of amide **3.156** and 1,2-diamine ligands **3.162** increase the catalyst efficiency and that stoichiometric amounts of preformed copper(I) amidates **3.157** react to form N-aryl lactams upon addition of a 1,2-diamine ligand and aryl iodide **3.158**, it was proposed that the catalytically active species in the reaction is

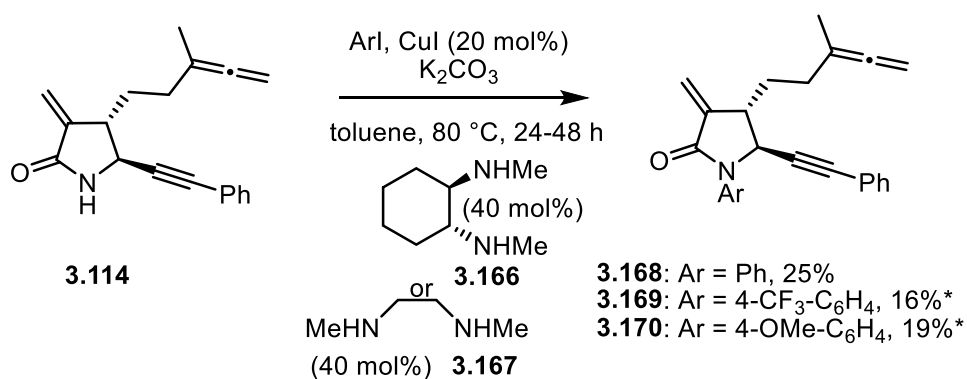
copper(I) amidate **3.157** (Scheme 3.36).²¹² In stoichiometric reactions, copper(I) amidates existed as oligomers **3.161** in solution, as shown by broad peaks in the ¹H NMR spectrum, which sharpened upon addition of a 1,2-diamine **3.162** to form a single, monomeric species with a copper to amide ratio of 1:1. The copper(I) amidate oligomers **3.161** exist in rapid equilibrium with the catalytically active copper(I) amidate **3.157** and the copper(I)-ligated diamine complex **3.160**.

Buchwald and coworkers observed that electron-deficient aryl iodides underwent the N-arylation more rapidly than electron-rich or electron neutral aryl iodides for both stoichiometric and catalytic reactions.²¹² The relatively low ρ -value of +0.48 derived from the Hammett plot of *para*-substituted aryl iodides and the low enthalpy of activation ($\Delta H^\ddagger = 6.8$ kcal/mol) suggest that little bond cleavage or build-up of negative charge occurs in the transition state for aryl iodide activation, implying that oxidative addition is not the rate-determining step in the second stage of N-arylation; in contrast, oxidative addition of Pd(0) has a ρ value of 2.3 and enthalpy of activation equal to 18.4 kcal/mol and is the rate determining step.²¹² This led to the proposal that the rate determining step in stage 2 of the copper(I) catalyzed N-arylation with aryl iodides is either copper(II)-radical anion formation to give complex **3.163** or η^2 complex formation to give **3.164**. In the first case, radical anion-copper(II) complex **3.163** could undergo rapid halide transfer to copper(II), radical combination to form copper(III) species, and reductive elimination to provide *N*-aryl lactam **3.159**. Electron-deficient aryl iodides would facilitate the initial single electron transfer from copper to the aryl iodide in this case.²¹² Alternatively, slow formation of an η^2 complex **3.164** followed by fast oxidative addition to give **3.165** and fast reductive elimination to provide *N*-aryl lactam **3.159** is possible. In this case, electron-deficient aryl iodides could facilitate formation of the η^2 complex by lowering the LUMO of the aryl iodide.



Buchwald reported that potassium carbonate was superior to potassium phosphate or cesium carbonate when N-arylation reactions were performed with aryl bromides because N-arylation of the 1,2-diamine ligand led to catalyst deactivation when the less reactive aryl bromides were used and that stronger bases increased the amount of N-arylated diamine.¹⁷³ Thus, it was proposed that sterically hindered lactam **3.114** would slow the reaction with aryl iodides. N-arylation of **3.114** with iodobenzene was initially attempted in toluene at 80 °C for 24-48 h with potassium carbonate as the base and *N,N*-dimethylcyclohexyldiamine (**3.166**) as the diamine ligand, but only 16-27% yield of N-aryl lactam **3.168** was obtained along with 20-25% recovered

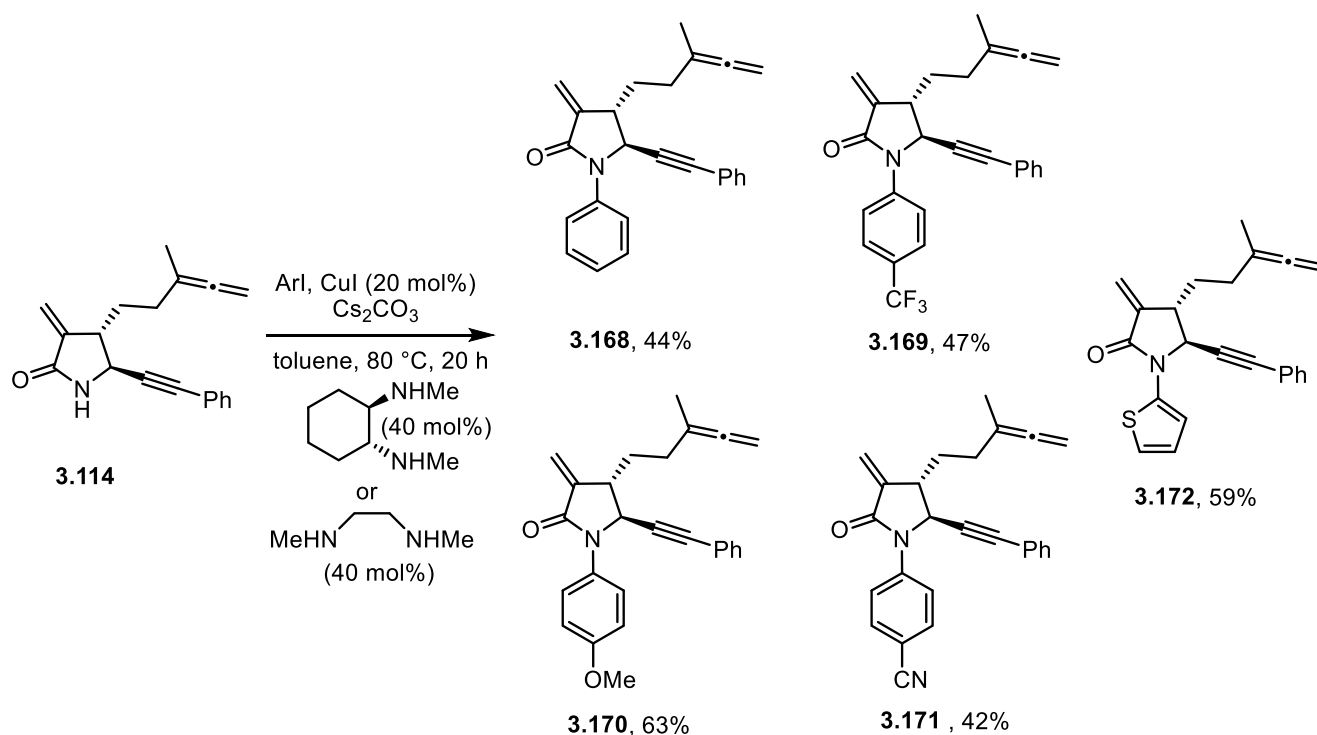
starting material (Scheme 3.37). Using a less bulky diamine ligand, *N,N*-dimethylethylenediamine (**3.167**), the active copper-ligated diamine was expected to react faster with lactam **3.114**, but this gave similar yields as *N,N*-dimethylcyclohexyldiamine **3.166**. Similar yields were also obtained when the amount of copper iodide and 1,2-diamine ligand were increased to 30-40 mol% CuI and 60-80 mol% ligand.



Scheme 3.37. *N*-Arylation of lactams with potassium carbonate as a base.

A stronger base should facilitate formation of the copper-lactam complex (e.g. **3.157**, Scheme 3.36). Thus, *N*-arylation of allene-yne **3.114** was performed with cesium carbonate as a base. This provided *N*-phenyl lactam **3.168** in 44% yield and complete conversion of the starting material based on TLC analysis. The lactam nitrogen was arylated with various aryl iodides using these optimized conditions: 20 mol% copper iodide, 40 mol% *N,N*-dimethylethylenediamine, 1.2 equiv aryl iodide, 2 equiv cesium carbonate, and 1 equiv lactam **3.114** were stirred in toluene at 80 °C in a sealed tube, under a nitrogen atmosphere for 20 h. These conditions allowed the installation of electron withdrawing and an electron donating groups, affording *N*-aryl lactams **3.168-3.172** in 42-63% yield (Scheme 3.38). Arylation with 4-iodobenzotrifluoride, 4-iodoanisole, and 4-iodobenzonitrile provided lactams **3.168-3.171** in 47, 63, and 42% yields, respectively.

Arylation of lactam **3.114** with 2-iodothiophene demonstrates the feasibility of installing a heteroaryl substituent using this methodology. Compounds **3.168-3.172** could be identified by disappearance of the broad singlet resonance between 5-7 ppm in the ^1H NMR, corresponding to the hydrogen on the lactam nitrogen, as well as new resonances in the aromatic region of the ^1H NMR spectra. The increased conversion of starting material to *N*-aryl lactam when cesium carbonate was used as a base compared to potassium carbonate suggests that formation of the copper(I)-amidate was slowed by the weaker base and that reaction with the aryl iodide was not the slow step, which is consistent with the studies by Buchwald on the less sterically hindered, unsubstituted 2-pyrrolidinone.

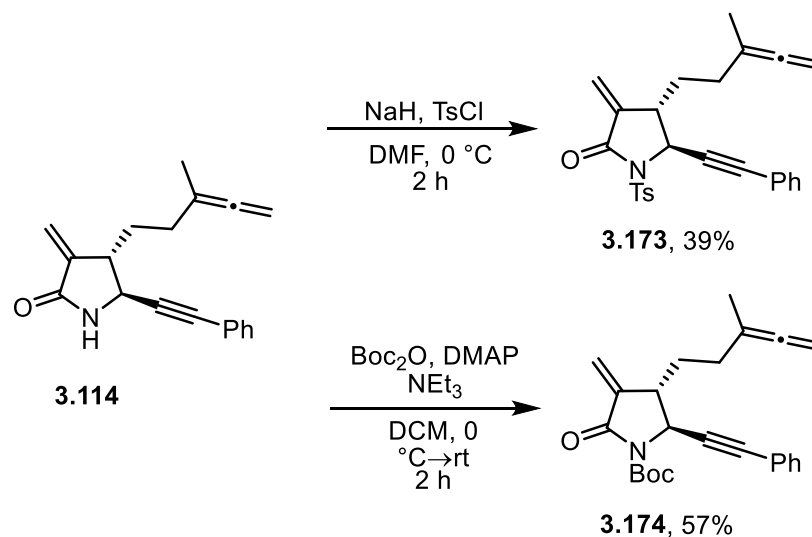


Scheme 3.38. *N*-Arylation of lactam-tethered allene-yne.

Arylation of the lactam nitrogen in tricycle **3.116** using Buchwald's copper or palladium catalyzed conditions resulted in recovery of starting material (80 °C) or decomposition (110 °C). These results are consistent with the crystal structure of tricycle **3.116** showing that the lactam nitrogen is hindered by the phenyl substituent of the cyclopentenone, which is why the *N*-arylation of this substrate failed (Figure 3.2).^{173, 211}

In addition to the *N*-aryl lactams above, lactams with stronger electron withdrawing groups on the nitrogen were proposed to significantly increase the electrophilicity of the α -methylene- γ -lactam Michael acceptor. Moreover, if lactam tethered allene-ynes were tolerant to deprotonation and nucleophilic addition to an electrophile, then the substrates available by a late stage modification methodology would include *N*-aryl, *N*-acyl, and *N*-alkyl lactams. Tosyl lactam **3.173** was formed in 39% yield by deprotonation of the lactam nitrogen of **3.114** and addition to tosyl chloride (Scheme 3.39). This reaction resulted in some reaction of the sodium hydride with the α -methylene, as noted by disappearance of the α -methylene hydrogens from the ¹H NMR of some byproducts. Other unidentified decomposition products resulted in this low yield. Although these yields were moderate, these substrates demonstrated the moderate stability of our lactam-tethered allene-ynes to a strong base (NaH) and to nucleophilic acyl substitution reactions. Further optimization of substitution reactions involving deprotonation of the secondary amide with a strong base are needed for these reactions to be synthetically useful. However, this provided a substrate with a strong electron withdrawing group for thiol reactivity and bioactivity studies. As tert-butyl carbonate is a common amide protecting group, its stability to the APKR was of interest. An A^{1,3}-interaction between the tert-butyl group and the phenyl ring of the APKR product was expected, and we wished to examine the feasibility of bulky nitrogen substituents as well as carbonates as substrates in the APKR. Towards this end, the nitrogen of lactam **3.114** was protected

with a carbonate group using di-tert-butyl dicarbonate, triethylamine, and dimethylaminopyridine to give carbonate **3.174** in 57% yield.

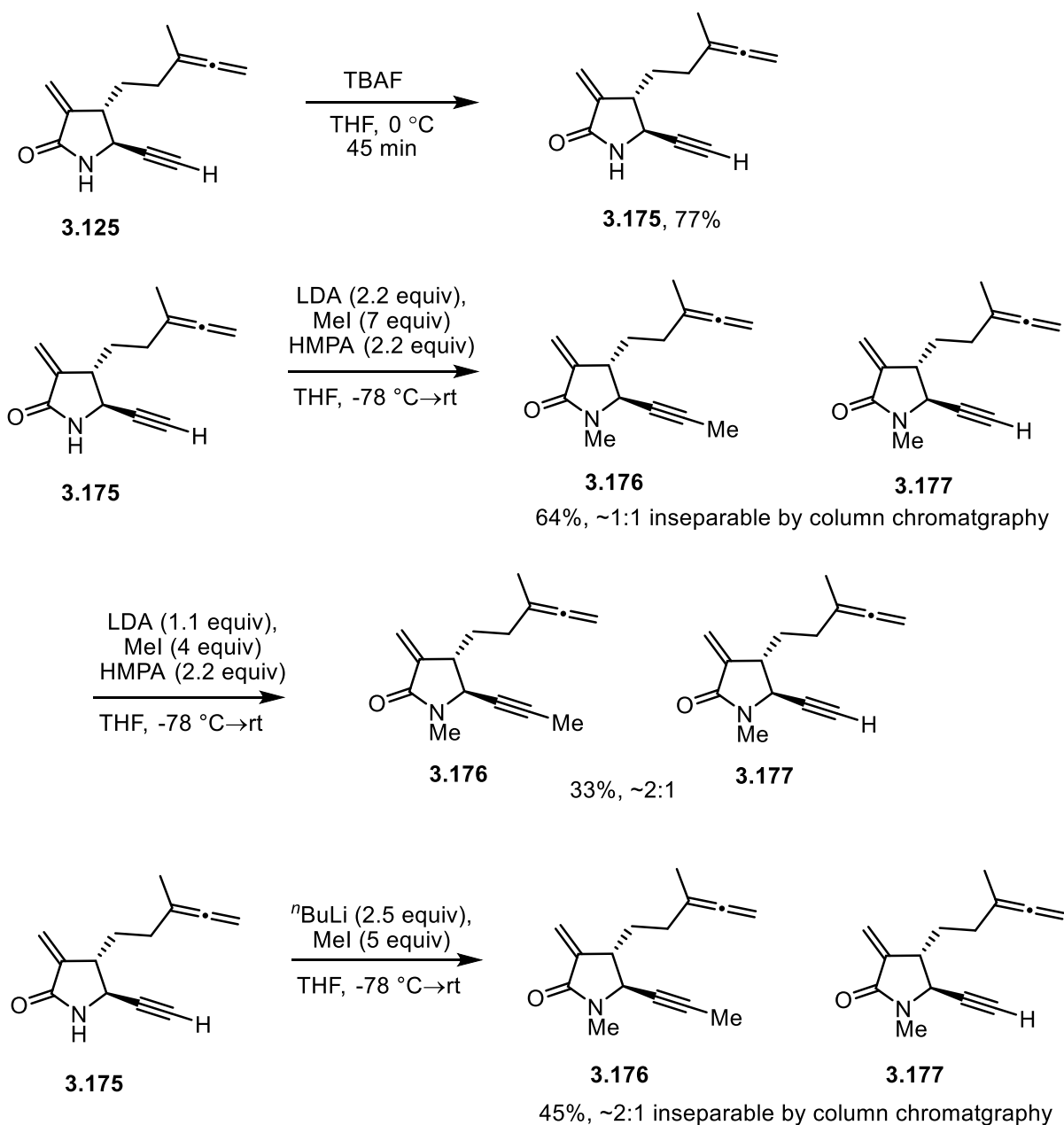


Scheme 3.39. Nucleophilic addition of lactams to electrophiles.

3.4.7. Modifications to the Alkyne Terminus

It was hypothesized that the alkyne could be modified by removing the triisopropyl silyl substituent and utilizing the resulting terminal alkyne to perform substitution or coupling reactions. Additionally, various alkyne substituents were pursued to examine the scope of the APKR with lactam-tethered allene-ynes. Installation of a methyl group at the terminus of the alkyne would provide tricycles that are identical to the 6,12-guaianolide skeleton with a lactam in place of the lactone (Section 3.1, Figure 3.1). The terminal alkyne could potentially be modified by Sonogashira coupling reactions to diversify the aryl substituent on the alkyne at a late stage in the synthetic sequence.

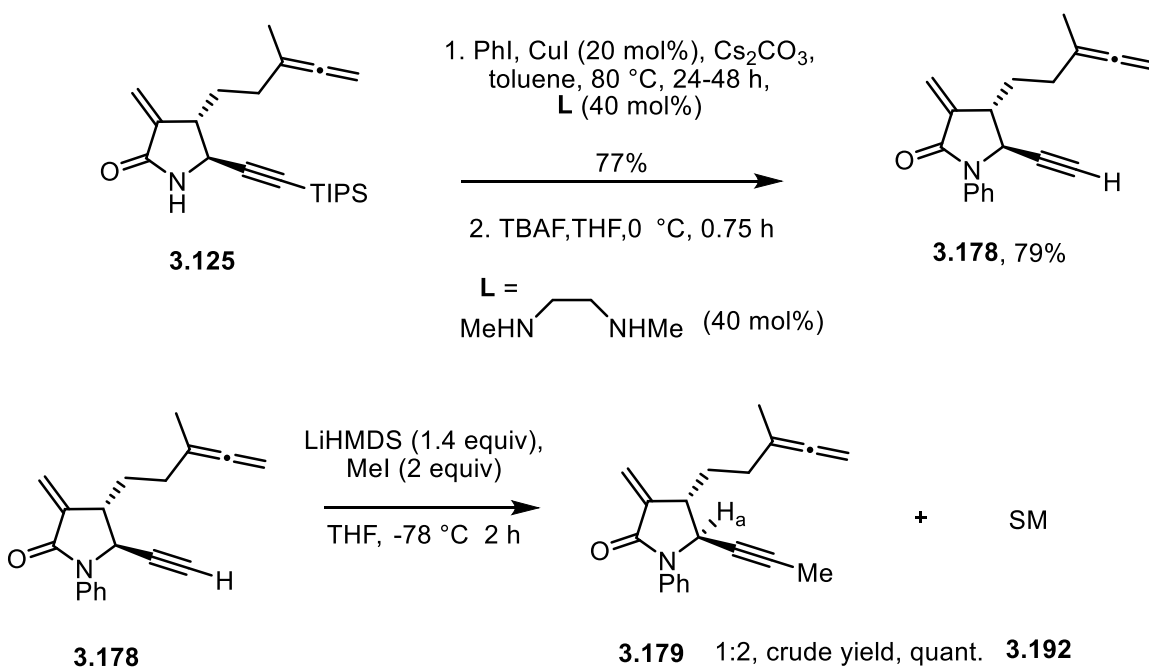
The TIPS group was removed from alkyne **3.125** to give the corresponding terminal alkyne **3.175** in 77% yield. ^1H NMR showed disappearance of the singlet resonance at 1.0 ppm corresponding to the hydrogens on the TIPS group, and a new doublet resonance appeared at 2.39 ppm for **3.175**, corresponding to the terminal alkyne hydrogen (Scheme 3.40). Bis-methylation of lactam **3.175** at the alkyne terminus and the lactam nitrogen was attempted by deprotonating this substrate with 2 equiv of lithium diisopropylamide (LDA) and reacting with methyl iodide, but an inseparable mixture of bismethylated lactam **3.176** and *N*-methylated lactam **3.177** were obtained in a 1:1 ratio and 64% overall yield. This mixture was subjected to LDA and methyl iodide a second time to achieve bismethylation, but an inseparable mixture of products **3.176** and **3.177** was obtained in a low yield of 33% and only a slightly better ratio of 2:1. *n*-Butyllithium was used as a base instead of LDA, but this gave a mixture of the mono and bismethylation in 45% yield and a 2:1 ratio; other unidentified impurities were also observed in the ^1H NMR spectrum.



Scheme 3.40. Modification of alkyne substituents.

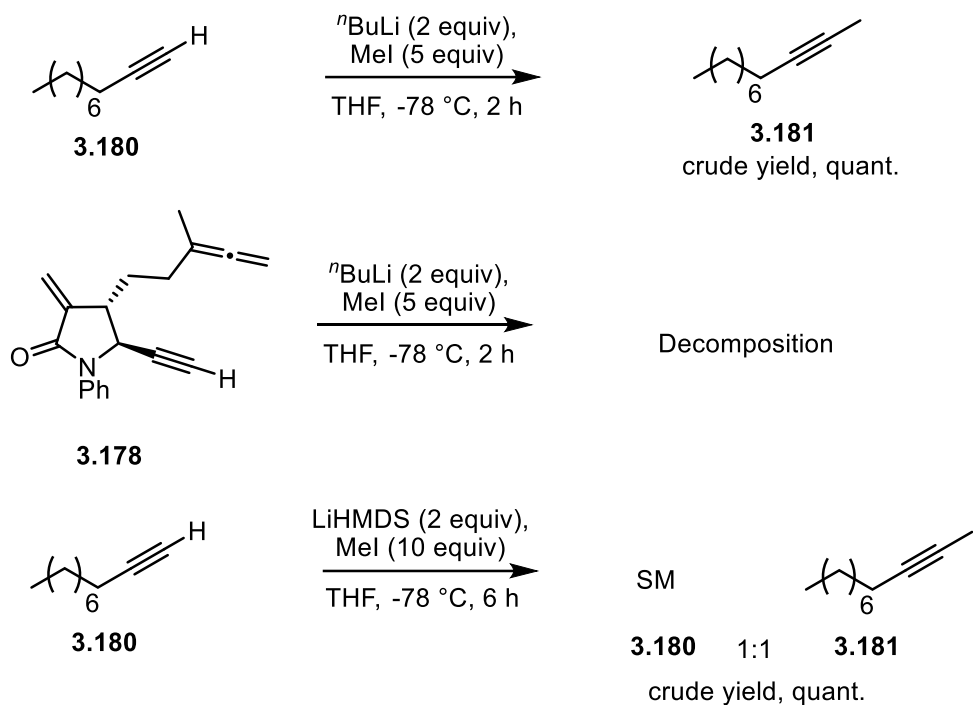
It was proposed that alkyne methylation would be easier to achieve if the lactam nitrogen was unreactive. Thus, arylation of the secondary amide of **3.125** under the arylation conditions discussed in the previous section afforded the N-arylated lactam in 77% yield (Scheme 3.41). The TIPS substituent of was removed with TBAF to afford terminal alkyne **3.178** 79% yield. The

tertiary amide of **3.178** was expected to be unreactive to the alkyne methylation conditions. As decomposition of alkynes containing a secondary amide was evident when strong bases were used, deprotonation of alkyne **3.178** was first attempted with lithium hexamethyldisilazane (LiHMDS) which is one of the weaker bases capable of deprotonating an alkyne. With methyl iodide as the electrophile, and keeping the reaction at $-78\text{ }^{\circ}\text{C}$, reaction of terminal alkyne **3.178** provided a 2:1 ratio of starting material to product **3.179** with a quantitative crude yield after aqueous work-up. This ratio was determined by integration of the resonances corresponding to the hydrogen at the γ -position of the lactam (labeled H_a) at 4.48 ppm for terminal alkyne **3.178** and 4.42 for internal alkyne **3.179**. Using similar conditions, but allowing the reaction to react for 2 h at $-78\text{ }^{\circ}\text{C}$ then warm to $0\text{ }^{\circ}\text{C}$ for 1 h resulted in decomposition, as evidenced by disappearance of the α -methylene resonances from the crude ^1H NMR spectrum. Using LDA as the base, as in the reaction above also resulted in decomposition and a 13% yield of an unknown byproduct that still retained the terminal alkyne.



Scheme 3.41. Alkyne methylation with tertiary amide.

Exploration of alkyne methylation with 1-decyne (**3.180**) demonstrated that the methylation of a terminal alkyne with methyl iodide and *n*BuLi as the base required about 2 h at -78 °C for complete methylation (Scheme 3.42). However, the use of a stronger base (*n*BuLi) with lactam **3.178** and keeping the reaction at -78 °C resulted in decomposition, where disappearance of the α -methylene resonances in the ¹H NMR was observed. For secondary amide **3.175** above, less decomposition was observed when *n*BuLi was used as the base. Deprotonation of the secondary amide should stabilize both the α -methylene and the lactam carbonyl from nucleophilic attack, which is why tertiary amide **3.178** is less stable to a strong base. When 1-decyne **3.180** was deprotonated with LiHMDS and methylated with methyl iodide, a 1:1 mixture of product to starting material was obtained after 6 h at -78 °C even when a large excess (10 equiv) of methyl iodide was used, indicating that this reaction is slow when kept at low temperatures. Indeed, many literature procedures that utilize methyl iodide as the alkylating reagent involve warming to 0 °C or rt. Investigations of alkyne methylation with a more reactive methylating reagent, methyl triflate, are ongoing, as these reactions proceed at low temperatures with LiHMDS as a base.²¹³

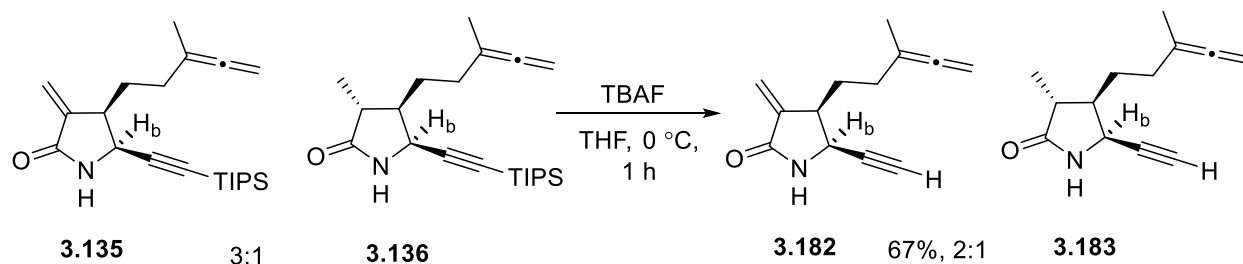


Scheme 3.42. Alkyne methylation at low temperatures with model substrate.

Procedures to methylate the terminal alkyne of lactam **3.175** or **3.178** are still being tested. An alternative method to synthesize methyl alkynes would be to install the methyl alkyne during the lactamization reaction by using 2-butyne as the aldehyde in place of phenyl or TIPS propynal, but late stage modification is more advantageous. Future work could also involve Sonagashira coupling on the terminal alkyne to install various alkenyl and aryl substituents.

Terminal alkynes of cis lactams were prepared analogously to the trans lactams. In one case, the TIPS substituent was removed from a mixture of alkynes (3:1) **3.135**:**3.136** with tetrabutylammonium fluoride (TBAF) to give terminal alkynes **3.182** and **3.183** in 67% yield, and a slightly decreased ratio of α -methylene lactam **3.182** to α -methyl lactam **3.183** from 3:1 in the starting material to 2:1 in the products; lactams **3.182** and **3.183** were still inseparable by column

chromatography Scheme 3.43). The ratio was determined by integration of H_b at 4.4 ppm for α -methylene lactam **3.182** and 4.2 ppm for α -methyl lactam **3.183** in the ¹H NMR spectrum.



Scheme 3.43. Removal of TIPS substituent from cis lactams to generate terminal alkynes.

3.5. ALLENIC PAUSON-KHAND REACTION OF α -METHYLENE- γ -LACTAM TETHERED ALLENE-YNES

With the α -methylene- γ -lactam-tethered allene-yne in hand, the scope of the allenic Pauson-Khand reaction was examined. 1,1-disubstituted allenes underwent the APKR to give the fused tricyclic structures **3.56**, **3.116**, **3.184-3.192** in yields of 41-79%. The typical conditions used in this reaction utilized 10 mole percent of rhodium biscarbonyl chloride, 1 atmosphere of carbon monoxide gas with toluene at 110 °C. The reaction was conducted by slow addition of an allene-yne to the rhodium catalyst over 1 h via a syringe pump and stirring for 0.5 h after addition of the allene-yne was complete.¹⁶³

In most cases, this gave complete consumption of the starting material as observed by TLC. As discussed in the feasibility studies, the *N*-methyl allene-yne **3.57** underwent the cyclocarbonylation reaction in 75% yield, and the allene-yne with an unsubstituted nitrogen, **3.114**, gave a similar yield of 79% (Table 3.3, entries 1-2). TIPS-substituted alkyne **3.125** afforded **3.184**

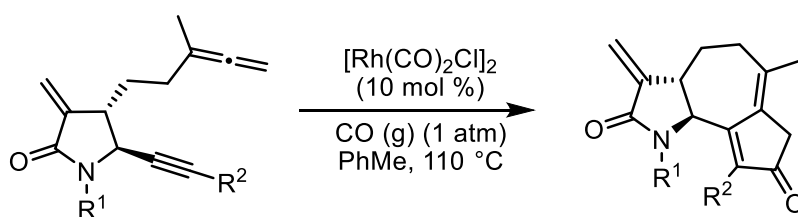
in 47% yield (entry 3). The longer reaction time for **3.125** vs **3.114** (4 h vs 1.5 h) is likely due to the developing A^{1,3} interaction between the TIPS group and the lactam. Moreover, a structurally related lactone-tethered-allene-yne with a less bulky trimethylsilyl group on the alkyne underwent an APKR in high yields and reaction times similar to a phenyl substituted alkyne.¹¹⁷ Terminal alkynes were tolerated well in the APKR as evidenced by the cyclocarbonylation reaction of allene-yne **3.175** to provide lactam **3.185** in 62% yield (entry 4). Allene-ynes **3.168-3.171** where tertiary amides were substituted with an *N*-phenyl, *N*-*para*-trifluoromethyl phenyl, *N*-*para*-cyanophenyl, , or *N*-*para*-methoxy phenyl gave yields of 69, 67, 72, and 76% of tricycles **3.186-3.189**, respectively (entries 5-8). The reaction time nor the yield were significantly impacted by the electronic nature of the aryl group on the lactam nitrogen. With a thiophene group on the nitrogen atom, allene-yne **3.172** provided lactam **3.190** in 67% yield demonstrating that heteroaryl groups are tolerated in this APKR (entry 8). The APKR of *N*-tosyl and *N*-Boc allenes **3.173** and **3.174** gave yields of 69 and 40% for tricycle formation, respectively (entries 9-10). The lower yield of lactam **3.192** is attributed to the thermal instability of the Boc group at 110 °C.²¹⁴

Entries 1-2 and 5-7 in Table 2 demonstrate that the APKR with a phenyl substituted alkyne is tolerant of alkyl, aryl (electron donating or withdrawing), sulfonyl, carbonate, and *N*-unsubstituted α -methylene- γ -lactam tethers. Entries 3-4 demonstrate the tolerance of TIPS-substitution and terminal alkynes in the APKR. The structure of the [5,7,5]-ring system of **3.116** was confirmed by X-ray crystallography (Figure 3.2). All compounds synthesized by the APKR are shown in Scheme 3.45.

In addition to the typical reaction conditions described above, the reaction was performed by adding the allene in a single portion to the rhodium catalyst and stirring for 1 h at 110 °C followed by cooling to rt and filtering through a plug of silica gel without the addition of polymer

bound triphenylphosphine for entries 1-2, 4, 10-11 in Table 1; yields of 75, 75, 42, 63, and 41% for entries 1, 2, 4, 10, and 11 under these conditions compared to yields of 75, 79, 62, 69, and 40%, respectively, under the slow addition conditions revealed that the yield was not significantly affected by slow addition of the allene or by rhodium scavenging with polymer bound triphenylphosphine. The exception to this was terminal alkyne **3.175**, which gave an improved yield under the more dilute conditions.

Table 3.3. Allenic Pauson-Khand Reaction (APKR) with trans-substituted α -methylene- γ -lactam tethered allene-yne.



Entry	Allene	R ¹	R ²	Time (min)	Prod.	Method A Yield (%)	Method B Yield (%) ^a
1	3.57	Me	Ph	90	3.56	75	75
2	3.114	H	Ph	90	3.116	79	75
3	3.125	H	TIPS	300	3.184	47	ND
4	3.175	H	H	90	3.185	62	42
5	3.168	Ph	Ph	90	3.186	69	ND
6	3.169	4-CF ₃ -C ₆ H ₄	Ph	90	3.187	67	ND
7	3.171	4-CN-C ₆ H ₄	Ph	120	3.188	72	ND
8	3.170	4-OMe-C ₆ H ₄	Ph	90	3.189	76	ND
9	3.172	2-thiophene	Ph	90	3.190	66	ND
10	3.173	Tosyl	Ph	90	3.191	69	63
11	3.174	Boc	Ph	90	3.192	40	41

These reactions were typically complete within 30 min after a slow addition of the allene to the rhodium catalyst over 1 h (Method A) a) Only minor changes in yields were observed when allene was added in a single portion and stirred for 1 h (Method B).

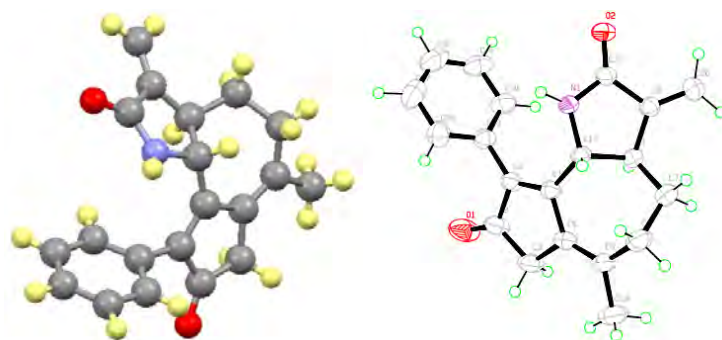
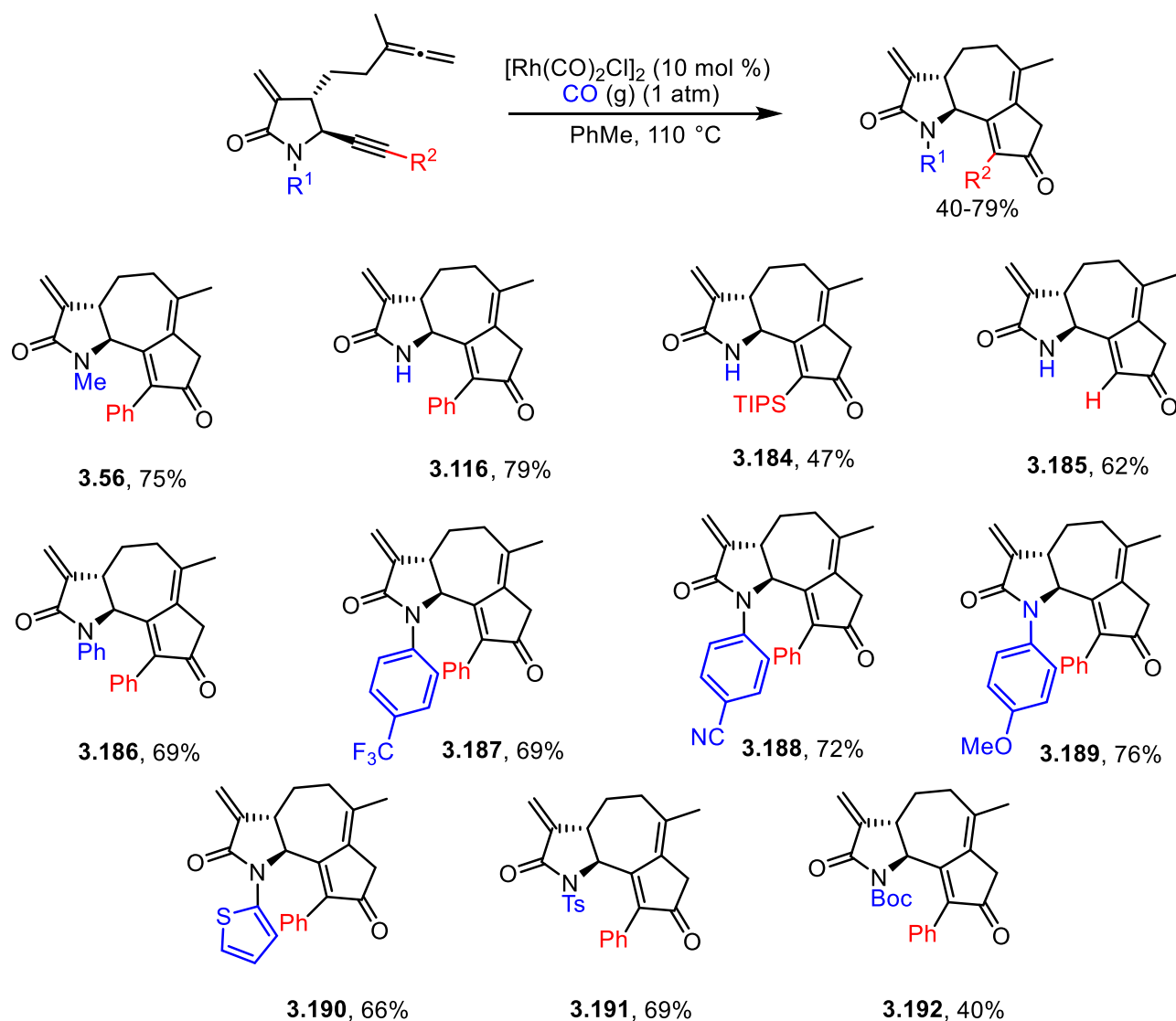
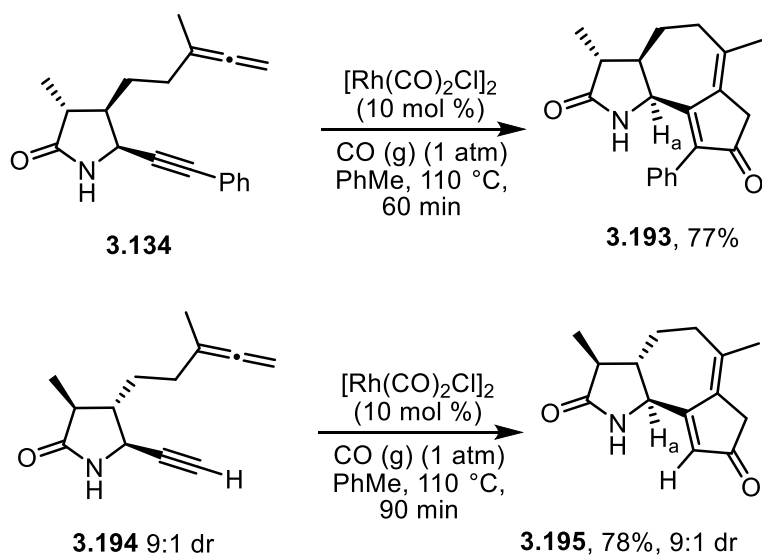


Figure 3.2. Crystal structure of tricyclic **3.116**, showing the trans lactam.



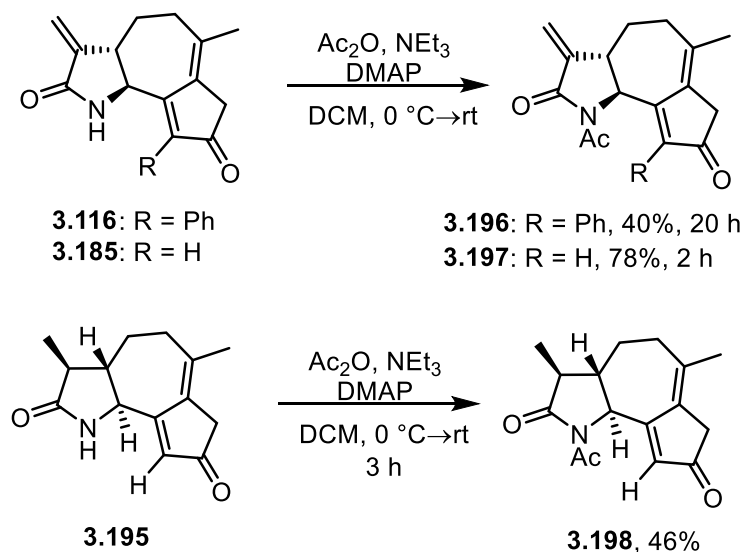
Scheme 3.44. APKR with trans-substituted α -methylene- γ -lactam tethered allene-ynes.

Next, the impact of the α -methylene group on the efficiency and facileness of the APKR was examined, using allene-yne **3.134** and **3.194** (Scheme 3.45). The α -methyl substituted lactam **3.134**, with cis substituted allene and alkyne groups, afforded the APKR product **3.193** in 77% yield in 60 min when the allene was added in a single portion to the rhodium catalyst. This demonstrated that the APKR can form cis-fused [5,7,5] ring systems and that the α -methylene did not impact the APKR. α -Methyl substituted lactam **3.194**, synthesized by removal of the TIPS group from allene-yne **3.126** with TBAF, underwent the APKR in 90 min to afford **3.195** in 78% yield as a 9:1 mixture of methyl diastereomers. A higher yield of **3.195** was obtained when compared to the corresponding trans α -methylene- γ -lactam **3.175** (78% vs 62%) with a terminal alkyne. The dr remained the same as the allene-yne starting materials where **3.193** was obtained as single diastereomer, and **3.195** was obtained with a 9:1 dr (determined by integration of H_a in the ¹H NMR spectrum which appeared as a doublet at 4.50 ppm for the major diastereomer and 4.56 ppm for the minor diastereomer). Since the resonances in the ¹H NMR of tricyclic products **3.193** and **3.195** were more distinct than the resonances in the allene-yne starting materials, the tricyclic products were used to determine the relative stereochemistry of the methyl substituent (see Section 3.6). The relative stereochemistry **3.193** and **3.195** was assigned by comparing calculated coupling constants to experimental coupling constants. It is predicted that the major diastereomer is the result of thermodynamic protonation of the intermediate copper enolate formed during the conjugate reduction of the α -methylene moiety by Stryker's reagent to give the α,β trans isomer.



Scheme 3.45. APKR with α -methyl lactams.

Acylation of secondary amide **3.116**, containing a phenyl substituent on the cyclopentenone ring, proceeded slowly (20 h to completion by TLC) to afford **3.196** in a 40% yield. Acylation of tricycles **3.185** and **3.195**, with no α -substituents on the cyclopentenone, reached completion in 2-3 h affording acylated lactams **3.197** and **3.198** in 78 and 46% yields, respectively.



Scheme 3.46. N-Acylation of tricyclic APKR products.

3.6. ASSIGNMENT OF RELATIVE STEREOCHEMISTRY OF α -METHYL- γ -LACTAMS BY CALCULATION AND NMR ANALYSIS

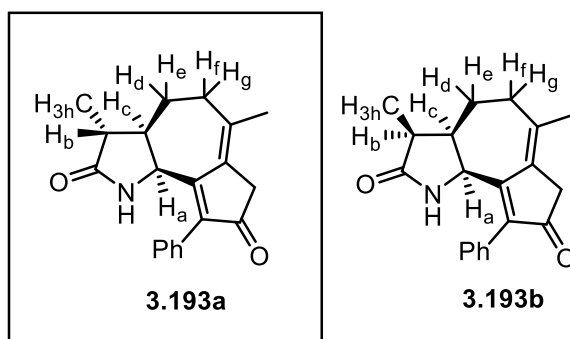
The stereochemistry of the methyl substituents of **3.193** and **3.195** was assigned by calculating the coupling constants for both possible isomers using Spartan. The lowest energy conformers were calculated using MMFF, and ^1H NMR data was calculated for the lowest energy conformer using B3LYP/6-31G* functionals. Cis-fused tricycle could have the stereochemistry shown in **3.193a**, where the methyl substituent is trans to the 7-membered ring or the stereochemistry shown in **3.193b** where the methyl substituent is on the same face as the 7-membered ring. The calculations indicated that **3.193a** with the methyl substituent on the opposite face as the 7-membered ring was 0.5 kcal/mol more stable than **3.193b**, and it was predicted that the more stable isomer would be the major diastereomer. This diastereomer would arise from conjugate reduction of the α -

methylene double bond followed by thermodynamic quenching of the resulting enolate. The calculated ^1H NMR coupling constants for the two possible methyl isomers were compared to the experimental coupling constants, and the calculated values for **3.193a** were closer to the experimental values. For H_a , the calculated coupling constant was 7.3 Hz for **3.193a** and 6.7 Hz for **3.193b**, while the experimental value was 7.6 Hz (Table 3.4, entry 1). For H_b , the experimental coupling constants of 2.4 and 7.2 Hz were closer to the calculated coupling constants for **3.193a**, 1.3 and 6.6 Hz, than they were to **3.193b**, 6.6 and 7.5 Hz (entry 2). The coupling constants could not be determined for H_c due to the complexity of the ^1H NMR spectrum and the calculated values for H_d , H_e , H_f , H_g , and H_h were not significantly different for the two possible isomers (entries 3-8). Thus, the relative stereochemistry with the methyl substituent trans to the 7-membered ring (**3.193a**) was assigned to the experimentally obtained compound based on the coupling constants of H_a and H_b .

The relative stereochemistry of the trans-fused lactam with an α -methyl substituent was determined analogously to the cis-fused lactam above. The two possible isomers **3.195a**, with the methyl substituent trans to the closest ring substituent, and **3.195b**, with the methyl group cis to the closest ring substituent are shown below (Table 3.5). Calculations from Spartan indicated that **3.195a** was 2.5 kcal/mol more stable than **3.195b**, and thus it was predicted that the relative stereochemistry would match that shown in **3.195a**. The calculated coupling constant for H_a of **3.195a** was 10.0 Hz which matched the experimental value, but the calculated coupling constant for H_a of **3.195b** was 9.7 Hz (Table 3.5, entry 1). The experimental coupling constants for H_b of 7.0 and 11.0 Hz were much closer to the calculated values of **3.195a** of 6.6 and 11.1 Hz than they were to the calculated coupling constants of **3.195b**, 6.6 and 8.8 Hz (entry 2). The experimental coupling constants for H_c did not match either of the calculated values well, while the calculated

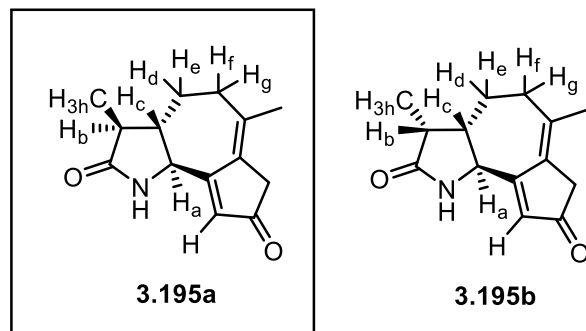
coupling constants for the remaining hydrogens were not significantly different between **3.195a** and **3.195b** (entries 3-8). Thus, the relative stereochemistry with the methyl substituent trans to the nearest ring substituent as shown in **3.195a** was assigned to the experimentally obtained product based on the coupling constants of H_a and H_b.

Table 3.4. ¹H NMR Calculations Compared to Experimental Data for **3.193**.



Entry	Hydrogen	Calculated δ 3.193a ppm	Calculated δ 3.193b ppm	Experimental δ ppm
1	H _a	4.95 ($J = 7.3$ Hz)	4.84 ($J = 6.7$ Hz)	4.98 ($J = 7.6$ Hz)
2	H _b	2.11 ($J = 1.3, 6.6$ Hz)	2.45 ($J = 6.6, 7.5$ Hz)	2.46 ($J = 2.4, 7.2$ Hz)
3	H _c	2.40 ($J = 1.3, 1.9, 5.1, 7.3$ Hz)	2.60 ($J = 1.6, 5.6, 6.7, 7.5$ Hz)	2.35-2.23 (m)
4	H _d	2.09 ($J = 0.8, 5.1, 12.9$ Hz)	1.99 ($J = 0.8, 1.6, 7.3$ Hz)	2.05 ($J = 4.6, 10.4, 14.0$ Hz)
5	H _e	1.76 ($J = 0.9, 1.9, 7.2$ Hz)	1.86 ($J = 0.8, 5.6, 12.8$ Hz)	2.35-2.23 (m)
6	H _f	2.74 ($J = 0.9, 12.9$ Hz)	2.70 ($J = 0.8, 12.8$ Hz)	2.55 ($J = 8.0, 11.2$ Hz)
7	H _g	2.05 ($J = 0.8, 7.2$ Hz)	2.03 ($J = 0.8, 7.3$ Hz)	1.84 ($J = 2.5, 6.0$ Hz)
8	H _h	1.20 ($J = 6.6$ Hz)	1.16 ($J = 6.6$ Hz)	1.22 ($J = 7.2$ Hz)

Table 3.5. ^1H NMR Calculations Compared to Experimental Data for **3.195**.

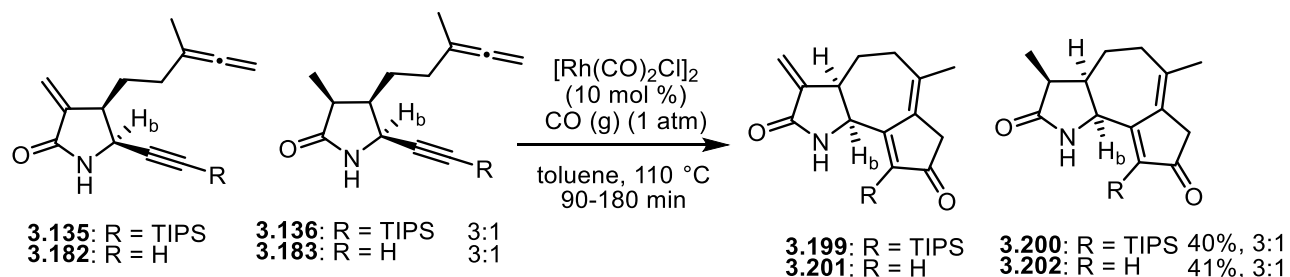


Entry	Hydrogen	Calculated δ 3.195a ppm	Calculated δ 3.195b ppm	Experimental δ ppm
1	H _a	4.41 ($J = 10.0$ Hz)	4.50 ($J = 9.7$)	4.51 ($J = 10.0$ Hz)
2	H _b	1.99 ($J = 6.6, 11.1$ Hz)	2.33 ($J = 6.6, 8.8$ Hz)	2.27 (7.0, 11.0 Hz)
3	H _c	1.93 ($J = 8.5, 9.2, 10.0, 11.1$ Hz)	2.39 ($J = 7.9, 8.8, 9.7, 9.9$ Hz)	2.21 ($J = 2.0, 6.5, 12.5$ Hz)
4	H _d	2.18 ($J = 4.7, 8.5, 12.5$ Hz)	1.82 ($J = 4.8, 7.9, 12.4$ Hz)	2.31-2.25 (m)
5	H _e	1.48 ($J = 2.4, 4.9, 9.2$ Hz)	1.78 ($J = 2.3, 5.0, 9.9$ Hz)	1.74 ($J = 3.0, 6.0, 9.5$ Hz)
6	H _f	2.67 ($J = 4.9, 12.5$ Hz)	2.61 ($J = 5.0, 12.4$ Hz)	2.73 ($J = 6.5, 11.5$ Hz)
7	H _g	1.95 ($J = 2.4, 4.7$ Hz)	1.99 ($J = 2.3, 4.8$ Hz)	1.91 ($J = 2.5, 7.5$ Hz)
8	H _h	1.13 ($J = 6.6$ Hz)	1.10 ($J = 6.6$ Hz)	1.19 ($J = 7.0$ Hz)

3.7. APKR WITH CIS-FUSED, LACTAM-TETHERED ALLENE-YNE SUBSTRATES

Although the only cis lactam-tethered allene-yne that was isolated as a pure compound was the α -methyl lactam **3.207** discussed above, mixtures of **3.135** and **3.136** or **3.182** and **3.183** were

subjected to the APKR slow addition conditions. Cis lactams with TIPS-substituted alkynes **3.135** and **3.136** (3:1), afforded a 3:1 mixture of tricyclic products **3.199** and **3.201** in 40% combined yield, a yield comparable to trans lactam **3.125** (Table 3.3, entry 3). The product ratio of **3.199** to **3.201** was determined by integration of H_b in the ¹H NMR spectrum which appeared as doublets at 5.01 and 4.65 ppm for **3.199** and **3.201**, respectively. Lactams **3.199** and **3.201** were separated for characterization purposes. An APKR time of 180 min was required for this TIPS-substituted alkyne, just like the trans lactam **3.125**. Terminal alkynes **3.182** and **3.183** (3:1), provided a 3:1 mixture of fused tricycles **3.201** and **3.202** in 41% combined yield. The product ratio of **3.201** to **3.202** was determined by integrating H_b, which appeared as doublets at 4.72 and 4.54 ppm for **3.201** and **3.202**, respectively. Based upon these two examples, there are only subtle differences between the cis and trans lactams in the APKR.



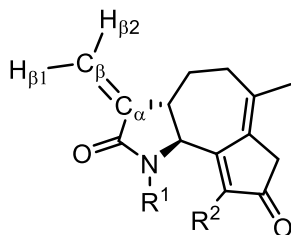
Scheme 3.47. APKR of mixtures of α -methylene and α -methyl- γ -lactams.

3.8. ANALYSIS OF ^{13}C AND ^1H NMR DATA FOR ESTIMATING THE ELECTROPHILIC REACTIVITY OF α -METHYLENE- γ -LACTAM GUAIANOLIDE ANALOGS

^{13}C NMR can be used to estimate the electrophilicity of a given carbon, where resonances shifted downfield correspond to more electrophilic carbon atoms. For example, scientists at Amgen showed that, for a series of *N*-aryl acrylamides containing electron-donating and electron-withdrawing aryl substituents, the chemical shift of the β -carbon and the β -hydrogen correlated well with the rate of glutathione (GSH) addition to these acrylamides (see Chapter 1 for rate data).⁹¹ The chemical shifts of the β -carbons ranged from 125.6-128.7 ppm and showed a correlation coefficient (R^2) of 0.80 to the rates of GSH addition to these acrylamides. The chemical shifts of the most downfield β -hydrogens ranged from 5.65-5.86 ppm and correlated to the rate of GSH addition with an R^2 of 0.71 for these structurally similar acrylamides.⁹¹ When more structurally diverse acrylamides were compared, such as *N*-aryl, *N*-alkyl and/or acrylamides with substituents at the α or β position of the alkene, the ^{13}C NMR chemical shifts of the α and β -carbons did not correlate to the rates of glutathione addition.⁹³

Based upon work described by Amgen, the chemical shifts of the α -carbons, β -carbons, and β -hydrogens were tabulated for tricyclic α -methylene- γ -lactams in Table 3.6 as the first step in establishing whether this data could be used to estimate electrophilic reactivity. The α and β carbons (C_α and C_β) were assigned based on the DEPT135 spectra, while the more downfield β -hydrogen was assigned as $\text{H}_{\beta 2}$. Overall, the results show that stronger electron withdrawing substituents on the nitrogen atom result in a downfield shift of the β -carbon that correlates to the expected electron withdrawing capacity of the substituent. For example, a methyl substituent and

a hydrogen on the lactam nitrogen showed chemical shifts of the β -carbon at 115.55 and 115.33 (entries 1-2); it was observed that the cyclopentenone substituent had little effect on the chemical shift of the β -carbon (compare entries 2, 3, and 5). Surprisingly, cis lactam **3.199** showed a significant increase in the chemical shift of the β -carbon from 115.73 ppm for trans lactam **3.184** to 118.48 ppm for **3.199**, potentially indicating that cis α -methylene- γ -lactams are more electrophilic than trans substituted α -methylene- γ -lactams (entries 3-4). This increase is likely due to strain in the product because, prior to the APKR, the cis and trans lactams had similar chemical shifts for C_β (117.2 for cis and 117.0 for trans). *N*-aryl lactams **3.186-3.189** had β -carbons that were shifted downfield relative to *N*-methyl or *N*-unsubstituted lactams **3.56, 3.116, 3.184-3.185**, and their chemical shifts ranged from 116.66 for *para*-methoxy aryl lactam **3.189** to 118.81 for *para*-cyano aryl lactam **3.188**; the chemical shifts increased with the electron withdrawing capacity of the aryl substituent (entries 6-9). Thiophene substituted lactam **3.190** had a β -carbon chemical shift of 117.77 ppm, which was further downfield than the electronically neutral phenyl substituted lactam **3.186** and electron-rich methoxy aryl substituted lactam **3.189** but further upfield than the electron-poor trifluoromethyl and cyano aryl substituted lactams **3.187** and **3.188** (compare entry 10 to entries 6-9). Substitution of the nitrogen atom with stronger electron withdrawing groups such as an acyl, tosyl, and carbonate substituent resulted in a downfield shift of the β -carbon compared to the *N*-aryl lactams; the chemical shifts of the β -carbons ranged from 119.48-121.43 for these strong electron-withdrawing nitrogen substituents (entries 11-13).

Table 3.6. ^{13}C and ^1H NMR data for α -methylene- γ -lactam guaianolide analogs.

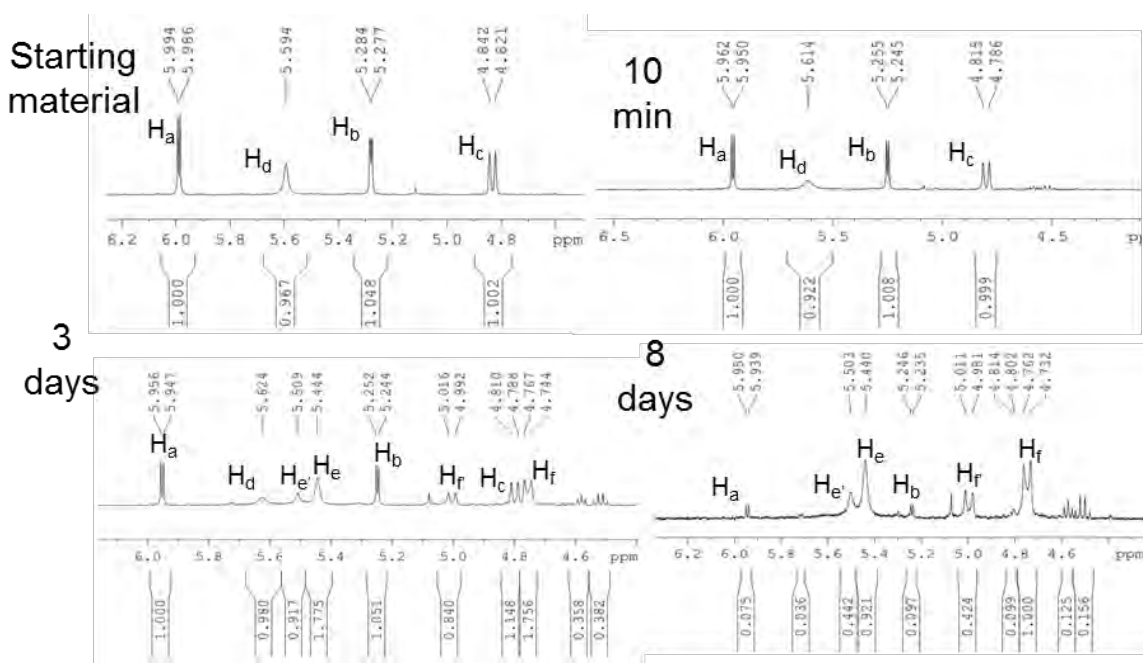
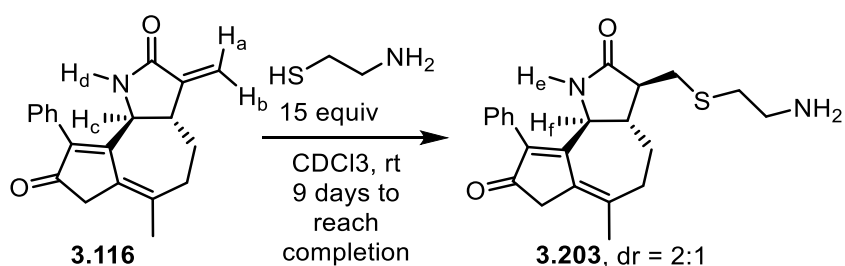
Entry	R ¹	R ²	Cmpd.	C _β (ppm)	C _α (ppm)	H _{β1} (ppm)	H _{β2} (ppm)
1	Me	Ph	3.56	115.55	143.18	6.101	5.339
2	H	Ph	3.116	115.33	143.14	5.983	5.272
3	H	TIPS	3.184	115.73	143.11	6.071	5.306
4	H ^a	TIPS ^a	3.199	118.48	143.43	6.211	5.463
5	H	H	3.185	115.77	143.86	6.061	5.316
6	Ph	Ph	3.186	117.11	143.64	6.243	5.505
7	4-CN-C ₆ H ₄	Ph	3.188	118.81	142.64	6.299	5.548
8	4-CF ₃ -C ₆ H ₄	Ph	3.187	118.15	143.05	6.281	5.518
9	4-OMe-C ₆ H ₄	Ph	3.189	116.66	143.73	6.215	5.441
10	2-thiophene	Ph	3.190	117.77	141.83	6.698	5.493
11	Ac	Ph	3.196	120.64	142.78	6.295	5.540
12	Tosyl	Ph	3.191	121.43	145.31	6.158	5.434
13	Boc	Ph	3.192	119.88	142.78	6.290	5.500

a) Cis-lactam

3.9. THIOL REACTIVITY OF α -METHYLENE- γ -LACTAMS

To measure the relative electrophilic reactivity of α -methylene- γ -lactams and to test whether the chemical shift of the β -carbon in the ^{13}C NMR was an accurate predictor of this, four different lactams were reacted with excess cysteamine, a thiol that purportedly mimics biothiols, in chloroform-*d* (see Chapter 1).⁷⁸ First, the α -methylene- γ -lactam **3.116** possessing an NH group was reacted with cysteamine (15 equiv) in chloroform-*d*. The progress of the hetero-Michael addition reaction was monitored by the disappearance of the α -methylene hydrogen resonances in the ^1H NMR (Scheme 3.49). Lactam **3.116** required 9 d for the complete disappearance of these

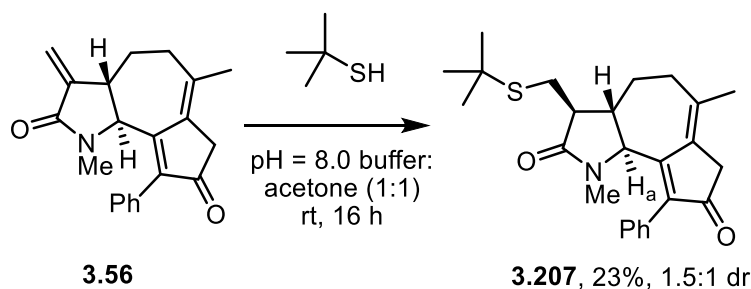
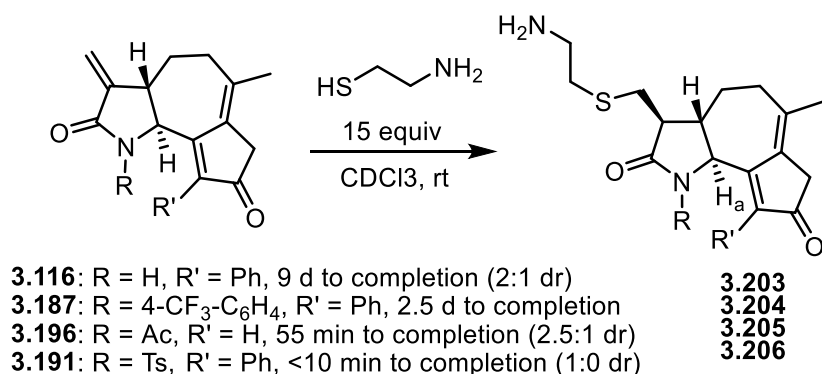
resonances. Two diastereomeric products were formed in a ratio of 2:1 as determined by integration of H_f and H_f . The major diastereomer (shown) is predicted based upon this being the most thermodynamically stable isomer.



Scheme 3.48. ^1H NMR monitoring of cysteamine addition to an α -methylene- γ -lactam.

The moderately electron withdrawing trifluoromethyl aryl substituted lactam **3.187** reacted completely with cysteamine in 2.5 d under the same conditions; the dr could not be determined due to impurities obscuring the resonance of H_a in the spectrum (Scheme 3.50). Lactam **3.196**, possessing a strong electron withdrawing acetyl group on the lactam nitrogen reacted completely

in 55 min, and lactam **3.191**, also containing a strongly electron withdrawing *N*-tosyl substituent, reacted completely in less than 10 min. The dr was determined by integration of H_a, and the major diastereomer was predicted to be the trans, trans isomers shown. Efforts to purify thiol adducts **3.203-3.206** to confirm structure were thwarted by their instability to column chromatography. Therefore, *N*-methyl lactam **3.56** was reacted with *tert*-butyl thiol in a buffered solution to form thiol adduct **3.207** in 23% yield as a 1.5:1 ratio of diastereomers. The thiol adduct **3.207** was purified by extraction into dichloromethane and full characterization of this mixture confirmed the structural identity of thiol adducts **3.203-3.207** and that only one equivalent of thiol was added to the exocyclic alkene of **3.207**.



Scheme 3.49. Thiol additions to α -methylene- γ -lactams.

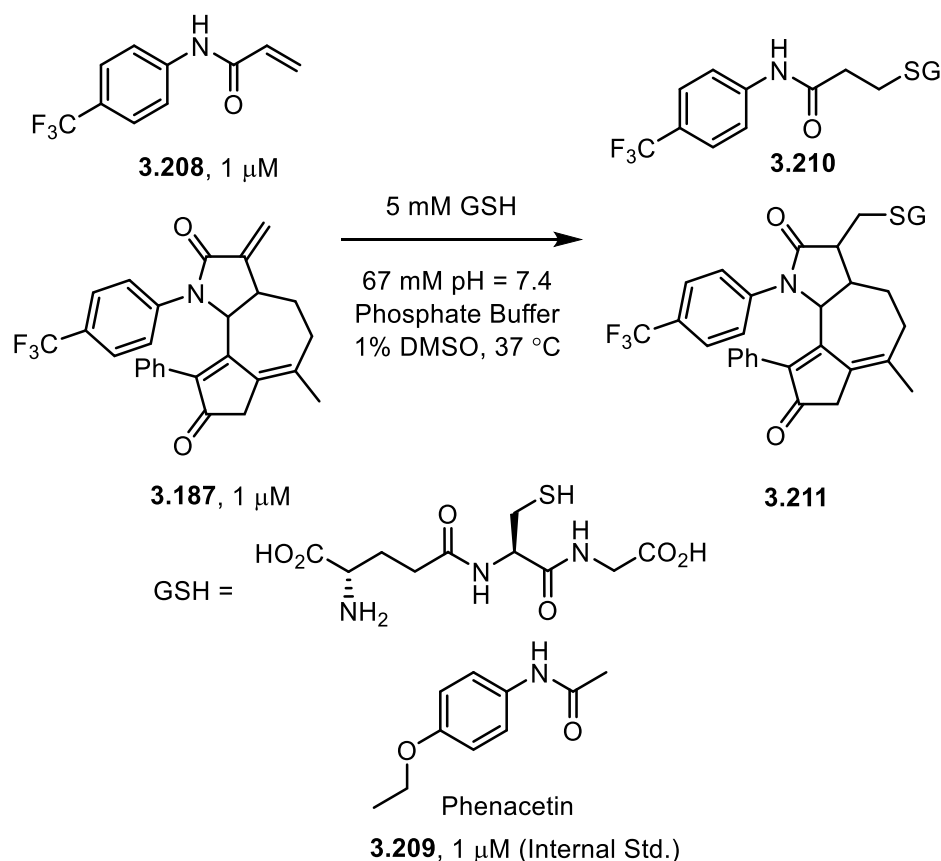
The chemical shift of β -carbon in the ¹³C NMR was the most accurate predictor of electrophilic reactivity, which consistently shifted further downfield as stronger electron-

withdrawing groups were installed. The chemical shift correlated well with the rate of cysteamine addition (compare entries 2, 8, 11, and 12, Table 3.6). The chemical shift of the α -carbon in the ^{13}C NMR did not correlate to the electrophilic reactivity of the α -methylene- γ -lactam. Indeed, in some cases the α -carbon was shifted upfield when electron withdrawing substituents were attached to the lactam nitrogen (compare entries 1 and 8 or entries 2 and 11, Table 3.6). The β -hydrogens tended to shift downfield as stronger electron withdrawing groups were installed on the lactam nitrogen (compare entries 1 and 7 or 2 and 8). However, *N*-aryl lactams had β -hydrogens which were further downfield than the *N*-tosyl and *N*-Boc lactams (compare entries 6 and 13 or entries 9 and 12).

3.9.1 Rate of Glutathione (GSH) Addition to an α -Methylene- γ -lactam: Rate Constant and Half-life

To measure the electrophilic reactivity of α -methylene- γ -lactams to known acrylamides, the rate of glutathione (GSH) addition to *N*-trifluoromethylaryl lactam **3.187** was benchmarked against the rate of known *N*-aryl acrylamide **3.208**. When acrylamide **3.208** was reacted with GSH in phosphate buffer at 37 °C (conditions meant to mimic a biological environment), the half-life was 39.5 min (Scheme 3.51).⁹¹ The consumption of electrophiles **3.208** and **3.187** was measured by calculating the peak area ratios (peak area electrophile/peak area of stable internal standard) from the mass spectrum relative to the stable internal standard, phenacetin (**3.209**). The relative abundance of the electrophiles was determined from the total ion concentration. Although this method does not give the actual concentrations of the electrophiles due to differences in ionization efficiencies, the decrease of the electrophile concentration over time can be determined since the

internal standard does not change. The rate constants were then calculated by fitting this data to the pseudo-first-order kinetic equation (Equation 3.1). Half-lives were calculated according to Equation 3.2. It was hypothesized that α -methylene- γ -lactams would react slower than acrylamides as alkyl substituents at the α -position of α,β -unsaturated carbonyls generally decrease the electrophilic reactivity.¹¹⁶ MS experiments were performed with the assistance of Dr. Bhaskar Ghodugu at the University of Pittsburgh.



Scheme 3.50. Experimental conditions to compare the rate of GSH addition to an acrylamide compared to an α -methylene- γ -lactam.

$$\ln([\textit{acrylamide}]) = -k_{\textit{pseudofirst}} t + \ln([\textit{acrylamide}]_0)$$

Equation 3.1. Rate equation for GSH addition to acrylamides (or α -methylene lactams).

$$t_{1/2} = \frac{\ln 2}{k_{\text{pseudo first}}}$$

Equation 3.2. Calculation of half-life from pseudo-first order rate constants.

The rate of glutathione addition to acrylamide **3.208** was calculated as 0.018 min^{-1} which corresponds to a half-life of 38.5 min (Figure 3.3, A), compared to the literature value of 39.5 min. Although the rate and half-life are close to the literature value, the y-intercept is expected to be 1 (observed y-intercept = -0.3835). This could be due to differences in the ionization efficiencies or differences in the initial concentrations of reagents. The rate of glutathione addition to tricycle **3.187** was calculated as 0.0162 min^{-1} , corresponding to a half-life of 42.8 min (Figure 3.3, B). As expected, α -methylene- γ -lactam-containing guaianolide analogs react slower with GSH than the corresponding acrylamides, although more examples are needed to confirm this observation.

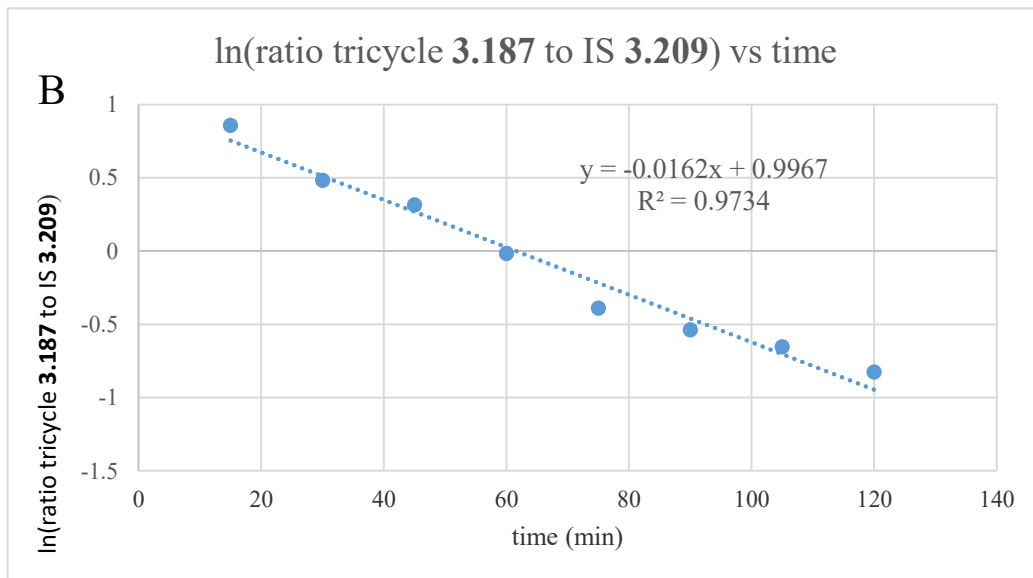
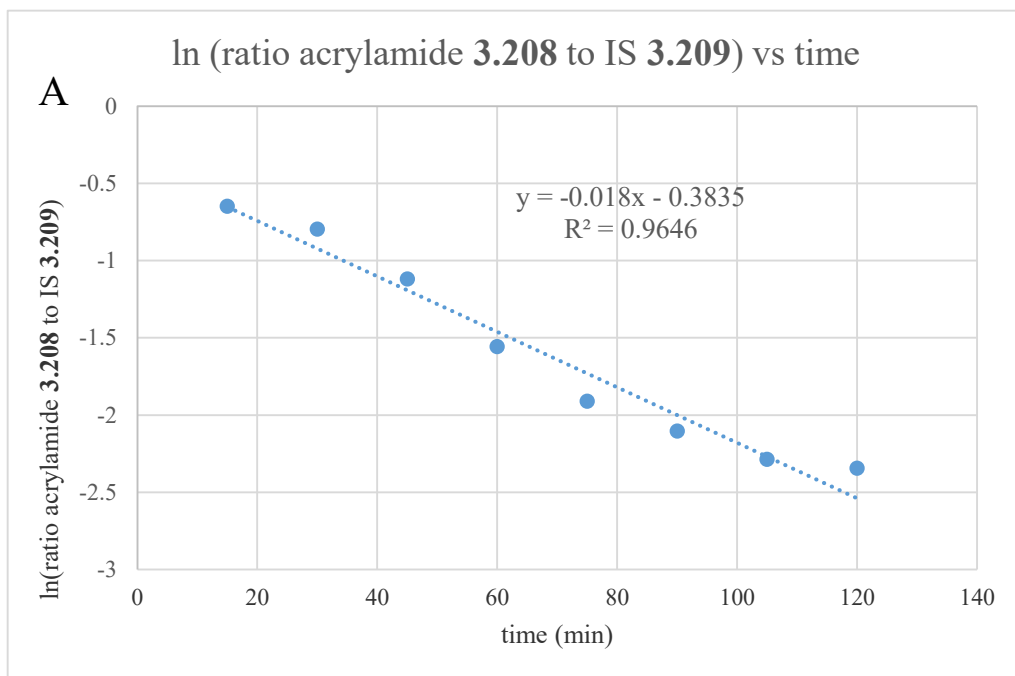


Figure 3.3: Depletion of acrylamide **3.208** (A) or tricycle **3.187** (B) over time.

The reaction mixture was prepared by adding 2 μL of each 1 mM DMSO stock solutions of acrylamide **3.208**, tricycle **3.187**, and phenacetin **3.209** to 1.794 mL of 67 mM phosphate buffer (pH = 7.4). This was divided into two 900 μL portions (1 control and 1 reaction). To the control

vial was added 100 μL of phosphate buffer. To the reaction vial was added 100 μL of 50 mM GSH solution (in phosphate buffer) and both were lowered into an oil bath set to 37 $^{\circ}\text{C}$ and allowed to react without stirring. Thus, the final concentrations of reagents in the reaction vial were: 1 μM of acrylamide **3.208**, 1 μM of tricycle **3.187**, 1 μM of phenacetin (**3.209**), and 5000 μM GSH all in 67 mM, pH = 7.4 phosphate buffer. Aliquots (50 μL) of the reaction mixture were taken every 15 min for 2 h, placed in an autosampler vial, and injected into a Thermo Scientific Q-Exactive Orbitrap MS with separation of the compounds by HPLC using the method described below. The ions were observed using single ion monitoring in ESI+ mode. The compounds were separated using a Thermo Scientific Hypersil GOLD column 1.9 μM (2.1 x 100 mm) using a gradient of 5-95% of 0.1% formic acid in acetonitrile (B) to 0.1% formic acid in water (A). Table 3.7 shows the time and gradient used for compound separation.

Table 3.7. Gradient of 0.1% formic acid in MeCN (B) to 0.1% formic acid in H₂O (A).

Time (min)	Mobile Phase B (%) = 0.1% formic acid in MeCN
1	5%
5	95%
6	95%
8	5%

3.10. BIOLOGICAL ACTIVITY OF α -METHYLENE- γ -LACTAM GUAIANOLIDE ISOSTERES: CYTOTOXICITY AND NF- κ B PATHWAY INHIBITION

Experiments in this section were performed by our collaborators in Professor Daniel Harki's laboratory at the University of Minnesota (John Widen, Henry Schares, Joseph Hexum)

3.10.1. Introduction to the NF- κ B Pathway

Inhibition of the NF- κ B (nuclear factor κ B) pathway promotes apoptosis, and this pathway is frequently overactive in cancer and inflammatory diseases.²⁶⁻²⁷ Thus, it represents a desirable drug target. Natural products and synthetic small molecules are known to inhibit the NF- κ B (nuclear factor κ B) pathway through a variety of mechanisms.^{21,26,151} One such mechanism is the alkylation of Cys38, located in the DNA-binding domain of p65 (also referred to as RelA), and this inhibits DNA binding of the NF- κ B heterodimer, made up of p50 and p65 subunits. Inhibition of DNA binding has been proposed as a general mechanism of action for inhibition of the NF- κ B pathway by guaianolides and other Michael acceptors.²⁵ Indeed, mutation of Cys38 to serine in p65 resulted in a protein that was resistant to DNA-binding inhibition by helenalin (**3.212**, Scheme 3.52).²¹⁵

Figure 3.4 summarizes the NF- κ B pathway and shows where in the pathway different compounds have been shown to inhibit.²⁶ The NF- κ B pathway is activated in response to numerous stimuli, which in turn activate the inhibitor of NF- κ B kinase (IKK). When NF- κ B is inactive, it is sequestered in the cytoplasm of the cell by the protein I κ B (inhibitor of NF- κ B). When IKK is activated, it phosphorylates I κ B, leading to degradation of I κ B by the proteasome. Upon degradation of I κ B, the p50/p65 heterodimer is released and is free to enter the nucleus where it

binds to DNA. Once bound to DNA, NF- κ B increases the rate of transcription for anti-apoptotic genes, as well as proteins involved in cell proliferation and cell invasion. The NF- κ B pathway can be inhibited at various stages. These include blocking stimuli that activate IKK (nonsteroidal anti-inflammatory drugs (NSAIDs), thalidomide), inhibition of I κ B phosphorylation by IKK, prevention of nuclear translocation (silibinin), and prevention of DNA-binding by the p50/p65 heterodimer (sesquiterpene lactones).

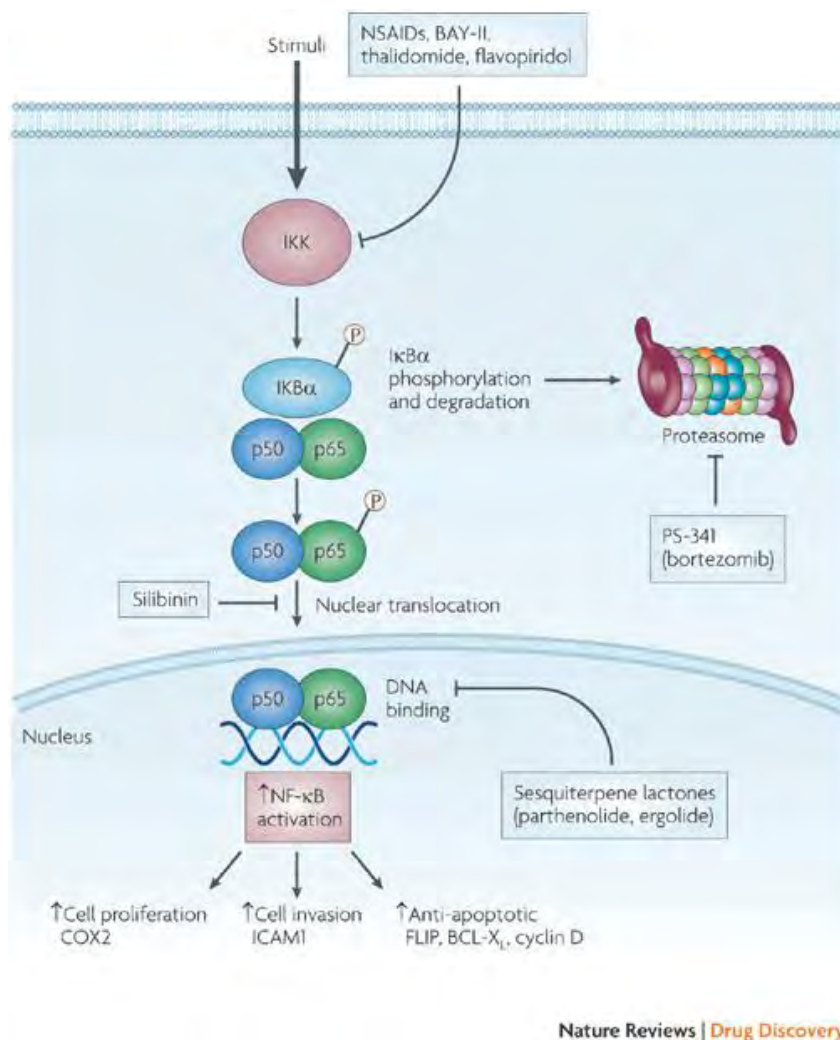
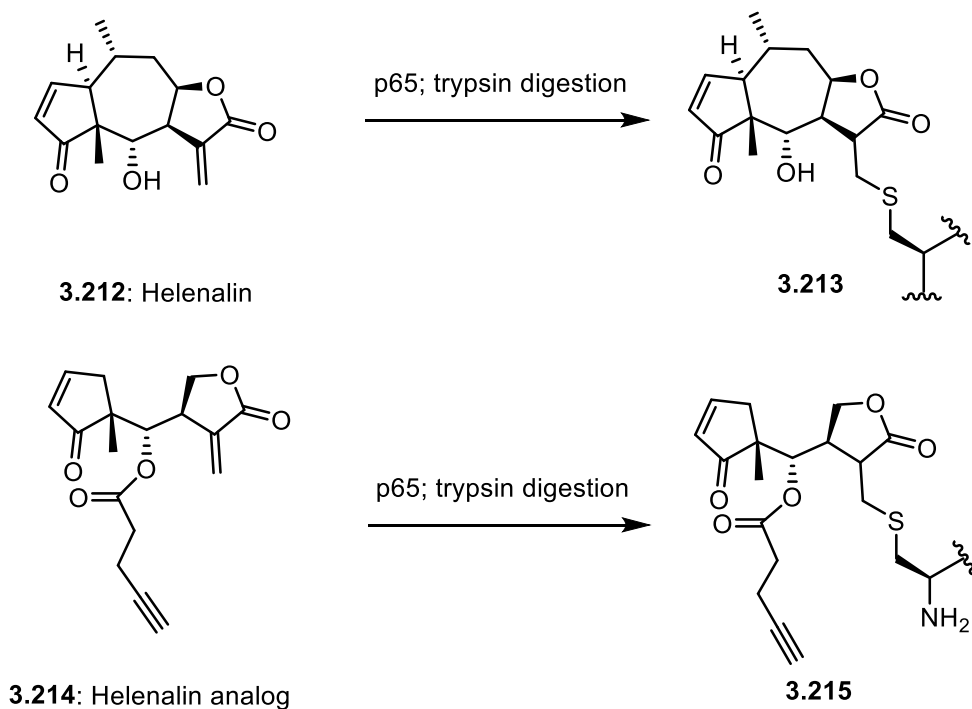


Figure 3.4. Summary of NF- κ B pathway with major points of inhibition. Reprinted with permission from Macmillan Publishers Ltd: *Nature Reviews Drug Discovery*, 2008, 7, 1031-1040, ©2008. DNA binding by the p50/p65 heterodimer is the most downstream process in the canonical NF- κ B signaling pathway. Inhibition of DNA-binding is favorable because targeting upstream

proteins results in off-target effects due to the involvement of those proteins in other cellular pathways.²⁷ Certain sesquiterpene lactones, such as helenalin (**3.212**) and simplified analog **3.214** inhibit the DNA binding of the p50/p65 transcription factor heterodimer by forming a covalent bond between the α -methylene- γ -lactone and the sulfhydryl group (Cys-38) of the p65 protein (Scheme 3.53).²¹⁶⁻²¹⁷ Covalent labeling of Cys38 on p65 was observed by MS analysis of peptide fragments after trypsin digestion. A peptide corresponding to YKC³⁸EGR bound to helenalin was detected, and a peptide corresponding to C³⁸EGR bound to simplified helenalin analog **3.214** was detected.²¹⁷ Protein pull-down studies also demonstrated that p65 was covalently labeled by **3.214**, but I κ B α , p50, and IKK α/β were not covalently labeled. Thus, covalent inhibition of p65 is a potential method for inhibiting the NF- κ B pathway.



Scheme 3.51. Reaction of helenalin or analog with Cys38 of p65.

3.10.2. Inhibition of the NF- κ B Pathway by α -Methylene- γ -lactam Guaianolide Analogs

Helenalin (**3.212**) is an 8,12-guaianolide; 6,12 guaianolides are thought to inhibit the NF- κ B pathway in a similar fashion. Previously, guaianolide analogs **3.216** and **3.217** containing an α -methylene- γ -lactone were synthesized in our lab and displayed inhibition of the NF- κ B pathway at low μ M levels, similar to the natural product parthenolide (**3.218**, Figure 3.5).¹¹⁸ Thus, it was hypothesized that α -methylene- γ -lactam guaianolide analogs would also inhibit the NF- κ B pathway and that this inhibition would occur through prevention of DNA-binding by the p50/p65 heterodimer. As discussed in Chapter 1 on thiol reactivity, α -methylene- γ -lactams are less reactive towards thiols than similar lactones. If alkylation of Cys38 on p65 is promoted by noncovalent interactions, the reduced electrophilic reactivity of α -methylene- γ -lactams would reduce the amount of off-target reactivity when compared to α -methylene- γ -lactones.²¹⁷ However, this reduced electrophilic reactivity could prevent or slow alkylation of Cys38 of p65, thus reducing or eliminating inhibition of the NF- κ B pathway by α -methylene- γ -lactams. This is why ability to tune the electrophilic reactivity of α -methylene- γ -lactams is important, as tunable guaianolide analogs could enable the development of α -methylene- γ -lactam guaianolide analogs that maximize covalent inhibition while minimizing off-target reactions.

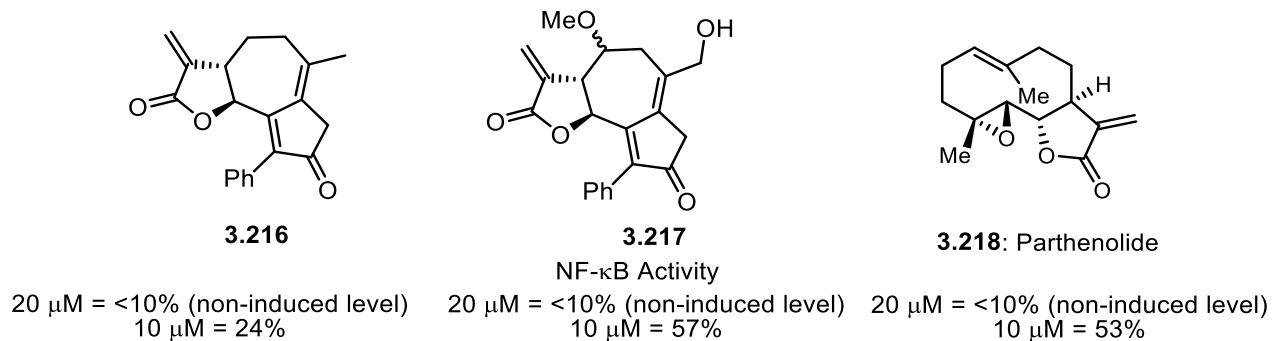


Figure 3.5. Synthetic guaianolide analogs and natural product parthenolide with remaining NF- κ B activity following treatment of cells with inhibitor.

Based on the ability of 6,12-guaianolides to inhibit the NF- κ B pathway, this pathway would provide a testing ground for comparisons of bioactivity between α -methylene- γ -lactams and α -methylene- γ -lactones, both in terms of NF- κ B inhibition and cytotoxicity. Experiments to determine inhibition of the NF- κ B pathway and cytotoxicity of α -methylene- γ -lactam guaianolide analogs was performed by our collaborators in the Harki laboratory (John Widen, Henry Schares, Joseph Hexum) at the University of Minnesota. NF- κ B inhibition was measured using a stably transfected A549 cell line containing a luciferase gene driven by NF- κ B activation. Induction of the NF- κ B pathway with TNF α (tumor necrosis factor α) results in an increase in reporter luminescence corresponding to NF- κ B activation. Upon inhibition of the NF- κ B pathway, reporter luminescence is decreased. Induced cells without inhibitor and non-induced cells were used as controls to measure the relative NF- κ B activity of cells treated with an inhibitor. Select compounds **3.56**, **3.185**, **3.186**, **3.187**, **3.189**, **3.191**, **3.196** were dosed at 50, 20, 10, and 5 μ M to cells before inducing with TNF- α for eight hours (Figure 3.6). These compounds were chosen to examine the effect of different nitrogen substituents (e.g. electron donating and electron withdrawing) on NF- κ B inhibition. Additionally, these compounds were tested for cytotoxicity at the same

concentrations by measuring the cell viability after 48 h using A549 cells and an Alamar blue assay. In this assay, A549 cells were treated with inhibitors **3.56**, **3.185**, **3.186**, **3.187**, **3.189**, **3.191**, **3.196** for 48 h (Figure 3.6).²¹⁸ At the 46 h mark, Alamar blue (cell viability reagent) was added to the cells. The Alamar blue assay evaluates the ability of metabolically active cells to convert resazurin (a nonfluorescent compound) to resorufin (a red fluorescent compound). The amount of fluorescence provides the number of live cells relative to a control which was not treated with any inhibitors. The goal was to explore the potential of α -methylene- γ -lactam guaianolide analogs as biologically active compounds and potentially discover a compound with good NF- κ B pathway inhibition and minimal toxicity. The hypothesis was that an α -methylene- γ -lactam with intermediate electrophilic reactivity would maximize NF- κ B inhibition and minimize cellular toxicity.

α -Methylene- γ -lactam **3.185** (NH) or **3.56** (NMe), did not inhibit the NF- κ B pathway at any concentration (5, 10, 20, 50 μ M) tested (Figure 3.6). These two lactams were also not cytotoxic as evidenced by cell viabilities above 80% when cells were treated with 50 μ M of **3.185** or **3.56** (Figure 3.7). α -Methylene- γ -lactams **3.186** (NPh) and **3.189** (N-4-OMe-C₆H₄) were also not cytotoxic at the highest concentration (50 μ M) tested. However, both lactams **3.186** and **3.189** showed weak inhibition of the NF- κ B pathway at 20 μ M, and at 50 μ M these compounds reduced NF- κ B activity to 54% or 60%, respectively, relative to the control. Lactam **3.191**, (NTs), reduced NF- κ B activity to 33% relative to induced levels at 5 μ M and to noninduced levels at 10 μ M. However, lactam **3.191** was cytotoxic, reducing cell viability by 20% at 5 μ M and by 36% at 10 μ M. α -Methylene- γ -lactam **3.196** (NAc) displayed NF- κ B inhibition with 59% remaining NF- κ B activity at 10 μ M and 29% remaining activity at 20 μ M. A concentration of 50 μ M **3.196** reduced NF- κ B activity to noninduced levels, but was cytotoxic with only 62% cell viability compared to

nontreated cells. The most promising biological activity was displayed by α -methylene- γ -lactam **3.187** (N-4-CF₃-C₆H₄). Lactam **3.187** reduced NF- κ B activity to 62% at 10 μ M, 21% at 20 μ M, and to non-induced levels (6%) at 50 μ M. Additionally, **3.187** was only minimally cytotoxic (88% cell viability relative to nontreated cells) at the highest concentration (50 μ M) tested. Figure 3.8 shows the correlation between NF- κ B activity and cellular toxicity for most α -methylene- γ -lactams tested by plotting the percentage of NF- κ B activity relative to the percentage of cell viability. Lactam **3.187**, containing the 4-trifluoromethyl phenyl substituent, is the outlier on this graph, where NF- κ B inhibition is not accompanied by an increase in cytotoxicity.

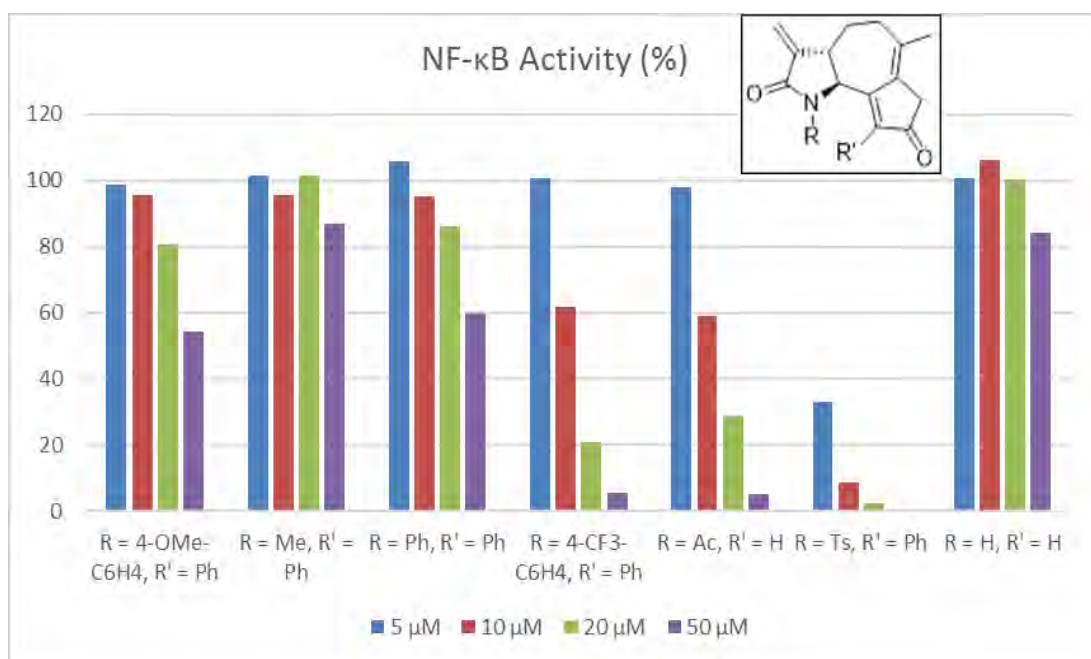


Figure 3.6. Graph of NF- κ B activity relative to induced levels for α -methylene- γ -lactams. In order the lactams are **3.189** (R = 4-OMe-C₆H₄), **3.56** (R = Me), **3.186** (R = Ph), **3.187** (R = 4-CF₃-C₆H₄), **3.196** (R = Ac), **3.191** (R = Ts), **3.185** (R = H).

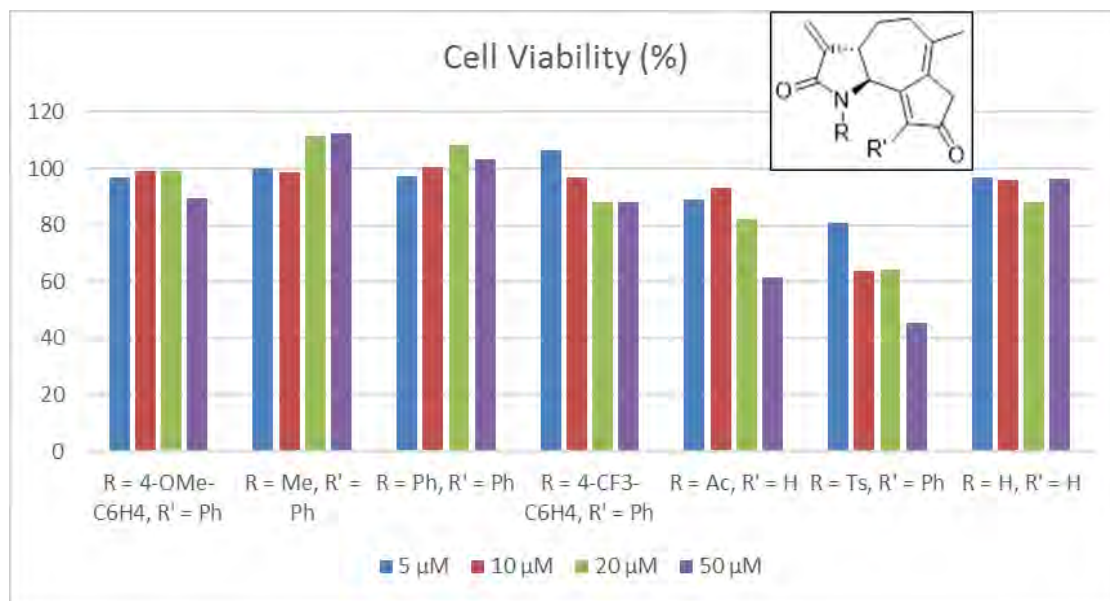


Figure 3.7. Graph of cell viability relative to nontreated cells for α -methylene- γ -lactams. In order the lactams are **3.189** (R = 4-OMe-C₆H₄), **3.56** (R = Me), **3.186** (R = Ph), **3.187** (R = 4-CF₃-C₆H₄), **3.196** (R = Ac), **3.191** (R = Ts), **3.185** (R = H).

In order to confirm that NF- κ B inhibition was not an artifact of the luciferase assay, α -methylene- γ -lactams were also tested for NF- κ B inhibition in HEK293 cells using a SEAP (secreted embryonic alkaline phosphatase) assay; similar NF- κ B inhibition was observed.²¹⁹ Cytotoxicity of HEK293 cells was also measured using the Alamar blue assay described above. In the SEAP assay, a decrease in alkaline phosphatase production corresponds to a decrease in NF- κ B activity. In this case, the alkaline phosphatase cleaves a phosphate from an indole phosphate to generate a chemiluminescent indole, much the same way that oxidation of luciferin by luciferase produces luminescence. These mechanistically distinct measurements of NF- κ B inhibition in two different cell lines provide confidence that the NF- κ B pathway is inhibited by α -methylene- γ -lactams.

In summary, α -methylene- γ -lactams containing electron withdrawing substituents (**3.187**, **3.196**, **3.191**) displayed comparable NF- κ B activity to the lactones **3.216** and **3.217** previously prepared in our lab (Figure 3.6 and 3.7). In the case of **3.187**, containing a 4-trifluoromethyl phenyl substituent, increased NF- κ B inhibition was not accompanied by increased cytotoxicity. Additionally, lactams containing a secondary amide (**3.185**), electron donating alkyl (**2.56**) or aryl (**3.189**) groups, and an electronically neutral phenyl group (**3.186**) were not cytotoxic even at high concentrations. Although, these lactams were inactive in the NF- κ B pathway, their lack of cytotoxicity means they could be used to inhibit other biological targets. Finally, inhibition of the NF- κ B pathway and cytotoxicity were related to the electrophilic reactivity of various α -methylene- γ -lactams. There is a correlation between time of reactivity with cysteamine in the ^1H NMR studies (see section 3.10) and amount of inhibition of the NF- κ B pathway for the derivatives **3.187**, **3.196**, and **3.191** where shorter reaction times relate to increased inhibitory activity. Additionally, compounds **3.196** and **3.191** that reacted rapidly with cysteamine (<10 min and 60 min to react completely, respectively) were cytotoxic, while **3.187**, which reacted more slowly with cysteamine (2.5 d to react completely) was not cytotoxic.

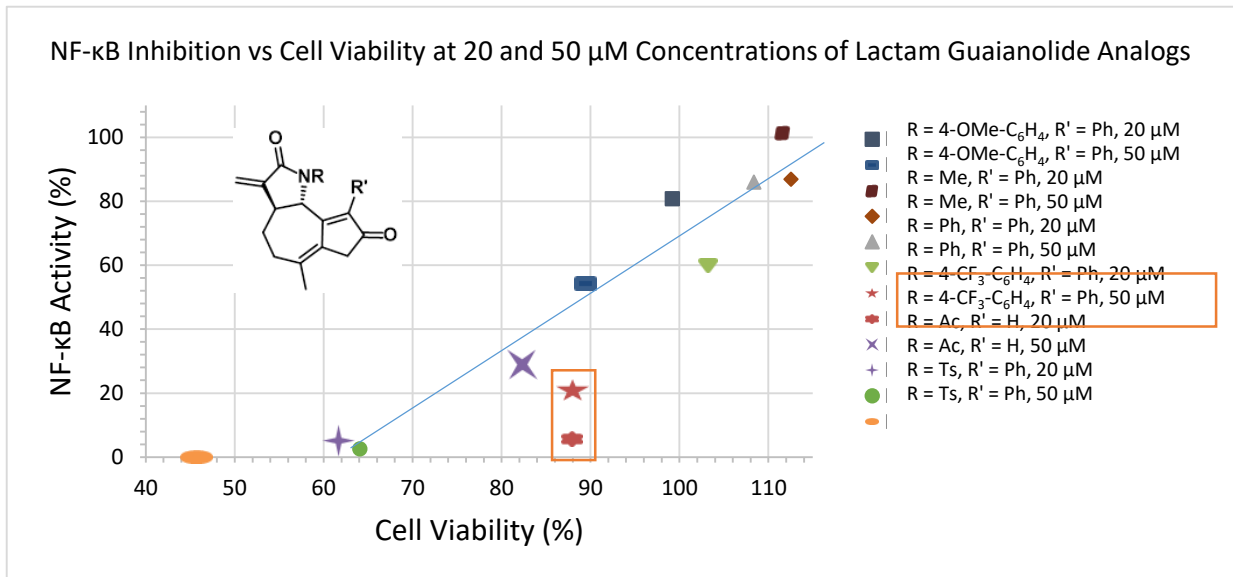


Figure 3.8. Plot of NF-κB activity and cellular toxicity for α-methylene-γ-lactams.

4.0. ALLENYL ACETATES IN THE ALLENIC PAUSON-KHAND REACTION WITH α -METHYLENE- γ -LACTAM-TETHERED ALLENE-YNES AND AN UNEXPECTED [2 + 2] CYCLOADDITION PRODUCT

4.1. INTRODUCTION

6,12-Guaianolides contain various degrees of oxidation, which is one representation of their molecular complexity when considering their synthetic accessibility. Oxidation level has been calculated by considering the 6,12-guaianolide skeleton **4.1** as having an oxidation level of zero (Figure 4.1). From this starting point, each additional alkene, hydroxyl, or ether attached directly to the guaianolide skeleton raises the oxidation level by 1; epoxides or carbonyls raise the oxidation level by 2.¹¹⁸ Thus, thapsigargin (**4.2**) and eupatochinilide VI (**4.3**) have oxidation levels of 7, moxartenolide (**4.4**) has an oxidation level of 6, ixerin (**4.5**) has an oxidation level of 5, arglabin (**4.6**) and leucodin (**4.7**) have oxidation levels of 4, and compressanolide (**4.8**) has an oxidation level of 2. Others have considered the oxidation level as the number of skeletal carbons with an oxygen substituent; alkenes are not counted.²²⁰ Thus, the guaianolide skeleton would have an oxidation level of 3, while thapsigargin would have an oxidation level of 9. Preparing more oxygenated [5,7,5]-guaianolide analogs would be beneficial because many guaianolide natural products contain higher oxidation levels. Using the principles of redox economy,²²¹ it was proposed that an APKR between allenyl acetates and an alkyne tethered by an α -methylene- γ -lactam would enable a redox economical method for the preparation of 6,12-guaianolide analogs containing an α -methylene- γ -lactam in place of the α -methylene- γ -lactone, with an additional α -acyloxy substituent on the cyclopentenone ring.

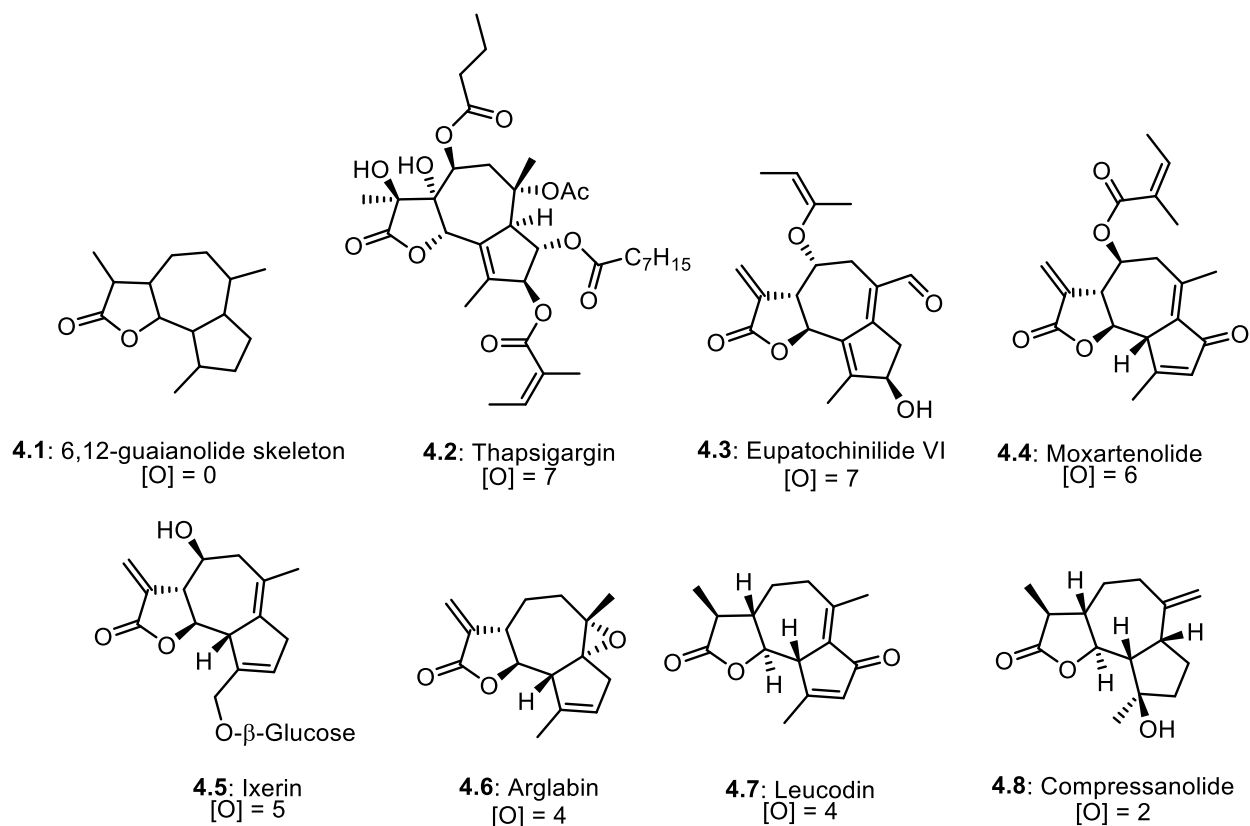
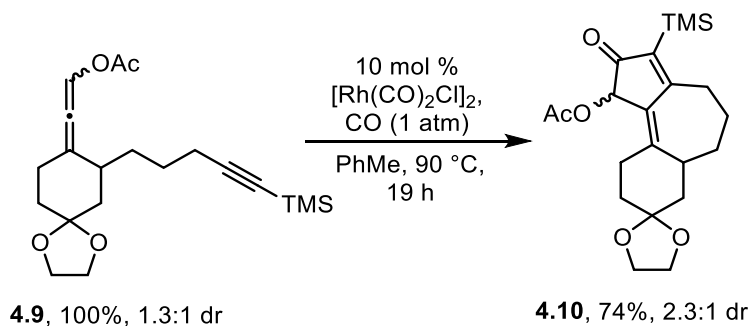


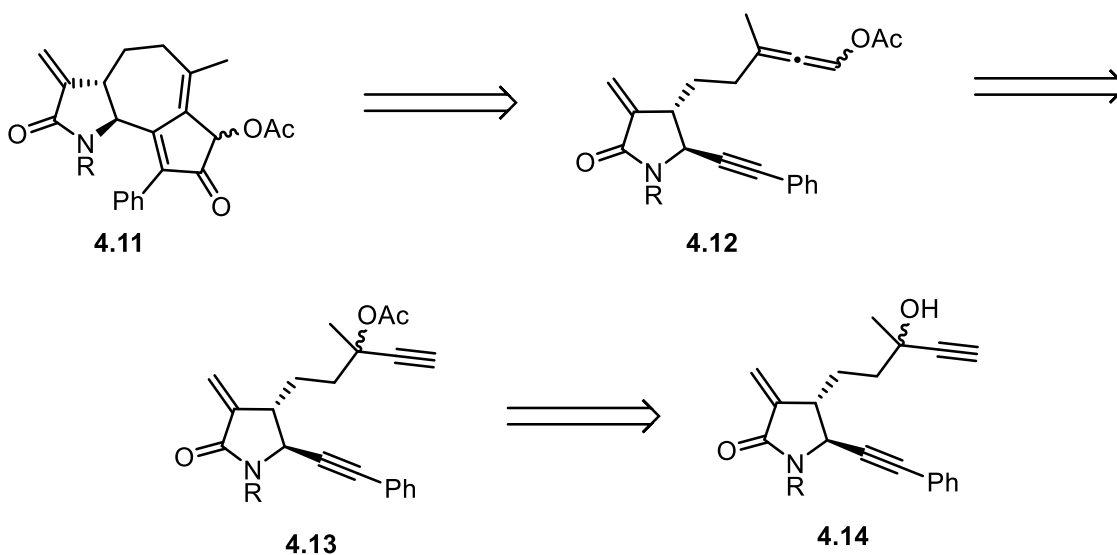
Figure 4.1. Oxidation level of naturally occurring 6,12-guaianolides.

Our group has previously demonstrated the ability of allenyl acetates to undergo the APKR to form α -acetoxy cyclopentenones.²²² For example, allenyl acetate **4.9** (1.3:1 dr) was subjected to rhodium biscarbonyl chloride dimer to form α -acetoxy cyclopentenone fused to 7-membered ring **4.10** with a 2.3:1 dr. This increase in diastereoselectivity is a result of the allenyl acetate undergoing a rapid scrambling of axial chirality.²²²



Scheme 4.1. APKR of allenyl acetate to form α -acetoxy cyclopentenone.

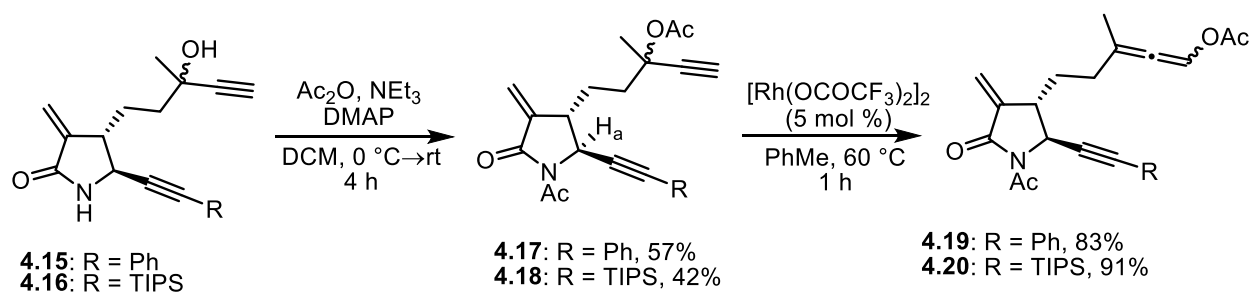
Thus, more highly oxygenated lactam analogs such as the [5,7,5]-guaianolide **4.11** was envisioned. Retrosynthetically, it was proposed that [5,7,5]-guaianolide analog **4.11** containing an α -acetoxy cyclopentenone could be formed from an APKR of **4.12** containing an α -methylene- γ -lactam tether between the alkyne and the allenyl acetate (Scheme 4.2). The allenyl acetate could be prepared from propargyl acetate **4.13** using a formal [3,3] sigmatropic rearrangement catalyzed by rhodium(II) trifluoroacetate dimer or gold(III) chloride, and this acetate would be generated by acetylation of propargyl alcohol **4.14**, whose synthesis was described in Chapter 3.



Scheme 4.2. Retrosynthetic analysis of lactam guaianolide analog **4.14**.

4.2. PREPARATION OF ALLENYL ACETATES FROM PROPARGYL ALCOHOLS

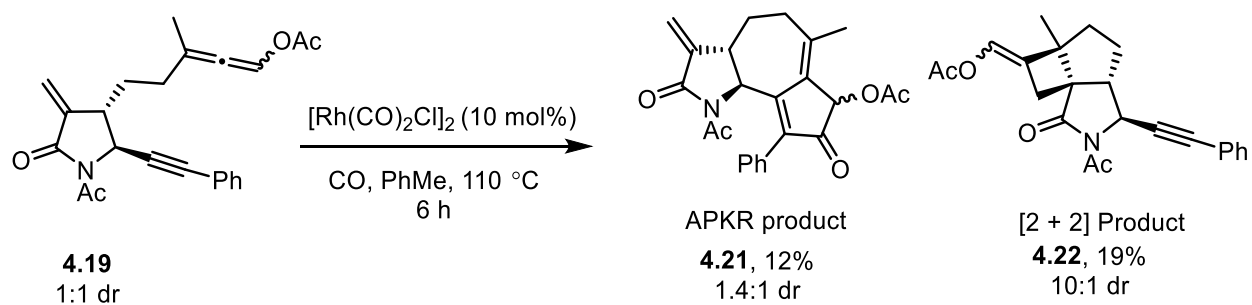
To prepare the allenyl acetate substrates for the APKR the hydroxyl group of **4.15** or **4.16** (synthesis in section 3.4) were acylated with acetic anhydride, triethylamine, and catalytic 4-dimethylaminopyridine. This reaction was accompanied by N-acylation to afford bisacylated products **4.17** or **4.18** in 57 and 42% yields, respectively (Scheme 4.3). Bisacylated products **4.17** and **4.18** were identified by the disappearance of the amide peaks at 6.98 or 5.90 ppm from **4.15** and **4.16**, respectively, and the appearance of two new methyl singlets at 1.99 ppm and 2.56 ppm for **4.17** and **4.18**, respectively, in the ^1H NMR spectrum. The ^1H NMR resonance corresponding to H_a shifted downfield from 4.3 to 4.9 ppm for **4.17** and from 4.1 to 4.6 ppm for **4.18**. Two new carbonyl carbon peaks in the ^{13}C NMR spectra at 171 and 166 ppm of **4.17** and **4.18** also demonstrated that bisacetylation had occurred. Attempts to shorten the reaction time in order to selectively acylate the alcohol over the amide nitrogen only led to mixtures of N-acylation (without O-acylation) and bisacylation, indicating that the nitrogen of the lactam was reacting faster than the tertiary alcohol. Nevertheless, these bisacylation **4.17** or **4.18** were reacted with rhodium(II) trifluoroacetate dimer (5 mol%) in toluene at 60 °C for 1 h to provide allenyl acetates **4.19** or **4.20** in yields of 83 and 91%, respectively. This demonstrated the feasibility of allenyl acetate formation in the presence of a tertiary amide. The allenyl acetates **4.19** and **4.20** could be identified by a disappearance of the alkynyl hydrogen singlet at 2.6 ppm from **4.17** and **4.18**, as well as a new allenyl hydrogen resonance at 7.3 ppm in the ^1H NMR spectra of both **4.19** and **4.20**. The central allene carbon was detected at 190 ppm in the ^{13}C NMR spectra.



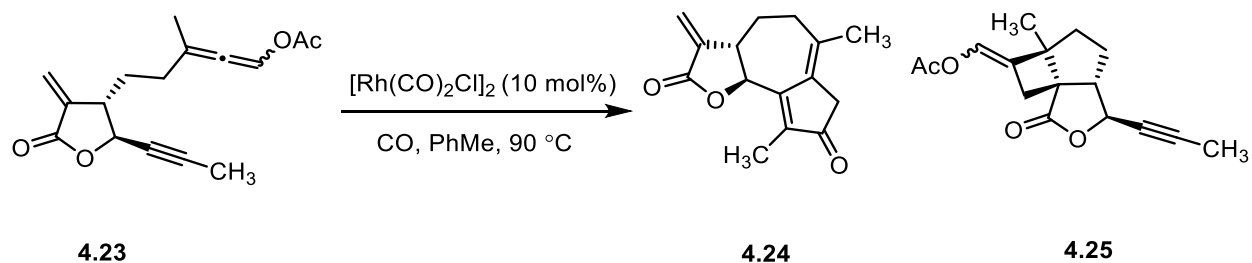
Scheme 4.3. Synthesis of allenyl acetates.

4.3. APKR OF ALLENYL ACETATES WITH *N*-ACETYL α -METHYLENE- γ -LACTAM TETHER

Allenyl acetate **4.19** was subjected to the typical APKR conditions using rhodium biscarbonyl chloride dimer (10 mol%) in toluene at 110 °C under a carbon monoxide atmosphere. This provided the APKR product **4.21** in only 12% yield as a 1.4:1 ratio of acetate diastereomers. A byproduct **4.22** arising from [2+2] cycloaddition between the proximal double bond of the allene and the α -methylene of the lactam was obtained in 19% yield (Scheme 4.4). The structure of the [2 + 2] cycloaddition product was confirmed by 2D NMR analysis (see Section 4.7). A similar product **4.25** was obtained as a byproduct by a former member of our group Dr. François Grillet. For example, **4.23** afforded a mixture of **4.24** and **4.25** under APKR conditions (Scheme 4.5). In this case, a crystal structure was obtained to confirm the structure of the [2 + 2] cycloaddition product (Figure 4.2).²²³ The NMR data for the lactone **4.25** and lactam **4.22** were similar, and the [2 + 2] cycloadduct structure was assigned by analogy to the lactone.



Scheme 4.4. APKR of allenyl acetate and alkyne tethered by an α -methylene- γ -lactam.



Scheme 4.5. APKR of allenyl acetate and alkyne tethered by an α -methylene- γ -lactone.

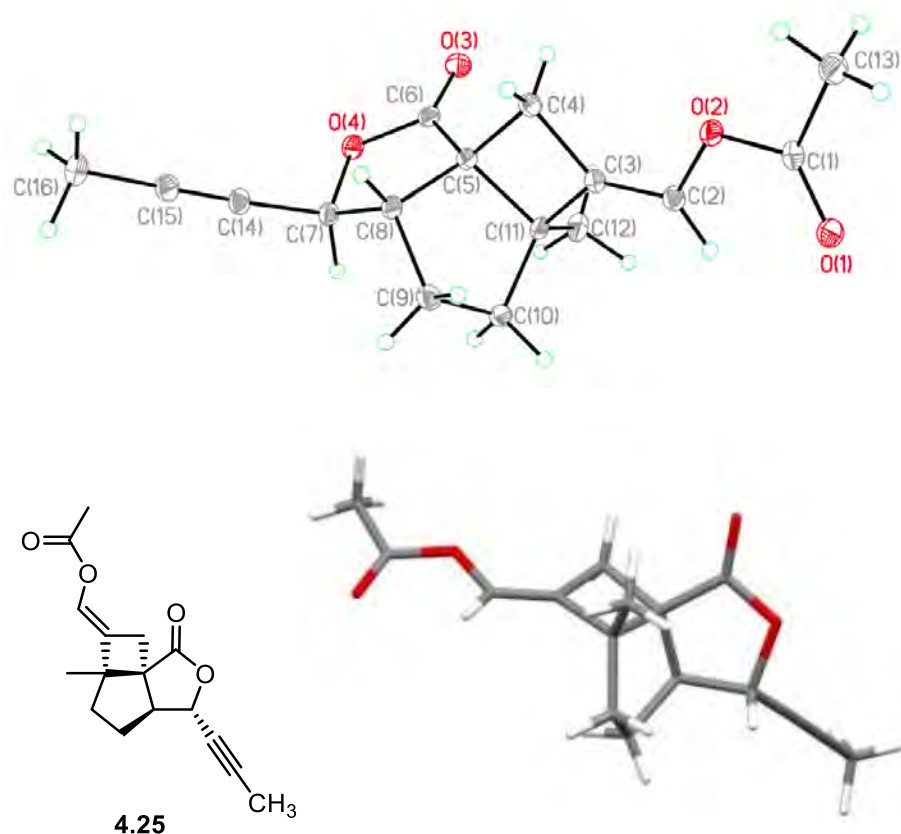
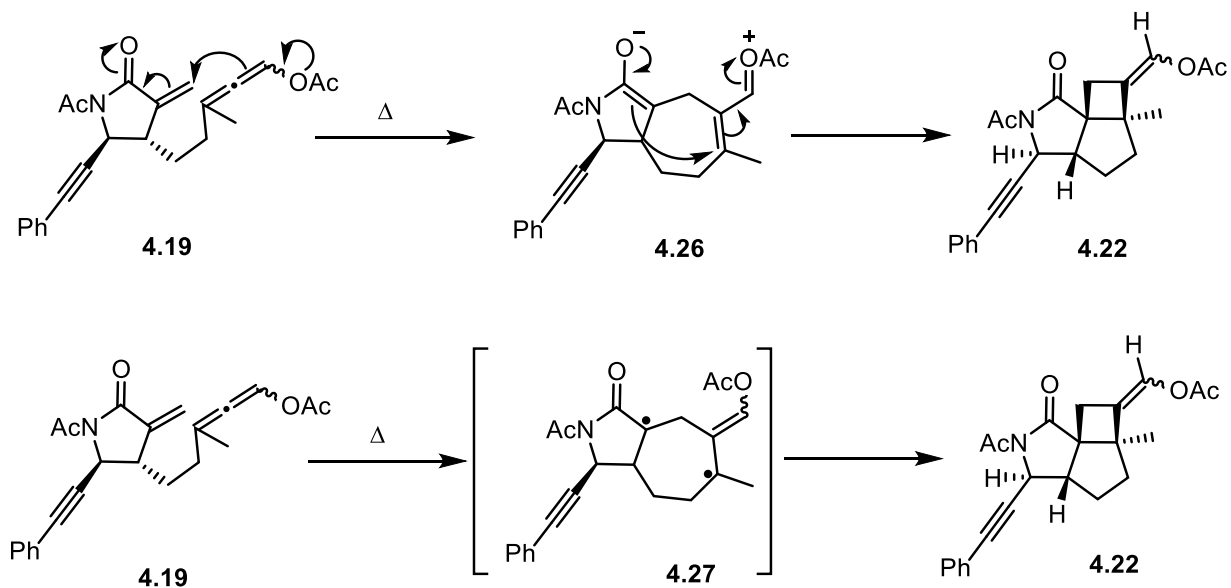


Figure 4.2: Crystal structure of [2 + 2] cycloaddition product from lactone.

4.4. PROPOSED MECHANISM FOR THE [2 + 2] CYCLOADDITION

The cycloaddition reaction is postulated to proceed via an initial carbon-carbon bond forming process between the electron-rich central carbon of the allene and the electron-deficient carbon of the α -methylene- γ -lactam to form the intermediate 7-membered ring **4.26** (Scheme 4.6). The resulting enolate **4.26** then forms a bond between the α -carbon of the γ -lactam and the methyl substituted alkene carbon to form the cyclobutane and the alkenyl acetate **4.22**. Thus, an electron-deficient alkene promotes the first step of the proposed mechanism. Alternatively, the [2 + 2] cycloaddition product could arise from a radical process, where initial bond formation between the

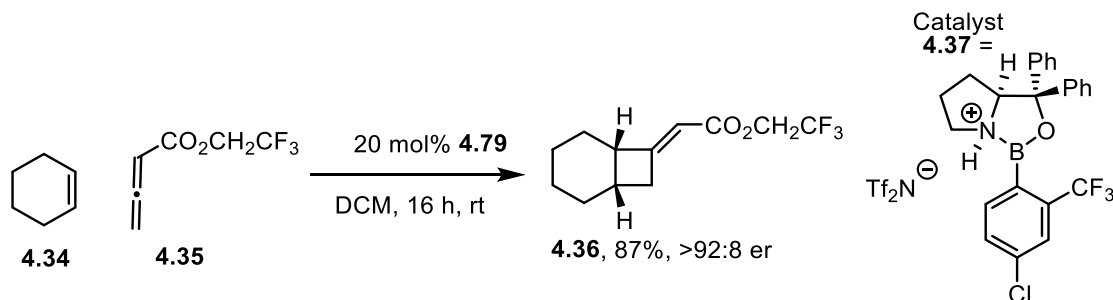
terminus of the alkene and the proximal allene double bond forms diradical intermediate **4.27**. Radical combination then affords the cyclobutane product **4.22**. Both radical and ionic process have been proposed for allene-alkene cycloadditions in the literature (for further discussion on mechanistic studies of allene-alkene cycloadditions in the literature see Section 4.8).



Scheme 4.6. Proposed mechanisms for cyclobutane formation.

The reaction of an allene and alkene to form cyclobutane derivatives via a [2 + 2] cycloaddition was reviewed in 2009 by Alcaide and coworkers.²²⁴ These reactions have been carried out under photochemical or thermal conditions as well as with Lewis acid or transition metal catalysis. Photochemical [2 + 2] cycloadditions of allenes and alkenes require an α,β -unsaturated carbonyl as the alkene portion to generate a diradical that reacts with the allene and involve irradiation with UV light between 250-300 nm. Although light was not excluded from our reactions with allenyl acetates, ambient light would not be expected to promote triplet enone formation.²²⁴⁻²²⁷

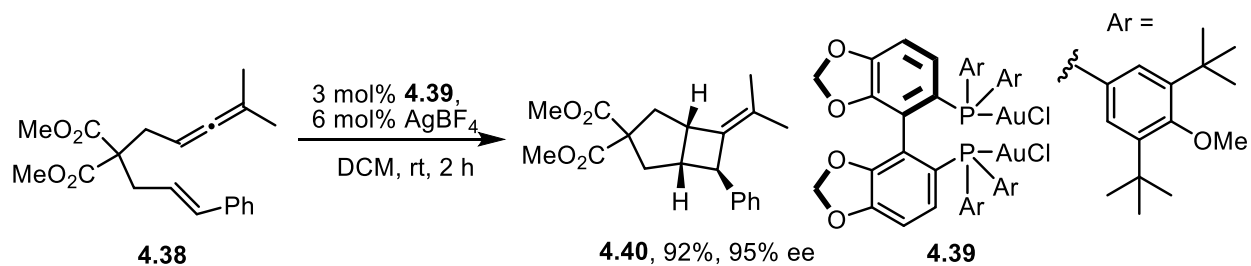
Lewis acid catalyzed allene-alkene cycloadditions between an electron-poor allenes and electron-rich alkenes are the most common.²²⁹ Recently, Brown and coworkers have reported enantioselective Lewis acid catalyzed, intermolecular cycloaddition of allenates with alkenes.²³⁰⁻²³¹ In this case trifluoroethyl allenate **4.35** was reacted with alkene **4.34** to give cyclobutane product **4.36** in an 87% yield and 90:10 er; internal, linear alkenes gave lower yields, but good enantiomeric ratios (Scheme 4.8).²³¹ In these cases, the Lewis acid is thought to activate the allenate for nucleophilic attack by the alkene, via short-lived ionic intermediates because lower yielding reactions were afforded with electron withdrawing substituents on the alkene.²²⁹⁻²³¹



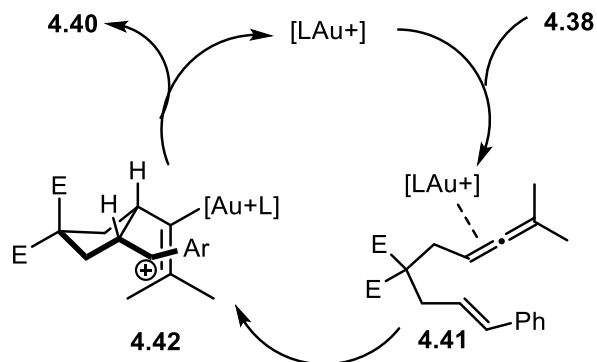
Scheme 4.8. Enantioselective, Lewis acid catalyzed [2 + 2] cycloaddition of alkenes and allenates.

In one example, using a cationic, gold catalyst (**4.39**), Toste and coworkers showed that alkyl substituted allenates such as **4.38** reacted intramolecularly with styrenyl alkenes to form bicyclo[3.2.0]heptanes, such as **4.40**, in good yields and enantioselectivities (Scheme 4.9).²³² The catalytic cycle involves a stepwise mechanism where a nucleophilic alkene adds to the gold(I) activated allene **4.41** to form carbocation intermediate **4.42** (Scheme 4.10).²³²⁻²³³ The vinyl gold species then reacts with the carbocation to form cyclobutane **4.40**. This mechanism was supported

by trapping the intermediate carbocation with methanol to give the corresponding cyclopentane. Other gold-catalyzed, enantioselective [2 + 2] cycloadditions of allenes and alkenes are thought to proceed through a similar mechanism.²³³⁻²³⁴



Scheme 4.9. Gold-catalyzed [2 + 2] cycloaddition of allenes and alkenes.



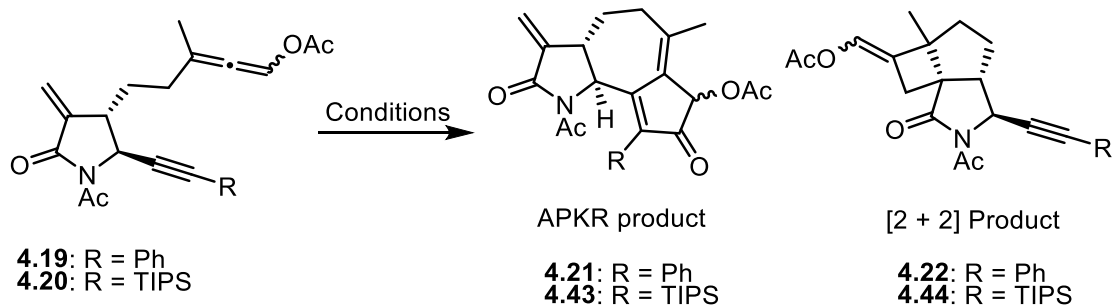
Scheme 4.10. Catalytic cycle for gold-catalyzed [2 + 2] cycloaddition of allenes and alkenes.

4.5. OPTIMIZATION OF CONDITIONS TO SELECTIVELY OBTAIN THE APKR PRODUCT OR THE [2 + 2] CYCLOADDITION PRODUCT FROM ALLENYL ACETATES WITH AN α -METHYLENE- γ -LACTAM TETHER

Different conditions were examined to selectively form the APKR product or the [2 + 2] product. These included lowering the temperature, changing the rhodium catalyst, changing the solvent, and decreasing the amount of carbon monoxide in the atmosphere. The results of these conditions are shown in Table 4.1. It was hypothesized that the [2 + 2] cycloaddition reaction was the result of a thermal-only process. Thus, removing the catalyst afforded a 71% yield of the [2 + 2] cycloadduct **4.22** in 71% yield (Table 4.1, entry 2). Using these same reaction conditions, **4.20** afforded a 51% yield of cycloadduct **4.44** and none of the APKR product **4.43** (entry 3). No efforts were made to further optimize the [2 + 2] cycloaddition. We next turned to developing conditions that would provide the APKR product in high yield. Lowering the temperature led to an increased yield of the [2 + 2] product **4.22** of 33%, but none of the APKR product **4.21** was obtained (entry 4). Changing the solvent from toluene to dichloroethane had a similar effect, providing the [2 + 2] product **4.22** in 45% yield with none of the APKR product **4.21** (entry 5). Activated rhodium catalysts that promote the APKR at lower temperatures and increase the rate of the APKR may increase the yield of the [5,7,5]-fused ring system. Previous work in our lab had showed that treatment of rhodium(I) biscarbonyl chloride dimer with triphenylphosphine and silver tetrafluoroborate (to form $\text{Rh}(\text{CO})_2(\text{PPh}_3)_2$) gave a catalyst that was active at lower temperatures and quickly formed APKR products with allenyl acetates. This active catalyst was reacted in a 10% carbon monoxide, 90% argon atmosphere, as 100% carbon monoxide leads to displacement of the triphenylphosphine ligand by carbon monoxide. With this activated catalyst at 50 °C, the

highest yield (25%) of the APKR product **4.21** was obtained as a 1.4:1 ratio of acetate diastereomers, but the [2 + 2] product **4.22** was still the major product obtained in 34% yield (entry 6). At room temperature, activated catalyst $\text{Rh}(\text{CO})_2(\text{PPh}_3)_2$ gave none of the APKR product **4.21**, 29% yield of [2 + 2] product **4.22**, and 17% of an α,β -unsaturated aldehyde arising from decomposition of the allenyl acetate (entry 5). As previous APKR with allenyl acetates were more successful with a silyl-substituted alkyne (TMS), it was proposed that lactam **4.20** with a TIPS substituent would increase the rate of the APKR. Thus, TIPS substituted alkyne **4.23** was subjected to typical APKR conditions with rhodium biscarbonyl chloride dimer. However, TIPS substituted alkyne **4.20** did not give any of the APKR product **4.43** under these conditions or with the activated catalyst at 50 °C (entries 8-9). The [2 + 2] product **4.44** was obtained in 56% yield at 110 °C with rhodium biscarbonyl chloride as the catalyst (entry 8). With the activated catalyst ($\text{Rh}(\text{CO})_2(\text{PPh}_3)_2$), a 13% yield of [2 + 2] product **4.44** was obtained along with 45% of the α,β -unsaturated aldehyde due to decomposition of the allenyl acetate (entries 8-9). This was not surprising, as the TIPS alkyne was shown to slow the APKR with 1,1-disubstituted allenes, and it is not expected to affect the rate of [2 + 2] cycloaddition (see Table 3.3, entry 3). Thus, thermal-only conditions to form the [2 + 2] cycloadduct selectively were identified. Efforts to find conditions for the selective formation of the APKR product were not pursued further because under all reaction conditions investigated, formation of the [2 + 2] product outcompeted the formation of the APKR suggesting that the Rh-catalyst may be functioning as a Lewis acid to facilitate the [2 + 2] cycloaddition.

Table 4.1. APKR or [2 + 2] cycloaddition with allenyl acetates.



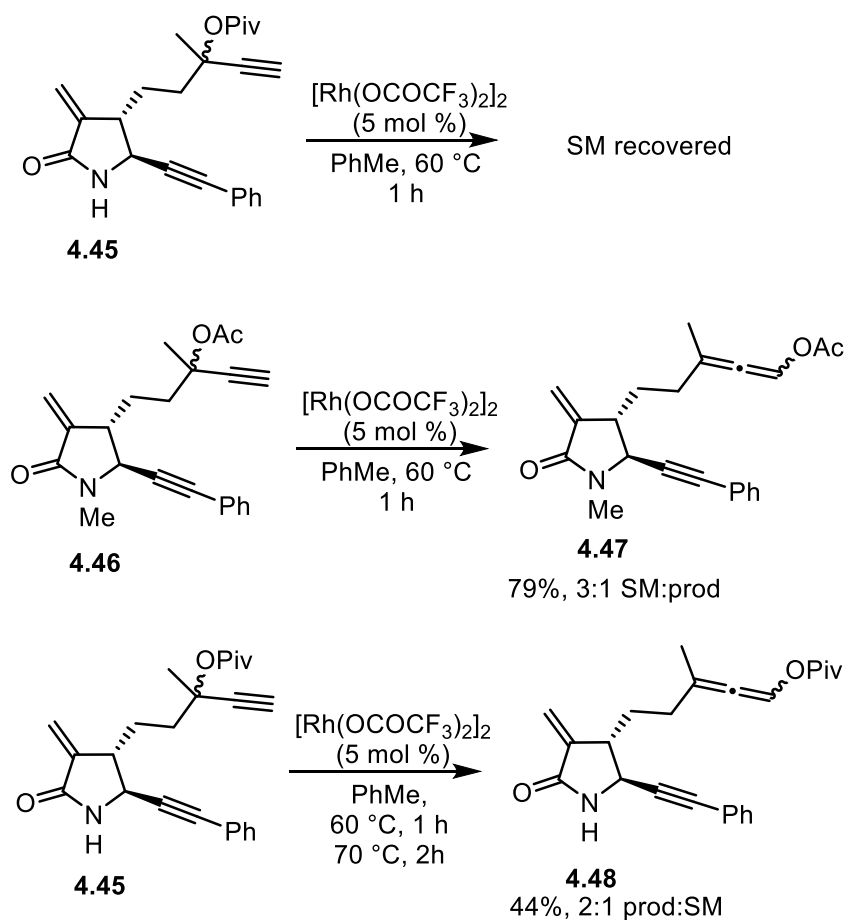
Entry	R =	Catalyst	Atmos- phere	Temp (°C)	Solvent	Time (h)	Yield PK (%)	Yield [2+2] (%)	Yield total (%)
1	Ph	[Rh(CO) ₂ Cl] ₂ (10 mol%)	CO	110	PhMe	6	12	19	31
2	Ph	None	N ₂	110	PhMe	4	0	71	71
3	TIPS	None	N ₂	110	PhMe	5	0	51	51
4	Ph	[Rh(CO) ₂ Cl] ₂ (10 mol%)	CO	70-90	PhMe	7	0	33	33
5	Ph	[Rh(CO) ₂ Cl] ₂ (10 mol%)	CO	90	DCE	6	0	45	45
6	Ph	[Rh(CO) ₂ Cl] ₂ (10 mol%), PPh ₃ (30 mol %), AgBF ₄ (22 mol %)	10% CO in Ar	50	DCE	2	25	34	60
7	Ph	[Rh(CO) ₂ Cl] ₂ (10 mol%), PPh ₃ (30 mol %), AgBF ₄ (22 mol %)	10% CO in Ar	25	DCE	4	0	29	46*
8	TIPS	[Rh(CO) ₂ Cl] ₂ (10 mol%)	CO	110	PhMe	2	0	56	56
9	TIPS	[Rh(CO) ₂ Cl] ₂ (10 mol%), PPh ₃ (30 mol %), AgBF ₄ (22 mol %)	10% CO in Ar	50	DCE	2	0	13	58*

* The remainder of the overall yield was due to α,β -unsaturated aldehyde formation from decomposition of the allenyl acetate.

4.6. DESIGN AND SYNTHESIS OF LESS-ELECTRON DEFICIENT α -METHYLENE- γ -LACTAMS FOR ALLENIC PAUSON-KHAND REACTIONS USING ALLENYL ACETATES

Since both the α -methylene- γ -lactone **4.23** and the *N*-acetyl α -methylene- γ -lactams **4.19-4.20** contain an electron-deficient alkene, and the proposed reaction mechanism is stepwise ionic, it was proposed that a less electron deficient alkene may suppress the [2 + 2] cycloaddition reaction. To test this hypothesis, the syntheses of allenyl acetates or pivalates with an unsubstituted or methylated lactam nitrogen were pursued, as these systems have less electrophilic alkenes, as evidenced by the slower rate of thiol addition to an *N*-unsubstituted lactam (Section 3.10). As mentioned above, selective O-acylation was difficult due to competitive N-acylation, thus the corresponding pivalate **4.45** was formed as discussed in Chapter 3. Based on previous results in our lab, the pivalate and various other acyloxy groups undergo the formal [3,3] sigmatropic rearrangement catalyzed by rhodium(II) trifluoroacetate dimer to the corresponding allenyl acyloxy systems. However, when pivalate **4.45** was reacted with catalytic rhodium(II) trifluoroacetate dimer, only starting material was recovered, quantitatively (Scheme 4.11). Because the unsubstituted lactam nitrogen may deactivate the catalyst by coordination of the secondary amide to rhodium, *N*-methyl lactam **4.46** was subjected to the rhodium catalyzed rearrangement. This system afforded similar results with a 79% overall yield consisting of a 3:1 ratio of recovered starting material to allenyl acetate **4.47**. Similarly, the reaction of unsubstituted NH lactam **4.45** afforded the desired allenyl pivalate in an inseparable 2:1 ratio of desired product **4.48** to starting material **4.45**, but only a 44% yield was obtained, which was attributed to decomposition of the starting material or product. The ratio of product to starting material was

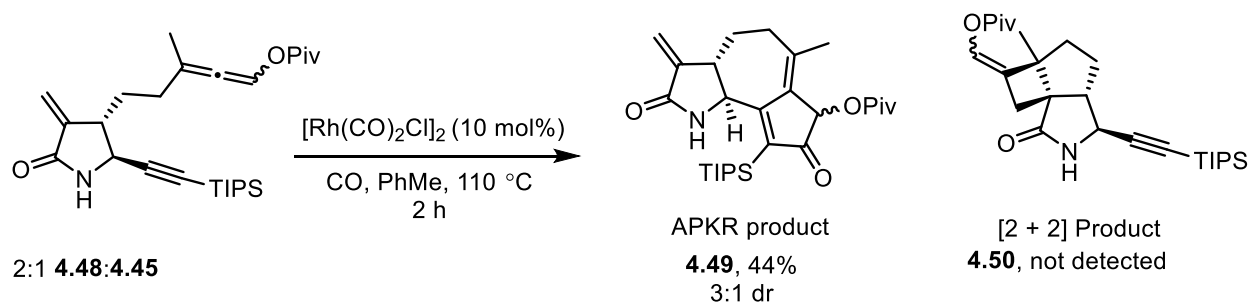
determined by integration of the allenyl pivalate hydrogen at 7.31 ppm and the terminal alkyne hydrogen at 2.53 ppm of the ^1H NMR spectrum. The diastereomeric ratio was unable to be determined due to overlapping resonances in the ^1H NMR of the starting material and product.



Scheme 4.11. Formation allenyl pivalates or acetates with *N*-unsubstituted or *N*-methyl lactams.

Since allenyl pivalate **4.48** was unable to be separated from propargyl pivalate **4.45**, the mixture was subjected to the typical APKR conditions. Allenyl pivalate **4.48** (2:1 with **4.45**) was reacted with rhodium biscarbonyl chloride dimer in toluene at 110 $^\circ\text{C}$ for 2 h to afford tricycle **4.49** in 44% yield and a 3:1 dr and no [2 + 2] product **4.50** (Scheme 4.12). The dr was determined

by integration of the proton resonance α to the pivaloyloxy group which appeared as a singlet at 5.66 ppm for the major diastereomer and 5.54 ppm for the minor diastereomer. This result suggests that allenic Pauson-Khand reactions between allenyl pivalates and alkynes with an α -methylene- γ -lactam tether containing only weakly electrophilic alkenes are possible without formation of the [2 + 2] product. However, the formation of allenyl pivalates attached to *N*-unsubstituted lactams still requires optimization. One possibility for this is to perform the rearrangement with a gold(III) chloride catalyst instead of the rhodium(II) trifluoroacetate dimer.



Scheme 4.12. APKR of allenyl pivalate with *N*-unsubstituted lactam tether.

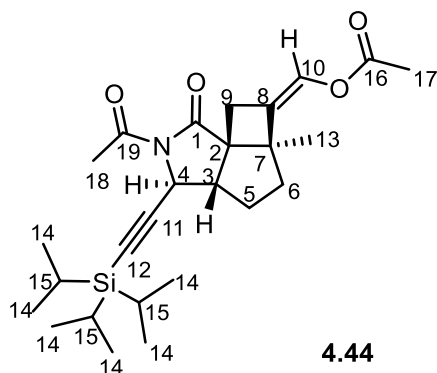
4.7. STRUCTURE CONFIRMATION OF THE [2 + 2] CYCLOADDITION PRODUCT BY 2D NMR ANALYSIS

The structure of tricyclic compound **4.44** was determined by ¹H, ¹³C, DEPT, HSQC, HMBC, and COSY NMR analyses. This NMR data is presented in Table 4.2, while key COSY and HMBC correlations are summarized in Figure 4.3. The compound showed the same exact mass as the starting material **4.20**, suggesting that a skeletal reorganization had occurred. Absence of the allenyl and alkenyl resonances in ¹H NMR spectrum strongly suggested a reaction between these two groups. Additionally, an upfield shift of the hydrogen at position 4 from 5.59 ppm in the SM **4.20** to 4.19 ppm in the product **4.44** was observed. A triplet at 7.02 ppm resulted from an upfield

shift of the allenyl acetate hydrogen of the SM from 7.32 ppm. Two new doublet of doublets appeared at 3.30 and 2.43 ppm and were assigned to geminal hydrogen atoms at position 9 on the cyclobutane ring; coupling constants of 2.7 Hz and COSY analysis showed that these two hydrogen atoms were coupled to the triplet at 7.02 ppm and to each other. This geminal coupling is indicative of a cyclobutane or cyclopentane ring. The hydrogen at position 3 in the SM **4.20** was a multiplet at 3.0 ppm and shifted upfield to become the triplet at 2.71 ppm in the product **4.44**. Two methyl singlets were observed in the ^1H NMR spectrum at 2.50 and 2.13 ppm, similar to the two acetyl methyl groups of the starting material. The third methyl singlet shifted from 1.83 ppm in the SM to 1.20 ppm in the product, suggesting it was no longer connected to an alkene. Multiplets at 2.25 and 2.03 ppm showed COSY correlations to the triplet at 2.71 ppm, demonstrating that these hydrogen atoms were at position 5; these multiplets also showed COSY correlations to the doublet of doublets at 1.92 ppm and the doublet of triplets at 1.55 ppm, so these resonances were assigned to the protons at position 6 of the product **4.44**. DEPT and HSQC spectra confirmed that position 5 was a CH_2 group correlating to the ^1H NMR resonances for geminal hydrogens at 2.25 and 2.03, while the resonances at 1.92 and 1.55 were a CH_2 corresponding to position 6. A singlet at 1.04 ppm of the ^1H NMR integrates for 21 and corresponds to the hydrogens of the triisopropyl silyl group.

^{13}C NMR showed three carbonyl peaks at 174.4, 170.3, and 167.9 ppm corresponding to the lactam carbonyl and the two acetyl groups. The central allene carbon of the allenyl acetate SM **4.20** at 189.7 was gone. Only two olefin resonances were observed at 129.2 and 126.6 ppm compared to five olefin resonances in the SM (189.9, 142.7, 122.5, 114.7, and 110.8), indicating that the allene and α -methylene of the lactam were transformed in the reaction. The alkyne carbon resonances at 105.3 and 85.6 ppm did not change from SM to product. Two new quaternary

carbons at 59.9 and 57.2 ppm were identified from their absence in HSQC and DEPT spectra. The acetyl methyl groups (positions 17 and 18) were identified as the peaks at 21.0 and 25.4 ppm by their single HMBC correlations to the carbonyl peaks at 170.3 and 167.9 ppm (positions 16 and 19) respectively, and HSQC correlations to the ^1H NMR resonances at 2.50 and 2.13 ppm. HSQC and DEPT helped identify the carbons at positions 3 and 4 as the resonances at 51.2 and 51.6 ppm. HSQC was also used to assign the ^{13}C NMR resonance at 20.7 to the methyl group at position 15 and the resonance at 28.4 ppm to position 9 in the product **4.44**.

Table 4.2. NMR Data for [2 + 2] cycloaddition product **4.44**.

Position	δ_C , Type	δ_H , mult., (J in Hz)	HMBC	COSY
1	174.4, C			
2	59.9, C			
3	51.2, CH	2.71, t, (7.0)	4, 6, 9, 11	H-4, H-5a,b
4	51.6, CH	4.19, d, (7.5)	5, 11, 12	H-3
5	30.0, CH ₂	a 2.29-2.22, m b 2.05-2.01, m	2, 6, 7	H-3, H-5b, H-6a,b H-3, H-5a, H-6a,b
6	38.5, CH ₂	a 1.92, dd, (6.5, 13.3) b 1.56, dt, (6.5, 13.3)	7, 8, 13	H-5a,b, H-6b H-5a,b, H-6a
7	57.2, C			
8	126.7, C			
9	28.4, CH ₂	a 3.30, dd, (2.7, 17.0) b 2.43, dd, (2.7, 17.0)	1, 4, 8, 10	H-9b, H-10 H-9a
10	129.2, CH	7.02, t, (2.7)	8, 9	H-9a,b
11	105.4, C			
12	85.6, C			
13	20.7, CH ₃	1.20, s	2, 6, 7, 8,	
14	18.7, CH ₃	1.04, s	15	
15	11.2, CH	1.04, s	14	
16	167.9, C			
17	21.0, CH ₃	2.13, s	19	
18	25.4, CH ₃	2.50, s	16	
19	170.3, C			

The key HMBC correlations show that the hydrogen at C-3 correlates to the carbons at C-4, 6, 9, and 11 and the hydrogen at position 4 correlates to the carbon at C-5 and the two alkyne carbons at C-11 and 12. The hydrogens at C-5 correlate to quaternary carbons 2 and 7, as do the hydrogens of the methyl group at C-15. The hydrogens at C-13 correlate to the alkene carbon at position 8, as do the hydrogens from C-9 and 6. The hydrogens on C-9 correlate to the carbonyl C-1 and the alkene C-10.

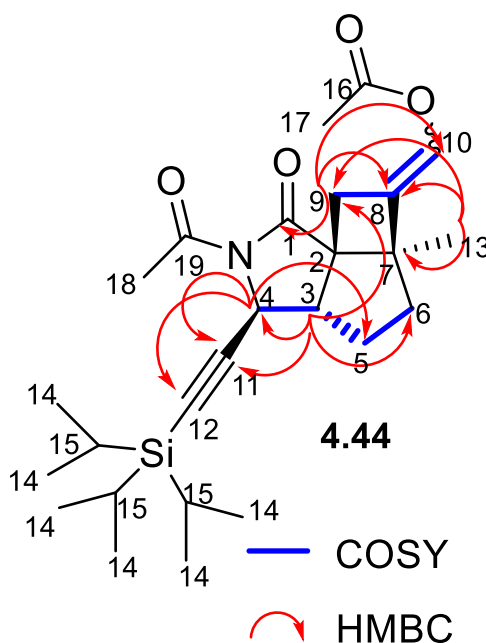


Figure 4.3. Important COSY and HMBC correlations used to confirm the structure of [2 + 2] cycloaddition product.

4.8. CONCLUSION

These literature examples are representative of the different conditions to promote the [2 + 2] cycloaddition between an allene and an alkene to form cyclobutane derivatives. Various

mechanisms are invoked in the [2 + 2] cycloadditions of allenes and alkenes depending on the conditions. These mechanisms involve diradicals, under photochemical and thermal conditions, or ionic intermediates under Lewis acidic or gold-catalyzed conditions. Although ionic intermediates are less commonly invoked in thermally-induced reactions, the presence of the acetate on the allene of our substrates is unprecedented in the literature on [2 + 2] cycloadditions of allenes. Considering that the [2 + 2] cycloaddition appears to be shut down with less electrophilic alkenes, it is more likely that the electron-rich allenyl acetate adds to the α -methylene- γ -lactam via an ionic process rather than a diradical process. Considering that the cycloaddition occurred at rt in the presence of a rhodium catalyst, the cationic rhodium(I) could be acting as a Lewis acid by coordinating to the lactam carbonyl, and thus increasing the electrophilicity of the α -methylene moiety.

The [2 + 2] cycloaddition of allenyl acetates with electron poor alkenes could offer a useful method for methylenecyclobutane formation, although further study is needed to examine the scope and synthetic utility of this reaction. Additionally, it was shown that the APKR could be favored over the [2 + 2] cycloaddition when less electron poor α -methylene- γ -lactams, such as those containing a secondary amide, were subjected to the APKR conditions

APPENDIX A

EXPERIMENTAL PROCEDURES AND COMPOUND CHARACTERIZATION DATA

1. General Methods
2. General Procedures
 - i. General Procedure A: α -Methylene Lactam Formation from Allylboronate
 - ii. General Procedure B: Hydrolysis of Ketal
 - iii. General Procedure C: Addition of Ethynyl Magnesium Bromide to Ketone
 - iv. Acetylation of Alcohol with Triethylamine, Dimethylaminopyridine, and Acetic Anhydride
 - v. General Procedure D: Formation of Propargyl Pivalate from Propargyl Alcohol
 - vi. General Procedure E: Conversion of Propargyl Ester to 1,1-Disubstituted Allenes Using (Triphenylphosphine)copper Hydride Hexamer

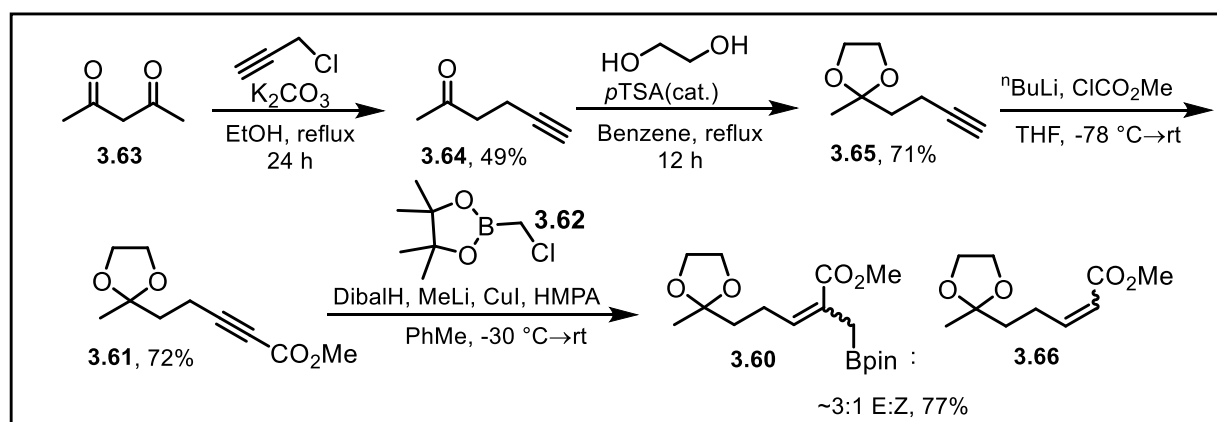
- vii. **General Procedure F: Removal of Triisopropyl silyl (TIPS) Substituent from Alkyne**
- viii. **Protection of Lactam Nitrogen with *tert*-Butyl Carbonate**
- ix. **General Procedure G: Arylation of Lactam Nitrogen with Aryl Iodides**
- x. **General Procedure H: Allenic Pauson-Khand Reaction (Slow Addition of Allene-yne to Rhodium(I) Catalyst)**
- xi. **General Procedure I: Alternative Procedure for Allenic Pauson-Khand Reaction**
- xii. **General Procedure J: Acetylation of Lactam Nitrogen**
- xiii. **General Procedure K: Monitoring the Reaction of α -Methylene- γ -lactams with Cysteamine by ^1H NMR**
- xiv. **Hetero-Michael Addition of *tert*-Butyl Thiol to an α -Methylene- γ -lactam**
- xv. **General Procedure L: Formation of Allenyl Acetates via Formal [3,3] Sigmatropic Rearrangement of Propargyl Acetates**
- xvi. **Allenic Pauson-Khand Reaction of Allenyl Acetates Accompanied by a [2+2] Cycloaddition**

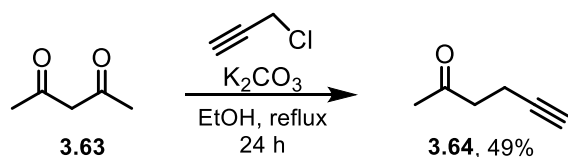
General Methods

Commercially available compounds were used as received unless otherwise noted. Dichloromethane (DCM), tetrahydrofuran (THF), and diethyl ether (Et₂O) were purified by passing through alumina using the Sol-Tek ST-002 solvent purification system. Triethylamine was distilled from calcium hydride (CaH₂) and stored over 4 Å molecular sieves. Acetic

anhydride (Ac₂O) was shaken with phosphorus pentoxide (P₂O₅), decanted, fractionally distilled from anhydrous potassium carbonate (K₂CO₃) and stored over 4 Å molecular sieves. Hexamethylphosphoramide (HMPA) was vacuum distilled from CaH₂ and stored over 4 Å molecular sieves. Deuterated chloroform (CDCl₃) was stored over anhydrous K₂CO₃. All reaction temperatures designated are bath temperatures. Silica gel (40-63 μm particle size, 60 Å pore size) purchased from Sorbent Technologies was used for the purification of compounds by flash chromatography. TLC analyses were performed on Silicycle SiliaPlate G silica gel glass plates (250 μm thickness). ¹H NMR and ¹³C NMR spectra were recorded on Bruker Avance 300 MHz, 400 MHz, or 500 MHz spectrometers. Spectra were referenced to residual chloroform (7.26 ppm, ¹H, 77.16 ppm, ¹³C). Chemical shifts are reported in ppm, multiplicities are indicated by s (singlet), bs (broad singlet), d (doublet), t (triplet), q (quartet), p (pentet), and m (multiplet). Coupling constants, *J*, are reported in hertz (Hz). All NMR spectra were obtained at rt unless otherwise specified. IR spectra were obtained using a Nicolet Avatar E.S.P. 360 FT-IR. ESI mass spectroscopy was performed on a Waters Q-TOF Ultima API, Micromass UK Limited high resolution mass spectrometer.

Synthesis of Allylboronate xx





Hex-5-yn-2-one (3.64): Hexynone **3.64** was synthesized according a literature procedure.¹⁷⁴ A flame-dried, 250-mL, single-necked, round-bottomed flask, equipped with a magnetic stir bar, septum, and nitrogen inlet needle was charged with 2,4-pentanedione **3.63** (30 mL, 290 mmol) and ethanol (120 mL, 2.2 M). Propargyl chloride (37 mL, 260 mmol) was added via syringe followed by potassium carbonate (48 g, 350 mmol) in a single portion. The septum was removed and a reflux condenser equipped with a septum and nitrogen inlet needle was attached, and the reaction was heated to reflux in an 85 °C oil bath for 24 h. Upon completion of the reaction as observed by TLC, the mixture was cooled to rt and filtered via vacuum filtration to remove the solids. The solid was washed with ethyl acetate. Ethyl acetate and ethanol were removed by simple distillation at atmospheric pressure. The residue was diluted with diethyl ether (100 mL), transferred to a separatory funnel, washed with deionized water (50 mL), then brine (50 mL), dried over magnesium sulfate, gravity filtered, and concentrated by simple distillation at atmospheric pressure. The residue was further purified by simple, vacuum distillation (45 mmHg, 85-90 °C) to give 12.5 g of product in a 49% yield. The spectral data matched literature values.¹⁷⁴

Data for 3.64: (PAJ 6-104, 12.5 g, 49%)

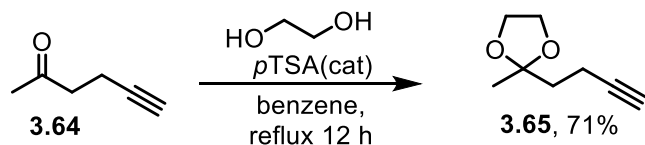
¹H NMR (300 MHz, CDCl₃)

δ 2.67, (t, *J* = 7.2 Hz, 2H), 2.42 (dt, *J* = 2.7, 7.1 Hz, 2H), 2.16 (s, 3H), 1.93 (t, *J* = 2.7 Hz, 1H) ppm

¹³C NMR (100 MHz, CDCl₃)

δ 206.3, 82.7, 68.6, 42.0, 29.8, 12.8 ppm

TLC $R_f = 0.46$ (25% EtOAc/hexanes) [silica gel, UV, KMnO₄]



2-(But-3-ynyl)-2-methyl-1,3-dioxolane (3.65). Following a procedure analogous to that previously reported,¹⁷⁵ a flame-dried, 200-mL, single-necked, round-bottomed flask equipped with a magnetic stir bar was charged with hex-5-yn-2-one **3.64** (12.5 g, 131 mmol), benzene (130 mL), ethylene glycol (8.8 mL, 160 mmol), and *p*-toluenesulfonic acid (0.497 g, 2.61 mmol) in that order. A Dean-Stark trap and reflux condenser were attached and the solution was refluxed in a 100 °C oil bath. After 15 h, TLC showed complete consumption of the starting material. The solution was allowed to cool to rt, diluted with diethyl ether (80 mL), transferred to a separatory funnel, then washed successively with saturated sodium bicarbonate (100 mL) and brine (100 mL). The organic layer was dried over magnesium sulfate, gravity filtered, and diethyl ether and benzene were removed by simple distillation at atmospheric pressure. Following the removal of solvent, the product was purified by vacuum distillation at 30 mmHg. Two fractions were collected, the first contained benzene with trace amounts of product (bp = 40-50 °C) and the second contained product with less than 10% benzene (bp = 113-120 °C, 13.0 g, 71%), as determined by integration of the benzene resonance at 7.19 and terminal alkyne resonance at 1.87 ppm.

Data for 3.65: (PAJ 6-106, 13.0 g, 71%)

¹H NMR (300 MHz, CDCl₃)

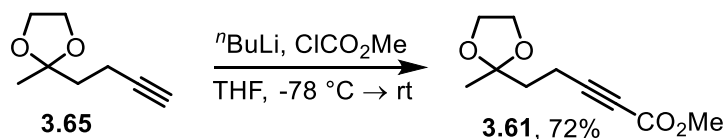
δ 3.96-3.86 (m, 4H), 2.25 (dt, $J = 2.7, 7.5$ Hz, 2H), 1.92-1.88 (m, 2H), 1.87 (s, 1H) 1.30 (s, 3H) ppm

¹³C NMR (100 MHz, CDCl₃)

δ 109.2, 84.5, 67.9, 65.0 (2C), 38.1, 23.9, 13.3 ppm

TLC

R_f = 0.55 (25% EtOAc/hexanes) [silica gel, UV, KMnO₄]



Methyl 5-(2-methyl-1,3-dioxolan-2-yl)pent-2-ynoate (3.61): Following a procedure analogous to that previously reported,¹⁷⁶ a flame-dried, 200-mL, single-necked, round-bottomed flask under a nitrogen atmosphere equipped with a magnetic stir bar, septum, and nitrogen inlet needle, was charged with alkyne **3.65** (2.10 g, 15.0 mmol) and tetrahydrofuran (75 mL) then cooled to $-78\text{ }^\circ\text{C}$. *n*-Butyl lithium (1.6 M in hexanes, 11.3 mL, 18.0 mmol) was added dropwise to the solution of alkyne via syringe and the reaction was stirred for an additional 30 min at $-78\text{ }^\circ\text{C}$ after the addition was complete. Methyl chloroformate (1.5 mL, 19.5 mmol) was added dropwise via syringe and stirred for 30 min at $-78\text{ }^\circ\text{C}$ before allowing the reaction to warm to rt for 3 h when it was complete by TLC. The reaction was quenched by addition of saturated aqueous ammonium chloride (30 mL) and the solution was transferred to a separatory funnel. The layers were separated, and the aqueous layer was extracted with diethyl ether (3 x 50 mL). The organic layers were combined, washed with brine (50 mL), dried over magnesium sulfate, gravity filtered, concentrated by rotary evaporation ($30\text{ }^\circ\text{C}$) and purified by silica gel flash column chromatography eluting with 20% diethyl ether in hexanes to yield alkynoate **3.61** (2.14 g, 72%) as a clear liquid.

Data for 3.61: (PAJ 6-62, 2.14 g, 72%)

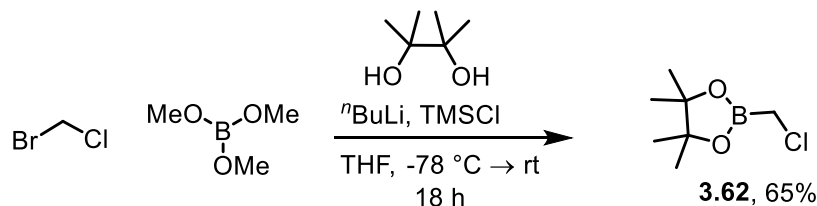
¹H NMR (300 MHz, CDCl₃)

δ 3.98-3.89 (m, 4H), 3.74 (s, 3H), 2.42 (t, $J = 7.9\text{ Hz}$, 2H), 1.95 (t, $J = 7.9\text{ Hz}$, 2H), 1.31 (s, 3H) ppm

^{13}C NMR (100 MHz, CDCl_3)

δ 154.4, 108.8, 89.7, 72.7, 65.0 (2C), 52.7, 36.9, 24.0, 13.6 ppm

TLC R_f = 0.23 (20% Et_2O /hexanes) [silica gel, UV, KMnO_4]



2-(Chloromethyl)-4,4,5,5-tetramethyl-1,3,2-dioxaborolane (3.62): Following a procedure analogous to those previously reported,¹⁸¹ a flame-dried, single-necked, 250-mL, round-bottomed flask equipped with a stir-bar, septum, and nitrogen inlet needle was charged with trimethyl borate (8.6 mL, 77 mmol) and bromochloromethane (5.5 mL, 85 mmol) and cooled to -78 °C. *n*-Butyl lithium (1.6 M in hexanes, 53 mL, 85 mmol) was added dropwise via syringe pump over 35 min. Upon completion of addition, the solution was maintained at -78 °C for an additional 30 min. Chlorotrimethylsilane (12 mL, 92 mmol) was added dropwise at -78 °C and the reaction was allowed to warm to rt by removal of the dry ice/acetone bath. The reaction stood for 16 h (without stirring), then pinacol (10.0 g, 85 mmol) was added and the reaction was stirred for 1 h at rt. The reaction was poured into a separatory funnel containing water (100 mL) and diethyl ether (100 mL). The organic layer was separated, washed with brine (50 mL), dried over magnesium sulfate, gravity filtered, concentrated by rotary evaporation (37 °C) and the residue transferred to a 25-mL, single-necked, round-bottomed flask. This residue was fractionally distilled under reduced pressure (14 mmHg, 108-115 °C) using a short, jacketed vigreux fractionating column connected to a short-path distillation head to give chloromethylpinacol boronate **3.62** as a colorless liquid (8.89 g, 65%).

Data for 3.62: (PAJ 6-66, 8.89 g, 65%)

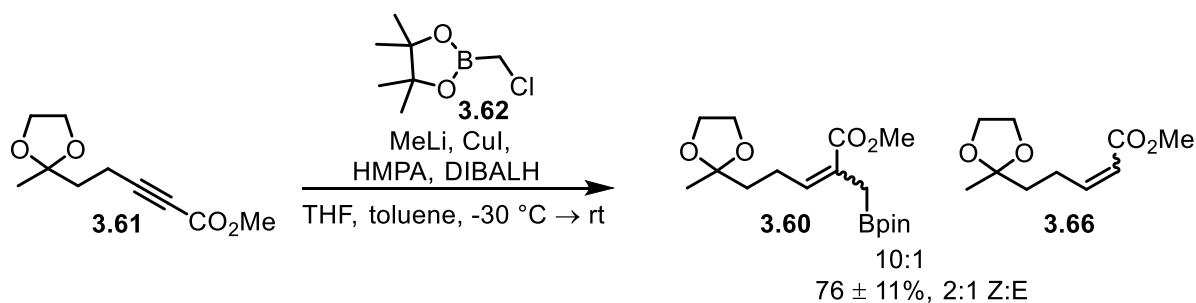
¹H NMR (300 MHz, CDCl₃)
 δ 2.94 (s, 2H), 1.28 (s, 12H) ppm

¹³C NMR (100 MHz, CDCl₃)
 δ 84.7, 24.8 (4C) ppm

¹¹B NMR (128 MHz, CDCl₃)
 δ 31.42 ppm

IR 3459, 2980, 2935, 1352, 1273, 1143 cm⁻¹

TLC *R_f* = 0.45 (10% Et₂O/hexanes) [silica gel, KMnO₄]



Methyl 5-(2-methyl-1,3-dioxolan-2-yl)-2-((4,4,5,5-tetramethyl-1,3,2-dioxaborolan-2-yl)methyl)pent-2-enoate (3.60): Prepared using a procedure analogous to that previously reported.^{117, 137} A flame-dried, 100-mL, single-necked, round-bottomed flask equipped with a magnetic stir bar, septum, and nitrogen inlet needle was charged with copper iodide (48 mg, 0.25 mmol) and tetrahydrofuran (8.4 mL), then cooled to -30 °C. Methyl lithium (1.6 M solution in diethyl ether, 0.16 mL, 0.25 mmol) was added dropwise over 1 min. Upon completion of addition the solution was maintained at -30 °C for an additional 20 min at which time it became dark brown to black in color. Toluene (18 mL) was added slowly to the reaction mixture over 10 min via syringe, followed by hexamethylphosphoramide (0.88 mL, 5.1 mmol, distilled from calcium hydride and stored over 4 Å molecular sieves). Diisobutylaluminum hydride (1 M solution in hexanes, 3.8 mL, 3.8 mmol) was added dropwise via syringe over 10 min at -30 °C, a

temperature that was maintained for an additional 2 h. Alkynoate **3.61** (500 mg, 2.52 mmol) in toluene (12 mL) was added dropwise to the reaction mixture over 10 min via syringe, and the solution was allowed to warm to -20 °C, a temperature that was maintained for 5 h. The reaction was difficult to monitor by TLC, as the alkene byproduct and alkyne starting material had the same R_f, so aliquots were taken and ¹H NMR was used to follow the reaction progress. Freshly distilled chloromethyl pinacol boronate **3.62** (623 mg, 3.53 mmol) in toluene (6 mL) was added dropwise via syringe over 5 min to the solution and this was allowed to warm to rt and stirred 16 h. The reaction was diluted with diethyl ether (10 mL) and slowly quenched by dropwise addition of 1 N hydrochloric acid (2 mL) over 5 min. The layers were separated, and the organic layer was washed sequentially with 1 N hydrochloric acid (3 x 3 mL), saturated aqueous sodium bicarbonate (1 x 5 mL), water (2 x 5 mL), and brine (1 x 10 mL), dried over magnesium sulfate, gravity filtered, concentrated by rotary evaporation, and eluted through a plug of silica gel with 20% diethyl ether in hexanes to yield allylboronate **3.60** (755 mg, 88%) as a pale yellow oil and a 2:1 ratio of Z:E isomers. The Z:E ratio was determined by integration of the alkene resonances at 5.92 ppm for the Z-isomer and 6.71 for the E-isomer. The allylboronate **3.60** was contaminated with about 5% of alkene byproducts **3.66** (2:1 Z:E), as determined by integration of the alkene resonances at 6.25 (dt) and 5.75 (dt) ppm for the Z-alkene and 6.96 (dt) and 5.90 (dt) for the E-alkene. Purification of the allylboronate **3.60** from the alkene **3.66** by column chromatography resulted in significantly decreased yields of the allylboronate, so the mixture was generally taken on to the next step.

This reaction was repeated 10 times with an average yield of 76 ± 11% and gave Z:E ratios of 2:1 to 3:1. The amount of alkene byproduct generally ranged from 10-20%, and this reaction could be performed on gram scale. For example, alkynoate **3.61** (3.02 g, 15.1 mmol),

chloromethylpinacolboronate **3.62** (3.74 g, 21.2 mmol), copper iodide (288 mg, 1.51 mmol), methyl lithium (1.5 M in Et₂O, 1.1 mL, 1.5 mmol), diisobutylaluminum hydride (1 M in hexanes, 23 mL, 23 mmol), hexamethylphosphoramide (5.3 mL, 30 mmol), toluene (216 mL), and THF (50 mL) provided allylboronate **3.60** (3.73 g, 73%, 2:1 Z:E containing ~10% of the alkene byproduct) as a pale yellow oil.

Data for **3.60**: (PAJ 6-74 755 mg, 88%, Characterized as a mixture of Z:E isomers, resonances for Z-isomer; PAJ 8-20, 3.32 g, 64%, 2:1 Z:E; PAJ 7-138, 1.35 g, 78%, 2:1 Z:E)

¹H NMR (400 MHz, CDCl₃)

δ 5.92 (t, *J* = 7.6 Hz, 1H), 3.92-3.88 (m, 4H), 3.67 (s, 3H), 2.56 (app q, *J* = 7.6 Hz, 2H), 1.81 (d, *J* = 13.6 Hz, 2H), 1.77-1.71 (m, 2H), 1.30 (s, 3H), 1.20 (s, 12H)

E-isomer, where distinguishable

6.71 (t, *J* = 7.6 Hz, 1H), 2.25-2.19 (m, 2H)

¹³C NMR (100 MHz, CDCl₃)

δ 168.2, 142.9, 140.6, 129.3, 128.0, 109.9, 83.4, 64.8 (2C), 51.2, 38.6, 24.8, 24.0 (4C) ppm

E-isomer

δ 168.7, 142.9, 141.0, 129.2, 128.0, 109.6, 83.3, 64.8 (2C), 51.7, 37.8, 24.7, 23.7 (4C) ppm

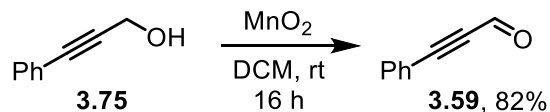
IR (thin film)

2981, 2884, 2240, 1716, 1645, 1437, 1351, 1257, 1145, 1055 cm⁻¹

HRMS TOF MS ES+ [M+H]: C₁₇H₃₀BO₆

Calc: 341.21300 Found: 341.21183

TLC *R_f* = 0.31 (25% EtOAc/hexanes) [silica gel, UV, *p*-anisaldehyde stain]



3-Phenylpropynal (3.59): Propynal **3.59** was prepared as previously described and the spectral data matched that reported.²³⁵ Active γ -manganese dioxide was prepared from manganese sulfate and potassium permanganate according to the previously reported method.²³⁶ Alternatively, propynal **3.59** was prepared according to the procedure for TIPS propynal (*vide infra*) in similar yields.¹⁸³

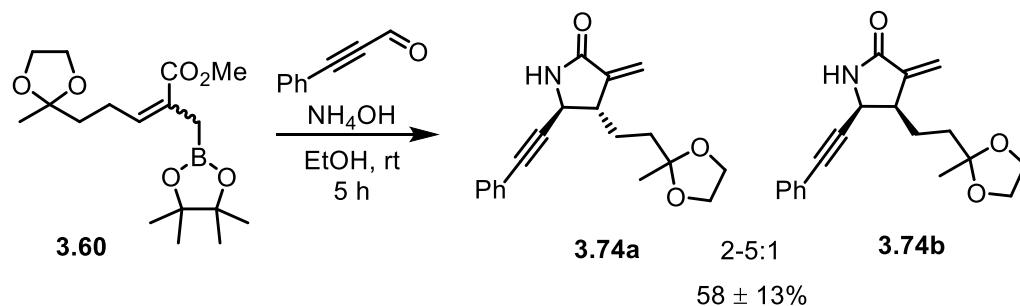
Data for 3.59: (PAJ 7-14, 75%)

¹H NMR (400 MHz, CDCl₃)

δ 9.43 (s, 1H), 7.62-7.60 (m, 2H), 7.51-7.47 (m, 1H), 7.43-7.39 (m, 2H) ppm

¹³C NMR (100 MHz, CDCl₃)

δ 177.0, 133.4 (2C), 131.4, 128.9 (2C), 119.6, 95.3, 88.6 ppm



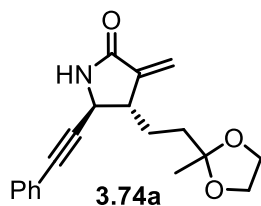
General Procedure A: α -Methylene Lactam Formation from Allylboronate

This procedure was modified from the procedure reported by Hall and Elford.¹³⁶ A 5-mL, single-necked, round-bottomed flask equipped with a magnetic stir bar, septum, and nitrogen inlet needle was charged with 3-phenyl-1-propynal (72 mg, 0.55 mmol) and ethanol (1 mL). Ammonium hydroxide (28-30% ammonia in water, 0.74 mL) was added via syringe in a single portion. The nitrogen inlet needle was removed and the reaction was stirred for 20 min at rt. Allylboronate **3.60** (171 mg, 0.50 mmol, 2:1 Z:E) in ethanol (1 mL) was added dropwise to the

solution over 1 min and the reaction was stirred in the sealed flask for 5 h at rt. TLC showed consumption of the allylboronate, and the reaction was quenched by slow addition 1 N HCl (~5 mL) until the pH was 1.5-2 (pH paper). The resulting solution was transferred to a separatory funnel and extracted with diethyl ether (4 x 10 mL). The combined organic layers were washed with brine (10 mL), dried over magnesium sulfate, gravity filtered, concentrated by rotary evaporation, and purified by silica gel flash column chromatography eluting with 30-50% ethyl acetate in hexanes to give lactams **3.74a** (trans) and **3.74b** (cis) (96 mg, 59%) in a 4:1 ratio. In some cases, the trans lactam was taken on as a single isomer or alternatively the mixture of trans and cis lactams could be taken on as a mixture and separated after formation of propargyl pivalates **3.113a** (trans) and **3.113b** (cis) with no difference in yields. The ratio of trans:cis isomeric ratio varied from 2-5:1. This reaction could be performed on a partially purified mixture of allylboronate **3.60** and alkene **3.66** isomers without significant effects on the yield, although purification became difficult when the allylboronate contained more than ~20% of alkene byproducts.

This reaction was repeated 11 times with an average yield of $58 \pm 13\%$. The ratio of trans:cis lactams ranged from 3:1 to 5:1, although the starting allylboronate was generally 2:1. It is unclear what the ratio of lactam products did not reflect the ratio of the starting allylboronate. This reaction could be performed on gram scale and 2 N HCl was also used to quench the reaction in some cases. For example, allylboronate **3.60** (1.66 g, 4.86 mmol, 2:1 Z:E), phenyl propynal **3.59** (696 mg, 5.35 mmol), ammonium hydroxide (28-30% NH₃, 7.2 mL), and ethanol (20 mL) provided lactam **3.74a,b** (1.38 g, 86%, 5:1 trans:cis) as a brown oil after column chromatography. Another example using allylboronate **3.60** (1.48 g, 4.35 mmol, 2:1 Z:E), phenyl propynal **3.59** (623 mg, 4.79 mmol), ammonium hydroxide (28-30% NH₃, 6.7 mL), and ethanol

(18 mL) provided 3 fractions after column chromatography: pure trans lactam **3.74a** (349 mg, 24%), a predominantly trans mixture of lactams **3.74a,b** (380 mg, 27%, 3:1 trans:cis), and a predominantly cis mixture of lactams **3.74b** (75 mg, 5%, 2:1 cis:trans).



(4S*,5S*)-4-(2-(2-Methyl-1,3-dioxolan-2-yl)ethyl)-3-methylene-5-(phenylethynyl)pyrrolidin-2-one (3.74a):

Data for 3.74a: (PAJ 6-80B trans, 96 mg total, 59% overall, 2:1 trans:cis; Data for trans isomer, some baseline impurities were observed in the NMR spectra; PAJ 8-22, 1.38 g, 86%, 5:1 trans:cis; PAJ 7-32, 349 mg, 24%, trans, 380 mg, 27%, trans:cis 3:1, 75 mg, 5%, cis:trans 2:1)

¹H NMR (300 MHz, CDCl₃)

δ 7.40-7.31 (m, 2H), 7.30-7.27 (m, 3H), 7.04 (bs, 1H), 6.10 (d, *J* = 2.8 Hz, 1H), 5.40, (d, *J* = 1.6 Hz, 1H), 4.24, (d, *J* = 4.0 Hz, 1H), 3.98-3.89 (m, 4H), 3.11-3.09 (m, 1H), 1.88-1.71 (m, 4H), 1.33 (s, 3H) ppm

¹³C NMR (100 MHz, CDCl₃)

δ 169.7, 142.2, 131.8 (2C), 128.7, 128.4 (2C), 122.3, 117.3, 109.7, 87.8, 84.5, 64.8 (2C), 48.8, 46.8, 35.8, 28.2, 24.1 ppm

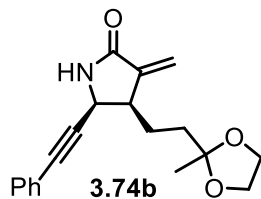
IR (thin film)

2983, 1703, 1659, 1491, 1324, 1063 cm⁻¹

HRMS TOF MS ES+ [M+H]: C₁₉H₂₂NO₃

Calc: 312.1594 Found: 312.1585

TLC *R_f* = 0.17 (50% EtOAc/hexanes) [silica gel, UV, *p*-anisaldehyde stain]



(4R*,5S*)-4-(2-(2-Methyl-1,3-dioxolan-2-yl)ethyl)-3-methylene-5-(phenylethynyl)pyrrolidin-2-one (3.74b):

Data for 3.74b: (PAJ 6-80B cis, 96 mg, 59%, 2:1 trans:cis overall, Data for cis isomer contaminated with about 30% of the trans isomer and some other baseline impurities)

¹H NMR (400 MHz, CDCl₃)

δ 7.41-7.38 (m, 3H), 7.31-7.28 (m, 2H), 6.31 (br s, 1H), 6.11 (d, *J* = 2.4 Hz, 1H), 5.39 (d, *J* = 2.4 Hz, 1H), 4.67 (d, *J* = 8.0 Hz, 1H), 3.93-3.87 (m, 4H), 3.12-3.08 (m, 1H), 1.94-1.84 (m, 2H), 1.76-1.66 (m, 2H), 1.33 (s, 3H) ppm

¹³C NMR (100 MHz, CDCl₃)

δ 170.3, 141.8, 131.8 (2C), 129.0, 128.5 (2C), 122.3, 117.1, 109.9, 86.7, 85.0, 64.8, 64.7, 47.7, 42.7, 36.4, 24.7, 24.1 ppm

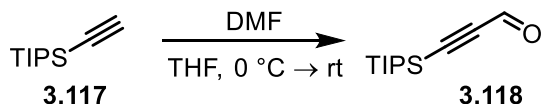
IR (thin film)

2983, 2245, 1704, 1659, 1490, 1321, 1269, 1062 cm⁻¹

HRMS TOF MS ES+ [M+H]: C₁₉H₂₂NO₃

Calc: 312.1594 Found: 312.1586

TLC *R_f* = 0.32 (50% EtOAc/hexanes) [silica gel, UV, *p*-anisaldehyde]



3-(Triisopropylsilyl) propiolaldehyde (3.118): Aldehyde **3.118** was prepared as previously described and the spectral data matched.¹⁸³

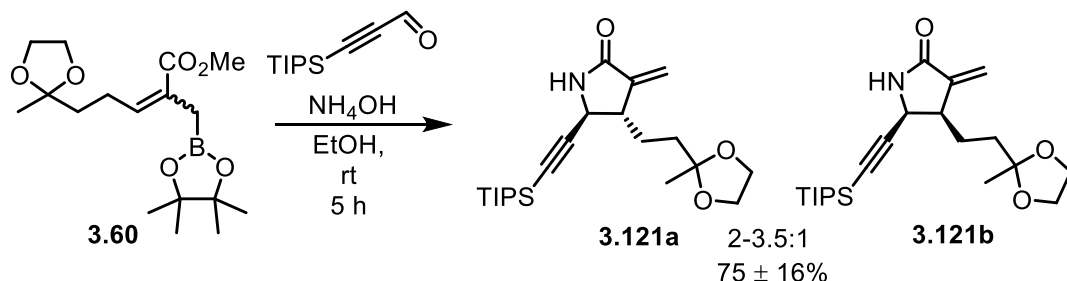
Data for **3.118**: (PAJ 7-2, 99%)

$^1\text{H NMR}$ (400 MHz, CDCl_3)

δ 9.2 (s, 1H), 1.12-1.07 (m, 21H) ppm

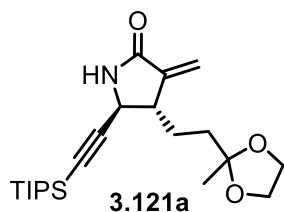
$^{13}\text{C NMR}$ (100 MHz, CDCl_3)

δ 176.8, 104.6, 101.0, 18.6, 11.1 ppm



Prepared according to general procedure A. 3-(Triisopropylsilyl) propionaldehyde (340 mg, 1.62 mmol) ethanol (6 mL), ammonium hydroxide (28-30% ammonia, 2.2 mL), allylboronate **3.60** (500 mg, 1.47 mmol, 15% alkene **3.66**, 2:1 Z:E) were stirred for 5 h. The reaction was quenched with 2 N HCl (10 mL), then extracted with diethyl ether (3 x 20 mL). Column chromatography (gradient elution with 10-40% ethyl acetate in hexanes) provided trans-lactam **3.121a** (126 mg, 18%), cis-lactam **3.121b** (23 mg, 3%, contaminated with 25% trans isomer), and a 2.3:1 trans:cis mixture (217 mg, 31%) as yellow oils in a 53% overall yield and a ratio of 3.5:1 trans:cis lactams. The trans and cis isomers were separated for characterization, but in other cases the trans and cis isomers were not separated but taken on as a mixture.

This reaction was repeated 5 times with an average yield of $75 \pm 16\%$ and good be performed on gram scale. For example, allylboronate **3.60** (1.67 g, 4.86 mmol, 2:1 Z:E), triisopropylsilyl propynal **3.118** (1.13 g, 5.35 mmol), ammonium hydroxide (28-30% NH_3 , 7.2 mL), ethanol (20 mL), provided lactam **3.121a,b** (1.72 g, 90%, 2:1 trans:cis) as a brown oil after column chromatography.



(4S*,5S*)-4-(2-(2-Methyl-1,3-dioxolan-2-yl)ethyl)-3-methylene-5-((triisopropylsilyl)ethynyl)pyrrolidin-2-one (3.121a):

Data for 3.121a: (PAJ 7-16, 366 mg, 53% overall, 3.5:1 trans:cis; Data for pure trans isomer; PAJ 8-120, 1.72 g, 90%, 2:1 trans:cis)

¹H NMR (400 MHz, CDCl₃)

δ 6.06 (d, *J* = 2.6 Hz, 1H), 6.02 (br s, 1H), 5.37 (d, *J* = 2.6 Hz, 1H), 4.02 (d, *J* = 5.2 Hz, 1H), 3.98-3.87 (m, 4H), 3.01-2.97 (m, 1H), 1.91-1.78 (m, 3H), 1.75-1.63 (m, 1H), 1.31 (s, 3H), 1.05 (s, 21H)

¹³C NMR (100 MHz, CDCl₃)

δ 169.3, 142.0, 117.0, 109.6, 106.0, 86.2, 64.9 (2C), 48.9, 47.4, 36.2, 27.7, 25.0, 18.7 (6C), 11.2 (3C)

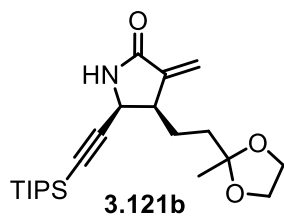
IR (thin film)

2943, 2175, 1708, 1660, 1462, 1376, 1325, 1150, 1063

HRMS TOF MS ES+ [M+H]: C₂₂H₃₈NO₃Si

Calc: 392.2616 Found: 392.2616

TLC *R_f* = 0.30 (50% EtOAc/hexanes) [silica gel, UV, KMnO₄]



(4R*,5S*)-4-(2-(2-Methyl-1,3-dioxolan-2-yl)ethyl)-3-methylene-5-((triisopropylsilyl)ethynyl)pyrrolidin-2-one (3.121b):

Data for 3.121b: (PAJ 7-16, 366 mg, 53% overall, 3.5:1 trans:cis; NMR for cis isomer contaminated with 25% of the trans isomer)

¹H NMR (300 MHz, CDCl₃)

δ 6.23 (br s, 1H), 6.05 (d, *J* = 2.0 Hz, 1H), 5.34 (d, *J* = 2.0 Hz, 1H), 4.45 (d, *J* = 7.6 Hz, 1H), 3.95-3.79 (m, 4H), 3.00-2.97 (m, 1H), 1.90-1.82 (m, 3H), 1.80-1.70 (m, 1H), 1.31 (s, 3H), 1.02 (s, 21H) ppm

¹³C NMR (100 MHz, CDCl₃)

δ 170.3, 142.1, 116.8, 103.2, 109.9, 88.4, 64.8, 64.7, 47.9, 42.8, 36.4, 24.3, 23.9, 18.7 (6C), 11.2 (3C) ppm

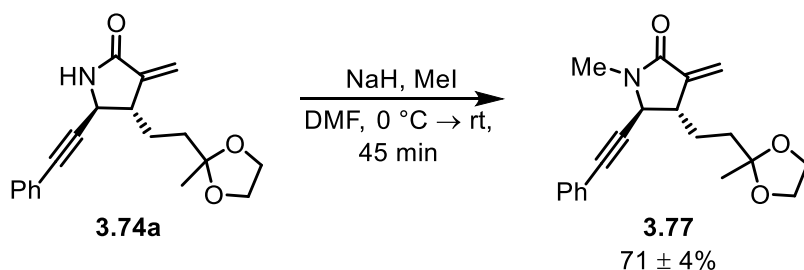
IR (thin film)

3213, 2866, 2175, 1660, 1377, 1221, 1143, 1112 cm⁻¹

HRMS TOF MS ES+ [M+H]: C₂₂H₃₈NO₃Si

Calc: 392.2616 Found: 392.2616

TLC *R_f* = 0.21 (50% EtOAc/hexanes) [silica gel, UV, *p*-anisaldehyde]



(4S*,5S*)-1-Methyl-4-(2-(2-methyl-1,3-dioxolan-2-yl)ethyl)-3-methylene-5-

(phenylethynyl)pyrrolidin-2-one (3.77): A flame-dried, 10-mL, single-necked, round-bottomed flask equipped with a magnetic stir bar, septum, and nitrogen inlet needle was charged with

trans-lactam **3.74a** (337 mg, 1.03 mmol) dissolved in dimethylformamide (5.2 mL) and cooled to 0 °C in an ice bath. Sodium hydride (60% in mineral oil, 62 mg, 1.5 mmol) was added in a single portion and the reaction was stirred 15 min at 0 °C. Iodomethane (0.13 mL, 2.1 mmol) was added dropwise over 1 min and the reaction was stirred at 0 °C for 15 min before removing the ice bath and allowing the reaction to warm to rt for 15 min. TLC showed consumption of the starting material, so it was quenched by pouring into a separatory funnel containing saturated aqueous ammonium chloride solution (20 mL). The mixture was extracted with diethyl ether (3 x 25 mL). The organic layers were combined, washed with brine (10 mL), dried over magnesium sulfate, gravity filtered, concentrated by rotary evaporation, and purified by filtration through a plug of silica gel (elution with 50% ethyl acetate and hexanes) to provide the *N*-methyl lactam **3.77** (225 mg, 67%) as a yellow oil.

This reaction was repeated 3 times with an average yield of $71 \pm 4\%$. In one case ketal **3.74a** (430 mg, 1.3 mmol, 4:1 trans:cis), sodium hydride (60% in mineral oil, 105 mg, 2.6 mmol), iodomethane (0.21 mL, 3.3 mmol), and DMF (7 mL) provided ketal **3.77** (321 mg, 71%, 4:1 trans:cis) as a yellow oil after column chromatography.

Data for **3.77**: (PAJ 6-192, 225 mg, 67%, contaminated with 6% of the cis isomer and some other baseline impurities; 7-106, 321 mg, 71%, 4:1 trans:cis)

¹H NMR (400 MHz, CDCl₃)

δ 7.42-7.40 (m, 2H), 7.34-7.31 (m, 3H), 6.08 (d, $J = 2.4$ Hz, 1H), 5.36 (d, $J = 2.4$ Hz, 1H), 4.12 (d, $J = 4.0$ Hz, 1H), 3.99-3.90 (m, 4H), 3.05-3.04 (m, 1H), 3.03 (s, 3H), 1.87-1.69 (m, 4H), 1.33 (s, 3H)

¹³C NMR (100 MHz, CDCl₃)

δ 167.2, 142.3, 131.8 (2C), 128.9, 128.5 (2C), 122.2, 116.4, 109.7, 86.2, 85.7,
64.9 (2C), 55.4, 44.6, 35.9, 29.8, 28.5, 24.1

IR (thin film)

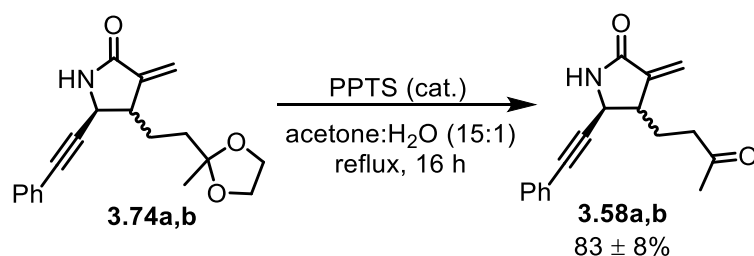
2925, 1697, 1660, 1427, 1396, 1145, 1082 cm^{-1}

HRMS TOF MS ES+ [M+H]: $\text{C}_{20}\text{H}_{24}\text{NO}_3$

Calc: 326.1751 Found: 326.1752

TLC R_f = 0.39 (75% EtOAc/hexanes) [silica gel, UV, *p*-anisaldehyde]

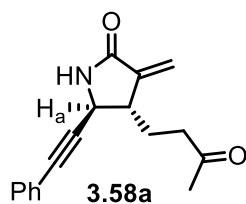
General Procedure B: Hydrolysis of Ketal



A 10-mL, single-necked, round-bottomed flask equipped with a magnetic stir bar was charged with ketal **3.74a,b** (100 mg, 0.304 mmol, 5:1 trans:cis), acetone (4 mL), and water (0.3 mL). Pyridinium *para*-toluene sulfonate (38 mg, 0.152 mmol) was added in a single portion, a reflux condenser capped with a septum and nitrogen inlet needle was attached and the reaction was refluxed for 16 h in a 70 °C oil bath. Upon completion of the reaction as observed by TLC, the reaction was allowed to cool to rt, diluted with ethyl acetate (20 mL), transferred to a separatory funnel, then washed consecutively with water (2 x 5 mL) and brine (1 x 5 mL), dried over magnesium sulfate, gravity filtered, concentrated by rotary evaporation, then eluted through a plug of silica gel with 75% ethyl acetate in hexanes to yield ketone **3.58a,b** (63 mg, 73%, 5:1 trans:cis) as a light yellow oil. In larger scale reactions, acetone was removed by rotary evaporation prior to dilution with ethyl acetate. The product contained 16% of the cis lactam

isomer by integration of the trans lactam resonance for H_a at 4.21 ppm and the cis lactam resonance of H_a at 4.68 ppm.

This reaction was repeated 9 times with an average yield of 83 ± 8%. The trans and cis isomers were generally taken on as a mixture and only isolated for characterization. This reaction could be performed on gram scale. For example, ketal **3.74a,b** (1.66 g, 5.33 mmol, 3:1 trans:cis), pyridinium *para*-toluenesulfonate (670 mg, 2.7 mmol), acetone (72 mL), and water (4 mL) provided ketone **3.58a,b** (1.3 g, 91%, 3:1 trans:cis) as a pale yellow oil after column chromatography.



(4S*,5S*)-3-Methylene-4-(3-oxobutyl)-5-(phenylethynyl)pyrrolidin-2-one (3.58a):

Data for 3.58a: (PAJ 6-150, 63 mg, 73%, NMR contained 16% of the cis isomer)

¹H NMR (300 MHz, CDCl₃)

δ 7.38-7.37 (m 2H), 7.32-7.29 (m, 3H), 6.77 (br s, 1H). 6.11 (d, *J* = 2.4 Hz, 1H), 5.40 (d, *J* = 2.4 Hz, 1H), 4.21 (d, *J* = 4.8 Hz, 1H), 3.16-3.08 (m, 1H), 2.64 (t, *J* = 7.8 Hz, 2H), 2.14 (s, 3H), 2.14-2.13 (m, 1H), 1.92-1.80 (m, 1H) ppm

Cis isomer: 4.68 (d, *J* = 7.5 Hz, 1H)

¹³C NMR (100 MHz, CDCl₃)

δ 207.5, 169.5, 141.8, 131.8 (2C), 128.9, 128.5 (2C), 122.1, 117.4, 87.4, 84.9, 48.8, 46.1, 39.9, 30.3, 27.0 ppm

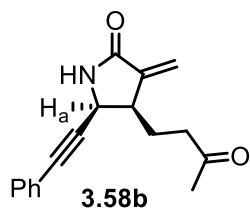
IR (thin film)

3434, 2088, 1643 cm⁻¹

HRMS TOF MS ES+ [M+H]: C₁₇H₁₈NO₂

Calc: 268.1344 Found: 268.1332

TLC *R_f* = 0.32 (75% EtOAc/hexanes) [silica gel, UV, *p*-anisaldehyde]



(4*R,5*S**)-3-methylene-4-(3-oxobutyl)-5-(phenylethynyl)pyrrolidin-2-one (3.58b)**: Prepared according to general procedure B. Ketal **3.74a,b** (426 mg, 1.30 mmol, 3:1 trans:cis), pyridinium *para*-toluene sulfonate (163 mg, 0.648 mmol), acetone (18 mL), and deionized water (1 mL) provided ketone **3.58a,b** (307 mg, 88%, 3:1 trans:cis) as a clear oil after filtration through silica gel (elution with 50% ethyl acetate in hexanes). The cis isomer was isolated for characterization.

Data for 3.58b: (7-46, 3:1 trans:cis, 307 mg, 88% overall, NMR for cis isomer contained 10% trans isomer)

¹H NMR (300 MHz, CDCl₃)

δ 7.39-7.37 (m 2H), 7.34-7.30 (m, 3H), 6.39 (br s, 1H). 6.13 (d, *J* = 2.3 Hz, 1H), 5.42 (d, *J* = 2.3 Hz, 1H), 4.70 (d, *J* = 7.5 Hz, 1H), 3.17-3.13 (m, 1H), 2.72-2.58 (m, 2H), 2.16 (s, 3H), 2.15-2.09 (m, 2H) ppm

¹³C NMR (100 MHz, CDCl₃)

δ 207.9, 169.9, 141.5, 131.9 (2C), 129.0, 128.6 (2C), 122.0, 117.6, 87.2, 84.6, 47.5, 41.7, 40.5, 30.2, 24.5 ppm

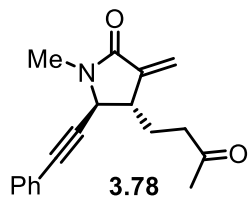
IR (thin film)

3245, 2927, 1708, 1657, 1418, 1360, 1273, 1166 cm⁻¹

HRMS TOF MS ES+ M+H]: C₁₇H₁₈NO₂

Calc: 268.1332 Found: 268.1327

TLC $R_f = 0.28$ (75% EtOAc/hexanes) [silica gel, UV, *p*-anisaldehyde]



(4S*,5S*)-1-Methyl-3-methylene-4-(3-oxobutyl)-5-(phenylethynyl)pyrrolidin-2-one (3.78):

Prepared according to general procedure B. trans-Ketal **3.77** (290 mg, 0.882 mmol, contaminated with 6% cis isomer), pyridinium *para*-toluene sulfonate (111 mg, 0.441 mmol), acetone (12 mL), and water (0.6 mL) provided the product **3.78** (164 mg, 66%) as a yellow oil after column chromatography. Another example of this reaction used ketal **3.77** (490 mg, 1.4 mmol, 5:1 trans:cis), pyridinium *para*-toluenesulfonate (180 mg, 0.72 mmol, acetone (19 mL), and water (1 mL) to provide trans ketone **3.78** (310 mg, 73%, 19:1 trans:cis) and cis ketone (not shown, 18 mg, 4%, 7:1 cis:trans) each as clear oils after column chromatography.

Data for 3.78: (PAJ 6-196, 164 mg, 66%, NMR contaminated with ~5% of cis isomer; PAJ 7-108, 328 mg, 77% total)

^1H NMR (500 MHz, CDCl_3)

δ 7.42-7.40 (m, 2H), 7.35-7.32 (m, 3H), 6.11 (d, $J = 2.5$ Hz, 1H), 5.36 (d, $J = 2.5$ Hz, 1H), 4.08 (d, $J = 4.5$ Hz, 1H), 3.08-3.04 (m, 1H), 3.03 (s, 3H), 2.66-2.63 (app. t, $J = 7.5$ Hz, 2H), 2.17 (s, 3H), 2.12-2.04 (m, 1H), 1.90-1.84 (m, 1H) ppm

^{13}C NMR (125 MHz, CDCl_3)

δ 207.5, 167.1, 142.0, 131.9 (2C), 129.0, 128.6 (2C), 122.1, 116.5, 86.1, 85.9, 55.4, 44.1, 40.1, 30.3, 28.5, 27.3 ppm

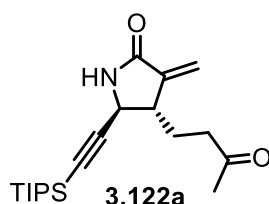
IR (thin film)

2924, 1696, 1424, 1396, 1265 cm⁻¹

HRMS TOF MS ES+ M+H]: C₁₈H₂₀NO₂

Calc: 282.1489 Found: 282.1489

TLC R_f = 0.48 (50% EtOAc/hexanes) [silica gel, UV, *p*-anisaldehyde]



(4S*,5S*)-3-Methylene-4-(3-oxobutyl)-5-((triisopropylsilyl)ethynyl)pyrrolidin-2-one

(3.122a): Prepared according to general procedure B. Ketal **3.121a** (120 mg, 0.306 mmol, pure trans), pyridinium *para*-toluene sulfonate (39 mg, 0.15 mmol), acetone (4.1 mL), and water (0.3 mL) provided ketone **3.122a** (74 mg, 70%) as a pale yellow oil after filtration through a plug of silica (elution with 50% ethyl acetate in hexanes).

This reaction was repeated 6 times with an average yield of $73 \pm 9\%$. The cis and trans isomers were generally taken on as a mixture but were isolated for characterization in some cases. The trans:cis ratio reflected the ratio of the starting ketal. This reaction could be performed on gram scale with good yields. For example, ketal **3.121a,b** (1.74 g, 4.4 mmol, 2:1 trans:cis), pyridinium *para*-toluenesulfonate (552 mg, 2.2 mmol), acetone (60 mL), and water (3 mL) provided ketone **3.122a,b** (1.05 g, 68%, 2:1 trans:cis) as a pale yellow oil after column chromatography. Another example used ketal **3.121a,b** (350 mg, 0.89 mmol, 2:1 trans:cis), pyridinium *para*-toluenesulfonate (112 mg, 0.45 mmol), acetone (13 mL), and water (1 mL) to provide ketone **3.122a,b** (265 mg, 85%, 1.5:1 trans:cis) as a clear oil after column chromatography.

Data for **3.122a**: (PAJ 7-20, 74 mg, 70%; 8-124, 1.05 g, 2:1 trans:cis; 7-146, 265 mg, 85%, 1.5:1 trans:cis)

¹H NMR (400 MHz, CDCl₃)

δ 6.26 (br s, 1H), 6.08 (d, *J* = 2.6 Hz, 1H), 5.38 (dd, *J* = 2.6 Hz, 0.8 Hz, 1H), 4.00 (d, *J* = 4.8 Hz, 1H), 3.03-2.97 (m, 1H), 2.68-2.58 (m, 2H), 2.16 (s, 3H), 2.15-2.06 (m, 1H), 1.85-1.75 (m, 1H), 1.05 (s, 21H) ppm

¹³C NMR (100 MHz, CDCl₃)

δ 207.3, 169.1, 141.6, 117.2, 105.9, 86.5, 48.9, 46.6, 40.3, 30.1, 26.9, 18.7 (6C), 11.2 (3C) ppm

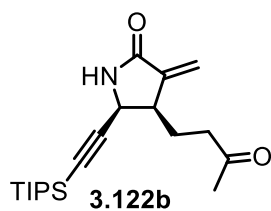
IR (thin film)

2943, 2865, 2175, 1709, 1659, 1463, 1366, 1323 cm⁻¹

HRMS TOF MS ES+ [M+H]: C₂₀H₃₄O₂NSi

Calc: 348.2359 Found: 348.2373

TLC *R_f* = 0.48 (75% EtOAc/hexanes) [silica gel, UV, *p*-anisaldehyde]



(4R*,5S*)-3-Methylene-4-(3-oxobutyl)-5-((triisopropylsilyl)ethynyl)pyrrolidin-2-one

(3.122b): Prepared according to general procedure B. Ketal **3.121a,b** (1.72 g, 4.39 mmol, 4:1 trans:cis), pyridinium *para*-toluene sulfonate (552 mg, 2.20 mmol), acetone (60 mL), and deionized water (3 mL) provided ketone **3.122a,b** (1.22 g, 80%, 4:1 trans:cis) and ketone **3.122a,b** (30 mg, 2%, 5:1 cis:trans) each as a pale yellow oil after column chromatography (gradient elution with 25-75% ethyl acetate in hexanes).

Data for 3.122b: (PAJ 8-28, 1.25 g, 80%, 4:1 trans:cis, NMR contained ~20% of trans isomer)

¹H NMR (400 MHz, CDCl₃)

δ 6.48 (br s, 1H), 6.07 (d, *J* = 2.4 Hz, 1H), 5.37 (d, *J* = 2.4 Hz, 1H), 4.46 (d, *J* = 8.0 Hz, 1H), 3.04-2.99 (m, 1H), 2.69-2.51 (m, 2H), 2.14 (s, 3H), 2.13-1.97 (m, 2H), 1.0 (s, 21H) ppm

¹³C NMR (100 MHz, CDCl₃)

δ 207.5, 170.0, 141.5, 117.3, 102.8, 88.8, 47.5, 41.3, 40.5, 30.0, 24.3, 18.6 (6C), 11.2 (3C) ppm

IR (thin film)

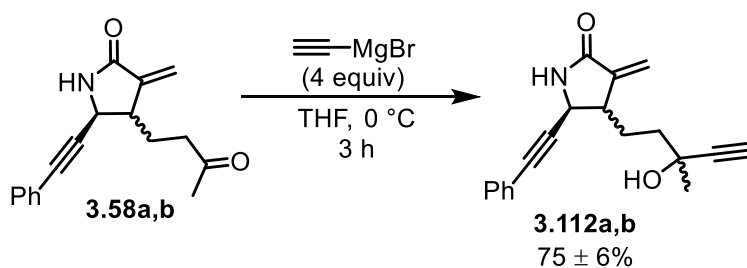
3175, 2909, 2832, 2145, 1690, 1639, 1446, 1348, 1308, 1257, 1151 cm⁻¹

HRMS TOF MS ES+ [M+H]: C₂₀H₃₄O₂NSi

Calc: 348.2353 Found: 348.2363

TLC *R_f* = 0.41 (75% EtOAc/hexanes) [silica gel, UV, *p*-anisaldehyde]

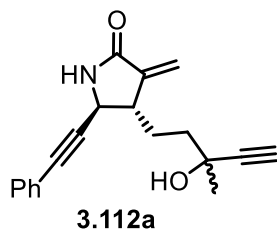
General Procedure C: Addition of Ethynyl Magnesium Bromide to Ketone



A flame-dried, 100-mL, single-necked, round-bottomed flask equipped with a magnetic stir bar, a septum, and a nitrogen inlet needle was charged with ketone **3.58a,b** (558 mg, 2.08 mmol, ~3:1 trans:cis) dissolved in tetrahydrofuran (25 mL). The solution was cooled to 0 °C in an ice bath, then ethynyl magnesium bromide (0.5 M solution in tetrahydrofuran, 17 mL, 8.5 mmol) was added dropwise via syringe over 15 min. The reaction was stirred for 3 h at 0 °C,

then quenched at 0 °C by dropwise addition of 1 N HCl (25 mL). The resulting solution was transferred to a separatory funnel and extracted with diethyl ether (4 x 40 mL). The organic layers were combined, washed with brine (20 mL), dried over magnesium sulfate, gravity filtered, concentrated by rotary evaporation, and purified by silica gel flash column chromatography eluting with 40-60% ethyl acetate in hexanes to provide trans propargyl alcohol **3.112a** (41 mg, 7%), cis propargyl alcohol **3.112b** (1 mg, 1%, cis), and a 4:1 trans:cis mixture of propargyl alcohols **3.112a,b** (385 mg, 63%) each as clear oils and a 1:1 ratio of diastereomers as determined by ¹³C NMR.

The cis and trans isomers were generally taken on as a mixture, but were separated for characterization in some cases. This reaction was repeated 6 times with an average yield of 75 ± 6% and the trans:cis ratio of propargyl alcohol products reflected the ratio of the ketone starting material. This reaction could be performed on gram scale. For example, ketone **3.58a,b** (1.30 g, 4.9 mmol, 3:1 trans:cis), ethynyl magnesium bromide (0.5 M in THF, 38 mL, 19 mmol), and THF (60 mL) provided propargyl alcohols **3.112a,b** (1.13 g, 78%, 3:1 trans:cis) as a clear oil after column chromatography. Another example using ketone **3.58a,b** (640 mg, 2.4 mmol, 4:1 trans:cis), ethynyl magnesium bromide (0.5 M in THF, 19 mL, 9.5 mmol), and THF (29 mL) provided propargyl alcohols **3.112a,b** in two fractions (528 mg, 75%, 6:1 trans:cis, and 39 mg, 6%, 2:1 cis:trans) each as clear oils after column chromatography.



(4S*,5S*)-4-(3-Hydroxy-3-methylpent-4-ynyl)-3-methylene-5-(phenylethynyl)pyrrolidin-2-one (3.112a):

Data for 3.112a: (PAJ 7-62, 426 mg total, 70%, 4:1 trans:cis; PAJ 9-24, 1.13 g, 78%, 3:1 trans:cis; PAJ 8-32, 528 mg, 75%, 6:1 trans:cis, 39 mg, 6%, 2:1 cis:trans)

¹H NMR (500 MHz, CDCl₃)

δ 7.40-7.38 (m, 2H), 7.31-7.27 (m, 3H), 6.98 (br s, 1H), 6.12 (d, *J* = 2.0 Hz, 1H), 5.43 (d, *J* = 2.0 Hz, 1H), 4.26 (d, *J* = 4.5 Hz, 1H), 3.14-3.11 (m, 1H), 2.62 (br s, 1H), 2.46 (s, 1H), 2.04-1.96 (m, 1H), 1.90-1.79 (m, 3H), 1.52 (s, 3H) ppm

Et₂O detected at 3.48 and 1.21 ppm

¹³C NMR (125 MHz, CDCl₃)

δ 169.8, 142.0, 131.8 (2C), 128.8, 128.5 (2C), 122.2, 117.6, 117.5*, 87.7, 87.4, 84.7, 72.01, 71.97*, 67.67, 67.65*, 48.9, 48.8*, 46.80, 46.78*, 39.9, 39.8*, 30.3, 30.2*, 28.9, 28.8* ppm

*Discernible signals for one of two diastereomers

Et₂O detected at 65.9 and 15.2 ppm

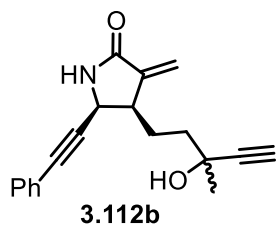
IR (thin film)

3448, 1652, 1156 cm⁻¹

HRMS TOF MS ES+ [M+H]: C₁₉H₂₀NO₂

Calc: 294.1489 Found: 294.1477

TLC *R_f* = 0.36 (75% EtOAc/hexanes) [silica gel, UV, *p*-anisaldehyde]



(4R*,5S*)-4-(3-Hydroxy-3-methylpent-4-yn-1-yl)-3-methylene-5-(phenylethynyl)pyrrolidin-2-one (3.112b):

Data for **3.112b**: (PAJ 7-62, 426 mg, 4:1 trans:cis, NMR contained ~15% of the trans isomer)

¹H NMR (500 MHz, CDCl₃)

δ 7.41-7.39 (m, 2H), 7.33-7.27 (m, 3H), 6.19 (br s, 1H), 6.13 (d, *J* = 2.3 Hz, 1H), 5.44 (d, *J* = 2.3 Hz, 1H), 5.42 (d, *J* = 2.0 Hz, 1H)*, 4.70 (d, *J* = 7.5 Hz, 1H), 4.69 (d, *J* = 8.0 Hz, 1H)*, 3.16-3.13 (m, 1H), 2.36 (s, 1H), 2.16 (s, 1H)*, 2.14-2.06 (m, 2H), 1.95-1.90 (m, 1H), 1.84-1.78 (m, 1H), 1.53 (s, 3H) ppm

¹³C NMR (125 MHz, CDCl₃)

δ 170.2, 141.7, 131.9 (2C), 131.85*(2C), 129.0, 128.9*, 128.6 (2C), 128.5*, 122.2, 122.0*, 117.3, 117.2*, 87.3, 87.2*, 85.0, 84.9*, 72.1, 71.9*, 68.0, 67.8*, 47.74, 47.71*, 47.4, 46.2*, 42.74, 42.71*, 40.55, 40.51*, 30.4, 30.3*, 30.2, 30.1* ppm

*Discernible signals for one of two diastereomers

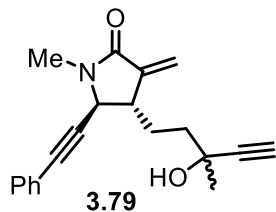
IR (thin film)

2929, 2231, 2145, 1686, 1660, 1490, 1435, 1400, 1276, 1082 cm⁻¹

HRMS TOF MS ES+ [M+H]: C₁₉H₂₀NO₂

Calc: 294.1489 Found: 294.1477

TLC *R_f* = 0.29 (75% EtOAc/hexanes) [silica gel, UV, *p*-anisaldehyde]



(4S*,5S*)-4-(3-Hydroxy-3-methylpent-4-ynyl)-1-methyl-3-methylene-5-

(phenylethynyl)pyrrolidin-2-one (3.79): Prepared according to general procedure C. Ketone **3.78** (310 mg, 1.04 mmol, trans:cis 7:1), THF (14 mL) and ethynyl magnesium bromide (0.5 M

solution in THF, 6.3 mL, 3.1 mmol) provided propargyl alcohol **3.79** (198 mg, 62%, trans:cis 7:1, 1:1 ratio of diastereomers) as a white, sticky solid after column chromatography (gradient elution with 20-60% ethyl acetate in hexanes). The diastereomeric ratio is based on the ^{13}C NMR, as the diastereomers were indistinguishable by ^1H NMR.

Data for 3.79: (PAJ 7-114, 198 mg, 62%, trans:cis 7:1, NMR contaminated with about 7% of the ketone starting material)

^1H NMR (400 MHz, CDCl_3)

δ 7.42-7.39 (m, 2H), 7.34-7.31 (m, 3H), 6.09 (d, $J = 2.6$ Hz, 1H), 5.38 (d, $J = 2.6$ Hz, 1H), 4.13 (d, $J = 4.0$ Hz, 1H), 3.07-3.05 (m, 1H), 3.03 (s, 3H), 2.47 (s, 1H), 2.28 (br s, 1H), 2.06-1.95 (m, 1H), 1.87-1.78 (m, 3H), 1.53 (s, 3H) ppm

^{13}C NMR (100 MHz, CDCl_3)

δ 167.2, 142.14, 142.12*, 131.9 (2C), 128.9, 128.5 (2C), 122.1, 116.64, 116.66*, 87.2, 86.1, 85.9, 72.13, 72.09*, 67.8, 67.7*, 55.4, 55.3*, 44.6, 44.5*, 39.9, 39.8*, 30.4, 30.3*, 29.2, 29.0*, 28.6 ppm

*Discernible signals for one of two diastereomers

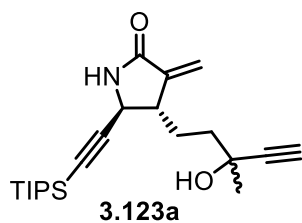
IR (thin film)

3298, 2979, 2929, 2231, 2108, 1680, 1659, 1490, 1432, 1292, 1159, 1084 cm^{-1}

HRMS TOF MS ES+ $[\text{M}+\text{H}]$: $\text{C}_{20}\text{H}_{22}\text{NO}_2$

Calc: 308.1651 Found: 308.1658

TLC $R_f = 0.60$ (50% EtOAc/hexanes) [silica gel, UV, *p*-anisaldehyde]



(4S*,5S*)-4-(3-Hydroxy-3-methylpent-4-ynyl)-3-methylene-5-

((triisopropylsilyl)ethynyl)pyrrolidin-2-one (3.123a): Prepared according to general procedure C. Ketone **3.122a** (270 mg, 0.78 mmol, pure trans), ethynyl magnesium bromide (0.5 M solution in tetrahydrofuran, 6.2 mL, 3.1 mmol), and tetrahydrofuran (9.3 mL) yielded the propargyl alcohol **3.123a** (265 mg, 91%) as a pale yellow oil and a 1:1 mixture of diastereomers based on the ¹³C NMR.

This reaction was repeated 5 times with an average yield of 82 ± 9% and the trans:cis ratio remained the same as the starting material. For example, ketone **3.122a,b** (2.30 g, 6.62 mmol, 2.3:1 trans:cis), ethynyl magnesium bromide (0.5 M in THF, 53 mL, 27 mmol), and THF (79 mL) provided propargyl alcohol **3.123a,b** (2.25 g, 6.02 mmol, 2.3:1 trans:cis) in 91% yield.

Data for 3.123a: (PAJ 7-44, 265 mg, 91%, 1:1 mixture of diastereomers)

¹H NMR (500 MHz, CDCl₃)

δ 6.09 (d, *J* = 3.0 Hz, 1H), 5.90 (br s, 1H), 5.41 (s, 1H), 4.05 (d, *J* = 5.0 Hz, 1H), 3.05-3.04 (m, 1H), 2.47 (s, 1H)*, 2.46 (s, 1H), 2.16-2.03 (m, 1H), 1.93-1.77 (m, 4H), 1.24 (s, 3H), 1.05 (s, 21H) ppm

¹³C NMR (125 MHz, CDCl₃)

δ 169.1, 141.8, 117.13, 117.09*, 105.9, 87.2, 87.1*, 86.4, 72.1, 67.80, 67.77*, 49.0, 48.9*, 47.4, 47.3*, 30.5, 30.3*, 28.45, 28.40*, 25.0, 18.7 (6C), 11.2 (3C) ppm

*Discernible signals for one of two diastereomers

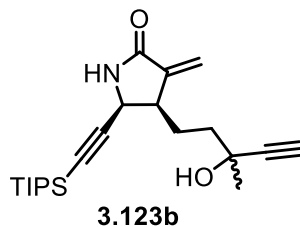
IR (thin film)

2943, 2865, 1703, 1660, 1462, 1323, 1260, 1093, 1019 cm⁻¹

HRMS TOF MS ES+ [M+H]: C₂₂H₃₆NO₂Si

Calc: 374.2515 Found: 374.2508

TLC $R_f = 0.33$ (50% EtOAc/hexanes) [silica gel, UV, *p*-anisaldehyde]



(4R*,5S*)-4-(3-Hydroxy-3-methylpent-4-yn-1-yl)-3-methylene-5-

((triisopropylsilyl)ethynyl)pyrrolidin-2-one (3.123b): Prepared according to general procedure

C. Ketone **3.122a,b** (1.22 g, 3.51 mmol, 4:1 trans:cis), ethynyl magnesium bromide (0.5 M solution in THF, 28 mL, 14 mmol), and THF (42 mL) provided trans propargyl alcohol **3.123a,b** (1.07 g, 82%, 4:1 trans:cis) and cis propargyl alcohol **3.123b,a** (52 mg, 4%, 2:1 cis:trans) each as a white sticky solid after column chromatography (gradient elution with 50-75% ethyl acetate in hexanes). The ratio of diastereomers was estimated to be about 1.5:1 based on the ratio of ^{13}C NMR peaks, but the peaks could not be separately integrated in the ^1H NMR.

Data for 3.123b: (PAJ 8-34, 1.12 g, 86%, ~4:1 trans:cis overall, NMR contained ~56% of trans isomer)

^1H NMR (400 MHz, CDCl_3)

δ 6.52 (br s, 1H), 6.06 (d, $J = 1.8$ Hz, 1H), 5.38 (d, $J = 1.8$ Hz, 1H), 4.48 (app t, $J = 6.6$ Hz, 1H), 3.04-3.00 (m, 1H), 2.42 (s, 1H), 2.41*(s, 1H), 2.04-1.95 (m, 2H), 1.89-1.75 (m, 2H), 1.50 (s, 3H), 1.49* (s, 3H), 1.02 (s, 21H) ppm

^{13}C NMR (100 MHz, CDCl_3)

δ 170.3, 170.2*, 141.8, 117.2, 116.9*, 103.2, 103.0*, 88.7, 88.5*, 87.7, 87.3*, 72.0, 71.7*, 67.9, 67.7*, 48.0, 47.9*, 42.8, 42.7*, 40.4, 40.2*, 30.2, 30.0*, 25.2, 25.0*, 18.70 (6C), 18.67*, 11.2 (3C) ppm

*Discernible signals for one of two diastereomers

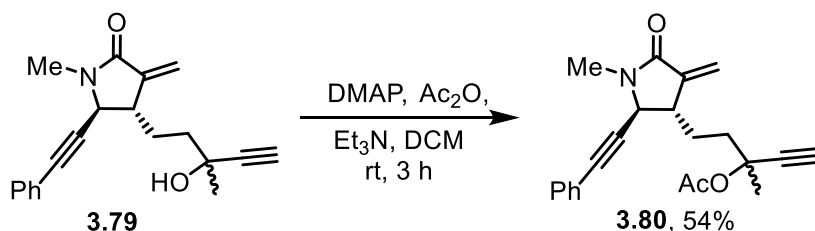
IR (thin film)

2943, 2246, 2172, 1703, 1658, 1544, 1462, 1321, 1172, 1072 cm^{-1}

HRMS TOF MS ES+ [M+H]: $\text{C}_{22}\text{H}_{36}\text{NO}_2\text{Si}$

Calc:308.1651 Found: 308.1658

TLC $R_f = 0.22$ (50% EtOAc/hexanes) [silica gel, UV, *p*-anisaldehyde]



3-Methyl-5-((2*S,3*S**)-1-methyl-4-methylene-5-oxo-2-(phenylethynyl)pyrrolidin-3-yl)pent-**

1-yn-3-yl acetate (3.80**):** A flame-dried, 5-mL, single-necked, round-bottomed flask equipped with a stir bar, septum, and nitrogen inlet needle was charged with dimethylaminopyridine (DMAP, 4 mg, 0.03 mmol) and propargyl alcohol **3.79** (86 mg, 0.27 mmol) dissolved in DCM (1.3 mL) and cooled to 0 °C. Triethylamine (0.37 mL, 2.7 mmol) was added dropwise via syringe over 2 min, followed by dropwise addition of acetic anhydride (0.12 mL, 1.3 mmol) over 1 min via syringe. The ice bath was removed, and the mixture was allowed to warm to rt for 3 h. TLC showed consumption of the starting material, so the mixture was diluted with DCM (25 mL) and transferred to a separatory funnel. The organic layer was washed with saturated aqueous ammonium chloride (5 mL), then brine (5 mL), dried over magnesium sulfate, gravity filtered, concentrated by rotary evaporation, and purified by flash column chromatography on silica gel (gradient elution with 40-50% ethyl acetate in hexanes) to provide lactam **3.80** (50 mg, 54%) as a clear oil and a 1:1 ratio of diastereomers based on ratio of peaks in the ^{13}C NMR.

Using acetic anhydride and following general procedure D (see below) 30% of acetate **3.80** was obtained after column chromatography.

Data for 3.80: (PAJ 6-206, 50 mg, 54%)

¹H NMR (400 MHz, CDCl₃)

δ 7.42-7.40 (m, 2H), 7.34-7.29 (m, 3H), 6.13 (d, *J* = 2.4 Hz, 1H), 5.37 (d, *J* = 2.4 Hz, 1H), 4.11 (d, *J* = 4.0 Hz, 1H), 3.08-3.05 (m, 1H), 3.03 (s, 3H), 2.58 (s, 1H), 2.16-2.07 (m, 1H), 2.03 (s, 3H), 1.98-1.81 (m, 3H), 1.70 (s, 3H) ppm

¹³C NMR (100 MHz, CDCl₃)

δ 169.42, 169.39*, 167.1, 142.0, 131.9 (2C), 129.0, 128.5 (2C), 122.1, 116.6, 116.5*, 86.0, 83.42, 83.39*, 74.51, 74.48*, 74.02, 74.00*, 55.3, 55.2*, 44.5, 44.4*, 38.23, 38.19*, 28.63, 28.57, 28.5, 26.71, 26.66*, 22.01 ppm

*Discernible signals for one of two diastereomers

IR (thin film)

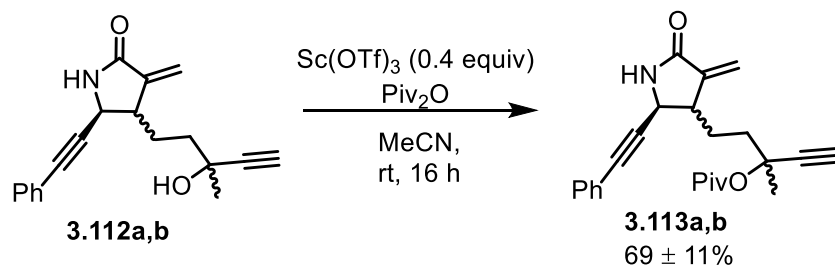
3292, 2937, 2243, 2120, 1742, 1697, 1661, 1427, 1243, 1173, 1082 cm⁻¹

HRMS TOF MS ES+ [M+H]: C₂₂H₂₄NO₃

Calc: 350.1751 Found: 350.1751

TLC *R_f* = 0.26 (50% EtOAc/hexanes, [silica gel, UV, KMnO₄])

General Procedure D: Formation of Propargyl Pivalate from Propargyl Alcohol

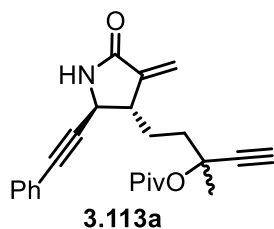


This reaction was generally performed on a mixture of cis and trans propargyl alcohols **3.112a,b** and separated after this reaction as the pivalates **3.113a,b** were the most easily separable cis and trans lactam isomers.

A flame-dried, 10-mL test tube equipped with a magnetic stir bar, septum, and nitrogen inlet needle was charged with propargyl alcohol **3.112a** (56 mg, 0.18 mmol, pure trans) dissolved in acetonitrile (0.72 mL). Trimethyl acetic anhydride (0.05 mL, 0.2 mmol) was then added via syringe followed by scandium(III) trifluoromethanesulfonate (36 mg, 0.073 mmol). The reaction was stirred at rt for 16 h. TLC showed consumption of the starting material, so the reaction was diluted with diethyl ether (20 mL), transferred to a separatory funnel, then washed with saturated sodium bicarbonate solution (10 mL). The aqueous layer was extracted with diethyl ether (2 x 10 mL), the organic layers were combined, washed with brine, dried over magnesium sulfate, gravity filtered, concentrated by rotary evaporation, and purified by silica gel flash column chromatography (gradient elution with 15-30% ethyl acetate in hexanes) to provide propargyl pivalate **3.113a** (54 mg, 76%) as a clear oil. The diastereomers were not distinguishable by ¹H NMR. ¹³C NMR showed a 1:1 mixture of diastereomers.

This reaction was repeated 7 times with a yield of 69 ± 11%. The ratio of isolated trans:cis products reflected the ratio of the propargyl alcohol starting materials. For example, propargyl alcohol **3.112a,b** (368 mg, 1.25 mmol, 3.5:1 trans:cis), pivalic anhydride (0.36 mL, 1.8 mmol), scandium(III) trifluoromethanesulfonate (246 mg, 0.50 mmol), and MeCN (5 mL) provided trans pivalate **3.113a** (299 mg, 61%) and cis pivalate **3.113b** (79 mg, 16%) after column chromatography. Another example, propargyl alcohol **3.112a,b** (1.13 g, 3.85 mmol, 3:1 trans:cis), pivalic anhydride (0.94 mL, 4.62 mmol), scandium(III) trifluoromethanesulfonate (758 mg, 1.54 mmol), and acetonitrile (15 mL) provided trans pivalate **3.113a** (490 mg, 34%), cis

pivalate **3.113b** (163 mg, 11%), and a 4:1 trans:cis mixture (176 mg, 12%) each as a clear oil after column chromatography.



3-Methyl-5-((2S*,3S*)-4-methylene-5-oxo-2-(phenylethynyl)pyrrolidin-3-yl)pent-1-yn-3-yl pivalate (3.113a**):**

Data for **3.113a**: (PAJ 6-160, 54 mg, 76%; PAJ 7-184, 299 mg trans, 79 mg cis, 77% total; PAJ 9-26, 490 mg trans, 163 mg cis, 176 mg mix, 57% total)

¹H NMR (500 MHz, CDCl₃)

δ 7.35-7.34 (m, 2H), 7.27-7.21 (m, 3H), 6.98 (s, 1H), 6.08 (d, *J* = 2 Hz, 1H), 5.36 (s, 1H), 4.21 (d, *J* = 4.5 Hz, 1H), 3.10-3.09 (m, 1H), 2.50 (s, 1H), 2.12-2.04 (m, 1H), 1.95-1.90 (m, 2H), 1.84-1.77 (m, 1H), 1.64 (s, 3H), 1.13 (s, 9H) ppm

¹³C NMR (125 MHz, CDCl₃)

δ 176.6, 169.6, 142.0, 131.8 (2C), 128.8, 128.4 (2C), 122.2, 117.3, 117.2*, 87.5, 84.8, 83.52, 83.47*, 74.0, 73.9*, 73.7, 73.6*, 48.8, 48.7*, 46.7, 39.3, 38.34, 38.27*, 28.2, 27.1 (3C), 26.6 ppm

*Discernible signals for one of two diastereomers

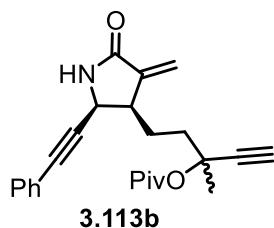
IR (thin film)

2926, 1702, 1711, 1456, 1153 cm⁻¹

HRMS TOF MS ES⁺ [M+H]: C₂₄H₂₈NO₃

Calc: 378.2064 Found: 378.2049

TLC *R_f* = 0.47 (50% EtOAc/hexanes) [silica gel, UV, KMnO₄]



3-Methyl-5-((2S*,3R*)-4-methylene-5-oxo-2-(phenylethynyl)pyrrolidin-3-yl)pent-1-yn-3-yl pivalate (3.113b): Propargyl pivalate **3.113b** was prepared according to general procedure D. A mixture of propargyl alcohols **3.113a,b** (140 mg, 0.48 mmol, 5:1 trans:cis), trimethyl acetic anhydride (0.12 mL, 0.57 mmol), scandium(III) trifluoromethane sulfonate (94 mg, 0.19 mmol), and acetonitrile (1.9 mL) provided trans isomer **3.113a** (99 mg, 55%) as a clear oil, cis isomer **3.113b** (20 mg, 11%) as a clear oil, and a 2:1 trans:cis mixture (7 mg, 4%) as a clear oil after column chromatography (gradient elution with 15-30% ethyl acetate in hexanes). A 1.5:1 ratio of diastereomers was determined by integration of terminal alkyne resonances in the ¹H NMR at 2.48 (major) and 2.43 ppm (minor).

Data for 3.113b: (PAJ 7-68, 20 mg cis, 99 mg trans, 66% total, 5:1 trans:cis isolated ratio; PAJ 7-184, 299 mg trans, 79 mg cis, 77% total; PAJ 9-26, 490 mg trans, 163 mg cis, 176 mg mix, 57% total)

¹H NMR (500 MHz, CDCl₃)

δ 7.39-7.38 (m, 2H), 7.31-7.28 (m, 3H), 6.58 (br s, 1H), 6.57* (br s, 1H), 6.13 (m, 1H), 5.41-5.40 (m, 1H), 4.71 (d, *J* = 7.5 Hz, 1H), 4.70* (d, *J* = 7.5 Hz, 1H), 3.12-3.08 (m, 1H), 2.48 (s, 1H), 2.43* (s, 1H), 2.17-2.14 (m, 1H), 2.09-2.01 (m, 3H), 1.68 (s, 3H), 1.45*(s, 9H), 1.11 (s, 9H) ppm

¹³C NMR (125 MHz, CDCl₃)

δ 176.7, 170.20, 170.15*, 141.8, 141.7*, 131.9 (2C), 128.9, 128.4 (2C) 122.20, 122.18*, 117.1, 87.03, 86.99*, 84.9, 84.8*, 83.8, 83.5*, 74.2, 73.9*, 73.7, 73.5*,

47.8, 42.70, 42.68*, 30.32, 39.30*, 39.1, 39.0*, 27.1 (3C), 26.7, 26.6*, 25.0,
24.8* ppm

*Discernible signals for one of two diastereomers

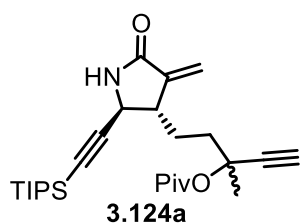
IR (thin film)

2974, 2934, 1705, 1660, 1491, 1479, 1444, 1322, 1285, 1150, 1103 cm^{-1}

HRMS TOF MS ES+ [M+H]: $\text{C}_{24}\text{H}_{28}\text{NO}_3$

Calc: 378.2064 Found: 378.2068

TLC R_f = 0.37 (50% EtOAc/hexanes) [silica gel, UV, KMnO_4]



3-Methyl-5-((2S*,3S*)-4-methylene-5-oxo-2-((triisopropylsilyl)ethynyl)pyrrolidin-3-yl)pent-1-yn-3-yl pivalate (3.124a): Prepared according to general procedure D. Lactam **3.123a** (100 mg, 0.27 mmol, pure trans), scandium(III) trifluoromethanesulfonate (53 mg, 0.11 mmol), pivalic anhydride (0.07 mL, 0.35 mmol), and acetonitrile (1.1 mL) provided pivalate **3.124a** (118 mg, 96%) as a clear oil after column chromatography (gradient elution with 20-50% ethyl acetate in hexanes). ^{13}C NMR showed a 1:1 mixture of diastereomers.

This reaction was repeated following general procedure D. Lactam **3.123a,b** (230 mg, 0.62 mmol, 2.5:1 trans:cis), scandium(III) trifluoromethanesulfonate (121 mg, 0.25 mmol), pivalic anhydride (0.16 mL, 0.80 mmol), and acetonitrile (2.5 mL) provided trans pivalate **3.124a** (110 mg, 39%) and cis pivalate **3.124b** (44 mg, 16%) as clear oils after column chromatography in a total yield of 55%. Another repetition on a 1 g scale is shown below for formation of cis pivalate **3.124b**.

Data for **3.124a**: (PAJ 7-50, 118 mg, 96%; PAJ 7-152, 110 mg, 39% trans, 55% total, 2.5:1 trans:cis; PAJ 8-38, 565 mg, 43% trans, 59% total, 4:1 trans:cis)

¹H NMR (500 MHz, CDCl₃)

6.49 (s, 1H), 6.08 (d, *J* = 2.6 Hz, 1H), 5.38 (d, *J* = 2.6 Hz, 1H), 5.37* (d, *J* = 2.4 Hz, 1H), 4.05 (d, *J* = 5.2 Hz, 1H), 4.04* (d, *J* = 5.2 Hz, 1H), 3.05-3.01 (m, 1H), 2.532 (s, 1H), 2.527* (s, 1H), 2.15-1.90 (m, 2H), 1.88-1.76 (m, 2H), 1.67 (s, 3H), 1.18 (s, 9H), 1.02 (s, 21H) ppm

¹³C NMR (125 MHz, CDCl₃)

176.6, 169.4, 141.83, 141.81*, 117.0, 116.9*, 105.75, 105.74*, 86.4, 83.43, 83.40*, 73.9, 73.8*, 73.65, 73.60*, 49.0, 48.9*, 47.0, 39.3, 38.73*, 38.69, 38.57*, 27.9, 27.8*, 27.3 (3C), 27.2* (3C), 26.51, 26.49*, 18.7 (6C), 11.2 (3C) ppm

*Discernible signals for one of two diastereomers

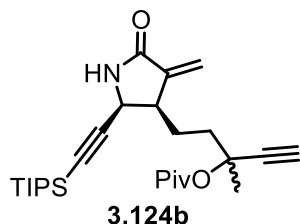
IR (thin film)

2943, 2866, 1709, 1660, 1462, 1367, 1325, 1285, 1101 cm⁻¹

HRMS TOF MS ES+ [M+H]: C₂₇H₄₄NO₃Si

Calc: 458.3090 Found: 458.3059

TLC *R_f* = 0.37 (25% EtOAc/hexanes) [silica gel, UV, KMnO₄]



3-Methyl-5-((2*S,3*R**)-4-methylene-5-oxo-2-((triisopropylsilyl)ethynyl)pyrrolidin-3-**

yl)pent-1-yn-3-yl pivalate (3.124b): Propargyl pivalate **3.124b** was prepared according to general procedure D. Propargyl alcohol **3.123a,b** (1.07 g, 2.87 mmol, 4:1 trans:cis), pivalic

anhydride (0.70 mL, 3.5 mmol), scandium (III) trifluoromethanesulfonate (565 mg, 1.15 mmol), and acetonitrile (12 mL) provided trans lactam **3.124a** (565 mg, 43%), cis lactam **3.124b** (139 mg, 11%), and a 2:1 trans:cis mixture (72 mg, 5%) each as a clear oil after column chromatography (gradient elution with 5-25% ethyl acetate in hexanes). A 1.7:1 ratio of diastereomers was determined by integration of methylene hydrogen resonances in the ^1H NMR at 5.38 ppm for the major diastereomer and 5.40 ppm for the minor diastereomer.

Data for 3.124b: (PAJ 8-38, 139 mg, 11% cis, 59% total, 4:1 trans:cis; PAJ 7-152, 110 mg, 39%, 55% total, 2.5:1 trans:cis)

^1H NMR (500 MHz, CDCl_3)

δ 6.10 (app t, $J = 2.8$ Hz, 1H), 5.84 (br s, 1H), 5.40 (d, $J = 2.0$ Hz, 1H), 5.38*(d, $J = 1.5$ Hz, 1H), 4.51 (app t, $J = 7.0$ Hz, 1H), 3.05-3.02 (m, 1H), 2.52 (s, 1H), 2.51*(s, 1H), 2.08-1.96 (m, 3H), 1.93-1.88 (m, 1H), 1.68 (s, 3H), 1.66*(s, 3H), 1.183 (s, 9H), 1.177*(s, 9H), 1.04 (s, 21H), 1.03*(s, 21H) ppm

^{13}C NMR (125 MHz, CDCl_3)

δ 176.7, 169.85, 169.77*, 141.65, 141.61*, 117.3, 117.2*, 103.04, 102.99*, 89.0, 88.9*, 83.9, 83.4*, 74.3, 73.9*, 73.8, 73.4*, 47.9, 42.8, 42.6*, 39.4, 39.3*, 39.0, 38.8*, 27.20 (3C), 27.19*, 26.6, 26.3*, 25.0, 24.8*, 18.7 (6C), 11.2 (3C) ppm

*Discernible signals for one of two diastereomers

IR (thin film)

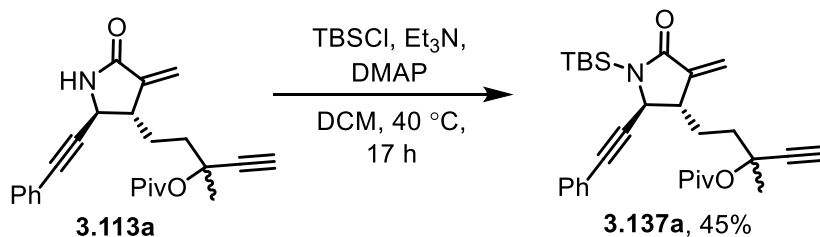
3270, 2909, 2832, 2219, 2150, 1684, 1640, 1445, 1308 cm^{-1}

HRMS TOF MS ES+ [M+H]: $\text{C}_{27}\text{H}_{44}\text{NO}_3\text{Si}$

Calc: 458.3085 Found: 458.3095

TLC

$R_f = 0.29$ (25% EtOAc/hexanes) [silica gel, UV, KMnO_4]



5-((2S*,3S*)-1-(tert-Butyldimethylsilyl)-4-methylene-5-oxo-2-(phenylethynyl)pyrrolidin-3-

yl)-3-methylpent-1-yn-3-yl pivalate (3.137a**):** A flame-dried, 25-mL, round-bottomed flask equipped with a stir bar, septum, and nitrogen inlet needle was charged with lactam **3.113a** (110 mg, 0.29 mmol) and dichloromethane (10 mL). *tert*-Butyl silyl chloride (439 mg, 2.9 mmol), triethylamine (0.61 mL, 4.4 mmol), and dimethylaminopyridine (4 mg, 0.03 mmol) were added to the lactam solution in that order. A reflux condenser was attached, sealed with a septum, and the system evacuated and filled with nitrogen (3x) then the solution was lowered into a 40 °C oil bath and stirred for 17 h. TLC analysis showed consumption of the starting material so the reaction was concentrated by rotary evaporation, then purified by silica gel flash column chromatography eluting with 5-10% ethyl acetate in hexanes. The desired silyl lactam **3.137a** was isolated as a clear oil (64 mg, 45%) and some loss of the silyl group during chromatography was observed (42 mg starting material recovered).

Data for **3.137a**: (PAJ 8-196, 64 mg, 45%, unknown impurities present, peaks reported for 1 of 2 diastereomers)

$^1\text{H NMR}$ (400 MHz, CDCl_3)

δ 7.37-7.34 (m, 2H), 7.31-7.29 (m, 3H), 6.09 (d, $J = 1.6$ Hz, 1H), 5.39 (app s, 1H), 4.17 (app t, $J = 2.0$ Hz, 1H), 3.08-3.06 (m, 1H), 1.92-1.79 (m, 4H), 1.67 (s, 3H), 1.17 (s, 9H), 1.02 (s, 9H), 0.08 (s, 6H) ppm

$^{13}\text{C NMR}$ (100 MHz, CDCl_3)

δ 176.7, 174.4, 143.7, 131.6 (2C), 128.7, 128.5 (2C), 122.6, 117.6, 89.9, 84.6, 83.6, 83.5, 74.0, 73.7, 53.3, 47.6, 39.4, 38.6, 29.9, 25.8 (3C), 18.1 (3C), -3.5 (2C) ppm

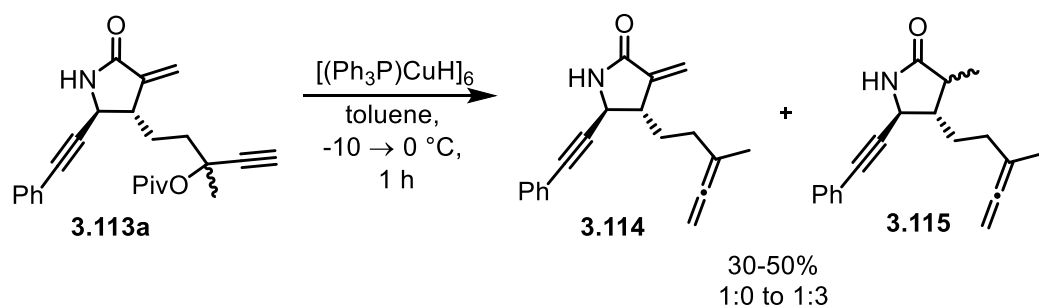
IR (thin film)

3307, 2957, 2248, 1735, 1692, 1660, 1479, 1395, 1149, 1090 cm^{-1}

HRMS TOF MS ES+ [M+H]: $\text{C}_{30}\text{H}_{42}\text{NO}_3\text{Si}$

Calc: 492.2929 Found: 492.2904

TLC R_f = 0.57 (25% EtOAc/hexanes) [silica gel, UV, *p*-anisaldehyde]

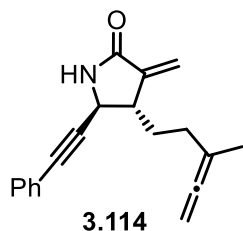


General Procedure E: Conversion of Propargyl Ester to 1,1-Disubstituted Allenes Using (Triphenylphosphine)copper Hydride Hexamer

A flame-dried, 15-mL, round-bottomed flask equipped with a stir bar, septum, and nitrogen inlet needle was charged with propargyl pivalate **3.113a** (107 mg, 0.272 mmol), toluene (7 mL), and deionized water (0.01 mL). This solution was degassed by bubbling nitrogen through the solution for 10 min, then the solution was cooled to $-10 \text{ } ^\circ\text{C}$. (Triphenylphosphine)copper hydride hexamer (533 mg, 0.272 mmol) was weighed in a glove box under a N_2 atmosphere, removed, and added to the degassed solution in a single portion. The flask was evacuated and filled with nitrogen (3x) and stirred under nitrogen for 2 h. Completion of the reaction was observed by a ^1H NMR aliquot which showed the disappearance of the terminal alkyne proton at 2.5 ppm. The reaction was quenched by pouring the reaction mixture

into a cooled (0 °C) solution of saturated ammonium chloride. The mixture was diluted with Et₂O (10 mL) and stirred open to air for 30 min, then poured into a separatory funnel and extracted with diethyl ether (3 x 10 mL). The organic layers were dried over magnesium sulfate, filtered through a plug of silica gel eluting with diethyl ether, concentrated by rotary evaporation, then purified by silica gel flash column chromatography eluting with 15-30% ethyl acetate in hexanes to give 1,1-disubstituted allene **3.114** (24 mg, 33%) as a clear oil.

Initially when performing the allene formation with an older bottle of Stryker's reagent purchased from Sigma-Aldrich (90%) and had been stored in the glovebox, we did not see any reduction of the α -methylene, but when a new bottle from Acros (97%) was used, significant amounts of the reduced product (~1:1 desired to reduced) were obtained. Lowering the temperature to -10 °C gave better ratios near 10:1 of the desired product to the reduced product. Other commercial sources and batches of Stryker's reagent (Sigma-Aldrich 90%, Acros 97%) or Stryker's reagent synthesized from copper (II) acetate, triphenylphosphine, and diphenylsilane¹⁸⁹ gave similar ratios and yields when the reaction was conducted at -10 °C. However, the ratio of products varied significantly (from 1:1 to 10:1) when the reaction was performed at rt. It should also be noted that the sources of Stryker's reagent varied in appearance: Acros (97%) was bright to dark orange depending on batch, Sigma-Aldrich (90%) was brick red to light brown depending on batch, and freshly prepared Stryker's reagent¹⁸⁹ was a reddish orange color similar to that purchased from Acros.



(4S*,5S*)-3-Methylene-4-(3-methylpenta-3,4-dienyl)-5-(phenylethynyl)pyrrolidin-2-one

(3.114):

Data for 3.114: (PAJ 7-82, 24 mg, 33%)

¹H NMR (400 MHz, CDCl₃)

δ 7.41-7.38 (m, 2H), 7.33-7.30 (m, 3H), 6.77 (br s, 1H), 6.11 (d, *J* = 2.2 Hz, 1H),
5.41 (d, *J* = 2.2 Hz, 1H), 4.66-4.64 (m, 2H), 4.26 (d, *J* = 4.0 Hz, 1H), 3.17-3.16
(m, 1H), 2.15-2.08 (m, 2H), 1.92-1.86 (m, 1H), 1.81-1.74 (m, 1H), 1.71 (t, *J* = 3.2
Hz, 3H) ppm

¹³C NMR (100 MHz, CDCl₃)

δ 206.1, 169.7, 142.2, 131.8 (2C), 128.8, 128.5 (2C), 122.3, 117.3, 97.7, 87.8,
84.5, 75.3, 49.0, 46.4, 31.9, 29.9, 19.1 ppm

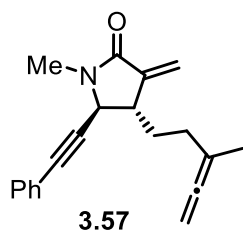
IR (thin film)

2922, 1741, 1736, 1445, 1372, 1270, 1216, 1110, 1042 cm⁻¹

HRMS TOF MS ES+ [M+H]: C₁₉H₂₀NO

Calc: 278.1539 Found: 278.1533

TLC *R_f* = 0.44 (50% EtOAc/hexanes) [silica gel, UV, vanillin]



(4S*,5S*)-1-Methyl-3-methylene-4-(3-methylpenta-3,4-dien-1-yl)-5-

(phenylethynyl)pyrrolidin-2-one (3.57): Prepared according to general procedure E. Propargyl acetate **3.80** (69 mg, 0.20 mmol), (triphenylphosphine)copper hydride hexamer (385 mg, 0.196 mmol), toluene (5.0 mL), and deionized water (0.01 ml) provided allene **3.57** (30 mg, 53%) as a

clear oil after column chromatography (gradient elution with 10-20% ethyl acetate in hexanes). Some baseline impurities from triphenylphosphine byproducts of Stryker's reagent were observed in the aromatic regions of the ^1H and ^{13}C NMR spectra.

Data for 3.57: (PAJ 7-134, 30 mg, 53%)

^1H NMR (500 MHz, CDCl_3)

δ 7.41-7.40 (m, 2H), 7.34-7.30 (m, 3H), 6.07 (d, $J = 1.5$ Hz, 1H), 5.35 (s, 1H), 4.66- 4.64 (m, 2H), 4.11 (d, $J = 4.0$ Hz, 1H), 3.08 (app br s, 1H), 3.03 (s, 3H), 2.14-2.08 (m, 2H), 1.90-1.84 (m, 1H), 1.77-1.73 (m, 1H), 1.71 (t, $J = 3.0$ Hz, 3H) ppm

^{13}C NMR (125 MHz, CDCl_3)

δ 201.2, 167.3, 142.4, 131.9 (2C), 128.9, 128.5 (2C), 122.2, 116.3, 97.7, 86.2, 85.7, 75.2, 55.5, 44.2, 32.2, 30.0, 28.5, 19.1 ppm

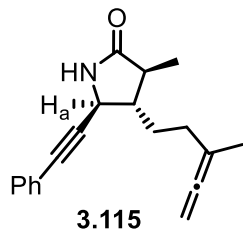
IR (thin film)

2078, 1633, 1414, 1381, 1260, 1058 cm^{-1}

HRMS TOF MS ES+ $[\text{M}+\text{H}]$: $\text{C}_{20}\text{H}_{22}\text{NO}$

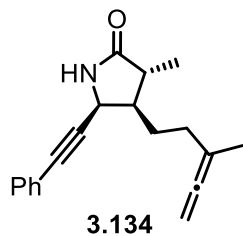
Calc: 292.1701 Found: 292.1712

TLC $R_f = 0.66$ (50% EtOAc/hexanes) [silica gel, UV, KMnO_4]



The reduced product **3.115** was never completely characterized, but was evident by the presence of a methyl doublet at 1.03 ppm and a doublet at 4.23 ppm corresponding to H_a in the

^1H NMR spectra of allene-yne **3.114**; similar resonances were observed for the reduced products with a TIPS-substituted alkyne **3.126** or terminal alkyne **3.208** (full characterization data below).



(4R*,5S*)-3-Methyl-4-(3-methylpenta-3,4-dien-1-yl)-5-(phenylethynyl)pyrrolidin-2-one

(3.134): Prepared according to general procedure E. Cis lactam **3.113b** (75 mg, 0.19 mmol), (triphenylphosphine)copper hydride hexamer (373 mg, 0.19 mmol), toluene (5 mL), water (0.01 mL) provided allene **3.134** (19 mg, 36%) after column chromatography (gradient elution with 15-25% ethyl acetate in hexanes) as a clear oil and as the only product.

Data for 3.134: (PAJ 7-192, 19 mg, 36%)

^1H NMR (500 MHz, CDCl_3)

δ 7.40-7.38 (m, 2H), 7.33-7.31 (m, 3H), 5.77 (br s, 1H), 4.64-4.61 (m, 2H), 4.51 (d, $J = 7.0$ Hz, 1H), 2.27-2.14 (m, 3H), 2.03-1.98 (m, 1H), 1.92-1.84 (m, 2H), 1.71 (t, $J = 3.0$ Hz, 3H), 1.20 (d, $J = 7.0$ Hz, 3H), ppm

^{13}C NMR (125 MHz, CDCl_3)

δ 206.3, 179.8, 131.8 (2C), 128.8, 128.5 (2C), 122.5, 97.8, 86.4, 85.3, 74.7, 47.6, 46.8, 40.3, 31.2, 28.0, 18.8, 13.8 ppm

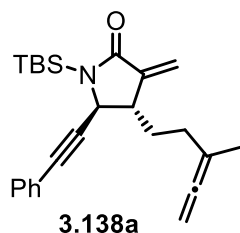
IR (thin film)

3245, 2895, 1937, 1681, 1426, 1361 cm^{-1}

HRMS TOF MS ES+ $[\text{M}+\text{H}]$: $\text{C}_{19}\text{H}_{22}\text{NO}$

Calc: 280.1696 Found: 280.1698

TLC $R_f = 0.33$ (50% EtOAc/hexanes) [silica gel, UV, vanillin]



(4S*,5S*)-1-(tert-Butyldimethylsilyl)-3-methylene-4-(3-methylpenta-3,4-dien-1-yl)-5-

(phenylethynyl)pyrrolidin-2-one (3.138a): Prepared according to general procedure E. Propargyl pivalate **3.137a** (55 mg, 0.11 mmol), (triphenylphosphine)copper hydride hexamer (220 mg, 0.11 mmol), toluene (3.0 mL), and deionized water (0.01 ml) provided allene **3.138a** (13 mg, 30%) as a pale yellow oil after column chromatography (gradient elution with 15-50% ethyl acetate in hexanes).

Data for 3.138a: (PAJ 8-198, 13 mg, 30%)

¹H NMR (400 MHz, CDCl₃)

δ 7.37-7.35 (m, 2H), 7.31-7.29 (m, 3H), 6.06 (d, *J* = 1.2 Hz, 1H), 5.37 (d, *J* = 1.2 Hz, 1H), 4.65 (app. q, *J* = 3.0 Hz, 2H), 4.17 (d, *J* = 2.0 Hz, 1H), 3.10-3.07 (m, 1H), 2.08-2.04 (m, 2H), 1.80-1.66 (m, 2H), 1.73 (t, *J* = 6.2 Hz, 3H), 1.02 (s, 9H), 0.41 (s, 3H), 0.39 (s, 3H) ppm

¹³C NMR (100 MHz, CDCl₃)

δ 206.2, 174.6, 144.0, 131.6 (2C), 128.6, 128.5 (2C), 122.7, 117.3, 97.6, 90.3, 84.4, 75.1, 53.5, 47.3, 33.1, 30.5, 30.0, 27.3, 25.8, 19.4, 19.0, -3.4, -4.7 ppm

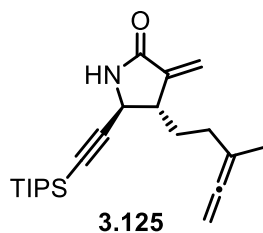
IR (thin film)

3307, 2923, 2235, 1959, 1692, 1661, 1469, 1352, 1252 cm⁻¹

HRMS TOF MS ES+ [M+H]: C₂₅H₃₄NOSi

Calc: 392.2404 Found: 392.2386

TLC *R_f* = 0.28 (25% EtOAc/hexanes) [silica gel, UV, KMnO₄]



(4S*,5S*)-3-Methylene-4-(3-methylpenta-3,4-dienyl)-5-

((triisopropylsilyl)ethynyl)pyrrolidin-2-one (3.125): Prepared according to general procedure E at -20 °C. Propargyl pivalate **3.124a** (110 mg, 0.24 mmol), (triphenylphosphine)copper hydride hexamer (424 mg, 0.22 mmol), and toluene (6 mL) yielded allenes **3.125** (39 mg, 46%) and **3.126** (9 mg, 11%) in a 4:1 ratio each as a clear oil after column chromatography (gradient elution with 5-25% ethyl acetate in hexanes). Other repetitions of this reaction gave 31-53% of the desired allene **3.125** with 0-31% of the reduced methylene product **3.126**.

Data for 3.125: (8-62, 39 mg, 46%, baseline impurities which appear to be from reduction of the allene or alkyne to an alkene and some triphenylphosphine byproducts from Stryker's reagent were present in ¹H and ¹³C NMR)

¹H NMR (400 MHz, CDCl₃)

δ 6.24 (br s, 1H), 6.05 (d, *J* = 2.4 Hz, 1H), 5.36 (d, *J* = 2.4 Hz, 1H), 4.66-4.63 (m, 2H), 4.03, (d, *J* = 4.8 Hz, 1H), 3.08-3.03 (m, 1H), 2.16-2.09 (m, 1H), 2.06-1.99 (m, 1H), 1.93-1.84 (m, 1H), 1.72-1.61 (m, 1H) 1.69 (t, *J* = 3.0 Hz, 3H), 1.04 (s, 21H) ppm

¹³C NMR (100 MHz, CDCl₃)

δ 206.0, 169.5, 142.1, 117.0, 106.2, 97.9, 86.1, 75.4, 49.1, 47.0, 31.7, 30.1, 19.2, 18.7 (6C), 11.2 (3C) ppm

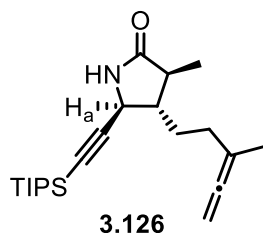
IR (thin film)

2926, 2865, 1704, 1658, 1462, 1324 cm⁻¹

HRMS TOF MS ES+ [M+H]: C₂₂H₃₆NOSi

Calc: 358.2561 Found: 358.2566

TLC *R_f* = 0.32 (25% EtOAc/hexanes) [silica gel, UV, KMnO₄]



(4S*,5S*)-3-Methyl-4-(3-methylpenta-3,4-dien-1-yl)-5-

((triisopropylsilyl)ethynyl)pyrrolidin-2-one (3.126): The ratio of diastereomers was determined by integration of the resonances for H_a at 4.02 ppm for the minor diastereomer and 3.95 ppm for the major diastereomer.

Data for 3.126: (PAJ 8-62, 9 mg, 11%, 8.3:1 dr, peaks reported for major diastereomer only)

¹H NMR (500 MHz, CDCl₃)

δ 5.77 (br s, 1H), 4.64-4.62 (m, 2H), 3.95 (d, *J* = 8.0 Hz, 1H), 2.18-2.11 (m, 1H), 2.09-2.01 (m, 3H), 1.80-1.74 (m, 1H), 1.69 (t, *J* = 2.7 Hz, 3H), 1.69-1.60 (m, 1H), 1.24 (d, *J* = 10.5 Hz, 3H), 1.05 (s, 21H) ppm

¹³C NMR (125 MHz, CDCl₃)

δ 206.0, 178.5, 106.3, 98.2, 85.9, 75.3, 51.5, 49.7, 42.4, 31.1, 31.0, 19.1, 18.7 (6C), 15.1, 11.3 (3C) ppm

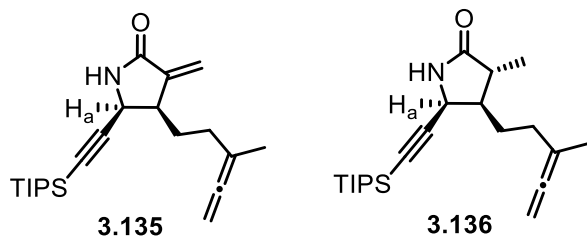
IR (thin film)

2908, 2831, 2156, 1961, 1685, 1443 cm⁻¹

HRMS TOF MS ES+ [M+H]: C₂₂H₃₈NOSi

Calc: 360.2717 Found: 360.2708

TLC *R_f* = 0.38 (35% EtOAc/hexanes) [silica gel, UV, vanillin]



(4R*,5S*)-3-Methylene-4-(3-methylpenta-3,4-dien-1-yl)-5-

((triisopropylsilyl)ethynyl)pyrrolidin-2-one (3.135): Prepared according to general procedure

E. Propargyl pivalate **3.124b** (40 mg, 0.087 mmol), (triphenylphosphine)copper hydride hexamer (170 mg, 0.087 mmol), toluene (2.2 mL), and deionized water (0.01 ml) provided allene **3.135** (11 mg, 35%) as a clear oil after column chromatography (gradient elution with 5-15% ethyl acetate in hexanes). Baseline impurities were detected from reduction of the allene and/or alkyne to an alkene and from triphenylphosphine byproducts of Stryker's reagent. This reaction was repeated according to general procedure E. Propargyl pivalate **3.124b** (135 mg, 0.29 mmol), (triphenylphosphine)copper hydride hexamer (578 mg, 0.29 mmol), toluene (7.4 mL), and deionized water (0.01 ml) provided allene **3.135** and reduced methylene lactam **3.136** (2.5:1, 26 mg, 25% overall yield) as a clear oil after column chromatography. The ratio was determined by integration of Ha next to the nitrogen which appeared as a doublet at 4.5 ppm for lactam **xx** and as a doublet at 4.3 ppm for the reduced methylene compound **xx**.

Data for 3.135: (PAJ 7-156, 11 mg, 35%; PAJ 8-40, 26 mg, 25%)

¹H NMR (400 MHz, CDCl₃)

δ 6.06 (d, *J* = 2.4 Hz, 1H), 6.04 (br s, 1H), 5.46 (d, *J* = 2.4 Hz, 1H), 4.63-4.61 (m, 2H), 4.48 (d, *J* = 7.6 Hz, 1H), 3.07-3.03 (m, 1H), 2.15-2.03 (m, 2H), 2.00-1.87 (m, 2H), 1.69 (t, *J* = 3.0 Hz, 3H), 1.01 (s, 21H) ppm

¹³C NMR (100 MHz, CDCl₃)

δ 206.2, 170.2, 141.8, 116.9, 103.1, 97.7, 88.4, 75.0, 47.8, 41.8, 30.4, 27.6, 19.0,
18.7 (6C), 11.2 (3C) ppm

IR (thin film)

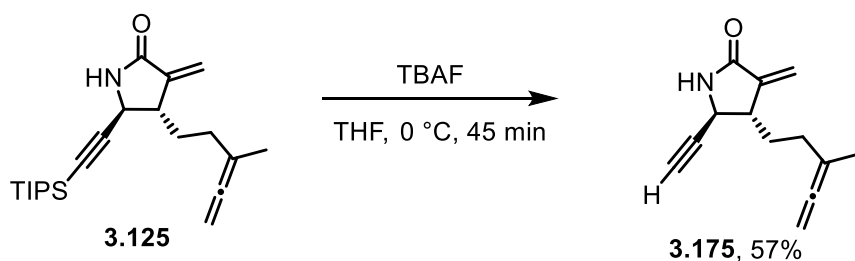
2942, 2176, 1960, 1709, 1660, 1463, 1324 cm^{-1}

HRMS TOF MS ES+ [M+H]: $\text{C}_{22}\text{H}_{36}\text{NOSi}$

Calc: 358.2561 Found: 358.2573

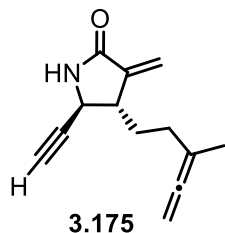
TLC R_f = 0.72 (50% EtOAc/hexanes) [silica gel, UV, *p*-anisaldehyde]

General Procedure F: Removal of TIPS Substituent from Alkyne



A flame-dried, 5-mL, round-bottomed flask equipped with a stir bar, septum, and nitrogen inlet needle was charged with TIPS allene **3.125** (38 mg, 0.11 mmol, pure trans) dissolved in THF (1.1 mL) and cooled to 0 °C in an ice water bath. Tetrabutylammonium fluoride (1 M solution in THF, 0.15 mL, 0.15 mmol) was added dropwise via syringe and the reaction was stirred for 45 minutes when TLC showed consumption of the starting material. Saturated aqueous ammonium chloride (2 mL) was added to the cooled reaction mixture to quench the reaction and the biphasic mixture was transferred to a separatory funnel. The aqueous layer was extracted with ethyl acetate (4 x 5 mL). The combined organic layers were washed with brine (1 x 5 mL), dried over magnesium sulfate, gravity filtered, concentrated by rotary evaporation, and purified by silica gel flash column chromatography (gradient elution with 25-75% ethyl acetate in hexanes) to provide allene **3.175** (12 mg, 57%) as a clear oil. This reaction

was repeated according to the above procedure. TIPS allene **3.125** (40 mg, 0.11 mmol, pure trans), tetrabutylammonium fluoride (1 M solution in THF, 0.17 mL, 0.17 mmol), THF (1.1 mL) provided allene **3.175** (18 mg, 82%) as a clear oil after column chromatography



(4S*,5S*)-5-Ethynyl-3-methylene-4-(3-methylpenta-3,4-dien-1-yl)pyrrolidin-2-one (3.175):

Data for 3.175: (PAJ 8-56, 12 mg, 57%; PAJ 7-168A, 18 mg, 82%; PAJ 8-66, 14 mg, 93%; PAJ 8-88, 11 mg, 85%)

¹H NMR (400 MHz, CDCl₃)

δ 6.79 (br s, 1H), 6.07 (d, *J* = 2.2 Hz, 1H), 5.38 (d, *J* = 2.2 Hz, 1H), 4.65-4.63 (m, 2H), 4.02 (dd, *J* = 2.0, 4.0 Hz, 1H), 3.09-3.05 (m, 1H), 2.39 (d, *J* = 2.0 Hz, 1H), 2.10-2.02 (m, 2H), 1.88-1.80 (m, 1H), 1.73-1.71 (m, 1H), 1.70 (t, *J* = 3.0 Hz, 3H)
ppm

¹³C NMR (100 MHz, CDCl₃)

δ 206.1, 169.7, 141.9, 117.4, 97.6, 82.7, 75.3, 72.9, 48.1, 46.1, 31.9, 29.8, 19.0
ppm

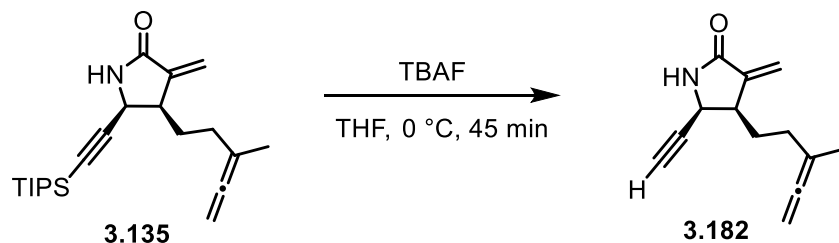
IR (thin film)

2094, 1936, 1633, 1411, 1308, 1061 cm⁻¹

HRMS TOF MS ES+ [M+H]: C₁₃H₁₆NO

Calc: 202.1226 Found: 202.1227

TLC *R_f* = 0.36 (50% EtOAc/hexanes) [silica gel, UV, *p*-anisaldehyde]



(4R*,5S*)-5-Ethynyl-3-methylene-4-(3-methylpenta-3,4-dien-1-yl)pyrrolidin-2-one (3.182):

Prepared according to general procedure F. TIPS allene **3.135** (11 mg, 0.031 mmol, pure cis), tetrabutylammonium fluoride (1 M solution in THF, 0.05 mL, 0.05 mmol), THF (0.31 mL) provided allene **3.182** (4 mg, 67%) as a clear oil after column chromatography (gradient elution with 50-75% ethyl acetate in hexanes). This reaction was repeated according to general procedure F. TIPS allene **3.135** (14 mg, 0.039 mmol), tetrabutylammonium fluoride (1 M solution in THF, 0.06 mL, 0.06 mmol), THF (0.4 mL) provided allene **3.182** (7 mg, 75%) as a clear oil after column chromatography.

Data for 3.182: (PAJ 7-162, 4 mg, 67% contaminated with 17% lactam with reduced methylene and some baseline impurities; PAJ 8-44, 6 mg, 67%; PAJ 7-168B, 7 mg, 75%)

¹H NMR (500 MHz, CDCl₃)

δ 6.13 (br s, 1H), 6.09 (d, *J* = 2.5 Hz, 1H), 5.38 (d, *J* = 2.5 Hz, 1H), 4.65-4.63 (m, 2H), 4.46 (dd, *J* = 7.5, 2.0 Hz, 1H), 3.10-3.08 (m, 1H), 2.42 (d, *J* = 2.0 Hz, 1H), 2.14-2.04 (m, 2H), 1.97-1.89 (m, 2H), 1.72 (t, *J* = 3.2 Hz, 3H) ppm

¹³C NMR (125 MHz, CDCl₃)

δ 206.3, 170.1, 141.5, 117.1, 97.5, 79.9, 75.2, 74.8, 46.9, 41.5, 30.5, 27.5, 18.8 ppm

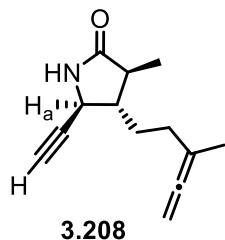
IR (thin film)

2898, 2101, 1937, 1647, 1422, 1395, 1373, 1242, 1086 cm⁻¹

HRMS TOF MS ES+ [M+H]: C₁₃H₁₆NO

Calc: 202.1226 Found: 202.1231

TLC $R_f = 0.34$ (50% EtOAc/hexanes) [silica gel, UV, *p*-anisaldehyde]



(4S*,5S*)-5-Ethynyl-3-methyl-4-(3-methylpenta-3,4-dien-1-yl)pyrrolidin-2-one (3.208):

Prepared according to general procedure F. Lactam **3.126** (26 mg, 0.072 mmol, 8:1 dr), tetrabutylammonium fluoride (1M in THF, 0.11 mL, 0.10 mmol), and THF (0.8 mL) yielded terminal alkyne **3.208** (14 mg, 86%) as a clear oil after column chromatography (gradient elution with 25-50% ethyl acetate in hexanes) and as an 8:1 mixture of diastereomers as determined by integration of the resonances for H_a at 3.93 for the minor diastereomer and 3.92 for the major diastereomer.

Data for 3.208: (PAJ 8-74, 14 mg, 86%, 8:1 dr, peaks reported for major diastereomer only)

¹H NMR (500 MHz, CDCl₃)

δ 6.04 (br s, 1H), 4.65-4.63 (m, 2H), 3.92 (dd, $J = 7.5, 1.7$ Hz, 1H), 2.39 (d, $J = 1.7$ Hz, 1H), 2.17-2.01 (m, 4H), 1.79-1.68 (m, 2H), 1.70 (t, $J = 3.2$ Hz, 3H), 1.24 (d, $J = 7.0$ Hz, 3H) ppm

¹³C NMR (125 MHz, CDCl₃)

δ 206.1, 178.7, 98.0, 82.8, 75.3, 72.8, 50.6, 48.8, 42.2, 31.0, 30.7, 19.0, 15.3 ppm

IR (thin film)

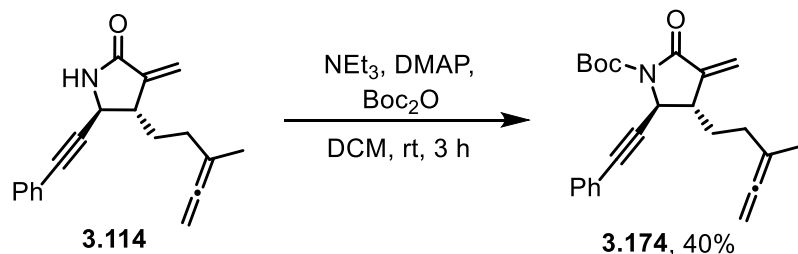
3190, 2889, 2060, 1936, 1679, 1440, 1364 cm⁻¹

HRMS TOF MS ES+ [M+H]: C₁₃H₁₈NO

Calc: 204.1383 Found: 204.1378

TLC

$R_f = 0.24$ (50% EtOAc/hexanes) [silica gel, UV, vanillin]



tert-Butyl

(4*S**,5*S**)-3-methylene-4-(3-methylpenta-3,4-dien-1-yl)-2-oxo-5-

(phenylethynyl)pyrrolidine-1-carboxylate (**3.174**): A 5-mL, flame-dried, test tube equipped with a stir bar, septum, and nitrogen inlet needle was charged with allene-ynone **3.114** (15 mg, 0.054 mmol) and dichloromethane (0.3 mL). Dimethylaminopyridine (1 mg, 0.008 mmol) was added and the solution was cooled to 0 °C. Triethylamine (0.08 mL, 0.5 mmol) was added dropwise followed by addition of di-*tert*-butyl dicarbonate (59 mg, 0.27 mmol) in a single portion. The ice bath was removed and the solution was allowed to warm to rt and stirred for 2 h. After consumption of the starting material was observed by TLC, the solution was diluted with dichloromethane (15 mL), transferred to a separatory funnel, and washed sequentially with saturated aqueous ammonium chloride (5 mL) and brine (5 mL). The organic layer was dried over magnesium sulfate, gravity filtered, concentrated by rotary evaporation, and purified by silica gel flash column chromatography (gradient elution with 5-25% ethyl acetate in hexanes) to provide allene-ynone **3.174** (8 mg, 40%) as a clear oil. This reaction was repeated according to the procedure above. Lactam **3.114** (23 mg, 0.083 mmol), dimethylaminopyridine (1 mg, 0.008 mmol), triethylamine (0.12 mL, 0.83 mmol), di-*tert*-butyl dicarbonate (90 mg, 0.41 mmol), and dichloromethane (0.4 mL) provided lactam **3.174** (17 mg, 54%) as a pale yellow oil after column chromatography.

Data for **3.174**: (PAJ 7-6, 8 mg, 40%; PAJ 6-198, 17 mg, 54%)

¹H NMR (500 MHz, CDCl₃)

δ 7.38-7.36 (m, 2H), 7.31-7.29 (m, 3H), 6.30 (d, *J* = 1.7 Hz, 1H), 5.54 (d, *J* = 1.7 Hz, 1H), 4.67-4.65 (m, 3H), 3.08-3.05 (m, 1H), 2.07-2.05 (m, 2H), 1.80-1.71 (m, 2H), 1.71 (t, *J* = 3.2 Hz, 3H), 1.57 (s, 9H) ppm

¹³C NMR (125 MHz, CDCl₃)

δ 206.3, 165.6, 149.9, 142.1, 131.8 (2C), 128.7, 128.5 (2C), 122.4, 121.6, 97.4, 87.5, 84.0, 83.7, 75.3, 52.8, 43.6, 32.8, 29.8, 28.2 (3C), 19.0 ppm

IR (thin film)

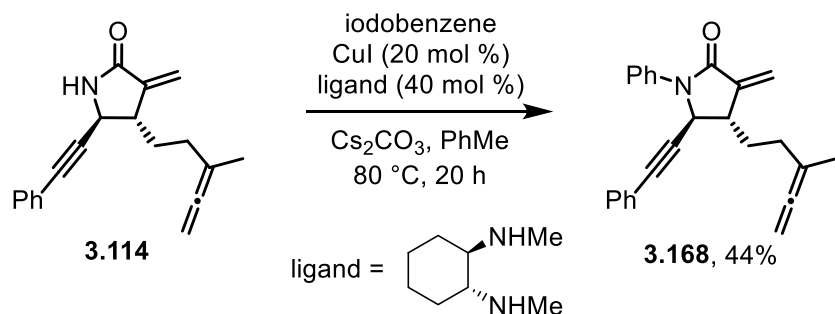
2969, 2915, 1793, 1759, 1717, 1401, 1302, 1153 cm⁻¹

HRMS TOF MS ES+ [M+H]: C₂₄H₂₈NO₃

Calc: 378.2069 Found: 378.2082

TLC *R_f* = 0.69 (50% EtOAc/hexanes) [silica gel, UV, *p*-anisaldehyde]

General Procedure G: Arylation of Lactam Nitrogen with Aryl Iodides



This procedure was modified from the method reported by Buchwald and coworkers for the amidation of aryl halides.¹⁷³ A flame-dried, 10-mL test tube equipped with a magnetic stir bar was charged with copper iodide (4 mg, 0.02 mmol) and cesium carbonate (50 mg, 0.15 mmol). The test tube was capped with a septum, then evacuated and filled with nitrogen (3x). Iodobenzene (13 μL, 0.11 mmol) and *trans*-*N,N'*-dimethylcyclohexane-1,2-diamine (8 μL, 0.05 mmol), were added via syringe. Lactam **3.114** (21 mg, 0.076 mmol) was dissolved in toluene

(0.8 mL) and added to the test tube containing the other reagents via syringe. The test tube was evacuated and filled with nitrogen (3x), and the nitrogen inlet needle was removed. The test tube was then placed in an 80 °C oil bath for 20 h. TLC showed formation of a new product. The reaction was cooled to rt, filtered through a plug of silica gel eluting with 50% ethyl acetate in hexanes, concentrated, then purified by silica gel flash column chromatography eluting with 5-15% ethyl acetate in hexanes to give lactam **3.168** as a clear oil (12 mg, 44%).

Alternatively, *N,N'*-dimethylethylenediamine was used as the copper ligand with little difference in yield. When potassium carbonate was used as the base instead of cesium carbonate, lower yields and incomplete conversion to the product was observed. For example, lactam **3.114** (10 mg, 0.033 mmol), iodobenzene (5 μ L, 0.04 mmol), copper iodide (5 mg, 0.03 mmol), *trans-N,N'*-dimethylcyclohexane-1,2-diamine (4 μ L, 0.03 mmol) potassium carbonate (10 mg, 0.065 mmol), and toluene (0.4 mL) provided lactam **3.168** (3 mg, 27%, PAJ 8-6) as a clear oil after column chromatography.

(4S*,5S*)-3-Methylene-4-(3-methylpenta-3,4-dien-1-yl)-1-phenyl-5-(phenylethynyl)pyrrolidin-2-one (3.168):

Data for 3.168: (PAJ 8-204, 12 mg, 44%)

¹H NMR (400 MHz, CDCl₃)

δ 7.77-7.75 (m, 2H), 7.44-7.40 (m, 2H), 7.30-7.20 (m, 6H), 6.25 (d, $J = 2.2$ Hz, 1H), 5.51 (d, $J = 2.2$ Hz, 1H), 4.69-4.66 (m, 3H), 3.26-3.23 (m, 1H), 2.18-2.13 (m, 2H), 1.91-1.83 (m, 2H), 1.73 (t, $J = 3.2$ Hz, 3H) ppm

¹³C NMR (100 MHz, CDCl₃)

δ 206.2, 166.3, 143.0, 138.3, 131.8 (2C), 129.0 (2C), 128.8 (2C), 128.4, 125.7, 122.2 (2C), 118.4, 97.6, 87.1, 85.8, 76.8, 75.4, 55.1, 44.6, 32.5, 30.0, 19.1 ppm

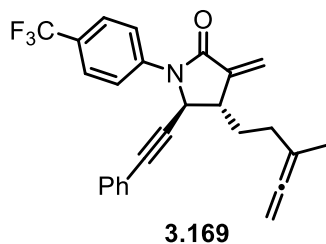
IR (thin film)

2924, 2227, 1959, 1701, 1660, 1498, 1372 cm⁻¹

HRMS TOF MS ES+ [M+H]: C₂₅H₂₄NO

Calc: 354.1852 Found: 354.1837

TLC R_f = 0.86 (50% EtOAc/hexanes) [silica gel, UV, vanillin]



(4S*,5S*)-3-Methylene-4-(3-methylpenta-3,4-dien-1-yl)-5-(phenylethynyl)-1-(4-

(trifluoromethyl)phenyl)pyrrolidin-2-one (3.169): Prepared according to general procedure G with potassium carbonate as base instead of cesium carbonate. Lactam **3.114** (24 mg, 0.087 mmol), 4-benzotrifluoride (0.02 mL, 0.1 mmol), copper iodide (2 mg, 0.02 mmol), *N,N'*-dimethylethylenediamine (4 μL, 0.04 mmol), cesium carbonate (57 mg, 0.17 mmol), and toluene (0.9 mL) provided lactam **3.169** (17 mg, 47%) as a clear oil after column chromatography (gradient elution with 5-10% ethyl acetate in hexanes). When potassium carbonate was used as a base only 14-16% of lactam **3.169** was isolated and 20-25% of the starting material was recovered (PAJ 8-100, PAJ 8-192).

Data for 3.169: (PAJ 9-36, 17 mg, 47%, NMR contaminated with about 13% of the compound with the α-methylene of the lactam reduced)

¹H NMR (400 MHz, CDCl₃)

δ 7.96 (d, *J* = 8.6 Hz, 2H), 7.67 (d, *J* = 8.6 Hz, 2H), 7.32-7.28 (m, 5H), 6.29 (d, *J* = 2.0 Hz, 1H), 5.56 (d, *J* = 2.0 Hz, 1H), 4.72 (d, *J* = 3.2 Hz, 1H), 4.68-4.66 (m,

2H), 3.29-3.26 (m, 1H), 2.19-2.13 (m, 2H), 1.90-1.83 (m, 2H), 1.73 (t, $J = 3.0$ Hz, 3H) ppm

^{13}C NMR (100 MHz, CDCl_3)

δ 206.2, 166.5, 142.5, 141.3, 131.8 (2C), 129.1 (2C), 128.5 (2C), 127.2, 126.08 (q, $J = 4.0$ Hz, 1C), 125.6, 121.9, 121.2 (2C), 119.5, 97.5, 86.3, 75.5, 54.7, 44.5, 32.5, 29.9, 19.1 ppm

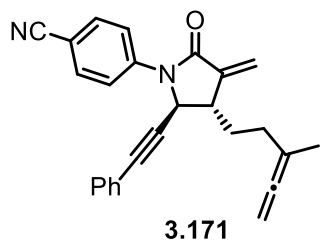
IR (thin film)

2942, 2381, 1715, 1325, 1213, 1122, 1068 cm^{-1}

HRMS TOF MS ES+ $[\text{M}+\text{H}]$: $\text{C}_{26}\text{H}_{23}\text{F}_3\text{NO}$

Calc: 422.17263 Found: 422.17102

TLC $R_f = 0.86$ (50% EtOAc/hexanes) [silica gel, UV, vanillin]



4-((4S*,5S*)-3-Methylene-4-(3-methylpenta-3,4-dien-1-yl)-2-oxo-5-

(phenylethynyl)pyrrolidin-1-yl)benzotrile (3.171): Prepared according to general procedure

G. Lactam **3.114** (33 mg, 0.12 mmol), 4-iodobenzotrile (38 mg, 0.17 mmol), copper iodide (5 mg, 0.02 mmol), *N,N'*-dimethylethylenediamine (5 μL , 0.05 mmol), cesium carbonate (78 mg, 0.24 mmol), and toluene (1.2 mL) provided lactam **3.171** (19 mg, 42%) as a pale yellow oil after column chromatography (gradient elution with 5-15% ethyl acetate in hexanes).

Data for 3.171: (PAJ 9-46, 19 mg, 42%)

^1H NMR (400 MHz, CDCl_3)

δ 7.99 (app dd, $J = 2.0, 6.8$ Hz, 2H), 7.70 (app dd, $J = 2.0, 6.8$ Hz, 2H), 7.33-7.28 (m, 5H), 6.30 (d, $J = 2.2$ Hz, 1H), 5.59 (d, $J = 2.2$ Hz, 1H), 4.71 (d, $J = 3.2$ Hz, 1H), 4.68-4.66 (m, 2H), 3.28-3.27 (m, 1H), 2.17-2.13 (m, 2H), 1.89-1.83 (m, 2H), 1.73 (t, $J = 3.2$ Hz, 3H) ppm

^{13}C NMR (125 MHz, CDCl_3)

δ 206.2, 166.5, 142.2, 133.0 (2C), 131.8 (2C), 129.2, 128.5 (2C), 121.6, 121.0 (2C), 120.0, 118.9, 108.11, 97.4, 86.5, 85.9, 75.5, 54.4, 44.3, 32.4, 29.9, 19.1 ppm

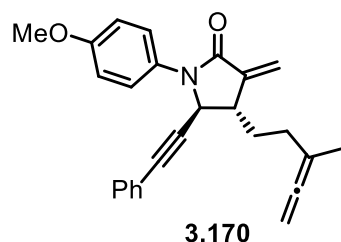
IR (thin film)

3432, 2101, 1642, 1511 cm^{-1}

HRMS TOF MS ES+ $[\text{M}+\text{H}]$: $\text{C}_{26}\text{H}_{23}\text{N}_2\text{O}$

Calc: 379.1732 Found: 379.1735

TLC $R_f = 0.43$ (25% EtOAc/hexanes) [silica gel, UV, vanillin]



(4S*,5S*)-1-(4-Methoxyphenyl)-3-methylene-4-(3-methylpenta-3,4-dien-1-yl)-5-

(phenylethynyl)pyrrolidin-2-one (3.170): Prepared according to general procedure G. Lactam **3.114** (29 mg, 0.11 mmol), 4-iodoanisole (37 mg, 0.16 mmol), copper iodide (4 mg, 0.02 mmol), *N,N'*-dimethylethylenediamine (5 μL , 0.04 mmol), cesium carbonate (68 mg, 0.21 mmol), and toluene (1 mL) provided lactam **3.170** (25 mg, 63%) as a pale yellow oil after column chromatography (gradient elution with 5-20% ethyl acetate in hexanes). This reaction was first performed according to general procedure G with potassium carbonate as a base. Lactam **3.114** (20 mg, 0.072 mmol), 4-iodoanisole (20 mg, 0.087 mmol), copper iodide (3 mg, 0.01 mmol),

N,N'-dimethylethylenediamine (4 μ L, 0.03 mmol), potassium carbonate (20 mg, 0.14 mmol), and toluene (0.72 mL) provided lactam **3.170** (5 mg, 19%) as a pale yellow oil after column chromatography; 25% (5 mg) of starting material **3.114** was also recovered (PAJ 8-118).

Data for **3.170**: (PAJ 9-30, 25 mg, 63%)

^1H NMR (500 MHz, CDCl_3)

δ 7.60 (d, $J = 8.7$ Hz, 2H), 7.32-7.27 (m, 5H), 6.94 (d, $J = 8.7$ Hz, 2H), 6.22 (d, $J = 1.5$ Hz, 1H), 5.48 (d, $J = 1.5$ Hz, 1H), 4.68-4.66 (m, 2H), 4.62 (d, $J = 3.0$ Hz, 1H), 3.82 (s, 3H), 3.27-3.21 (m, 1H), 2.18-2.13 (m, 2H), 1.93-1.82 (m, 2H), 1.73 (t, $J = 2.7$ Hz, 3H) ppm

^{13}C NMR (125 MHz, CDCl_3)

δ 206.3, 166.3, 157.7, 143.1, 131.8 (2C), 131.3, 128.8, 128.4 (2C), 124.5 (2C), 122.3, 117.8, 114.3 (2C), 97.7, 87.3, 85.8, 75.3, 55.7, 55.6, 44.7, 32.5, 30.0, 19.1 ppm

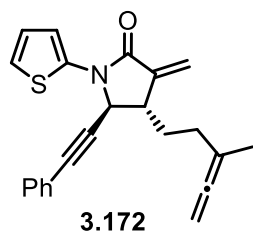
IR (thin film)

2924, 1995, 1697, 1512, 1377, 1300, 1249 cm^{-1}

HRMS TOF MS ES+ $[\text{M}+\text{H}]$: $\text{C}_{26}\text{H}_{26}\text{NO}_2$

Calc: 384.1958 Found: 384.1968

TLC $R_f = 0.59$ (50% EtOAc/hexanes) [silica gel, UV, Vanillin]



(4S*,5S*)-3-Methylene-4-(3-methylpenta-3,4-dien-1-yl)-5-(phenylethynyl)-1-(thiophen-2-yl)pyrrolidin-2-one (3.172): Prepared according to general procedure G. Lactam **3.114** (21 mg,

0.076 mmol), copper iodide (3 mg, 0.02 mmol), *trans*-N,N'-dimethylcyclohexane-1,2-diamine (5 μ L, 0.03 mmol), cesium carbonate (50 mg, 0.15 mmol), iodothiophene (12 μ L, 0.10 mmol), and toluene (0.8 mL) provided lactam **3.172** (15 mg, 56%) as a pale yellow oil after column chromatography (5-10% ethyl acetate in hexanes gradient elution). This reaction was repeated according to general procedure G. Lactam **3.114** (23 mg, 0.083 mmol), copper iodide (3 mg, 0.02 mmol), *trans*-N,N'-dimethylcyclohexane-1,2-diamine (4 μ L, 0.03 mmol), cesium carbonate (52 mg, 0.16 mmol), iodothiophene (10 μ L, 0.11 mmol), and toluene (0.8 mL) provided lactam **3.172** (19 mg, 63%) as a pale yellow oil after column chromatography

Data for 3.172: (PAJ 8-206, 15 mg, 56%; PAJ 9-40, 19 mg, 63%)

$^1\text{H NMR}$ (400 MHz, CDCl_3)

δ 7.38-7.36 (m, 2H), 7.32-7.28 (m, 3H), 7.03-7.02 (m, 1H), 6.97-6.94 (m, 2H), 6.27 (d, $J = 2.0$ Hz, 1H), 5.54 (d, $J = 2.0$ Hz, 1H), 4.70 (d, $J = 2.8$ Hz, 1H), 4.68-4.66 (m, 2H), 3.34-3.29 (m, 1H), 2.15-2.11 (m, 2H), 1.84 (app q, $J = 7.6$ Hz, 2H), 1.73 (t, $J = 3.2$ Hz, 3H) ppm

$^{13}\text{C NMR}$ (125 MHz, CDCl_3)

δ 206.2, 164.3, 141.5, 139.4, 131.9 (2C), 129.0, 128.5 (2C), 124.2, 122.0, 119.3, 119.2, 113.0, 97.4, 86.1, 86.0, 75.4, 55.4, 44.9, 33.2, 29.8, 19.1 ppm

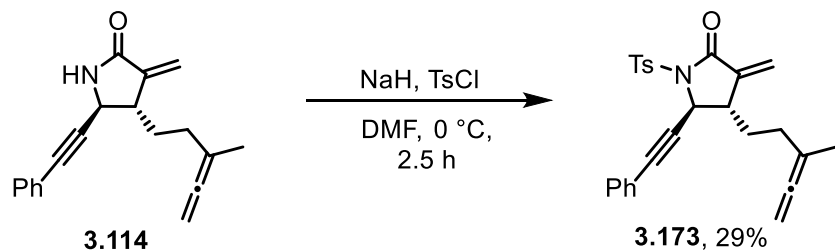
IR (thin film)

2924, 2227, 1959, 1695, 1534, 1451, 1399 cm^{-1}

HRMS TOF MS ES+ [$\text{M}+\text{H}$]: $\text{C}_{23}\text{H}_{22}\text{NOS}$

Calc: 360.1417 Found: 360.1401

TLC $R_f = 0.58$ (25% EtOAc/hexanes) [silica gel, UV, *p*-anisaldehyde]



(4S*,5S*)-3-Methylene-4-(3-methylpenta-3,4-dien-1-yl)-5-(phenylethynyl)-1-

tosylpyrrolidin-2-one (3.173): A flame-dried test tube equipped with a stir bar, septum, and nitrogen inlet needle was charged with lactam **3.114** (20 mg, 0.07 mmol) and DMF (0.75 mL) and cooled to 0 °C under a nitrogen atmosphere. Sodium hydride (60% dispersion in mineral oil, 6 mg, 0.14 mmol) was added in a single portion and the reaction mixture was stirred for 15 min at 0 °C. *para*-Toluene sulfonyl chloride (28 mg, 0.14 mmol) was then added in a single portion, the ice bath was removed, and the solution was allowed to warm to rt for 2.5 h. TLC analysis revealed consumption of the starting material, and the reaction was quenched by pouring it into a separatory funnel containing saturated aqueous ammonium chloride (5 mL). The aqueous layer was extracted with ethyl acetate (3 x 10 mL). The organic layers were combined, dried over magnesium sulfate, gravity filtered, concentrated by rotary evaporation, and purified by silica gel flash column chromatography eluting with 10-25% ethyl acetate in hexanes. Lactam **3.173** was obtained as a pale yellow oil (9 mg, 29%). This reaction was repeated, but it was kept at 0 °C for 1 h after addition of *para*-toluene sulfonyl chloride, then allowed to warm to rt for 1 h before quenching. Lactam **3.114** (18 mg, 0.069 mmol), sodium hydride (60% dispersion in mineral oil, 5 mg, 0.1 mmol), *para*-toluene sulfonyl chloride (25 mg, 0.13 mmol), and DMF (0.7 mL) provided lactam **3.173** (14 mg, 48%) as a yellow oil after column chromatography; some unidentified contaminants were observed in the ¹H NMR. Additional purification by column chromatography provided allene-yne **3.186** (4 mg, 18%) as a clear oil.

Data for **3.173**: (PAJ 8-4, 9 mg, 29%; PAJ 8-82, 14 mg, 48% (impure) and 4 mg, 18% (pure))

¹H NMR (500 MHz, CDCl₃)

δ 8.08 (d, *J* = 8.0 Hz, 2H), 7.25-7.28 (m, 5H), 7.22 (d, *J* = 8.0 Hz, 2H), 6.23 (d, *J* = 1.7 Hz, 1H), 5.54 (d, *J* = 1.7 Hz, 1H), 4.98 (d, *J* = 1.5 Hz, 1H), 4.68-4.67 (m, 2H), 3.11-3.08 (m, 1H), 2.38 (s, 3H), 2.08-2.05 (m, 2H), 1.88-1.84 (m, 1H), 1.74-1.69 (m, 1H), 1.71 (t, *J* = 3.3 Hz, 3H) ppm

¹³C NMR (125 MHz, CDCl₃)

δ 206.3, 164.9, 145.3, 141.1, 135.6, 131.9 (2C), 131.7, 129.8 (2C), 129.5 (2C), 128.5 (2C), 122.6, 121.9, 97.2, 86.3, 85.9, 75.4, 53.6, 45.5, 32.8, 29.8, 21.8, 19.0 ppm

IR (thin film)

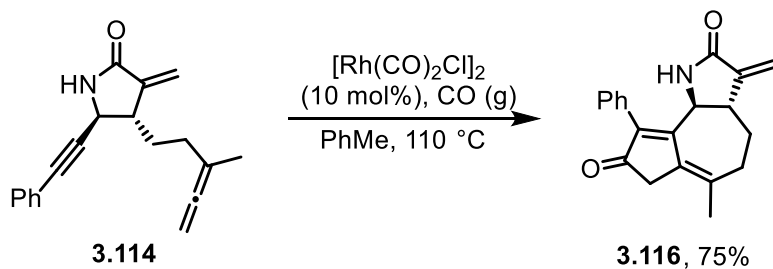
2891, 2218, 1937, 1697, 1579, 1429, 1356, 1160, 1078, 804, 750 cm⁻¹

HRMS TOF MS ES+ [M+H]: C₂₆H₂₆NO₃S

Calc: 432.1628 Found: 432.1641

TLC *R_f* = 0.66 (25% EtOAc/hexanes) [silica gel, UV, vanillin]

General Procedure H: Allenic Pauson-Khand Reaction (Slow Addition of Allene-Yne to Rhodium Catalyst)



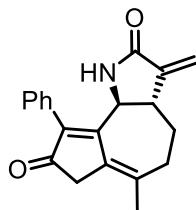
A flame-dried, 10-mL, 2-necked round-bottomed flask equipped with a magnetic stir bar, condenser capped with septum, and a septum was charged with rhodium dicarbonyl chloride

dimer (2 mg, 0.004 mmol) and toluene (3.4 mL). The apparatus was evacuated via a needle attached to a vacuum line for 2-3 seconds then filled with carbon monoxide (3x) via a needle attached to a balloon, then lowered into a prewarmed oil bath set to 110 °C. The allene-yne **3.114** (13 mg, 0.044 mmol) was dissolved in toluene (1.1 mL) and added dropwise to the stirring solution of rhodium dicarbonyl chloride dimer over 1 h using a syringe pump. After the addition was complete, the reaction was stirred an additional 30 min at 110 °C and TLC showed consumption of the starting material. The reaction was removed from the oil bath and allowed to cool to rt, then polymer bound triphenylphosphine (3 mmol/g, 60 mg) was added and stirred 4 h. The polymer was removed by vacuum filtration, then the solution was concentrated, and purified by silica gel flash column chromatography with gradient elution using 25-75% ethyl acetate in hexanes to yield tricycle **3.116** as a white solid (9 mg, 64%). This reaction was repeated according to the procedure above. Allene-yne **3.114** (21 mg, 0.076 mmol), rhodium dicarbonyl chloride dimer (3 mg, 0.008 mmol), and toluene (7.6 mL) provided tricycle **3.116** (19 mg, 79%) as a white solid after column chromatography. The compound was crystallized by vapor diffusion using ethyl acetate and pentanes, and X-ray crystallography confirmed the structure and trans stereochemistry of the lactam substituents.

General Procedure I: Alternative Procedure for Allenic Pauson-Khand Reaction

To a flame-dried, 2-necked, 25-mL round-bottomed flask equipped with a septum, condenser capped with a septum, and a magnetic stir bar was added rhodium dicarbonyl chloride dimer (4 mg, 0.01 mmol) and toluene (7 mL). The apparatus was evacuated via a needle attached to a vacuum line for 2-3 seconds and filled with carbon monoxide (3x) via a needle attached to a balloon, then lowered into a prewarmed oil bath set to 110 °C with stirring. Allene **3.114** (30 mg, 0.11 mmol) was then dissolved in toluene (4 mL) and added to the stirring solution of rhodium

catalyst via syringe in a single portion and the reaction was stirred 1 h. Consumption of the starting material was observed by TLC, and the crude reaction mixture was concentrated by rotary evaporation. The crude residue was purified by silica gel flash column chromatography eluting with a gradient of 30-75% ethyl acetate in hexanes to give tricycle **3.116** as a white solid (25 mg, 75%).



3.116

(3aS*,9bS*)-6-Methyl-3-methylene-9-phenyl-3,3a,4,5-tetrahydro-1H-azuleno[4,5-b]pyrrole-2,8(7H,9bH)-dione (3.116):

Data for 3.116: (PAJ 6-176, 9 mg, 64%; PAJ 7-84, 19 mg, 79%; PAJ 7-200, 25 mg, 75%)

¹H NMR (400 MHz, CDCl₃)

δ 7.46-7.40 (m, 3H), 7.25-7.24 (m, 2H), 5.98 (d, *J* = 3.2 Hz, 1H), 5.58 (br s, 1H), 5.27 (d, *J* = 3.2 Hz, 1H), 4.82 (d, *J* = 8.4 Hz, 1H), 3.18, 3.11 (ABq, *J* = 20.0 Hz, 2H), 3.05-3.02 (m, 1H), 2.77-2.72 (m, 1H), 2.42-2.35 (m, 2H), 1.99 (s, 3H), 1.91-1.83 (m, 1H) ppm

¹³C NMR (100 MHz, CDCl₃)

δ 202.0, 168.6, 165.5, 143.1, 140.8, 135.7, 131.8, 131.3, 129.3 (4C), 128.4, 115.3, 56.2, 44.3, 40.9, 31.8, 26.6, 24.8 ppm

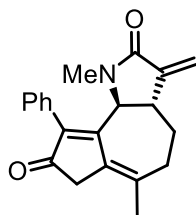
IR (thin film)

3419, 2950, 2865, 1697, 1675, 1460, 1380, 1305, 1201 cm⁻¹

HRMS TOF MS ESI+ [M + H]: C₂₀H₂₀NO₂

Calcd: 306.1489 Found: 306.1479

TLC $R_f = 0.22$ (75% EtOAc/hexanes) [silica gel, UV, *p*-anisaldehyde]



3.56

(3aS*,9bS*)-1,6-Dimethyl-3-methylene-9-phenyl-1,3a,4,5,7,9b-hexahydro-2H-azuleno[4,5-b]pyrrole-2,8(3H)-dione (3.56): Prepared according to general procedure H. Allene **3.57** (30 mg, 0.1 mmol), rhodium dicarbonyl chloride dimer (4 mg, 0.009 mmol), and toluene (8.6 mL) provided tricycle **3.56** (24 mg, 75%) as a white solid after column chromatography (gradient elution with 25-75% ethyl acetate in hexanes).

Data for 3.56: (PAJ 7-136, 24 mg, 75%)

¹H NMR (400 MHz, CDCl₃)

δ 7.33-7.31 (m, 3H), 7.11-7.10 (m, 2H), 6.10 (d, $J = 3.2$ Hz, 1H), 5.34 (d, $J = 3.2$ Hz, 1H), 4.52 (d, $J = 8.0$ Hz, 1H), 3.17, 3.10 (ABq, $J = 21.2$ Hz, 2H), 3.20-3.07 (m, 1H), 2.93-2.84 (m, 1H), 2.57-2.46 (m, 1H), 2.42 (app dd, $J = 4.2, 16.2$ Hz, 1H), 2.01 (s, 3H), 1.99 (s, 3H), 1.96-1.88 (m, 1H) ppm

¹³C NMR (100 MHz, CDCl₃)

δ 202.8, 168.8, 165.5, 143.2, 137.6, 136.6, 130.6, 130.3 (2C), 128.4, 127.7 (2C), 115.6, 62.1, 41.7, 40.5, 32.3, 30.4, 29.8, 28.5, 25.8 ppm

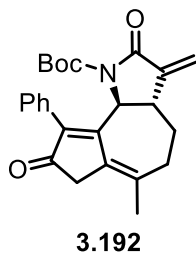
IR (thin film)

2885, 1670, 1638, 1422, 1378, 1296, 1257, 1141, 1080 cm⁻¹

HRMS TOF MS ESI+ [M + H]: C₂₁H₂₂NO₂

Calc: 320.1645 Found: 320.1651

TLC $R_f = 0.36$ (75% EtOAc/hexanes) [silica gel, UV, *p*-anisaldehyde]



***tert*-Butyl (3a*S**,9b*S**)-6-methyl-3-methylene-2,8-dioxo-9-phenyl-2,3,3a,4,5,7,8,9b-octahydro-1*H*-azuleno[4,5-*b*]pyrrole-1-carboxylate (3.192):** Prepared according to general procedure H. Allene-yne **3.174** (7 mg, 0.018 mmol), rhodium dicarbonyl chloride dimer (1 mg, 0.002 mmol), and toluene (1.9 mL) provided tricycle **3.192** (3 mg, 40%) as a pale yellow solid after column chromatography (gradient elution with 15-50% ethyl acetate in hexanes). Tricycle **3.192** was also prepared according to general procedure I. Allene-yne **3.174** (16 mg, 0.042 mmol), rhodium dicarbonyl chloride dimer (2 mg, 0.004 mmol), and toluene (4.2 mL) provided tricycle **3.192** (7 mg, 41%) as a pale yellow solid after column chromatography.

Data for 3.192: (PAJ 7-4, 3 mg, 40%; PAJ 6-204, 7 mg, 41%)

^1H NMR (500 MHz, CDCl_3)

δ 7.35-7.27 (m, 3H), 7.05-7.04 (m, 2H), 6.29 (d, $J = 3.5$ Hz, 1H), 5.50 (d, $J = 3.5$ Hz, 1H), 5.12 (d, $J = 9.0$ Hz, 1H), 3.17 (d, $J = 21.0$ Hz, 1H), 3.17, 3.06 (ABq, $J = 21.0$ Hz, 2H), 3.14-3.11 (m, 1H), 3.01-2.92 (m, 1H), 2.56-2.50 (m, 1H), 2.43-2.39 (m, 1H), 2.00 (s, 3H), 1.95-1.92 (m, 1H), 1.18 (s, 9H) ppm

^{13}C NMR (125 MHz, CDCl_3)

δ 202.7, 165.0, 164.8, 150.4, 142.8, 137.9, 135.7, 131.0 (2C), 130.6, 130.2, 127.9 (2C), 119.9, 83.5, 60.5, 58.5, 40.6, 39.8, 31.9, 28.9, 27.9 (3C), 25.7

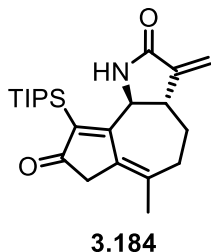
IR (thin film)

2969, 2915, 1793, 1757, 1717, 1401, 1302, 1153 cm^{-1}

HRMS TOF MS ESI+ [M + H]: $\text{C}_{25}\text{H}_{28}\text{NO}_4$

Calc: 406.2013 Found: 406.2013

TLC $R_f = 0.65$ (50% EtOAc/hexanes, [silica gel, UV, *p*-anisaldehyde])



(3aS*,9bS*)-6-Methyl-3-methylene-9-(triisopropylsilyl)-3,3a,4,5-tetrahydro-1H-

azuleno[4,5-b]pyrrole-2,8(7H,9bH)-dione (3.184): Prepared according to general procedure H.

Allene-yne **3.125** (20 mg, 0.056 mmol), rhodium dicarbonyl chloride dimer (2 mg, 0.006 mmol), and toluene (5.7 mL) provided tricycle **3.184** (11 mg, 50%) as a clear oil after column chromatography (gradient elution with 15-30% ethyl acetate in hexanes). This reaction was repeated according to general procedure H. Allene-yne **3.125** (25 mg, 0.078 mmol), rhodium dicarbonyl chloride dimer (3 mg, 0.008 mmol), and toluene (8 mL) provided tricycle **3.184** (11 mg, 41%) as a white solid after column chromatography.

Data for 3.184: (PAJ 7-78, 11 mg, 50%; PAJ 8-58, 11 mg, 41%)

^1H NMR (300 MHz, CDCl_3)

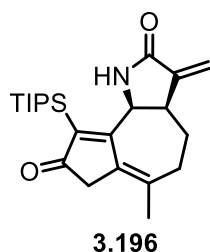
δ 6.19 (br s, 1H), 6.07 (d, $J = 3.1$ Hz, 1H), 5.31 (d, $J = 3.1$ Hz, 1H), 4.65 (d, $J = 8.1$ Hz, 1H), 3.05-3.00 (m, 1H), 3.0 (s, 2H), 2.99-2.65 (m, 1H), 2.45-2.27 (m, 2H), 1.95 (s, 3H), 1.90-1.80 (m, 1H), 1.63-1.53 (m, 3H), 1.13 (d, $J = 2.0$ Hz, 9H), 1.09 (d, $J = 2.0$ Hz, 9H) ppm

¹³C NMR (100 MHz, CDCl₃)
δ 208.2, 179.9, 169.3, 143.1, 137.9, 134.1, 133.9, 115.7, 56.8, 44.2, 41.4, 31.9,
27.1, 25.4, 19.5 (3C), 19.4 (3C), 13.0 (3C) ppm

IR (thin film)
2943, 2881, 1719, 1688, 1518, 1504 cm⁻¹

HRMS TOF MS ESI+ [M + H]: C₂₃H₃₆NO₂Si
Calc: 386.2510 Found: 386.2515

TLC *R_f* = 0.37 (50% EtOAc/hexanes) [silica gel, UV, *p*-anisaldehyde]



(3aR*,9bS*)-6-Methyl-3-methylene-9-(triisopropylsilyl)-1,3a,4,5,7,9b-hexahydro-2H-azuleno[4,5-b]pyrrole-2,8(3H)-dione (3.196): Prepared according to general procedure H. Allene **3.135** (3:1 mixture of α -methylene lactam and α -methyl lactam, 10 mg, 0.028 mmol), rhodium dicarbonyl chloride dimer (1 mg, 0.003 mmol), and toluene (2.8 mL) provided tricycle **3.196** (2 mg, 40%) as a white solid after column chromatography (gradient elution with 15-30% ethyl acetate in hexanes).

Data for 3.196: (PAJ 8-42, 2 mg, 40%; PAJ 8-50, 40%)

¹H NMR (500 MHz, CDCl₃)
δ 6.21 (d, *J* = 1.5 Hz, 1H), 5.50 (br s, 1H), 5.46 (app s, 1H), 5.01 (d, *J* = 7.5 Hz, 1H), 3.40 (app br s, 1H), 3.12, 3.00 (ABq, *J* = 20.5 Hz, 2H), 2.50-2.44 (m, 1H),

2.14-2.08 (m, 2H), 1.92-1.88 (m, 1H), 1.82 (s, 3H), 1.54-1.48 (m, 3H), 1.07-1.04 (m, 18H) ppm

¹³C NMR (126 MHz, CDCl₃)

δ 208.7, 176.6, 170.1, 143.6, 143.4, 139.3, 131.2, 118.5, 56.8, 44.3, 41.5, 35.2, 31.8, 24.4, 19.2 (2C), 19.1 (2C), 18.7 (2C), 12.3 (3C) ppm

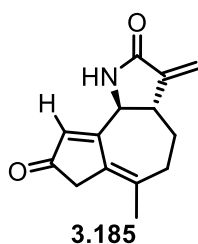
IR (thin film)

2909, 2833, 1688, 1640, 1445, 1135 cm⁻¹

HRMS TOF MS ES+ [M+H]: C₂₃H₃₆NO₂Si

Calc: 386.2510 Found: 386.2422

TLC R_f = 0.33 (50% EtOAc/hexanes) [silica gel, UV, *p*-anisaldehyde]



(3aS*,9bS*)-6-Methyl-3-methylene-1,3a,4,5,7,9b-hexahydro-2H-azuleno[4,5-b]pyrrole-

2,8(3H)-dione (3.185): Prepared according to general procedure H. Allene-yne **3.175** (12 mg, 0.060 mmol), rhodium dicarbonyl chloride dimer (3 mg, 0.006 mmol), and toluene (6 mL) provided **3.185** (9 mg, 64%) as a white solid after column chromatography (gradient elution with 50-100% ethyl acetate in hexanes). This reaction was repeated according to general procedure H. Allene-yne **3.175** (17 mg, 0.085 mmol), rhodium dicarbonyl chloride dimer (4 mg, 0.008 mmol), and toluene (8.6 mL) provided tricycle **3.185** (8 mg, 42%) as a white solid after column chromatography.

Data for 3.185: (PAJ 8-60, 9 mg, 64%; PAJ 7-172, 8 mg, 42%)

¹H NMR (500 MHz, CDCl₃)

δ 7.86 (br s, 1H), 6.14 (s, 1H), 6.06 (d, $J = 3.0$ Hz, 1H), 5.32 (d, $J = 3.0$ Hz, 1H), 4.58 (d, $J = 8.5$ Hz, 1H), 3.00 (s, 2H), 2.86-2.82 (m, 1H), 2.76-2.71 (m, 1H), 2.42-2.31 (m, 2H), 1.94 (s, 3H), 1.93-1.87 (m, 1H) ppm

^{13}C NMR (126 MHz, CDCl_3)

δ 204.0, 173.0, 170.7, 143.9, 137.1, 131.6, 126.6, 115.8, 56.1, 43.4, 41.3, 32.0, 26.8, 24.9 ppm

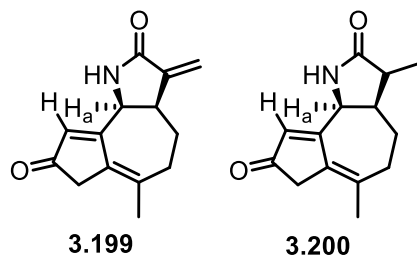
IR (thin film)

2895, 1685, 1556, 1420, 1327, 1231, 1149 cm^{-1}

HRMS TOF MS ES+ [$\text{M}+\text{H}$]: $\text{C}_{14}\text{H}_{16}\text{NO}_2$

Calc: 230.1179 Found: 230.1176

TLC $R_f = 0.15$ (100% EtOAc) [silica gel, UV, *p*-anisaldehyde]



(3aR*,9bS*)-6-Methyl-3-methylene-1,3a,4,5,7,9b-hexahydro-2H-azuleno[4,5-b]pyrrole-2,8(3H)-dione (3.199) and (3aR*,9bS*)-3,6-dimethyl-1,3a,4,5,7,9b-hexahydro-2H-azuleno[4,5-b]pyrrole-2,8(3H)-dione (3.200): Prepared according to general procedure I. Allene **3.182** (10 mg, 0.05 mmol, 5:1 ratio of **3.182** to reduced α -methylene compound **3.183**), rhodium dicarbonyl chloride dimer (2 mg, 0.005 mmol), and toluene (5 mL) provided **3.199** and **3.200** (4 mg, 40%) as a white solid in a 3:1 ratio after column chromatography (gradient elution with 50-100% ethyl acetate in hexanes). Preparation according to general procedure H on a 0.03 mmol scale of **3.182** (2:1 **3.182** to reduced α -methylene compound **3.183**) gave a similar yield of

43% (2:1 **3.199** to reduced α -methylene compound **3.200**). The ratio was determined by integration of the resonance for H_a which appeared as a doublet at 4.73 for **3.199** and 4.52 for **3.200**.

Data for 3.199: (PAJ 7-176, 4 mg, 40%, Data reported for major product only; PAJ 8-48, 3 mg, 57%)

¹H NMR (400 MHz, CDCl₃)

δ 7.21-6.90 (br s, 1H), 6.13 (s, 1H), 6.06 (d, $J = 2.6$ Hz, 1H), 5.33 (d, $J = 2.6$ Hz, 1H), 4.73 (d, $J = 9.2$ Hz, 1H), 3.51-3.46 (m, 1H), 3.10, 2.99 (ABq, $J = 20.8$ Hz, 2H), 2.50-2.22 (m, 4H), 1.93 (s, 3H) ppm

¹³C NMR (100 MHz, CDCl₃)

δ 203.6, 170.6, 142.3, 141.7, 137.7, 131.2, 126.4, 56.4, 44.8, 42.7, 41.2, 28.1, 24.8, 24.2 ppm

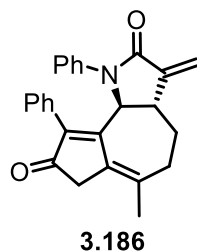
IR (thin film)

2909, 1715, 1688, 1640, 1445, 1351, 1135 cm⁻¹

HRMS TOF MS ES+ [M+H]: C₁₄H₁₆NO₂

Calc: 230.1179 Found: 230.1166

TLC $R_f = 0.08$ (75% EtOAc/hexanes) [silica gel, UV, *p*-anisaldehyde]



(3aS*,9bS*)-6-Methyl-3-methylene-1,9-diphenyl-1,3a,4,5,7,9b-hexahydro-2H-azuleno[4,5-b]pyrrole-2,8(3H)-dione (3.186): Prepared according to general procedure I. Allene-yne **3.168**

(11 mg, 0.031 mmol), rhodium dicarbonyl chloride dimer (1.2 mL of a 1 mg/mL toluene solution, 0.003 mmol), and toluene (3.1 mL) provided tricycle **3.186** (8 mg, 67%) as a white solid after column chromatography (gradient elution with 25-50% ethyl acetate in hexanes). This reaction was repeated according to general procedure I. Allene-yne **3.168** (3 mg, 0.008 mmol), rhodium dicarbonyl chloride dimer (0.5 mL of a 1 mg/mL solution in toluene), and toluene (0.5 mL) provided tricycle **3.186** (2 mg, 66%) as a white solid after column chromatography.

Data for **3.186**: (PAJ 9-4, 8 mg, 67%; PAJ 8-8, 2 mg, 66%)

¹H NMR (500 MHz, CDCl₃)

δ 7.10-7.07 (m, 1H), 7.02-6.97 (m, 2H), 6.96-6.94 (m, 2H), 6.91-6.90 (m, 1H), 6.89-6.86 (m, 2H), 6.53-6.52 (m, 2H), 6.24 (d, *J* = 3.3 Hz, 1H), 5.46 (d, *J* = 3.3 Hz, 1H), 5.34 (d, *J* = 8.0 Hz, 1H), 3.31-3.29 (m, 1H), 3.17, 3.08 (ABq, *J* = 21.0 Hz, 2H), 3.08-3.02 (m, 1H), 2.63-2.60 (m, 1H), 2.52-2.47 (m, 1H), 2.05 (s, 3H), 2.08-2.03 (m, 1H) ppm

¹³C NMR (126 MHz, CDCl₃)

δ 202.5, 166.4, 163.3, 143.6, 139.4, 137.6, 136.4, 130.6, 130.5, 129.6 (2C), 128.1 (2C), 127.5, 127.4 (2C), 124.1, 119.3 (2C), 117.1, 59.1, 40.9, 40.6, 32.4, 28.7, 25.9 ppm

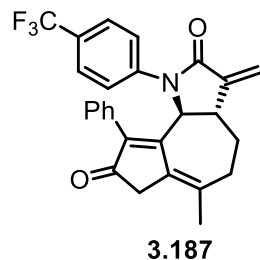
IR (thin film)

2891, 1675, 1631, 1477, 1356 cm⁻¹

HRMS TOF MS ES+ [M+H]: C₂₆H₂₄NO₂

Calc: 382.1802 Found: 382.1807

TLC *R_f* = 0.35 (50% EtOAc/hexanes) [silica gel, UV, *p*-anisaldehyde]



(3aS*,9bS*)-6-Methyl-3-methylene-9-phenyl-1-(4-(trifluoromethyl)phenyl)-1,3a,4,5,7,9b-hexahydro-2H-azuleno[4,5-b]pyrrole-2,8(3H)-dione (3.187): Prepared according to general procedure H. Allene-yne **3.169** (17 mg, 0.04 mmol), rhodium dicarbonyl chloride dimer (2 mg, 0.004 mmol), and toluene (4 mL) provided tricycle **3.187** (13 mg, 72%) as a white solid after column chromatography (gradient elution with 15-50% ethyl acetate in hexanes). Tricycle **3.187** was also prepared according to general procedure I. Allene-yne **3.169** (6 mg, 0.01 mmol), rhodium dicarbonyl chloride dimer (0.5 mL of a 1 mg/mL solution in toluene), and toluene (0.9 mL) provided tricycle **3.187** (4 mg, 67%) as a white solid after column chromatography.

Data for 3.187: (PAJ 9-38, 13 mg, 72%; PAJ 8-108, 4 mg, 67%)

¹H NMR (500 MHz, CDCl₃)

δ 7.20 (app d, *J* = 8.5 Hz, 2H) 7.10 (app t, *J* = 7.5 Hz, 1H), 7.00 (app d, *J* = 9.0 Hz, 4H), 6.50 (app br s, 2H), 6.28 (d, *J* = 3.5 Hz, 1H), 5.52 (d, *J* = 3.5 Hz, 1H), 5.33 (d, *J* = 8.5 Hz, 1H), 3.34-3.31 (m, 1H), 3.17, 3.10 (ABq, *J* = 21.0 Hz, 2H), 3.09-3.02 (m, 1H), 2.66-2.59 (m, 1H), 2.53-2.49 (m, 1H), 2.10-1.99 (m, 1H), 2.06 (s, 3H) ppm

¹³C NMR (125 MHz, CDCl₃)

δ 202.3, 166.5, 162.5, 143.0, 140.4, 139.3, 136.9, 130.38, 130.36, 129.6 (2C), 127.6 (2C), 127.5 (2C), 125.8, 125.6 (q, *J* = 32.5 Hz, 1C), 125.2 (q, *J* = 3.7 Hz, 1C), 122.8, 119.3, 118.2, 59.1, 40.9, 40.5, 32.3, 28.6, 25.9 ppm

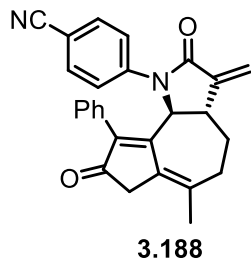
IR (thin film)

2930, 1698, 1615, 1325, 1168, 1117 cm^{-1}

HRMS TOF MS ES+ [M+H]: $\text{C}_{27}\text{H}_{23}\text{NO}_2\text{F}_3$

Calc: 450.1675 Found: 450.1655

TLC $R_f = 0.36$ (50% EtOAc/hexanes) [silica gel, UV, vanillin]



4-((3aS*,9bS*)-6-Methyl-3-methylene-2,8-dioxo-9-phenyl-2,3,3a,4,5,7,8,9b-octahydro-1H-azuleno[4,5-b]pyrrol-1-yl)benzotrile (3.188): Prepared according to general procedure H. Allene-yne **3.171** (17 mg, 0.045 mmol), rhodium dicarbonyl chloride dimer (2 mg, 0.0045 mmol), and toluene (4.5 mL) provided tricycle **3.188** (13 mg, 72%) as a light yellow solid after column chromatography (gradient elution with 15-35% ethyl acetate in hexanes).

Data for 3.188: (PAJ 9-48, 13 mg, 72%)

^1H NMR (400 MHz, CDCl_3)

δ 7.27-7.25 (m, 2H), 7.13-7.11 (m, 1H), 7.09-7.03 (m, 4H), 6.53 (app br s, 2H), 6.30 (d, $J = 3.4$ Hz, 1H), 5.55 (d, $J = 3.4$ Hz, 1H), 5.31 (d, $J = 8.4$ Hz, 1H), 3.35-3.31 (m, 1H), 3.19, 3.10 (ABq, $J = 21.0, 36.6$ Hz, 2H), 3.06-3.01 (m, 1H), 2.68-2.59 (m, 1H), 2.55-2.49 (m, 1H), 2.10-2.03 (m, 1H), 2.08 (s, 3H) ppm

^{13}C NMR (100 MHz, CDCl_3)

δ 202.1, 166.6, 162.2, 142.6, 141.4, 139.2, 137.0, 132.1 (2C), 130.3, 130.2, 129.7 (2C), 127.8, 127.5 (2C), 119.6 (2C), 119.0, 118.8, 107.0, 58.9, 40.8, 40.5, 32.2, 28.6, 25.9 ppm

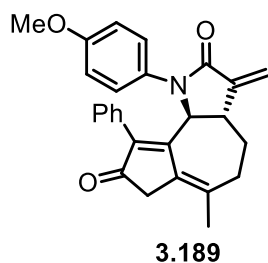
IR (thin film)

2925, 2854, 2224, 1704, 1659, 1604, 1509, 1345, 1179 cm^{-1}

HRMS TOF MS ES+ [M+H]: $\text{C}_{27}\text{H}_{23}\text{N}_2\text{O}_2$

Calc: 407.1754 Found: 406.1753

TLC R_f = 0.27 (50% EtOAc/hexanes) [silica gel, UV, *p*-anisaldehyde]



(3aS*,9bS*)-1-(4-Methoxyphenyl)-6-methyl-3-methylene-9-phenyl-1,3a,4,5,7,9b-hexahydro-2H-azuleno[4,5-b]pyrrole-2,8(3H)-dione (3.189): Prepared according to general procedure I. Allene-yne **3.170** (6 mg, 0.2 mmol), rhodium dicarbonyl chloride dimer (0.5 mL of a 1 mg/mL toluene solution, 0.001 mmol), and toluene (1.3 mL) provided tricycle **3.189** (5 mg, 76%) as a white solid after column chromatography (gradient elution with 15-35% ethyl acetate in hexanes). This product was also prepared according to general procedure H. Allene-yne **3.170** (25 mg, 0.065 mmol), rhodium biscarbonyl chloride dimer (3 mg, 0.006 mmol), and toluene (6.6 mL) to provide tricycle **3.189** (20 mg, 77%) as a white solid after column chromatography.

Data for 3.189: (PAJ 8-122, 5 mg, 76%; PAJ 9-32, 20 mg, 77%)

^1H NMR (500 MHz, CDCl_3)

δ 7.12-7.10 (m, 1H), 7.06-7.03 (m, 2H), 6.79-6.77 (m, 2H), 6.58-6.57 (m, 2H), 6.51-6.49 (m, 2H), 6.22 (d, $J = 3.2$ Hz, 1H), 5.45 (d, $J = 3.2$ Hz, 1H), 5.31 (d, $J = 8.5$ Hz, 1H), 3.72 (s, 3H), 3.31-3.28 (m, 1H), 3.17, 3.08 (ABq, $J = 21.0$ Hz, 2H), 3.09-3.01 (m, 1H), 2.62-2.58 (m, 1H), 2.51-2.46 (m, 1H), 2.10-2.00 (m, 1H), 2.05 (s, 3H) ppm

^{13}C NMR (125 MHz, CDCl_3)

δ 202.4, 166.2, 163.4, 156.3, 143.7, 139.3, 136.4, 131.2, 130.7, 129.6 (2C), 127.6, 127.4 (2C), 120.6 (2C), 116.7, 113.5 (2C), 59.2, 55.6, 41.0, 40.6, 32.4, 29.9, 28.7, 25.8 ppm

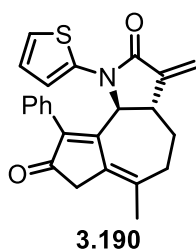
IR (thin film)

2924, 1700, 1511, 1250 cm^{-1}

HRMS TOF MS ES+ $[\text{M}+\text{H}]$: $\text{C}_{27}\text{H}_{26}\text{NO}_3$

Calc: 412.1907 Found: 412.1901

TLC $R_f = 0.23$ (50% EtOAc/hexanes) [silica gel, UV, vanillin]



(3aS*,9bS*)-6-Methyl-3-methylene-9-phenyl-1-(thiophen-2-yl)-1,3a,4,5,7,9b-hexahydro-2H-azuleno[4,5-b]pyrrole-2,8(3H)-dione (3.190): Prepared according to general procedure I. Allene-yne **3.172** (12 mg, 0.033 mmol), rhodium biscarbonyl chloride dimer (1.3 mL of a 1 mg/mL toluene solution, 0.003 mmol), and toluene (3.3 mL) provided tricycle **3.190** (7 mg, 54%) as a pale yellow solid after column chromatography (gradient elution with 25-50% ethyl

acetate in hexanes). This product was also synthesized following general procedure H. Allene-
yne **3.172** (18 mg, 0.050 mmol), rhodium biscarbonyl chloride dimer (2 mg, 0.005 mmol), and
toluene (5 mL) provided tricycle **3.190** (15 mg, 79%) as a pale yellow solid after column
chromatography.

Data for 3.190: (PAJ 9-2, 7 mg, 54%; PAJ 9-44, 15 mg, 79%)

¹H NMR (400 MHz, CDCl₃)

δ 7.10-7.04 (m, 3H), 6.70 (dd, *J* = 1.4, 5.4 Hz, 1H), 6.65-6.59 (m, 3H), 6.25 (d, *J*
= 3.6 Hz, 1H), 6.24 (d, *J* = 3.2 Hz, 1H), 5.49 (d, *J* = 3.2 Hz, 1H), 5.16 (d, *J* = 8.0
Hz, 1H), 3.40-3.34 (m, 1H), 3.21, 3.12 (ABq, *J* = 21.0 Hz, 2H), 3.08-2.98 (m,
1H), 2.69-2.58 (m, 1H), 2.55-2.48 (m, 1H), 2.06 (s, 3H), 2.03-1.99 (m, 1H) ppm

¹³C NMR (100 MHz, CDCl₃)

δ 202.4, 164.6, 163.1, 141.8, 139.5, 139.0, 136.2, 130.4, 130.1, 129.3 (2C), 127.8,
127.2 (2C), 123.0, 119.2, 117.8, 111.8, 60.8, 41.9, 40.5, 32.2, 28.5, 25.9 ppm

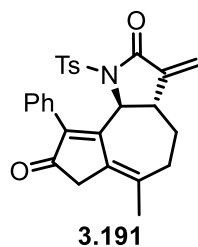
IR (thin film)

3434, 1693, 1575, 1360, 1305 cm⁻¹

HRMS TOF MS ES+ [M+1]: C₂₄H₂₂NO₂S

Calc: 388.1366 Found: 388.1357

TLC *R_f* = 0.31 (50% EtOAc/hexanes) [silica gel, UV, *p*-anisaldehyde]



**(3aS*,9bS*)-6-Methyl-3-methylene-9-phenyl-1-tosyl-1,3a,4,5,7,9b-hexahydro-2H-
azuleno[4,5-b]pyrrole-2,8(3H)-dione (3.191):** Prepared according to general procedure I.

Allene-yne **3.173** (4 mg, 0.009 mmol), rhodium biscarbonyl chloride dimer (0.5 mL of a 1 mg/mL toluene solution, 0.001 mmol), and toluene (1 mL) provided tricycle **3.191** (3 mg, 75%) as a white solid after column chromatography (gradient elution with 25-50% ethyl acetate in hexanes). This reaction was repeated according to general procedure I. Allene-yne **3.173** (9 mg, 0.02 mmol), rhodium biscarbonyl chloride (1 mg, 0.002), and toluene (2.1 mL) provided tricycle **3.191** (6 mg, 67%) as a white solid after column chromatography.

Data for 3.191: (PAJ 8-84, 3 mg, 75%; PAJ 8-10, 6 mg, 67%)

¹H NMR (500 MHz, CDCl₃)

δ 7.64 (d, *J* = 8.5 Hz, 2H), 7.40-7.38 (m, 3H), 7.21 (d, *J* = 8.5 Hz, 2H), 7.12 (app
br s, 2H), 6.16 (d, *J* = 3.5 Hz, 1H), 5.43 (d, *J* = 3.5 Hz, 1H), 5.07 (d, *J* = 8.5 Hz,
1H), 3.23-3.22 (m, 1H), 3.23, 3.10 (ABq, *J* = 20.5 Hz, 2H), 2.96-2.86 (m, 1H),
2.56-2.47 (m, 1H), 2.43-2.38 (m, 1H), 2.37 (s, 3H), 2.01 (s, 3H), 1.80-1.74 (m,
1H) ppm

¹³C NMR (125 MHz, CDCl₃)

δ 202.6, 166.5, 164.6, 145.3, 140.7, 139.3, 134.8, 134.7, 132.0, 131.4 (2C), 130.9,
130.4, 129.7 (2C), 128.5 (2C), 127.8 (2C), 121.4, 60.2, 41.5, 40.7, 31.9, 29.3,
25.7, 21.8 ppm

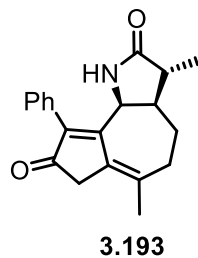
IR (thin film)

2888, 1714, 1674, 1358, 1160 cm⁻¹

HRMS TOF MS ES+ [M+H]: C₂₇H₂₆NO₄S

Calc: 460.1577 Found: 460.1577

TLC *R_f* = 0.23 (50% EtOAc/hexanes) [silica gel, UV, vanillin]



(3aR*,9bS*)-3,6-Dimethyl-9-phenyl-1,3a,4,5,7,9b-hexahydro-2H-azuleno[4,5-b]pyrrole-2,8(3H)-dione (3.193): Prepared according to general procedure I. Allene-yne **3.134** (17 mg, 0.061 mmol), rhodium dicarbonyl chloride dimer (3 mg, 0.0061 mmol), and toluene (6 mL) yielded tricycle **3.193** (14 mg, 77%) as a white solid after purification by column chromatography (gradient elution with 50-100% ethyl acetate in hexanes).

Data for 3.193: (PAJ 7-196, 14 mg, 77%)

¹H NMR (400 MHz, CDCl₃)

δ 7.44-7.38 (m, 3H), 7.17-7.15 (m, 2H), 5.21 (br s, 1H), 4.98 (d, *J* = 7.6 Hz, 1H), 3.19, 3.12 (ABq, *J* = 20.8 Hz, 2H), 2.59-2.46 (m, 2H), 2.35-2.24 (m, 2H), 2.09-2.02 (m, 1H), 1.90 (s, 3H), 1.86-1.81 (m, 1H), 1.22 (d, *J* = 7.2 Hz, 3H) ppm

¹³C NMR (100 MHz, CDCl₃)

δ 202.5, 179.8, 163.0, 144.7, 140.9, 131.2, 129.5 (2C), 129.0, 128.8 (2C), 128.7, 55.3, 45.6, 42.4, 42.1, 32.7, 31.9, 24.2, 15.6 ppm

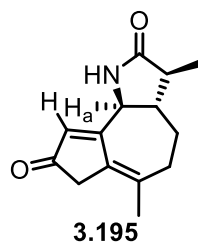
IR (thin film)

3374, 2902, 1673, 1431 cm⁻¹

HRMS TOF MS ES+ [M+H]: C₂₀H₂₂NO₂

Calc: 308.1645 Found: 308.1649

TLC *R_f* = 0.15 (75% EtOAc/hexanes) [silica gel, UV, vanillin]



(3aS*,9bS*)-3,6-Dimethyl-1,3a,4,5,7,9b-hexahydro-2H-azuleno[4,5-b]pyrrole-2,8(3H)-dione

(3.195): Prepared according to general procedure H. Allene-yne **3.194** (12 mg, 0.059 mmol, 9:1 ratio of diastereomers), rhodium dicarbonyl chloride dimer (2 mg, 0.005 mmol), and toluene (5 mL) provided tricycle **3.195** (11 mg, 78%) as a white solid after column chromatography (gradient elution with 25-100% ethyl acetate in hexanes). The ratio of diastereomers was determined to be 7:1 based on integration of the resonances for H_a which appeared as doublets at 4.56 (minor) and 4.51 (major), and the major diastereomer is depicted in **3.195**.

Data for 3.195: (PAJ 8-76, 11 mg, 78%)

¹H NMR (500 MHz, CDCl₃)

δ 7.47 (br s, 1H)*, 7.36 (br s, 1H), 6.10 (s, 1H)*, 6.07 (s, 1H), 4.56 (d, *J* = 10.5 Hz, 1H)*, 4.51 (d, *J* = 10.0 Hz, 1H), 3.00 (s, 2H), 2.76-2.70 (m, 1H), 2.31-2.18 (m, 3H), 1.91 (s, 3H), 1.95-1.87 (m, 1H), 1.77-1.70 (m, 1H), 1.20 (d, *J* = 7.0 Hz, 3H) ppm

*Minor diastereomer where distinguishable

¹³C NMR (126 MHz, CDCl₃)

δ 204.0, 179.5, 173.3, 137.5, 131.2, 126.6, 57.1*, 56.6, 47.3, 45.0, 42.0*, 41.5*, 41.4, 33.3*, 32.7, 28.1, 24.8, 23.7*, 13.8, 12.0* ppm

IR (thin film)

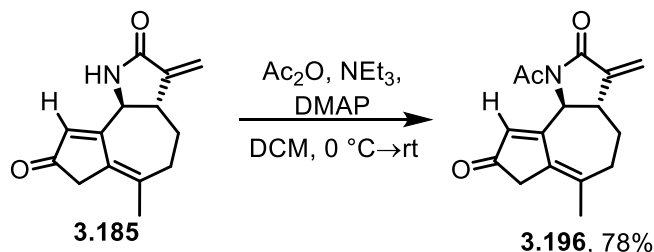
3196, 2893, 1680, 1553, 1438, 1231, 1156 cm⁻¹

HRMS TOF MS ES⁺ [M+H]⁺: C₁₄H₁₈NO₂

Calc: 232.1259 Found: 232.1339

TLC $R_f = 0.11$ (100% EtOAc) [silica gel, UV, *p*-anisaldehyde]

General Procedure J: Acetylation of Lactam Nitrogen



(3a*S**,9b*S**)-1-Acetyl-6-methyl-3-methylene-1,3a,4,5,7,9b-hexahydro-2H-azuleno[4,5-

b]pyrrole-2,8(3H)-dione (3.196): A flame-dried test tube equipped with a stir bar, septum, and nitrogen inlet needle was charged with tricyclic **3.185** (8 mg, 0.03 mmol) dissolved in DCM (0.4 mL). Dimethylaminopyridine (1 mg, 0.008 mmol) was added and the solution was cooled to $0\text{ }^\circ\text{C}$. Triethylamine (0.05 mL, 0.3 mmol) was added dropwise via syringe followed by dropwise addition of acetic anhydride (0.02 mL, 0.2 mmol) via syringe. The reaction was allowed to warm to rt with stirring for 2 h, and TLC showed consumption of starting material. The reaction was diluted with DCM (10 mL) and transferred to a separatory funnel. The organic layer was washed with saturated ammonium chloride (5 mL), brine (5 mL), dried over magnesium sulfate, gravity filtered, concentrated by rotary evaporation, and purified by silica gel flash column chromatography (gradient elution with 50-75% ethyl acetate in hexanes) to provide *N*-acetyl lactam **3.196** (7 mg, 78%) as a white, sticky solid.

Data for 3.196: (PAJ 8-68, 7 mg, 78%)

^1H NMR (400 MHz, CDCl_3)

δ 6.27 (d, $J = 3.6$ Hz, 1H), 5.63 (s, 1H), 5.49 (d, $J = 3.6$ Hz, 1H), 5.03 (d, $J = 9.2$ Hz, 1H), 3.02, 2.94 (ABq, $J = 20.8$ Hz, 2H), 2.89-2.75 (m, 2H), 2.65 (s, 3H), 2.56-2.41 (m, 1H), 2.37-2.31 (m, 1H), 1.94 (s, 3H), 1.87-1.79 (m, 1H) ppm

^{13}C NMR (100 MHz, CDCl_3)

δ 203.6, 172.4, 171.9, 167.6, 142.4, 136.1, 131.8, 126.9, 120.3, 57.8, 41.0, 39.6, 31.2, 27.7, 25.8, 24.9 ppm

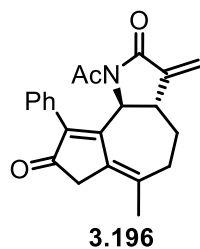
IR (thin film)

2890, 1710, 1653, 1555, 1351, 1299, 1145 cm^{-1}

HRMS TOF MS ES+ $[\text{M}+\text{H}]$: $\text{C}_{16}\text{H}_{18}\text{NO}_3$

Calc: 272.1281 Found: 272.1277

TLC $R_f = 0.57$ (100% EtOAc) [silica gel, UV, *p*-anisaldehyde]



(3aS*,9bS*)-1-Acetyl-6-methyl-3-methylene-9-phenyl-1,3a,4,5,7,9b-hexahydro-2H-azuleno[4,5-b]pyrrole-2,8(3H)-dione (3.196): Prepared according to general procedure J, except that the reaction was not complete after 5 h, so it was stirred for 20 h at rt. Tricycle **3.116** (9 mg, 0.03 mmol), dimethylaminopyridine (1 mg, 0.008 mmol), triethylamine (0.04 mL, 0.3 mmol), acetic anhydride (0.02 mL, 0.2 mmol), and DCM (0.2 mL) provided *N*-acetyl lactam **3.196** (6 mg, 60%) as a pale yellow solid after column chromatography (gradient elution with 15-50% ethyl acetate in hexanes).

Data for 3.196: (PAJ 7-124, 6 mg, 60%)

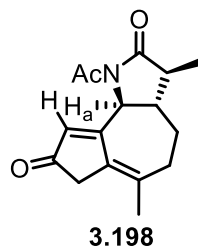
¹H NMR (500 MHz, CDCl₃)
δ 7.35-7.29 (m, 3H), 7.04-6.49 (app br s, 2H), 6.29 (d, *J* = 3.2 Hz, 1H), 5.54 (d, *J* = 3.2 Hz, 1H), 5.16 (d, *J* = 8.5 Hz, 1H), 3.17, 3.06 (ABq, *J* = 21.0 Hz, 2H), 3.12-3.10 (m, 1H), 2.99-2.91 (m, 1H), 2.59-2.51 (m, 1H), 2.44-2.39 (m, 1H), 2.00 (s, 3H), 1.91-1.88 (m, 1H), 1.59 (s, 3H) ppm

¹³C NMR (126 MHz, CDCl₃)
δ 202.7, 171.8, 166.4, 164.5, 142.8, 138.3, 135.8, 131.2, 131.0 (2C), 130.6, 127.8 (2C), 120.6, 57.4, 40.5, 39.7, 31.8, 29.7, 28.6, 25.7, 23.9 ppm

IR (thin film)
3390, 2892, 1689, 1355, 1273, 1164 cm⁻¹

HRMS TOF MS ES+ [M+H]: C₂₂H₂₂NO₃
Calc: 348.1521 Found: 348.1518

TLC *R_f* = 0.31 (50% EtOAc/hexanes) [silica gel, UV, KMnO₄]



(3aS*,9bS*)-1-Acetyl-3,6-dimethyl-1,3a,4,5,7,9b-hexahydro-2H-azuleno[4,5-b]pyrrole-2,8(3H)-dione (3.198): Prepared according to general procedure J; TLC showed consumption of the starting material after 6.5 h. Tricycle **3.195** (11 mg, 0.05 mmol, 9:1 ratio of diastereomers), dimethylaminopyridine (1 mg, 0.008 mmol), triethylamine (0.07 mL, 0.5 mmol), acetic anhydride (0.02 mL), and DCM (0.5 mL) provided *N*-acetyl lactam **3.198** (6 mg, 46%) as a white solid after column chromatography (gradient elution with 25-75% ethyl acetate in hexanes) and

as a 4.75:1 mixture of diastereomers based on integration of the resonances corresponding to H_a appearing as doublets at 5.08 (minor) and 5.02 (major)

Data for 3.198: (PAJ 8-78, 6 mg, 46%)

¹H NMR (500 MHz, CDCl₃)

δ 5.59 (s, 1H), 5.08 (d, *J* = 5.5 Hz, 1H)*, 5.02 (d, *J* = 10.5 Hz, 1H), 3.01, 2.94 (ABq, *J* = 21.0 Hz, 2H), 2.87-2.81 (m, 1H), 2.57 (s, 3H), 2.41-2.26 (m, 3H), 1.93 (s, 3H), 1.87-1.79 (m, 1H), 1.71-1.65 (m, 1H), 1.24 (d, *J* = 7.0 Hz, 3H) ppm

¹³C NMR (126 MHz, CDCl₃)

δ 203.7, 177.1, 172.5, 171.7, 136.5, 131.7, 127.1, 66.0, 58.3, 45.7, 42.3*, 41.0, 31.6, 29.0, 25.4, 24.7, 15.4*, 13.7 ppm

* Discernible signals for 1 of 2 diastereomers

IR (thin film)

2893, 1721, 1681, 1661, 1544, 1353, 1254 cm⁻¹

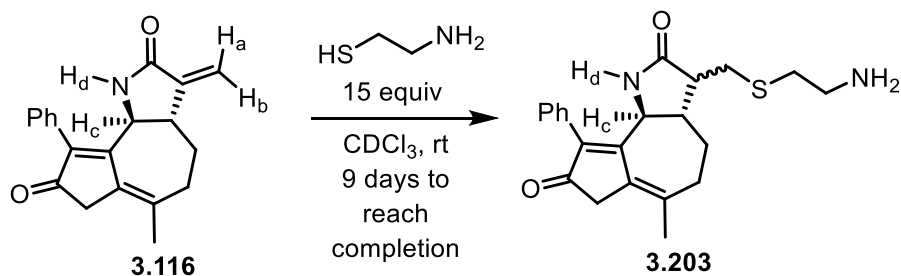
HRMS TOF MS ES+ [M+H]: C₁₆H₂₀NO₃

Calc: 274.1438 Found: 274.1438

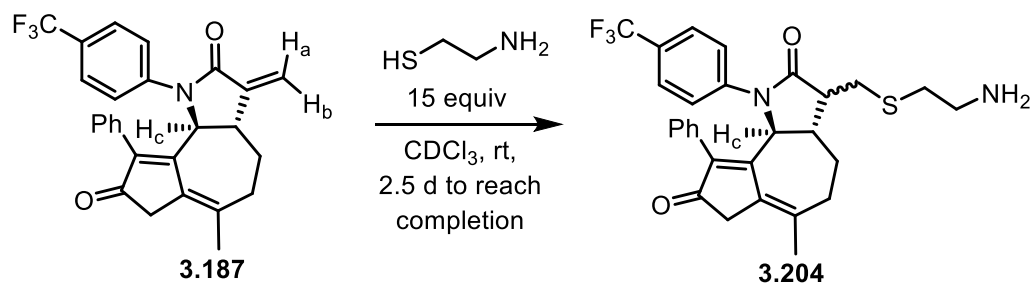
TLC *R_f* = 0.46 (75% EtOAc/hexanes) [silica gel, UV, vanillin]

General Procedure K: Monitoring the Reaction of α-Methylene-γ-Lactams with

Cysteamine by ¹H NMR

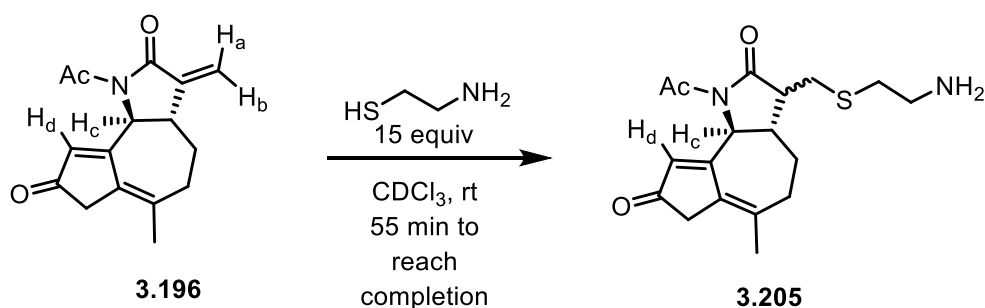


Tricyclic lactam **3.116** (8 mg, 0.03 mmol) was dissolved in chloroform-*d* (0.5 mL) and transferred to an NMR tube. Cysteamine (30 mg, 0.4 mmol) was dissolved in chloroform-*d* separately, transferred to the NMR tube containing lactam **3.116** via pipet and the NMR tube was capped and shaken vigorously by hand for 2 min. The ^1H NMR was monitored for the disappearance of the methylene hydrogen resonances (H_a and H_b) which appeared as doublets at 5.99 ppm and 5.28 ppm. Integration of the methylene hydrogen resonances showed about 5% remaining starting material after 8 days and this remained the same at 9 days. Product formation was first observed after 24 h at rt where new resonances for the amide hydrogen (H_d , 5.51 and 5.44) and the hydrogen on the carbon next to the nitrogen (H_c , 5.01 and 4.75) were detected indicating the formation of 2 diastereomers in about a 2:1 ratio. The products were unable to be isolated for structural confirmation.

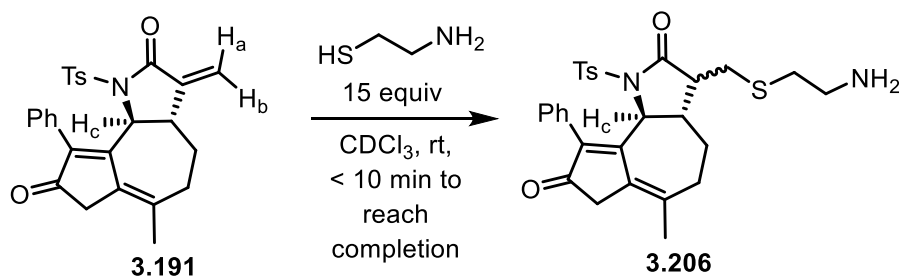


The reaction was monitored according to general procedure K. Tricyclic lactam **3.187** (2 mg, 0.004 mmol), cysteamine (5 mg, 0.07 mmol), and chloroform-*d* (0.7 mL) were used. Complete disappearance of the α -methylene resonances at 6.29 and 5.53 was observed after about 2.5 d. Minimal product formation was detected after 21 h, and it was observed that cysteamine had mostly oxidized to the disulfide, thus more cysteamine was added at this time point (10 mg, 0.15 mmol). H_c appeared at the same chemical shift for both the starting material **3.187** and the product **3.204**. Product formation was initially observed 2 h after this additional

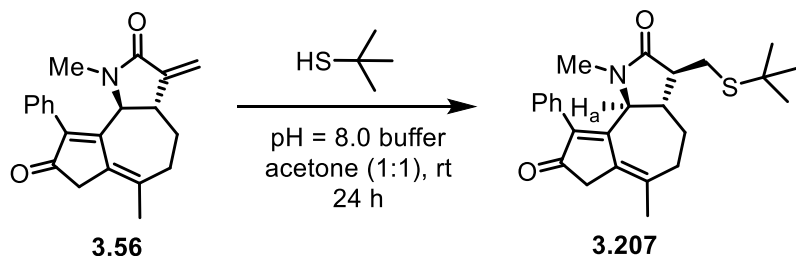
cysteamine was added (23 h total reaction time) by a new aromatic peak shifted upfield relative to the starting material at 6.89 ppm. The area of this peak increased over time as the area of the α -methylene resonances decreased. 32 h after additional cysteamine was added (53 h total), the α -methylene resonances decreased. 32 h after additional cysteamine was added (53 h total), the α -methylene resonances were nearly gone and further measurements became difficult due to the large amount of cysteamine and disulfide present in the reaction, so complete adduct formation was estimated as about 2.5 days.



This reaction was monitored according to general procedure K. Tricyclic lactam **3.196** (2 mg, 0.006 mmol), cysteamine (7 mg, 0.09 mmol), and chloroform-*d* (1 mL) were used. Complete disappearance of the α -methylene resonances at 6.26 and 5.48 was observed after 55 min. Significant product formation (more than 50% SM reacted) was observed in less than 10 min as two new peaks, corresponding to two diastereomers, for H_c (5.18 and 5.03) and H_d (5.56 and 5.57) were observed as a 2:1 ratio of diastereomers and a 2.3:1 ratio of products to starting material.



This reaction was monitored according to general procedure K. Tricyclic lactam **191** (2 mg, 0.004 mmol), cysteamine (5 mg, 0.07 mmol), and chloroform-*d* (0.7 mL) were used. Complete disappearance of the α -methylene resonances at 6.17 and 5.44 was observed in less than 10 min. Only a single resonance was observed for H_c, suggesting that a single diastereomer was formed.



(3aS*,9bS*)-3-((*tert*-Butylthio)methyl)-1,6-dimethyl-9-phenyl-1,3a,4,5,7,9b-hexahydro-2H-azuleno[4,5-b]pyrrole-2,8(3H)-dione (3.207): A 2-mL vial equipped with a magnetic stir bar was charged with tricyclic lactam **3.56** (10 mg, 0.03 mmol), *tert*-butyl thiol (0.02 mL, 0.2 mmol), acetone (0.5 mL), and phosphate buffered saline (pH = 8.0, 0.5 mL). The vial was capped with a septum and allowed to stir at rt for 24 h. Only starting material was detected by TLC analysis, so the pH was raised to 12 (pH paper) by addition of potassium hydroxide (2 mg, 0.04 mmol) and the starting material was consumed within 30 min as observed by TLC. The reaction was then poured into a separatory funnel containing deionized water (3 mL) and DCM (10 mL). The layers were separated. The aqueous layer was extracted with DCM (2 x 5 mL). The organic layers were combined, washed with brine (5 mL), dried over magnesium sulfate, filtered, and concentrated by rotary evaporation and purified by flash column chromatography on silica gel (gradient elution with 25-50% ethyl acetate in hexanes) to provide thiol adduct **3.207** (3 mg, 23%, 1.6:1 diastereomeric ratio) as a clear oil. Diastereomeric ratio determined by integration of

resonances corresponding to H_a at 4.66 (*J* = 10.0 Hz) for the minor diastereomer and 4.50 (*J* = 8.5 Hz) for the major diastereomer.

Data for 3.207: (PAJ 8-130, 3 mg, 23%, 1.6:1 dr)

¹H NMR (500 MHz, CDCl₃)

δ 7.33-7.27 (m, 3H), 7.23-7.21 (m, 2H), 4.66 (d, *J* = 10.0 Hz, 1H)*, 4.50 (d, *J* = 8.5 Hz, 1H), 3.17-3.07 (m, 3H), 2.94-2.79 (m, 2H), 2.75-2.69 (m, 1H), 2.51-2.41 (m, 2H), 2.37-2.30 (m, 2H), 1.98 (s, 3H), 1.90 (s, 3H), 1.37 (s, 9H) ppm

¹³C NMR (100 MHz, CDCl₃)

δ 202.92, 202.86*, 175.3, 166.1, 138.5, 137.7, 137.1, 130.8, 130.73*, 130.67 (2C), 128.5, 128.4*, 127.7 (2C), 127.6*, 62.7, 61.7*, 50.3, 44.2, 43.2*, 42.7, 42.6*, 40.6, 34.3, 33.4*, 32.6, 31.1, 31.0*, 30.8, 30.4*, 30.32, 30.30*, 29.4, 25.7, 25.6*, 21.0 ppm

* Discernible signals for 1 of 2 diastereomers

IR (thin film)

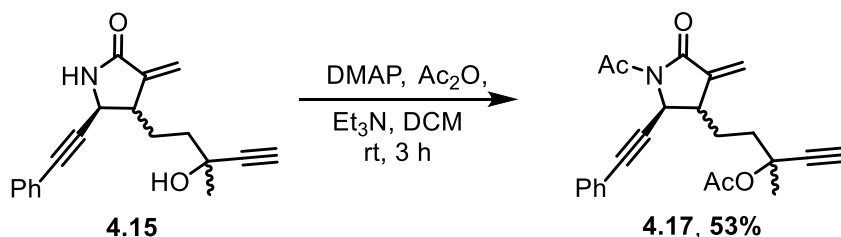
3407, 2927, 1686, 1445, 1079 cm⁻¹

HRMS TOF MS ES+ [M+H]: C₂₅H₃₂NO₂S

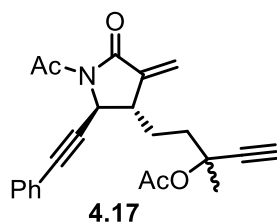
Calc: 410.2148 Found: 410.2144

TLC *R_f* = 0.32 (50% EtOAc/hexanes) [silica gel, UV, vanillin]

General Procedure K: Acetylation of Nitrogen and Oxygen



A flame dried, 5 mL round bottom flask under a nitrogen atmosphere equipped with a magnetic stir bar, a septum, and nitrogen inlet needle was charged with alcohol **4.15** (92 mg, 0.31 mmol, 4:1 trans:cis), dichloromethane (1.6 mL), and 4-dimethylaminopyridine (4 mg, 0.03 mmol), then cooled to 0 °C in an ice bath. Triethylamine (0.44 mL, 3.1 mmol) was added dropwise via syringe, followed by dropwise addition of acetic anhydride (0.15 mL, 1.6 mmol). The ice bath was removed and the reaction was allowed to warm to rt over 3 h. The reaction was transferred to a separatory funnel, diluted with dichloromethane (25 mL), washed sequentially with saturated aqueous ammonium chloride (10 mL) and brine (10 mL), dried over magnesium sulfate, filtered, concentrated by rotary evaporation, and purified by silica gel flash column chromatography eluting with 10-20% ethyl acetate in hexanes to yield the trans bis acetylated lactam **xx** (62 mg, 53%) as a clear oil and the cis bis acetylated lactam **4.17** (9 mg, 8%) as a clear oil.



5-((2S*,3S*)-1-Acetyl-4-methylene-5-oxo-2-(phenylethynyl)pyrrolidin-3-yl)-3-methylpent-1-yn-3-yl acetate (4.17):

Data for 4.17: (PAJ 7-64, 77 mg, 66% total, 7:1 trans:cis)

¹H NMR (400 MHz, CDCl₃)

δ 7.39-7.38 (m, 2H), 7.30-7.27 (m, 3H), 6.38 (d, *J* = 2.0 Hz, 1H), 5.66 (d, *J* = 2.0 Hz, 1H), 4.87 (d, *J* = 2.0 Hz, 1H), 3.11-3.08 (m, 1H), 2.62 (s, 3H), 2.58 (s, 0.5H), 2.57* (s, 0.5H), 2.11-2.06 (m, 1H), 2.03 (s, 3H), 1.91-1.76 (m, 3H), 1.69 (s, 3H)

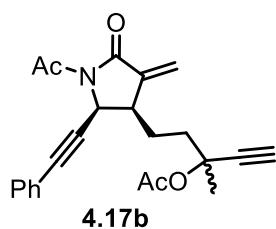
ppm

¹³C NMR (100 MHz, CDCl₃)
δ 171.0, 169.31, 169.29*, 166.3, 142.55, 142.49*, 132.0 (2C), 128.8, 128.4 (2C),
122.91, 122.88*, 122.2, 86.84, 86.81*, 84.1, 83.2, 83.1*, 74.24, 74.22*, 74.18,
51.2, 51.1*, 44.11, 44.06*, 38.4, 38.3*, 29.9, 29.8*, 26.67, 26.66*, 25.5, 22.0
ppm

IR (thin film)
3268, 2938, 1738, 1705, 1652, 1371, 1303, 1243, 1174, 1017 cm⁻¹

HRMS TOF MS ES+ [M+H]: C₂₃H₂₄NO₄
Calc: 378.1700 Found: 378.1684

TLC R_f = 0.29 (25% EtOAc/hexanes) [silica gel, UV, KMnO₄]



5-((2S*,3R*)-1-Acetyl-4-methylene-5-oxo-2-(phenylethynyl)pyrrolidin-3-yl)-3-methylpent-1-yn-3-yl acetate (4.17b):

Data for 4.17b: (PAJ 7-64, 77 mg, 66%, 7:1 trans:cis)

¹H NMR (400 MHz, CDCl₃)
δ 7.40-7.37 (m, 2H), 7.30-7.26 (m, 3H), 6.33 (d, J = 3.0 Hz, 1H), 5.59 (app t, J =
2.3 Hz, 1H), 5.32 (d, J = 8.0 Hz, 1H), 2.98-2.93 (m, 1H), 2.61 (s, 3H), 2.51 (s,
0.5H), 2.45* (0.5H), 2.26-2.06 (m, 4H), 2.06 (s (1.5H), 1.89* (s, 1.5H), 1.72 (s,
1.5H), 1.70* (s, 1.5H) ppm

¹³C NMR (100 MHz, CDCl₃)

δ 170.6, 169.38, 169.34*, 166.9, 142.83, 142.81*, 132.1 (2C), 128.9, 128.3 (2C), 122.2, 122.1*, 120.6, 85.97, 85.96*, 83.5, 83.31*, 83.29, 83.1*, 74.6, 74.3*, 74.2, 73.9*, 50.00, 49.98*, 40.8, 40.7*, 39.0, 38.6*, 29.8, 26.8, 26.7*, 25.4*, 23.5, 23.2*, 22.0, 21.8* ppm

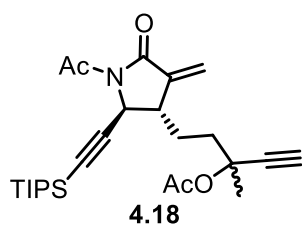
IR (thin film)

2932, 1715, 1685, 1447 cm^{-1}

HRMS TOF MS ES+ [M+H]: $\text{C}_{23}\text{H}_{24}\text{NO}_4$

Calc: 378.1700 Found: 378.1684

TLC R_f = 0.25 (25% EtOAc/hexanes) [silica gel, UV, KMnO_4]



5-((2S*,3S*)-1-Acetyl-4-methylene-5-oxo-2-((triisopropylsilyl)ethynyl)pyrrolidin-3-yl)-3-methylpent-1-yn-3-yl acetate (4.18): Prepared according to general procedure K; lactam **4.16** (85 mg, 0.23 mmol, 4:1 trans:cis), dichloromethane (1.2 mL), 4-dimethylaminopyridine (3 mg, 0.02 mmol), triethylamine (0.32 mL, 2.3 mmol), and acetic anhydride (0.11 mL, 1.1 mmol) provided bis acetylated lactam **4.18** (70 mg, 67%, 4:1 trans:cis) as clear oils after silica gel flash column chromatography.

Data for 4.18: (PAJ 7-34, 70 mg,, 67%, 4:1 trans:cis, 1:1 mixture of diastereomers)

^1H NMR (300 MHz, CDCl_3)

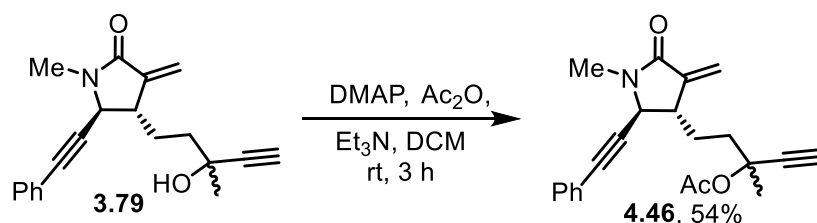
δ 6.31 (d, J = 3.0 Hz, 1H), 5.59 (d, J = 1.8 Hz, 1H), 4.60-4.59 (m, 1H), 2.98-2.92 (m, 1H), 2.55 (s, 3H), 2.54 (s, 1H), 2.06-2.01 (m, 1H), 2.00 (s, 3H), 1.98-1.71 (m, 3H), 1.69 (s, 3H), 1.01 (s, 21H) ppm

¹³C NMR (125 MHz, CDCl₃)
δ 170.7, 169.3, 166.3, 142.5, 122.4, 105.2, 85.7, 83.2, 74.2, 51.4, 51.3, 44.3, 38.5,
29.5, 26.6, 25.4, 21.9, 18.6 (6C), 11.1 (3C) ppm

IR (thin film)
3269, 2943, 2866, 2175, 1739, 1709, 1463, 1371, 1350, 1294, 1243, 1174 cm⁻¹

HRMS TOF MS ES+ [M+H]: C₂₆H₄₀NO₄Si
Calc: 458.2727 Found: 458.2728

TLC R_f = 0.67 (25% EtOAc/hexanes) [silica gel, UV, *p*-anisaldehyde]



3-Methyl-5-((2S*,3S*)-1-methyl-4-methylene-5-oxo-2-(phenylethynyl)pyrrolidin-3-yl)pent-1-yn-3-yl acetate (4.46): General procedure K was followed. Lactam **3.79** (86 mg, 0.27 mmol), triethylamine (0.37 mL, 2.7 mmol), dimethylaminopyridine (4 mg, 0.03 mmol), acetic anhydride (0.12 mL, 1.3 mmol), and DCM (1.3 mL) yielded lactam bis acetylated lactam **4.46** as a clear oil (50 mg, 54%)

Data for 4.46: (PAJ 6-206, 50 mg, 54%)

¹H NMR (400 MHz, CDCl₃)
δ 7.42-7.40 (m, 2H), 7.34-7.29 (m, 3H), 6.13 (d, *J* = 2.4 Hz, 1H), 5.37 (d, *J* = 2.4 Hz, 1H), 4.11 (d, *J* = 4 Hz, 1H), 3.08-3.05 (m, 1H), 3.03 (s, 3H), 2.58 (s, 1H), 2.16-2.07 (m, 1H), 2.03 (s, 3H), 1.98-1.81 (m, 3H), 1.70 (s, 3H)

¹³C NMR (100 MHz, CDCl₃)

δ 169.4, 167.1, 142.0, 131.9 (2C), 129.0, 128.5 (2C), 122.1, 116.6, 86.0, 83.4,
74.5, 74.0, 55.3, 44.5, 38.2, 28.6 (2C), 28.5, 26.7, 22.01

IR (thin film)

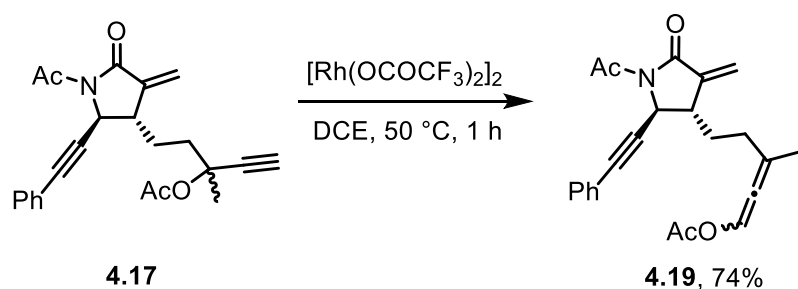
3292, 2937, 2243, 2120, 1742, 1697, 1661, 1427, 1243, 1173, 1082 cm^{-1}

HRMS TOF MS ES+ [M+H]: $\text{C}_{22}\text{H}_{24}\text{NO}_3$

Calc: 350.1751 Found: 350.1751

TLC R_f = 0.26 (50% EtOAc/hexanes, [silica gel, UV, KMnO_4])

General Procedure L: Formal [3,3] Sigmatropic Rearrangement of Propargyl Acetates



5-((2S*,3S*)-1-Acetyl-4-methylene-5-oxo-2-(phenylethynyl)pyrrolidin-3-yl)-3-methylpenta-1,2-dienyl acetate (4.19): A flame dried test tube equipped with a magnetic stir bar was charged with rhodium (II) trifluoroacetate dimer (6 mg, 0.008 mmol) in a nitrogen glove box, sealed with a septum, removed, and placed under nitrogen via a needle in a fume hood. Propargyl acetate **4.17** (62 mg, 0.16 mmol) was dissolved in degassed toluene (0.8 mL) then transferred to the tube containing the rhodium (II) trifluoroacetate dimer by syringe. The tube was evacuated and filled with nitrogen (3x), the nitrogen inlet needle was removed, and the solution was heated to 60 °C (sealed tube) in a prewarmed oil bath for 1 h. The solution was removed from the heat and allowed to cool to rt, then applied directly to a silica gel column and purified by flash column chromatography eluting with 5-15% ethyl acetate in hexanes to yield allenyl acetate **4.19** as a clear oil (46 mg, 74%).

Data for 4.19: (PAJ 7-70, 46 mg, 74%)

¹H NMR (400 MHz, CDCl₃)

δ 7.39-7.37 (m, 2H), 7.35-7.33 (m, 1H), 7.31-7.26 (m, 3H), 6.36 (app t, *J* = 2 Hz, 1H), 5.64 (d, *J* = 7.2 Hz, 0.5H), 5.63*(d, *J* = 7.2 Hz, 0.5H), 4.85 (s, 1H), 3.12-3.09 (m, 1H), 2.616 (s, 3H), 2.615* (s, 3H), 2.23-2.18 (m, 2H), 2.14 (s, 1.5H), 2.12* (s, 1.5H), 1.859 (s, 1.5H), 1.855* (s, 1.5H), 1.80 (m, 1H), 1.73-1.67 (m, 1H) ppm

¹³C NMR (125 MHz, CDCl₃)

δ 189.9, 189.8*, 171.09, 171.07*, 168.83, 168.79*, 166.4, 142.7, 142.6*, 132.0 (2C), 128.8, 128.4 (2C), 122.9, 122.8*, 122.3, 114.7, 114.6*, 110.8, 110.7*, 86.92, 86.90*, 84.1, 84.0*, 51.25, 51.18*, 43.72, 43.69*, 32.84, 32.78*, 31.6, 31.5*, 25.5, 21.0, 20.99, 20.93* ppm

*Discernible signals for one of two diastereomers

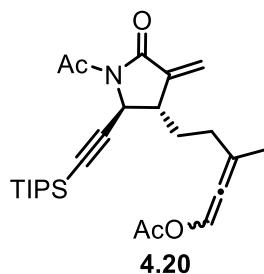
IR (thin film)

2922, 1741, 1491, 1445, 1372, 1270, 1216, 1110, 1042 cm⁻¹

HRMS TOF MS ES+ [M+H]: C₂₃H₂₄NO₄

Calc: 378.1700 Found: 378.1707

TLC *R_f* = 0.65 (40% EtOAc/hexanes, [silica gel, UV, *p*-anisaldehyde])



5-((2S*,3S*)-1-Acetyl-4-methylene-5-oxo-2-((triisopropylsilyl)ethynyl)pyrrolidin-3-yl)-3-methylpenta-1,2-dienyl acetate (4.20): General procedure L was followed. Rhodium (II) trifluoroacetate dimer (3 mg, 0.005 mmol), propargyl acetate **4.18** (43 mg, 0.094 mmol), and toluene (0.5 mL) were used. Purification by silica gel flash chromatography eluting with 5-10% ethyl acetate in hexanes yielded allenyl acetate **4.20** (42 mg, 97%) as a clear oil.

Data for 4.20: (PAJ 7-38, 42 mg, 97%)

¹H NMR (500 MHz, CDCl₃)

δ 7.32-7.31 (m, 1H), 6.31 (d, *J* = 2 Hz, 1H), 6.30*(d, *J* = 2 Hz, 1H), 5.59 (d, *J* = 1.5 Hz, 1H), 5.57*(d, *J* = 2 Hz, 1H), 4.61 (d, *J* = 1 Hz, 1H), 3.01-2.96 (m, 1H), 2.56 (s, 3H), 2.21-2.12 (m, 2H), 2.124 (s, 3H), 2.116* (s, 3H), 1.833 (s, 1.5H), 1.829* (s, 1.5H), 1.73-1.62 (m, 2H), 1.0 (s, 21H)

¹³C NMR (125 MHz, CDCl₃)

δ 189.7, 189.6*, 170.73, 170.72*, 168.81, 168.76*, 166.4, 142.7, 142.6*, 122.5, 122.4*, 114.8, 114.6*, 110.8, 110.7*, 105.3, 85.6, 85.5*, 51.32, 51.27*, 44.1, 43.9*, 32.7, 32.6*, 31.54, 31.51*, 25.3, 21.03, 21.01*, 20.9, 18.6 (6C), 11.1 (3C)

*Discernible signals for one of two diastereomers

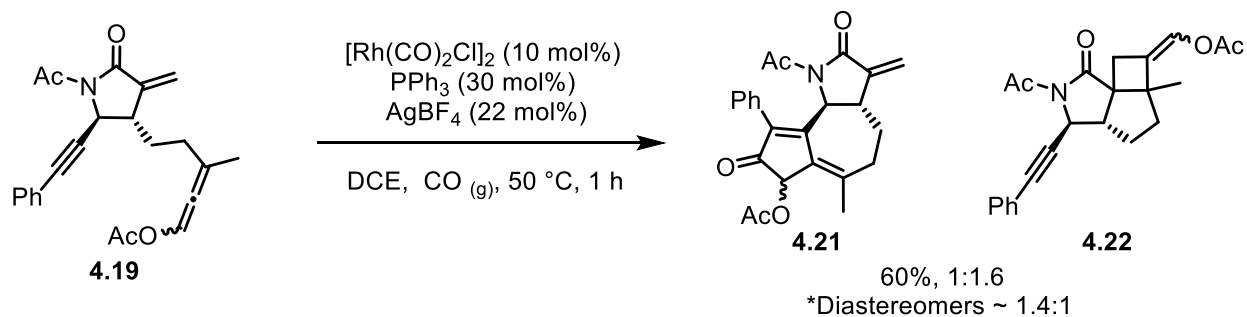
IR (thin film)

3266, 2931, 1715, 1447 cm⁻¹

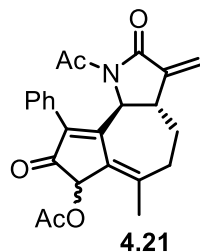
HRMS TOF MS ES+ [M+H]: C₂₆H₄₀NO₄Si

Calc: 458.2721 Found: 458.2742

TLC *R_f* = 0.52 (25% EtOAc/hexanes, [silica gel, UV, *p*-anisaldehyde])



A flame-dried test tube was charged with rhodium biscarbonyl chloride dimer (8 mg, 0.02 mmol) and dichloroethane (0.7 mL). Triphenylphosphine (17 mg, 0.06 mmol) was dissolved in dichloroethane (0.7 mL) and added to the rhodium and this was stirred 15 min under a nitrogen atmosphere. Silver tetrafluoroborate (9 mg, 0.05 mmol) was weighed into test tube in glove box, sealed with a septum, removed, and dissolved in dichloroethane (0.6 mL). The silver tetrafluoroborate solution was added dropwise over 5 min to the rhodium and triphenylphosphine solution. The stir plate was turned off and the precipitate was allowed to settle to the bottom of the test tube for 1 h, then the rhodium catalyst solution (1.1 mL, 0.01M in rhodium) was carefully removed via syringe, leaving the precipitate in the bottom of the test tube. This solution was transferred to a dry 5 mL round bottom flask under an atmosphere of 10% carbon monoxide in argon via syringe. A solution of allenyl acetate **4.19** (40 mg, 0.11 mmol) in dichloroethane (1.3 mL) was added via syringe to the rhodium catalyst solution, then this mixture was placed in a preheated oil bath at 50 °C and stirred for 2 h. The crude reaction mixture was filtered through a plug of silica gel eluting with 50% ethyl acetate in hexanes, concentrated, then purified by silica gel flash column chromatography (gradient elution with 15-45% ethyl acetate in hexanes) to provide [2 + 2] cycloaddition product **4.22** (15 mg, 34%) and Pauson-Khand product **4.21** (11 mg, 25%) each as pale yellow oils.



(3aS*,9bS*)-1-Acetyl-6-methyl-3-methylene-2,8-dioxo-9-phenyl-2,3,3a,4,5,7,8,9b-octahydro-1H-azuleno[4,5-b]pyrrol-7-yl acetate (4.21):

Data for 4.21: (PAJ 6-164, 11 mg, 25%)

¹H NMR (500 MHz, CDCl₃)

δ 7.38-7.31 (m, 3H), 7.01-6.89 (m, 2H), 6.31 (d, *J* = 3.5 Hz, 1H), 6.29* (d, *J* = 3.5 Hz, 1H), 5.82 (s, 1H), 5.59* (s, 1H), 5.56 (d, *J* = 3.5 Hz, 1H), 5.53* (d, *J* = 3.5 Hz, 1H), 5.23 (d, *J* = 8.5 Hz, 1H), 5.11* (d, *J* = 9.0 Hz, 1H), 3.22-3.15 (m, 1H), 3.12-3.17* (m, 1H), 3.06-2.99 (m, 2H), 2.61-2.57* (m, 2H), 2.40 (dt, *J* = 16.0, 5.0 Hz, 2H), 2.19 (s, 3H), 2.10* (s, 3H), 2.02 (s, 3H), 2.00* (s, 3H), 1.93-1.89* (m, 2H), 1.59 (s, 3H), 1.58* (s, 3H) ppm

¹³C NMR (125 MHz, CDCl₃)

δ 198.7, 198.4*, 171.8, 171.6*, 170.0, 169.7*, 166.2, 165.1*, 163.5, 142.6, 142.4*, 140.3, 139.7*, 135.4, 135.2*, 134.93*, 134.88, 134.83*, 131.0, 130.9*, 130.7, 130.42*, 130.38, 130.3*, 130.2, 128.3*, 128.1, 128.0*, 127.96, 127.8*, 121.0, 120.8*, 72.9, 70.4*, 57.4, 57.3*, 39.3, 39.1*, 32.7, 32.1*, 28.9, 28.7*, 25.2, 25.1*, 23.9, 23.8*, 20.8, 20.6* ppm

*Other diastereomer where distinguishable

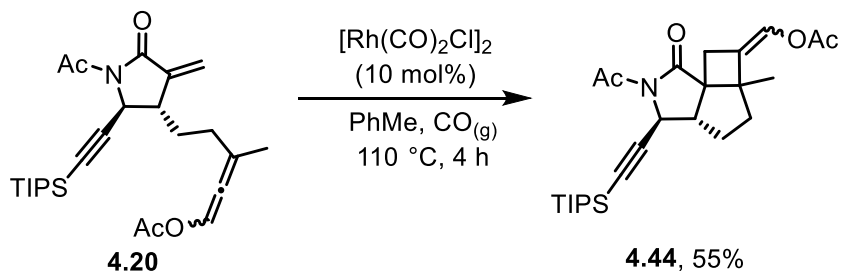
IR (thin film)

2926, 1735, 1709, 1438, 1371, 1281, 1227, 1171, 1119, 1041 cm⁻¹

HRMS TOF MS ES+ [M+H]: C₂₄H₂₄NO₅

Calc: 406.1654 Found: 406.1660

TLC *R_f* = 0.27 (50% EtOAc/hexanes) [silica gel, UV, *p*-anisaldehyde]



(Z)-((3*S,3*aS**)-2-Acetyl-5*a*-methyl-1-oxo-3-((triisopropylsilyl)ethynyl)hexahydro-1*H*-cyclobuta[1,5]cyclopenta[1,2-*c*]pyrrol-6(7*H*)-ylidene)methyl acetate (4.44):** A 2-neck, 15-mL, flame-dried round bottom flask equipped with a magnetic stir bar, a septum, and a condenser capped with a septum and attached to a vacuum line with a needle was charged with rhodium bis carbonyl chloride (4 mg, 0.009 mmol) and toluene (6.7 mL). The apparatus was evacuated and filled with CO(g) via a balloon (3x), then lowered into a preheated oil bath set to 110 °C. Allenyl acetate **4.20** (40 mg, 0.087 mmol) was dissolved in toluene (2 mL) and added slowly to the stirring mixture of rhodium bis carbonyl chloride via syringe pump over 1 h (2 mL/h). The reaction was stirred an additional 30 min after addition of the allenyl acetate **4.20** was complete, then an aliquot of the reaction mixture showed completion by ¹HNMR. The solution was allowed to cool to rt, filtered through a plug of silica gel eluting with 75% ethyl acetate in hexanes, then concentrated by rotary evaporation. The concentrated product was purified by silica gel flash column chromatography eluting with 5-75% ethyl acetate in hexanes to yield tricycle **4.44** as a clear oil (25 mg, 55%)

Alternatively, tricycle **4.44** was prepared in a similar yield under thermal conditions by dissolving allenyl acetate **4.20** (25 mg, 0.044 mmol) in toluene (4.4 mL) in a flame dry 10 mL

flask equipped with a reflux condenser and heating to 110 °C in an oil bath for 2.5 h. The solution was purified as described above by filtration through a plug of silica gel, concentration by rotary evaporation, and silica gel flash column chromatography to yield the title compound **4.44** as a clear oil (14 mg, 56%).

Data for 4.44: (PAJ 7-40, 25 mg, 55%) (Thermal conditions, PAJ 7-58, 14 mg, 56%)

¹H NMR (500 MHz, CDCl₃)

δ 7.01 (t, *J* = 3 Hz, 1H), 4.19 (d, *J* = 7.5 Hz, 1H), 3.29 (dd, *J* = 16.7 Hz, 3 Hz, 1H), 2.71 (t, *J* = 6.7 Hz, 1H), 2.50 (s, 3H), 2.43 (dd, *J* = 16.7 Hz, 3 Hz), 2.33-2.22 (m, 1H), 2.13 (s, 3H), 2.03 (dd, *J* = 12.5 Hz, 7.5 Hz, 1H), 1.93 (dd, *J* = 13.5 Hz, 6.5 Hz, 1H), 1.56 (dt, *J* = 13 Hz, 6.5 Hz, 1H), 1.20 (s, 3H), 1.03 (s, 21H) ppm

¹³C NMR (125 MHz, CDCl₃)

δ 174.4, 170.3, 167.9, 129.2, 126.7, 105.4, 85.6, 59.9, 57.2, 51.6, 51.2, 38.5, 30.0, 28.4, 25.5, 21.2, 20.8, 18.7 (6C), 11.2 (3C) ppm

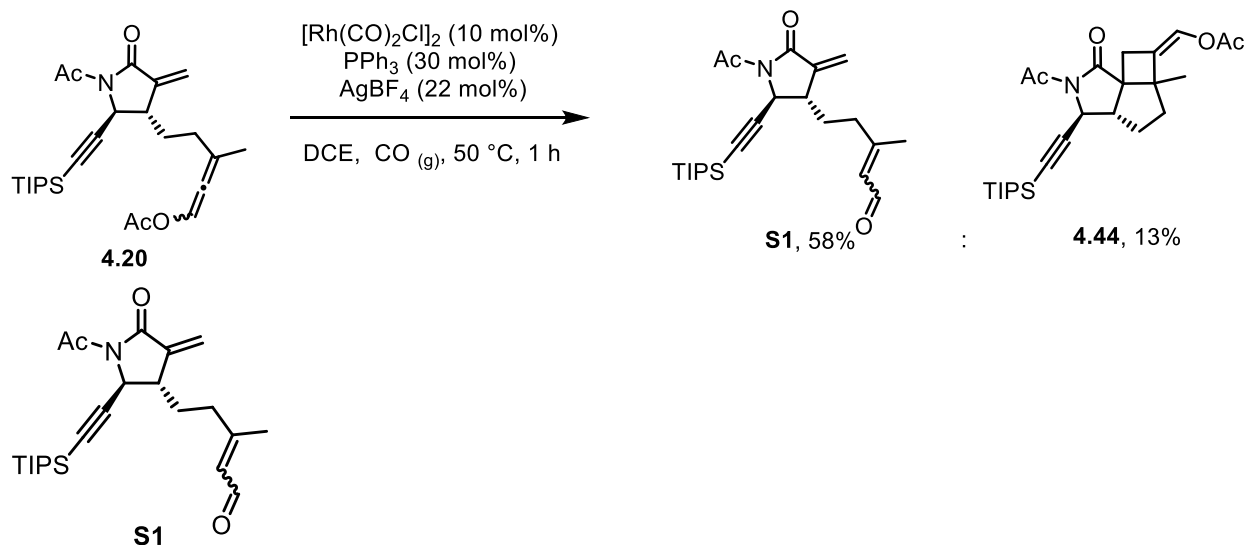
IR (thin film)

2943, 2865, 2176, 1740, 1710, 1463, 1371, 1313, 1300, 1269, 1214, 1096 cm⁻¹

HRMS TOF MS ES+ [M+H]: C₂₄H₂₄NO₅

Calc: 458.2727 Found: 458.2730

TLC *R_f* = 0.47 (50% EtOAc/hexanes) [silica gel, UV, *p*-anisaldehyde]



(E*)-5-((2S*,3S*)-1-Acetyl-4-methylene-5-oxo-2-((triisopropylsilyl)ethynyl)pyrrolidin-3-yl)-3-methylpent-2-enal (S1**):**

Data for **S1**: (PAJ 7-56, 32-34, Major isomer, 14 mg, 39%)

^1H NMR (500 MHz, CDCl_3)

δ 9.98 (d, $J = 8$ Hz, 1H), 6.35 (d, $J = 2$ Hz, 1H), 5.87 (d, $J = 8$ Hz, 1H), 5.61 (d, $J = 1.6$ Hz, 1H), 4.63 (d, $J = 2.4$ Hz, 1H), 2.96 (dt, $J = 7.6$ Hz, 2 Hz, 1H), 2.57 (s, 3H), 2.35-2.30 (m, 1H), 2.17 (d, $J = 1.2$ Hz, 3H), 1.78-1.71 (m, 2H), 1.01 (s, 21H) ppm

^{13}C NMR (125 MHz, CDCl_3)

δ 191.0, 170.7, 166.1, 161.4, 142.4, 127.8, 122.7, 104.9, 86.0, 51.1, 44.1, 37.1, 32.5, 25.3, 18.6, 17.9, 11.1 ppm

IR (thin film)

3406, 2943, 2865, 1736, 1707, 1674, 1463, 1372, 1288, 1160, 1110 cm^{-1}

HRMS TOF MS ES+ [$\text{M}+\text{H}$]: $\text{C}_{24}\text{H}_{24}\text{NO}_5$

Calc: 416.2616 Found: 416.2608

TLC $R_f = 0.27$ (50% EtOAc/hexanes) [silica gel, UV, *p*-anisaldehyde]

Data for S1: (PAJ 7-56, 30-31, Minor isomer, 7 mg, 19%)

$^1\text{H NMR}$ (500 MHz, CDCl_3)

δ 9.91 (d, $J = 7.6$ Hz, 1H), 6.37 (d, $J = 2$ Hz, 1H), 5.92 (d, $J = 7.6$ Hz, 1H), 5.63 (d, $J = 1.6$ Hz, 1H), 4.67 (d, $J = 2$ Hz, 1H), 3.03-2.99 (m, 1H), 2.68 (t, $J = 8.2$ Hz, 2H), 2.58 (s, 3H), 1.98 (d, $J = 1.2$ Hz, 3H), 1.85-1.68 (m, 2H), 1.01 (s, 21H) ppm

$^{13}\text{C NMR}$ (125 MHz, CDCl_3)

δ 190.0, 170.6, 166.0, 161.7, 142.3, 128.7, 122.8, 104.8, 86.1, 51.1, 44.6, 34.1, 29.8, 25.4, 25.2, 18.6 (6C), 11.1 (3C) ppm

IR (thin film)

2943, 2865, 2177, 1735, 1707, 1673, 1463, 1349, 1290 cm^{-1}

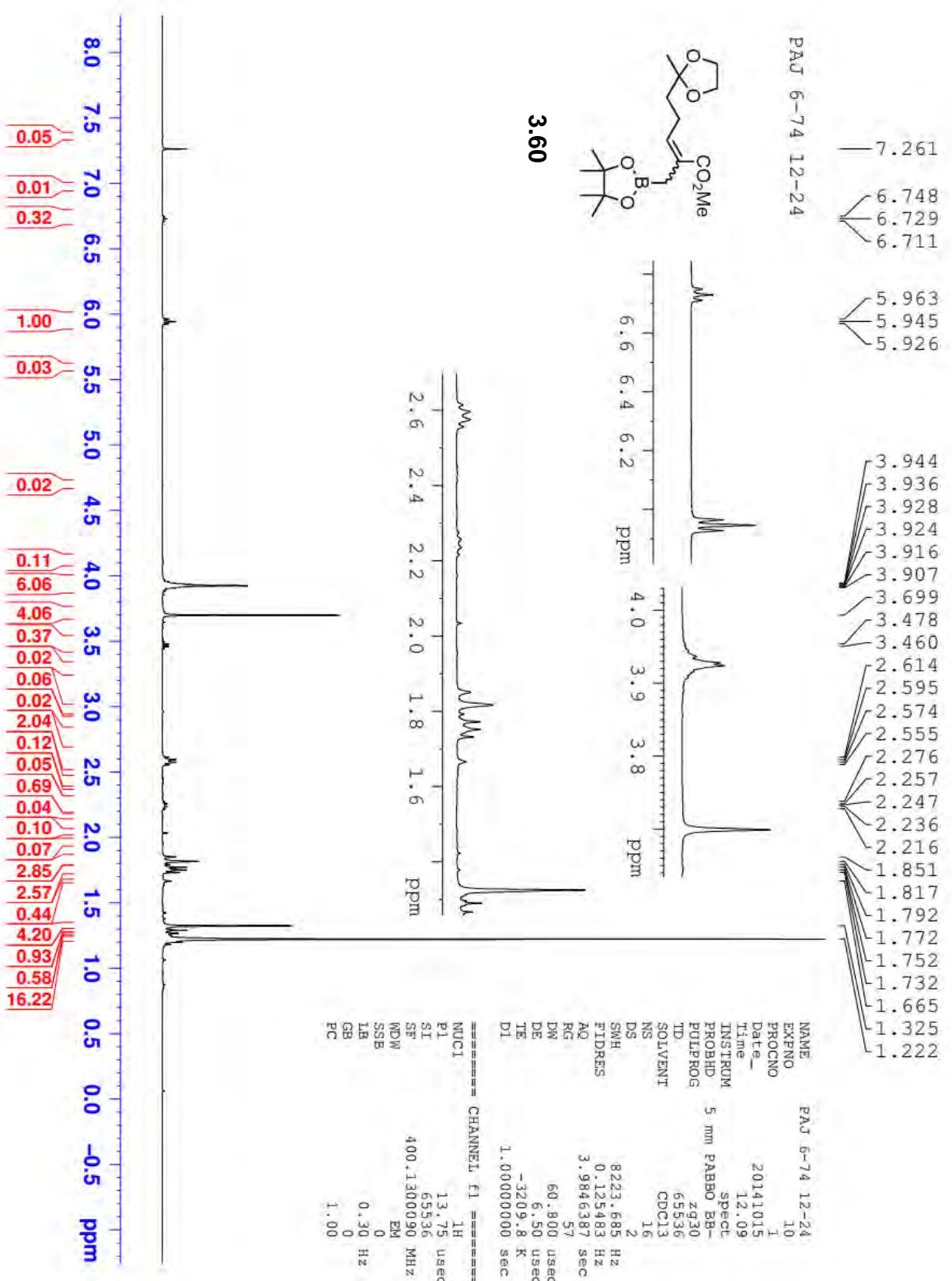
HRMS TOF MS ES+ [M+H]: $\text{C}_{24}\text{H}_{24}\text{NO}_5$

Calc: 416.2616 Found: 416.2605

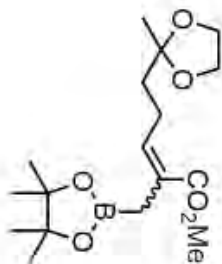
TLC $R_f = 0.34$ (50% EtOAc/hexanes) [silica gel, UV, *p*-anisaldehyde]

APPENDIX B

^1H AND ^{13}C NMR SPECTRA

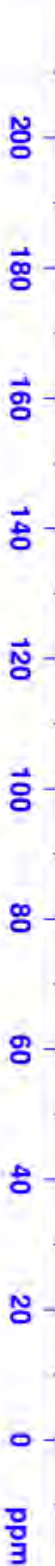


PAJ 6-74 12-24 CNMR



3.60

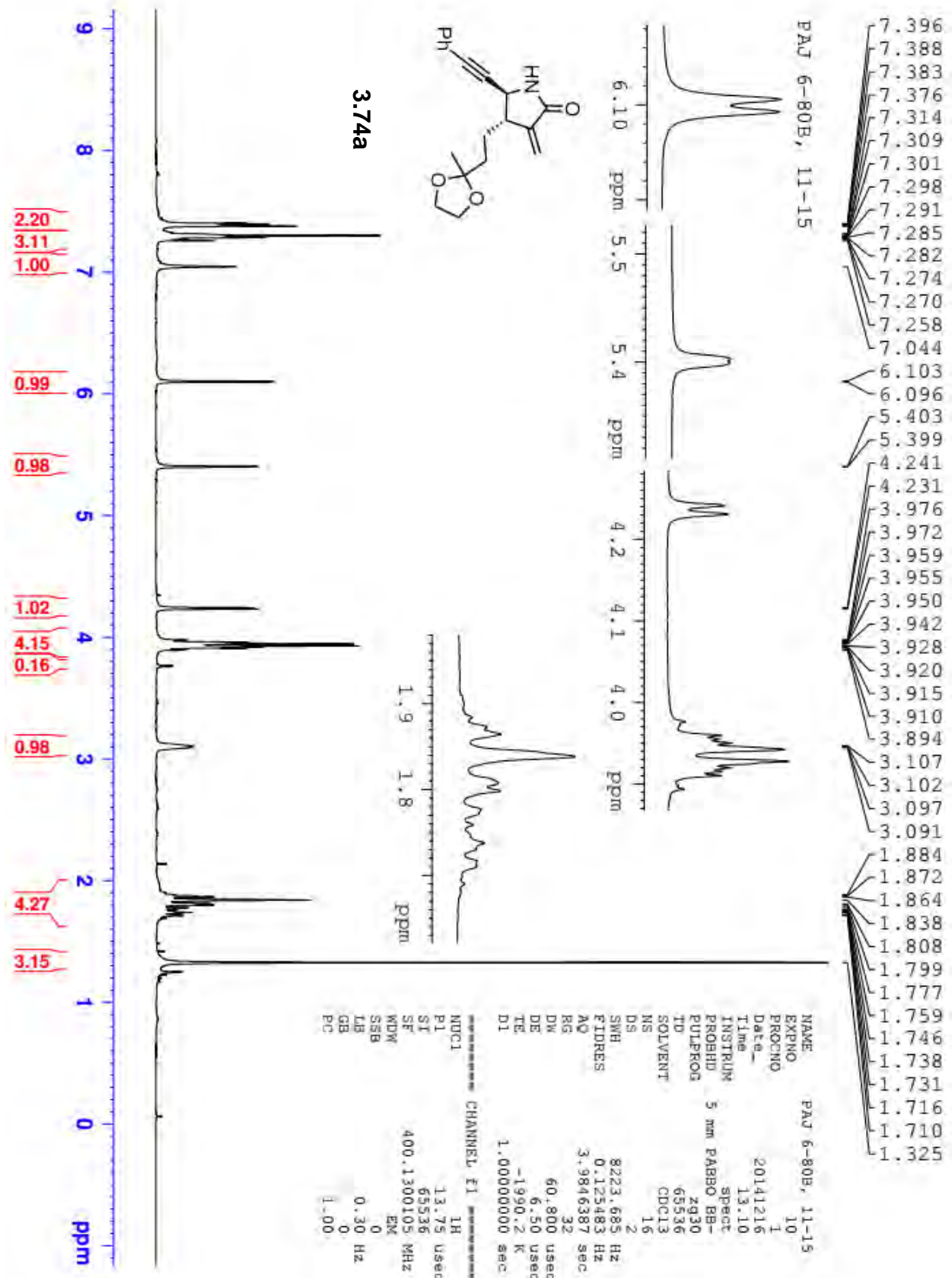
- 168.72
- 168.30
- 142.94
- 140.67
- 129.30
- 128.01
- 109.93
- 109.69
- 83.42
- 83.35
- 77.47
- 77.36
- 77.16
- 76.84
- 65.97
- 64.83
- 64.81
- 51.77
- 51.27
- 38.66
- 37.80
- 24.83
- 24.76
- 24.05
- 23.70
- 15.40

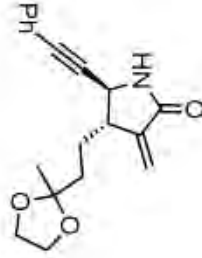


```

NAME          PAJ 6-74 12-24
EXPNO         11
PROCNO        1
Date_         20141015
Time          22.00
INSTRUM       spect
PROBHD        5 mm PABBO BB-
PULPROG       zgpg30
TD            65536
SOLVENT       CDCl3
NS            2048
DS            4
SWH           24038.461 Hz
FIDRES        0.366798 Hz
AQ            1.3631988 sec
RG            161
DM            20.800 usec
DE            6.50 usec
TE            -2440.0 K
D1            2.00000000 sec
D11           0.03000000 sec

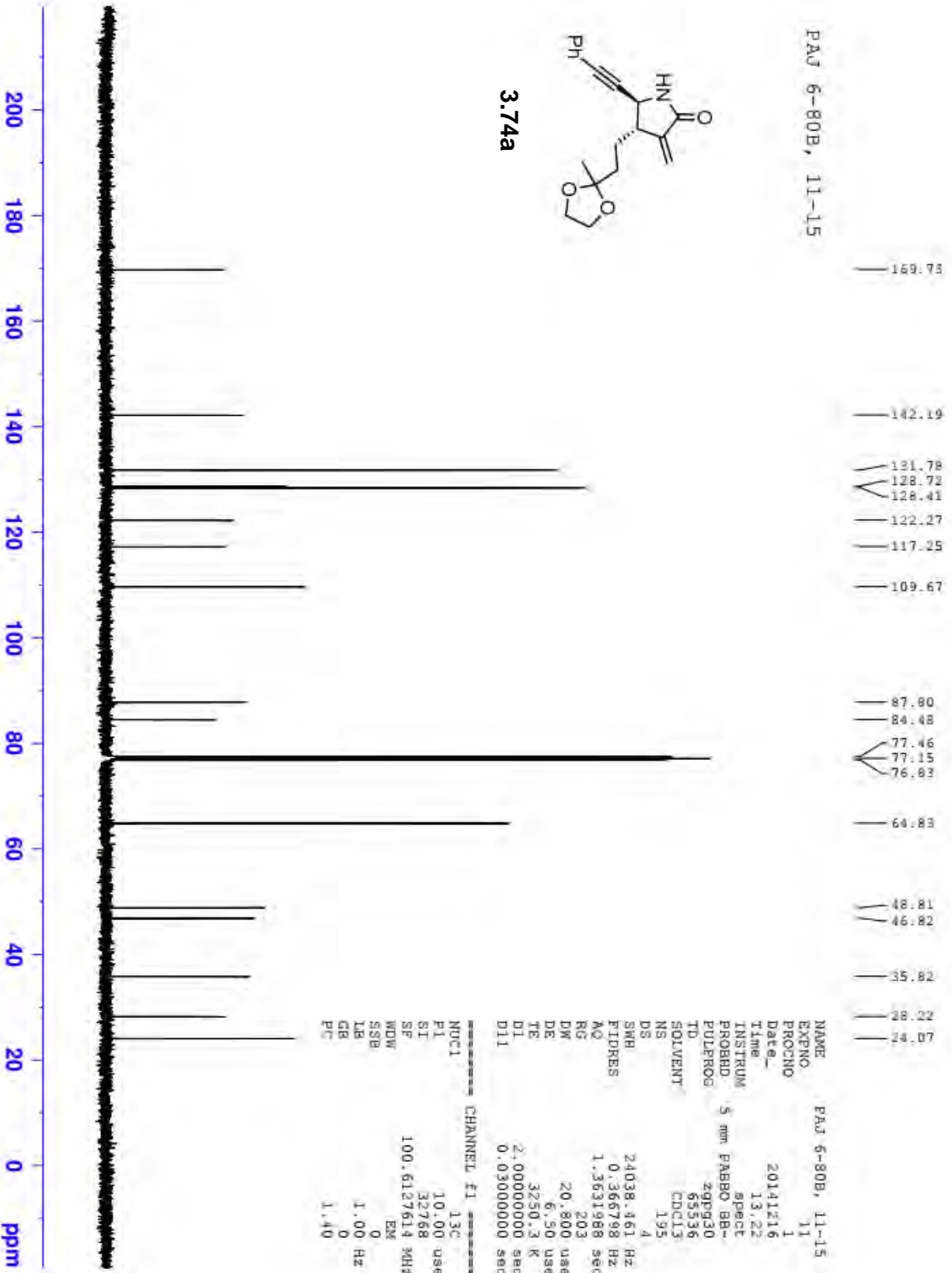
===== CHANNEL f1 =====
NUC1          13C
P1            10.00 usec
SI            32768
SE           100.6127559 MHz
WDW           EM
SSB           0
LB            1.00 Hz
GB            0
PC            1.40
  
```





3.74a

PAJ 6-80B, 11-15



```

NAME          PAJ 6-80B, 11-15
EXPNO         11
PROCNO        1
Date_         20111216
Time         13.22
INSTRUM       spect
PROBHD        5 mm PABBO BB-
PULPROG       zgpg30
TD            65536
SOLVENT       CDCl3
NS           195
DS            4
SWH           24038.461 Hz
FIDRES        0.366798 Hz
AQ           1.3631988 sec
RG            203
DW           20.800 usec
DE           6.50 usec
TE           3250.3 K
D1           2.00000000 sec
D11          0.03000000 sec

===== CHANNEL f1 =====
NUC1          13C
P1           10.00 usec
SI           32768
SF           100.6127614 MHz
WDW          EM
SSB          0
LB           1.00 Hz
GB           0
PC           1.40
  
```

PAJ 6-80B, 23-26

7.407
7.403
7.397
7.389
7.384
7.312
7.301
7.283
7.251

6.312
6.125
6.115
6.103
6.096

5.413
5.399
5.394

4.696
4.681
4.661
3.934
3.926

3.917
3.911
3.898
3.888
3.871

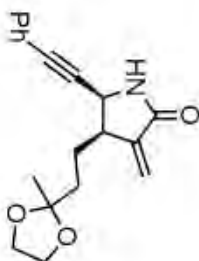
3.122
3.115
3.096
3.089
3.080

2.154
2.112
2.095
1.960
1.941

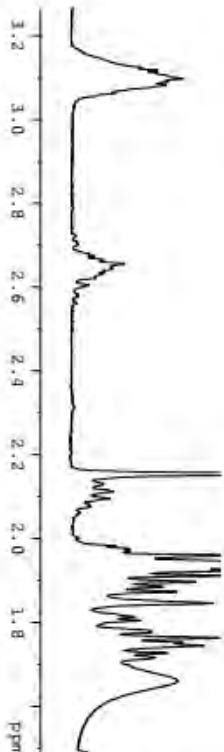
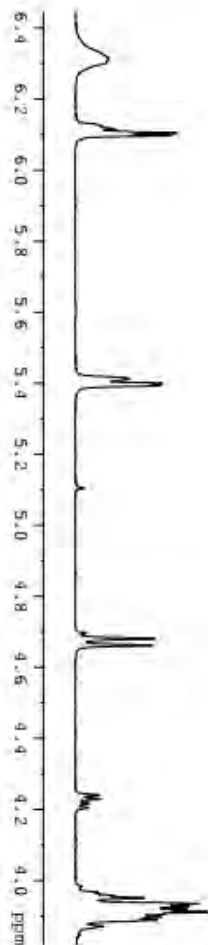
1.933
1.923
1.911
1.896
1.873

1.845
1.763
1.751
1.744
1.659

1.256
1.240

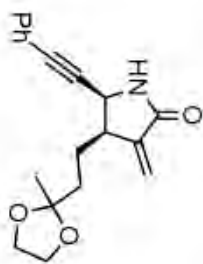


3.74b



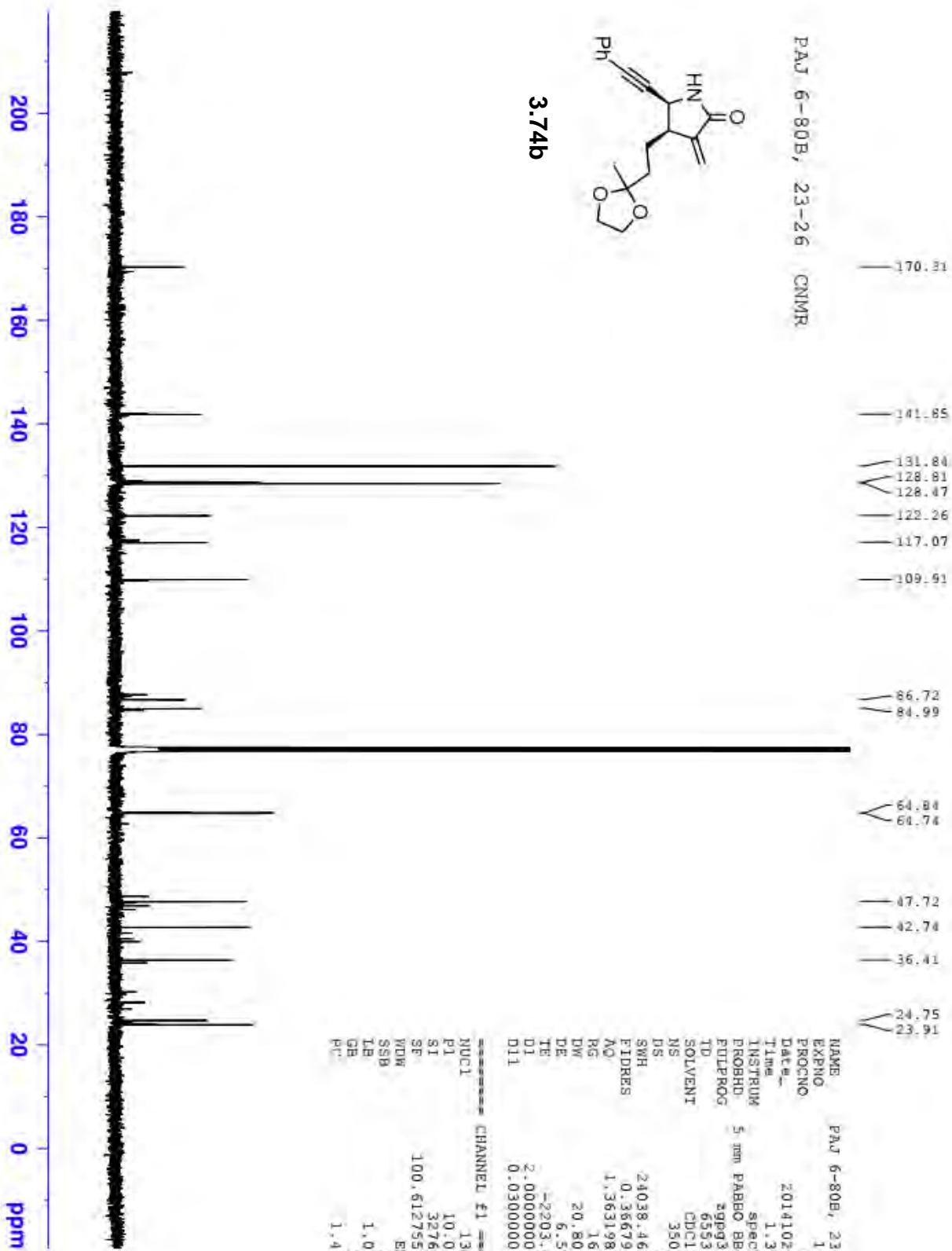
NAME PAJ 6-80B, 23-26
EXPNO 10
PROCNO 1
Date_ 20141028
Time 17.16
INSTRUM spect
PROBHD 5 mm PABBO BB-
PULPROG zg30
ID 65336
SOLVENT CDCl3
NS 16
DS 2
SMH 8223.685 Hz
FIDRES 0.125483 Hz
AQ 3.9846387 sec
RG 101
DW 60.800 usec
DE 6.50 usec
TE -1.4 K
D1 1.00000000 sec

CHANNEL F1
NUC1 1H
P1 13.75 usec
SI 65536
SF 400.1300129 MHz
WDW EM
SSB 0
LB 0.30 Hz
GB 0
PC 1.00



3.74b

PAJ 6-80B, 23-26 CNMR



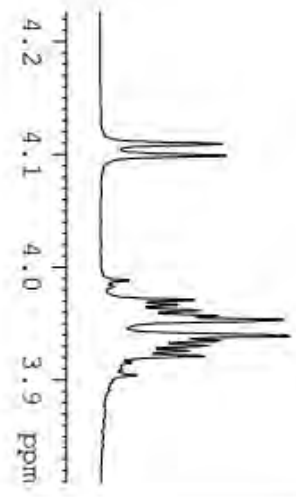
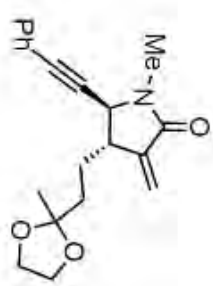
```

NAME      PAJ 6-80B, 23-26
EXPNO     11
PROCNO    1
Date_     20141029
Time      1.30
INSTRUM   spect
PROBHD    5 mm PABBO BB-
PULPROG   zgpg30
TD         65536
SOLVENT   CDCl3
NS         3500
DS         4
SWH        24038.461 Hz
FIDRES     0.366798 Hz
AQ         1.3631988 sec
RG         161
DE         20.800 usec
TE         -2203.4 K
D1         2.00000000 sec
D11        0.03000000 sec

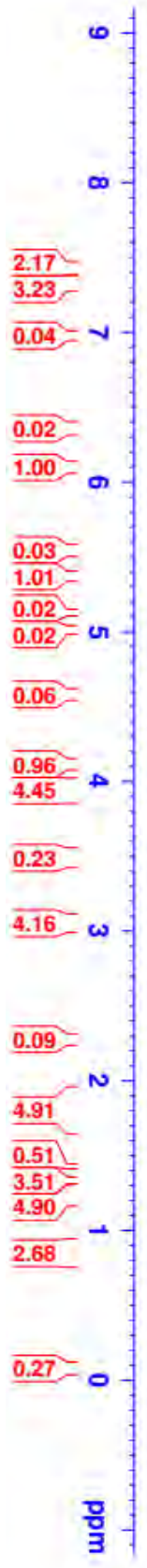
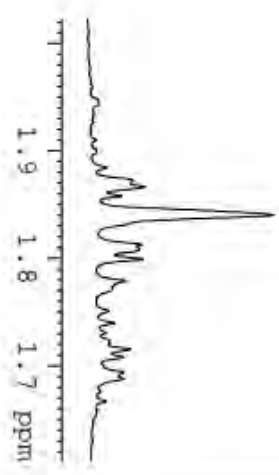
----- CHANNEL #1 -----
NUC1      13C
P1        10.00 usec
S1        32768
SE        100.6127557 MHz
WDW       EM
SSB       0
LB        1.00 Hz
GB        0
PC        1.40
  
```

PAJ 6-190, plug

- 7.421
- 7.417
- 7.412
- 7.408
- 7.404
- 7.397
- 7.337
- 7.333
- 7.327
- 7.324
- 7.313
- 7.311
- 7.309
- 7.263
- 6.087
- 6.081
- 5.362
- 5.356
- 4.109
- 4.099
- 3.988
- 3.971
- 3.966
- 3.961
- 3.957
- 3.953
- 3.939
- 3.935
- 3.930
- 3.926
- 3.921
- 3.915
- 3.904
- 3.046
- 3.031
- 1.872
- 1.866
- 1.858
- 1.840
- 1.812
- 1.809
- 1.799
- 1.778
- 1.739
- 1.721
- 1.715
- 1.708
- 1.693
- 1.687
- 1.427
- 1.334
- 1.252
- 1.202
- 0.876
- 0.068



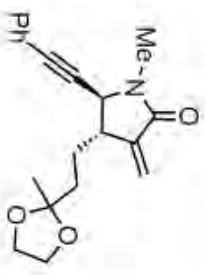
3.77



```

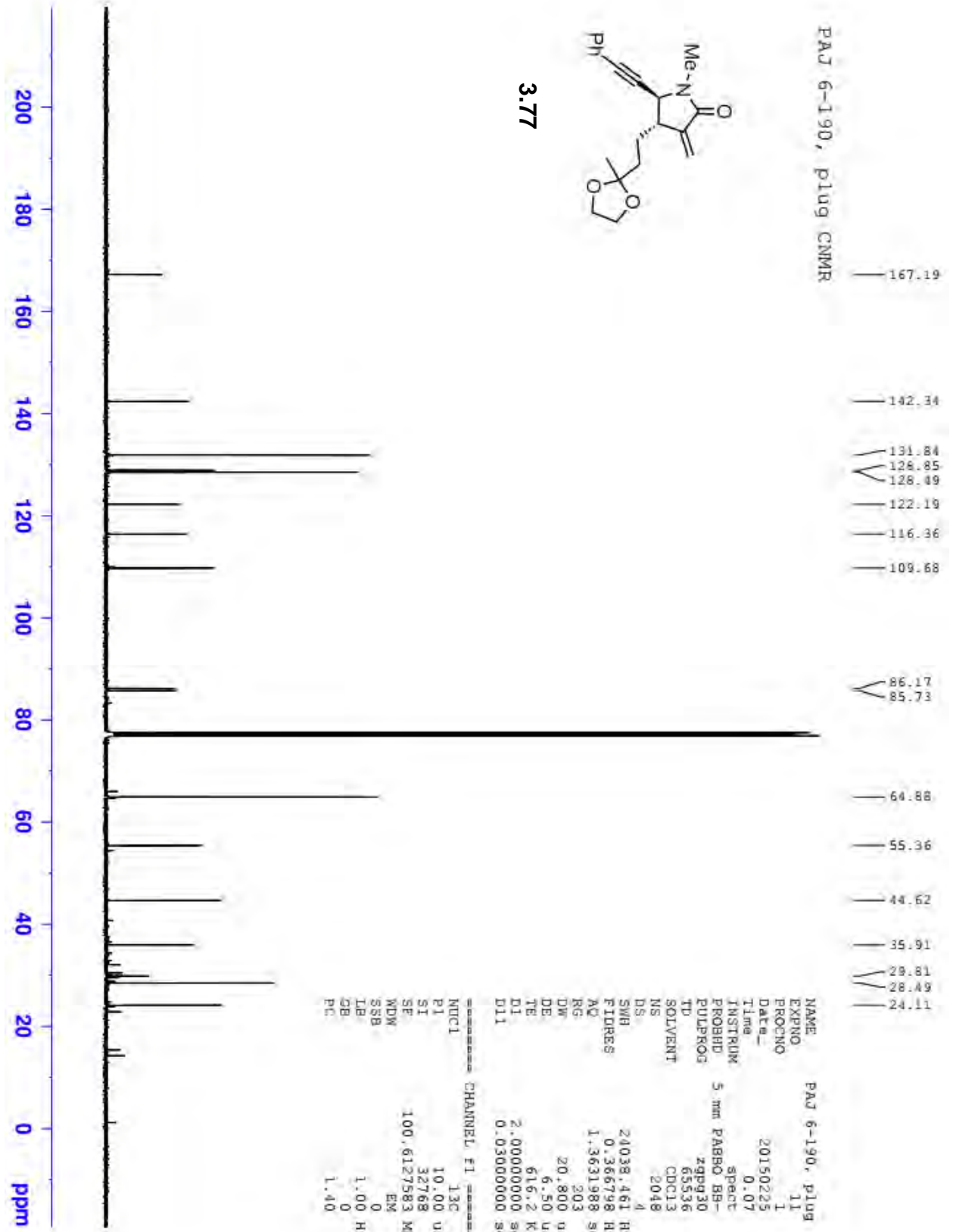
NAME      PAJ 6-190, plug
EXPNO     10
PROCNO    1
Date_     20150224
Time      10.10
INSTRUM   spect
PROBHD    5 mm PABBO BB-
PULPROG   zg30
TD         65536
ID         65536
SOLVENT   CDCl3
NS         16
DS         2
SMBR      8223.685 Hz
FIDRES    0.125483 Hz
AQ         3.9846387 sec
RG         32
DW         60.800 usec
DE         6.50 usec
TE         618.6 K
D1         1.00000000 sec

===== CHANNEL f1 =====
NUC1      1H
P1        13.75 usec
S1        65536
SP        400.1300095 MHz
WDW       EM
SSB       0
LB        0.30 Hz
GB        0
PC        1.00
  
```



3.77

PAJ 6-190, plus CNMR



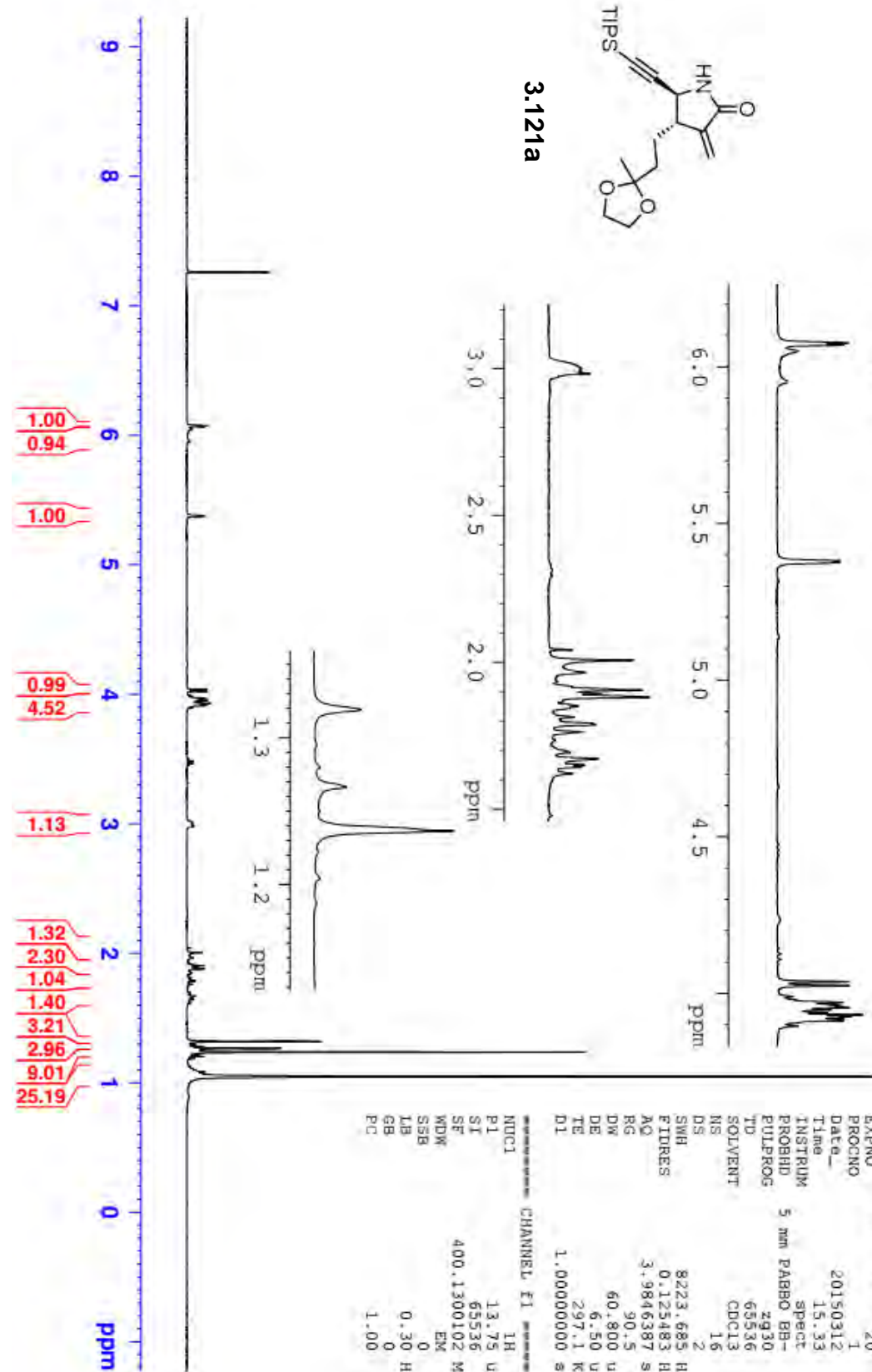
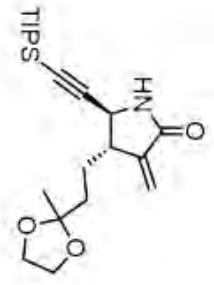
```

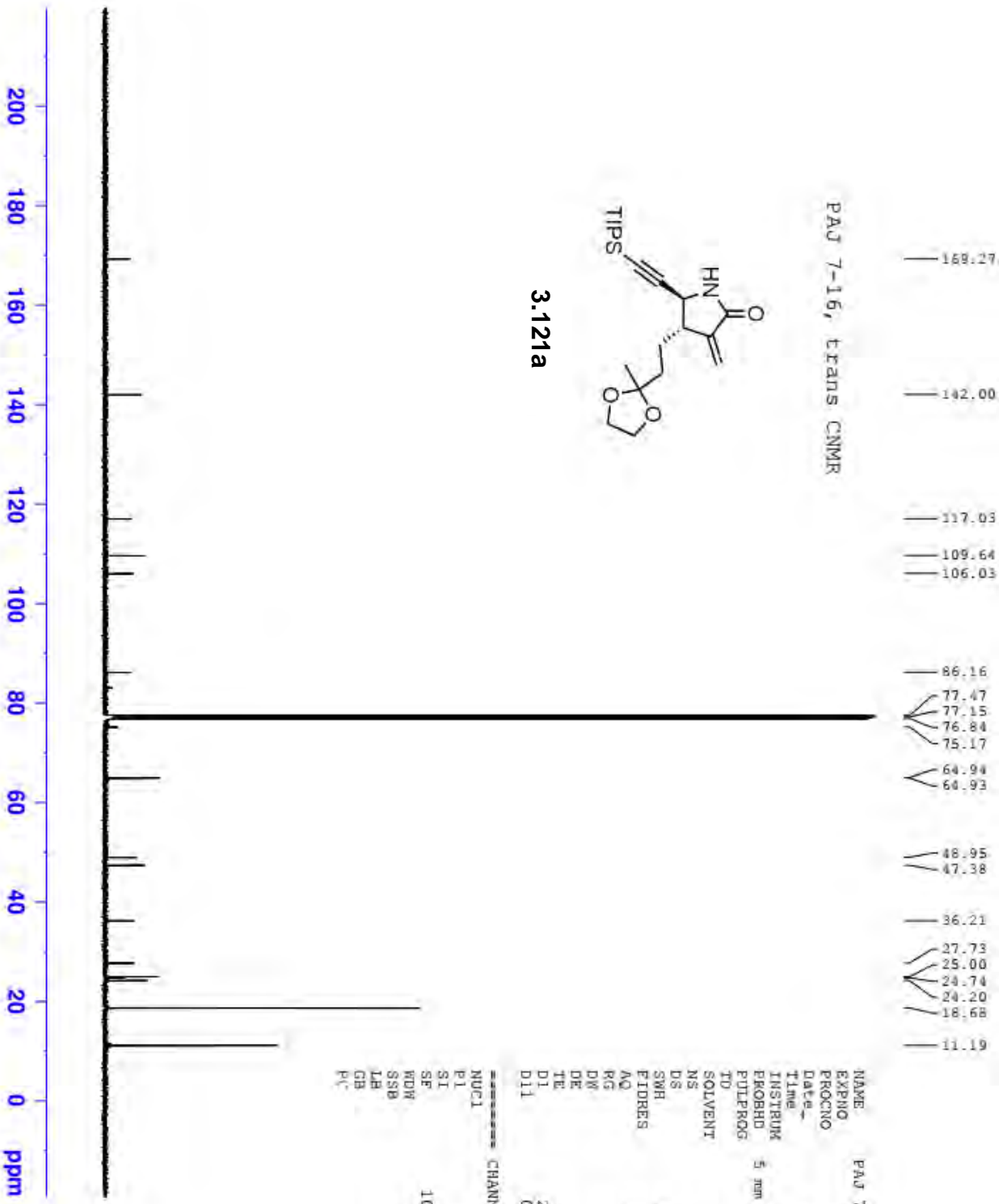
NAME          PAJ 6-190, plus
EXPNO         11
PROCNO        1
Date_         20150225
Time         0.07
INSTRUM       Spect
PROBHD        5 mm PABBO BB-
PULPROG       zgpg30
TD            65536
SOLVENT       CDCl3
NS            2048
DS            4
SWH           24038.461 Hz
FIDRES        0.366798 Hz
AQ            1.3631988 sec
RG            203
DW            20.800 usec
DE            6.50 usec
TE            316.2 K
D1            2.00000000 sec
D11           0.03000000 sec

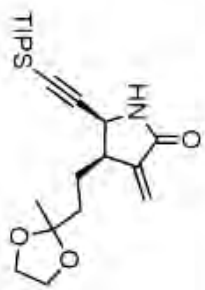
===== CHANNEL f1 =====
NUC1          13C
P1            10.00 usec
SI            32768
SF            100.6127583 MHz
WDW           EM
SSB           0
LB            1.00 Hz
GB            0
PC            1.40
  
```

PAJ 7-16, 18-40

7.261
6.075
6.069
6.050
5.951
5.381
5.379
5.376
4.037
4.025
3.990
3.979
3.971
3.963
3.958
3.954
3.947
3.938
3.931
3.925
3.921
3.916
3.913
3.896
3.009
2.998
2.989
2.981
2.041
2.005
1.964
1.916
1.904
1.892
1.879
1.849
1.812
1.791
1.786
1.762
1.697
1.691
1.670
1.658
1.649
1.642
1.620

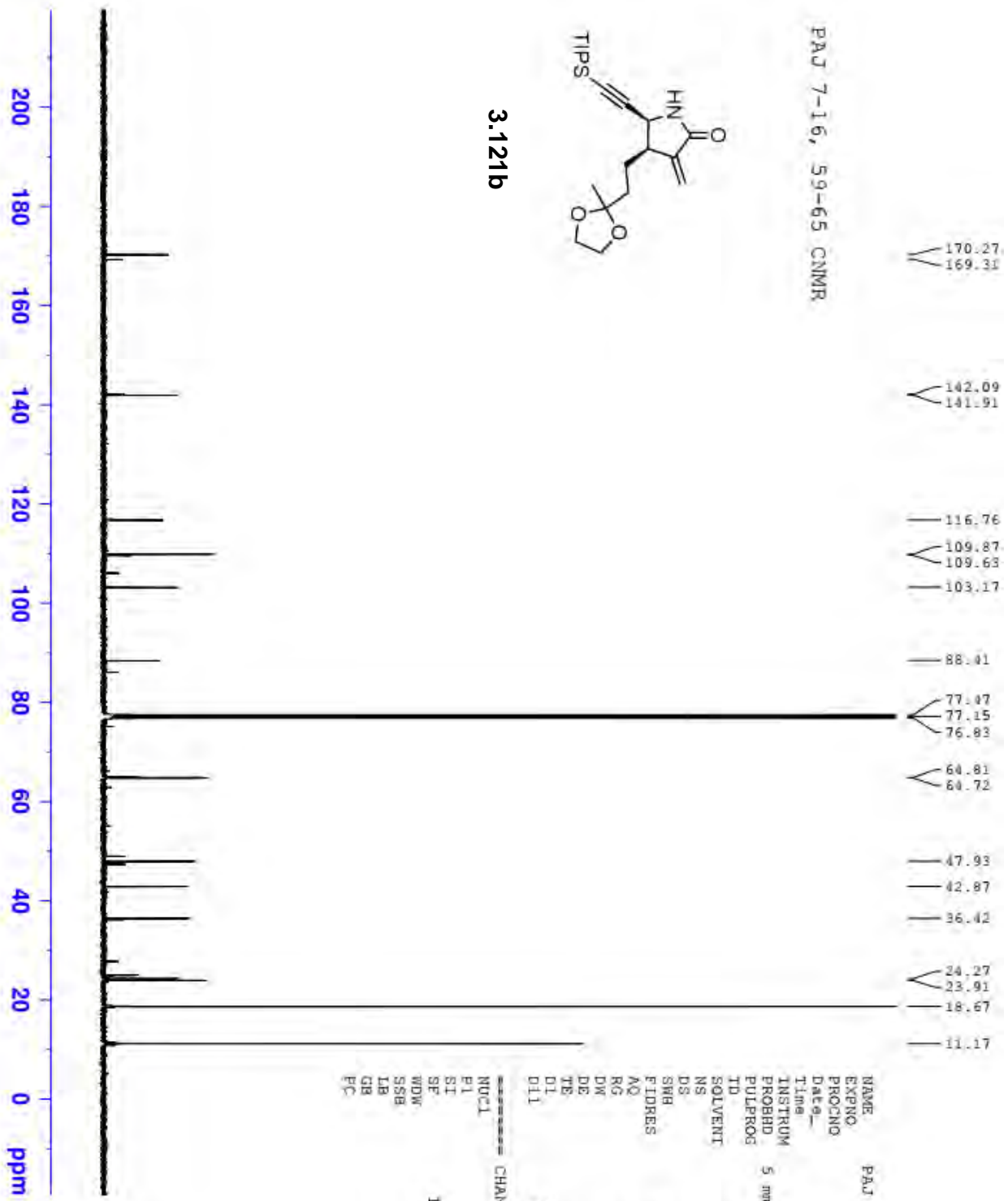






3.121b

PAJ 7-16, 59-65 CNMR



- 170.27
- 169.31
- 142.09
- 141.91
- 116.76
- 109.87
- 109.63
- 103.17
- 88.41
- 77.47
- 77.15
- 76.83
- 64.81
- 64.72
- 47.93
- 42.87
- 36.42
- 24.27
- 23.91
- 18.67
- 11.17

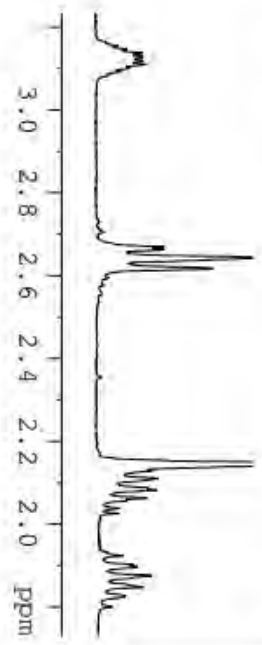
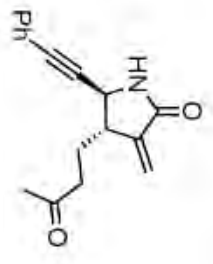
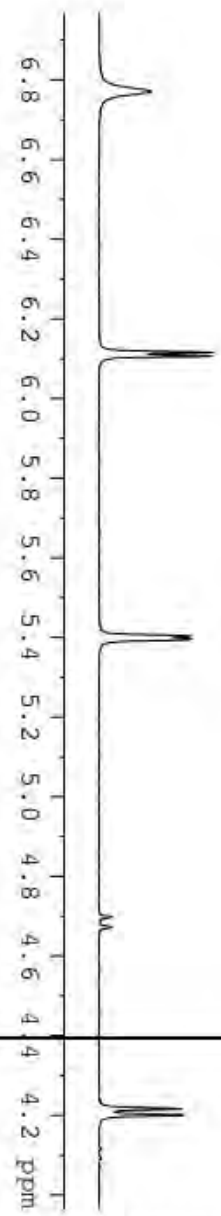
```

NAME          PAJ 7-16, 59-65
EXPNO         11
PROCNO        1
Date_         20150314
Time          22.37
INSTRUM       spect
PROBHD        5 mm PABBO BB-
PULPROG       zgpg30
TD            65536
SOLVENT       CDCl3
NS            2048
DS            4
SWH           24038.461 Hz
FIDRES        0.366798 Hz
AQ            1.3631988 sec
RG            203
DW            20.800 usec
DE            6.50 usec
TE            311.5 K
D1            2.00000000 sec
D11           0.03000000 sec

----- CHANNEL f1 -----
NUC1          13C
P1            10.00 usec
SI            32768
SF            100.6127572 MHz
WDW           EM
SSB           0
LB            1.00 Hz
GB            0
PC            1.30
  
```

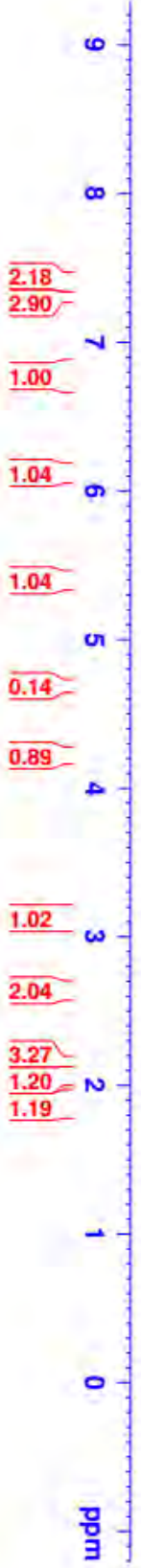
PAJ 6-150, plug

7.402
7.396
7.386
7.380
7.370
7.322
7.313
7.308
7.299
7.294
7.292
7.288
7.251
6.770
6.114
6.105
5.401
5.394
4.696
4.671
4.216
4.200
3.162
3.154
3.145
3.136
3.127
3.119
3.109
3.100
3.091
3.083
2.668
2.661
2.642
2.616
2.144
2.128
2.109
2.087
2.081
2.062
2.056
2.037
2.025
1.923
1.901
1.896
1.875
1.853
1.847
1.825
1.799



6.4:1 trans:cis

3.58a

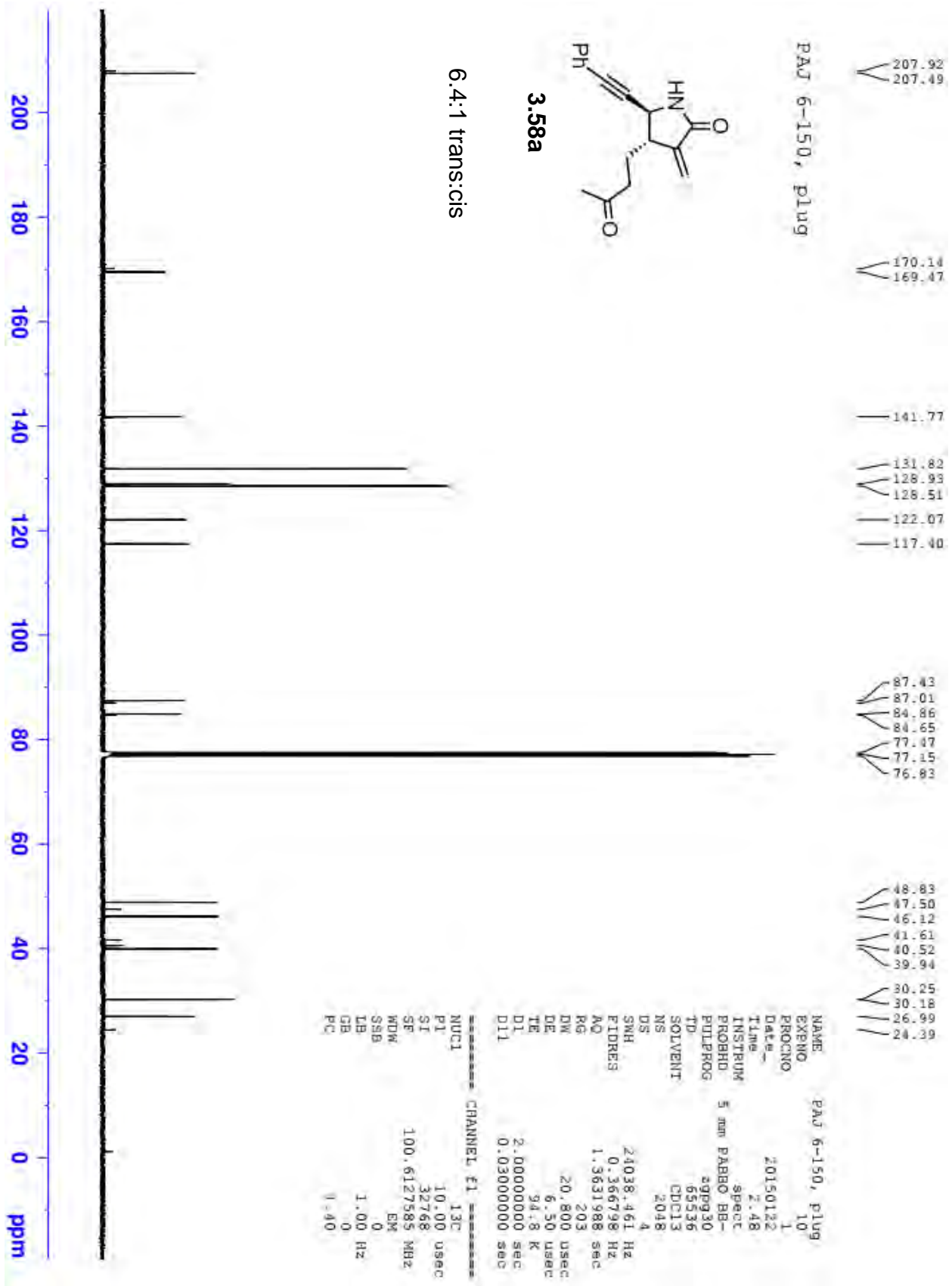


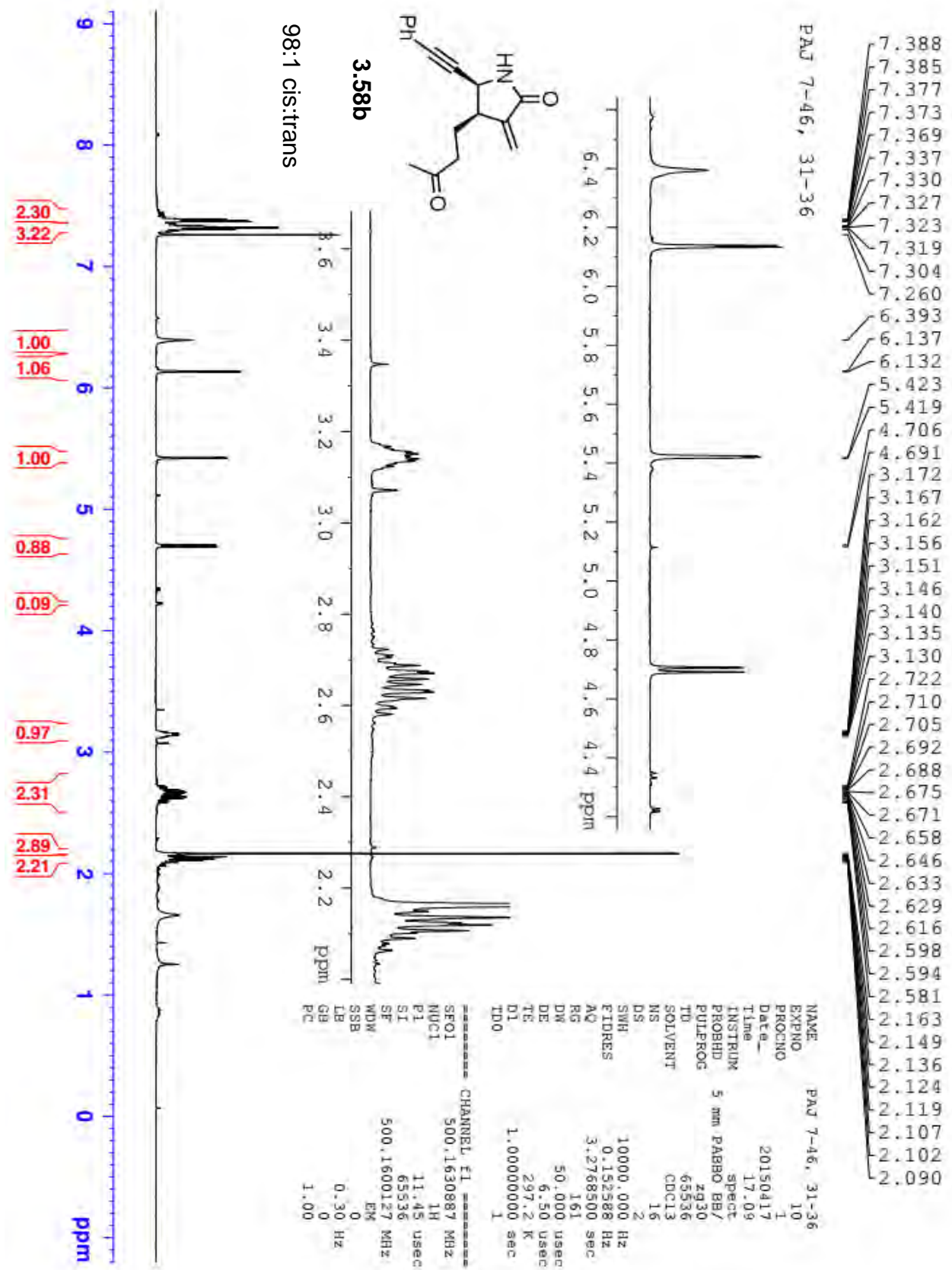
```

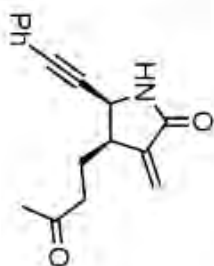
NAME          PAJ 6-150, plug
EXPNO         10
PROCNO        1
Date_         20150120
Time         14.32
INSTRUM       spect
PROBHD        5 mm QNP
PULPROG       zg30
TD            32768
SOLVENT       CDCl3
NS            16
DS            2
SWH           6188.15 Hz
FIDRES        0.188846 Hz
AQ            2.6477044 sec
RG            101
RG            101
AQ            101
DE            80.800 usec
DE            6.50 usec
TE            -929.3 K
D1            1.000000000 sec
TDO           1

===== CHANNEL f1 =====
SFO1          300.2318540 MHz
NUC1          1H
P1            12.71 usec
SI            32768
SP            300.2300109 MHz
WDW           EM
SSB           0
LB            0.10 Hz
GB            0
PC            1.00

```



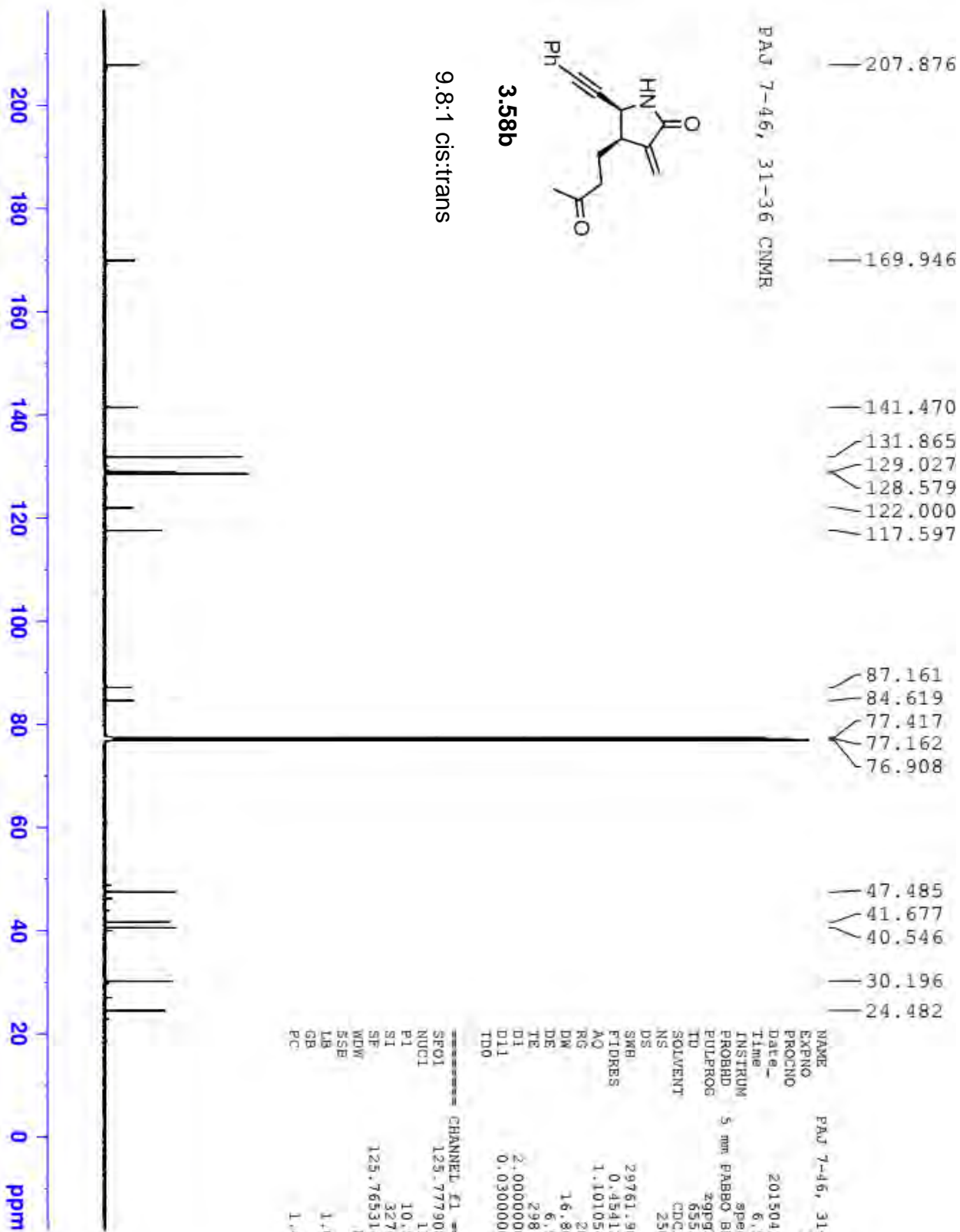




3.58b

9.8:1 cis:trans

PAJ 7-46, 31-36 CNMR



```

NAME          PAJ 7-46, 31-36
EXPNO         11
PROCNO        1
Date_         20150418
Time         6.51
INSTRUM       spect
PROBHD        5 mm PABBO BB/
PULPROG       zgpg30
TD            65536
SOLVENT       CDCl3
NS            2500
DS            2
SMB           29761.904 Hz
FIDRES        0.454131 Hz
AQ            1.1010548 sec
RG            203
DE            16.800 usec
TE            298.5 K
D1            2.00000000 sec
D11           0.03000000 sec
TD0           1
===== CHANNEL f1 =====
SFO1          125.7779086 MHz
NUC1          13C
P1            10.50 usec
SI            32768
SF            125.7653140 MHz
WDW           EM
SSB           0
LB            1.00 Hz
GB            0
PC            1.40

```

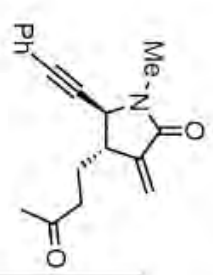
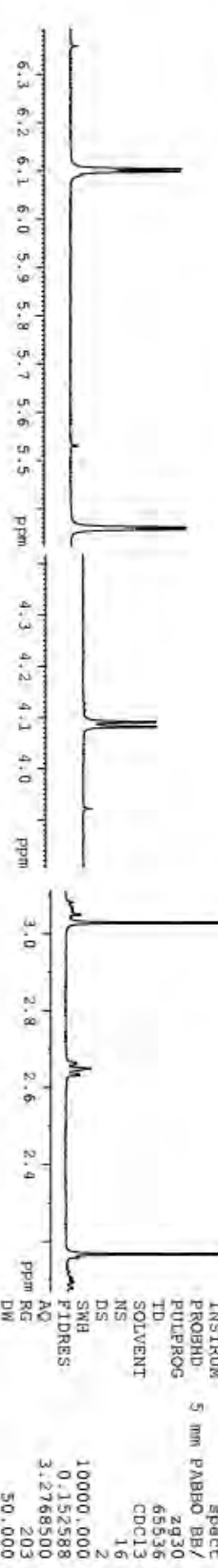
PAJ 6-196, Plug

7.422
7.419
7.411
7.407
7.403
7.353
7.344
7.338
7.329
7.326
7.324
7.259
6.103
6.098
5.362
5.357
4.091
4.082
3.080
3.073
3.067
3.062
3.057
3.048
3.041
3.028
2.664
2.660
2.649
2.634
2.167
2.159
2.121
2.110
2.106
2.100
2.094
2.078
2.066
2.062
2.051
2.051
2.043
1.902
1.889
1.886
1.873
1.873
1.856
1.843
1.254
0.879

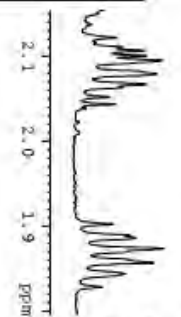
PAJ 6-196, Plug

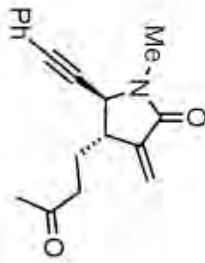
EXPNO 10
PROCNO 1
Date_ 20150227
Time 17.44
INSTRUM spect
PROBHD 5 mm PABBO BB/
PULPROG zg30
TD 65536
SOLVENT CDCl3
NS 16
DS 2
SWH 10000.000 Hz
AQ 0.1152588 Hz
RG 3.2768500 sec
FIDRES 203
AQ 50.000 usec
DE 6.50 usec
TE 298.9 K
D1 1.00000000 sec
TD0 1

CHANNEL F1 *****
SFO1 500.1630887 MHz
NUC1 1H
P1 11.45 usec
SI 65536
SE 500.1600117 MHz
WDW EM
SSB 0
LB 0.30 Hz
GB 0
PC 1.00



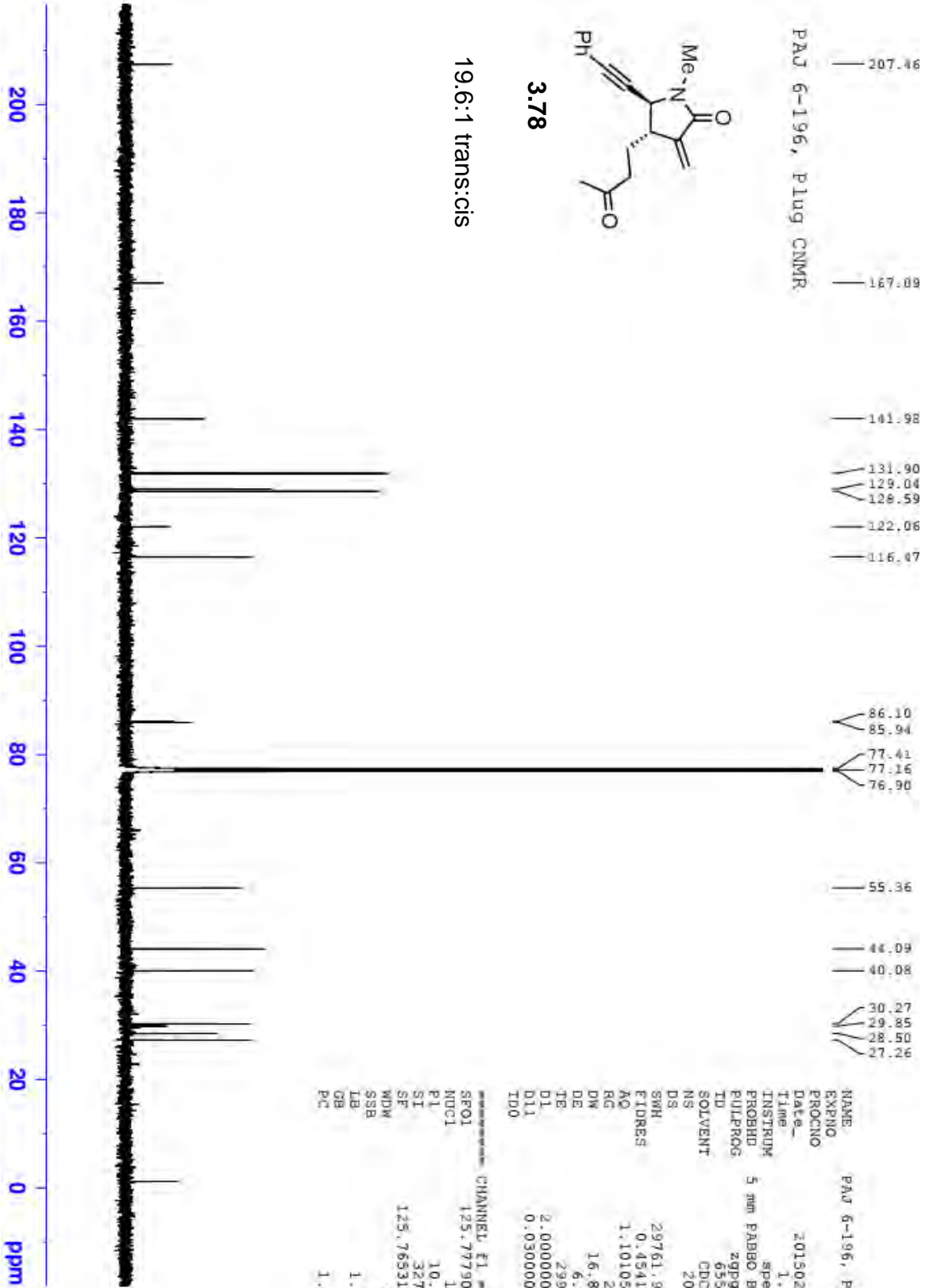
3.78
19.6:1 trans:cis





3.78

19.6:1 trans:cis



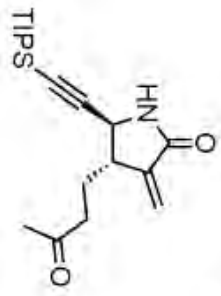
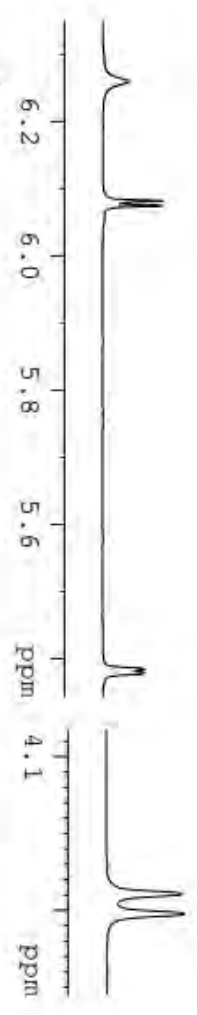
```

NAME      PAJ 6-196, Plug
EXPNO     1
PROCNO    1
DATE_     20150228
Time      1.34
INSTRUM   spect
PROBHD    5 mm PABBO BB/
PULPROG   zgpg30
TD         65536
SOLVENT   CDCl3
NS         2048
DS         2
SWH        29761.904 Hz
FIDRES     0.454131 Hz
AQ         1.1010548 sec
RG         203
DW         16.800 usec
DE         6.50 usec
TE         299.7 K
D1         2.00000000 sec
D11        0.03000000 sec
TD0        1

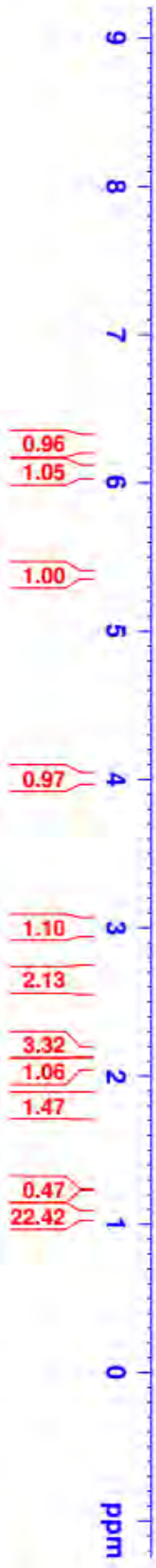
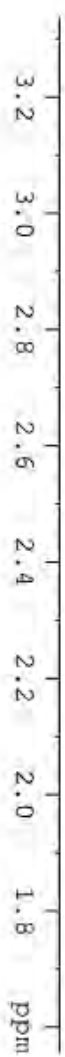
===== CHANNEL f1 =====
SFO1      125.7779086 MHz
NUC1      13C
P1        10.50 usec
SI        32768
SF        125.7653129 MHz
WDW       EM
SSB       0
LB        1.00 Hz
GB        0
PC        1.40
  
```

7.257
6.259
6.081
6.074
5.385
5.383
5.379
5.377
4.010
3.998
3.025
3.019
3.012
3.008
3.002
2.996
2.989
2.983
2.970
2.679
2.672
2.657
2.648
2.634
2.630
2.623
2.608
2.601
2.578
2.162
2.153
2.139
2.132
2.128
2.121
2.116
2.108
2.093
2.085
2.080
2.073
2.070
2.057
1.845
1.830
1.822
1.808
1.800
1.794
1.786
1.772
1.764
1.749
1.735
1.045

PAJ 7-20, trans



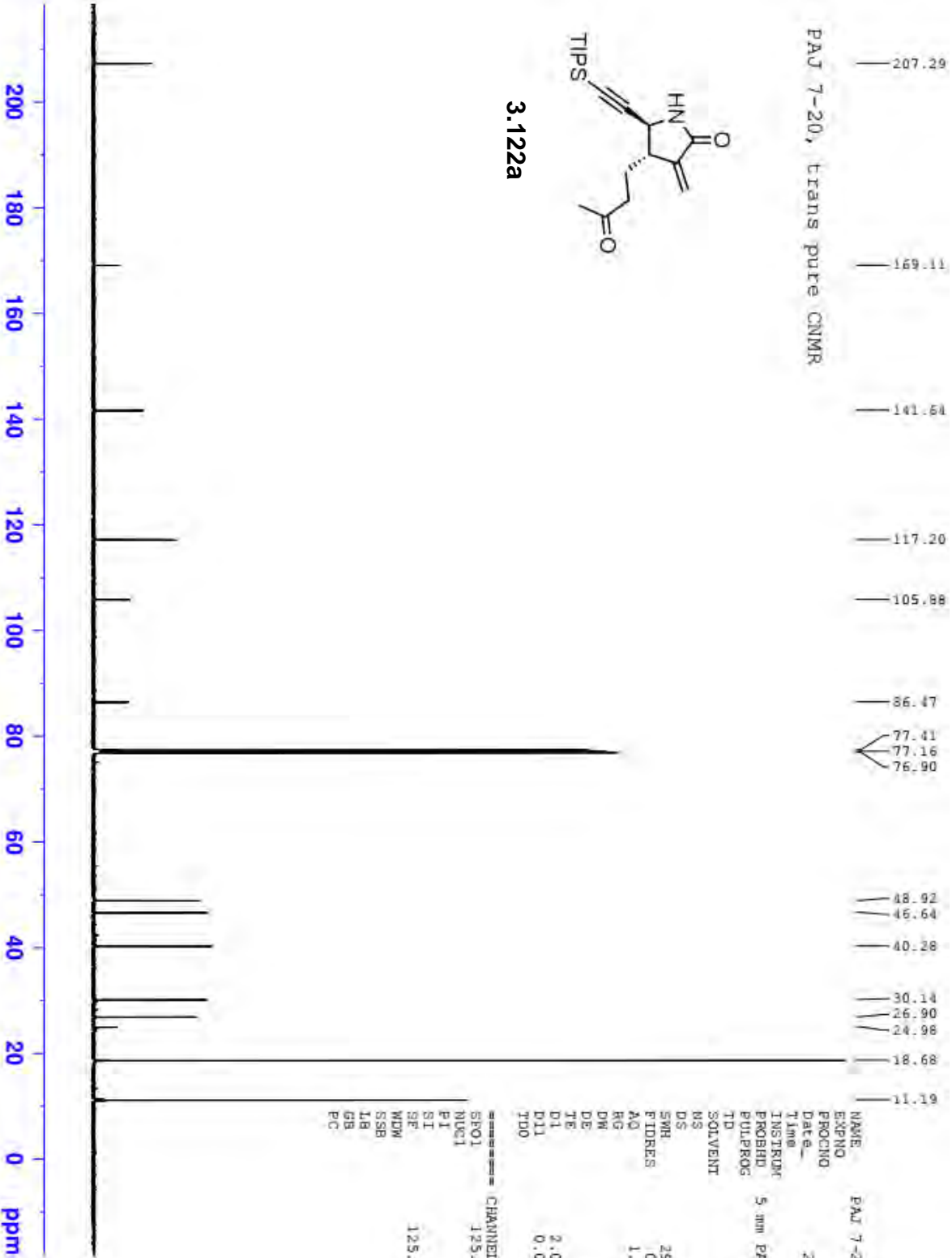
3.122a

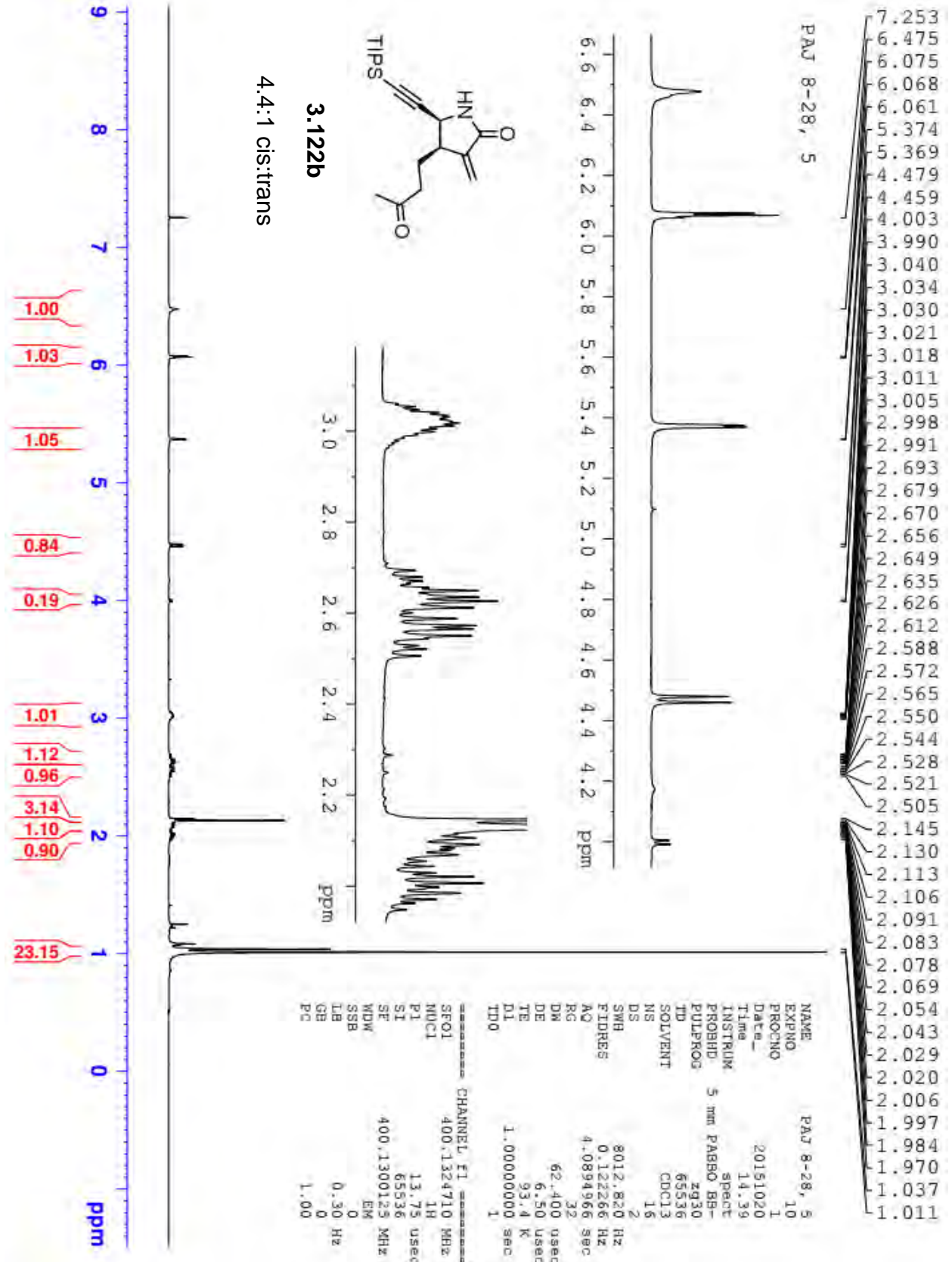


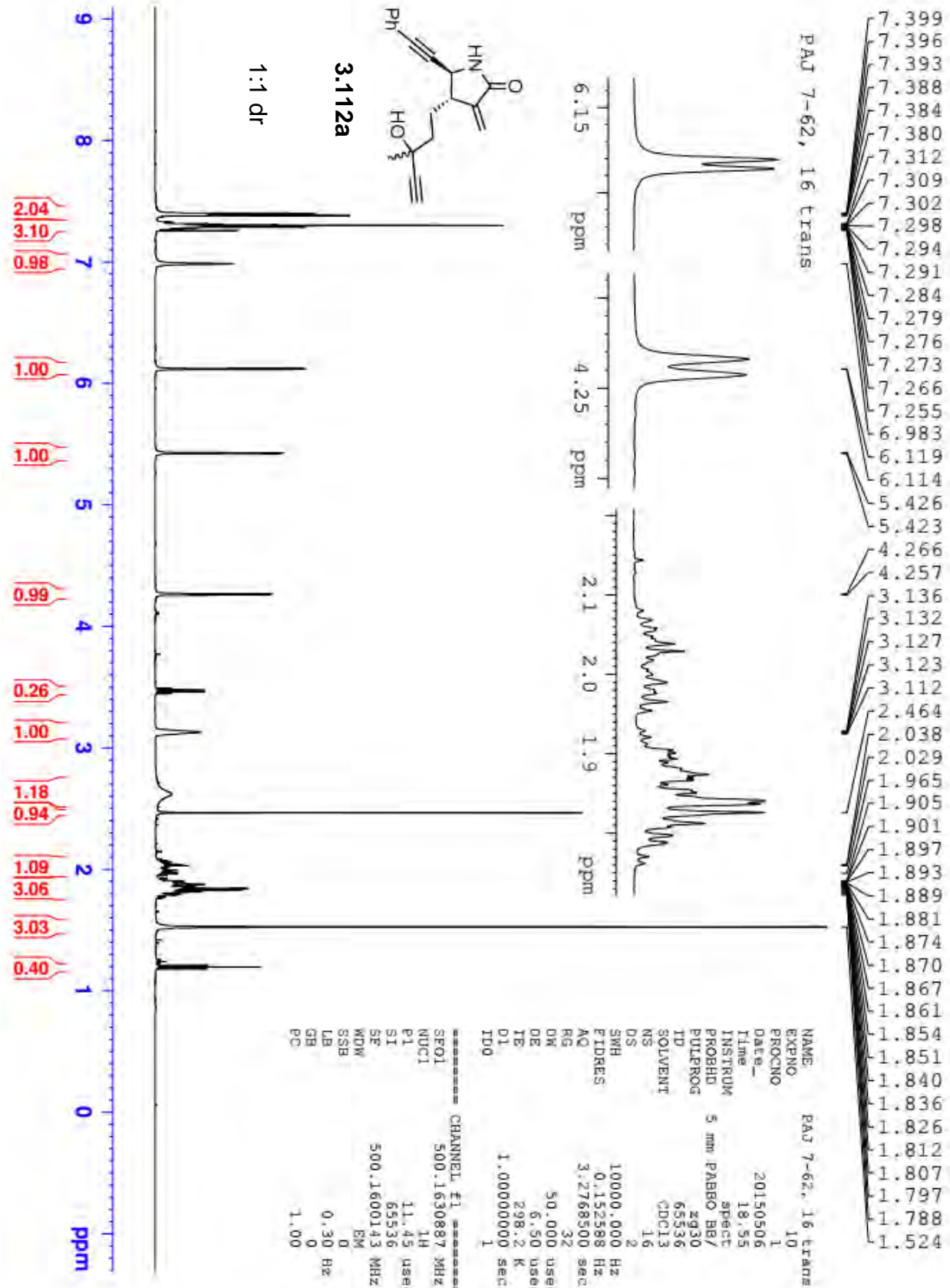
```

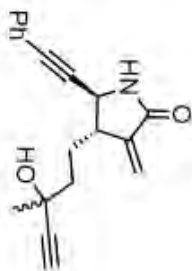
NAME          PAJ 7-20, trans
EXPNO         10
PROCNO        1
Date_         20150408
Time         15.21
INSTRUM       spect
PROBHD        5 mm PABBO BB-
PULPROG       zg30
TD            65536
FIDRES        0.125483 Hz
AQ            3.9846387 sec
RG            57
DE            60.800 usec
TE            92.0 K
D1            1.00000000 sec

===== CHANNEL f1 =====
NUC1          1H
P1            13.75 usec
SI            65536
SF            400.1300110 MHz
WDW           EM
SSB           0
L8            0.30 Hz
GB            0
PC            1.00
  
```





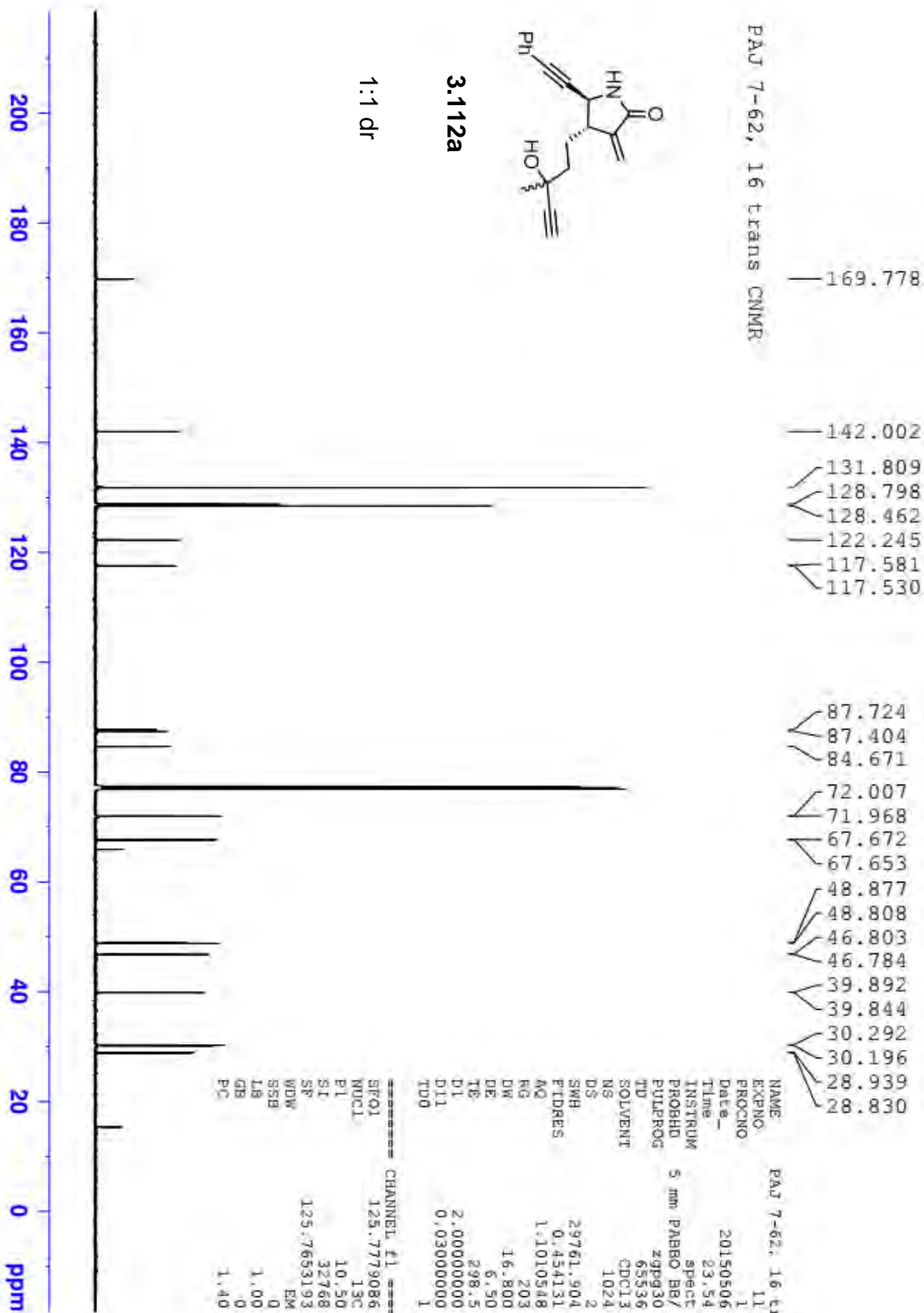


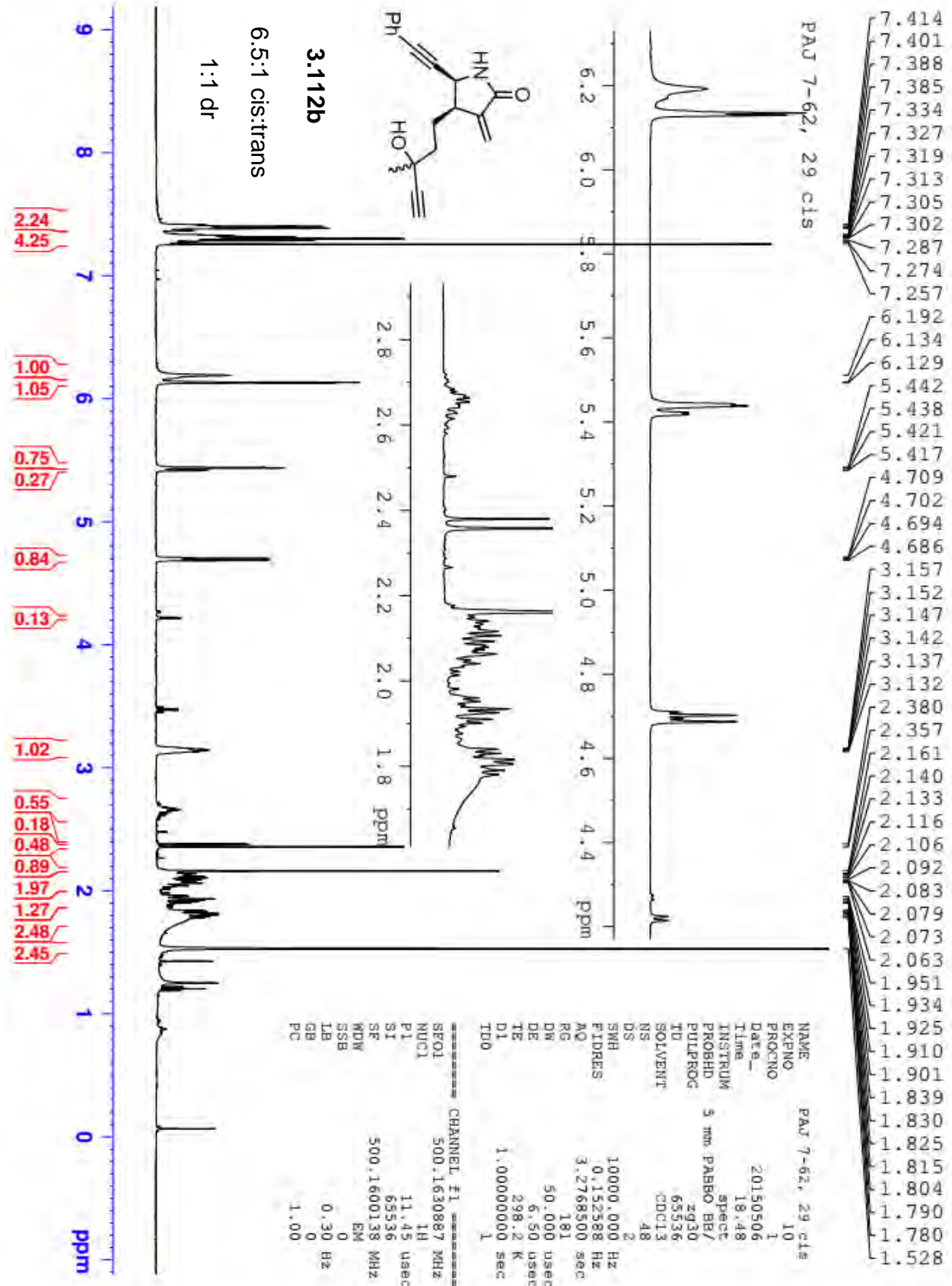


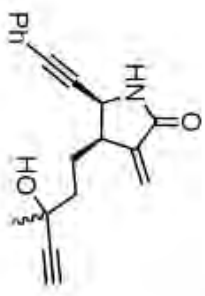
3.112a

1:1 dr

PAJ 7-62, 16 trans CNMR







PAJ 7-62, 29 cis CNMR

- 207.867
- 170.205
- 141.655
- 131.900
- 131.854
- 131.843
- 129.019
- 128.874
- 128.579
- 128.462
- 122.235
- 121.976
- 117.643
- 117.585
- 117.325
- 117.223
- 87.477
- 87.347
- 87.239
- 86.987
- 86.884
- 84.994
- 84.876
- 84.595
- 77.407
- 77.152
- 76.898
- 72.101
- 71.928
- 67.971
- 67.811
- 48.761
- 47.742
- 47.712
- 47.450
- 46.227
- 42.736
- 42.716
- 41.681
- 40.546
- 40.506
- 39.990
- 30.373
- 30.259
- 30.193
- 30.063
- 29.835

3.112b

6.5:1 cis:trans

1:1 dr



```

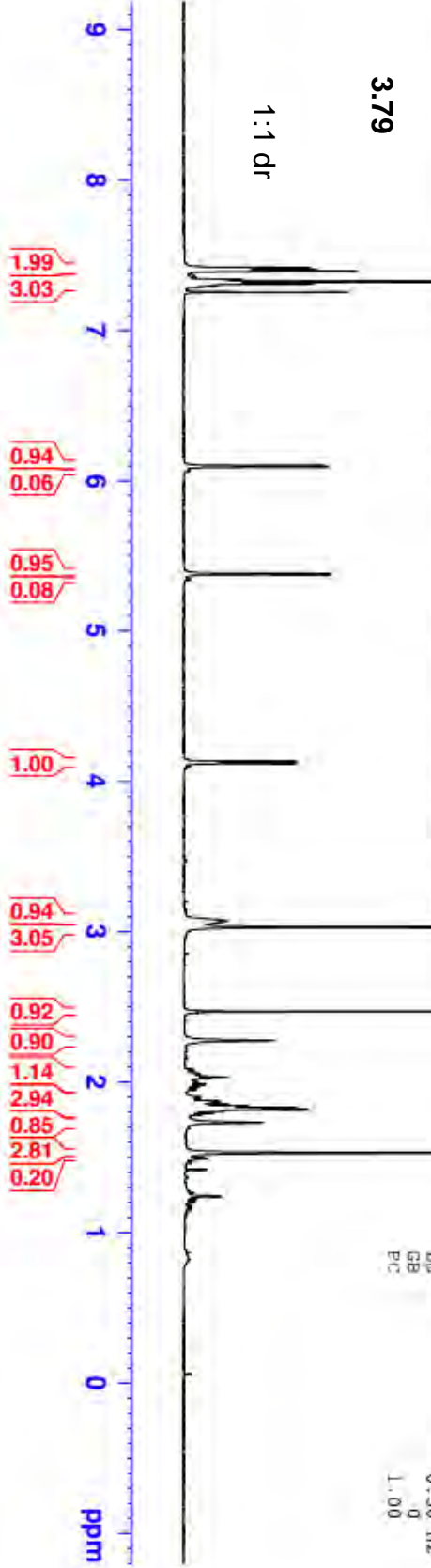
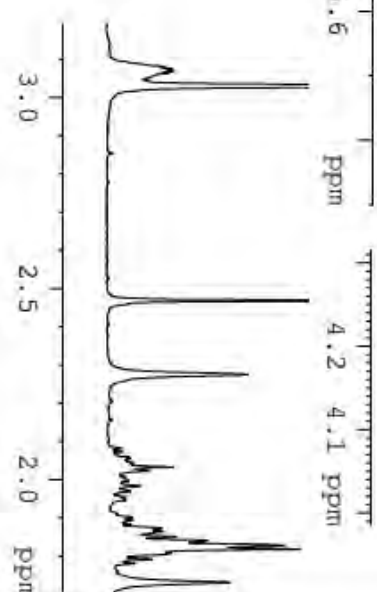
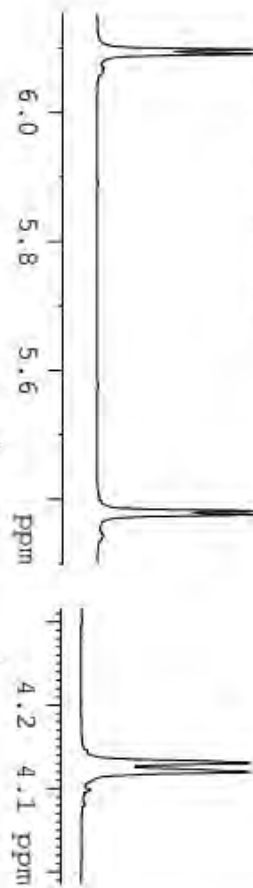
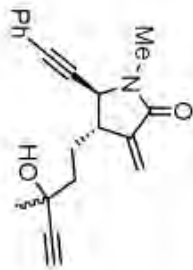
NAME: PAJ 7-62, 29 cis
EXPNO: 11
PROCNO: 1
Date_ : 20150507
Time: 2.38
INSTRUM: spect
PROBHD: 5 mm PABBO BH/
PULPROG: zgpg30
TD: 65536
SOLVENT: CDCl3
NS: 3000
DS: 2
SWH: 29761.904 HZ
FIDRES: 0.454131 HZ
AQ: 1.1010548 sec
RG: 203
DE: 16.800 usec
TE: 298.6 K
D1: 2.00000000 sec
D11: 0.03000000 sec
TD0: 1

===== CHANNEL f1 =====
SFO1: 125.7779086 MHz
NUC1: 13C
P1: 10.50 usec
SI: 32768
SE: 125.7653144 MHz
WDW: EM
SSB: 0
LB: 1.00 HZ
GB: 0
PC: 1.40

```

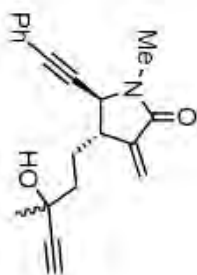
PAD 7-114, 35 trans

- 7.417
- 7.413
- 7.409
- 7.406
- 7.399
- 7.393
- 7.335
- 7.323
- 7.306
- 7.252
- 6.098
- 6.091
- 5.382
- 5.376
- 4.130
- 4.120
- 3.080
- 3.074
- 3.069
- 3.063
- 3.057
- 3.051
- 3.030
- 2.469
- 2.275
- 2.059
- 2.054
- 2.049
- 2.045
- 2.041
- 2.033
- 2.024
- 1.997
- 1.983
- 1.970
- 1.954
- 1.874
- 1.869
- 1.864
- 1.860
- 1.851
- 1.841
- 1.838
- 1.828
- 1.818
- 1.808
- 1.792
- 1.781
- 1.731
- 1.530



NAME PAD 7-114, 35 trans
 EXPNO 10
 PROCNO 1
 Date_ 20150616
 Time 17.22
 INSTRUM spect
 PROBHD 5 mm PABBO BB-
 PULPROG zg30
 TD 65536
 SOLVENT CDCl3
 NS 16
 DS 2
 SWH 8223.685 Hz
 FIDRES 0.125483 Hz
 AQ 3.9846387 sec
 RG 80.6
 DW 60.800 usec
 DE 6.50 usec
 TE 74.9 K
 D1 1.000000000 sec

CHANNEL F1
 NUCL 1H
 P1 13.75 usec
 SI 65536
 SE 400.1300134 MHz
 WDW EM
 SSB 0
 LB 0.30 Hz
 GB 0
 PC 1.00

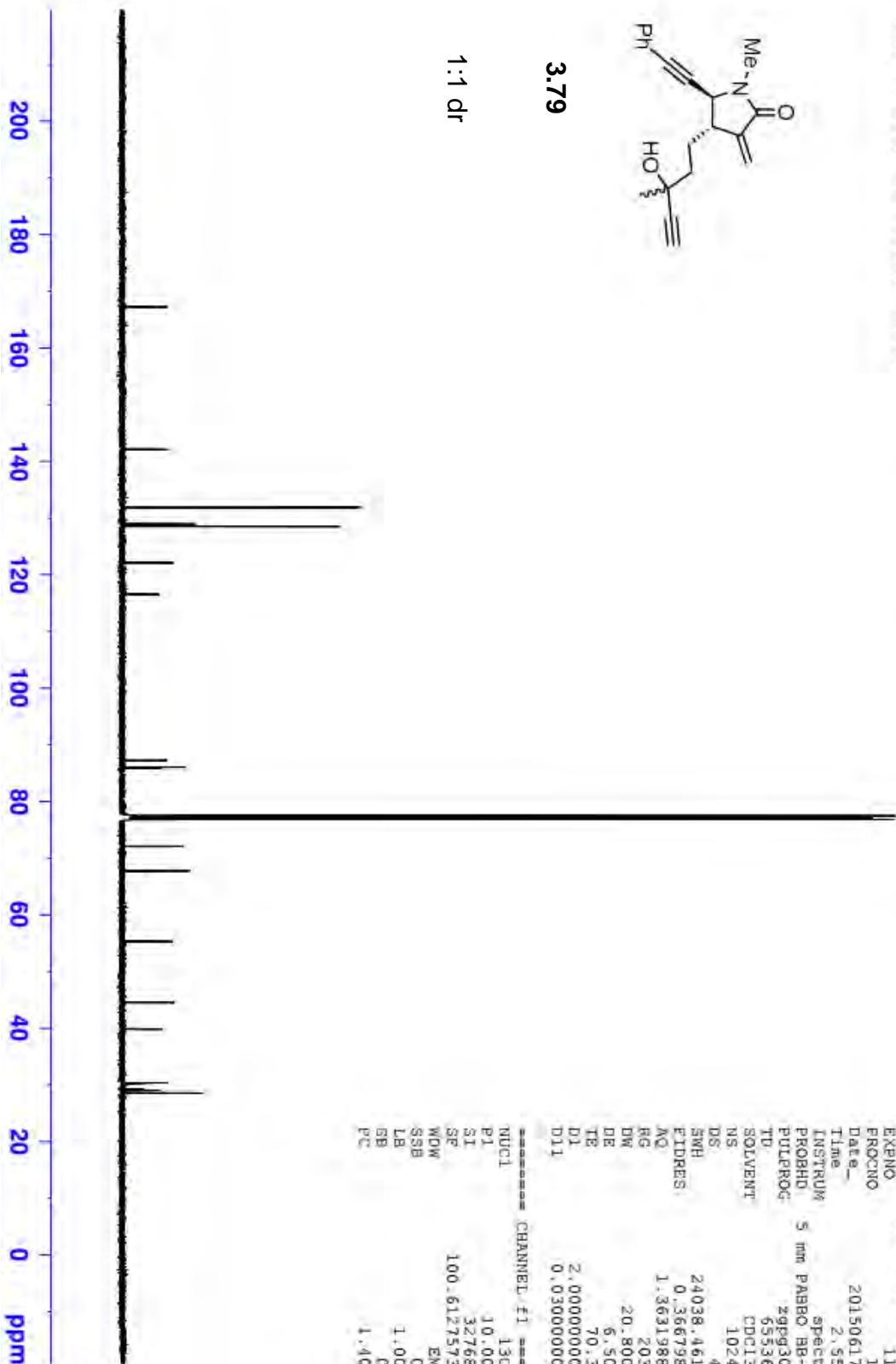


PAJ 7-114, 35 trans CNMR

- 167.25
- 142.14
- 142.12
- 131.86
- 128.93
- 128.53
- 122.12
- 116.64
- 116.57
- 87.23
- 86.05
- 85.89
- 77.49
- 77.17
- 76.85
- 72.13
- 72.09
- 67.77
- 67.74
- 55.42
- 55.31
- 44.57
- 44.54
- 39.90
- 39.81
- 30.38
- 30.38
- 29.20
- 29.04
- 28.56

3.79

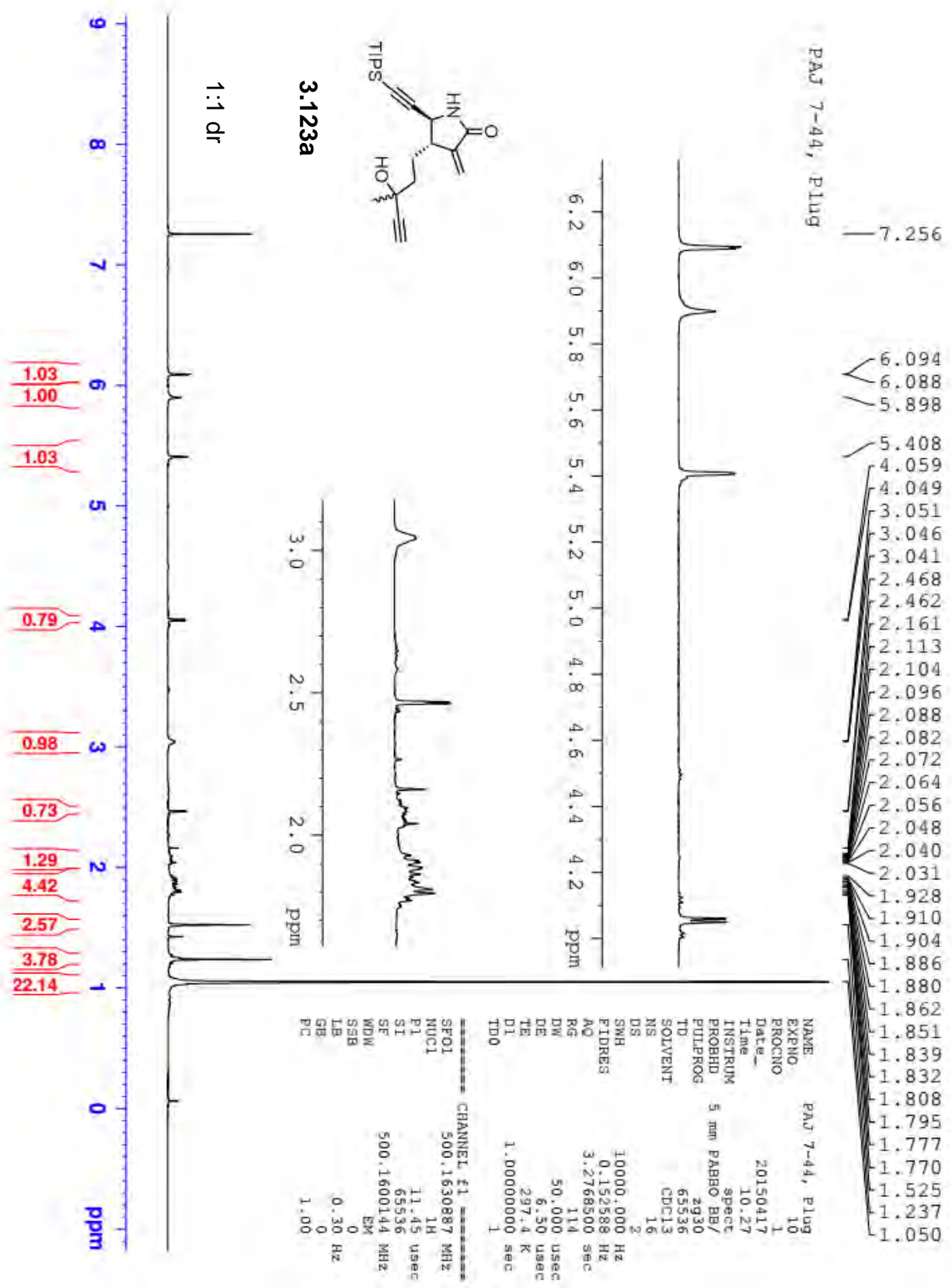
1:1 dr

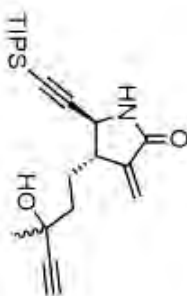


```

NAME          PAJ 7-114, 35 trans
EXPNO         11
PROCNO        1
Date_         20150617
Time          2.55
INSTRUM       spect
PROBHD        5 mm PABBO BB-
PULPROG       zgpg30
TD            65536
SOLVENT       CDCl3
NS            1024
DS            4
SWH           24038.461 Hz
FIDRES        0.366798 Hz
AQ            1.3631988 sec
RG            203
DE            20.800 usec
TE            70.3 K
D1            2.00000000 sec
D11           0.03000000 sec

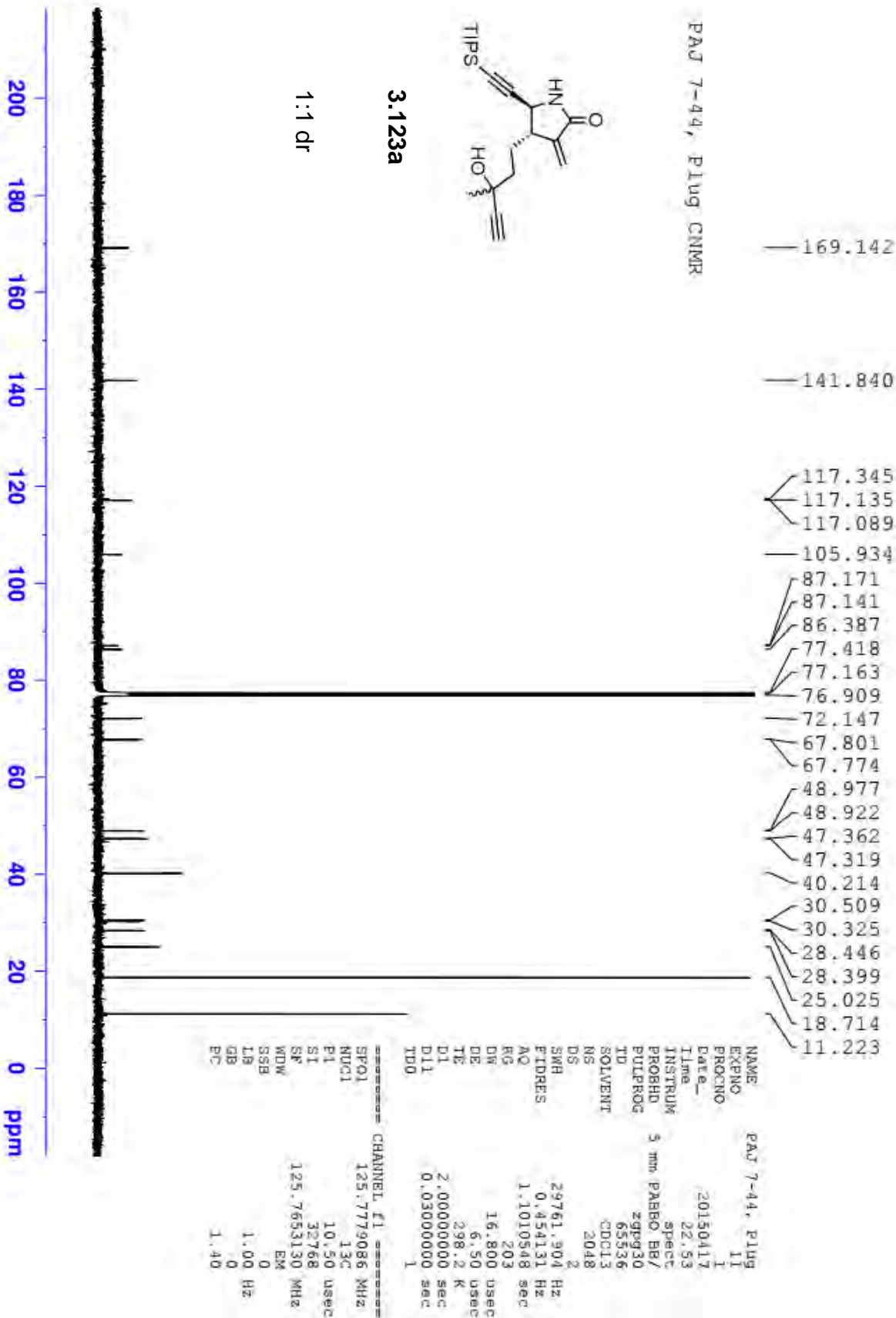
===== CHANNEL f1 =====
NUC1          13C
P1            10.00 usec
SI            32768
SF            100.6127573 MHz
WDW           EM
SSB           0
LB            1.00 Hz
GB            0
PC            1.40
  
```

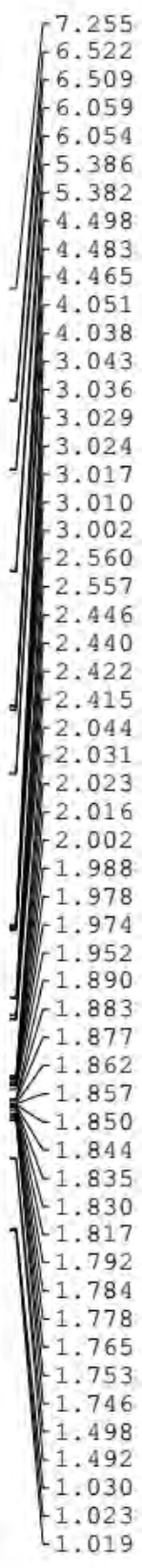




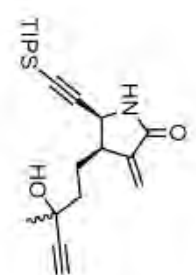
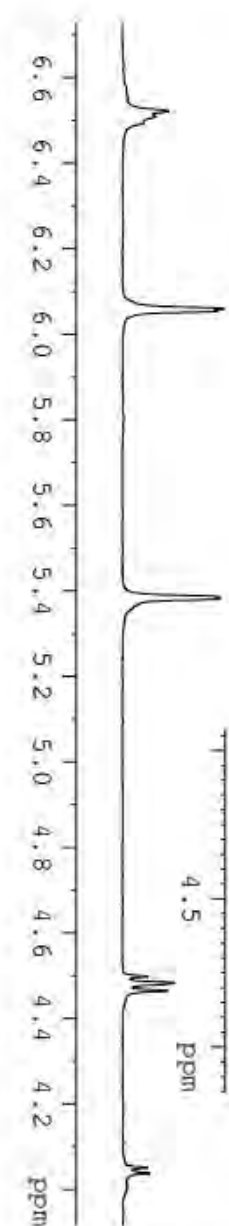
3.123a

1:1 dr





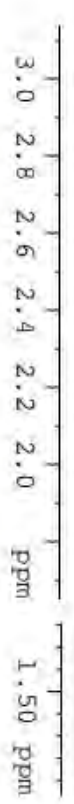
PAJ 8-34, 4



3.123b

1.8:1 cis:trans

1:1 dr



```

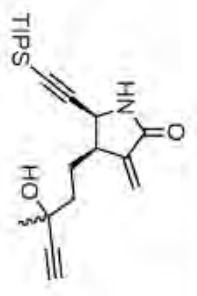
NAME          PAJ 8-34, 4
EXPNO         10
PROCNO        1
Date_         20151027
Time          15.21
INSTRUM       5 mm PABBO BB-
PROBHD        spect
PULPROG       zg30
TD            65536
SOLVENT       CDCl3
NS            16
DS            2
SWH           8012.820 Hz
FIDRES       0.122266 Hz
AQ           4.0894966 sec
RG           32
DE           62.400 usec
TE           97.2 K
D1           1.00000000 sec
TD0          1

----- CHANNEL f1 -----
SEQL          400.1324710 MHz
NUCL          1H
P1            13.75 usec
SI            65536
SF           400.1300115 MHz
MDW           EM
SSB           0
LB           0.30 Hz
GB           0
PC           1.00

```

- 170.35
- 170.33
- 169.45
- 142.00
- 141.83
- 117.16
- 117.02
- 116.92
- 105.99
- 103.19
- 103.02
- 88.65
- 88.50
- 87.66
- 87.32
- 86.15
- 77.47
- 77.16
- 76.84
- 72.02
- 71.95
- 71.70
- 67.89
- 67.66
- 67.60
- 49.03
- 47.98
- 47.93
- 47.28
- 42.82
- 42.67
- 40.41
- 40.19
- 30.24
- 29.97
- 25.18
- 25.04
- 24.85
- 18.70
- 18.67
- 11.16

PAJ 8-34, 4 CNMR2



3.123b

1.8:1 cis:trans

1:1 dr



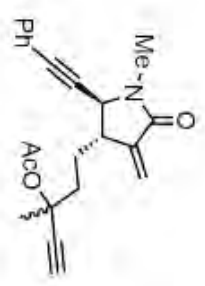
```

NAME          PAJ 8-34, 4
EXPNO         20
PROCNO        1
Date_         20151028
Time          0.32
INSTRUM       spect
PROBHD        5 mm FAREBO BB-
PULPROG       zgpg30
TD            65536
SOLVENT       CDCl3
NS            1024
DS            4
SWH           24038.461 Hz
FIDRES        0.366798 Hz
AQ            1.3631988 sec
RG            203
DW            20.800 usec
DE            6.50 usec
TE            300.2 K
D1            2.00000000 sec
D11           0.03000000 sec
TD0           1

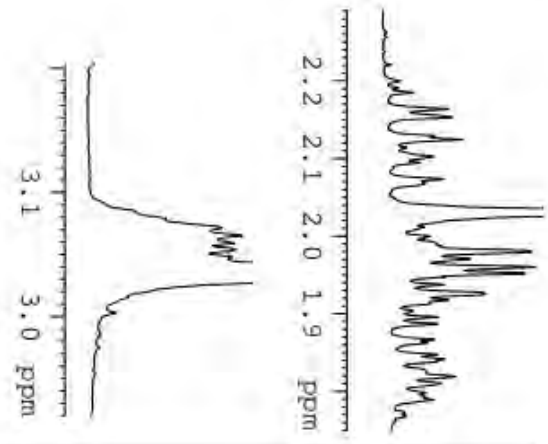
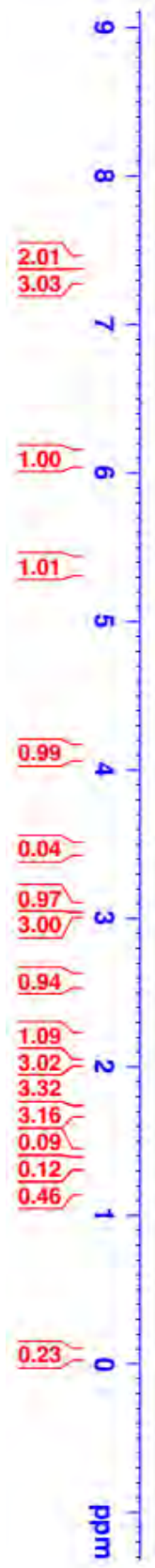
===== CHANNEL f1 =====
SFO1          100.6228293 MHz
NUC1          13C
P1            10.00 usec
SI            32768
SE            100.6127574 MHz
XWDW          EM
SSB           0
LMB           1.00 Hz
GB            0
PC            1.40
  
```

PAJ 6-206, 3-6

7.420
7.416
7.411
7.409
7.407
7.402
7.396
7.341
7.338
7.329
7.325
7.318
7.312
7.308
7.294
7.253
6.106
6.099
5.374
5.369
4.122
4.112
3.078
3.071
3.065
3.059
3.054
3.048
3.034
2.580
2.579
2.164
2.153
2.129
2.124
2.102
2.094
2.073
2.068
2.031
1.980
1.960
1.952
1.926
1.896
1.887
1.848
1.842
1.839
1.819
1.810
1.701
1.239
0.057

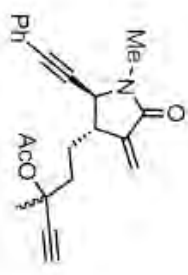


3.80
1:1 dr



NAME PAJ 6-206, 3-6
EXPNO 10
PROCNO 1
Date_ 20150305
Time 16.31
INSTRUM spect
PROBHD 5 mm PABBO BB-
PULPROG zg30
TR 65536
SOLVENT CDCl3
NS 16
DS 2
SWH 8223.685 Hz
FIDRES 0.125483 Hz
AQ 3.9846387 sec
RG 71.8
DM 60.800 usec
DE 6.50 usec
TE 94.8 K
D1 1.00000000 sec

CHANNEL F1
NUC1 1H
P1 13.75 usec
S1 65536
SF 400.1300135 MHz
WDW EM
SSB 0
LB 0.30 Hz
GB 0
PC 1.00



PAJ 6-206, 3-6 CNMR

- 169.42
- 169.39
- 167.10
- 142.04
- 131.85
- 128.96
- 128.54
- 122.10
- 116.57
- 116.53
- 85.96
- 83.42
- 83.39
- 77.48
- 77.37
- 77.16
- 76.84
- 74.51
- 74.48
- 74.02
- 74.00
- 55.30
- 55.22
- 44.48
- 44.42
- 38.23
- 38.19
- 28.63
- 28.57
- 28.53
- 26.71
- 26.66
- 22.01

3.80
1:1 dr



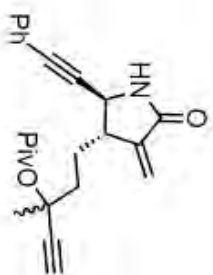
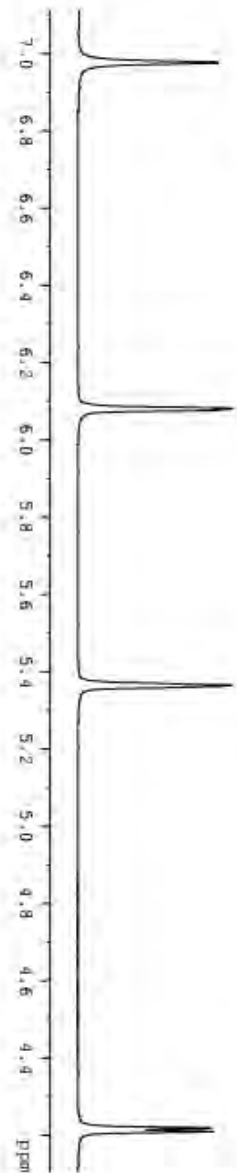
```

NAME          PAJ 6-206, 3-6
EXPNO         11
PROCNO        1
Date_         20150306
Time_         6.01
INSTRUM       spect
PROBHD        5 mm PABBO BB-
PULPROG       zgpg30
TD            65536
SOLVENT       CDCl3
NS            2048
DS            4
SMH           24038.461 Hz
FIDRES        0.366798 Hz
AQ            1.3631988 sec
RG            203
DW            20.800 usec
DE            6.50 usec
TE            96.5 K
D1            2.00000000 sec
D11           0.03000000 sec

===== CHANNEL F1 =====
NUC1          13C
P1            10.00 usec
SI            32768
SF            100.6127570 MHz
WDW           EM
SSB           0
LB            1.00 Hz
GB            0
PC            1.40
  
```

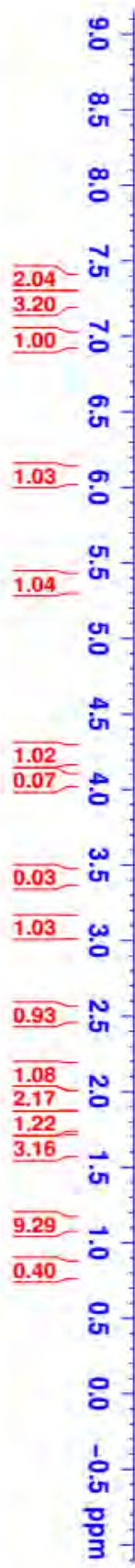
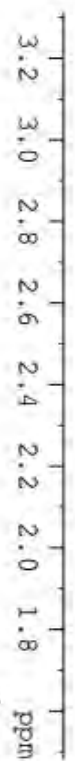
PAJ 6-160, 12-22

Chemical Shift (ppm)	Integration
7.352	
7.340	
7.336	
7.268	
7.255	
7.247	
7.240	
7.228	
7.207	
6.976	
6.081	
6.077	
5.364	
4.218	
4.209	
3.097	
3.093	
3.089	
2.499	
2.124	
2.107	
2.099	
2.082	
2.075	
2.064	
2.059	
2.041	
1.954	
1.940	
1.936	
1.925	
1.918	
1.909	
1.904	
1.896	
1.843	
1.823	
1.814	
1.805	
1.799	
1.781	
1.768	
1.766	
1.637	
1.125	



3.113a

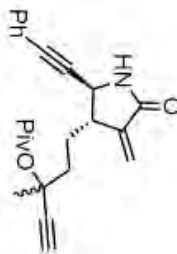
1:1 dr



NAME PAJ 6-160, 12-22
 EXPNO 10
 PROCNO 1
 Date_ 20150129
 Time 10.04
 INSTRUM spect
 PROBD 5 mm PABBO BB/
 PULPROG zg30
 TD 65536
 SOLVENT CDCl3
 NS 16
 DS 2
 SWH 10000.000 Hz
 FIDRES 0.152588 Hz
 AQ 3.2768500 sec
 RG 32
 DW 50.000 usec
 DE 6.50 usec
 TE 300.8 K
 D1 1.00000000 sec
 TD0 1

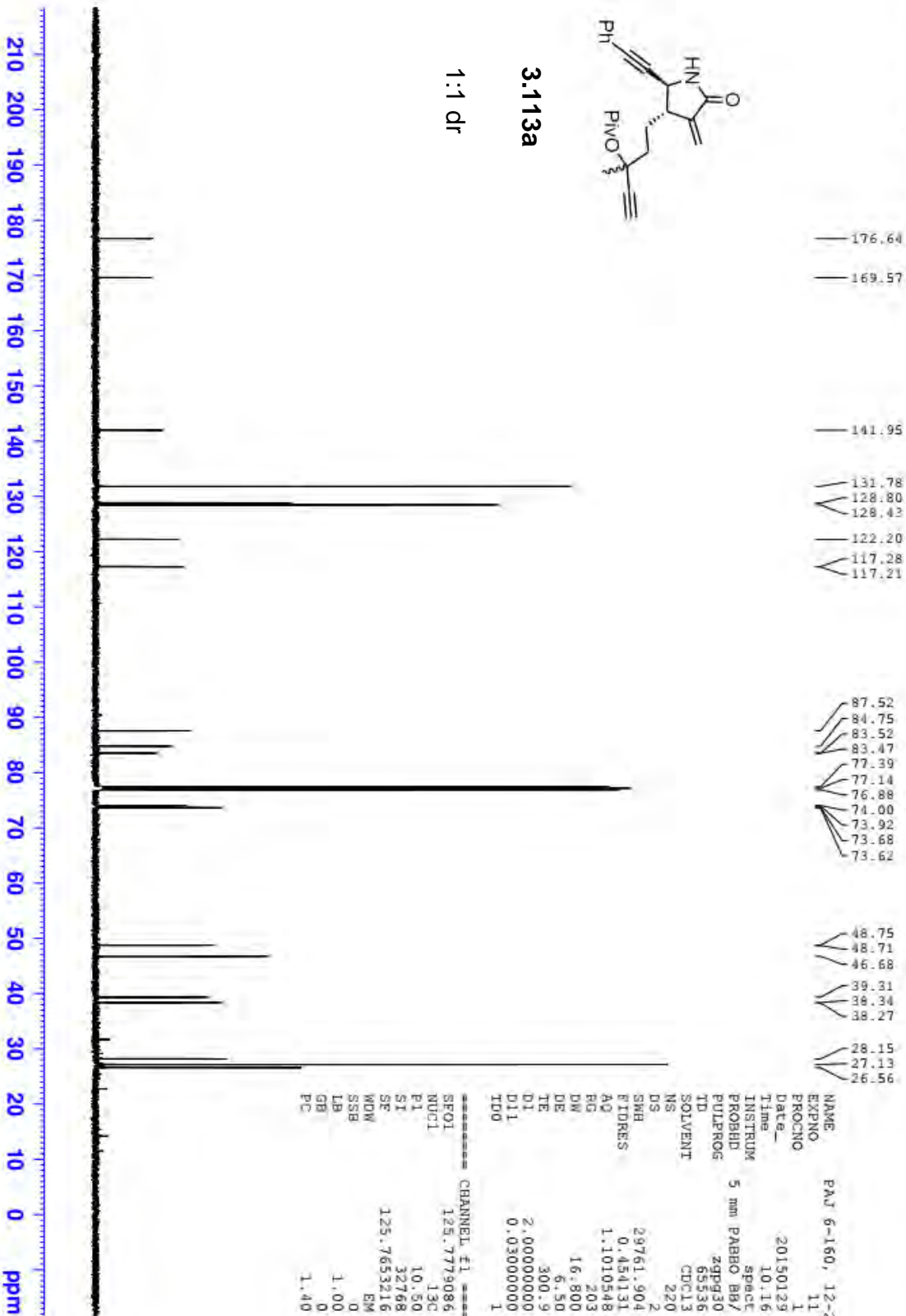
CHANNEL F1
 SF01 500.1630887 MHz
 NUC1 1H
 P1 11.45 usec
 SI 65536
 SF 500.1600385 MHz
 WDM EM
 SSB 0
 LB 0.30 Hz
 GB 0
 PC 1.00

PAD 6-160, 12-22 CNMR



3.113a

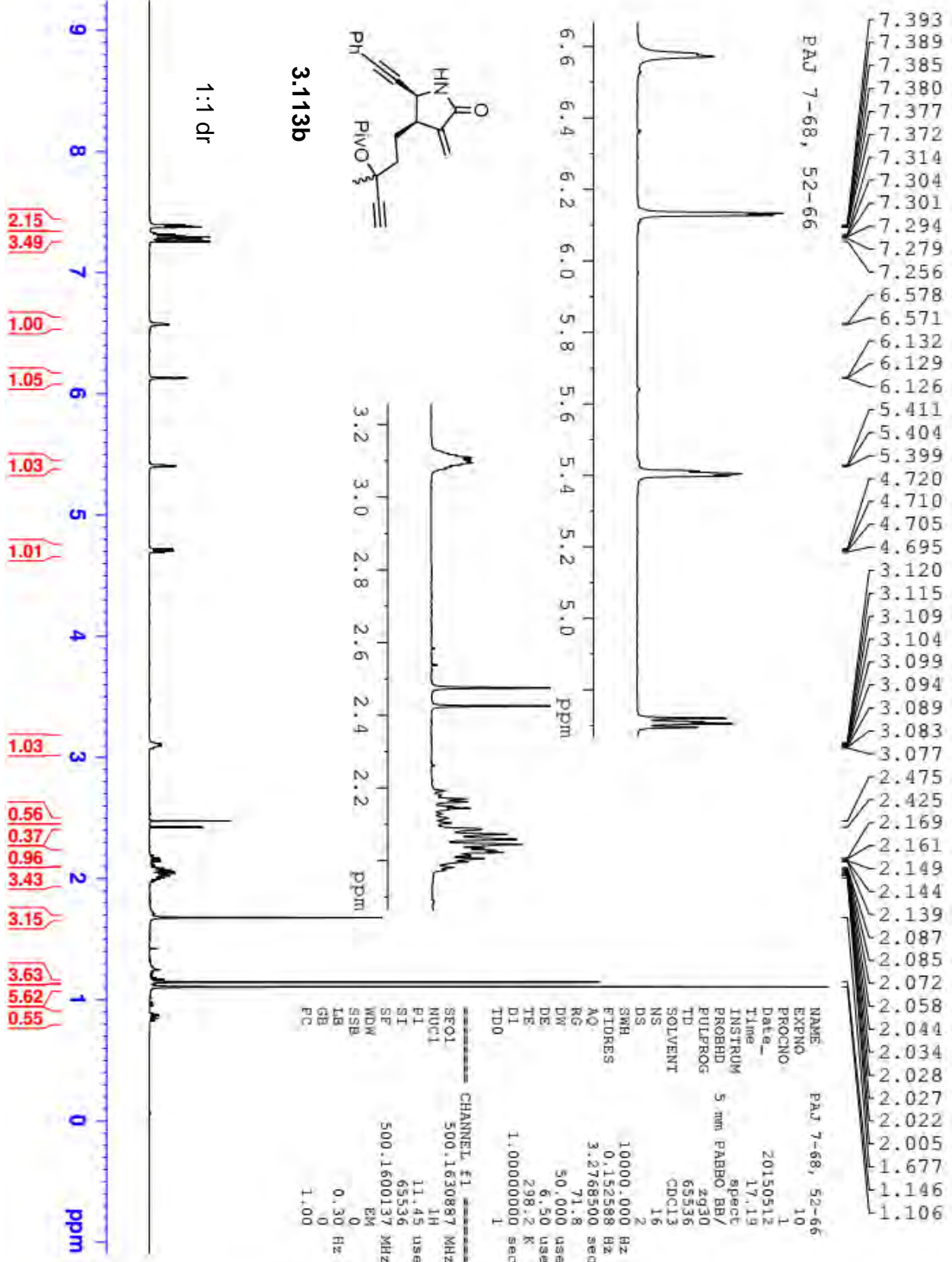
1:1 dr

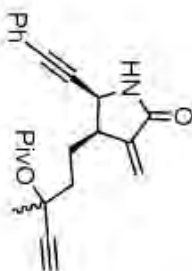


```

NAME          PAD 6-160, 12-22
EXPNO         11
PROCNO        1
Date_         20150129
Time         10.16
INSTRUM       spect
PROBHD        5 mm PABBO Bb/
PULPROG       zgpg30
TD            65536
FIDRES        0.454131 Hz
AQ            1.1010548 sec
RG            203
DE            16.800 usec
TE            300.9 K
D1            2.00000000 sec
D11           0.030000000 sec
TD0           1

===== CHANNEL f1 =====
SFO1          125.7779086 MHz
NUC1          13C
P1            10.50 usec
SI            32768
SF            125.7653216 MHz
WDW           EM
SSB           0
LB            1.00 Hz
GB            0
PC            1.40
  
```





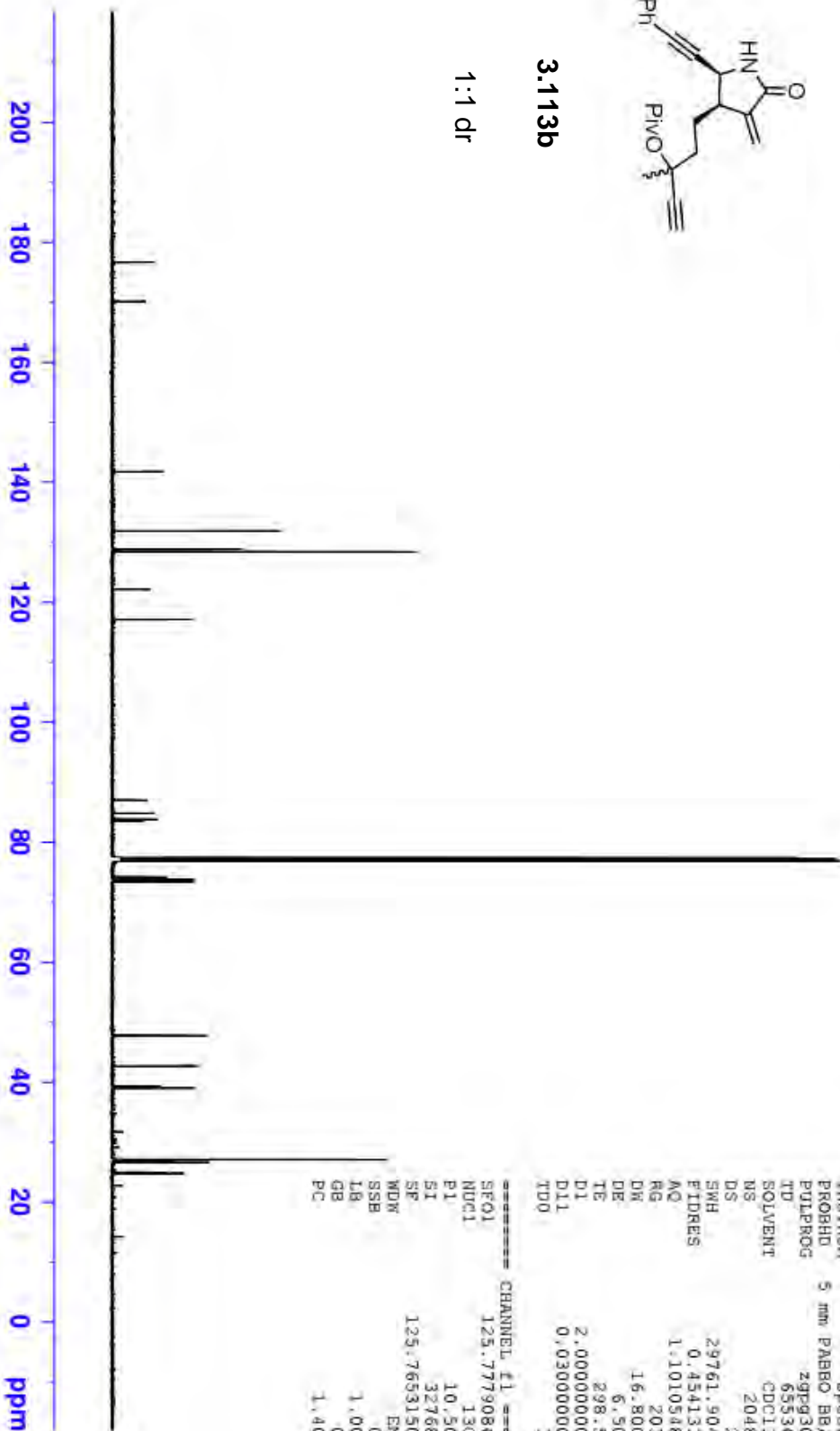
3.113b

1:1 dr

PAJ 7-68, 52-66 CNMR

176.712
170.204
170.152

141.802
141.749
131.910
131.887
128.890
128.442
122.202
122.179
117.148
87.033
86.989
84.893
84.848
83.839
83.528
77.415
77.160
76.906
74.198
73.852
73.687
73.463
47.781
42.700
42.679
39.324
39.297
39.058
39.035
27.140
27.101
26.731
26.640
24.988
24.788



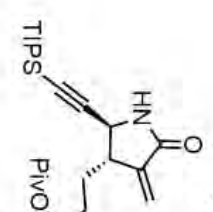
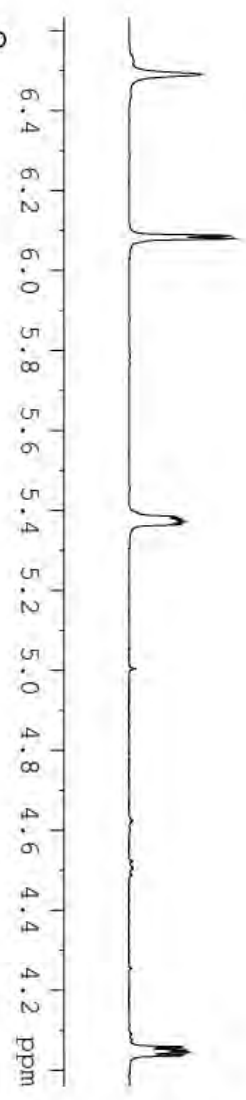
```

NAME          PAJ 7-68, 52-66
EXPNO         11
PROCNO        1
Date_         20150513
Time          4.52
INSTRUM       spect
PROBHD        5 mm PABBO BB/
PULPROG       zgpg30
TD            65536
SOLVENT       CDCl3
NS            2048
DS            2
SWH           29761.904 Hz
FIDRES       0.454131 Hz
AQ           1.1010548 sec
RG           203
DE           16.800 usec
TE           298.5 K
D1           2.00000000 sec
D11          0.03000000 sec
TD0          1

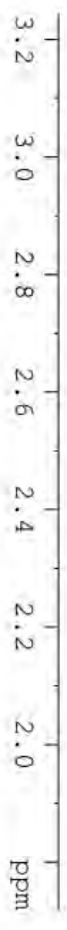
===== CHANNEL f1 =====
SFO1         125.7779086 MHz
NUC1         13C
P1           10.50 usec
SI           32768
SF           125.7653150 MHz
WDW          EM
SSB          0
LB           1.00 Hz
GB           0
PC           1.40
  
```

7.252
6.489
6.086
6.079
5.382
5.376
5.371
5.365
4.056
4.049
4.043
4.036
3.470
3.452
3.047
3.040
3.034
3.026
3.020
3.013
2.532
2.527
2.154
2.144
2.123
2.112
2.062
2.053
2.044
2.029
2.021
2.006
1.995
1.982
1.973
1.939
1.908
1.900
1.876
1.868
1.820
1.810
1.800
1.788
1.779
1.767
1.758
1.670

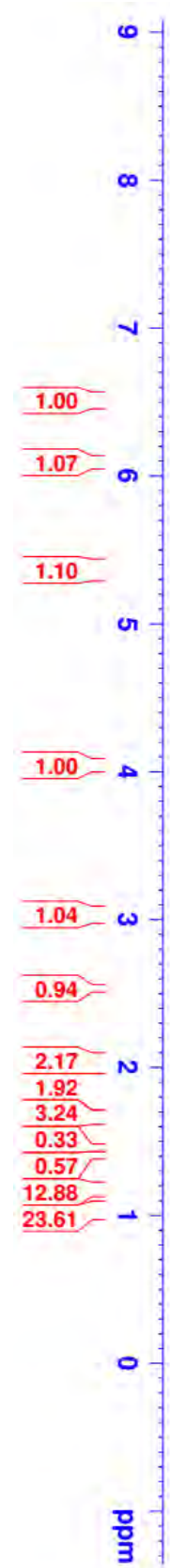
PAJ 7-50, 1-5



3.124a



1:1 dr

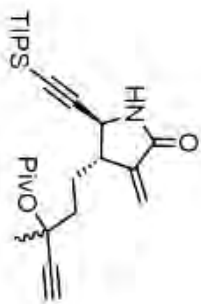


```

NAME          PAJ 7-50, 1-5
EXPNO         10
PROCNO        1
Date_         20150505
Time          17.36
INSTRUM       5 mm PABBO BB-
PROBHD        spect
PULPROG       zg30
TD            65536
SOLVENT       CDCl3
NS            16
DS            2
SMW           8223.685 Hz
FIDRES        0.125483 Hz
AQ            3.9846387 sec
RG            32
DM            60.800 usec
DE            6.50 usec
TE            91.3 K
D1            1.000000000 sec

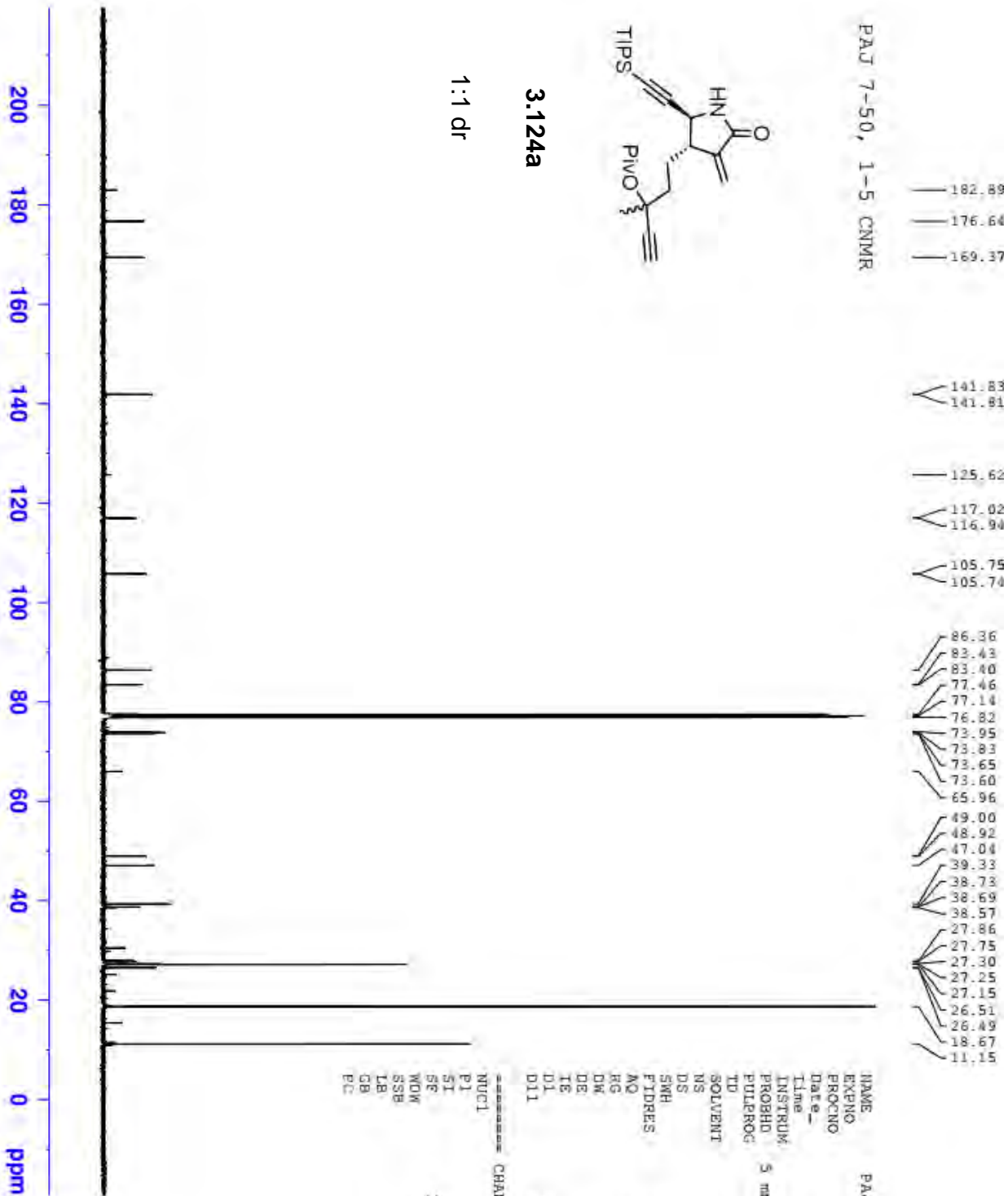
===== CHANNEL f1 =====
NUC1          1H
P1            13.75 usec
SI            65536
SF            400.1300132 MHz
WDW           EM
SSB           0
LB            0.30 Hz
GB            0
PC            1.00

```

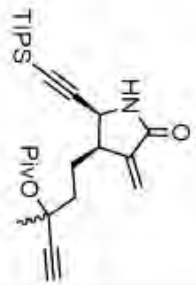
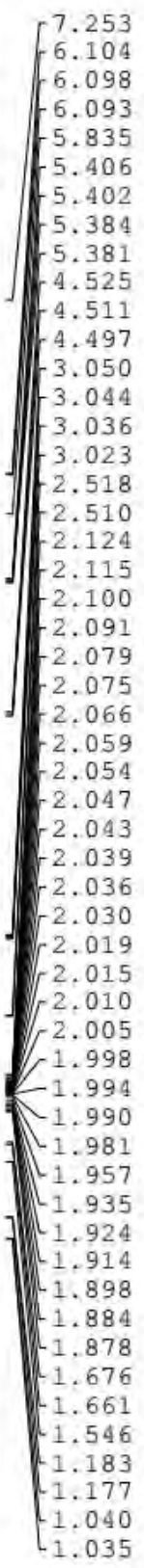


3.124a

1:1 dr

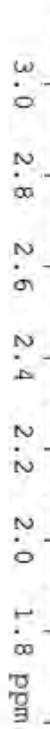


PAJ 8-38, cis, 65-75



3.124b

1:1 dr



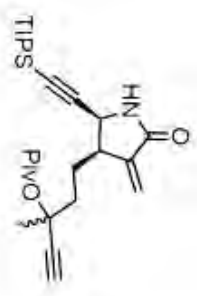
```

NAME          PAJ 8-38, cis, 65-75
EXPNO         10
PROCNO        1
Date_         20151028
Time         18.14
INSTRUM       spect
PROBHD        5 mm PABBO BB/
PULPROG       zg30
TD            65536
SOLVENT       CDCl3
NS            16
DS            2
SMH           10000.000 Hz
FIDRES        0.152888 Hz
AQ            3.2768500 sec
RG            203
DW            50.000 usec
DE            6.50 usec
TE            297.6 K
D1            1.00000000 sec
TD0           1

----- CHANNEL f1 -----
SFO1          500.1630887 MHz
NUC1          1H
P1            11.45 usec
S1            65536
SE           500.1600161 MHz
WDW           EM
SSB           0
LB            0.30 Hz
GB            0
PC            1.00
  
```

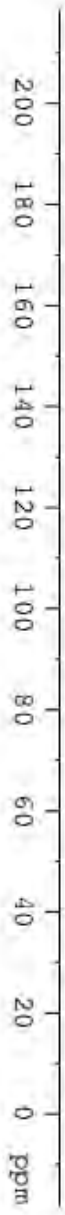
- 176.744
- 169.848
- 169.766
- 141.647
- 141.610
- 117.276
- 117.222
- 103.044
- 102.992
- 88.956
- 88.877
- 83.907
- 83.358
- 77.413
- 77.159
- 76.905
- 74.323
- 73.883
- 73.853
- 73.436
- 47.863
- 42.813
- 42.634
- 39.363
- 39.347
- 39.008
- 38.780
- 27.199
- 27.188
- 26.623
- 26.349
- 24.967

PAJ 8-38, 65-75 C1s CNMR



3.124b

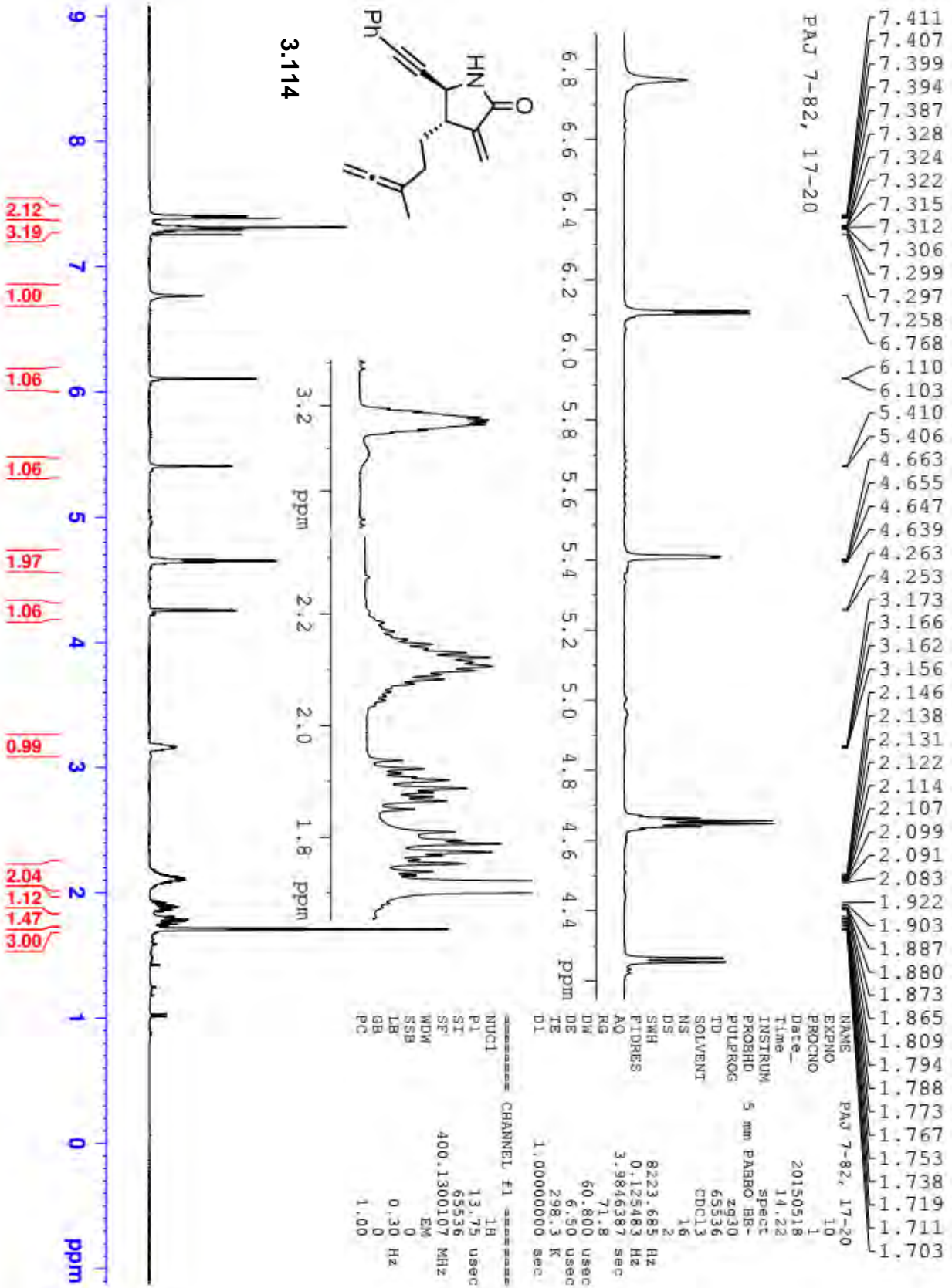
1:1 dr

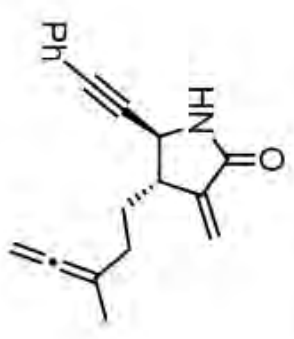


```

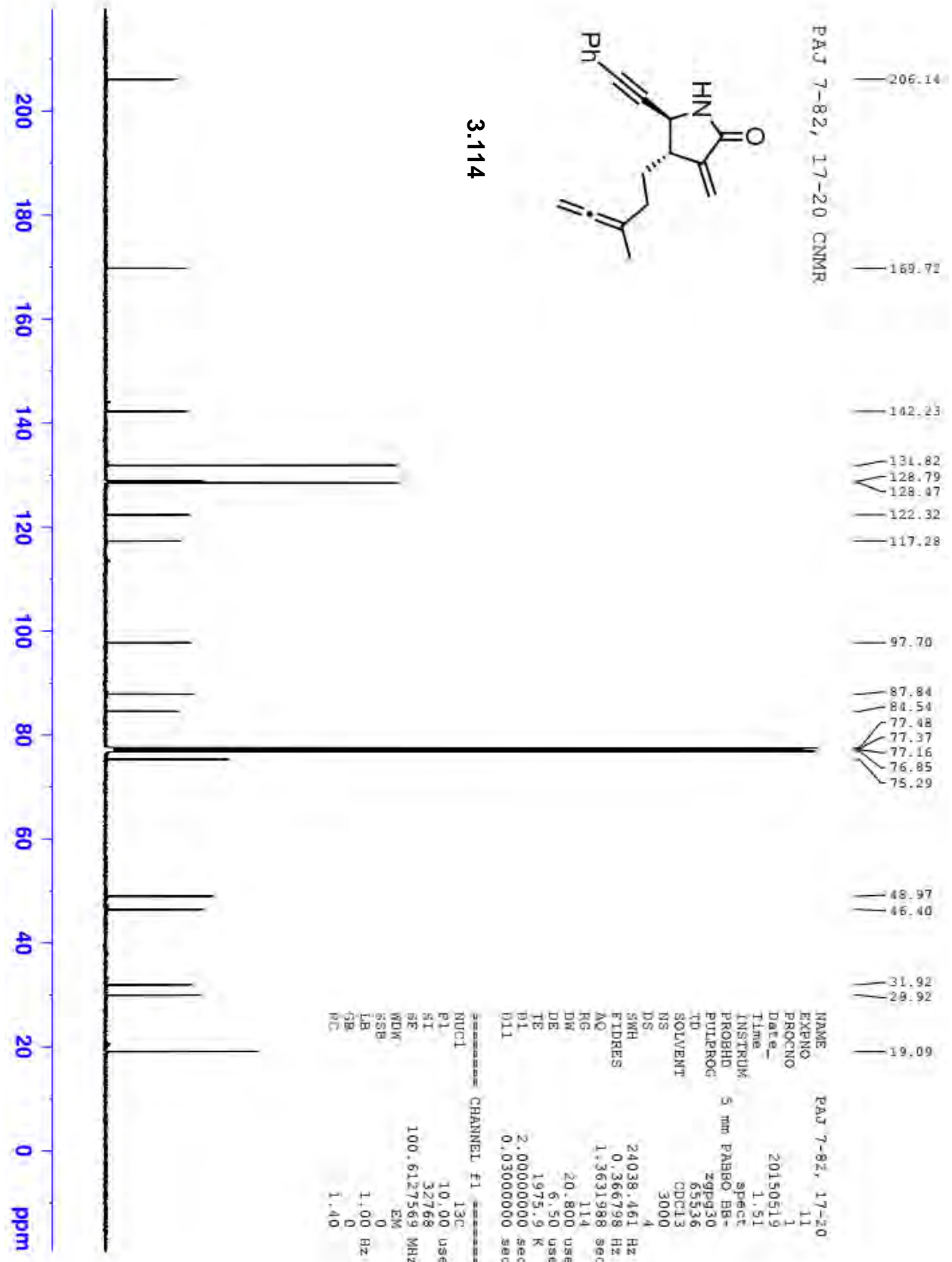
NAME          PAJ 8-38, 65-75 C1s
EXPNO         10
PROCNO        1
Date_         20151107
Time          4.07
INSTRUM       spect
PROBHD        5 mm PABBO BB/
PULPROG       zgpg30
TD            65536
SOLVENT       CDCl3
NS            3000
DS            2
SWH           29761.904 Hz
FIDRES        0.454131 Hz
AQ            1.1010548 sec
RG            203
DW            16.800 usec
DE            6.50 usec
TE            298.5 K
D1            2.00000000 sec
D11           0.03000000 sec
TD0           1

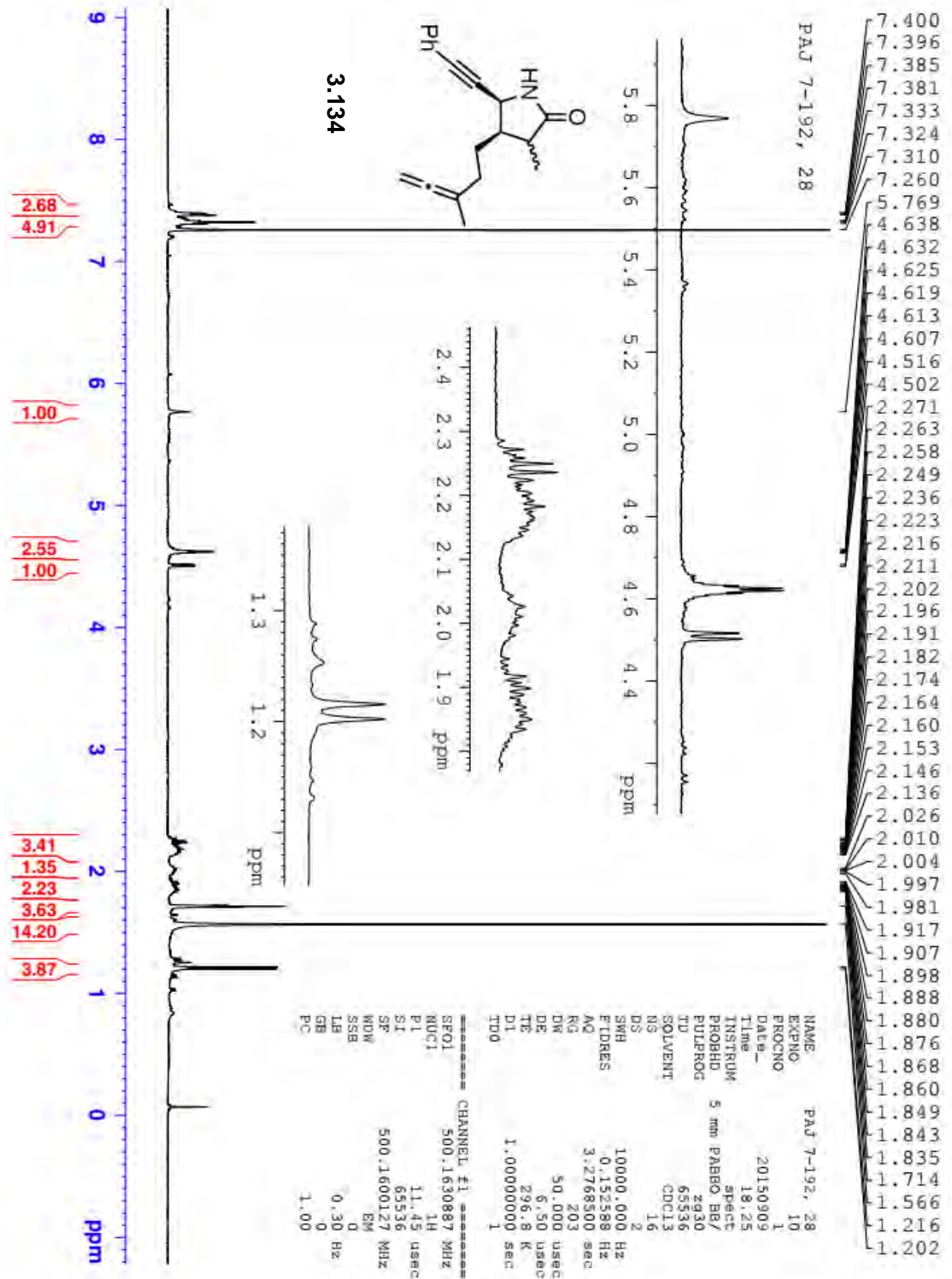
===== CHANNEL f1 =====
SFO1          125.7779086 MHz
NUC1          13C
P1            10.50 usec
SI            32768
SF            125.7653129 MHz
WDW           EM
SSB           0
LB            1.00 Hz
GB            0
PC            1.40
  
```

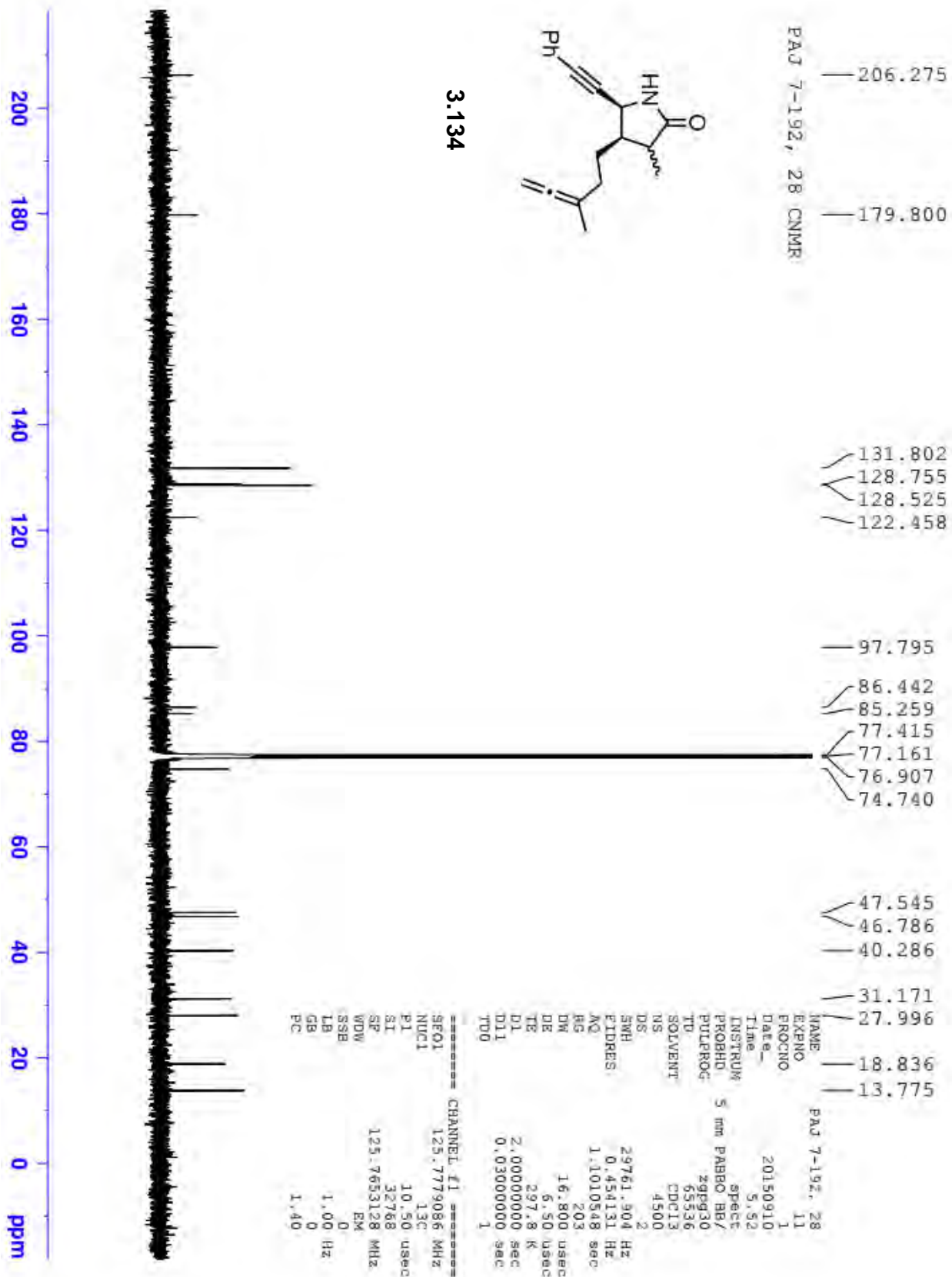




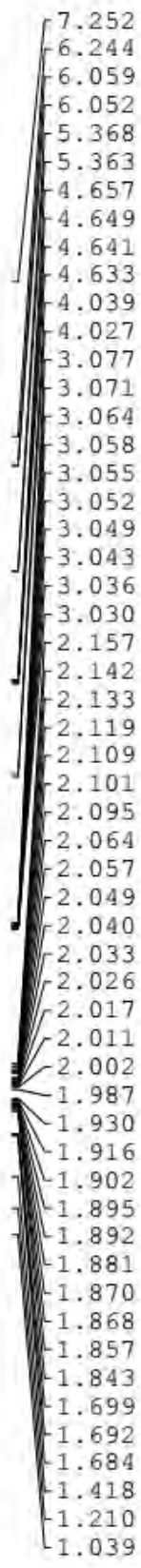
3.114



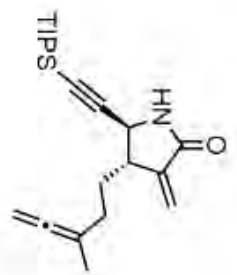
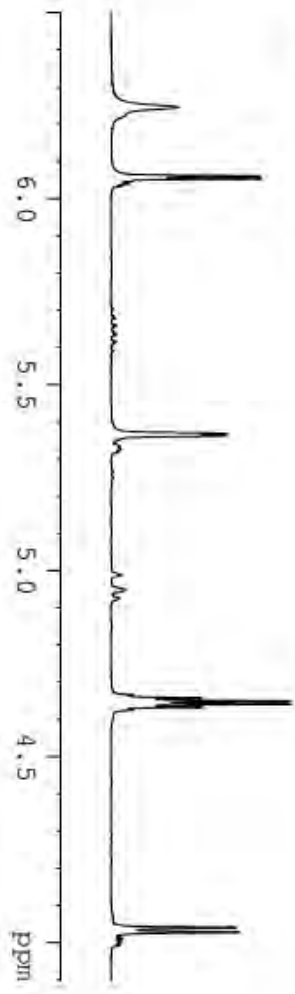




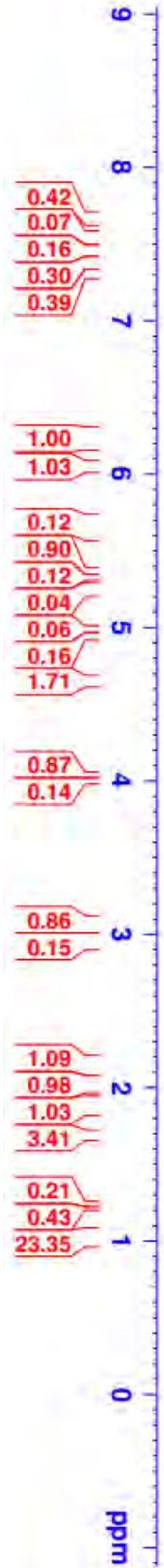
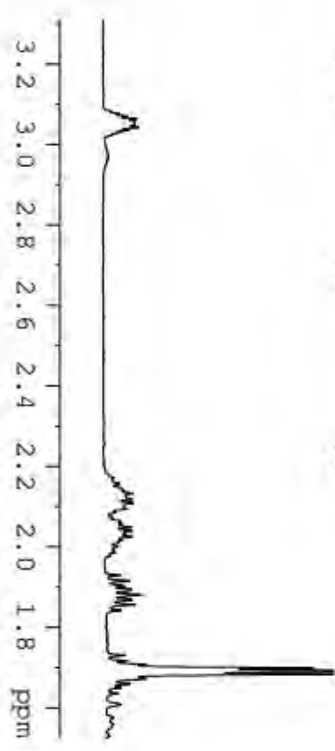
3.134



PAJ 7-74, 35-39



3.125



0.42
0.07
0.16
0.30
0.39

1.00
1.03

0.12
0.90
0.12
0.04
0.06
0.16
1.71

0.87
0.14

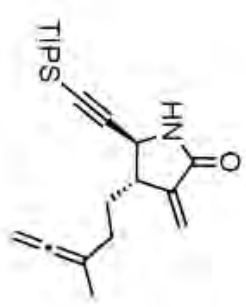
0.86
0.15

1.09
0.98
1.03
3.41

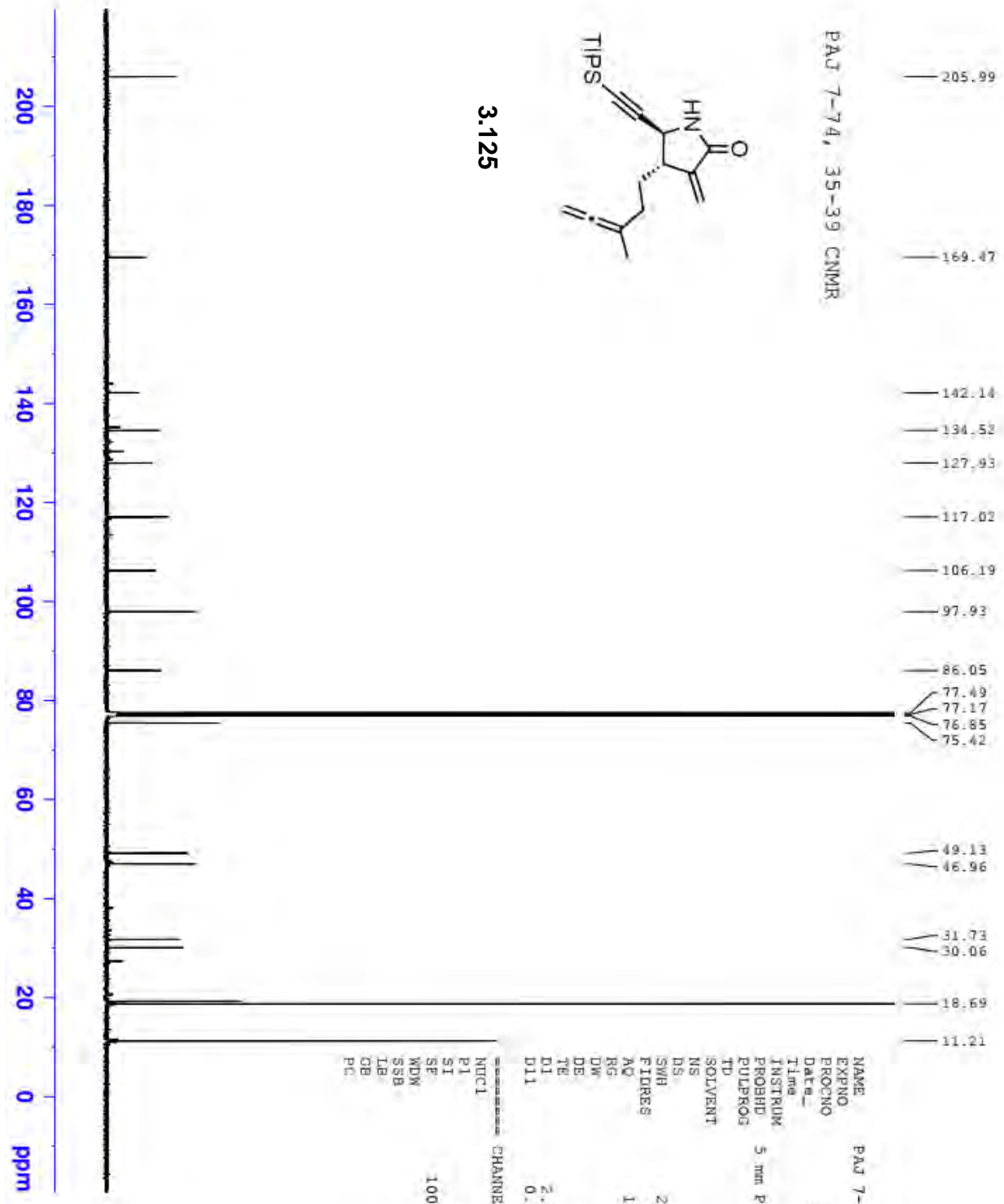
0.21
0.43
23.35

NAME: PAJ 7-74, 35-39
 EXPNO: 10
 PROCNO: 1
 Date_: 20150512
 Time: 14.34
 INSTRUM: 5 mm PABBO BB-
 PROBH1: spect
 PULPROG: zg30
 TD: 65536
 SOLVENT: CDCl3
 NS: 16
 DS: 2
 SWH: 8223.685 Hz
 FIDRES: 0.125483 Hz
 AQ: 3.9846387 sec
 RG: 57
 DW: 60.800 usec
 DE: 6.50 usec
 TE: 453.3 K
 D1: 1.00000000 sec

***** CHANNEL f1 *****
 NUC1: 1H
 P1: 13.75 usec
 ST: 65536
 SF: 400.1300128 MHz
 WDW: EM
 SSB: 0
 LB: 0.30 Hz
 GB: 0
 PC: 1.00



3.125



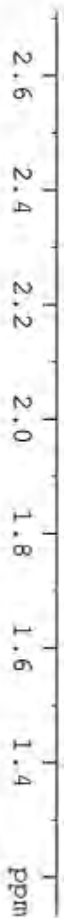
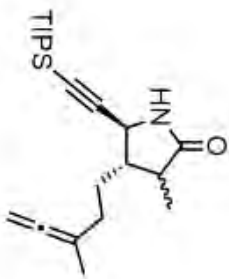
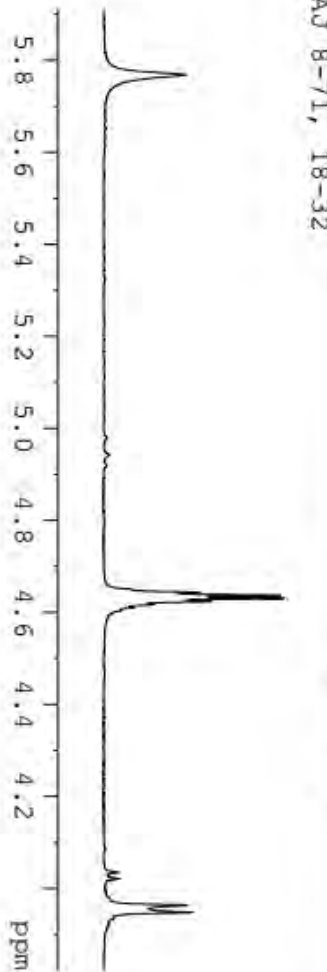
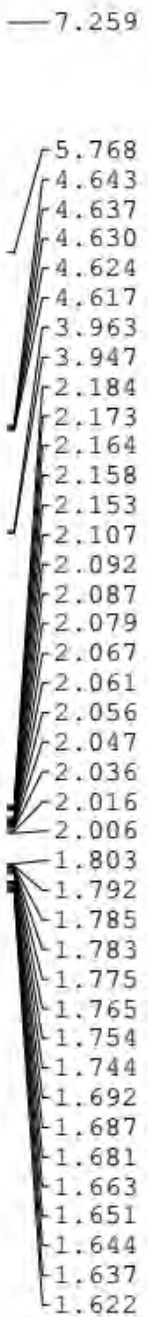
PAD 7-74, 35-39 CNMR

```

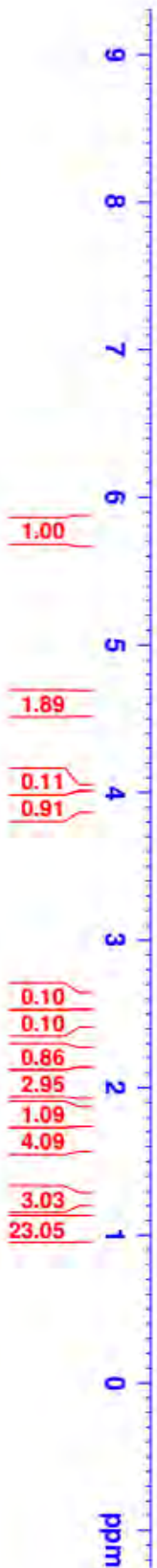
NAME          PAD 7-74, 35-39
EXPNO         11
PROCNO        1
Date_         20150513
Time          1.13
INSTRUM       spect
PROBHD        5 mm PABBO BB-
PULPROG       zgpg30
TD            65536
SOLVENT       CDCl3
NS            3056
DS            4
SWH           21038.461 Hz
FIDRES        0.366798 Hz
AQ            1.3631988 sec
RG            203
DE            20.800 usec
TE            -330.0 K
D1            2.00000000 sec
D11           0.03000000 sec

===== CHANNEL f1 =====
NUC1          13C
P1            10.00 usec
SI            32768
SF            100.6127547 MHz
WDW           EM
SSB           0
LB            1.00 Hz
GB            0
PC            1.40
  
```

PAJ 8-71, 18-32



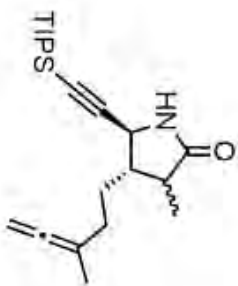
8.3:1 dr



```

NAME          PAJ 8-71, 18-32
EXPNO         10
PROCNO        1
Date_         20151210
Time         17.16
INSTRUM       spect
PROBHD        5 mm PABBO BB/
PULPROG       zg30
TD            65536
SOLVENT       CDCl3
NS            16
DS            2
SMH           10000.000 Hz
FIDRES        0.152588 Hz
AQ            3.2768500 sec
RG            90.5
DE            50.000 usec
TE            298.0 K
D1            1.00000000 sec
TD0           1

===== CHANNEL f1 =====
SFO1          500.1630887 MHz
NUC1          1H
P1            11.45 usec
SI            65536
SF            500.1600127 MHz
WDW           EM
SSB           0
LB            0.30 Hz
GB            0
PC            1.00
  
```



PAJ 8-71, 18-32 CNMR

- 206.010
- 178.520
- 106.333
- 98.195
- 85.879
- 77.415
- 77.161
- 76.907
- 75.300
- 51.461
- 49.720
- 42.404
- 31.122
- 31.043
- 19.139
- 18.702
- 15.076
- 11.250

3.126
8.3:1 dr



```

NAME          PAJ 8-71, 18-32
EXPNO         11
PROCNO        1
Date_         20151210
Time          23.20
INSTRUM       spect
PROBHD        5 mm PABBO BB/
PULPROG       zgpg30
TD            65536
SOLVENT       CDCl3
NS            1024
DS            2
SWH           29761.904 Hz
FIDRES        0.454131 Hz
AQ            1.1010548 sec
RG            203
DW            16.800 usec
DE            6.50 usec
TE            298.8 K
D1            2.00000000 sec
D11           0.03000000 sec
TD0           1

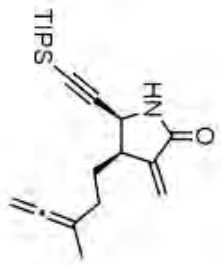
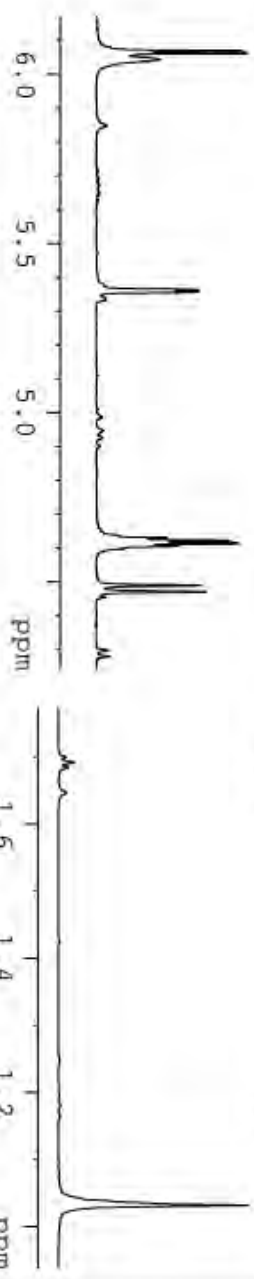
===== CHANNEL f1 =====
SFO1          125.7779086 MHz
NUC1          13C
P1            10.50 usec
SI            32768
SF            125.7653144 MHz
WDW           EM
SSB           0
L8            1.00 Hz
GB            0
PC            1.40

```

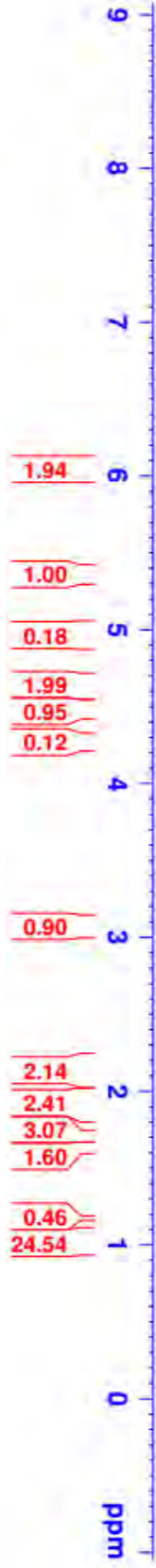
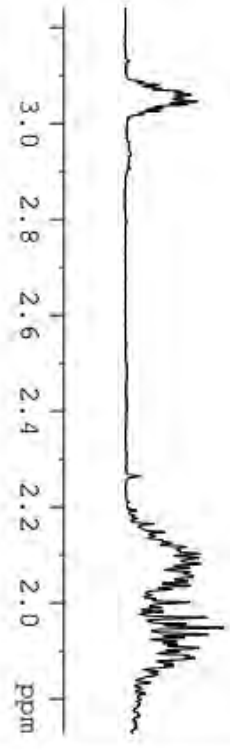
pa1 7-156, 22-28

- 7.257
- 6.067
- 6.060
- 6.042
- 5.362
- 5.357
- 4.628
- 4.621
- 4.613
- 4.605
- 4.489
- 4.470
- 4.295
- 4.279
- 3.073
- 3.066
- 3.059
- 3.052
- 3.046
- 3.039
- 3.033
- 2.165
- 2.148
- 2.140
- 2.125
- 2.117
- 2.103
- 2.094
- 2.082
- 2.056
- 2.045
- 2.036
- 2.029
- 2.001
- 1.970
- 1.956
- 1.948
- 1.934
- 1.927
- 1.919
- 1.913
- 1.906
- 1.899
- 1.891
- 1.885
- 1.873
- 1.868

- 1.699
- 1.691
- 1.684
- 1.646
- 1.181
- 1.164
- 1.031



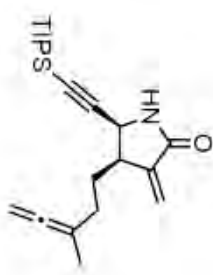
3.135



- 1.94
- 1.00
- 0.18
- 1.99
- 0.95
- 0.12
- 0.90
- 2.14
- 2.41
- 3.07
- 1.60
- 0.46
- 24.54

NAME pa1 7-156, 22-28
 EXPNO 10
 PROCNO 1
 Date_ 20150810
 Time 16.38
 INSTRUM spect
 PROBD 5 mm PABBO BB-
 PULPROG zg30
 TD 65536
 SOLVENT CDCl3
 NS 16
 DS 2
 SWH 8223.685 Hz
 FIDRES 0.125483 Hz
 AQ 3.9846387 sec
 RG 90.5
 DW 60.800 usec
 DE 6.50 usec
 TE 89.8 K
 D1 1.00000000 sec

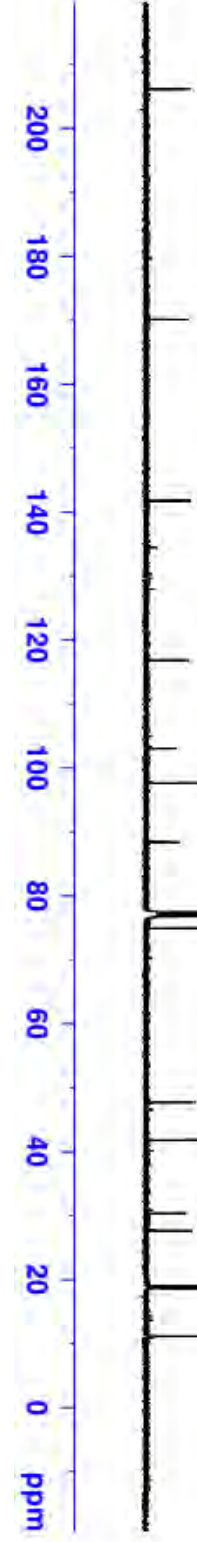
CHANNEL F1
 NUQ1 1H
 P1 13.75 usec
 S1 65536
 SE 400.1300107 MHz
 WDW EM
 SSB 0
 LB 0.30 Hz
 GB 0
 PC 1.00



paJ 7-156, 22-28 CNMR

- 206.16
- 170.16
- 141.82
- 116.86
- 103.08
- 97.67
- 88.43
- 77.47
- 77.35
- 77.15
- 76.83
- 74.96
- 47.75
- 41.82
- 30.36
- 27.65
- 18.99
- 18.70
- 18.66
- 11.19

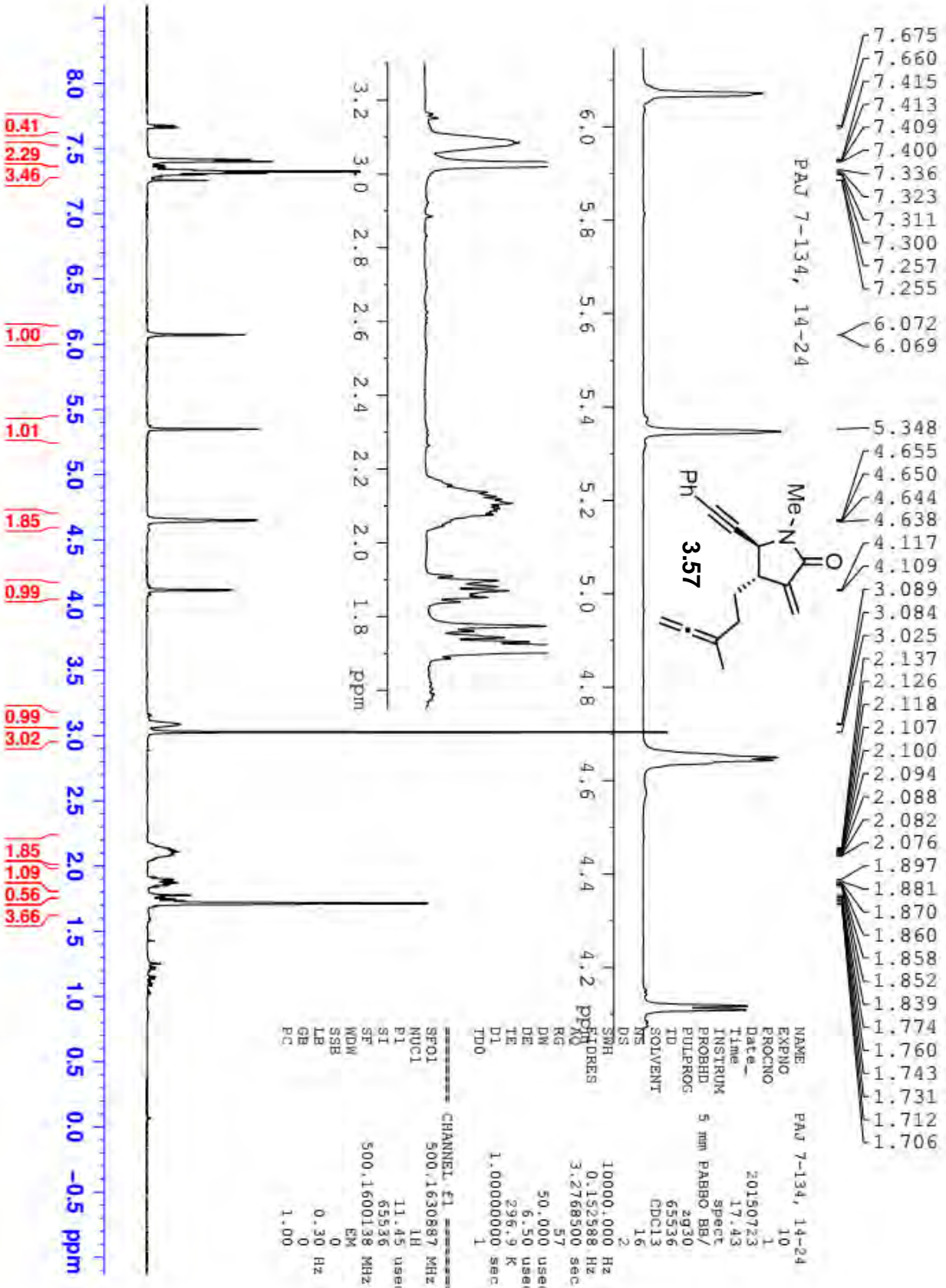
3.135

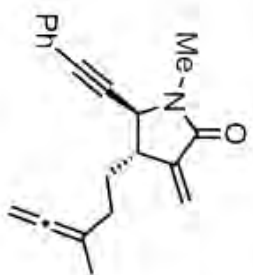


```

NAME      paJ 7-156, 22-28
EXPNO     11
PROCNO    1
Date_     20150811
Time      2.35
INSTRUM   spect
PROBRD    5 mm PABBO BB-
PULPROG   zgpg30
TD         65536
SOLVENT   CDCl3
NS         2048
DS         4
SWH        24038.461 Hz
FIDRES     0.366798 Hz
AQ         1.3631988 sec
RG         181
DW         20.800 usec
DE         6.50 usec
TE         301.2 K
D1         2.00000000 sec
D11        0.03000000 sec

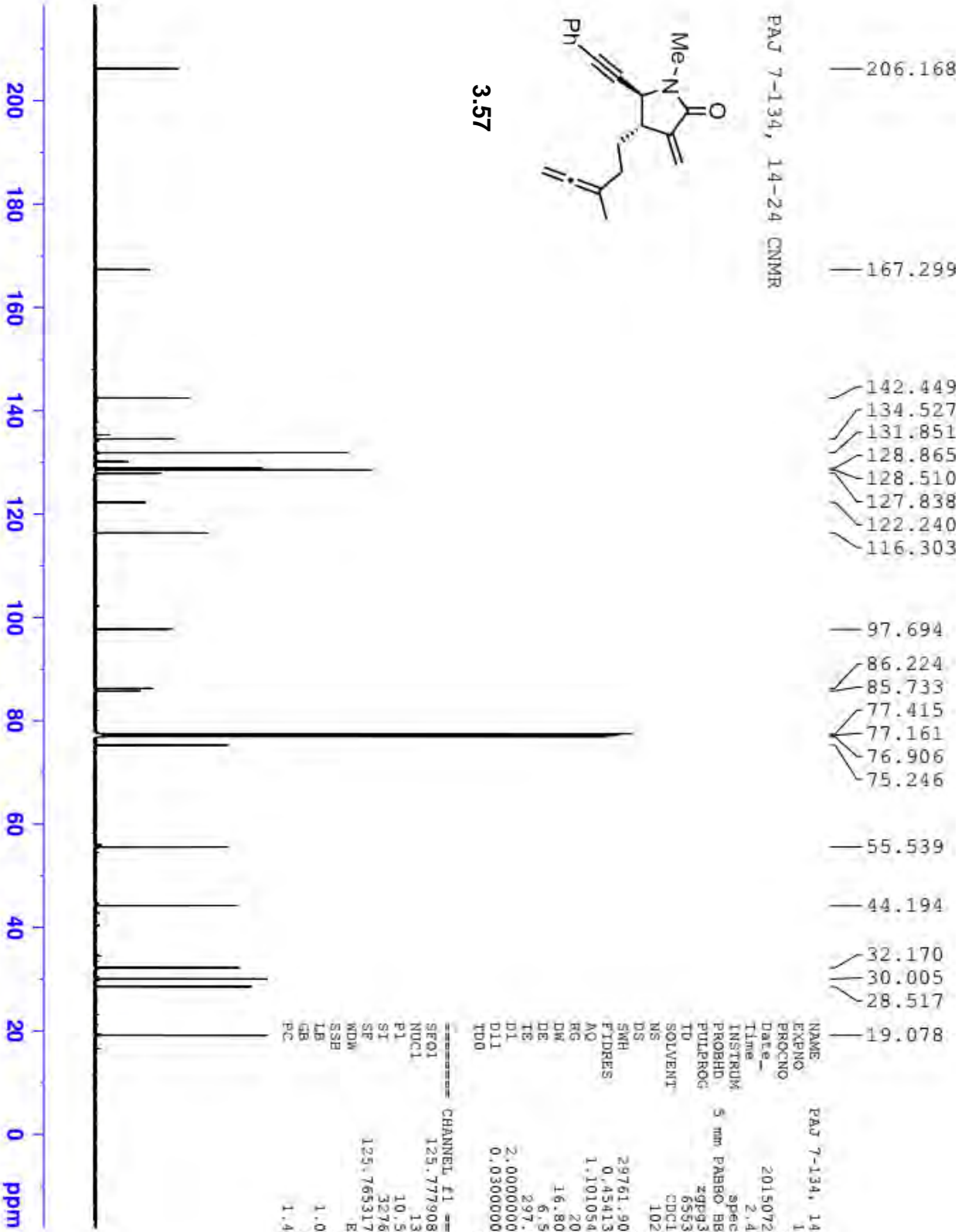
===== CHANNEL f1 =====
NUC1       13C
P1         10.00 usec
SI         32768
SF         100.6127561 MHz
WDW        EM
SSB        0
LB         1.00 Hz
GB         0
PC         1.40
  
```





3.57

PAJ 7-134, 14-24 CNMR



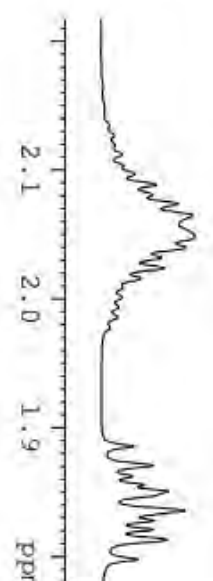
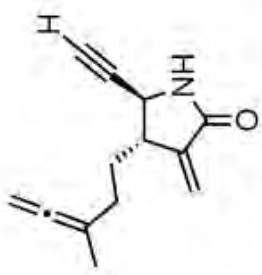
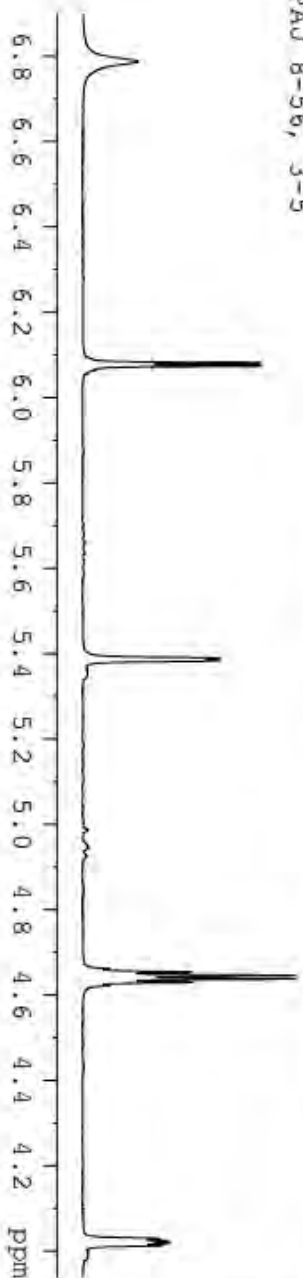
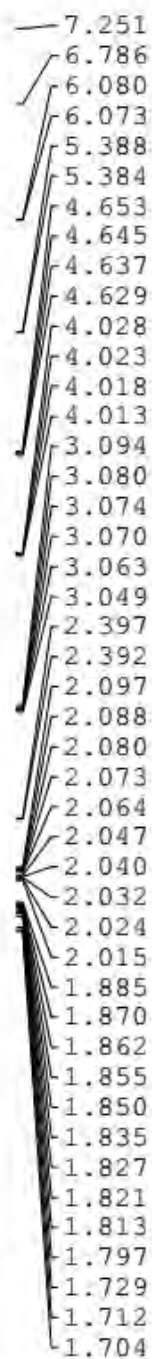
```

NAME          PAJ 7-134, 14-24
EXPNO         11
PROCNO        1
Date_         20150724
Time          2.40
INSTRUM       spect
PROBHD        5 mm PABBO BB/
PULPROG       zgpg30
TD            65536
SOLVENT       CDCl3
NS            1024
DS            2
SWH           29761.904 Hz
FIDRES        0.434131 Hz
AQ            1.1010548 sec
RG            203
DM            16.800 usec
DE            6.50 usec
TE            297.9 K
D1            2.00000000 sec
D11           0.03000000 sec
TD0           1

===== CHANNEL f1 =====
SFO1          125.7779086 MHz
NUC1          13C
P1            10.50 usec
SI            32768
SF            125.7653171 MHz
WDW           EM
SSB           0
LB            1.00 Hz
GB            0
PC            1.40

```

PAJ 8-56, 3-5



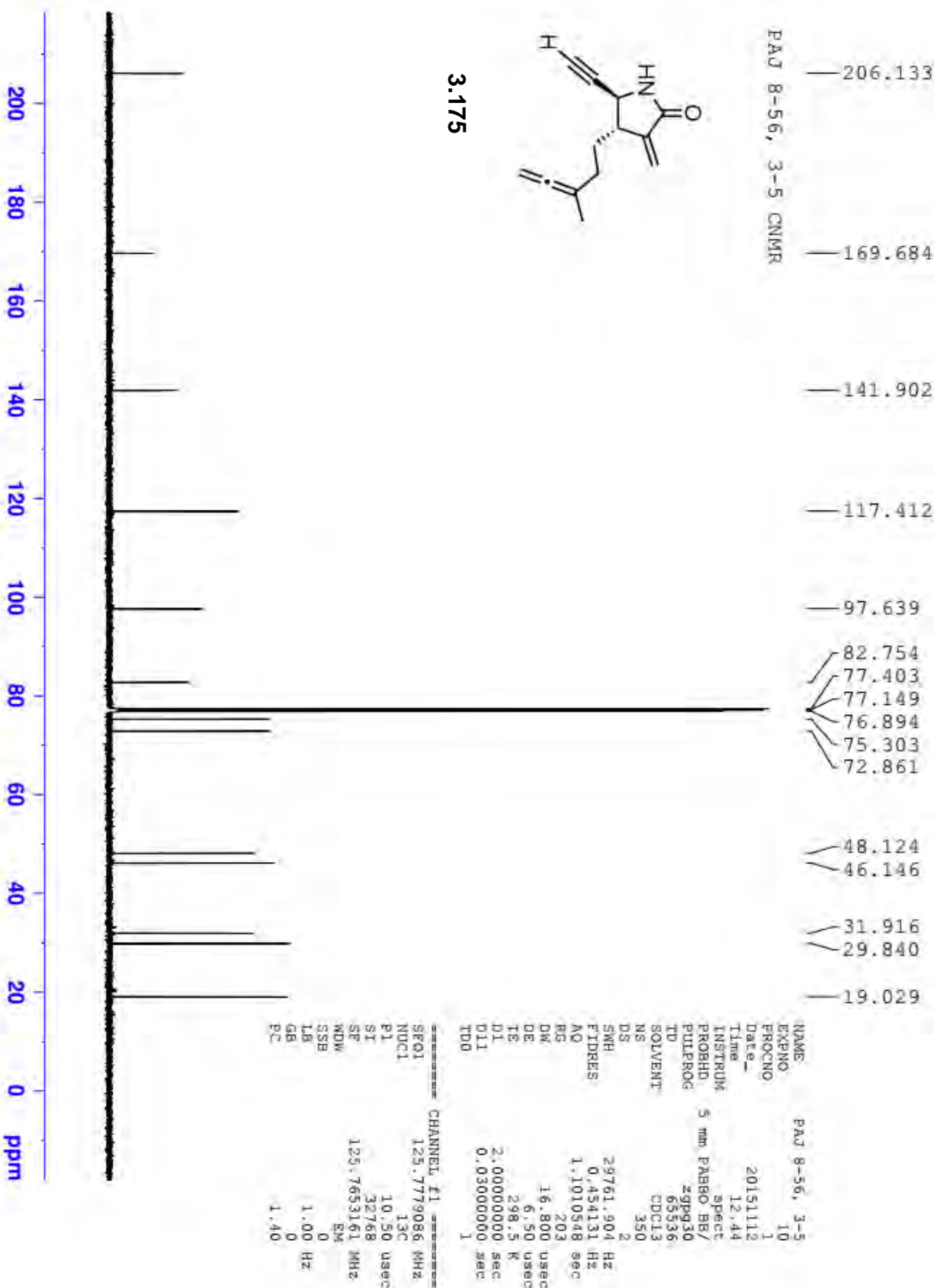
```

NAME          PAJ 8-56, 3-5
EXPNO         10
PROCNO        1
Date_         20151111
Time         17.54
INSTRUM       spect
PROBHD        5 mm PABBO BB-
PULPROG       zg30
TD            65536
SOLVENT       CDCl3
NS            16
DS            2
SWH           8223.685 Hz
FIDRES        0.125483 Hz
AQ            3.9846387 sec
RG            80.6
DM            60.800 usec
DE            6.50 usec
TE            37.7 K
D1            1.00000000 sec

===== CHANNEL f1 =====
NUC1          1H
P1            13.75 usec
SI            65536
SFO           400.1300130 MHz
WDW           EM
SSB           0
LB            0.30 Hz
GB            0
PC            1.00
  
```

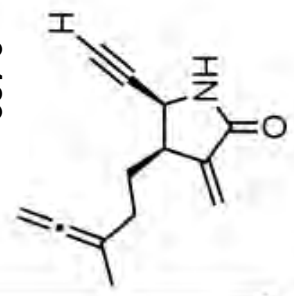
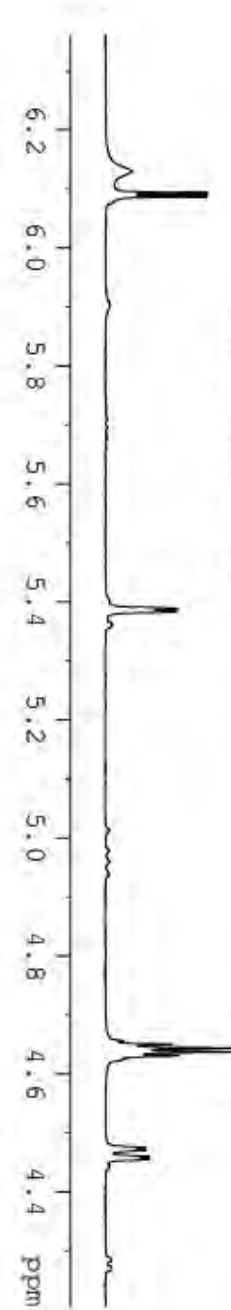
3.175





6.129
6.092
6.087
5.389
5.388
5.384
5.383
4.649
4.643
4.637
4.630
4.474
4.470
4.459
4.455
3.097
3.092
3.087
3.086
3.082
3.076
2.427
2.423
2.138
2.133
2.126
2.120
2.115
2.108
2.103
2.097
2.090
2.084
2.075
2.069
2.063
2.054
2.048
2.040
1.970
1.960
1.948
1.942
1.938
1.931
1.926
1.921
1.914
1.912
1.895
1.724
1.717
1.711
1.609

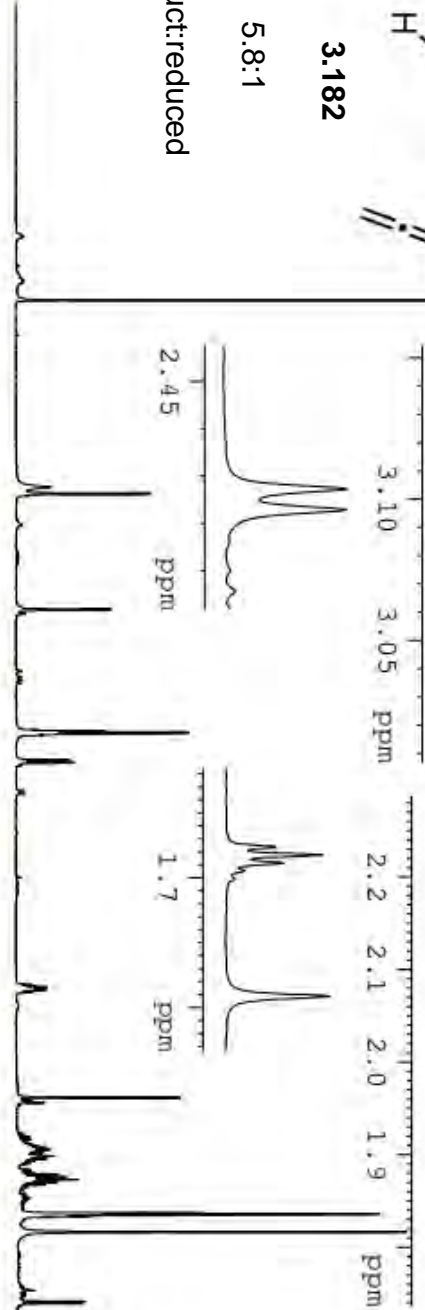
PAJ 7-162, 10-14



3.182

5.8:1

product: reduced

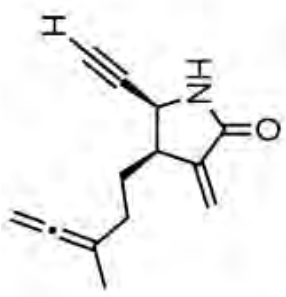


```

NAME          PAJ 7-162, 10-14
EXPNO         10
PROCNO        1
Date_         20150813
Time         17.35
INSTRUM       spect
PROBHD        5 mm PABBO BB/
PULPROG       zg30
TD            65536
SOLVENT       CDCl3
NS            16
DS            2
SWH           10000.000 Hz
FIDRES        0.152588 Hz
AQ            3.2768500 sec
RG            128
DW            50.000 usec
DE            6.50 usec
TE            296.8 K
D1            1.000000000 sec
TDO           1

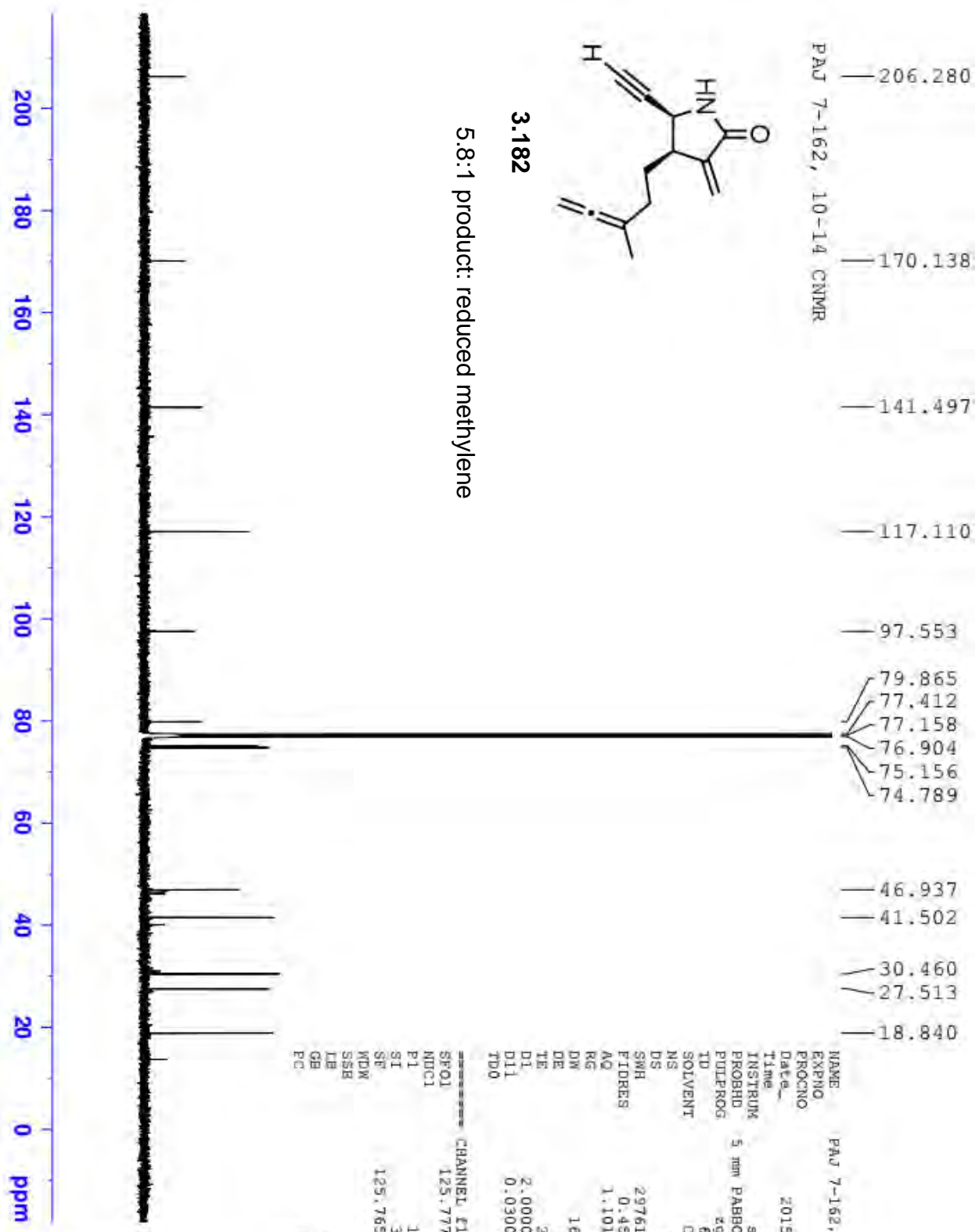
===== CHANNEL f1 =====
SFO1          500.1630887 MHz
NUC1           1H
P1            11.45 usec
SI            65536
SF            500.1600108 MHz
WDW           EM
SSB           0
LB            0.30 Hz
GB            0
PC            1.00

```



3.182

5:8:1 product: reduced methylene

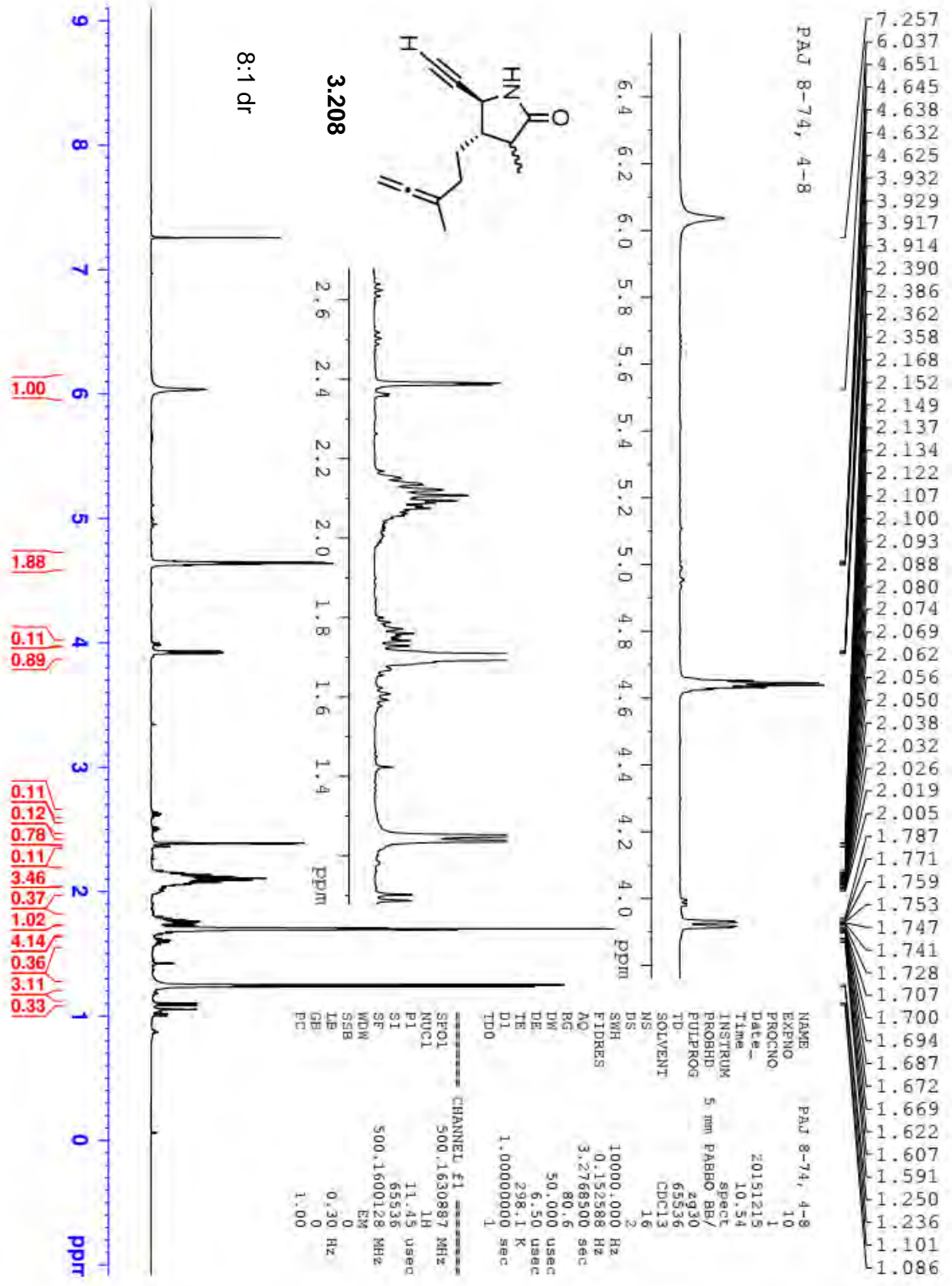


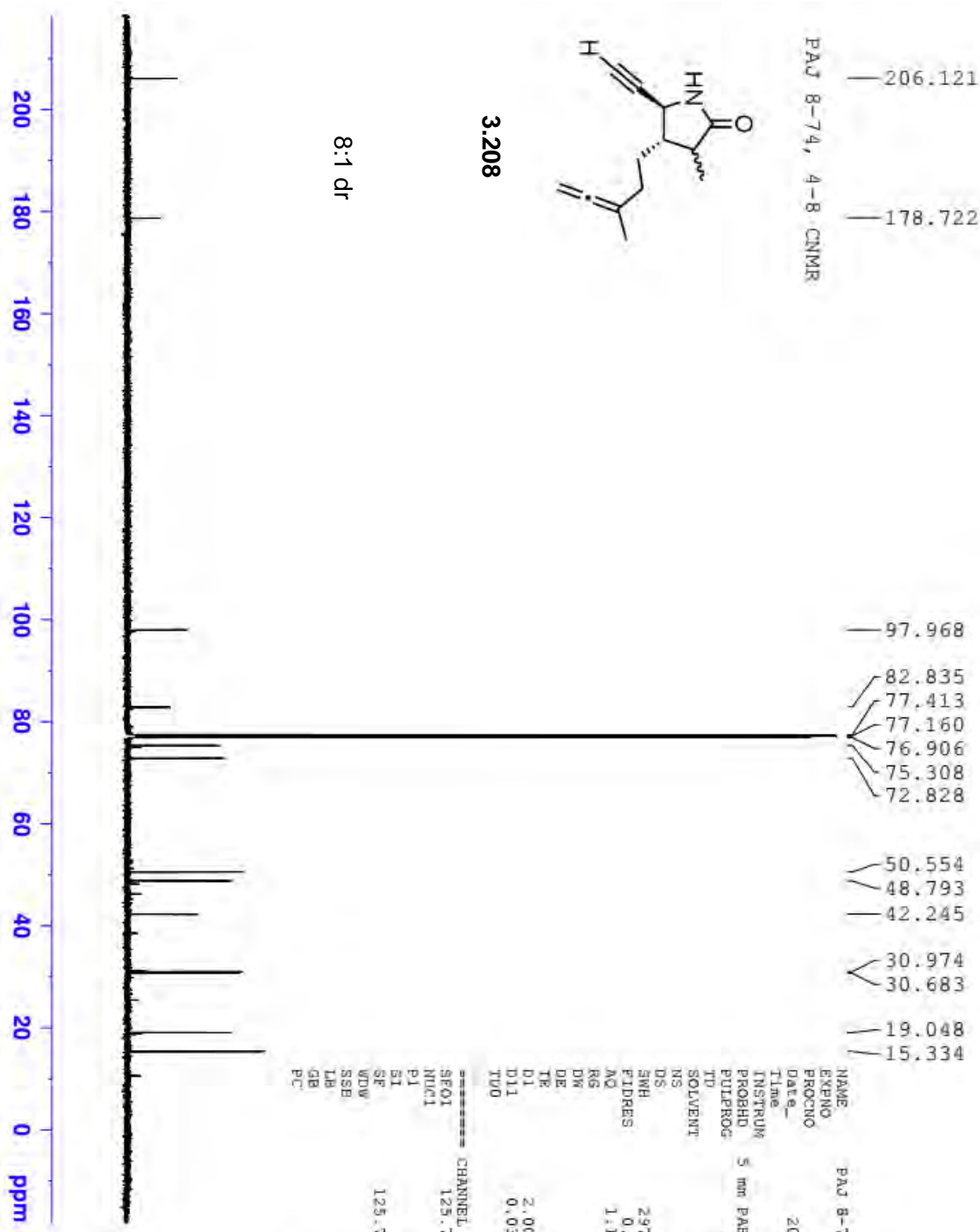
```

NAME PAJ 7-162, 10-14
EXPNO 11
PROCNO 1
Date_ 20150814
Time 5.14
INSTRUM spect
PROBHD 5 mm PABBO BB/
PULPROG zgpg30
TD 65536
SOLVENT CDCl3
NS 2048
DS 2
SMH 29761.904 Hz
FIDRES 0.454131 Hz
AQ 1.1010548 sec
RG 203
DW 16.800 usec
DE 6.50 usec
TE 298.1 K
D1 2.000000000 sec
D11 0.030000000 sec
TD0 1

----- CHANNEL f1 -----
SF01 125.7779086 MHz
NUC1 13C
P1 10.50 usec
SI 32768
SE 125.7653135 MHz
KDW EM
SSB 0
LB 1.00 Hz
GB 0
PC 1.40

```

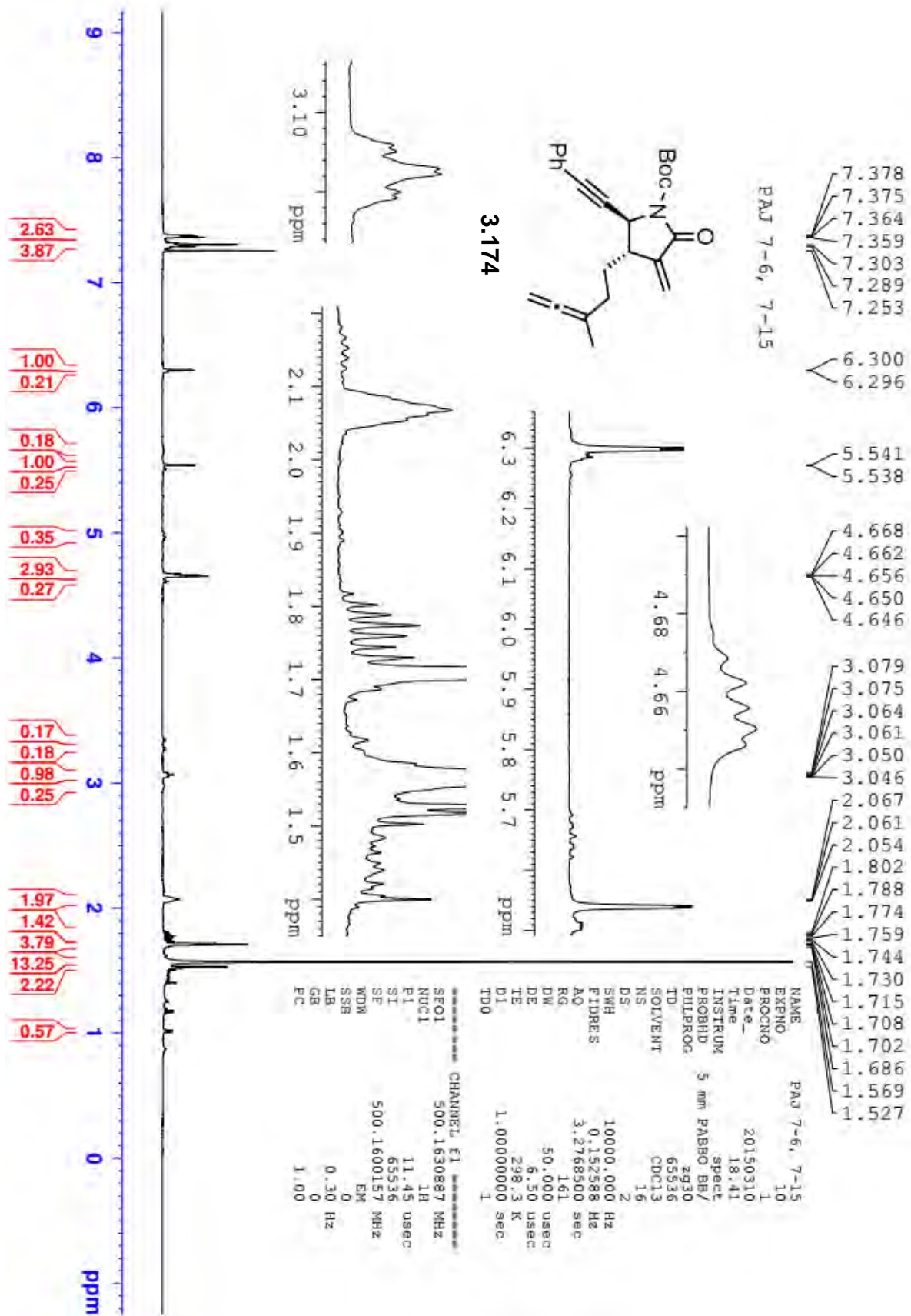


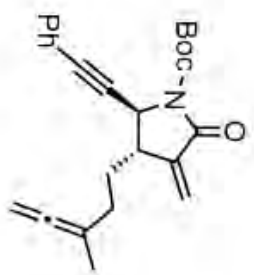


```

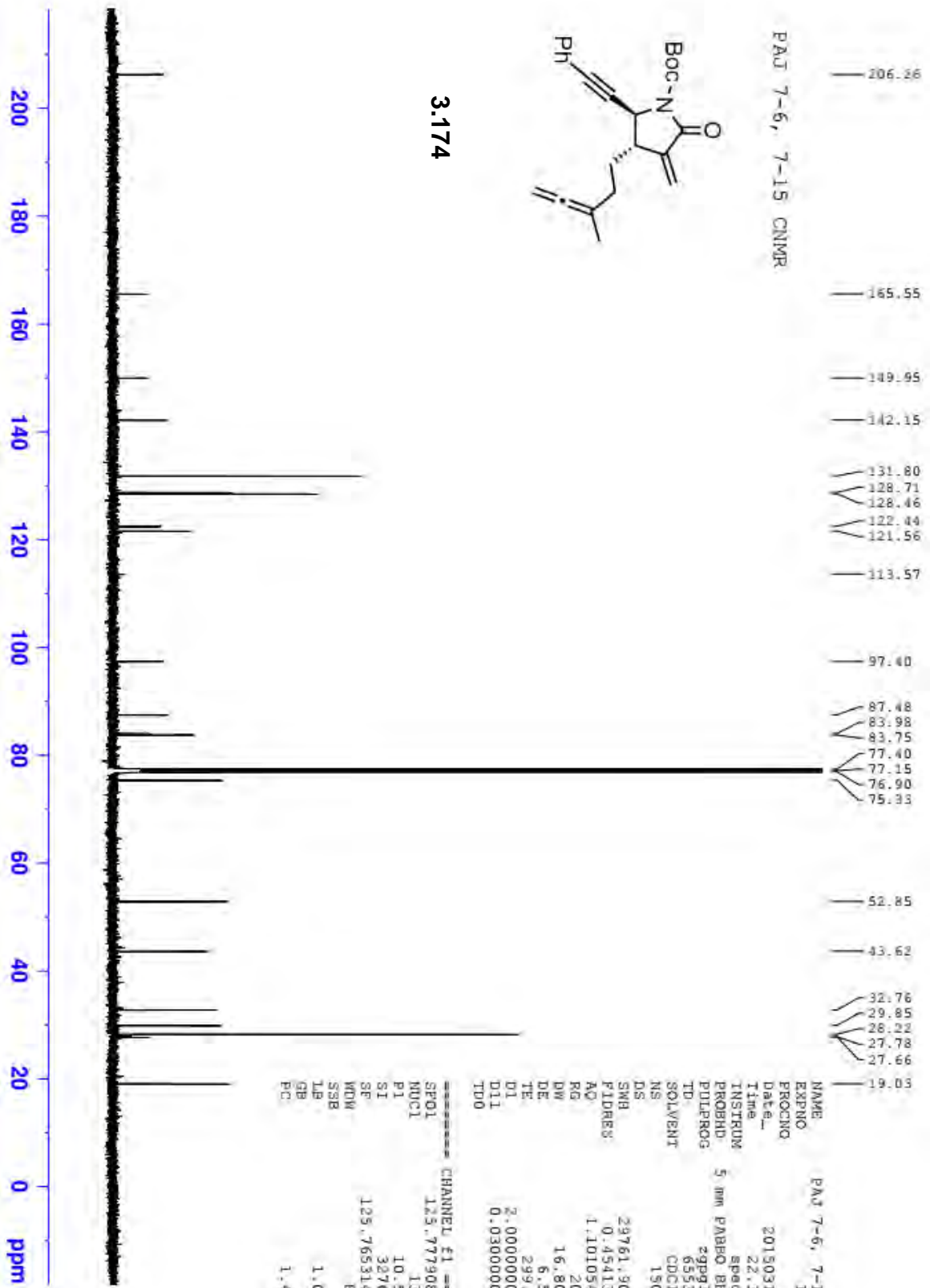
NAME          PAJ 8-74, 4-8
EXPNO         11
PROCNO        1
Date_         20151215
Time          11.17
INSTRUM       spect
PROBHD        5 mm PABBO BB/
PULPROG       zgpg30
TD            65536
SOLVENT       CDCl3
NS            400
DS            2
SWH           29761.904 Hz
FIDRES        0.454131 Hz
AQ            1.1010548 sec
RG            203
DM            16.800 usec
DE            6.50 usec
TE            298.8 K
D1            2.00000000 sec
D11           0.03000000 sec
TWO           1

===== CHANNEL f1 =====
SEOI          125.7779086 MHz
NUC1          13C
P1            10.50 usec
S1            32768
SF            125.7653139 MHz
WDW           EM
SSB           0
LB            1.00 Hz
GB            0
PC            1.40
  
```



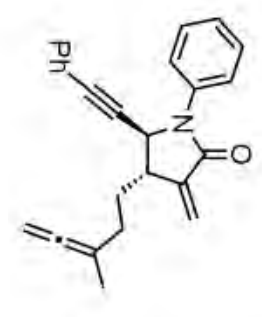
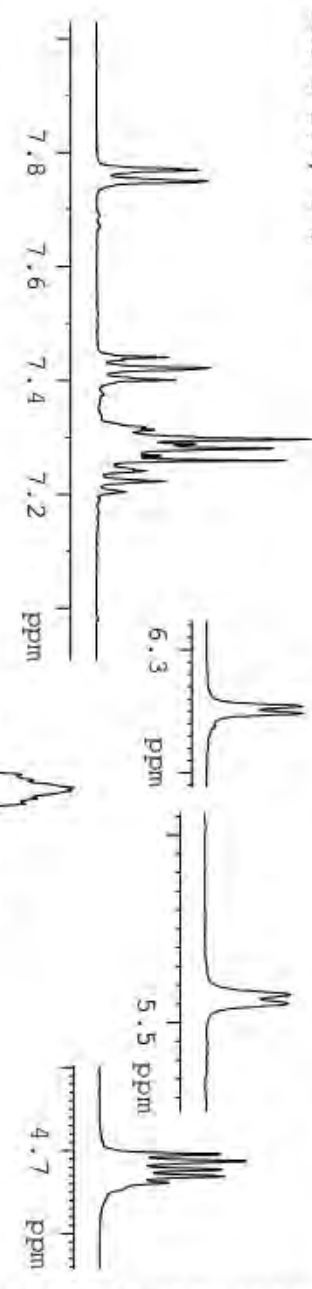


3.174

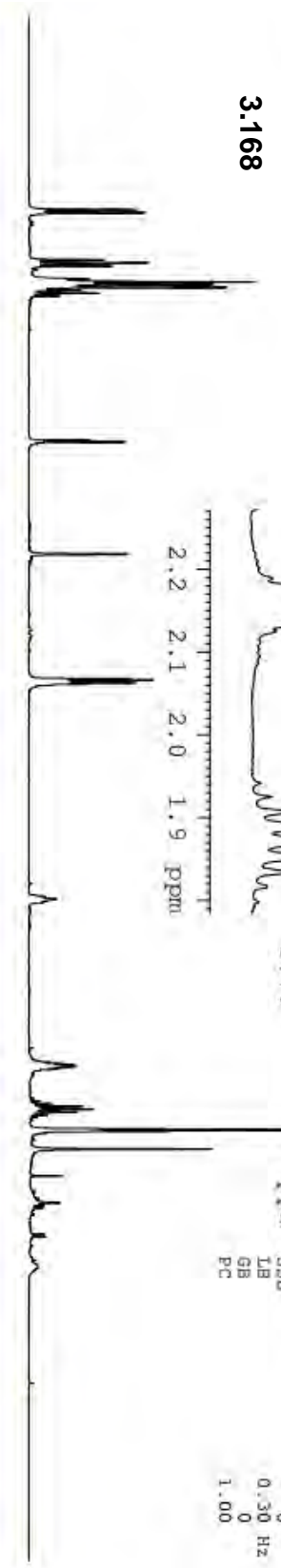


PAJ 8-204, 4-6

7.772
7.769
7.750
7.748
7.441
7.436
7.422
7.405
7.401
7.318
7.313
7.300
7.297
7.288
7.285
7.281
7.272
7.267
7.259
7.251
7.244
7.241
7.223
7.204
6.254
6.248
5.515
5.510
4.695
4.687
4.676
4.668
4.660
3.261
3.250
3.245
3.234
3.226
2.179
2.170
2.160
2.151
2.142
2.133
1.907
1.890
1.870
1.852
1.833
1.742
1.734
1.726
1.609
1.050
1.033



3.168



1.93
2.10
4.45
1.19

1.00

0.93
0.06
0.03
0.04
0.05
0.03
0.02
2.99

0.92

2.01
1.95
3.07
1.47

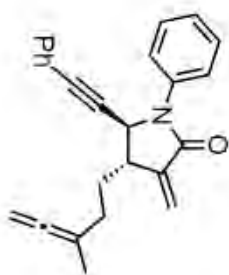
0.23

ppm

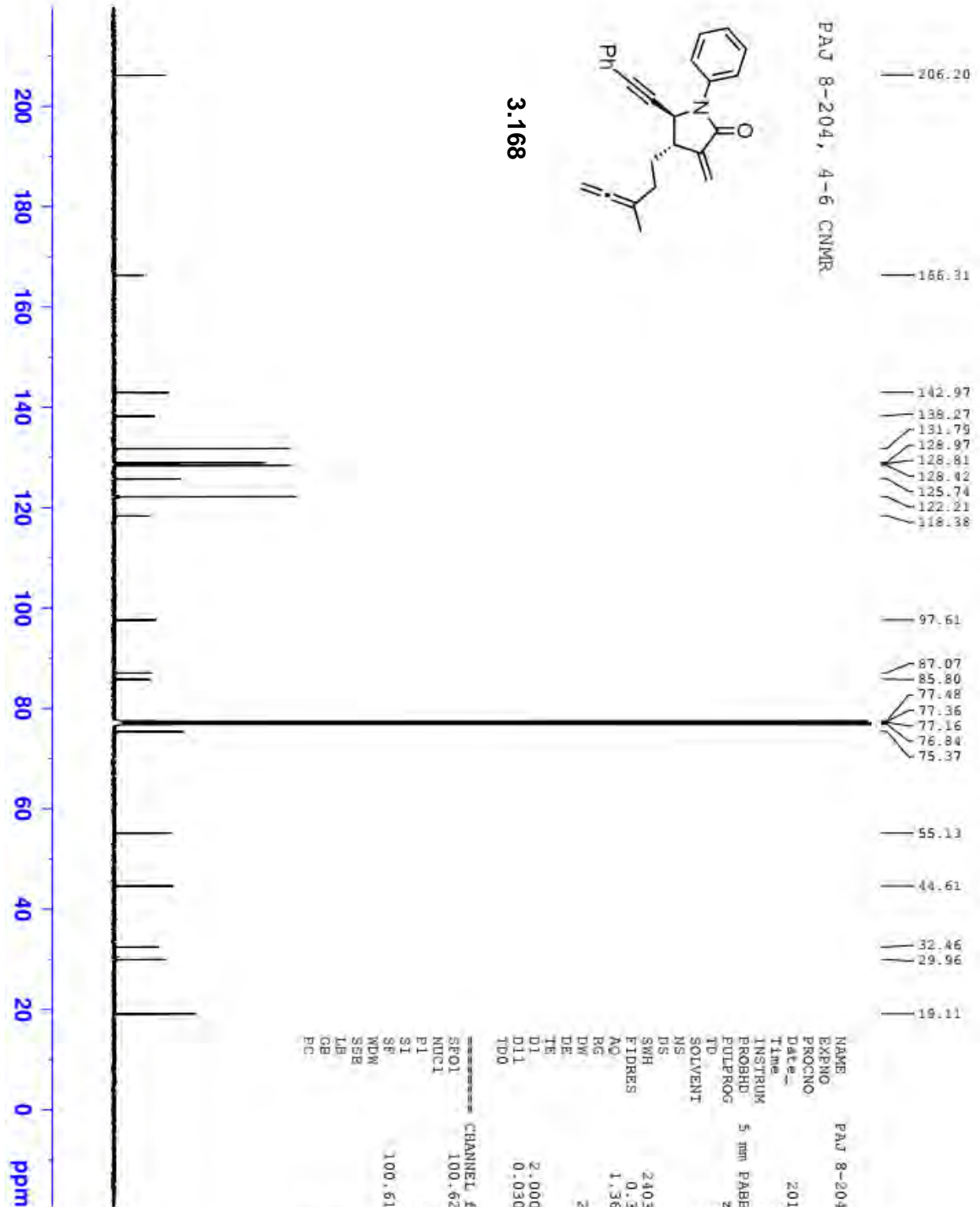
```

NAME          PAJ 8-204, 4-6
EXPNO         10
PROCNO        1
Date_         20160602
Time          11.38
INSTRUM       spect
PROBHD        5 mm PABBO BB-
PULPROG       zg30
TD            65536
SOLVENT       CDCl3
NS            16
DS            2
SWH           8012.820 Hz
FIDRES        0.122266 Hz
AQ            4.0894366 sec
RG            90.5
DE            62.400 usec
TE            300.2 K
D1            1.00000000 sec
TD0           1

----- CHANNEL f1 -----
SF01          400.1324710 MHz
NUC1          1H
P1            13.75 usec
SI            65536
SE            400.1300101 MHz
WDW           EM
SSB           0
LB            0.30 Hz
GB            0
PC            1.00
  
```



PAJ 8-204, 4-6 CNMR



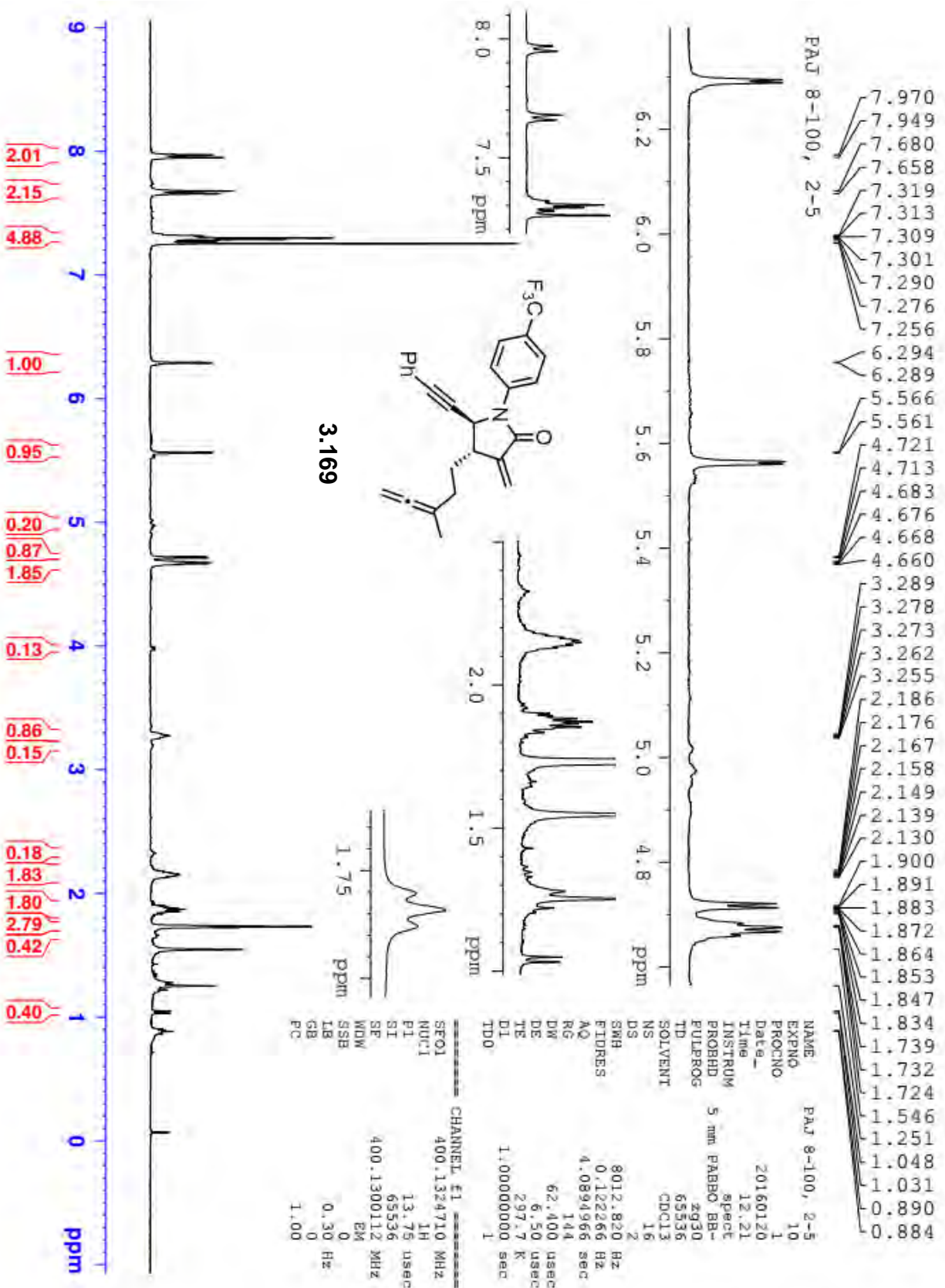
- 206.20
- 166.31
- 142.97
- 138.27
- 131.79
- 128.97
- 128.81
- 128.42
- 125.74
- 122.21
- 118.38
- 97.61
- 87.07
- 85.80
- 77.48
- 77.36
- 77.16
- 76.84
- 75.37
- 55.13
- 44.61
- 32.46
- 29.96
- 18.11

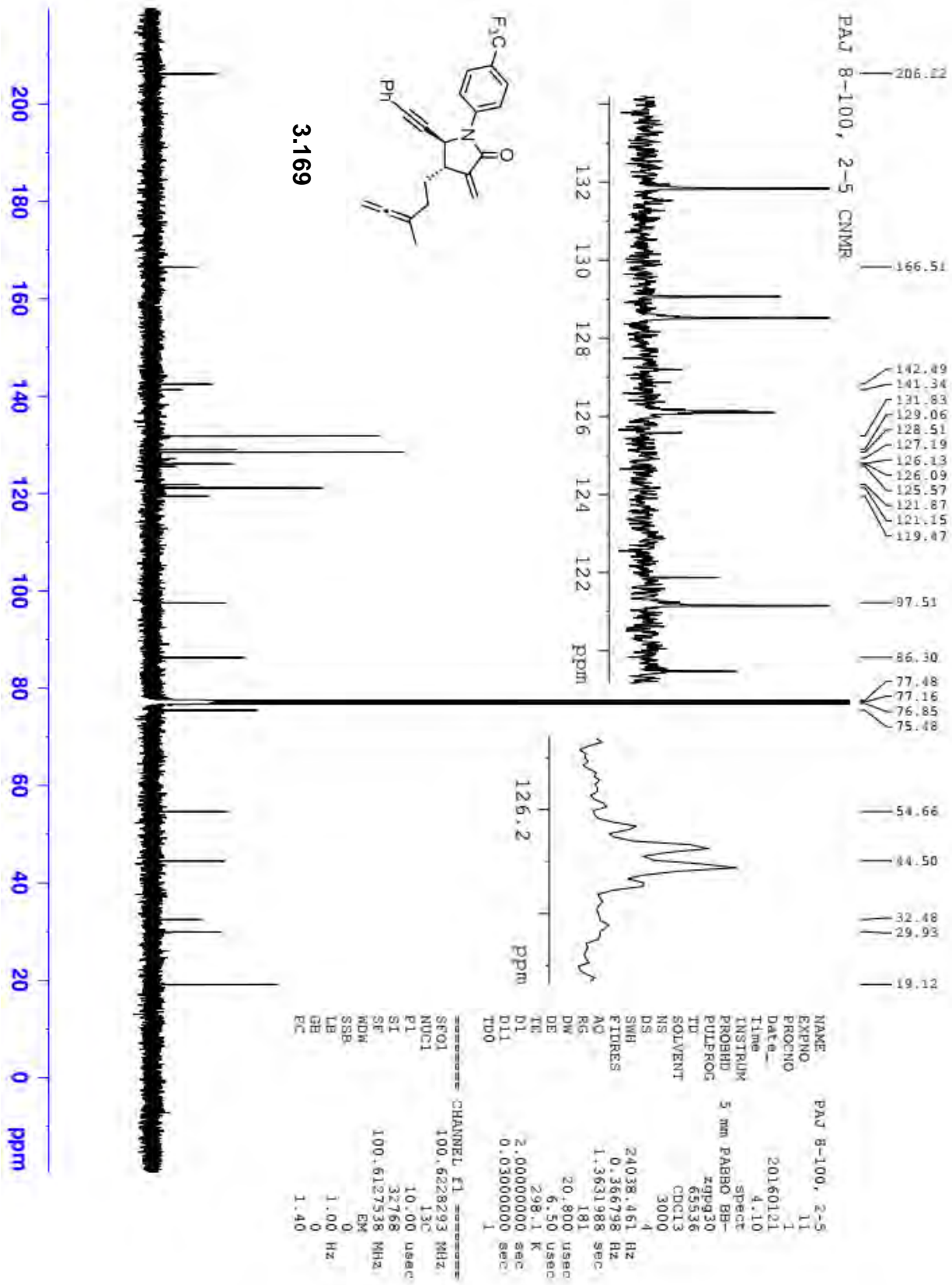
3.168

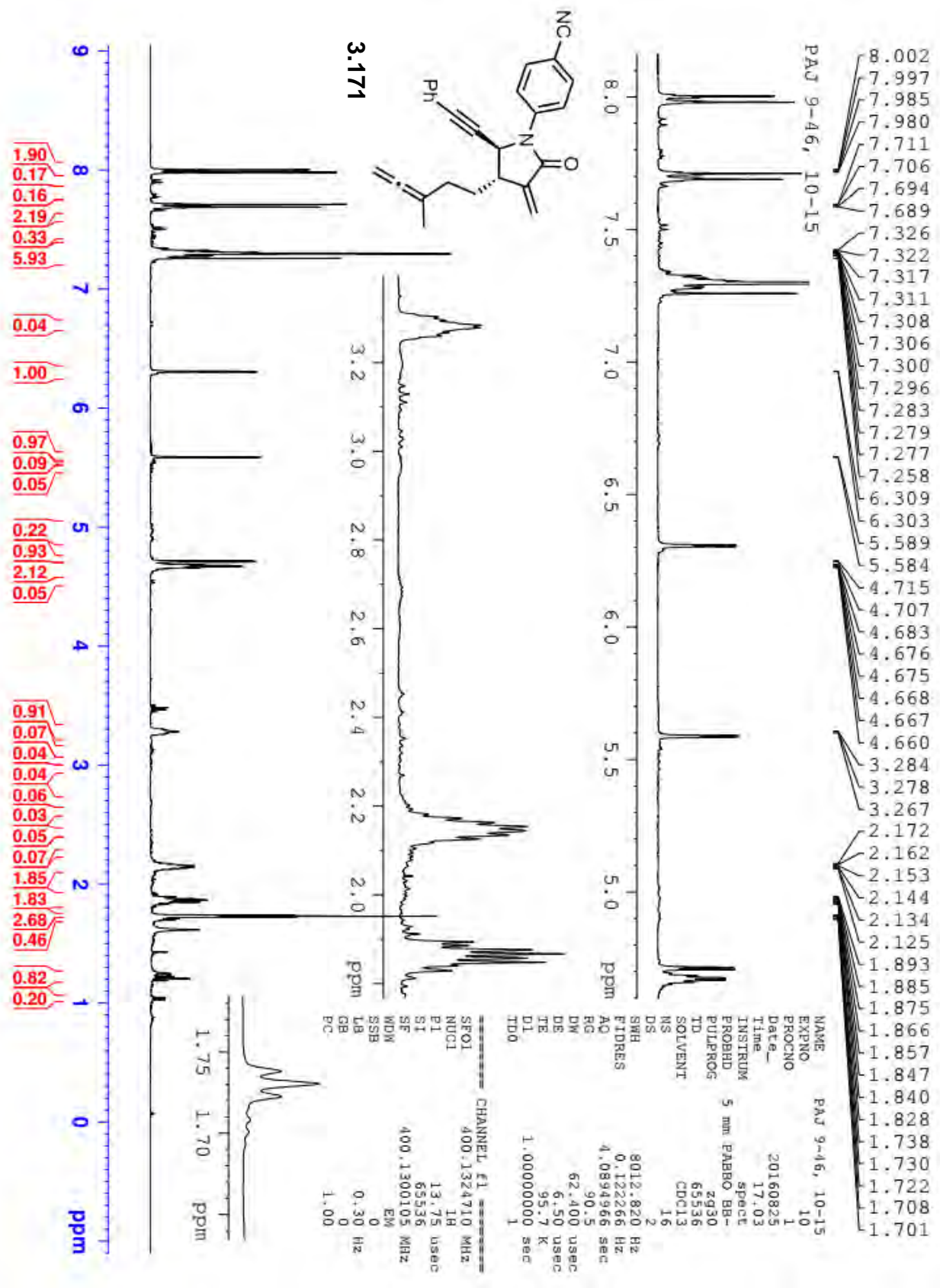
```

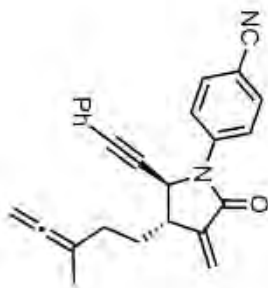
NAME          PAJ 8-204, 4-6
EXPNO         11
PROCNO        1
Date_         20160602
Time          22.56
INSTRUM       spect
PROBHD        5 mm F4BBO BB-
PULPROG       zgpg30
TD            65536
SOLVENT       CDCl3
NS            3000
DS            4
SWH           24038.461 Hz
FIDRES        0.366798 Hz
AQ            1.3631988 sec
RG            203
DE            20.800 usec
TE            6.50 usec
TE           95.9 K
D1            2.00000000 sec
D11           0.03000000 sec
TD0           1

===== CHANNEL f1 =====
SF01          100.6228293 MHz
NUC1          13C
P1            10.00 usec
S1            32768
SE            100.6127562 MHz
WDW           EM
SSB           0
LB            1.00 Hz
GB            0
PC            1.40
  
```

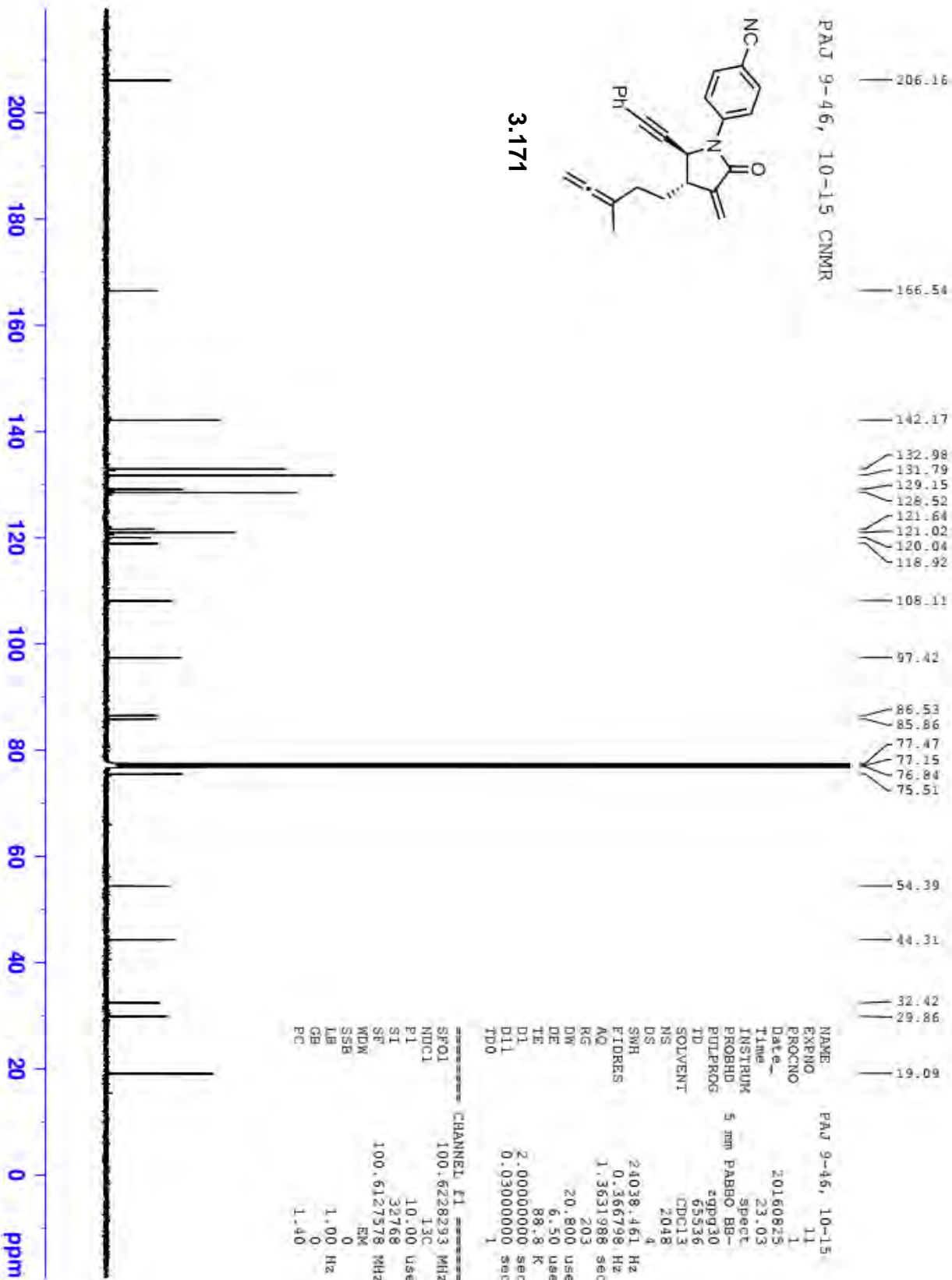


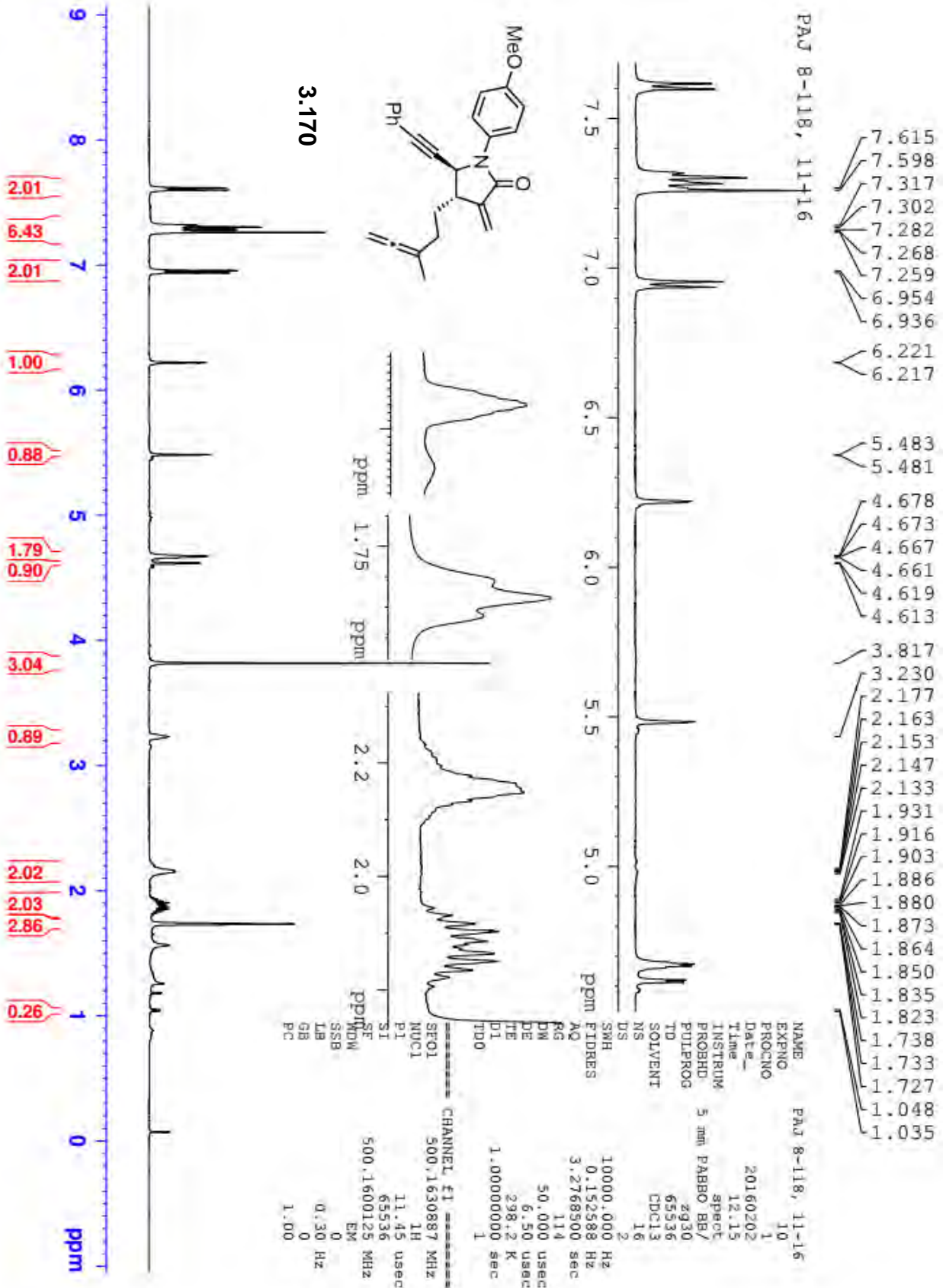


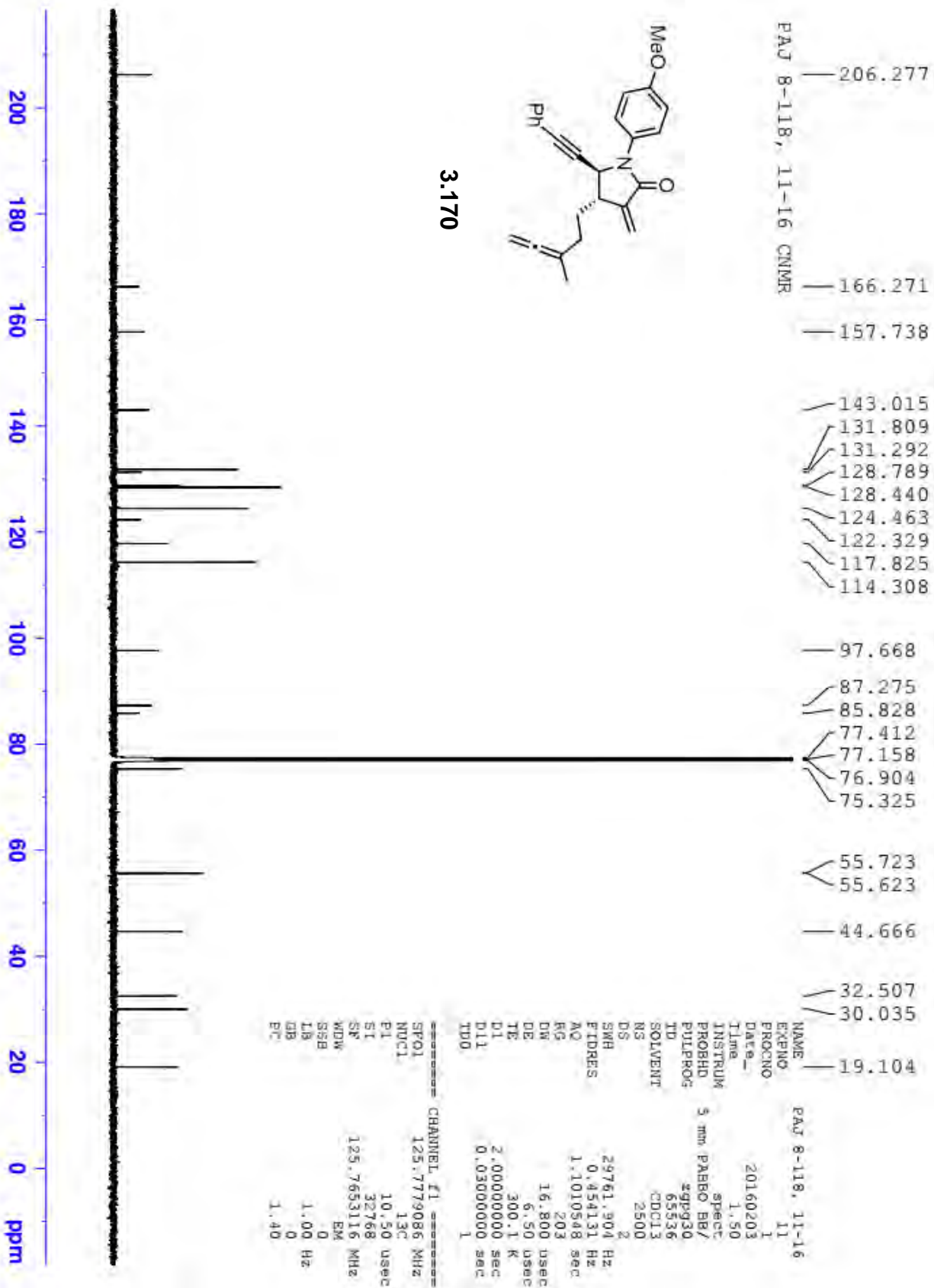




3.171

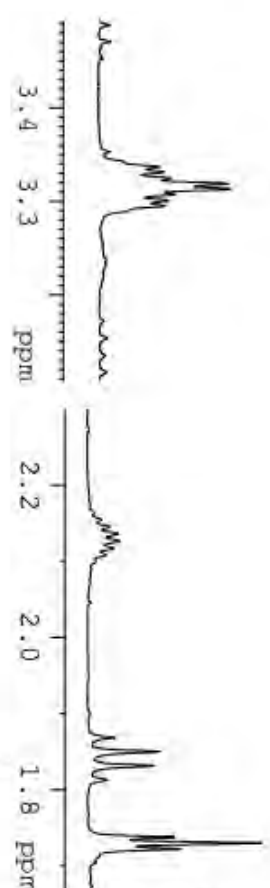
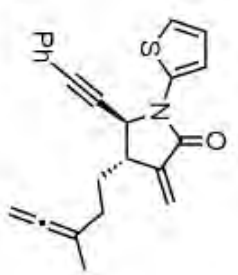
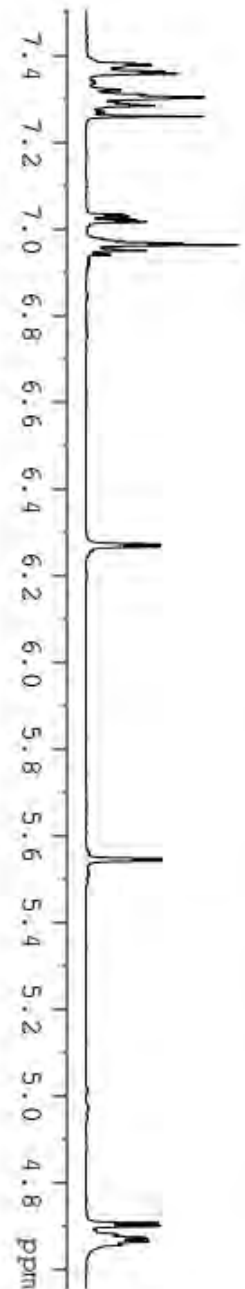






PAJ 8-206, 3-6

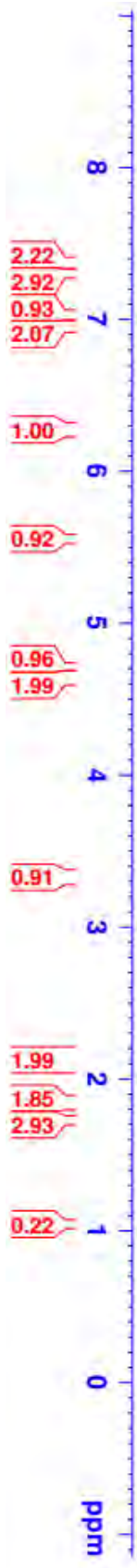
7.382
7.378
7.368
7.363
7.358
7.320
7.310
7.303
7.292
7.288
7.284
7.259
7.033
7.028
7.020
7.016
6.972
6.967
6.963
6.950
6.940
6.272
6.267
5.547
5.542
4.706
4.699
4.679
4.673
4.671
4.665
4.663
4.657
3.336
3.331
3.324
3.318
3.313
3.307
3.300
3.295
2.154
2.145
2.136
2.126
2.117
2.108
1.869
1.850
1.831
1.813
1.738
1.730
1.722

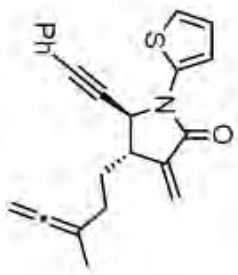


```

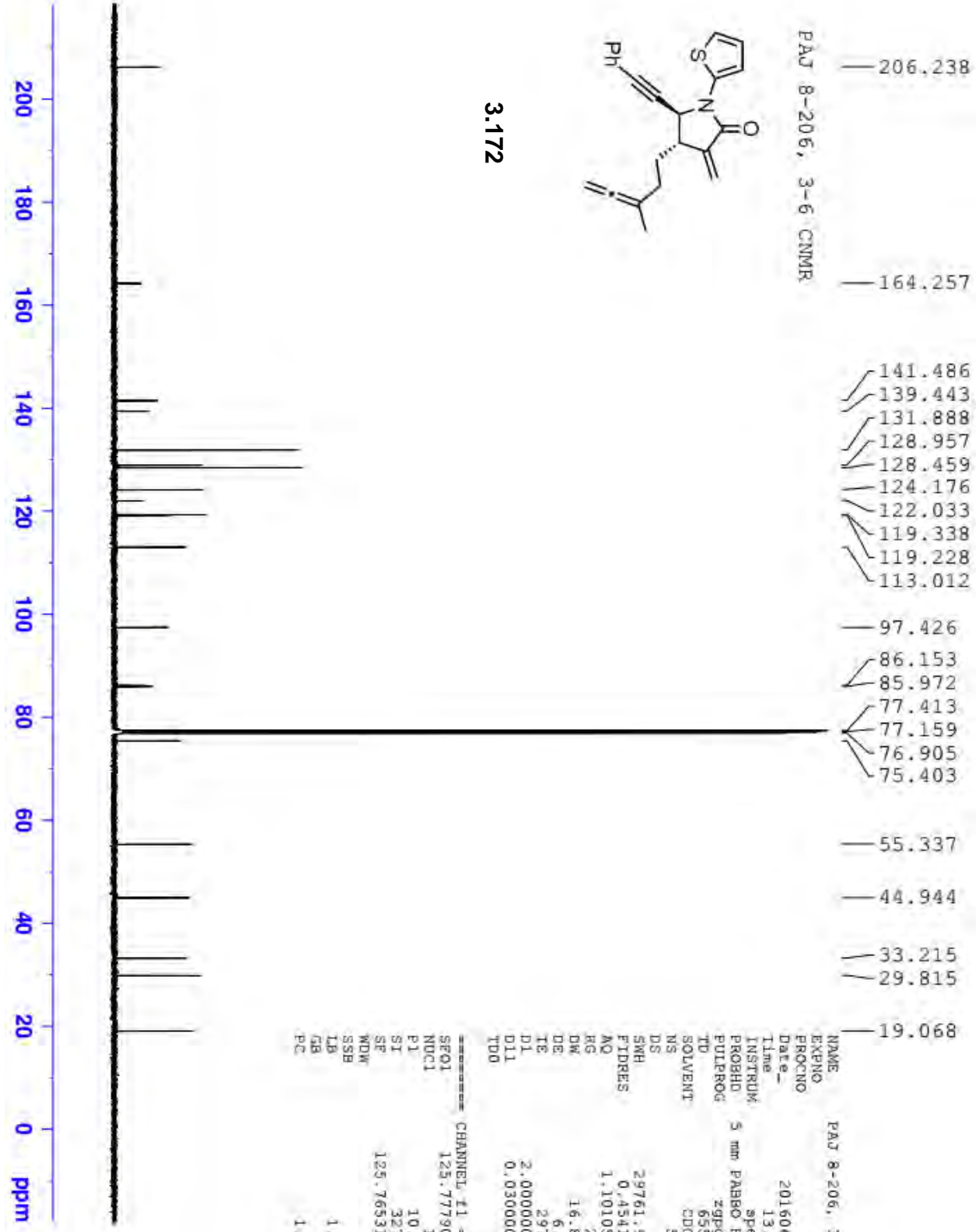
NAME          PAJ 8-206, 3-6
EXPNO         10
PROCNO        1
Date_         20160603
Time          13.02
INSTRUM       spect
PROBHD        5 mm PABBO BH-
PULPROG       zg30
TD            65536
SOLVENT       CDCl3
NS            16
DS            2
SWH           8012.820 Hz
FIDRES       0.122266 Hz
AQ           4.0894966 sec
RG           30.5
DW           62.400 usec
DE           6.50 usec
TE           96.3 K
D1           1.00000000 sec
TD0          1

===== CHANNEL f1 =====
SFO1         400.1324710 MHz
NUC1         1H
P1           13.75 usec
SI           65536
SF           400.1300102 MHz
WDW          EM
SSB          0
GB           0
PC           1.00
  
```





3.172

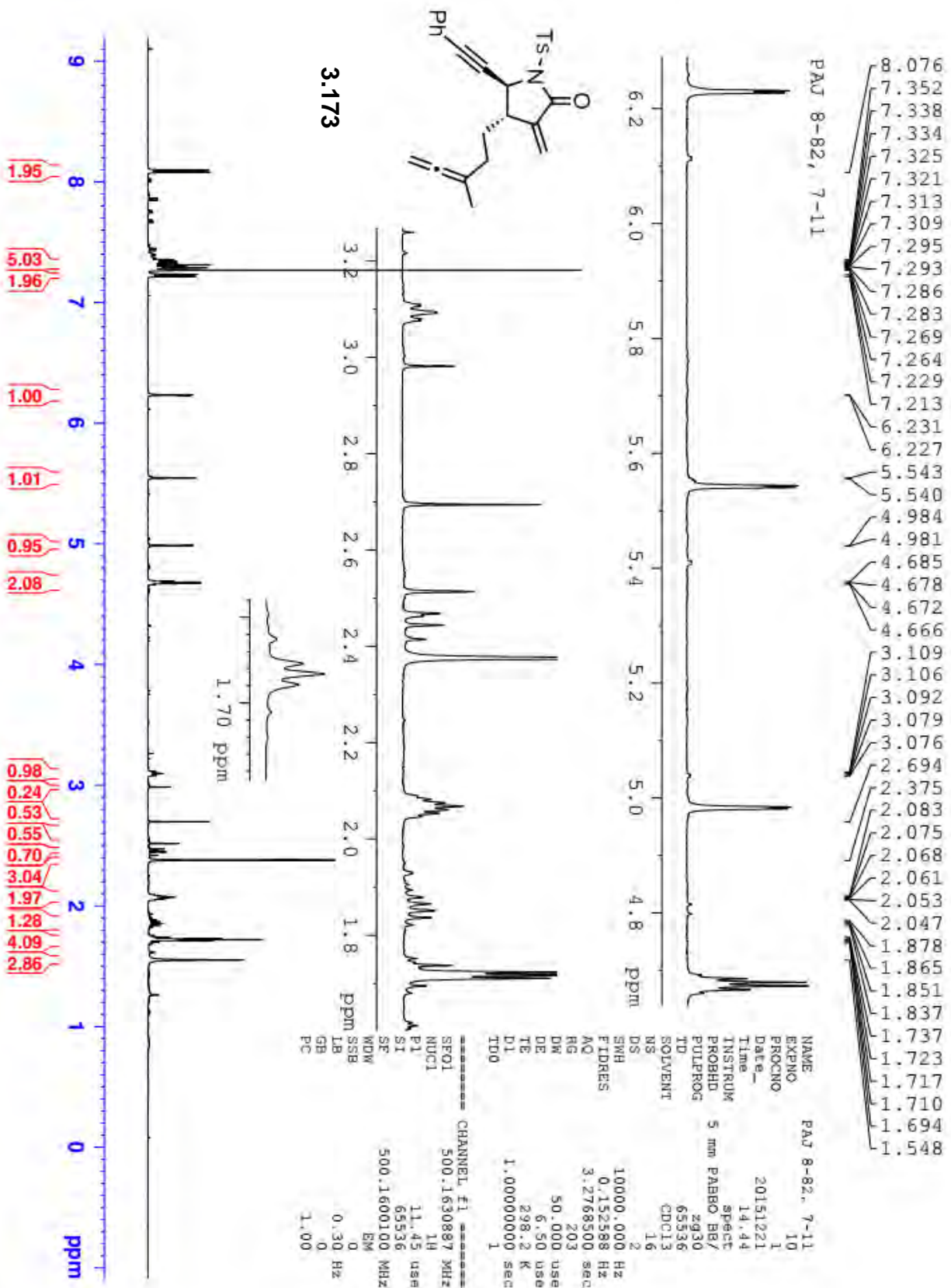


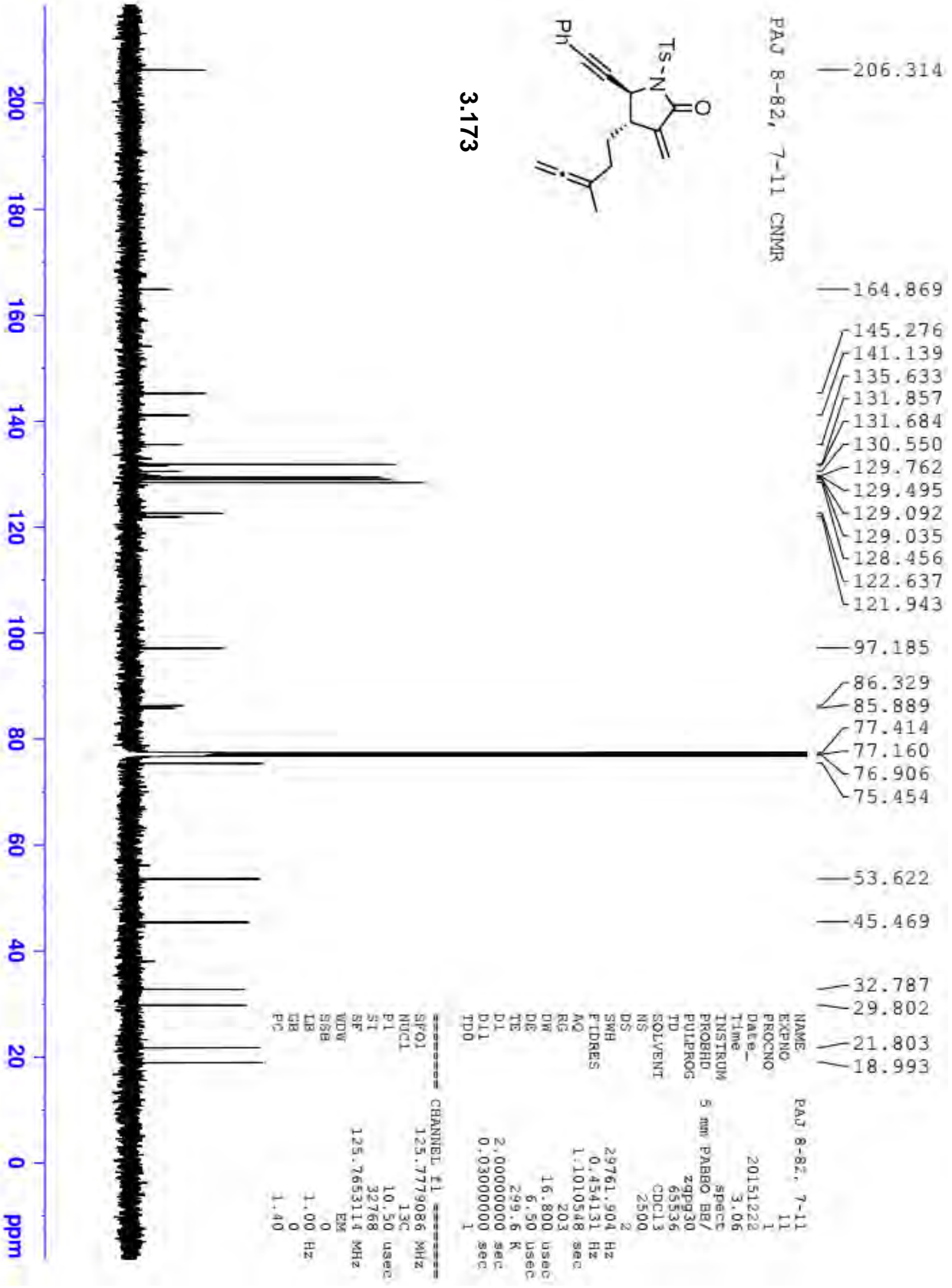
- 206.238
- 164.257
- 141.486
- 139.443
- 131.888
- 128.957
- 128.459
- 124.176
- 122.033
- 119.338
- 119.228
- 113.012
- 97.426
- 86.153
- 85.972
- 77.413
- 77.159
- 76.905
- 75.403
- 55.337
- 44.944
- 33.215
- 29.815
- 19.068

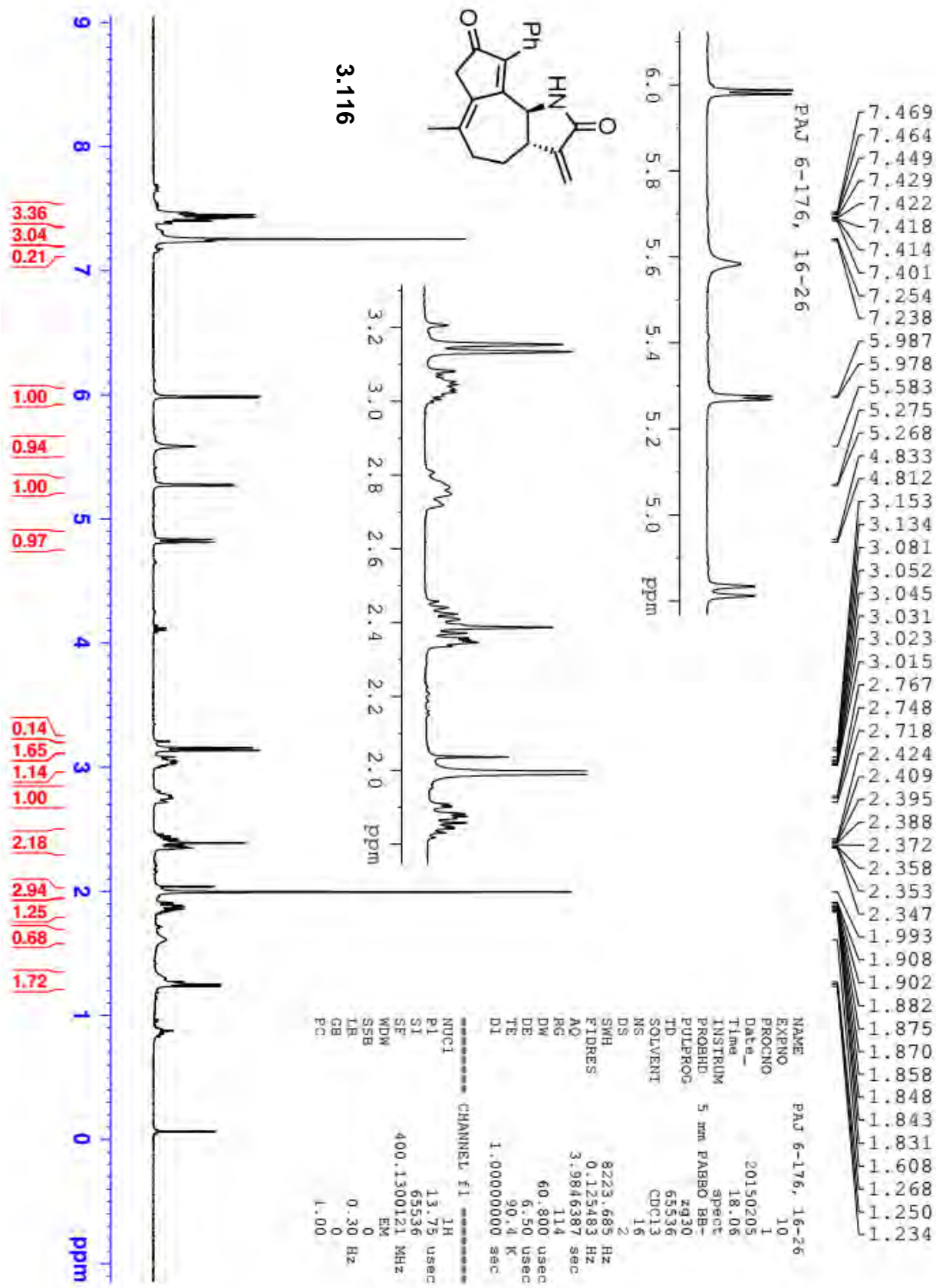
```

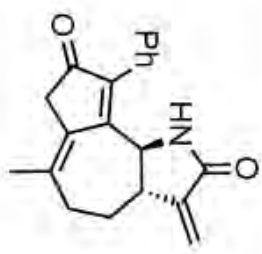
NAME          PAJ 8-206, 3-6
EXPNO         10
PROCNO        1
Date_         20160603
Time         13.49
INSTRUM       spect
PROBHD        5 mm PABBO BB/
PULPROG       zgpg30
TD            65536
SOLVENT       CDCl3
NS            500
DS            2
SMH           29761.904 HZ
FIDRES        0.454131 HZ
AQ            1.1010548 sec
RG            203
DW            16.800 usec
DE            6.50 usec
TE            297.1 K
D1            2.00000000 sec
D11           0.03000000 sec
TDO           1

----- CHANNEL f1 -----
SFO1          125.7779086 MHz
NUC1          13C
P1            10.50 usec
SI            32768
SF            125.7653156 MHz
WDW           EM
SSB           0
LB            1.00 Hz
GB            0
PC            1.40
  
```





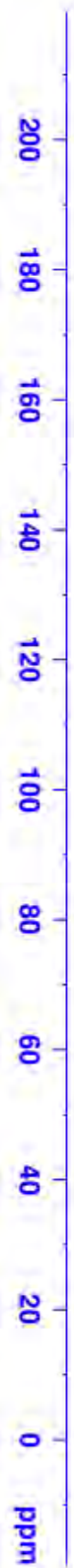




PAJ 6-176, 16-26 CNMR

- 202.03
- 168.57
- 165.51
- 143.14
- 140.81
- 135.73
- 131.85
- 131.28
- 129.31
- 128.37
- 115.33
- 77.48
- 77.36
- 77.16
- 76.84
- 56.16
- 44.27
- 40.94
- 31.78
- 26.58
- 24.75

3.116



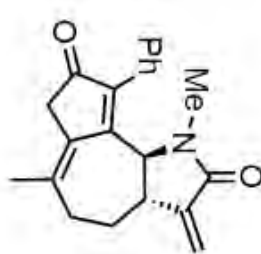
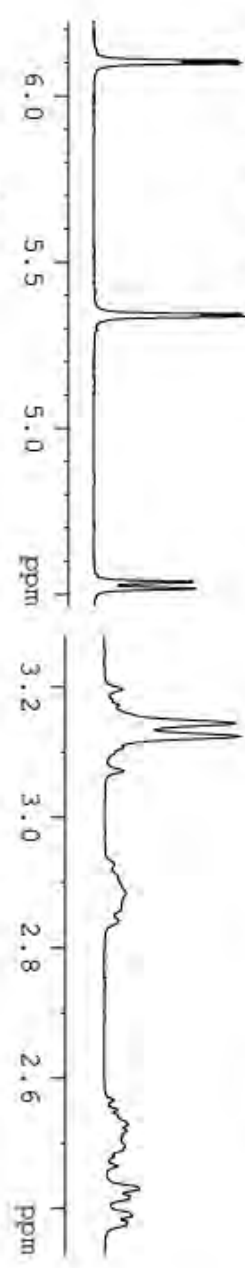
```

NAME PAJ 6-176, 16-26
EXPNO 11
PROCNO 1
DATE_ 20150206
Time 5.08
INSTRUM spect
PROBHD 5 mm PABBO BB-
PULPROG zgpg30
TD 65536
ID 65536
SOLVENT CDCl3
NS 2048
DS 4
SWH 24038.461 Hz
FIDRES 0.366798 Hz
AQ 1.3631988 sec
RG 203
DW 20.800 usec
DE 6.50 usec
TE 1815.7 K
D1 2.00000000 sec
D11 0.03000000 sec

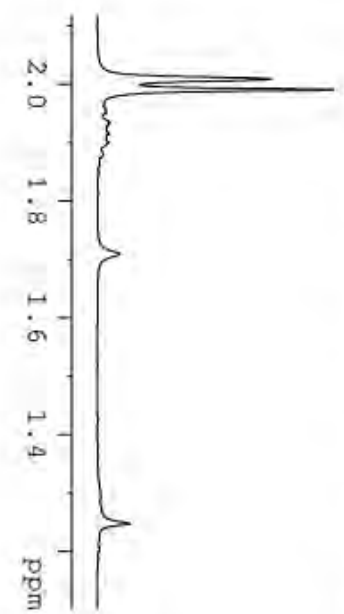
===== CHANNEL f1 =====
NUC1 13C
P1 10.00 usec
SI 32768
SF 100.6127550 MHz
WDW EM
SSB 0
LB 1.00 Hz
GB 0
PC 1.00
  
```

PAJ 7-136, 10-17

- 7.327
- 7.318
- 7.314
- 7.263
- 7.106
- 7.096
- 6.105
- 6.096
- 5.342
- 5.335
- 4.536
- 4.516
- 3.197
- 3.144
- 3.124
- 3.107
- 3.071
- 2.927
- 2.884
- 2.862
- 2.841
- 2.567
- 2.552
- 2.542
- 2.529
- 2.519
- 2.510
- 2.495
- 2.490
- 2.481
- 2.465
- 2.430
- 2.419
- 2.389
- 2.379
- 2.008
- 1.990
- 1.955
- 1.951
- 1.933
- 1.922
- 1.915
- 1.899
- 1.881
- 1.709
- 1.247



3.56

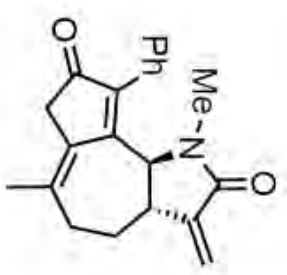


NAME PAJ 7-136, 10-17
 EXPNO 10
 PROCNO 1
 Date_ 20150729
 Time 17.26
 INSTRUM spect
 PROBRD PULPROG
 TD 2930
 SOLVENT CDC13
 NS 16
 DS 2
 SWH 8223.685 Hz
 FIDRES 0.125483 Hz
 AQ 3.9846387 sec
 RG 80.6
 DW 60.800 usec
 DE 6.50 usec
 TE 83.2 K
 D1 1.00000000 sec

CHANNEL F1
 NUCL 1H
 P1 13.75 usec
 S1 65536
 SF 400.1300088 MHz
 WDW EM
 SSB 0
 LB 0.30 Hz
 GB 0
 PC 1.00

- 202.77
- 168.82
- 165.51
- 143.18
- 137.64
- 136.62
- 130.60
- 130.53
- 130.33
- 128.43
- 127.70
- 115.55
- 77.47
- 77.15
- 76.83
- 62.32
- 41.67
- 40.51
- 32.26
- 30.42
- 28.81
- 28.54
- 28.29

PAJ 7-136, 10-17 CNMR



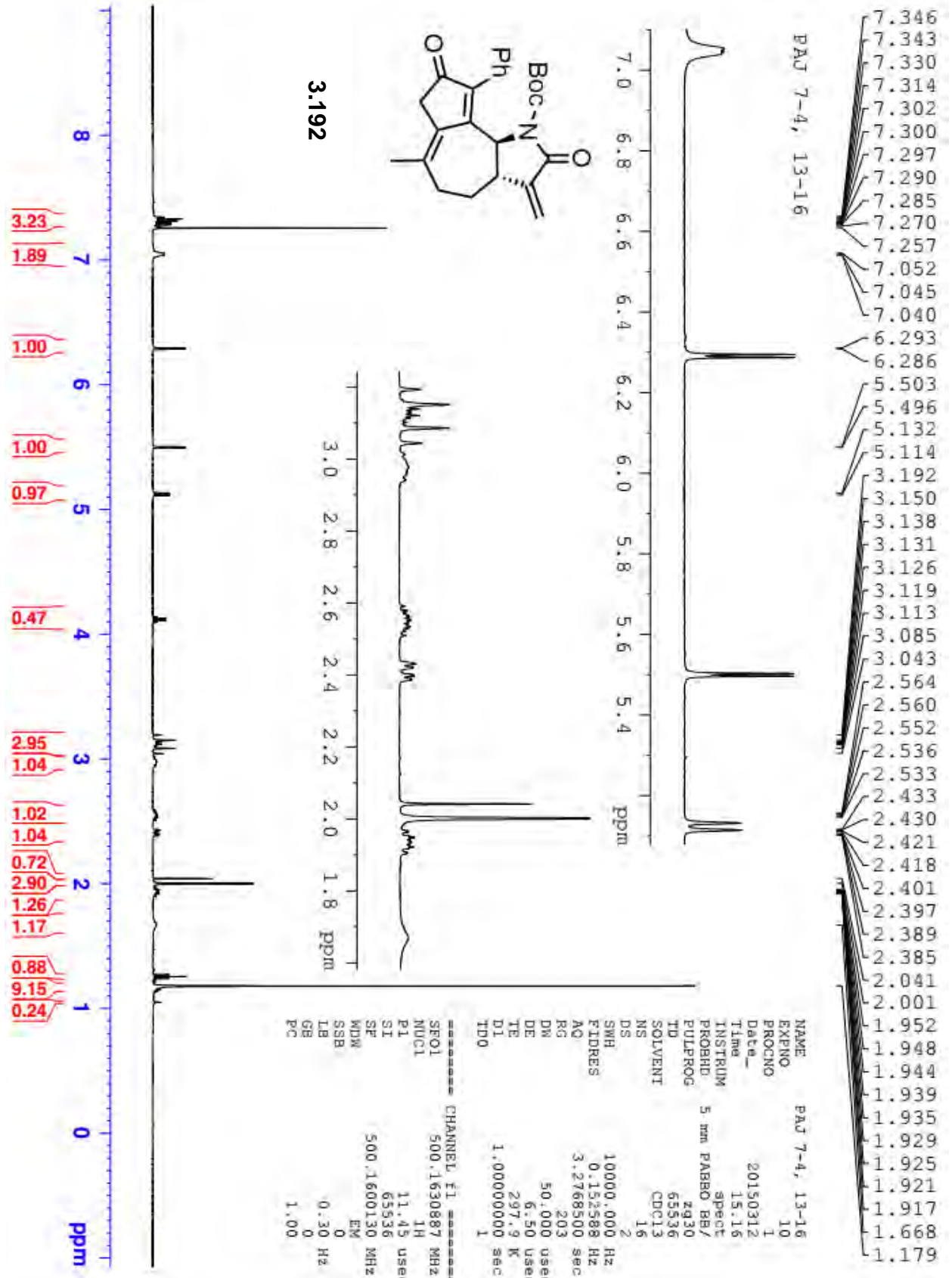
3.56

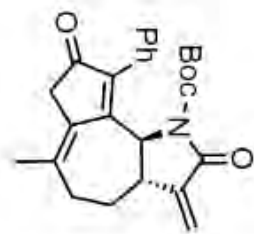


```

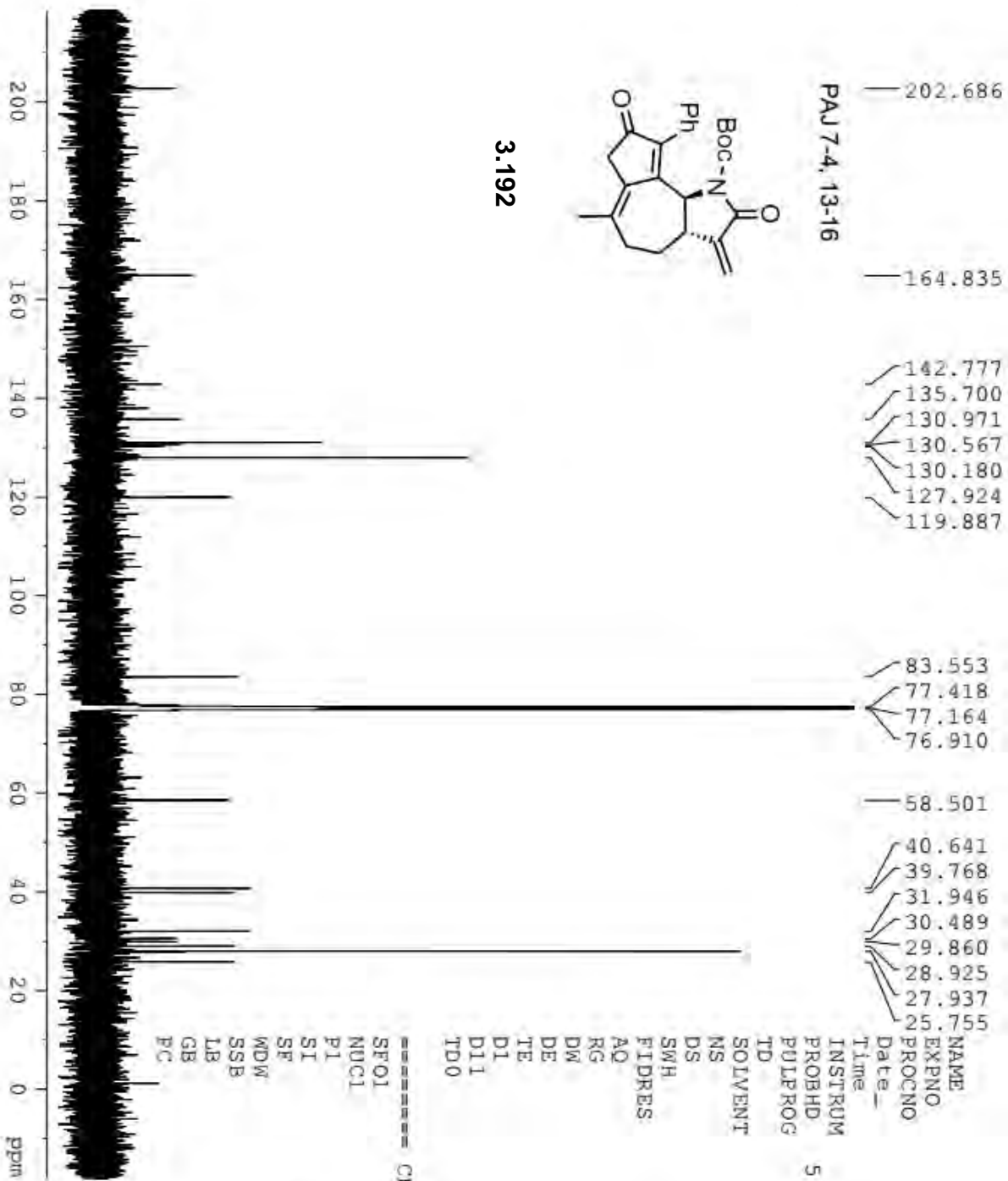
NAME          PAJ 7-136, 10-17
EXPNO         11
PROCNO        1
Date_         20150730
Time         3.03
INSTRUM       spect
PROBHD        5 mm PABBO BB-
PULPROG       zgpg30
TD            65536
FIDRES       0.365798 Hz
AQ           1.3631988 sec
RG           144
DW           20.800 usec
DE           6.50 usec
TE           300.2 K
D1           2.00000000 sec
D11          0.03000000 sec

----- CHANNEL f1 -----
NUC1          13C
P1           10.00 usec
S1           32768
SF           100.6127583 MHz
WDW          EM
SSB          0
LB           1.00 Hz
GB           0
PC           1.40
  
```





3.192

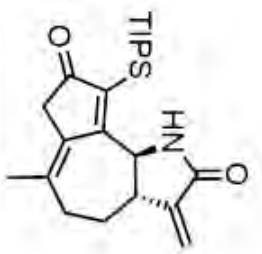
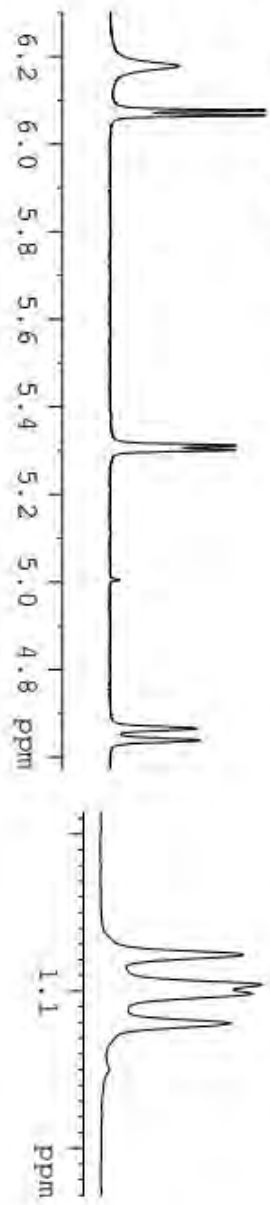
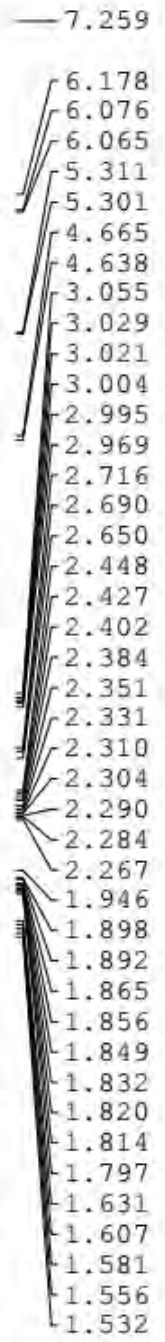


- 202.686
- 164.835
- 142.777
- 135.700
- 130.971
- 130.567
- 130.180
- 127.924
- 119.887
- 83.553
- 77.418
- 77.164
- 76.910
- 58.501
- 40.641
- 39.768
- 31.946
- 30.489
- 29.860
- 28.925
- 27.937
- 25.755

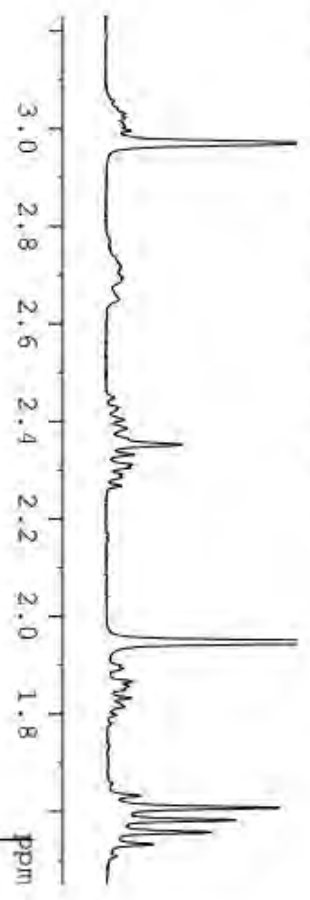
NAME	PAJ 7-4
EXPNO	11
PROCNO	1
Date_	20150522
Time	1.38
INSTRUM	5 mm PABBO BB/
PROBHD	zqpg30
PULPROG	gpg30
TD	65536
SOLVENT	CDCl3
NS	3000
DS	2
SWH	29761.904 Hz
FIDRES	0.454131 Hz
AQ	1.1010548 sec
RG	203
DW	16.800 use
DE	6.50 use
TE	298.7 K
D1	2.00000000 sec
D11	0.03000000 sec
TD0	1

***** CHANNEL F1 *****	
SFO1	125.7779086 MHz
NUC1	13C
PI	10.50 use
SI	32768
SF	125.7653120 MHz
WDW	EM
SSB	0
LB	1.00 Hz
GB	0
PC	1.40

PAJ 7-78, 32-43



3.184



```

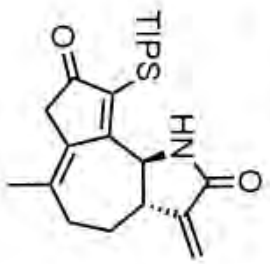
NAME          PAJ 7-78, 32-43
EXPNO         10
PROCNO        1
Date_         20150514
Time          17.13
INSTRUM       spect
PROBHD        5 mm QNP 1H/1
PULPROG       zg30
TD            32768
SOLVENT       CDCl3
NS            16
DS            2
SWH           6188.119 Hz
FIDRES       0.188846 Hz
AQ           2.6477044 sec
RG           144
DW           80.800 usec
DE           6.50 usec
TE           -927.7 K
DI           1.000000000 sec
TDO          1

----- CHANNEL f1 -----
SFO1          300.2318340 MHz
NUC1          1H
P1           12.71 usec
SI           32768
SF           300.2300091 MHz
WDW          EM
SSB          0
LB           0.10 Hz
GB           0
PC           1.00
  
```

208.24
 179.92
 169.34
 143.11
 137.93
 134.11
 133.85
 115.73
 77.46
 77.14
 76.82
 56.83
 44.20
 41.43
 31.92
 27.09
 25.36
 19.52
 19.42
 13.01



PAU 7-78, 23-43 CNMR



3.184

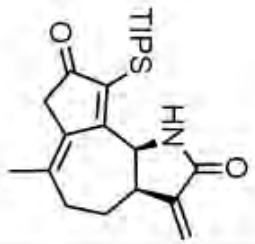


```

NAME PAU 7-78, 23-43
EXPNO 11
PROCNO 1
Date_ 20150516
Time 2.11
INSTRUM spect
PROBHD 5 mm PABBO BB-
PULPROG zgpg30
TD 65536
SOLVENT CDCl3
NS 3000
DS 4
SMR 24038.461 Hz
FIDRES 0.366798 Hz
AQ 1.3631988 sec
RG 144
DW 20.800 usec
DE 6.50 usec
TE 1515.8 K
D1 2.00000000 sec
D11 0.03000000 sec

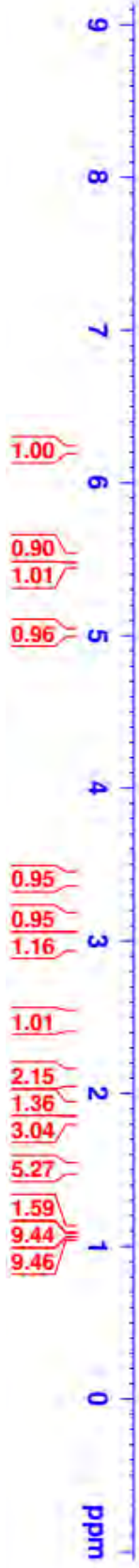
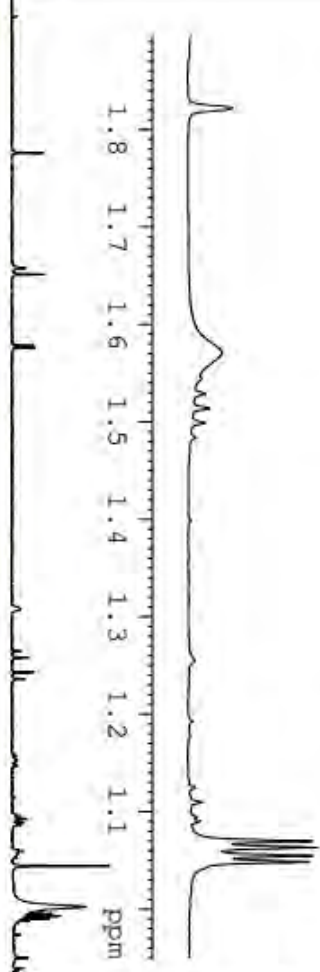
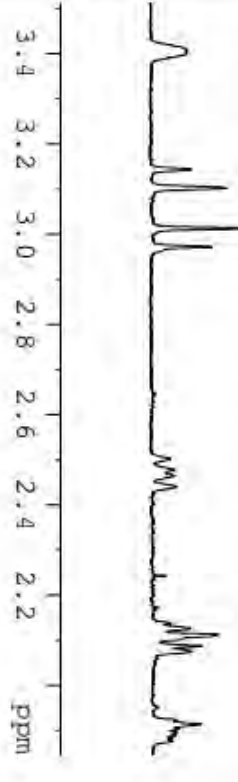
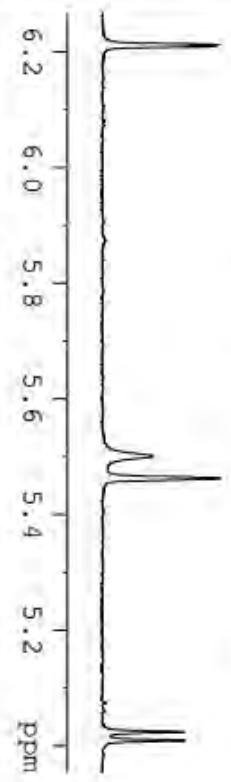
----- CHANNEL f1 -----
NUC1 13C
P1 10.00 usec
SI 32768
SF 100.6127570 MHz
WDW EM
SSB 0
LB 1.00 Hz
GB 0
PC 1.40
  
```

PAJ 8-42, 23-30



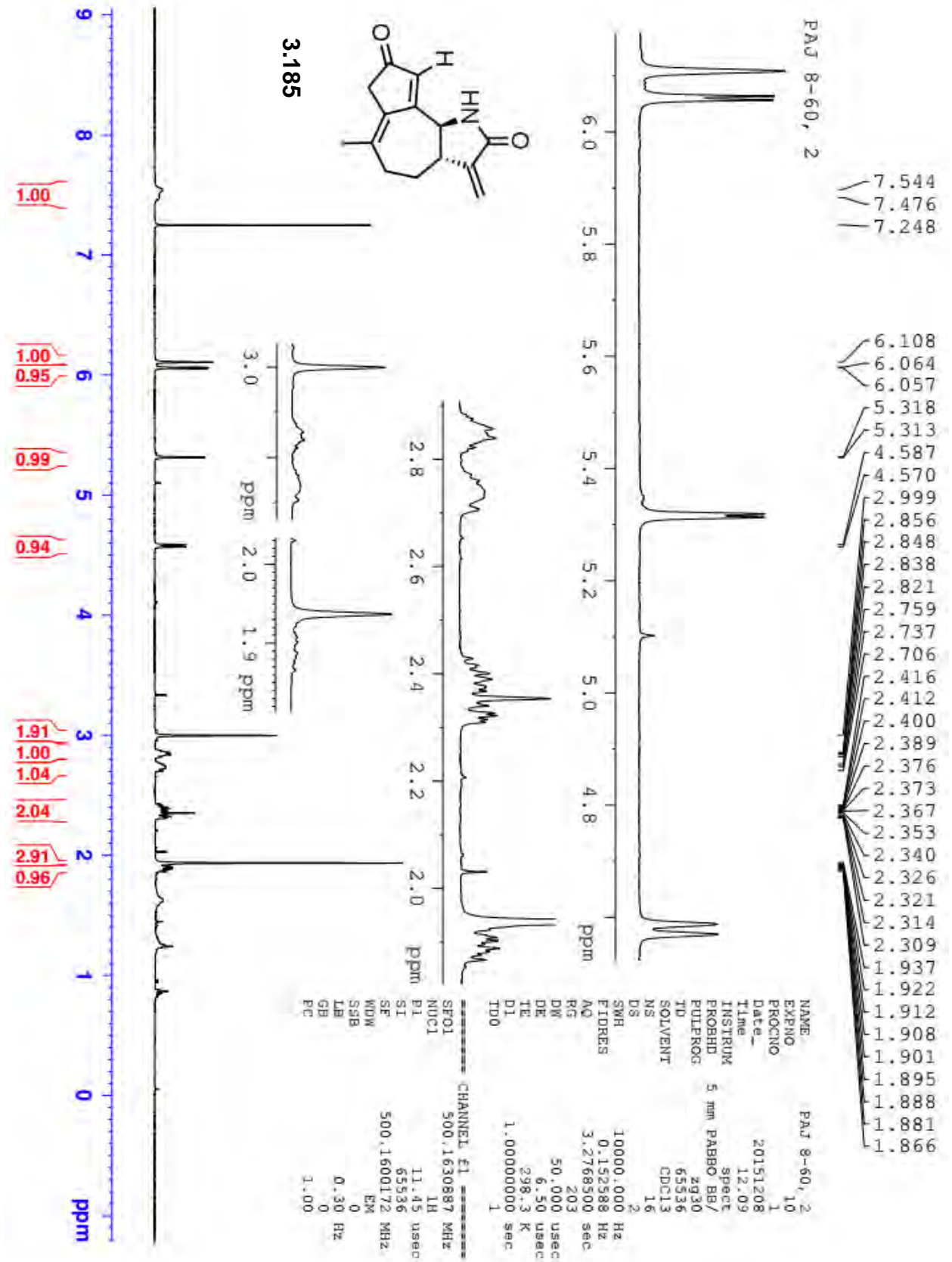
3.199

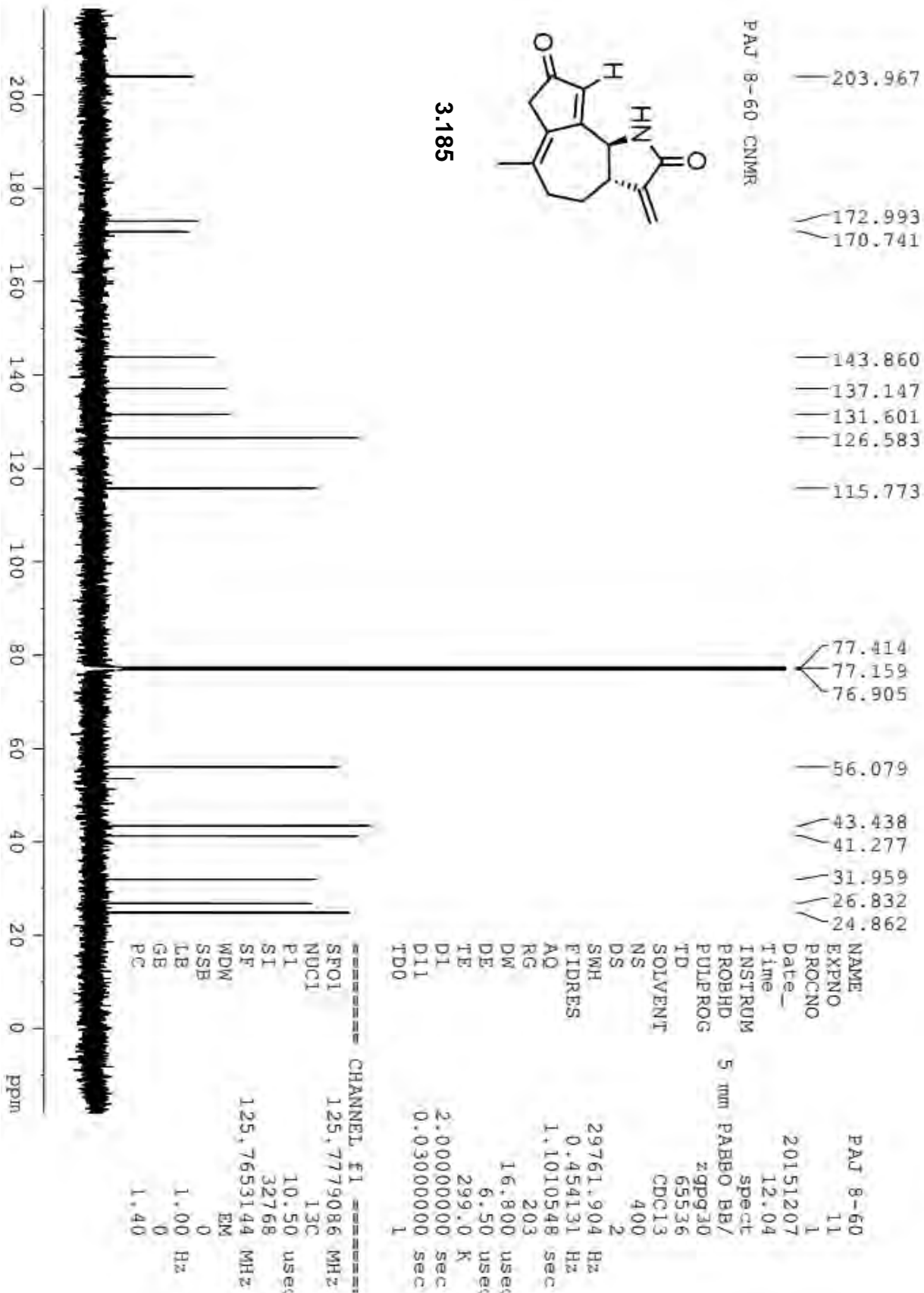
9.212	1.00
9.209	1.00
5.501	1.00
5.463	1.00
5.024	1.00
5.009	1.00
3.404	1.00
3.144	1.00
3.103	1.00
3.013	1.00
2.972	1.00
2.502	1.00
2.478	1.00
2.464	1.00
2.439	1.00
2.137	1.00
2.125	1.00
2.113	1.00
2.087	1.00
2.075	1.00
1.923	1.00
1.914	1.00
1.903	1.00
1.895	1.00
1.889	1.00
1.882	1.00
1.875	1.00
1.821	1.00
1.570	1.00
1.544	1.00
1.528	1.00
1.513	1.00
1.498	1.00
1.483	1.00
1.125	1.00
1.109	1.00
0.994	1.00
0.990	1.00
0.966	1.00

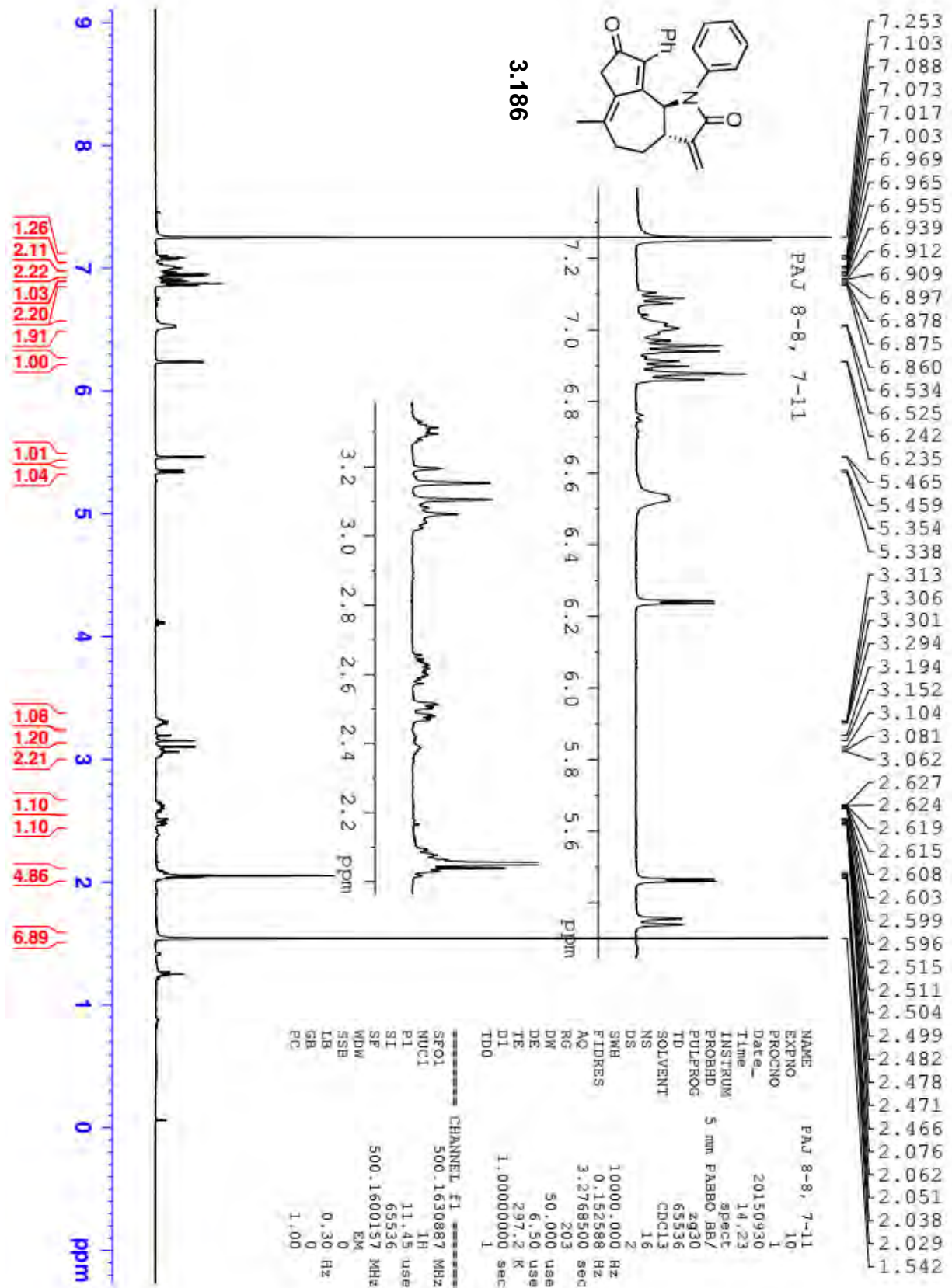


NAME PAJ 8-42, 23-30
 EXPNO 10
 PROCNO 1
 Date_ 20151104
 Time 9.56
 INSTRUM spect
 PROBHD 5 mm PABBO BB/
 PULPROG zg30
 TD 65536
 SOLVENT CDCl3
 NS 16
 DS 2
 SMF 10000.000 Hz
 FIDRES 0.152588 Hz
 AQ 3.2768500 sec
 RG 203
 DW 50.000 usec
 DE 6.50 usec
 TE 297.7 K
 D1 1.00000000 sec
 TD0 1

CHANNEL F1
 SFO1 500.1630887 MHz
 NUCL1 1H
 P1 11.45 usec
 SI 65536
 SF 500.1600119 MHz
 MDW EM
 SSB 0
 LB 0.30 Hz
 GB 0
 PC 1.00

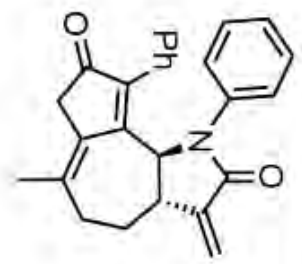




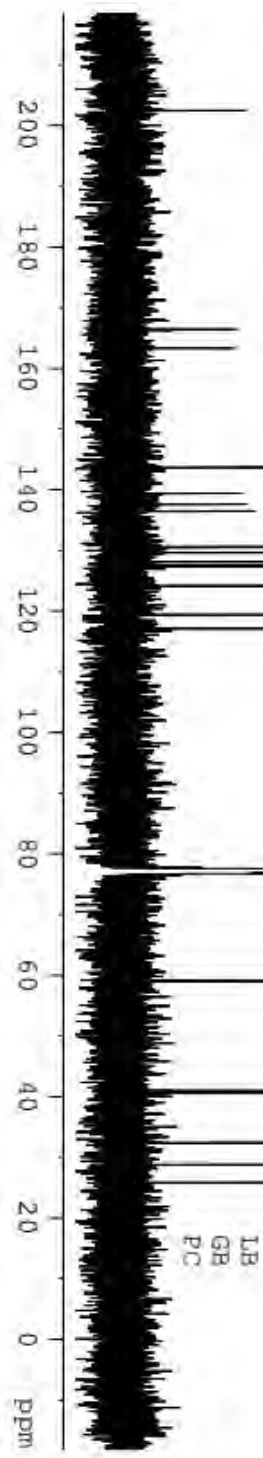


- 202.483
- 166.402
- 163.339
- 143.638
- 139.383
- 137.606
- 136.437
- 130.595
- 130.486
- 129.597
- 128.089
- 127.475
- 127.373
- 124.124
- 119.344
- 117.110
- 77.409
- 77.155
- 76.901
- 59.018
- 40.921
- 40.564
- 32.377
- 28.736
- 25.819

PAJ 8-8, 7-11 CNMR

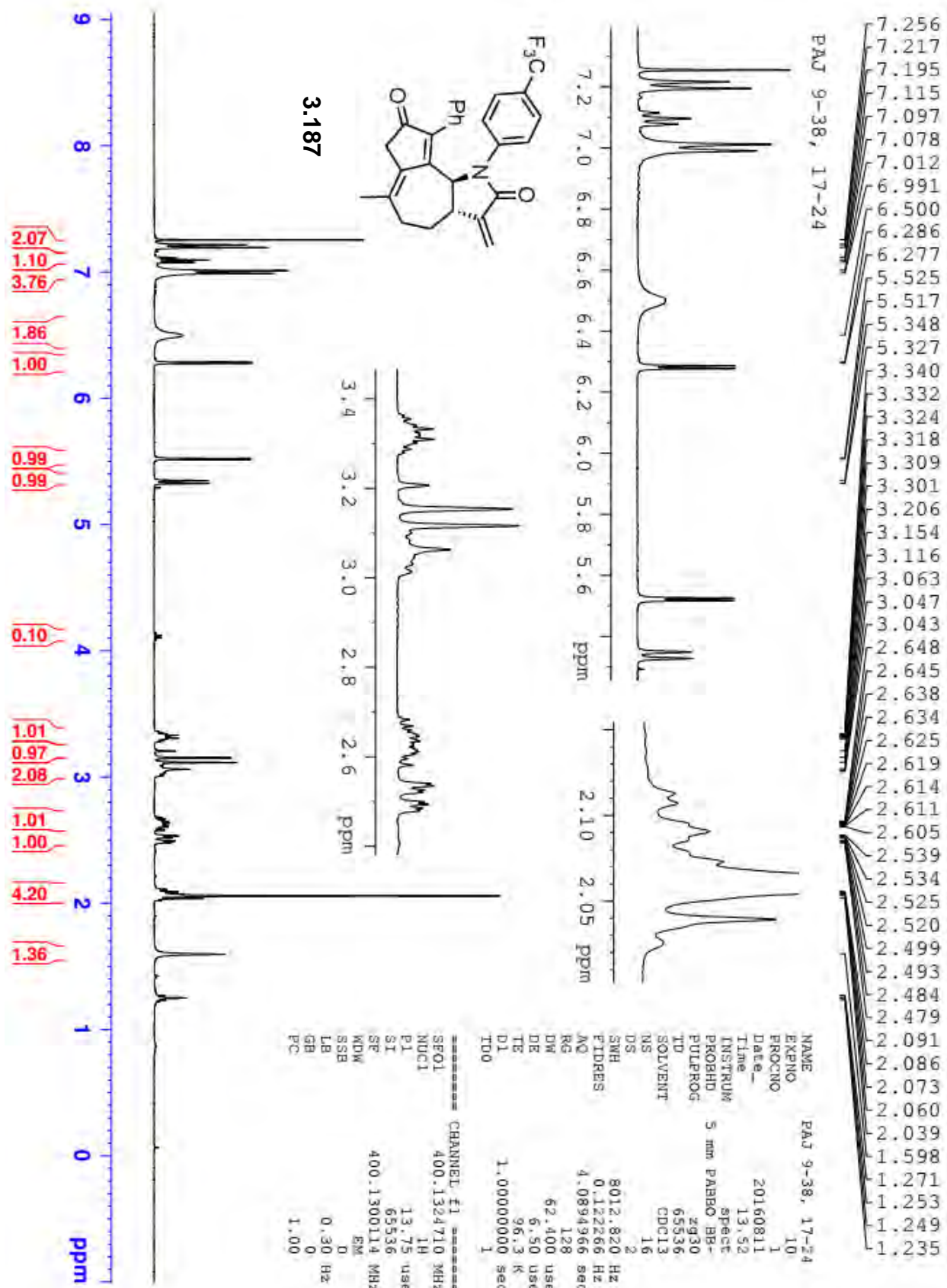


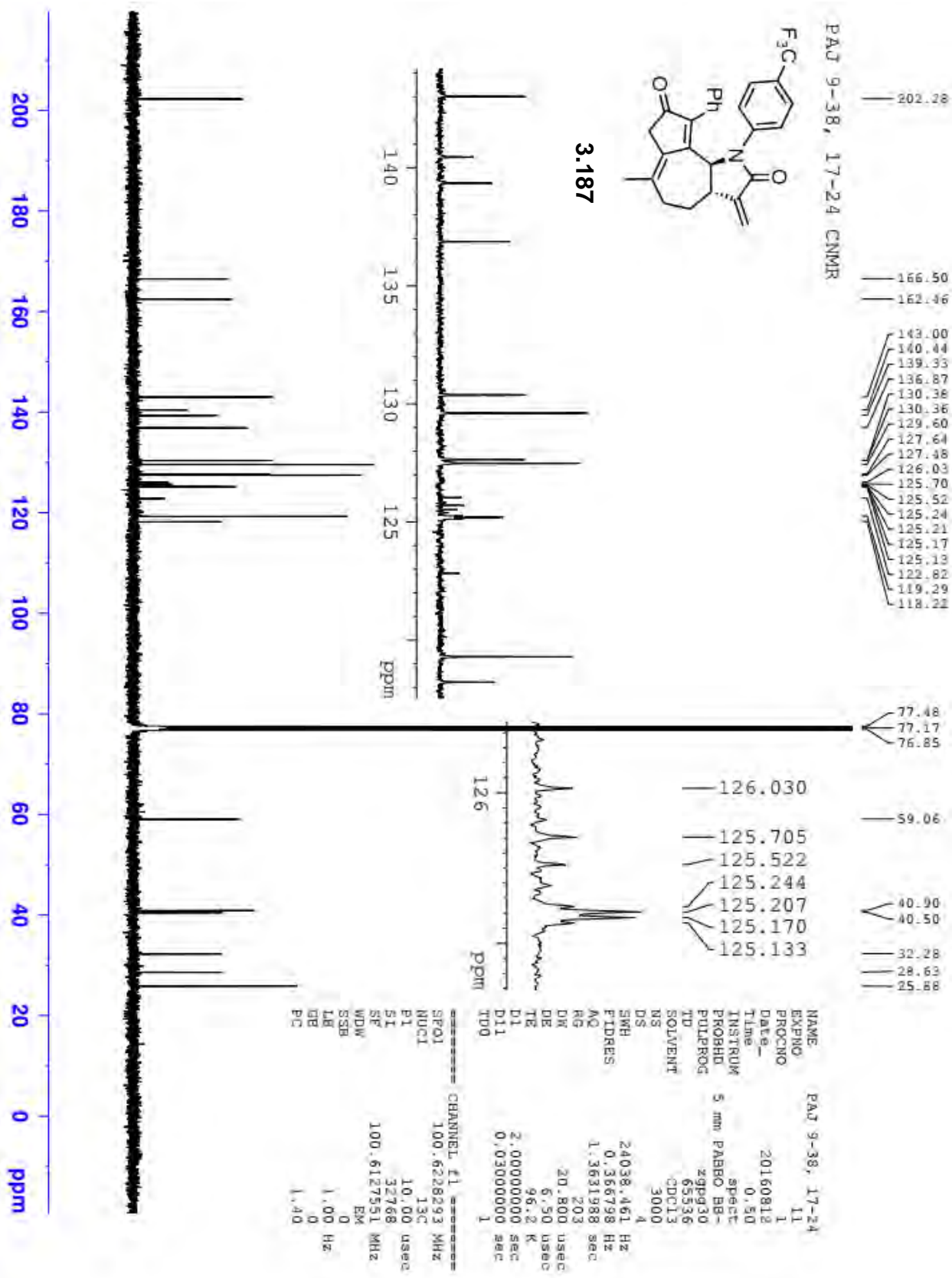
3.186

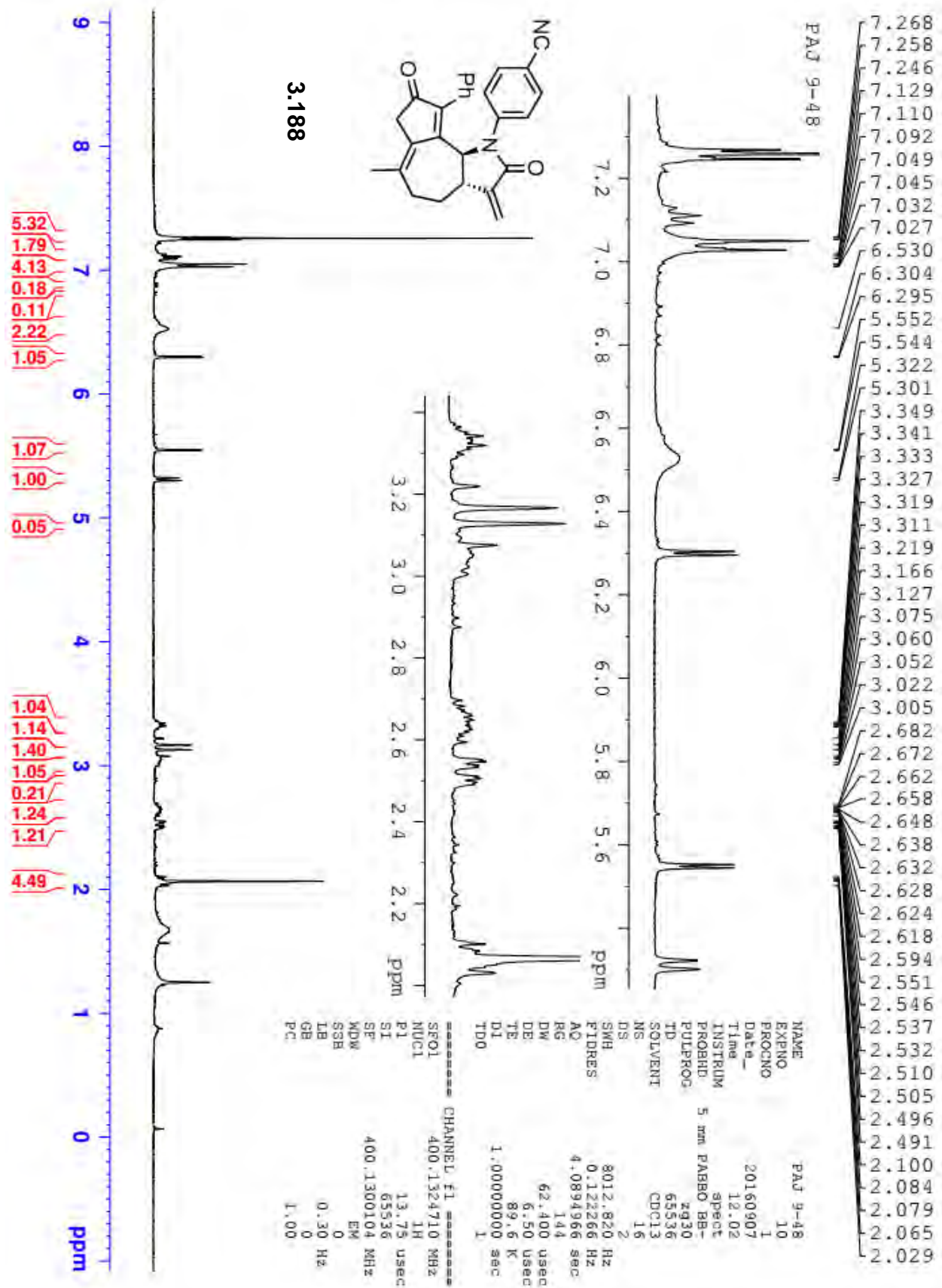


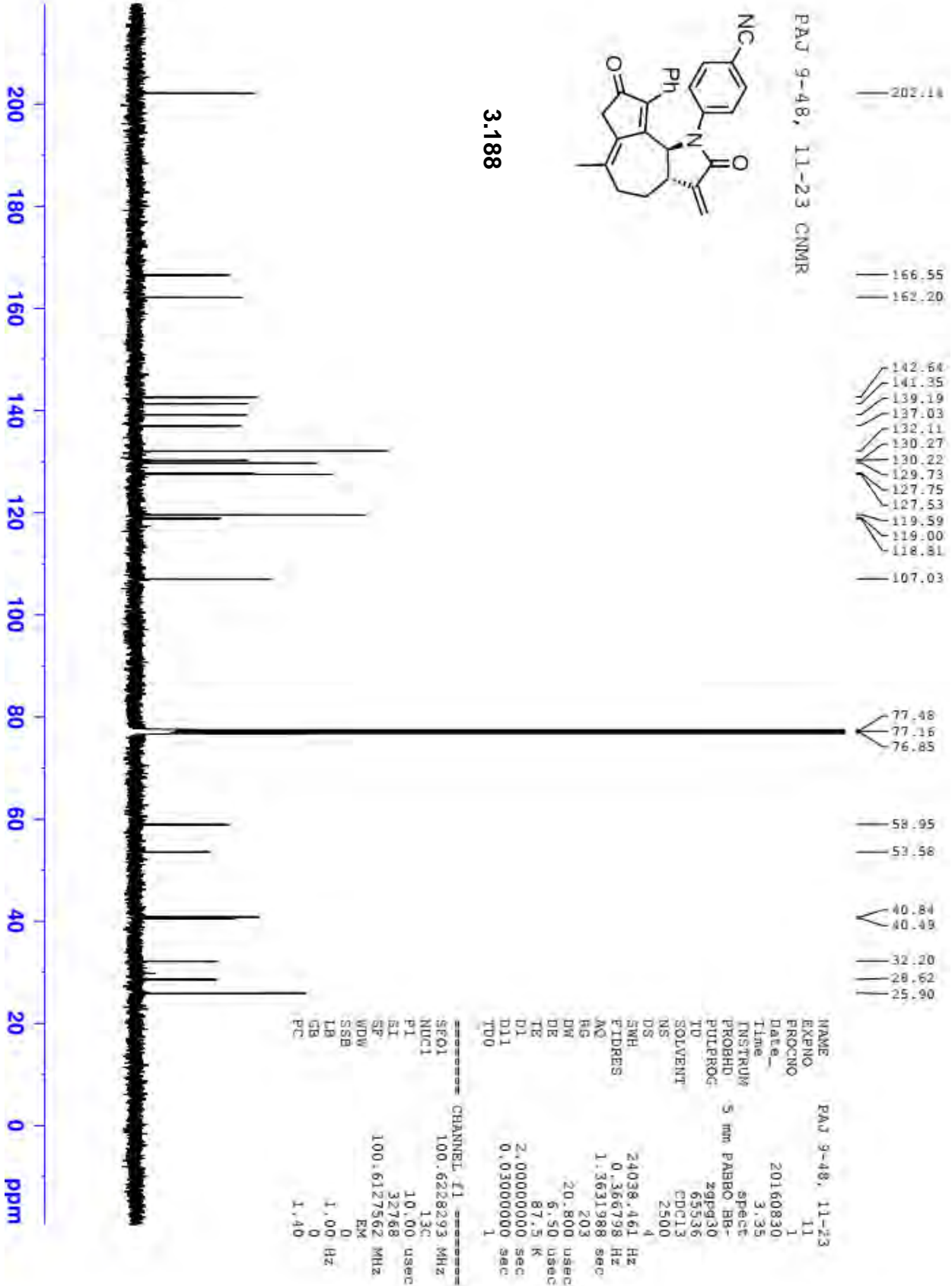
NAME	PAJ 8-8, 7-11
EXPNO	11
PROCNO	1
Date_	20151001
Time	2.31
INSTRUM	spect
PROBHD	5 mm PABBO BB/
PULPROG	zgpg30
TD	65536
SOLVENT	CDCl3
NS	4000
DS	2
SWH	29761.904 Hz
FIDRES	0.454131 Hz
AQ	1.1010548 sec
RG	203
DW	16.800 usec
DE	6.50 usec
TE	298.3 K
D1	2.00000000 sec
D11	0.03000000 sec
TD0	1

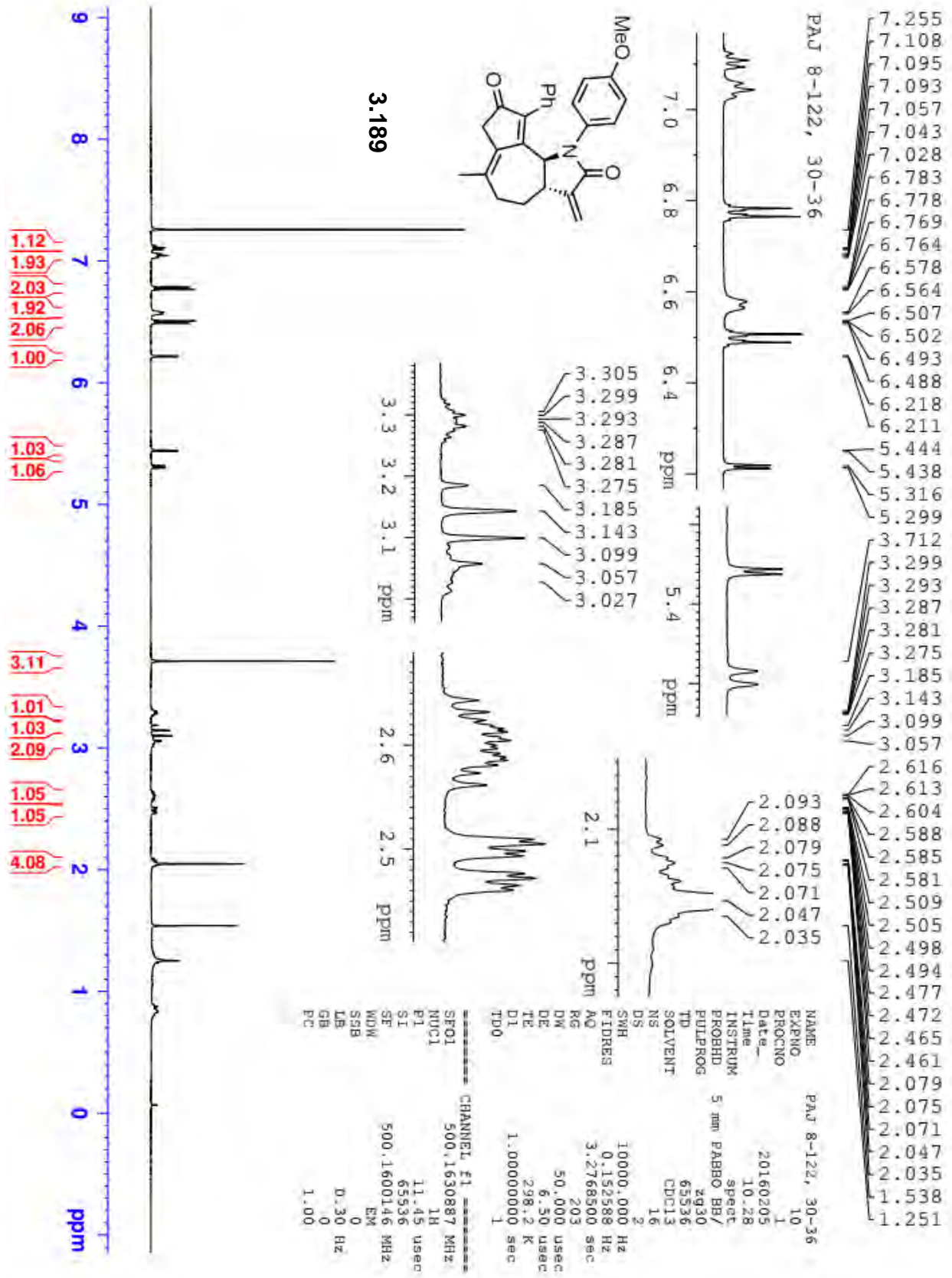
----- CHANNEL f1 -----	
SFO1	125.7779086 MHz
NUC1	13C
P1	10.50 usec
SI	32768
SF	125.7653131 MHz
WDW	EM
SSB	0
LB	1.00 Hz
GB	0
PC	1.40

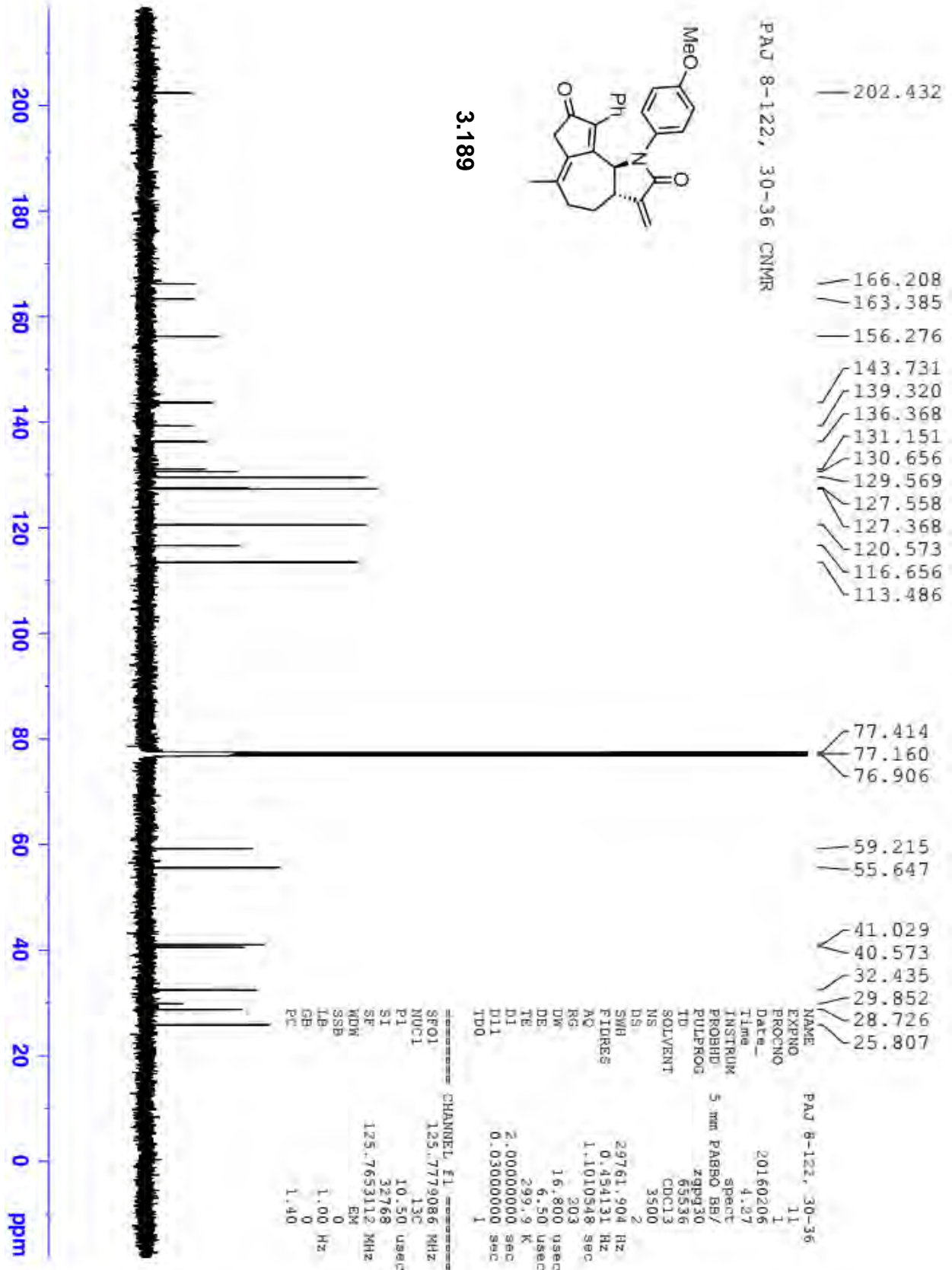












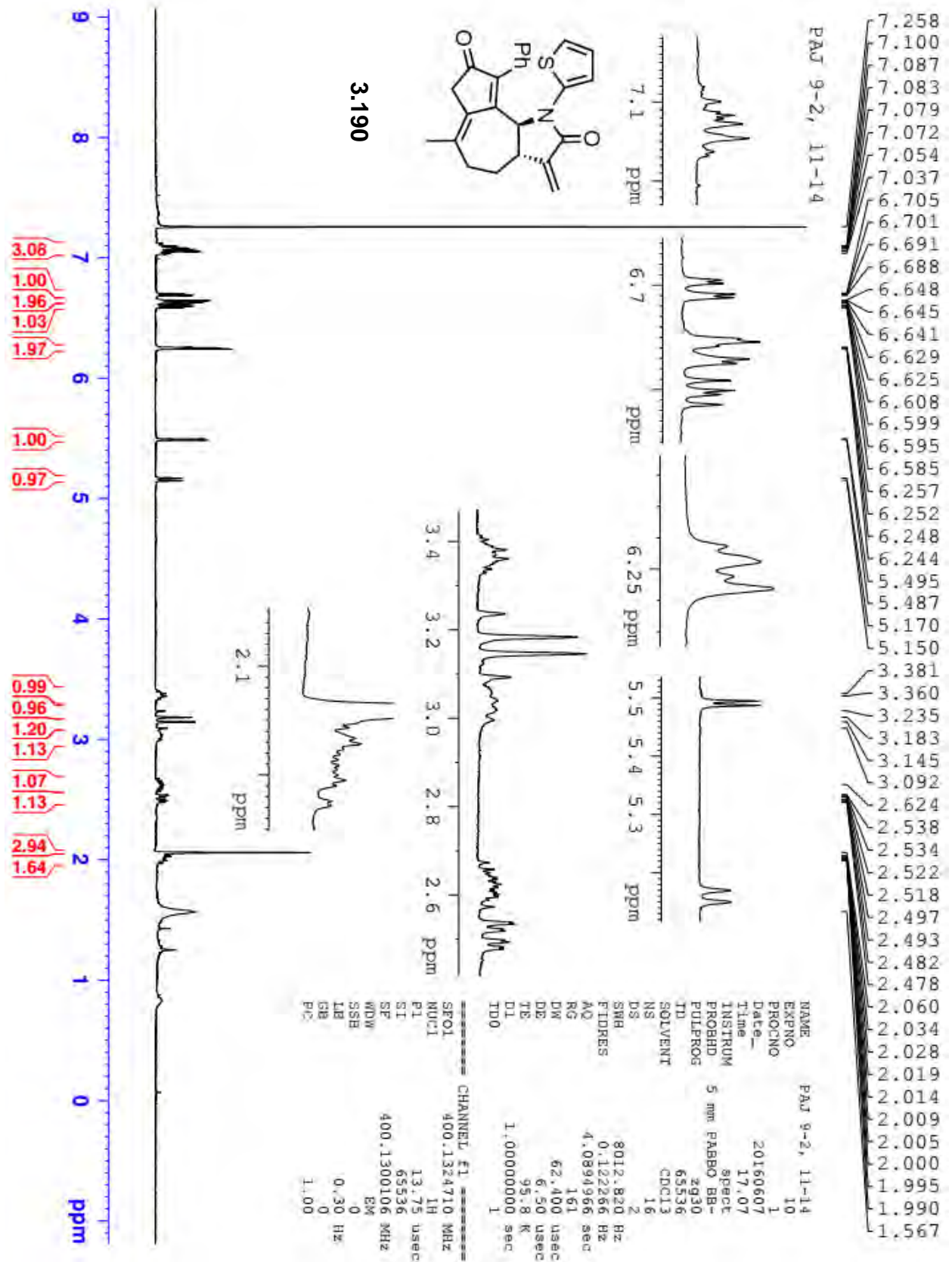
PAJ 8-122, 30-36 CNMR

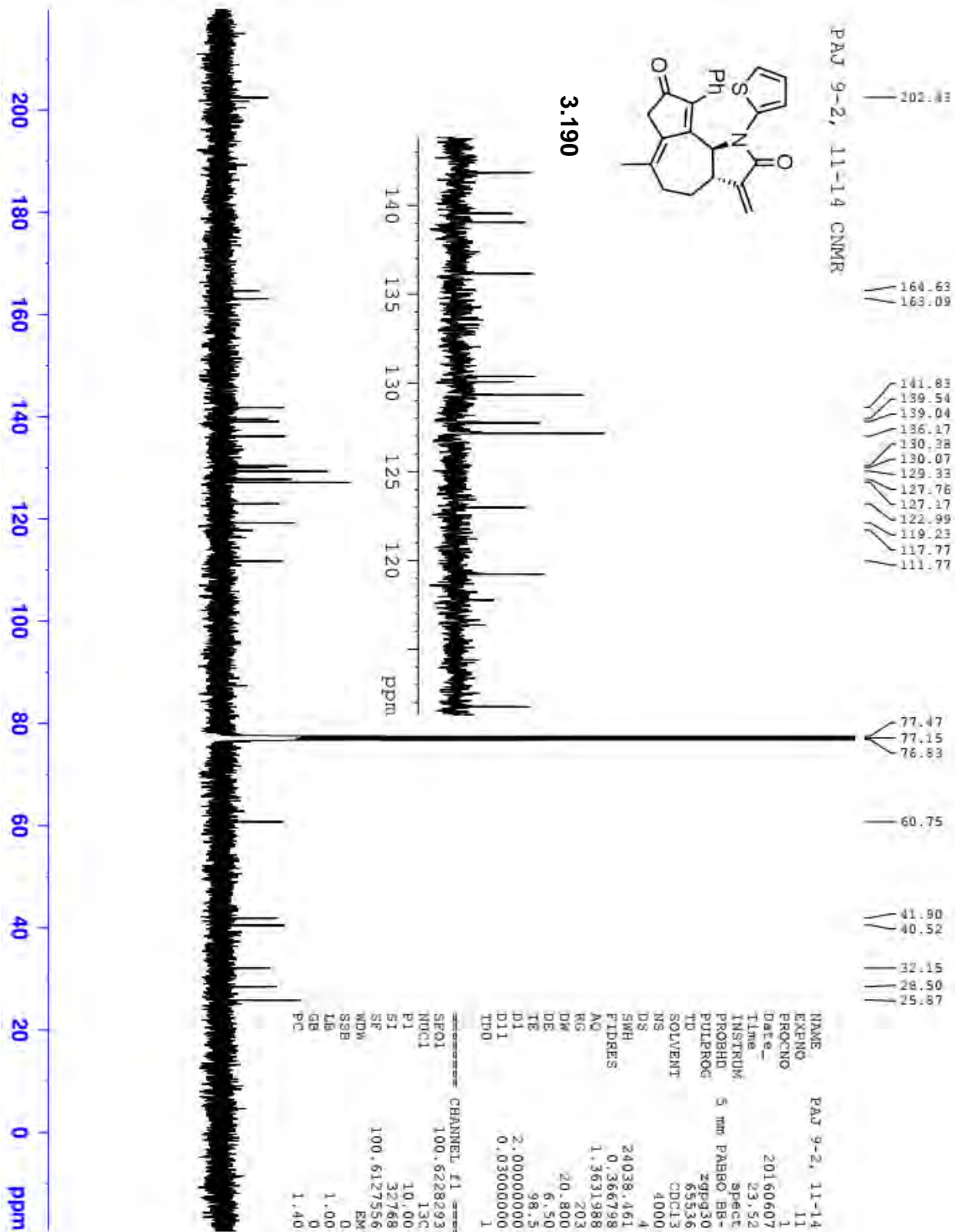
```

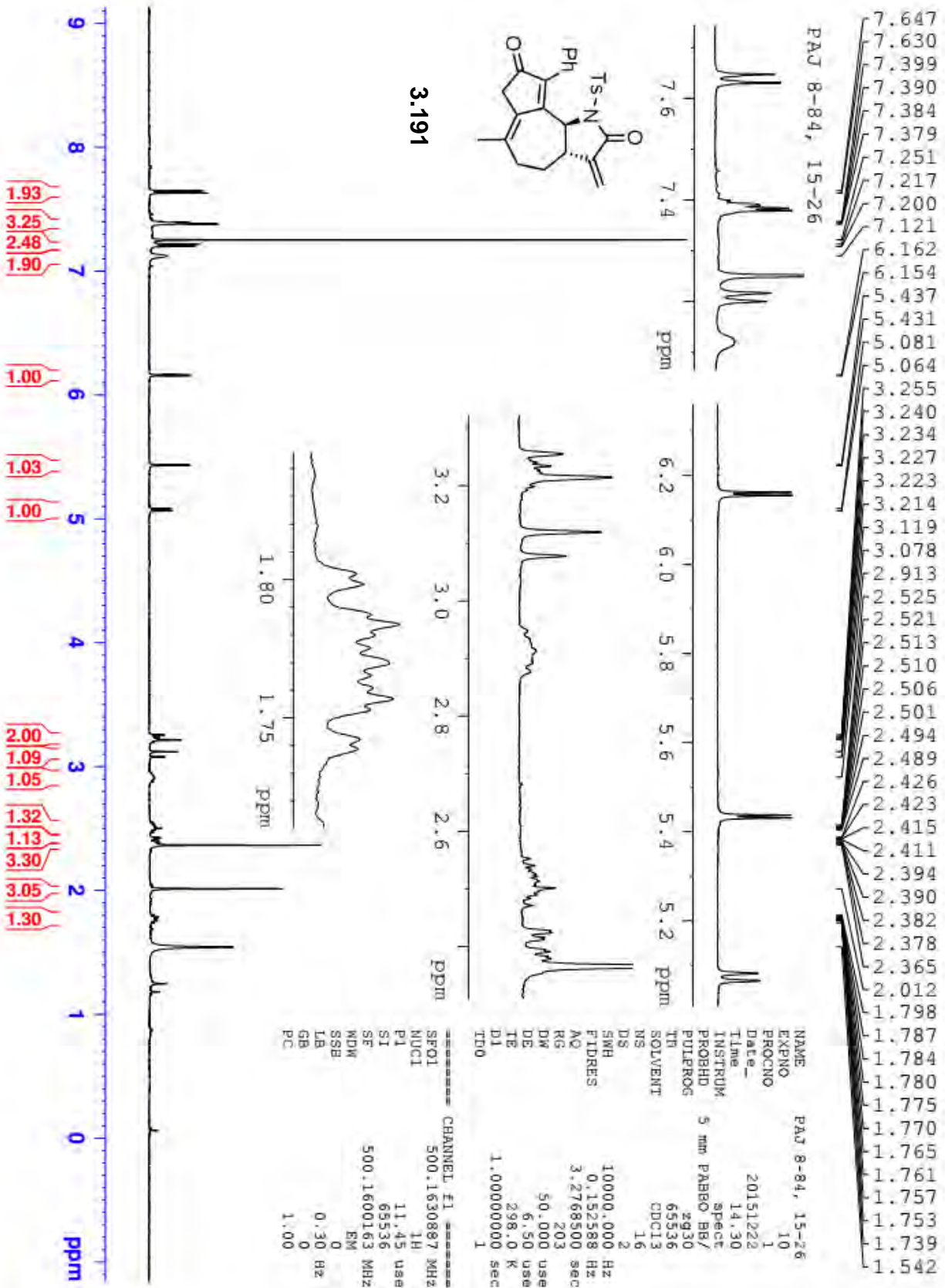
NAME          PAJ 8-122, 30-36
EXPNO         11
PROCNO        1
Date_         20160206
Time          4.27
INSTRUM       spect
PROBHD        5 mm PABBO BB/
PULPROG       zgpg30
ID            65536
SOLVENT       CDCl3
NS            3500
DS            2
SWH           29761.904 Hz
FIDRES        0.454131 Hz
AQ            1.1010548 sec
RG            203
DE            16.800 usec
TE            299.9 K
D1            2.00000000 sec
D11           0.03000000 sec
TD0           1
  
```

```

===== CHANNEL f1 =====
SFO1         125.7779086 MHz
NUC1         13C
P1           10.50 usec
SI           32768
SF           125.7653112 MHz
WDW          EM
SSB          0
LB           1.00 Hz
GB           0
PC           1.40
  
```

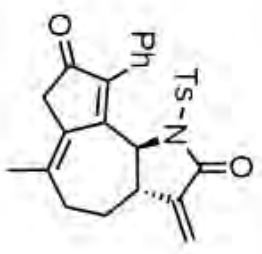




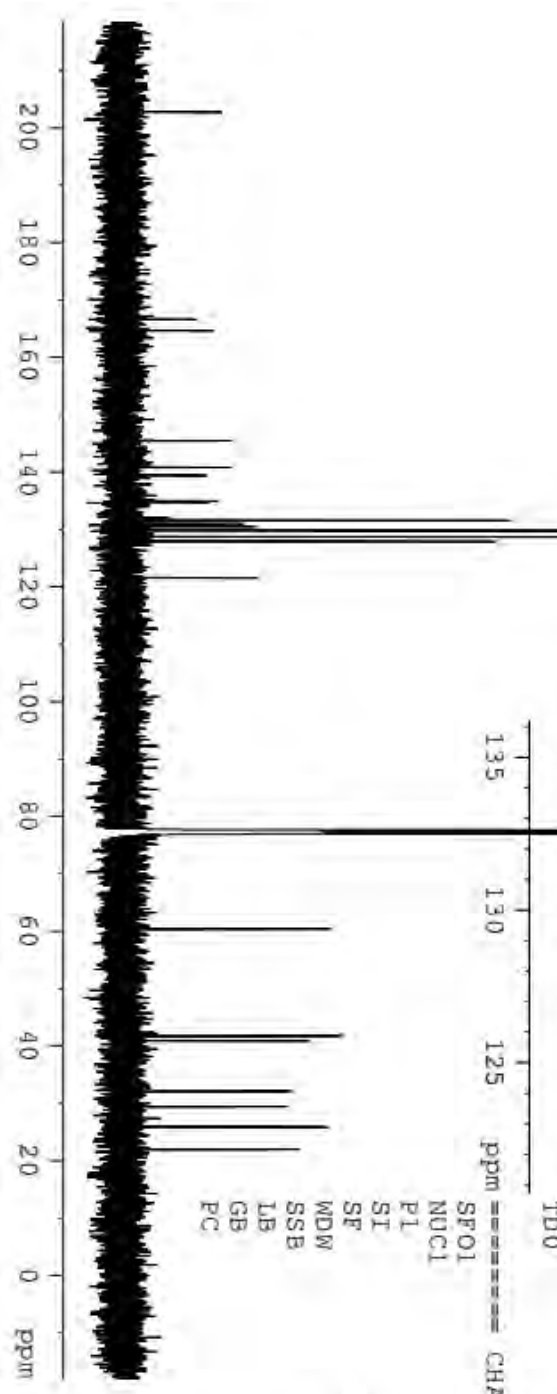


PAJ 8-84, 15-26 CNMR

- 202.621
- 166.468
- 164.551
- 145.308
- 140.708
- 139.286
- 134.846
- 134.662
- 131.429
- 130.871
- 130.373
- 129.693
- 128.544
- 127.786
- 121.432
- 77.408
- 77.154
- 76.900
- 60.199
- 41.527
- 40.676
- 31.949
- 29.252
- 25.728
- 21.764



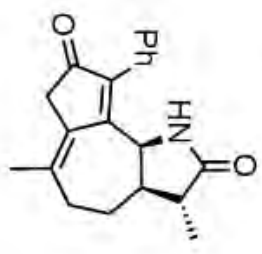
3.191



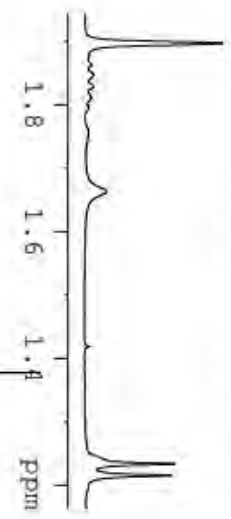
NAME	EXPNO	PROCNO	Date_	Time	INSTRUM	PROBHD	PULPROG	TD	SOLVENT	NS	DS	SWH	FTDRES	AQ	RG	DW	DE	TE	D1	D11	TD0
PAJ 8-84, 15-26	11	1	20151223	0.38	spect	5 mm PABBO BB/	zgpg30	65536	CDCl3	4000	2	29761.904 Hz	0.454131 Hz	1.1010548 sec	203	16.800 usec	6.50 usec	299.7 K	2.00000000 sec	0.03000000 sec	1
CHANNEL F1																					
SFO1																					
NOCL																					
PL																					
SI																					
SF																					
WDW																					
SSB																					
LB																					
GB																					
PC																					

PAJ 7-196, 30-40

- 7.441
- 7.423
- 7.420
- 7.405
- 7.381
- 7.377
- 7.362
- 7.252
- 7.173
- 7.170
- 7.153
- 5.309
- 4.991
- 4.972
- 3.218
- 3.166
- 3.147
- 3.124
- 3.095
- 2.586
- 2.559
- 2.539
- 2.510
- 2.495
- 2.483
- 2.477
- 2.464
- 2.351
- 2.332
- 2.304
- 2.285
- 2.280
- 2.267
- 2.261
- 2.249
- 2.244
- 2.055
- 2.047
- 2.032
- 2.020
- 1.897
- 1.862
- 1.847
- 1.829
- 1.811
- 1.663
- 1.233
- 1.215



3.193



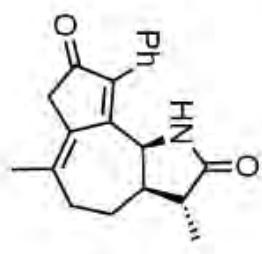
```

NAME          PAJ 7-196, 30-40
EXPNO         10
PROCNO        1
Date_         20150910
Time_         16.57
INSTRUM       spect
PROBHD        5 mm PABBO BB-
PULPROG       zg30
TD            65536
SOLVENT       CDCl3
NS            16
DS            2
SWH           8012.820 Hz
FIDRES       0.122266 Hz
AQ           4.0894966 sec
RG           101
DW           62.400 usec
DE           6.50 usec
TE           95.0 K
D1           1.00000000 sec
TD0          1

----- CHANNEL f1 -----
SEF01         400.1324710 MHz
NUC01         1H
P1           13.75 usec
SI           65536
SE           400.1300131 MHz
WDW          EM
SSB          0
LB           0.30 Hz
GB           0
PC           1.00
  
```

202.54
 179.79
 162.97
 144.67
 140.85
 131.15
 129.46
 128.98
 128.80
 128.72
 77.47
 77.15
 76.83
 55.27
 45.55
 42.36
 42.10
 32.72
 31.88
 24.20
 15.55

PAJ 7-196, 30-40 CNMR



3.193

200
180
160
140
120
100
80
60
40
20
0 ppm



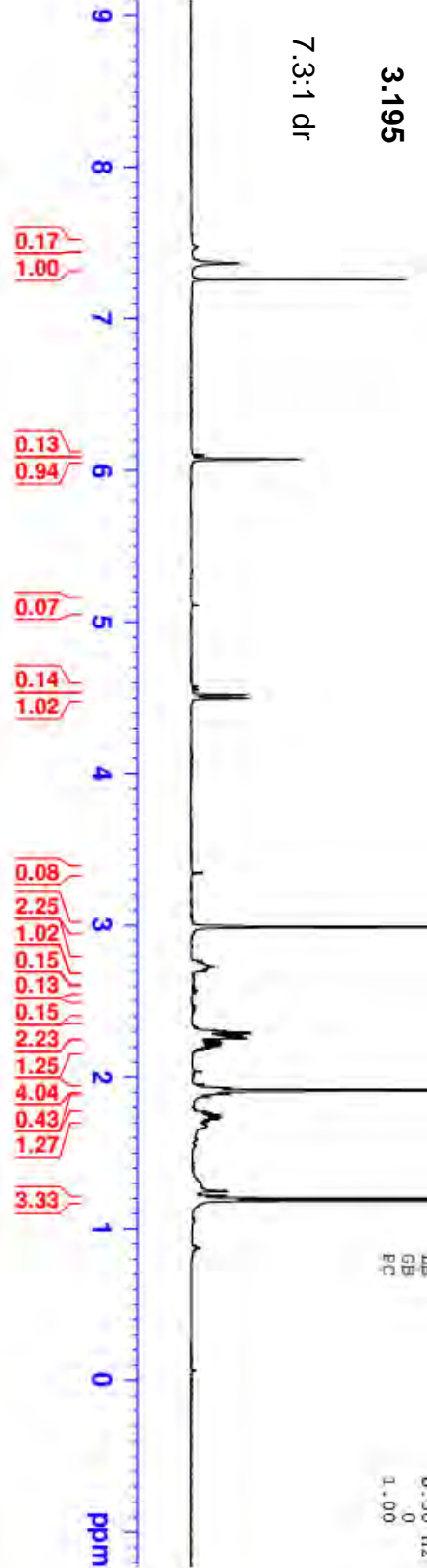
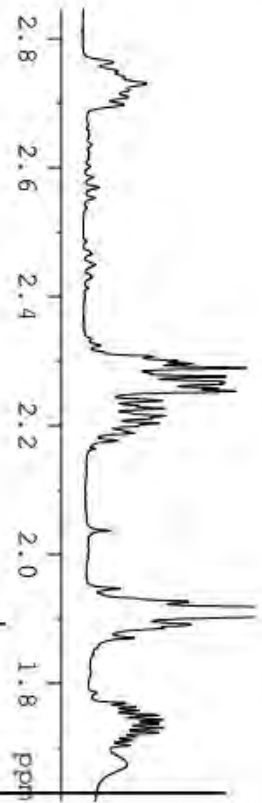
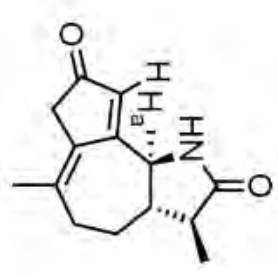
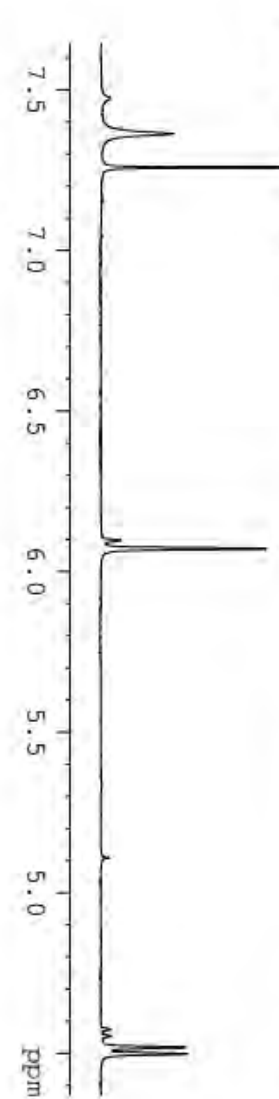
NAME Paj 7-196, 30-40
 EXPNO 11
 PROCNO 1
 Date_ 20150910
 Time 22.01
 INSTRUM spect
 PROBHD 5 mm PABBO BB-
 PULPROG zgpg30
 TD 65536
 SOLVENT CDCl3
 NS 2048
 DS 4
 SWH 24038.461 Hz
 FIDRES 0.366798 Hz
 AQ 1.3631988 sec
 RG 181
 DW 20.800 usec
 DE 6.50 usec
 TE 300.2 K
 D1 2.00000000 sec
 D11 0.03000000 sec
 TD0 1

----- CHANNEL f1 -----
 SFO1 100.6228293 MHz
 NUC1 13C
 P1 10.00 usec
 SI 32768
 SF 100.6127567 MHz
 WDW EM
 SSB 0
 LB 1.00 Hz
 GB 0
 PC 1.40

PAJ 8-76, 9-20

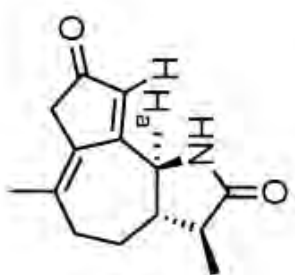
NAME PAF 8-76, 9-20
 EXPNO 10
 PROCNO 1
 Date 20151215
 Time 18.03
 INSTRUM spect
 PROBHD 5 mm PABBO BB/
 PULPROG zg30
 TD 65536
 SOLVENT CDCl3
 NS 16
 DS 2
 SWH 10000.000 Hz
 FIDRES 0.152588 Hz
 AQ 3.2768500 sec
 RG 101
 DW 50.000 usec
 DE 6.50 usec
 TE 297.9 K
 D1 1.00000000 sec
 TDO 1

----- CHANNEL f1 -----
 SF01 500.1630887 MHz
 NUC1 1H
 P1 11.45 usec
 SI 65536
 SF 500.1600131 MHz
 WDW EM
 SSB 0
 LB 0.30 Hz
 GB 0
 PC 1.00



3.195

7.3:1 dr



PAG 8-76, 9-20 CNMR

- 203.982
- 173.283
- 137.491
- 131.222
- 126.603
- 77.413
- 77.159
- 76.905
- 56.615
- 47.346
- 44.962
- 41.352
- 32.650
- 28.105
- 24.756
- 13.814

3.195
7.3:1 dr

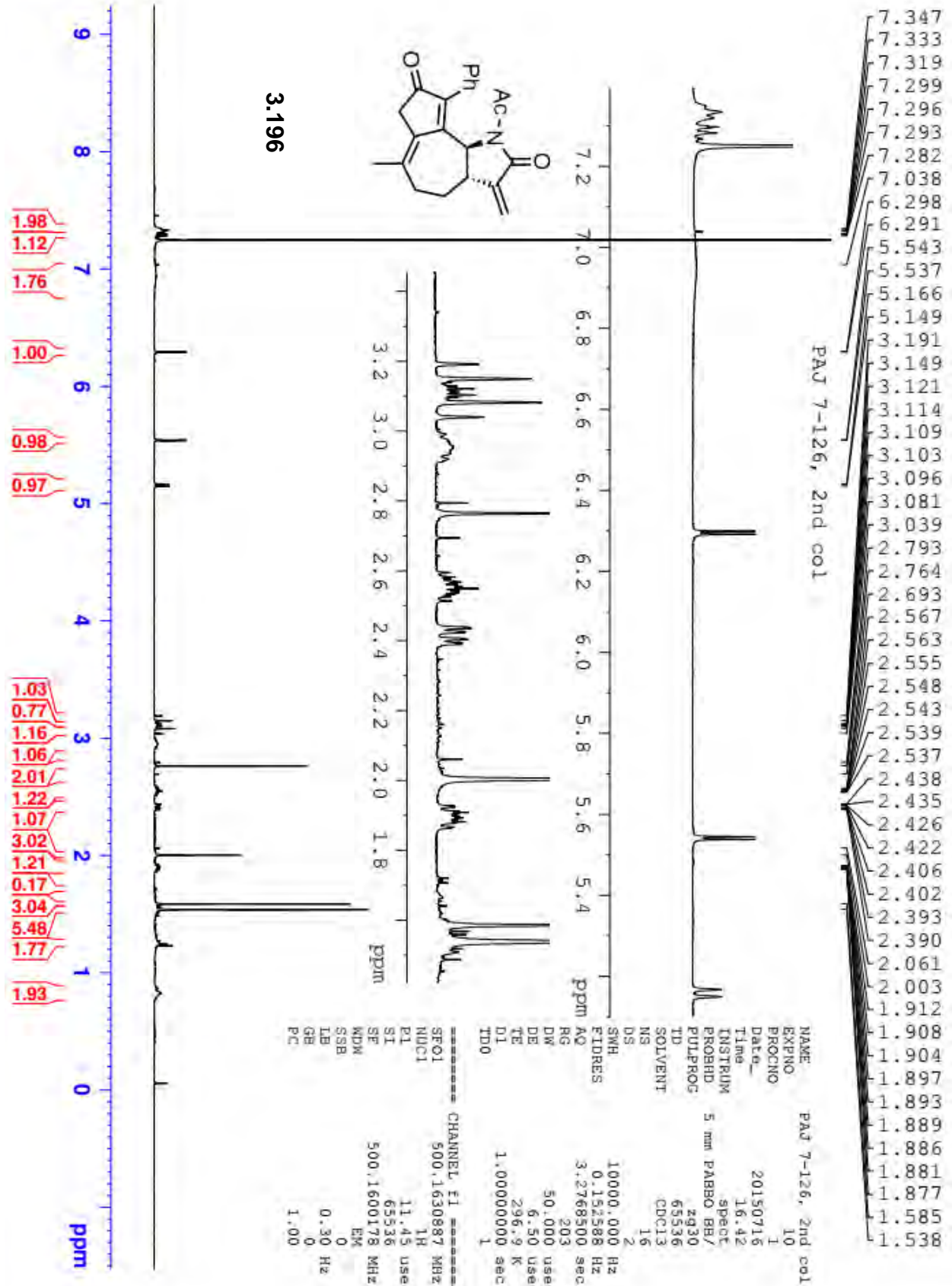


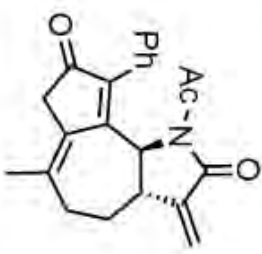
```

NAME          PAG 8-76, 9-20
EXPNO         11
PROCNO        1
Date_         20151215
Time         21.58
INSTRUM       spect
PROBHD        5 mm PABBO BB/
PULPROG       zgpg30
TD            65536
SOLVENT       CDCl3
NS            1024
DS            2
SWH           29761.904 Hz
FIDRES        0.454131 Hz
AQ            1.1010348 sec
RG            203
RG            203
DE            16.800 usec
DE            6.50 usec
TE            299.2 K
D1            2.00000000 sec
D11           0.03000000 sec
TD0           1

----- CHANNEL f1 -----
SFO1          125.7779086 MHz
NUC1          13C
P1            10.50 usec
S1            32768
SF            125.7653133 MHz
WDW           EM
SSB           0
LB            1.00 Hz
GB            0
PC            1.40

```





PAJ 7-126, 2nd col CNMR

- 202.668
- 171.803
- 166.414
- 164.488
- 142.759
- 138.256
- 135.827
- 131.166
- 131.011
- 130.597
- 127.840
- 120.636

- 77.405
- 77.151
- 76.898
- 57.400
- 40.459
- 39.735
- 31.846
- 29.717
- 28.614
- 25.711
- 23.855

3.196



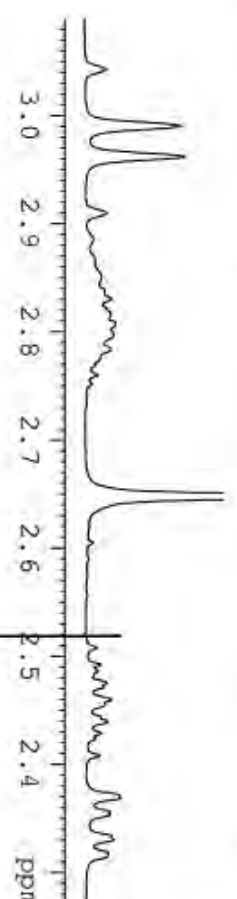
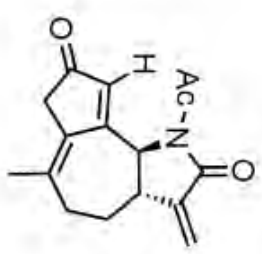
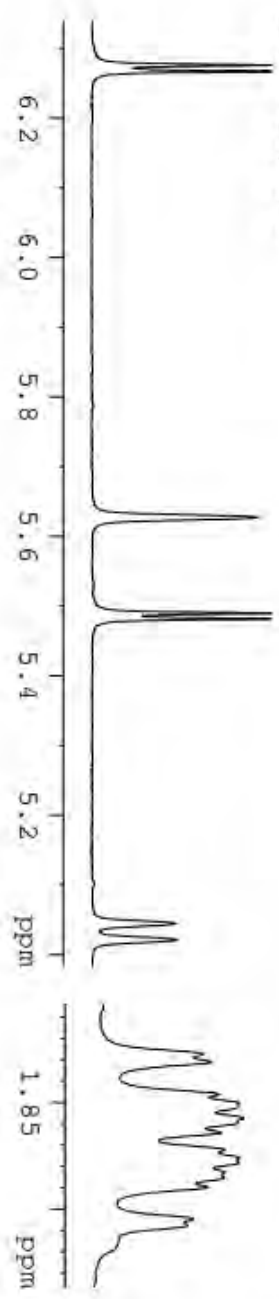
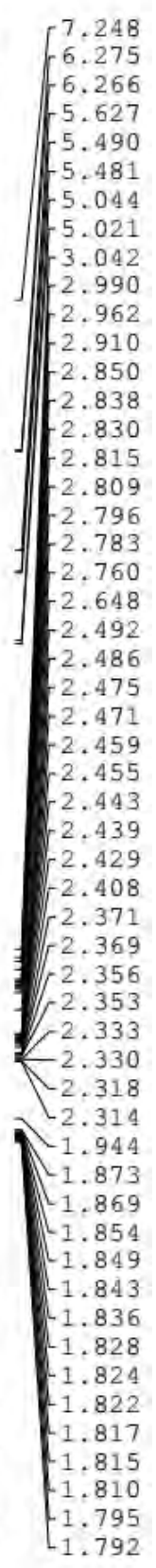
```

===== CHANNEL F1 =====
SFO1      125.7779086 MHz
NUC1      13C
P1         10.50 use
SI         32768
SF         125.7653132 MHz
WDW        EM
SSB        0
LB         1.00 Hz
GB         0
PC         1.40
  
```

```

NAME      PAJ 7-126, 2nd col
EXPNO     11
PROCNO    1
Date_     20150717
Time      3.21
INSTRUM   5 mm PABBO BB/
PROBHD    zgpg30
PULPROG   65536
TD         CDCl3
SOLVENT   4500
NS         2
DS         2
SWH        29761.904 Hz
FIDRES     0.454131 Hz
AQ         1.1010548 sec
RG         203
DW         16.800 use
DE         6.50 use
TE         298.0 K
D1         2.00000000 sec
D11        0.03000000 sec
TD0        1
  
```

PAJ 8-68, 2-5

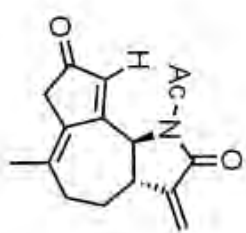


NAME PAJ 8-68, 2-5
 EXPNO 10
 PROCNO 1
 Date_ 20151208
 Time 17.21
 INSTRUM spect
 PROBHD 5 mm PABBO BB-
 PULPROG zg30
 TD 65536
 SOLVENT CDCl3
 NS 16
 DS 2
 SWH 8012.820 Hz
 FIDRES 0.122266 Hz
 AQ 4.0894966 sec
 RG 128
 DW 62.400 usec
 DE 6.50 usec
 TE 300.2 K
 D1 1.00000000 sec
 TDO 1

----- CHANNEL f1 -----
 SFO1 400.1324710 MHz
 NUC1 1H
 P1 13.75 usec
 SF 65536
 SI 400.1300145 MHz
 WDW EM
 SSB 0
 LB 0.30 Hz
 GB 0
 PC 1.00

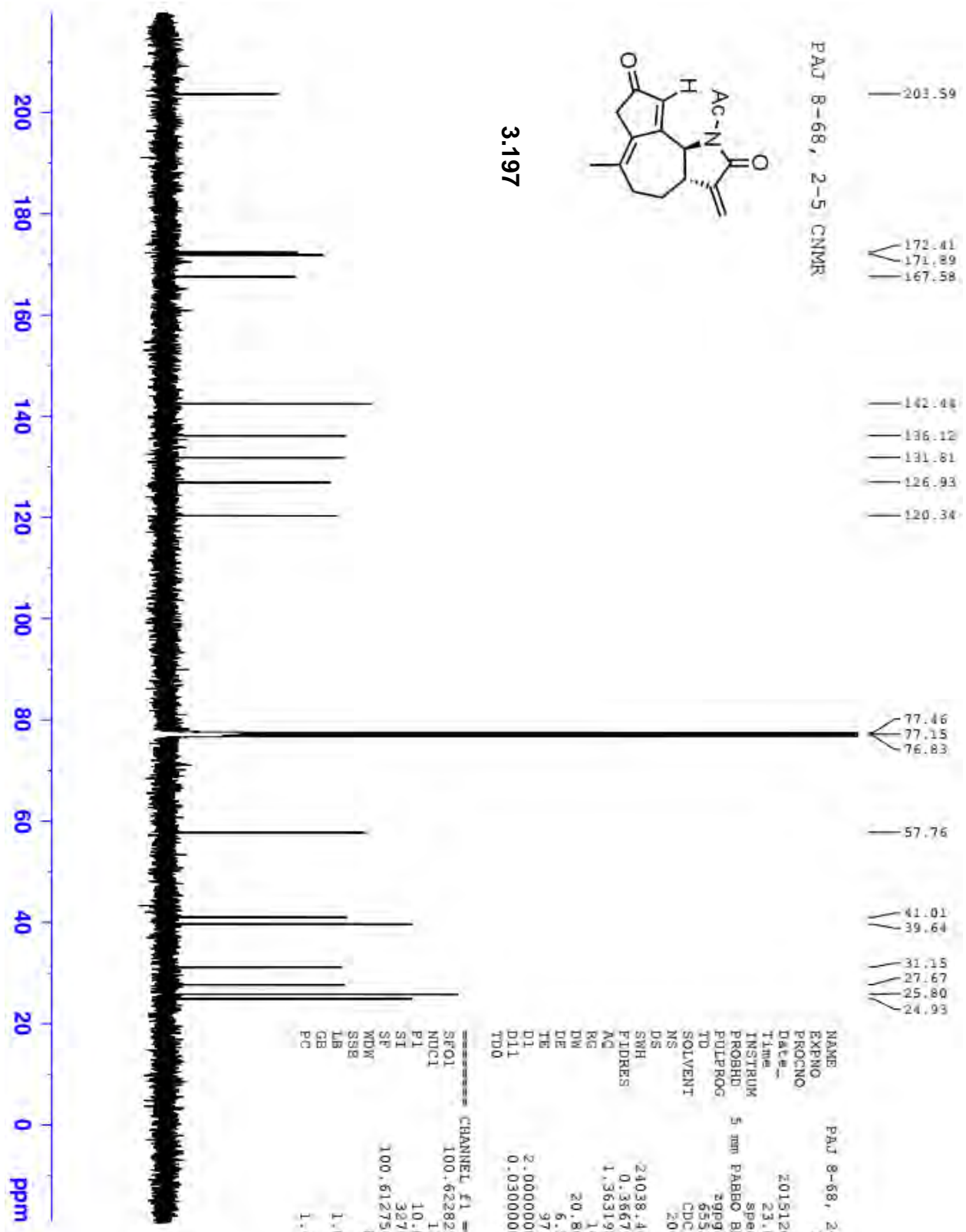
3.197





3.197

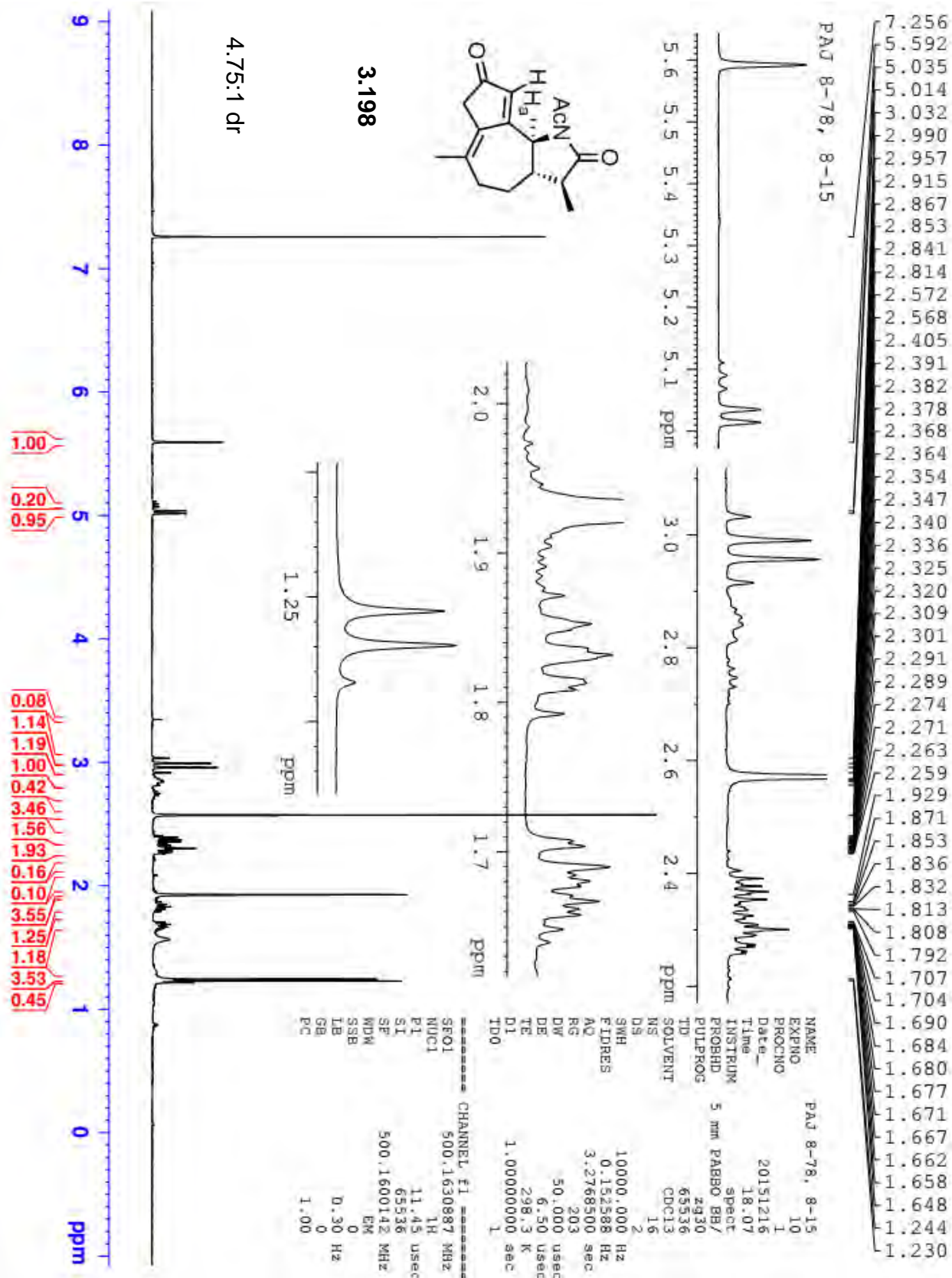
PAJ B-68, 2-5 CNMR

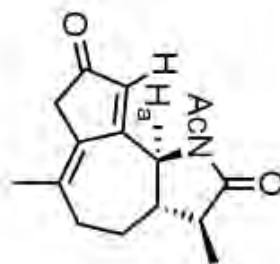


- 203.59
- 172.41
- 171.89
- 167.58
- 142.44
- 136.12
- 131.81
- 126.93
- 120.34
- 77.46
- 77.15
- 76.83
- 57.76
- 41.01
- 39.64
- 31.15
- 27.67
- 25.80
- 24.93

```

NAME          PAJ B-68, 2-5
EXPNO         11
PROCNO        1
Date_         20151208
Time          23.08
INSTRUM       spect
PROBHD        5 mm PABBO BB-
PULPROG       zgpg30
TD            65536
SOLVENT       CDCl3
NS            2048
DS            4
SWH           24038.461 Hz
FIDRES        0.366798 Hz
AQ            1.3631988 sec
RG            161
RG            161
DW            20.800 usec
DE            6.50 usec
TE            97.7 K
D1            2.00000000 sec
D11           0.03000000 sec
TD0           1
----- CHANNEL f1 -----
SFO1          100.62828293 MHz
NUC1          13C
P1            10.00 usec
SI            33768
SP            100.6127560 MHz
WDW           EM
SSB           0
LB            1.00 Hz
GB            0
PC            1.40
  
```



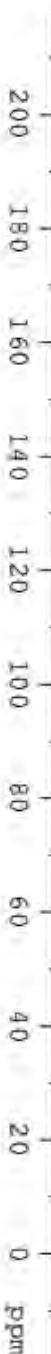


PAJ 8-78, 8-15 CNMR

- 203.712
- 177.103
- 172.459
- 171.672
- 136.454
- 131.660
- 127.058
- 77.414
- 77.160
- 76.905
- 65.988
- 58.262
- 45.682
- 42.331
- 41.048
- 31.576
- 29.030
- 25.441
- 24.725
- 15.416
- 13.666

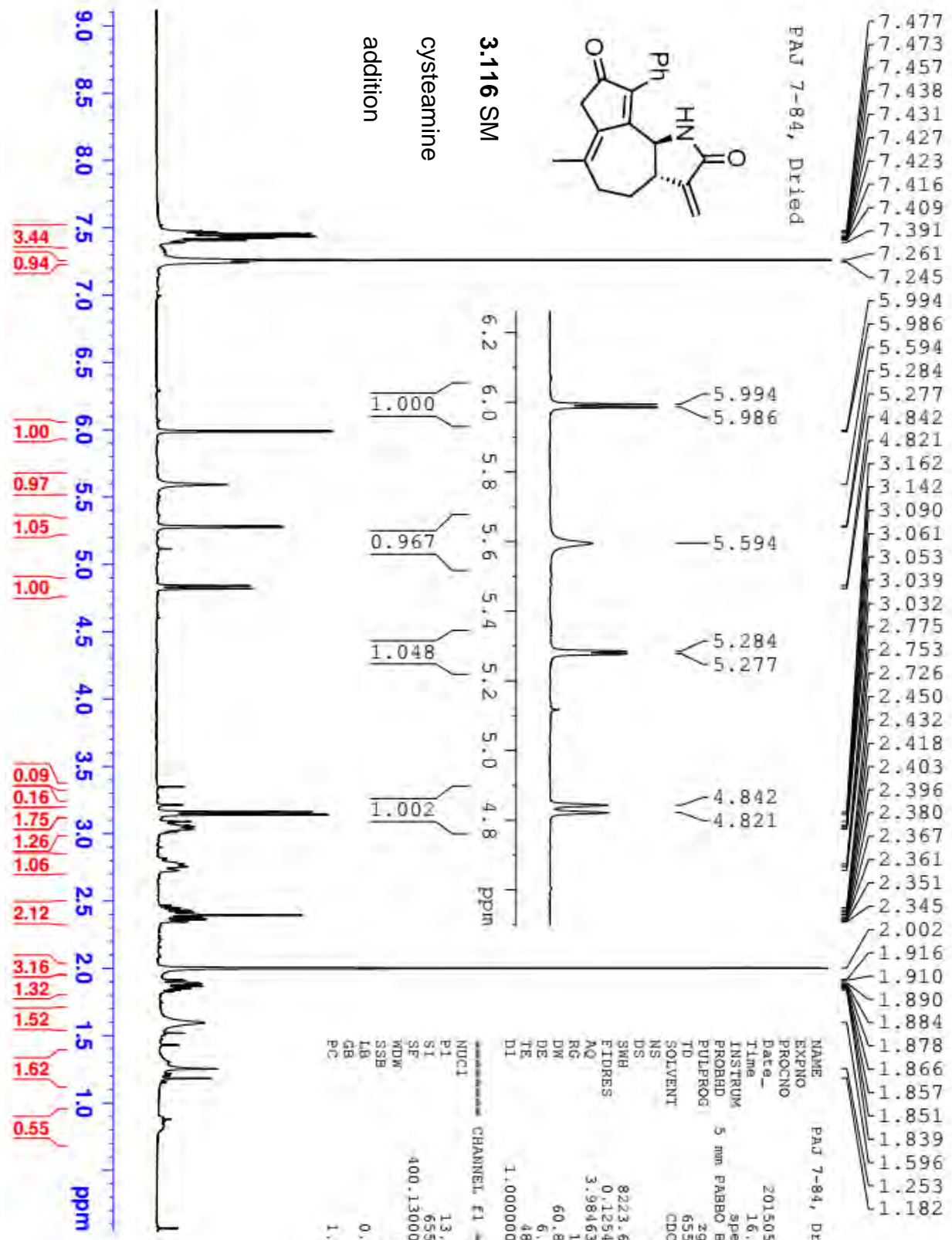
3.198

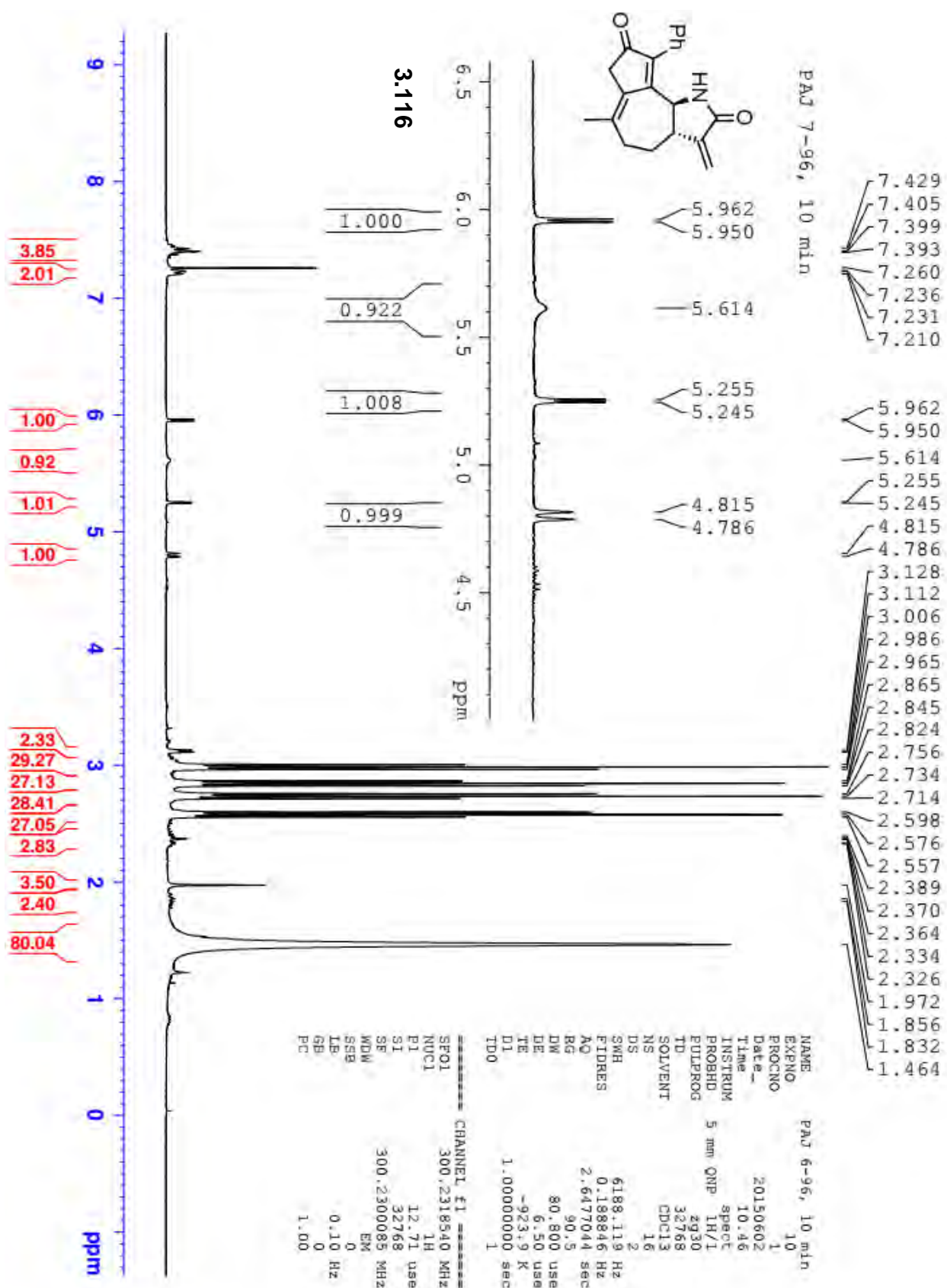
4.75:1 dr



NAME	PAJ 8-78, 8-15
EXPNO	11
PROCNO	1
Date_	20151217
Time	0.44
INSTRUM	spect
PROBHD	5 mm PABBO BB/
PULPROG	zgpg30
TD	65536
SOLVENT	CDCl3
NS	2500
DS	2
SWH	29761.904 Hz
FTDRES	0.454131 Hz
AQ	1.1010548 sec
RG	203
DW	16.800 use
DE	6.50 use
TE	299.3 K
DL	2.00000000 sec
D11	0.03000000 sec
TD0	1

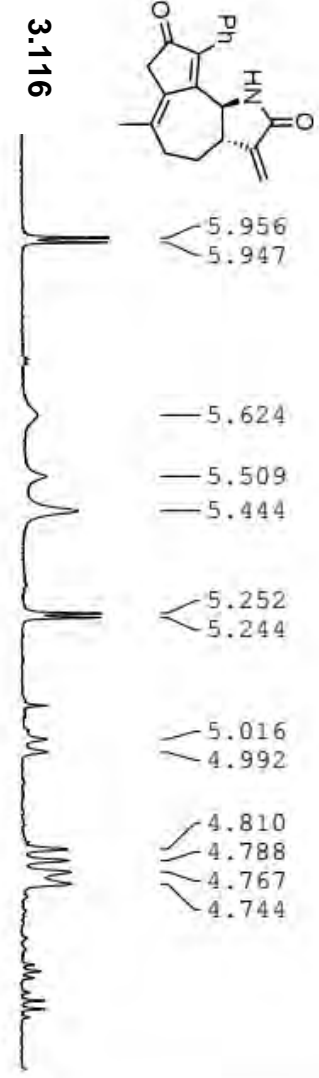
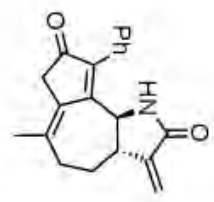
===== CHANNEL f1 =====	
SFO1	125.7779086 MHz
NUC1	13C
PL	10.50 use
SI	32768
SF	125.7653118 MHz
WDW	EM
SSB	0
LB	1.00 Hz
GB	0
PC	1.40



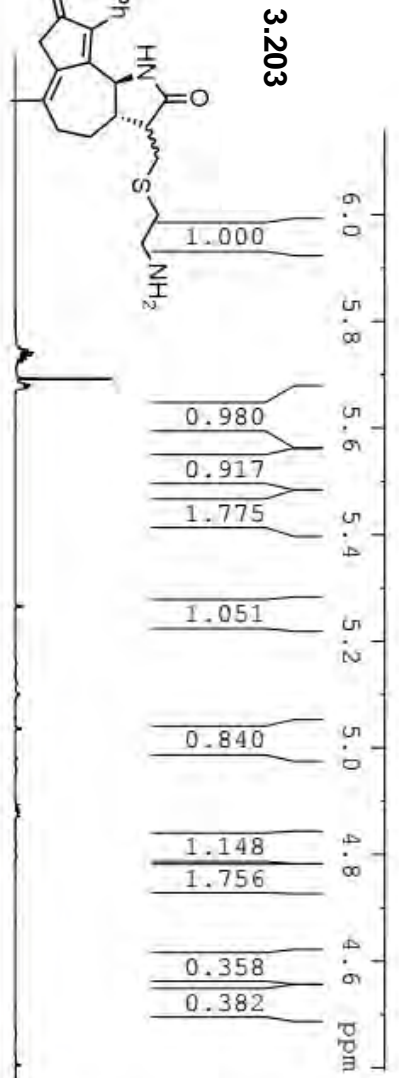
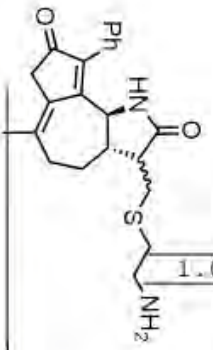


7.427
7.410
7.408
7.393
7.382
7.378
7.374
7.360
7.259
7.237
7.232
7.226
7.222
7.216
7.206
5.956
5.947
5.444
5.444
5.252
5.244
4.810
4.788
4.767
4.744
3.149
3.139
3.133
3.127
3.117
3.106
2.996
2.981
2.965
2.854
2.839
2.823
2.745
2.729
2.714
2.589
2.574
2.558
2.398
2.383
2.363
2.338
2.334
2.327
2.312
2.285
2.279
1.968
1.946
1.940
1.513

PAGE 7-96, 72h



NAME PAB 7-96, 72h
EXPNO 10
PROCNO 1
Date_ 20150605
Time 10.30
INSTRUM spect
PROBHD 5 mm PABBO BB-
PULPROG zg30
TD 65536
SOLVENT CDCl3
NS 16
DS 2
SWH 8223.685 Hz
FIDRES 0.125483 Hz
AQ 3.9846387 sec
RG 57
DE 60.800 usec
TE 288.5 K
D1 1.00000000 sec



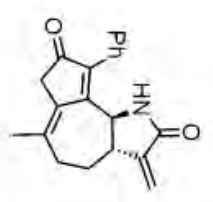
CHANNEL f1
NUC1 1H
P1 13.75 usec
SI 65536
SF 400.1300103 MHz
WDW EM
SSB 0
LB 0.30 Hz
GB 0
PC 1.00



2:1 dr

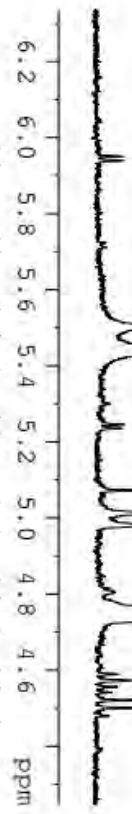
7.425
7.420
7.414
7.405
7.396
7.380
7.373
7.367
7.351
7.257
7.233
7.223
7.216
7.206
7.202
7.196
7.191
5.440
4.762
4.732
3.199
3.128
3.100
2.994
2.974
2.952
2.852
2.833
2.811
2.744
2.723
2.703
2.587
2.565
2.545
2.396
2.388
2.375
2.353
2.332
2.323
2.312
2.299
2.283
2.272
2.265
1.961
1.939
1.767
1.752
1.741
1.729
1.718
1.504

PAJ 7-96, 8 days



3.116

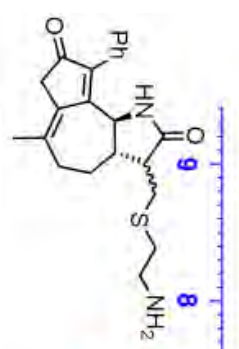
5.950
5.939
5.503
5.440
5.246
5.235
5.011
4.981
4.814
4.802
4.762
4.732



0.075
0.036
0.442
0.921
0.097
0.424
0.099
1.000
0.125
0.156

NAME Paj 7-96, 8 days
EXPNO 10
PROCNO 1
Date_ 20150610
Time 11.10
INSTRUM spect
PROBHD 5 mm QNP 1H/1
PULPROG zg30
TD 32768
SOLVENT CDCl3
NS 16
DS 2
SWH 6188.119 Hz
FIDRES 0.188846 Hz
AQ 2.6477044 sec
RG 80.6
DW 80.800 usec
DE 6.50 usec
TE -925.3 K
D1 1.00000000 sec
TD0 1

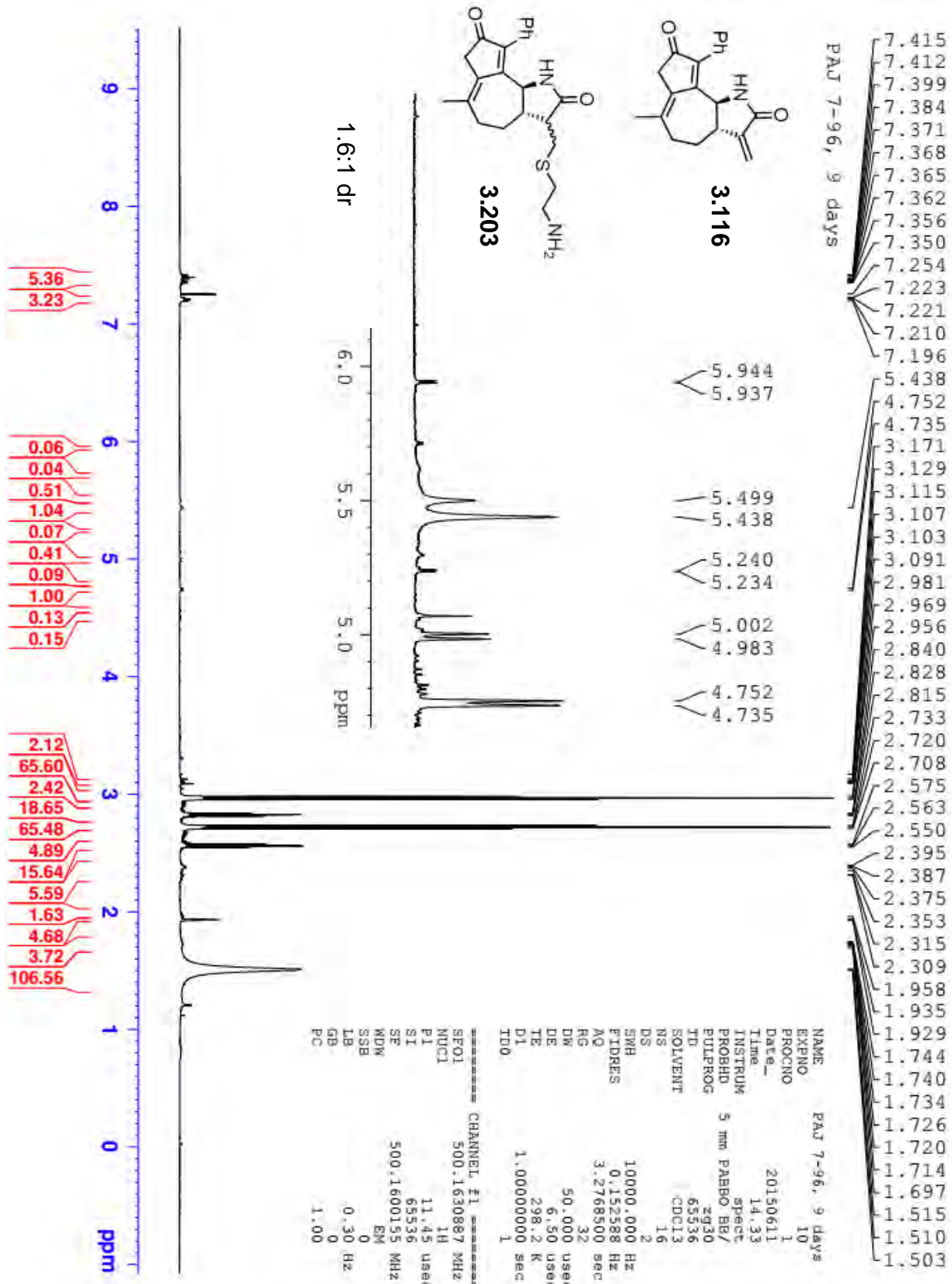
CHANNEL f1
SFO1 300.2318540 MHz
NUC1 1H
P1 12.71 usec
SI 32768
SE 300.2300093 MHz
WDW EM
SSB 0
LB 0.10 Hz
GB 0
PC 1.00



5.24
3.12
0.07
0.04
0.44
0.92
0.10
0.42
0.10
1.00
0.13
0.16
0.59
0.93
1.92
59.35
1.76
20.41
59.22
3.70
18.88
1.16
5.90
0.72
0.59
4.81
3.04
106.18

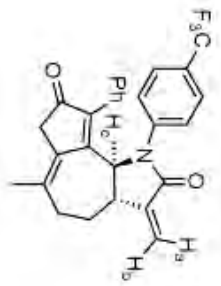
-1 ppm

3.203 2:1 dr



7.257
7.221
7.199
7.135
7.119
7.100
7.081
7.016
6.993
6.510
6.323
6.315
6.293
6.284
5.660
5.584
5.576
5.531
5.523
5.354
5.333
3.348
3.338
3.324
3.316
3.308
3.295
3.213
3.161
3.124
3.092
3.071
3.049
3.039
3.019
2.690
2.676
2.667
2.657
2.642
2.619
2.613
2.604
2.589
2.547
2.543
2.534
2.528
2.507
2.501
2.493
2.098
2.067
1.558

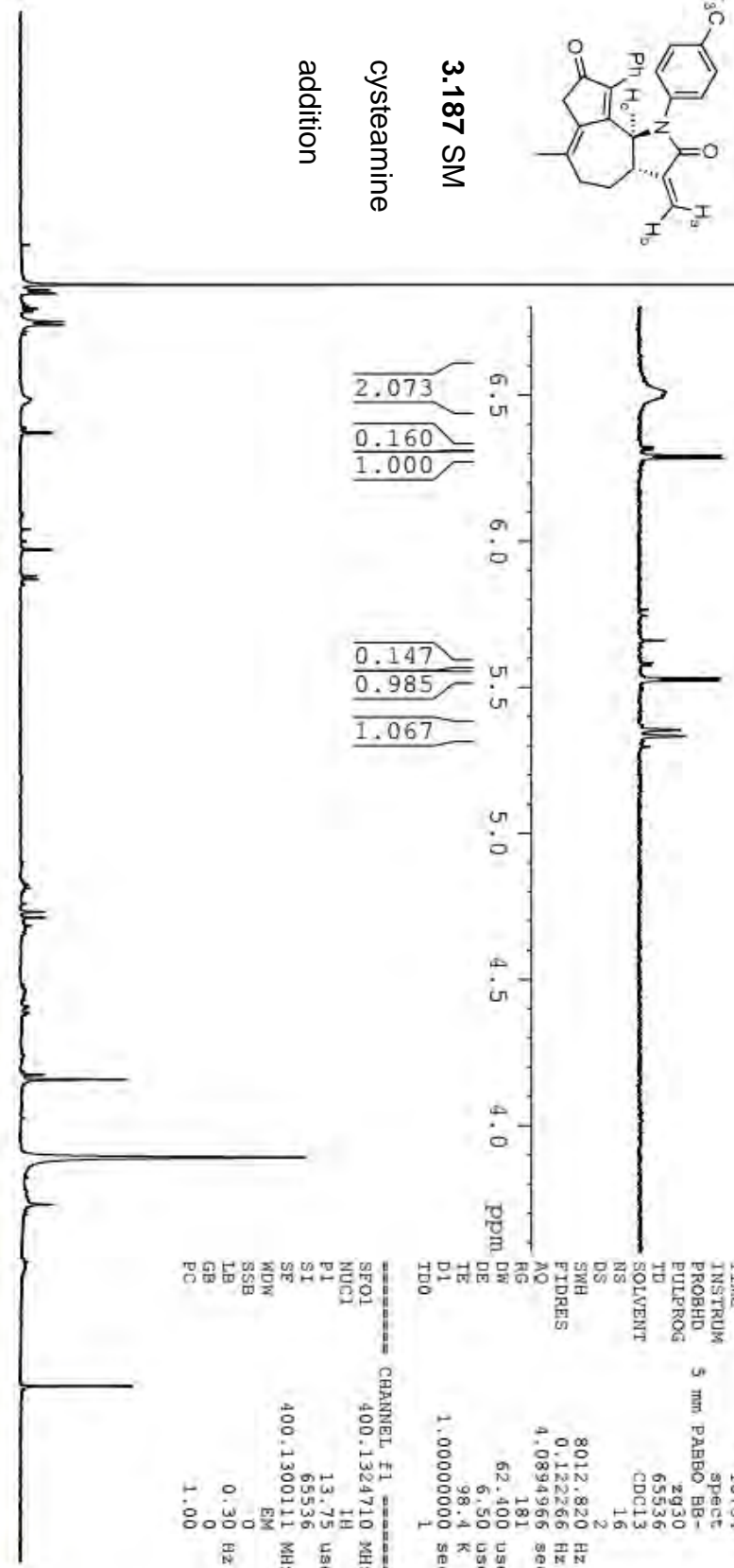
PAJ 9-10 SM



3.187 SM

cysteamine

addition



8
7
6
5
4
3
2
1
0
ppm

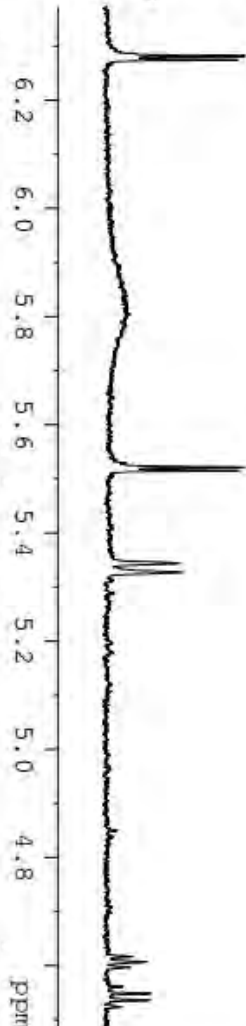
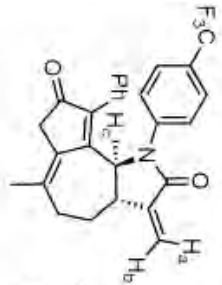
2.44
1.38
4.14
0.42
2.07
0.16
1.00
0.15
0.99
1.07
1.07
1.00
2.41
1.18
1.26
0.66
3.89

```

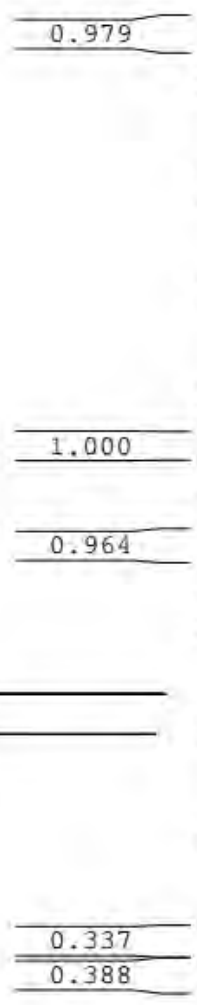
NAME          PAJ 9-10 SM
EXPNO         10
PROCNO        1
Date_         20160630
Time          10.54
INSTRUM       spect
PROBHD        5 mm PABBO BB-
PULPROG       zg30
TD            65536
FIDRES        0.122266 Hz
AQ            4.0894966 sec
RG            181
DS            2
SMH           8012.820 Hz
FIDRES        0.122266 Hz
DE            4.0894966 sec
TE            293.2 K
D1            62.400 usec
D2            6.50 usec
D3            98.4 K
TD0           1.000000000 sec
===== CHANNEL f1 =====
SFO1          400.1324710 MHz
NUC1          1H
P1            13.75 usec
SI            65536
SE            400.1300111 MHz
K0W           EM
SSB           0
LB            0.30 Hz
GB            0
PC            1.00
  
```

PAJ 9-10, 3 h

- 7.254
- 7.208
- 7.191
- 7.089
- 7.074
- 7.042
- 7.003
- 6.986
- 6.281
- 6.274
- 5.521
- 5.514
- 5.343
- 5.327
- 4.606
- 4.548
- 4.535
- 3.524
- 3.514
- 3.369
- 3.359
- 3.347
- 3.333
- 3.326
- 3.314
- 3.308
- 3.301
- 3.196
- 3.153
- 3.140
- 3.127
- 3.111
- 3.018
- 3.006
- 2.993
- 2.876
- 2.864
- 2.851
- 2.766
- 2.753
- 2.741
- 2.610
- 2.597
- 2.585
- 2.528
- 2.496
- 2.203
- 2.086
- 2.072
- 2.057
- 2.036
- 2.031
- 2.020
- 1.538
- 1.509



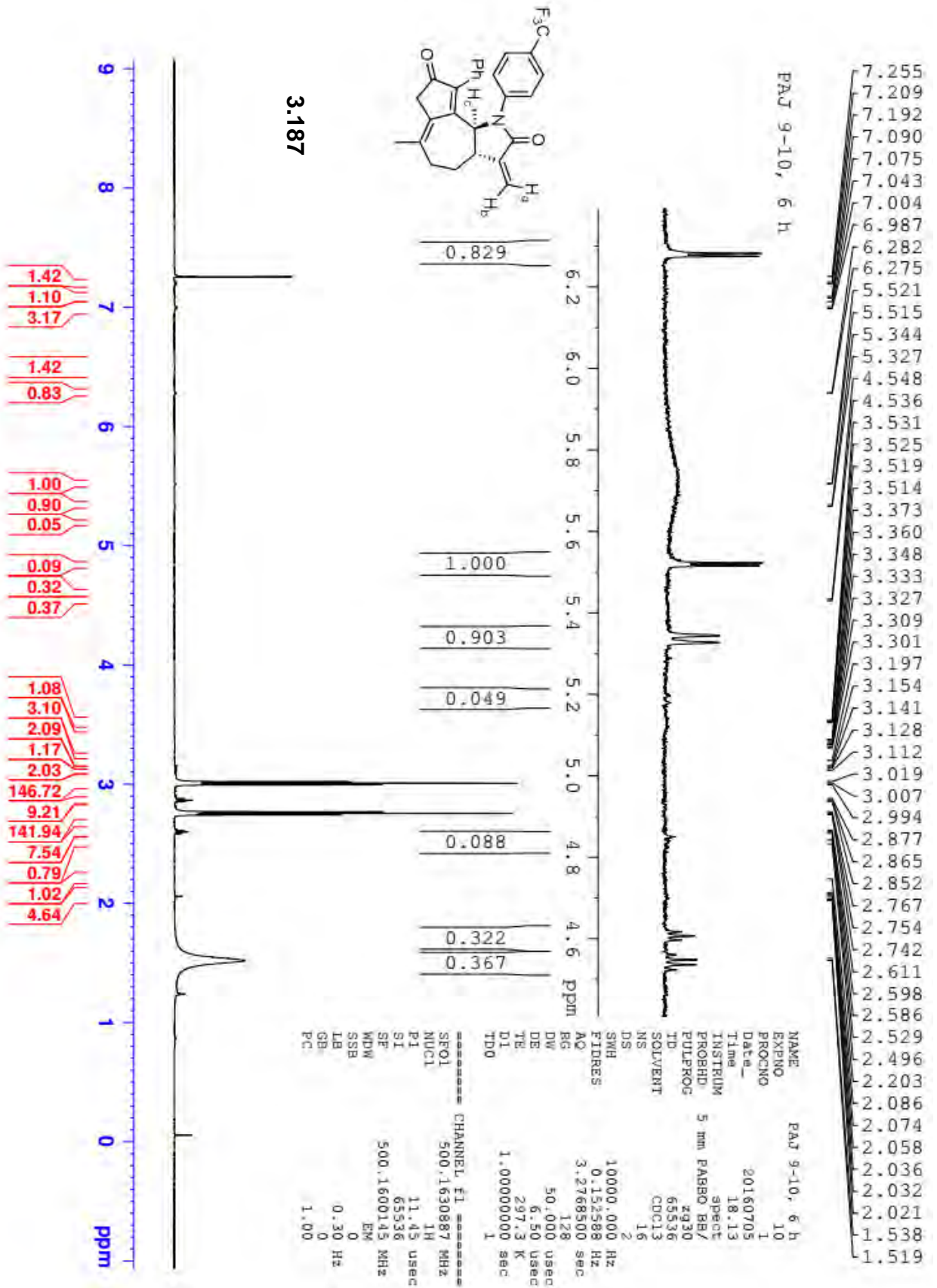
3.187



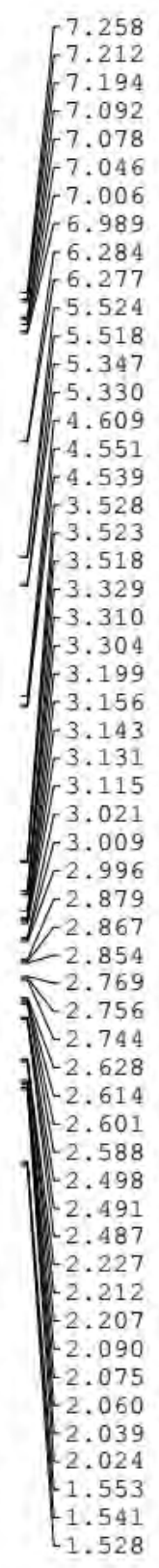
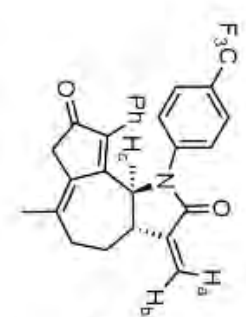
```

NAME          PAJ 9-10, 3 h
EXPNO         10
PROCNO        1
Date_         20160705
Time          15.11
INSTRUM       5 mm PABBO BB/
PROBHD        zg30
PULPROG       gms36
TD            65536
SOLVENT       CDCl3
NS            16
DS            2
SWH           10000.000 Hz
FIDRES        0.152588 Hz
AQ            3.2768500 sec
RG            181
RG            50.000 usec
DE            6.50 usec
TE            297.1 K
DL            1.000000000 sec
TD0           1

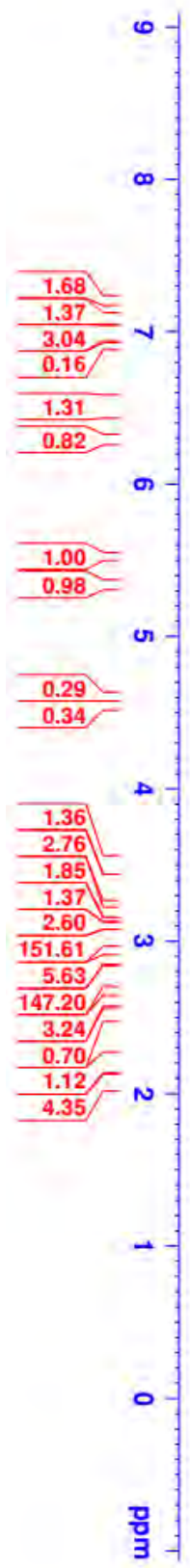
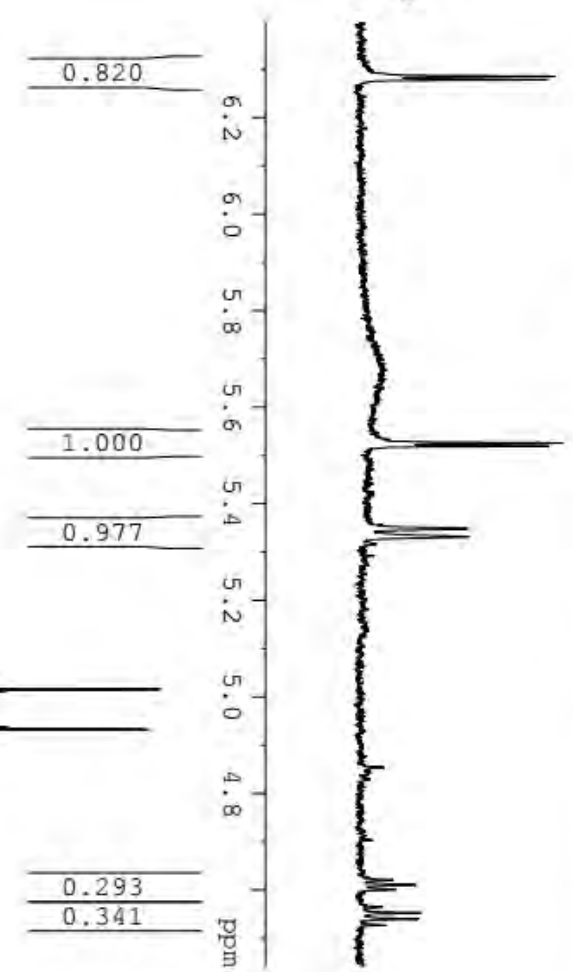
----- CHANNEL f1 -----
SFO1          500.1630887 MHz
NUC1          1H
P1            11.45 usec
SI            65536
SF            500.1600150 MHz
WDW           EM
SSB           0
LB            0.30 Hz
GB            0
PC            1.00
  
```



PAJ 9-10, 21 h



3.187

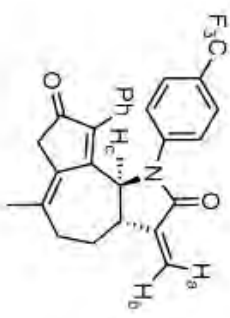
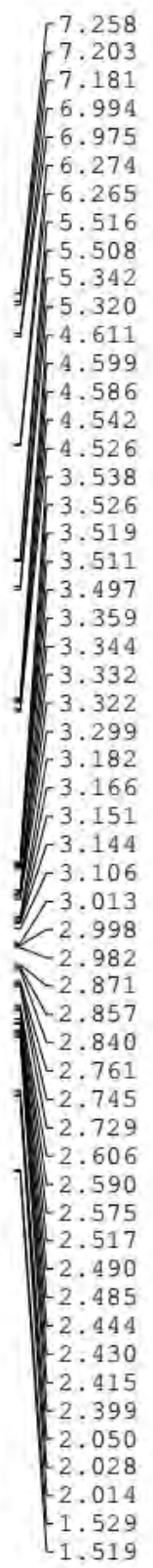


```

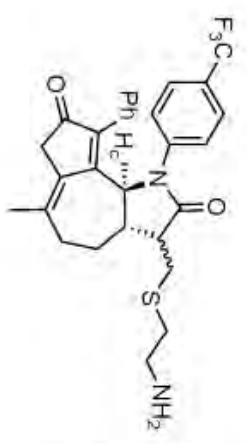
NAME          PAJ 9-10, 21 h
EXPNO         10
PROCNO        1
Date_         20160706
Time          9.28
INSTRUM       spect
PROBHD        5 mm PABBO BB/
PULPROG       zg30
TD            65536
SOLVENT       CDCl3
NS            16
DS            2
SWH           10000.000 Hz
FIDRES       0.152588 Hz
AQ           3.2768500 sec
RG           181
DW           50.000 usec
DE           6.50 usec
TE           296.4 K
D1           1.000000000 sec
TD0          1

===== CHANNEL f1 =====
SFO1          500.1630887 MHz
NUC1          1H
P1           11.45 usec
SI           65536
SE           500.1600132 MHz
WDM          EM
SSB          0
LB           0.30 Hz
GB           0
PC           1.00
  
```

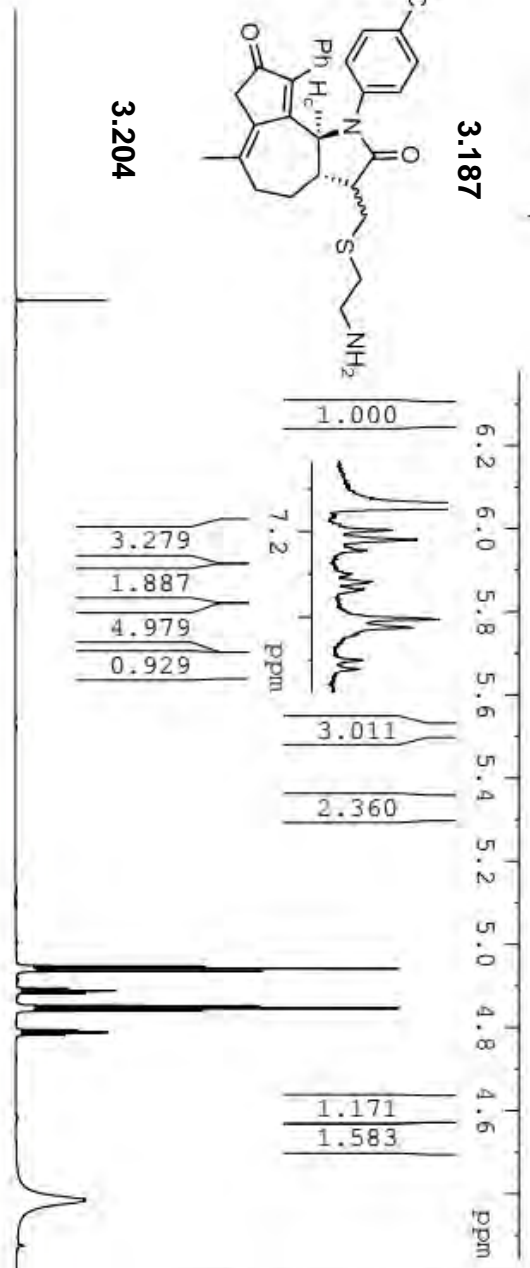
PAJ 9-10, 21 h, 2 h



3.187

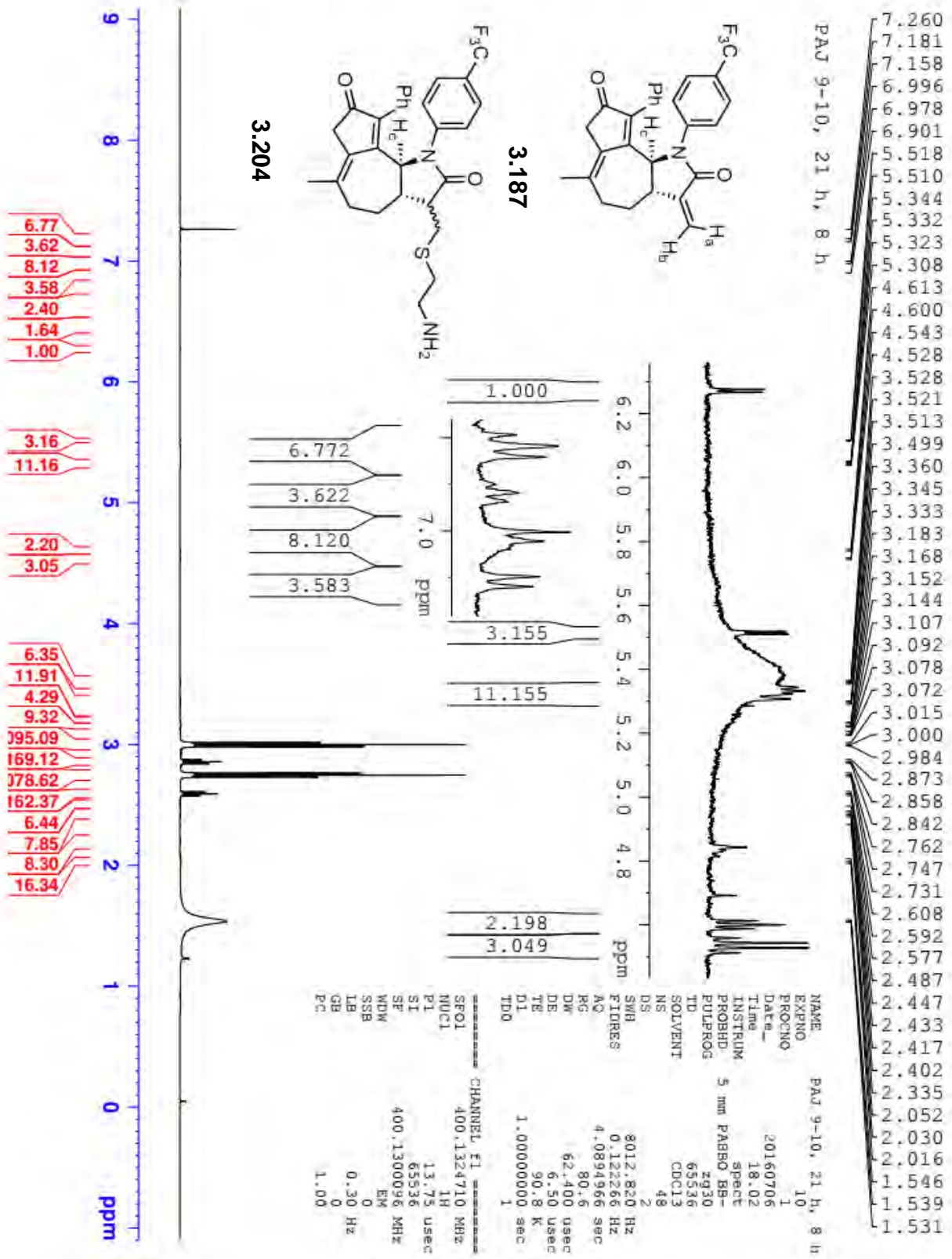


3.204

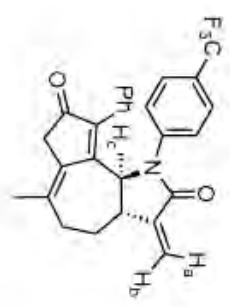
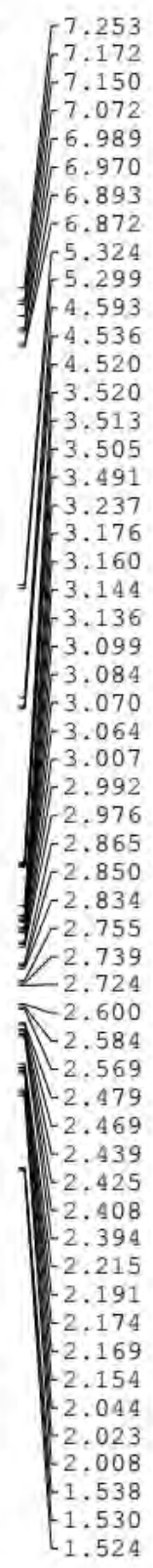


```

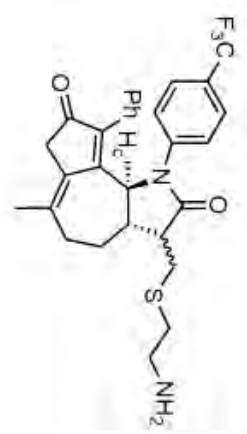
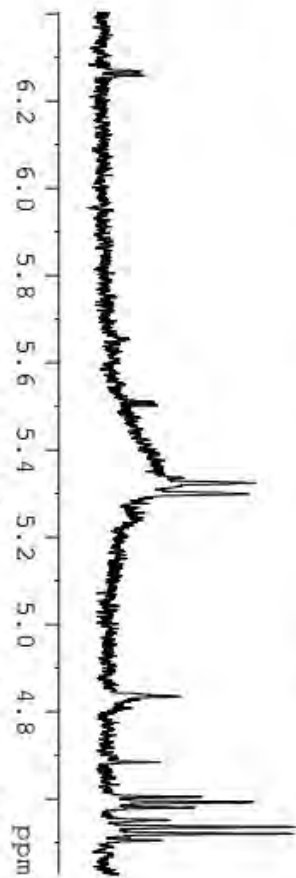
NAME          PAJ 9-10, 21 h, 2 h
EXPNO         10
PROCNO        1
Date_         20160706
Time          11.49
INSTRUM       5 mm PABBO BB-
PROBHD        spect
PULPROG       zg30
TD            65536
SOLVENT       CDCl3
RG            32
DS            2
SWH           8012.820 Hz
FIDRES       0.122266 Hz
AQ           4.0834966 sec
RG           80.6
DE           62.400 usec
TE           91.3 K
D1           1.00000000 sec
===== CHANNEL f1 =====
SFO1          400.1324710 MHz
NUC1          1H
P1           13.75 usec
SI           65536
SF           400.1300108 MHz
WDW          EM
SSB          0
LB           0.30 Hz
GB           0
PC           1.00
  
```



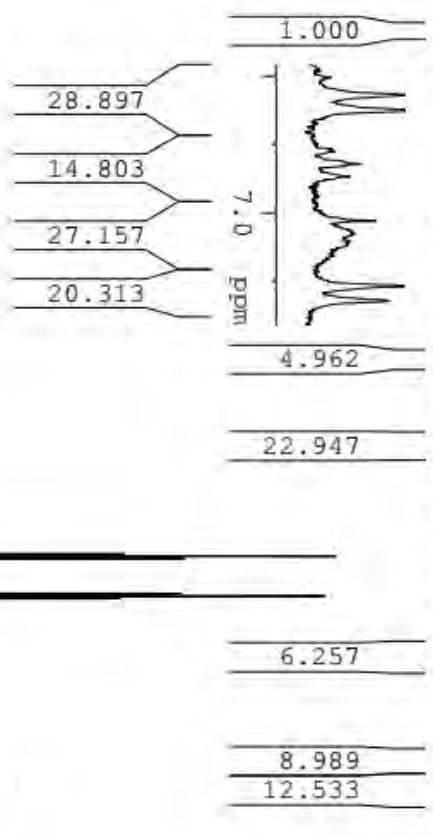
PAJ 9-10, 21 h, 24 h



3.187



3.204

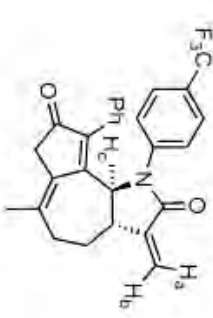
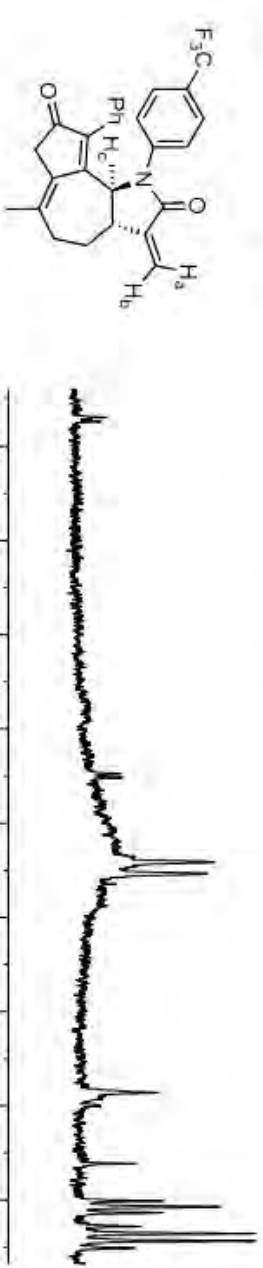


NAME PAJ 9-10, 21 h, 24 h
 EXPNO 10
 PROCNO 1
 Date_ 20160707
 Time 11.36
 INSTRUM spect
 PROBHID 5 mm PABBO BB-
 PULPROG zg30
 TD 65536
 SOLVENT CDCl3
 NS 16
 DS 2
 SFR 8012.820 Hz
 FIDRES 0.122266 Hz
 AQ 4.0894966 sec
 RG 80.6
 DW 62.400 usec
 DE 6.50 usec
 TE 300.2 K
 D1 91.0 sec
 D11 1.00000000 sec
 ID0 1

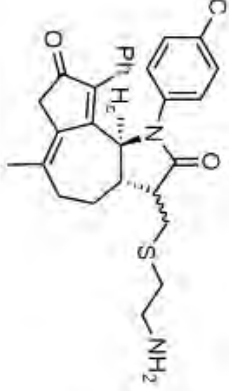
***** CHANNEL f1 *****
 SFO1 400.1324710 MHz
 NUC1 1H
 P1 13.75 usec
 SI 65536
 SF 400.1300128 MHz
 K1W EN
 SSB 0
 GB 0
 PC 1.00

PAJ 9-10, 21 h, 32 h

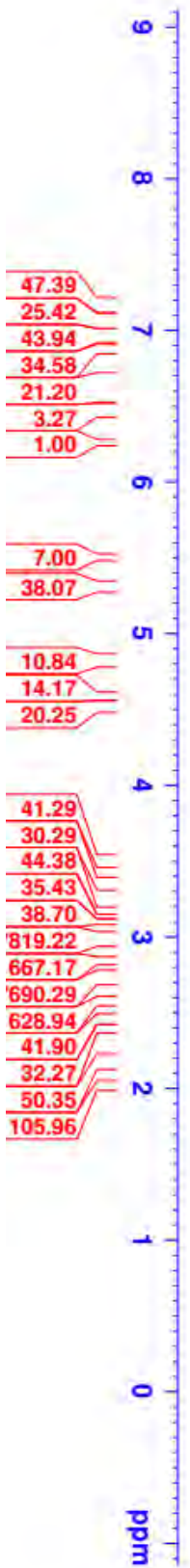
7.246
7.165
7.143
7.065
6.982
6.886
6.865
5.317
5.293
4.585
4.529
4.513
3.513
3.506
3.498
3.494
3.484
3.168
3.153
3.137
3.129
3.092
3.077
3.072
3.069
3.063
3.057
3.047
3.000
2.985
2.969
2.858
2.843
2.827
2.748
2.732
2.717
2.593
2.577
2.562
2.433
2.401
2.387
2.382
2.206
2.187
2.167
2.161
2.146
2.037
2.016
2.001
1.531
1.524
1.516



3.187



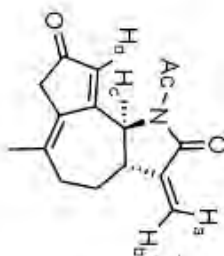
3.204



NAME PAJ 9-10, 21 h, 32 h
 EXPNO 10
 PROCNO 1
 Date_ 20160707
 Time 17.19
 INSTRUM spect
 PROBRD 5 mm PABBO BB-
 PULPROG zg30
 TD 65536
 SOLVENT CDCl3
 NS 32
 DS 2
 SWH 8012.820 Hz
 FIDRES 0.122266 Hz
 AQ 4.0834966 sec
 RG 80.6
 DW 62.400 usec
 DE 6.50 usec
 TE 300.2 K
 D1 90.7 K
 TD0 1.00000000 sec
 1

----- CHANNEL f1 -----
 SFO1 400.1324710 MHz
 NUC1 1H
 P1 13.75 usec
 SI 65536
 SF 400.1300157 MHz
 MDW EX
 SSH 0
 LB 0.30 Hz
 GB 0
 PC 1.00

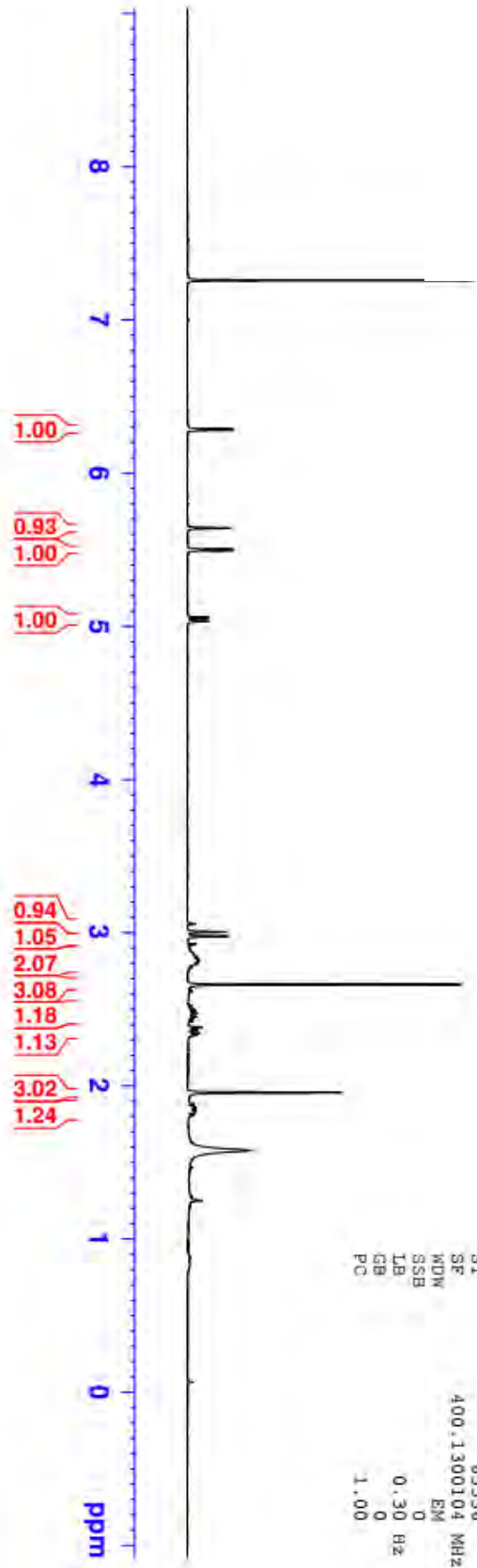
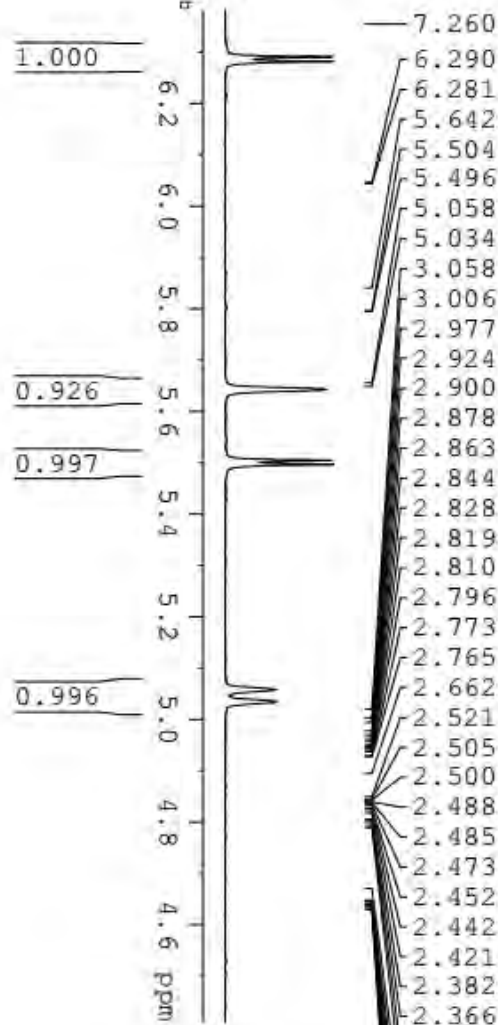
PAJ 9-6 SM



3.196 SM

cysteamine

addition



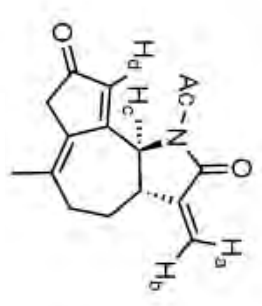
```

NAME          PAJ 9-6 SM
EXPNO         10
PROCNO        1
Date_         20160630
Time         10.43
INSTRUM       spect
PROBHD        5 mm PABBO BB-
PULPROG       zg30
TD            65536
SOLVENT       CDCl3
NS            16
DS            2
SWH           8012.820 Hz
FIDRES       0.122266 Hz
AQ           4.0894966 sec
RG            161
DW           62.400 usec
DE           6.50 usec
TE           297.9 K
D1           1.000000000 sec
TD0           1

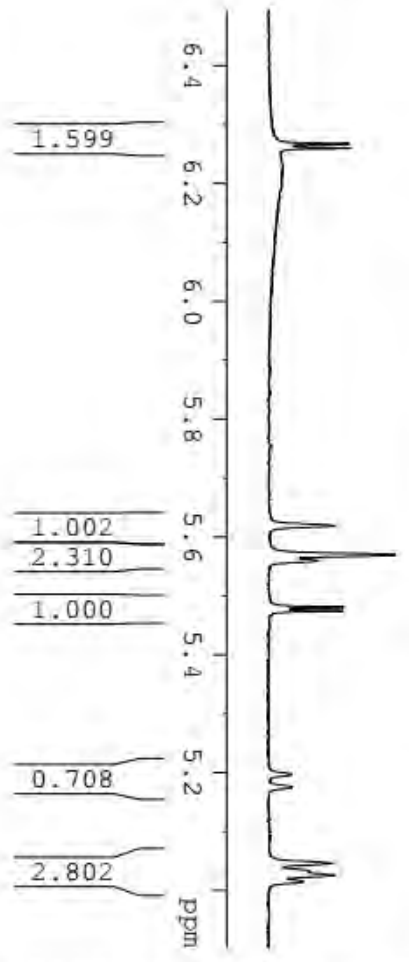
===== CHANNEL f1 =====
SFO1          400.1324710 MHz
NUC1          1H
P1            13.75 usec
SI            65536
SF           400.1300104 MHz
WDW          EM
SSB          0
LB           0.30 Hz
GB           0
PC           1.00
  
```

9.266
 9.259
 5.619
 5.569
 5.560
 5.481
 5.474
 5.197
 5.175
 5.046
 5.025
 5.015
 3.142
 3.130
 3.008
 2.996
 2.983
 2.867
 2.855
 2.842
 2.756
 2.743
 2.731
 2.600
 2.587
 2.575
 2.560
 2.472
 2.461
 2.446
 2.434
 2.418
 2.408
 2.404
 2.398
 2.392
 2.377
 2.358
 2.343
 2.324
 2.315
 2.292
 2.289
 2.281
 2.277
 2.261
 2.258
 2.249
 2.246
 2.191
 2.171
 2.151
 2.132
 1.935
 1.916

PAJ 9-6, 10 min



3.196



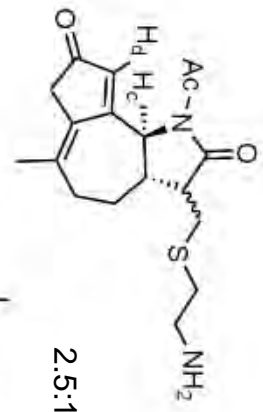
1.599

1.002
2.310
1.000

0.708

2.802

ppm



2.5:1 dr

3.205



1.60

1.00
2.31
1.00
0.71
2.80

0.29
0.41

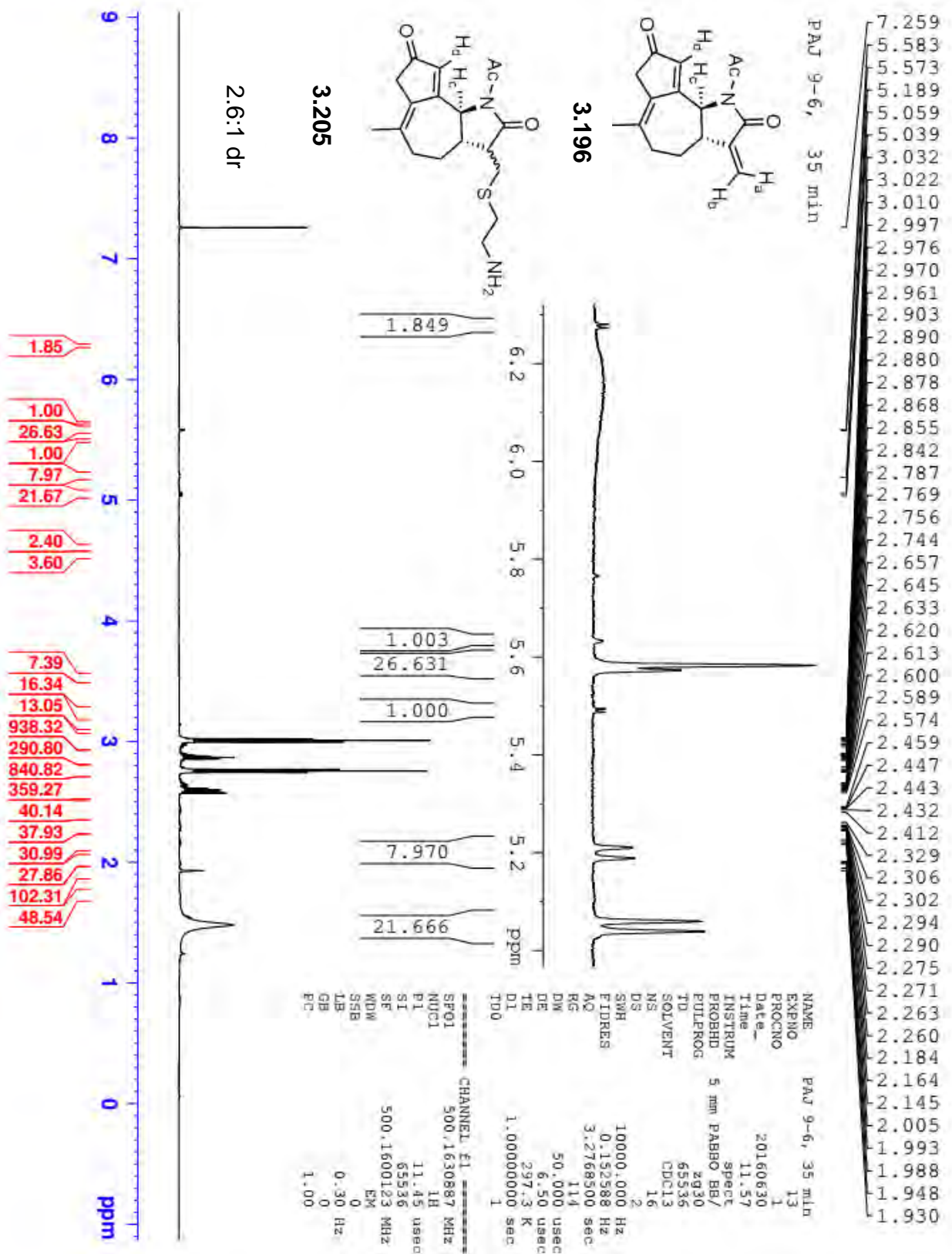
0.91
2.11
1.30
99.39
5.44
34.28
95.77
7.87
35.02
4.59
4.34
2.80
11.52

ppm

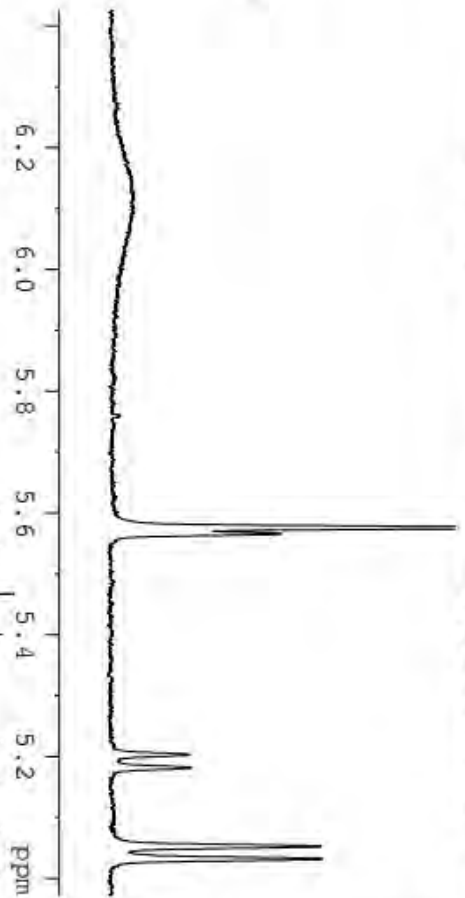
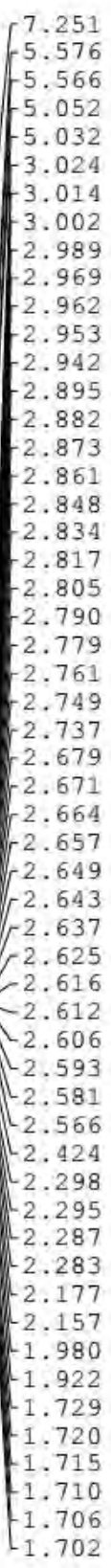
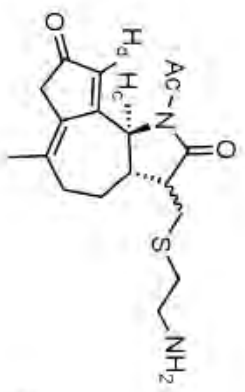
```

NAME          PAJ 9-6, 10 min
EXPNO         10
PROCNO        1
Date_         20160630
Time         11.34
INSTRUM       5 mm EABBO BB/
PROBHD        zg30
PULPROG       spect
TD            65536
SOLVENT       CDCl3
NS            16
DS            2
SWH           10000.000 Hz
FIDRES        0.152588 Hz
AQ            3.2768500 sec
RG            114
DE            50.000 usec
TE            297.3 K
D1            1.00000000 sec
TD0           1

===== CHANNEL f1 =====
SFO1          500.1630887 MHz
NUC1          1H
P1            11.45 usec
SI            65536
SF            500.1600193 MHz
WDW           EM
SSB           0
LB            0.30 Hz
GB            0
PC            1.00
  
```

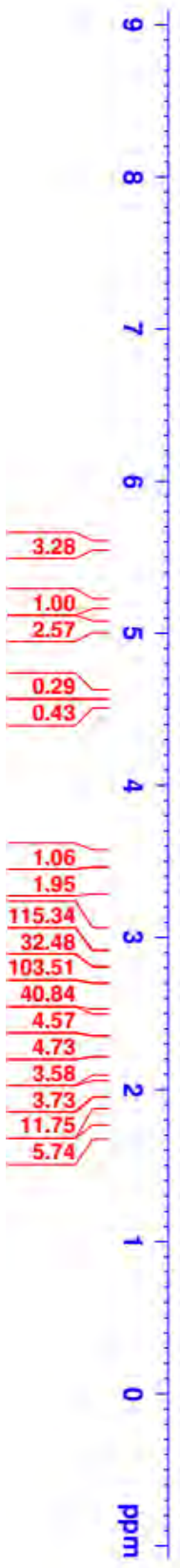


PAJ 9-6, 55 min



3.205

2.6:1 dr

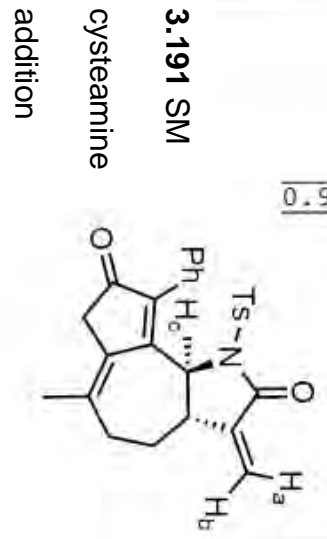


NAME PAJ 9-6, 55 min
 EXPNO 15
 PROCNO 1
 Date_ 20160630
 Time 12.17
 INSTRUM spect
 PROBD 5 mm PABBO BB/
 PULPROG zg30
 TD 65536
 FIDRES 0.152588 Hz
 AQ 3.2768500 sec
 RG 114
 DW 50.000 usec
 DE 6.50 usec
 TE 297.3 K
 D1 1.00000000 sec
 D10 1

CHANNEL F1
 SF01 500.1630887 MHz
 NUC1 1H
 P1 11.45 usec
 SI 65536
 SF 500.1600161 MHz
 WDW EM
 SSB 0
 LB 0.30 Hz
 GB 0
 PC 1.00

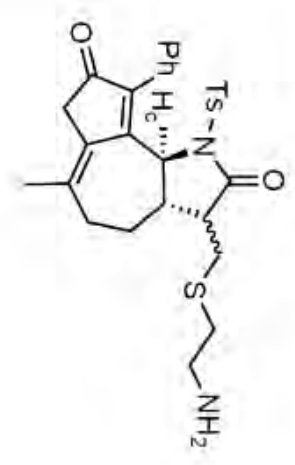
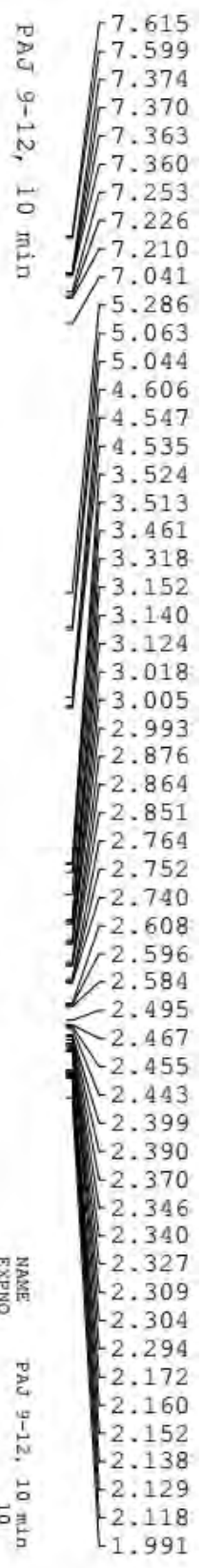
PAJ 9-12, SM

- 7.659
- 7.638
- 7.404
- 7.395
- 7.389
- 7.260
- 7.228
- 7.208
- 7.130
- 6.172
- 6.163
- 5.447
- 5.439
- 5.300
- 5.091
- 5.071
- 3.491
- 3.271
- 3.245
- 3.220
- 3.132
- 3.080
- 2.936
- 2.919
- 2.876
- 2.571
- 2.556
- 2.522
- 2.509
- 2.494
- 2.470
- 2.437
- 2.425
- 2.373
- 2.021



NAME PAJ 9-12, SM
 EXNO 10
 PROCNO 1
 DATE_ 20160630
 Time 13.35
 INSTRUM spect
 PROBD 5 mm PABBO BB-
 PULPROG zgpg30
 TD 65536
 ID CDC13
 SOLVENT CDCl3
 NS 16
 DS 2
 SWH 8012.820 Hz
 FIDRES 0.122266 Hz
 AQ 4.0894986 sec
 RG 181
 DW 62.400 usec
 DE 6.50 usec
 TE 97.2 K
 D1 1.00000000 sec
 TD0 1

----- CHANNEL f1 -----
 SFO1 400.1324710 MHz
 NUCL1 1H
 P1 13.75 usec
 SI 65536
 SF 400.1300105 MHz
 WDW EM
 SSB 0
 LB 0.30 Hz
 GB 0
 PC 1.00



3.206

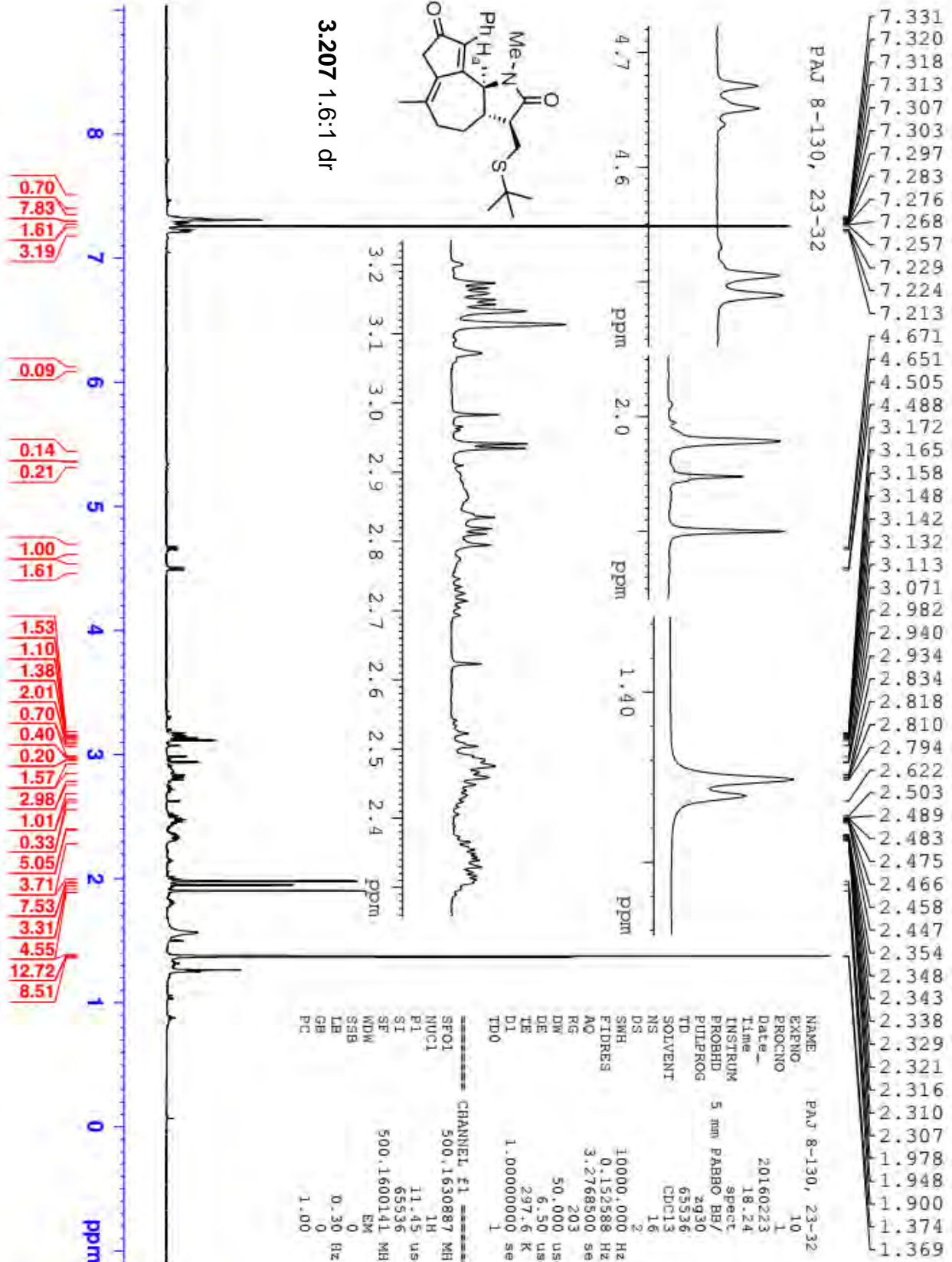


```

NAME          PAF 9-12, 10 min
EXPNO         10
PROCNO        1
Date_         20160630
Time         14.04
INSTRUM       spect
PROBHD        5 mm PABBO BB/
PULPROG       zg30
TD            65536
SOLVENT       CDCl3
NS            16
DS            2
SWH           10000.000 Hz
FIDRES        0.152588 Hz
AQ            3.2768500 sec
RG            181
DW            50.000 usec
DE            6.50 usec
TE            297.1 K
D1            1.00000000 sec
TD0           1

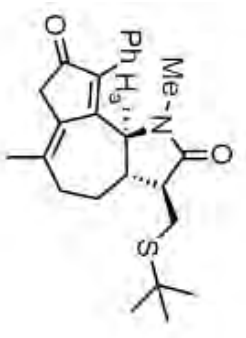
----- CHANNEL f1 -----
SE01          500.1630887 MRZ
NUC1          1H
P1            11.45 usec
SI            65536
SF            500.1600158 MHz
WDW           EM
SSB           0
LB            0.30 Hz
GB            0
PC            1.00

```



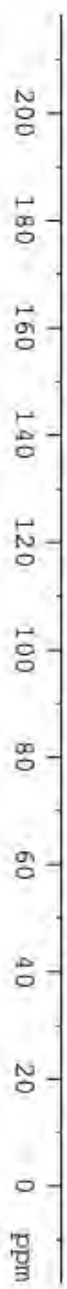
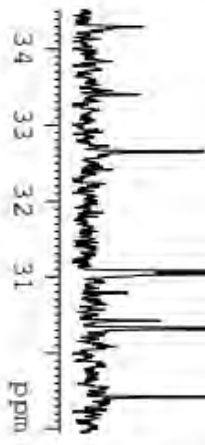
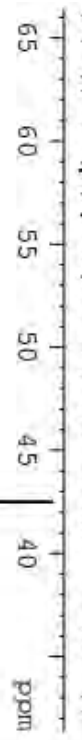
- 202.921
- 202.856
- 175.252
- 166.107
- 138.496
- 137.710
- 137.078
- 130.809
- 130.729
- 130.667
- 130.556
- 128.486
- 128.363
- 127.660
- 127.610
- 77.414
- 77.160
- 76.906
- 76.443
- 62.735
- 61.667
- 50.226
- 44.170
- 43.178
- 42.749
- 42.564
- 40.587
- 40.547
- 34.295
- 33.404
- 32.648
- 31.070
- 31.032
- 30.785
- 30.417
- 30.323
- 30.303

PAJ 8-130, 23-32 CNMR



1.6:1 dr

3.207

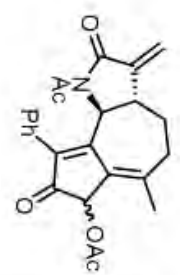
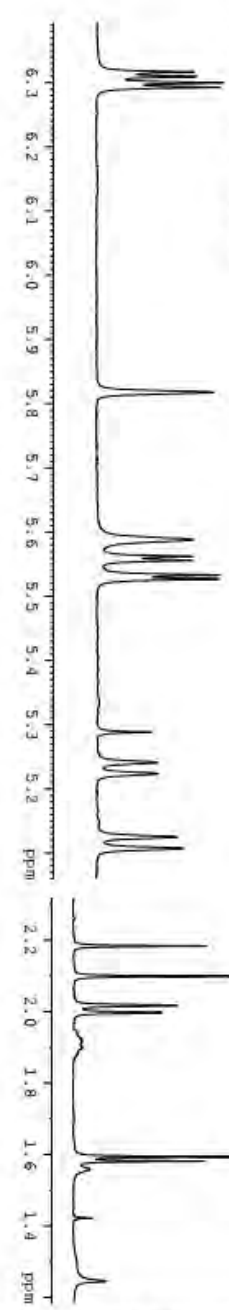


NAME	PAJ 8-130, 23-32
EXPNO	11
PROCNO	1
Date_	20160224
Time	0.15
INSTRUM	spec
PROBHD	5 mm PABBO BB/
PULPROG	zgpg30
TD	65536
SOLVENT	CDCl3
NS	3500
DS	2
SWH	29761.904 Hz
FIDRES	0.454131 Hz
AQ	1.1010548 sec
RG	203
DW	16.800 usec
DE	6.50 usec
TE	298.3 K
D1	2.00000000 sec
D11	0.03000000 sec
TD0	1

===== CHANNEL f1 =====	
SFO1	125.7779086 MHz
NUC1	13C
P1	10.50 usec
SI	32768
SF	125.7653125 MHz
WDW	EM
SSB	0
LB	1.00 Hz
GB	0
PC	1.40

PAJ 6-164, 21-28

NAME PAJ 6-164, 21-28
 EXPNO 10
 PROCNO 1
 Date_ 20150130
 Time 15:12
 INSTRUM spect
 PROBHD 5 mm PABBO BB/
 PULPROG zg30
 ID 65536
 SOLVENT CDCl3
 NS 16
 DS 2
 SWH 10000.000 Hz
 FIDRES 0.152388 Hz
 AQ 3.2768300 sec
 RG 161
 DW 50.000 usec
 DE 6.50 usec
 TE 299.2 K
 D1 1.00000000 sec
 TDO 1

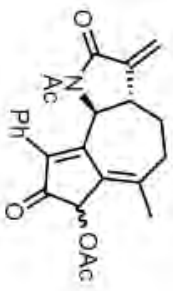
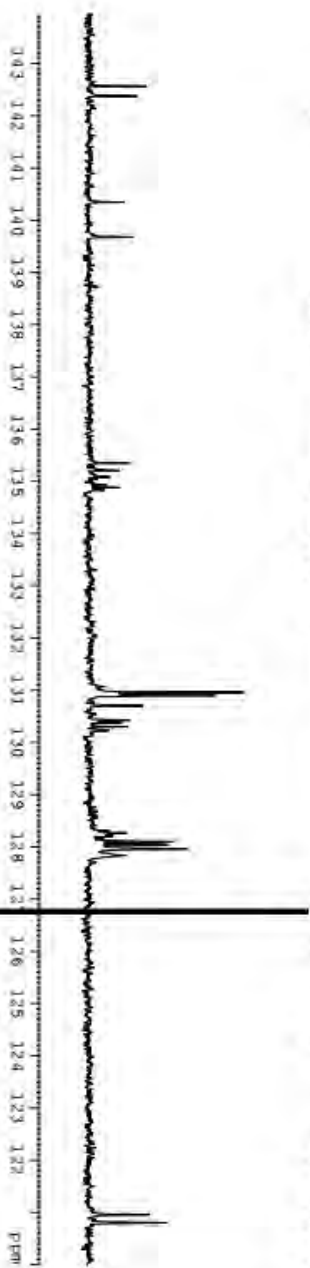


4.21
 1:4:1 dr



CHANNEL F1
 SFO1 500.1630887 MHz
 NUCL1 1H
 P1 11.45 usec
 SI 65536
 SE 500.1600169 MHz
 WDW EM
 SSB 0
 LB 0.30 Hz
 GB 0
 PC 1.00

PAJ 6-164, 21-28 CNMR



4.21

1.4:1 dr



72.91
70.40
57.38
57.29
39.32
39.08
32.74
32.07
29.84
28.89
28.72
25.21
25.14
23.85
23.77
20.89
20.80

NAME PAJ 6-164, 21-28
EXPNO 11
PROCNO 1
Date_ 20130131
Time 0.35
INSTRUM spect
PROBHD 5 mm PABBO BR/
PULPROG zgpg30
TD 65536
SOLVENT CDCl3
NS 4000
DS 2
SWH 29761.904 Hz
FIDRES 0.454131 Hz
AQ 1.1010548 sec
RG 203
DW 16.800 usec
DE 6.50 usec
TE 300.1 K
D1 2.00000000 sec
D11 0.03000000 sec
TD0 1

CHANNEL F1
SE01 125.7779086 MHz
NUC1 13C
P1 10.50 usec
SI 32768
SF 125.7653141 MHz
WDW EM
SSB 0
LB 1.00 Hz
GB 0
PC 1.40

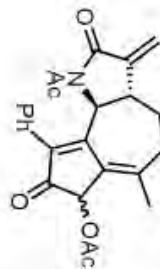
PAJ 6-164, 21-28 DEPT

134.74
130.81
130.75
130.09
127.96
127.90
127.82
127.68
120.82
120.67

72.76
70.25

57.23
57.14

39.18
38.94
32.60
31.93
28.75
28.58
25.07
25.01
23.71
23.64
20.66
20.50



4.21

1.4:1 dr

150 140 130 120 110 100 90 80 70 60 50 40 30 20 ppm



NAME PAJ 6-164, 21-28

EXPNO 12

PROCNO 1

Date_ 20150131

Time 0.52

INSTRUM 5 mm PABBO BB/

PROBHD deptsp135

PULPROG 65536

ID CDC13

SOLVENT 256

NS 4

DS 4

SWH 20161.291 Hz

FTDRES 0.307637 Hz

AO 1.6253428 sec

RG 203

DW 24.800 usec

DE 6.50 usec

TE 299.9 K

CNSTZ 145.0000000

D1 2.000000000 sec

D2 0.00344828 sec

D12 0.00002000 sec

TD0 1

CHANNEL F1

SFO1 125.7753927 MHz

NUC1 13C

P1 10.50 usec

P13 2000.00 usec

SI 32768

SF 125.7653320 MHz

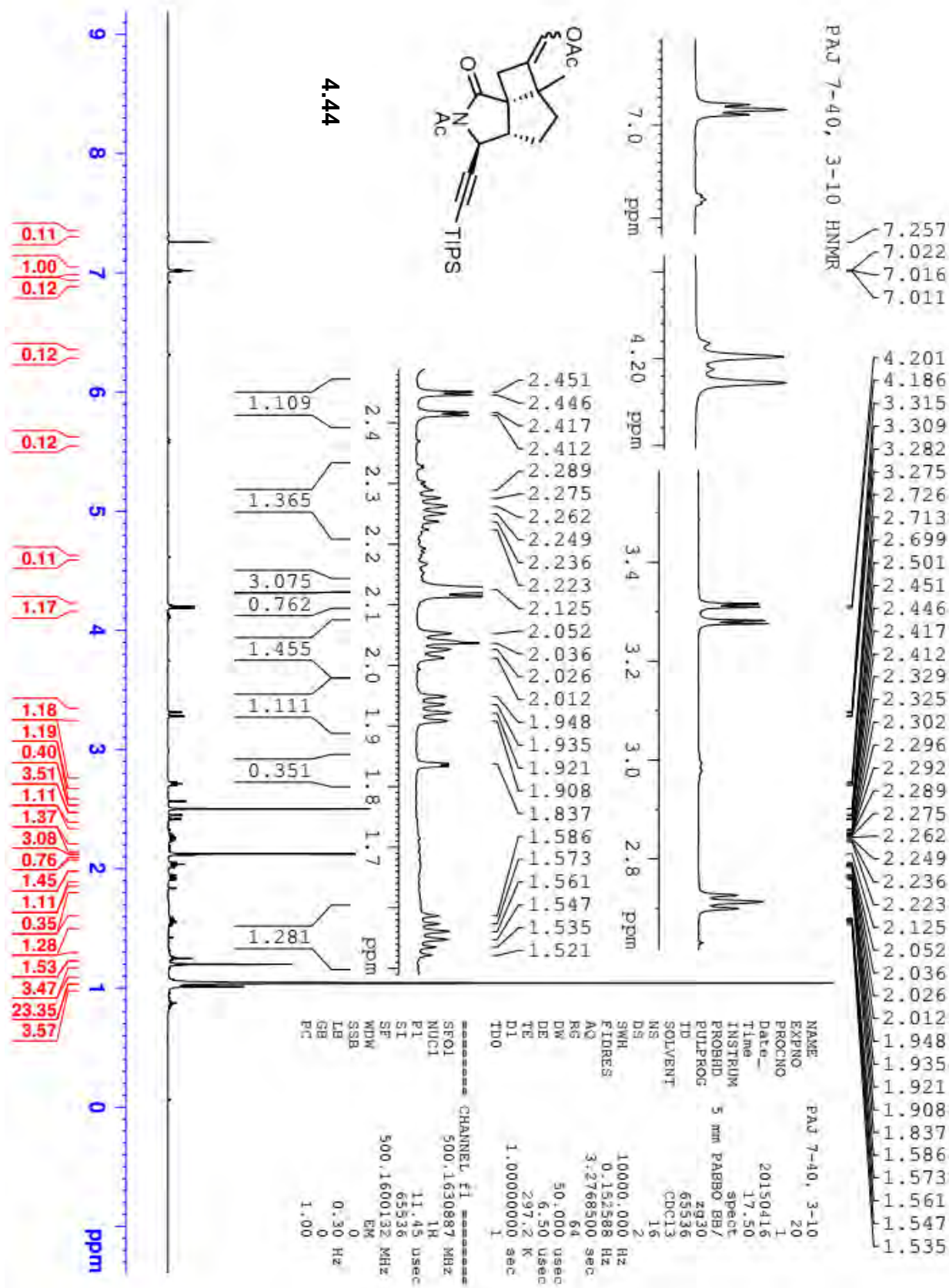
WDW EM

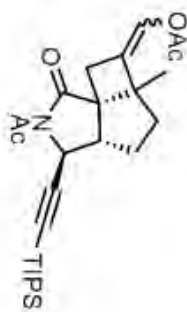
SAB 0

LB 1.00 Hz

GB 0

PC 1.40

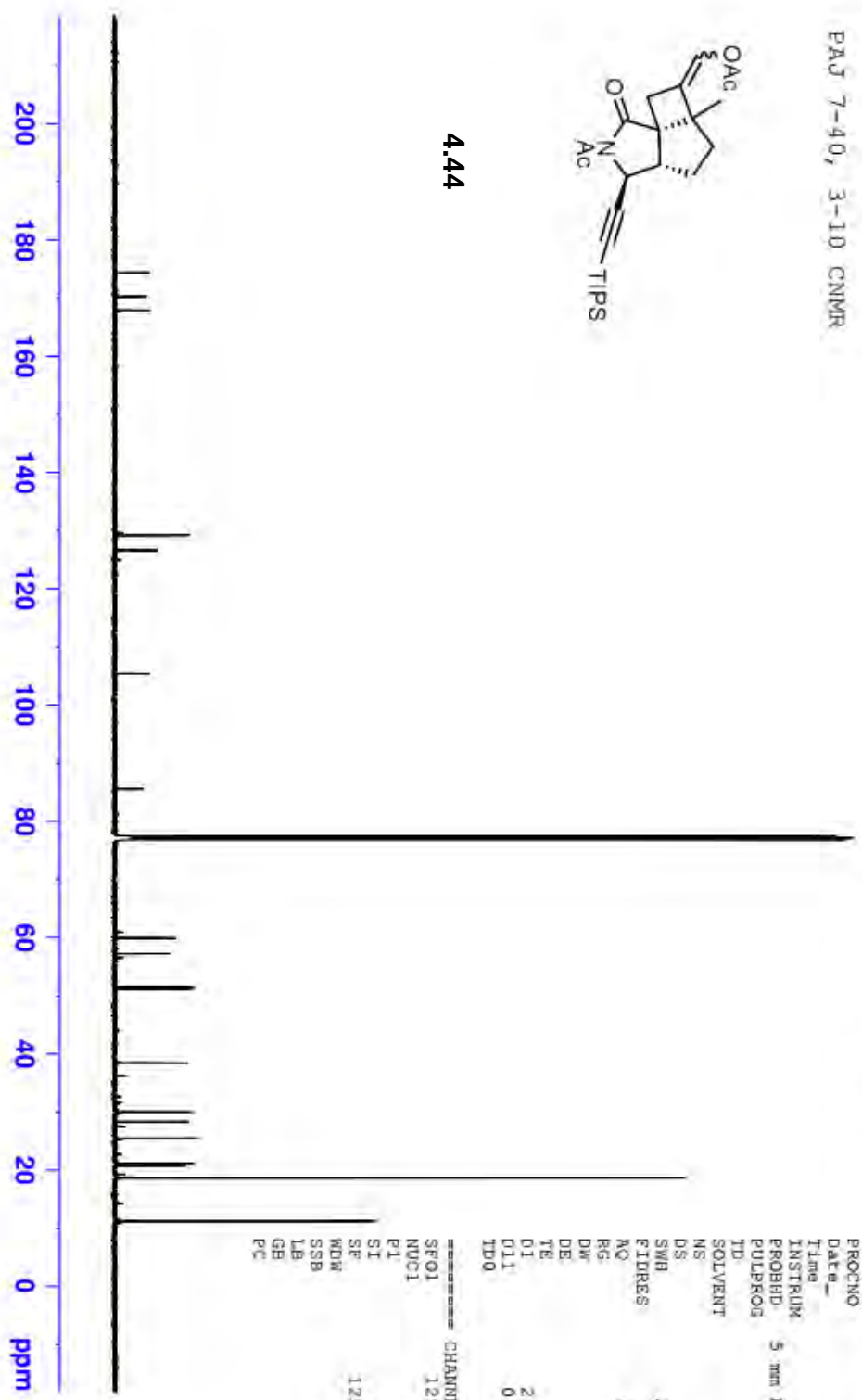




PAJ 7-40, 3-10 CNMR

- 174.443
- 170.303
- 167.931
- 129.247
- 126.651
- 105.411
- 85.627
- 77.413
- 77.159
- 76.906
- 59.936
- 57.271
- 51.603
- 51.213
- 38.475
- 30.047
- 28.361
- 25.512
- 21.191
- 20.793
- 18.692
- 11.247

4.44



NAME PAJ 7-40, 3-10
 EXPNO 11
 PROCNO 1
 Date_ 20150416
 Time 2.46
 INSTRUM spect
 PROBRD 5 mm PABBO BB/
 PULPROG zgpg30
 TD 65536
 SOLVENT CDCl3
 NS 2048
 DS 2
 SWH 29761.904 Hz
 FIDRES 0.454131 Hz
 AQ 1.1010548 sec
 RG 203
 DW 16.800 usec
 DE 6.50 usec
 TE 298.5 K
 O1 2.00000000 sec
 O11 0.03000000 sec
 TD0 1

CHANNEL #1 -----
 SFO1 125.7779086 MHz
 NUC1 13C
 P1 10.50 usec
 SI 32768
 SF 125.7653133 MHz
 WDW EM
 SSB 0
 LB 1.00 Hz
 GB 0
 PC 1.40

129.503
129.093

51.446
51.064

38.320
29.703
28.207
25.378
21.046
20.657
18.547
11.095

PAJ 7-40, 3-10 DEPT



4.44

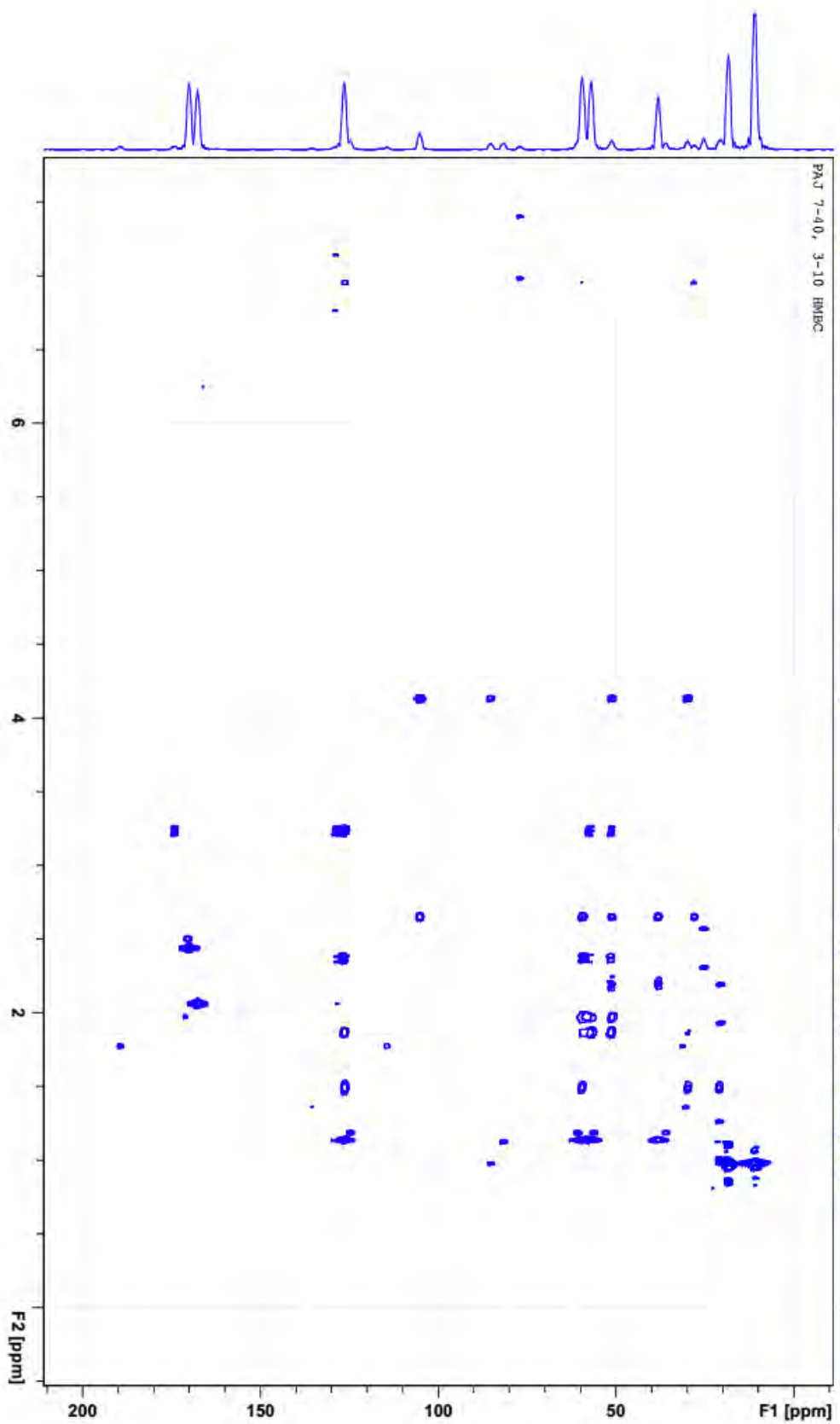
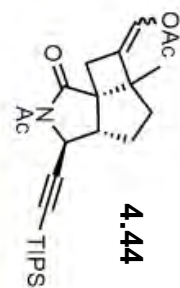


```

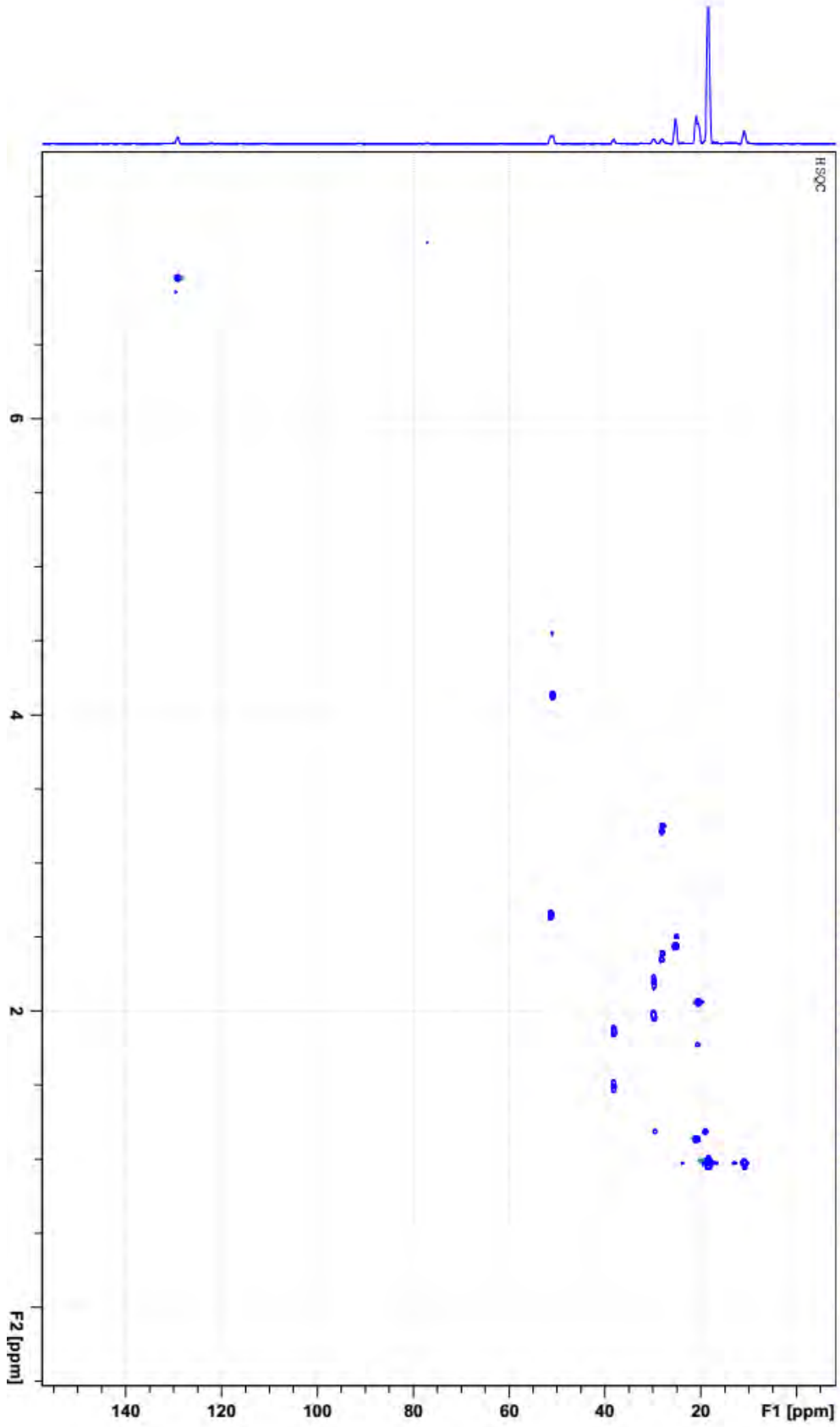
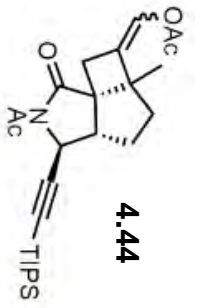
NAME          PAJ 7-40, 3-10
EXPNO         22
PROCNO        1
Date_         20150417
Time          5.44
INSTRUM       spect
PROBHD        5 mm PABBO BB/
PULPROG       deptsp135
TD            65536
SOLVENT       CDCl3
NS            256
DS            4
SWH           20161.291 Hz
FIDRES        0.307637 Hz
AQ            1.6253428 sec
RG            203
DW            24.800 usec
DE            6.50 usec
TE            297.9 K
CNS12         145,0000000
D1            2.00000000 sec
D2            0.00344828 sec
D12           0.00002000 sec
TD0           1

===== CHANNEL f1 =====
SE01          125.7753927 MHz
NUC1          13C
P1            10.50 usec
PL3           2000.00 usec
SI            32768
SF            125.7653320 MHz
WDW           EM
SSB           0
LB            1.00 Hz
GB            0
PC            1.40
  
```

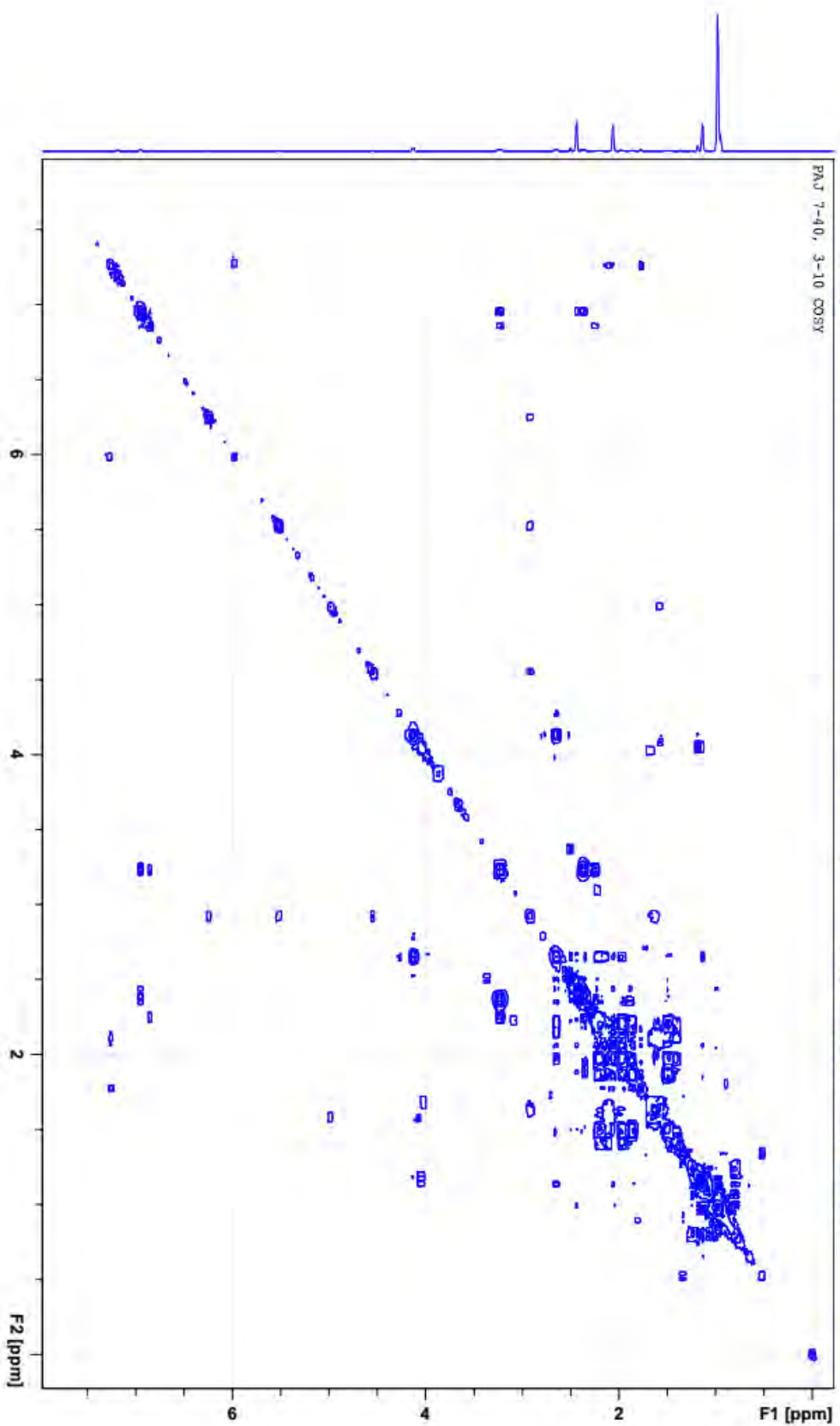
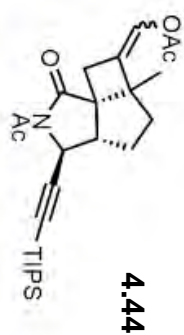
"PAJ 7-40, 3-10" 24 1 0: \2015 Brunmond



"PMU 7-40, 3-10" 31 1 D:\2015 Brummond



"PAU" 7-40, 3-10" 21 1 D: \2015 Bruumond



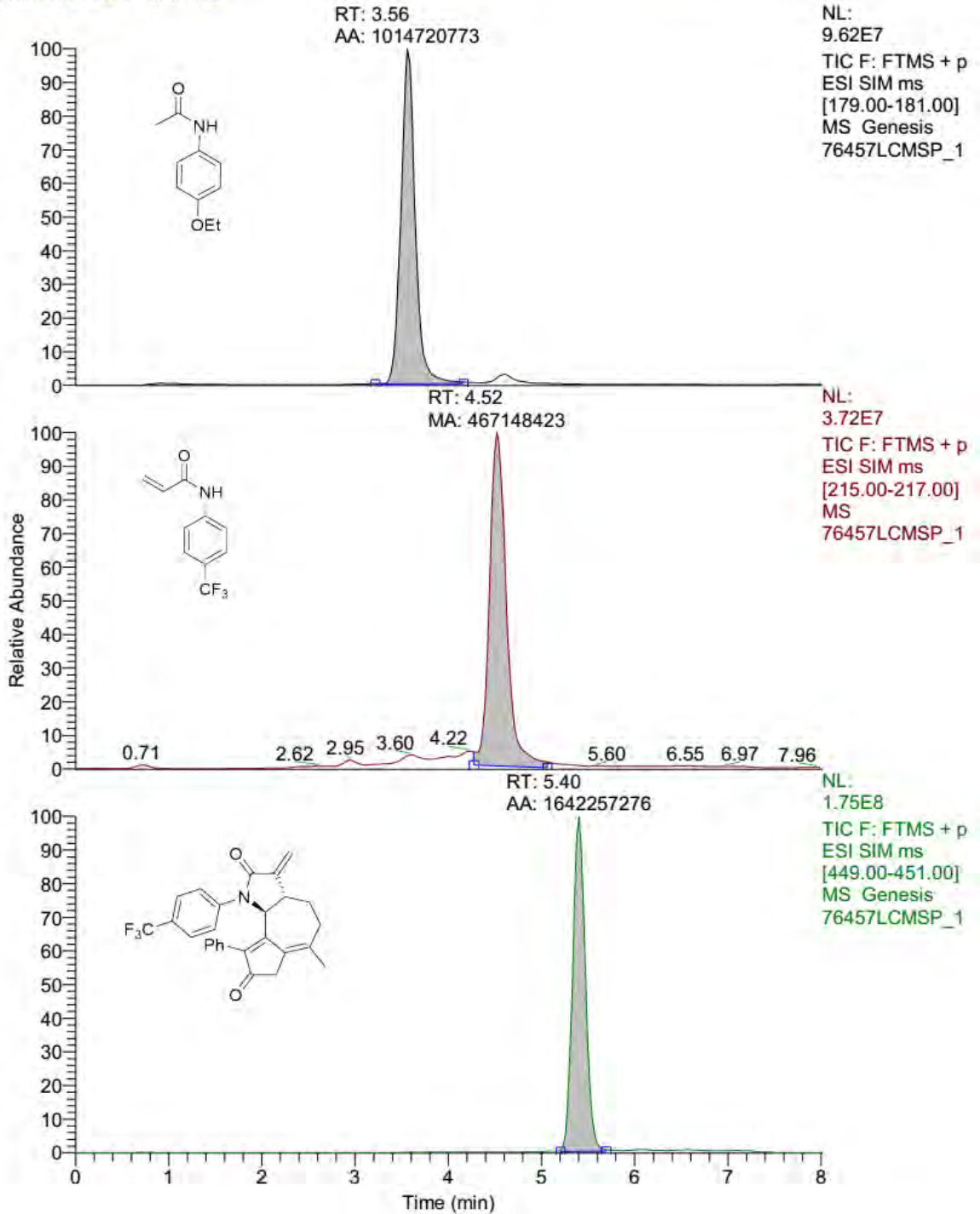
Mass Spectral Data from Rate Experiments with Glutathione

Starting material, control

C:\Xcalibur\...Jackson\76457LCMSP_1
Phosphate Buffer
RT: 0.00 - 8.01 SM: 11G

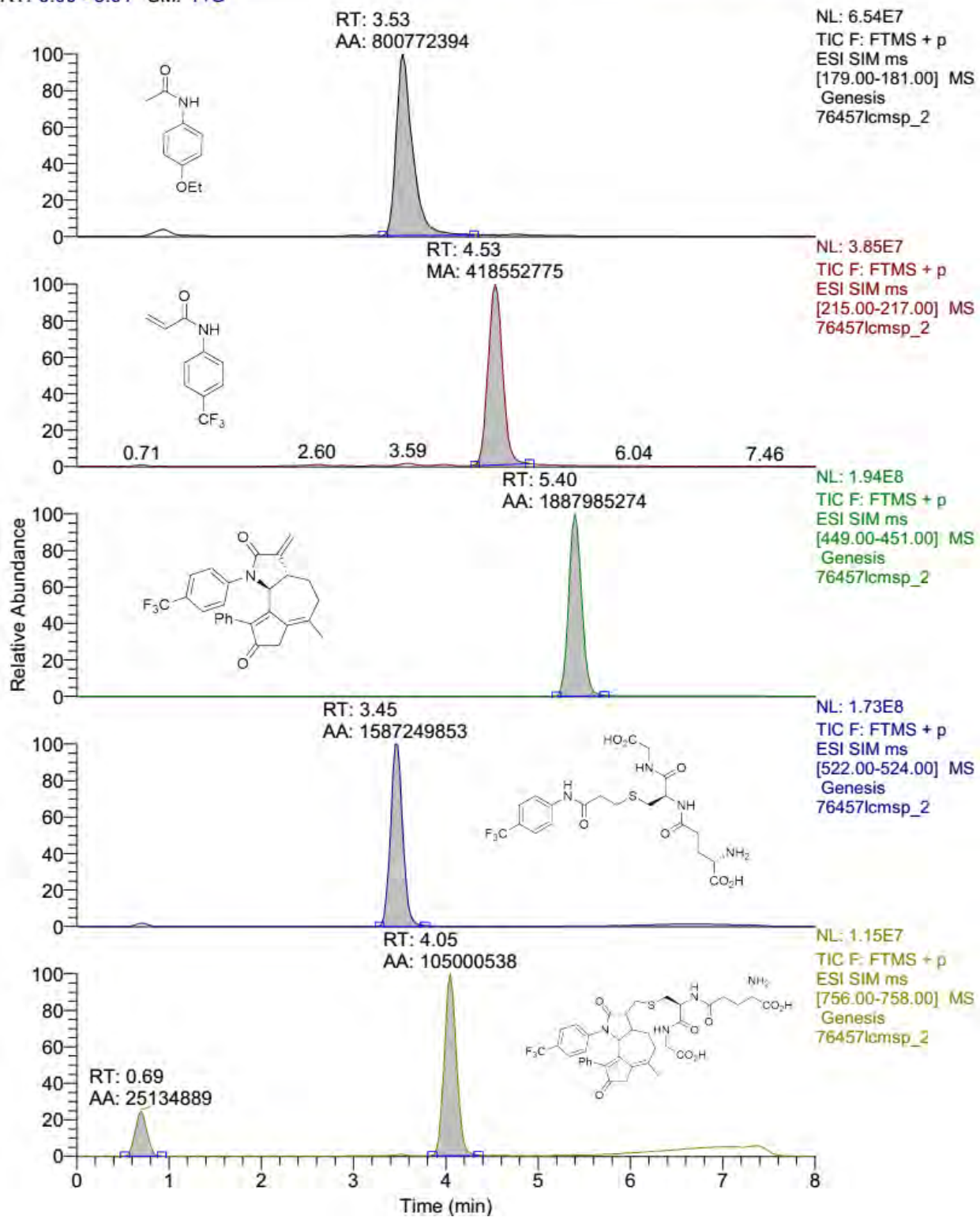
10/25/16 14:39:54

CONTROL



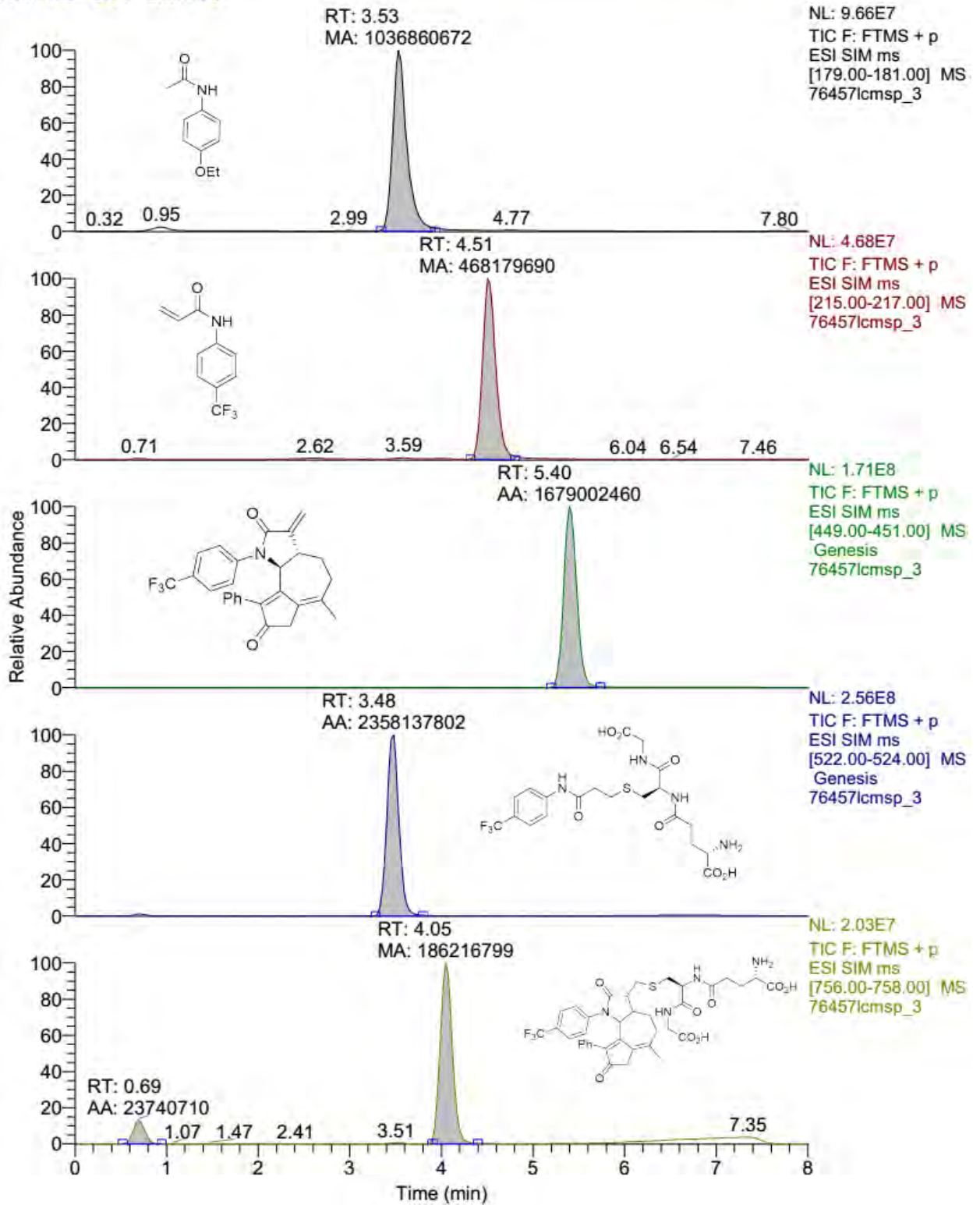
15 min

RT: 0.00 - 8.01 SM: 11G



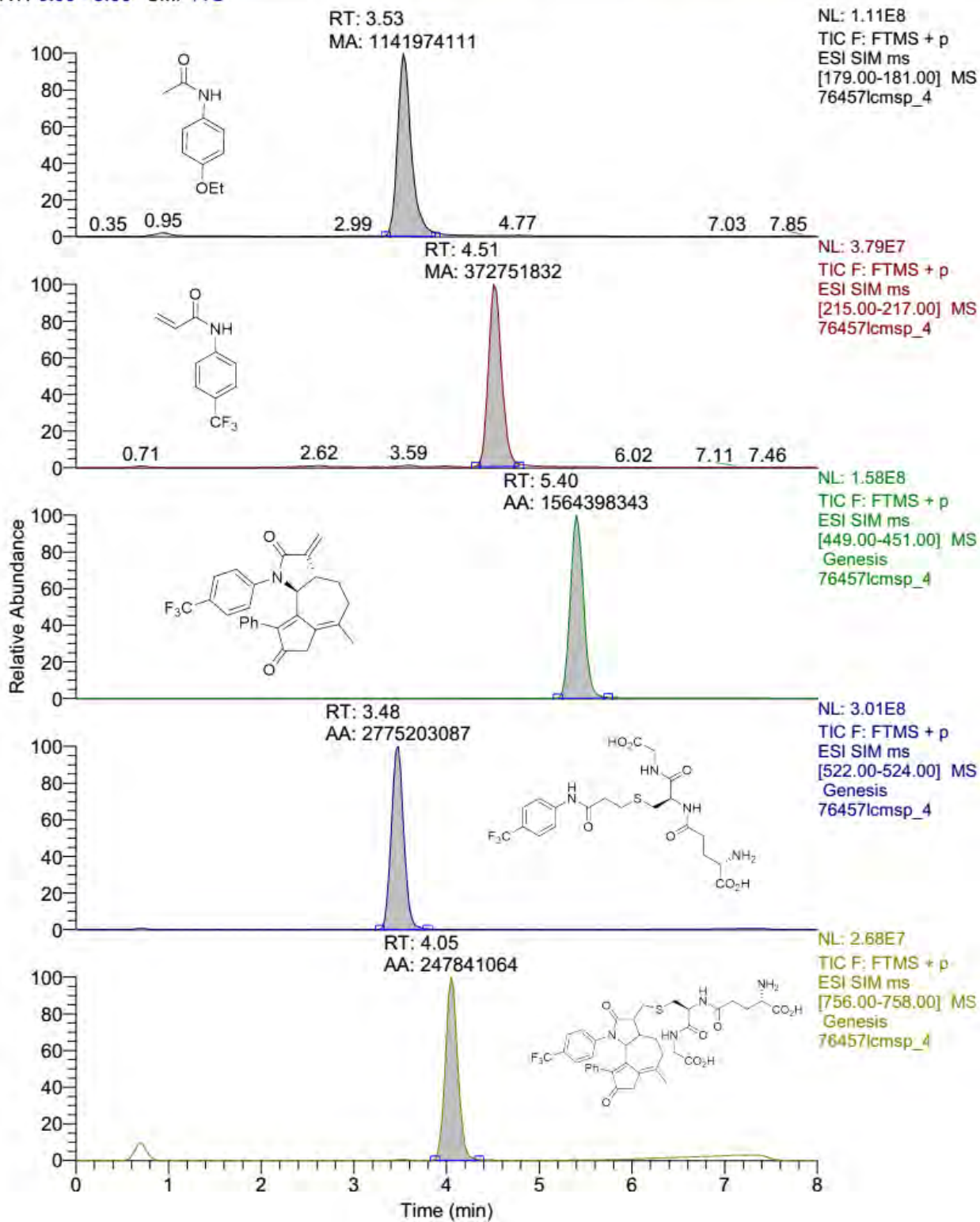
30 min

RT: 0.00 - 8.01 SM: 11G



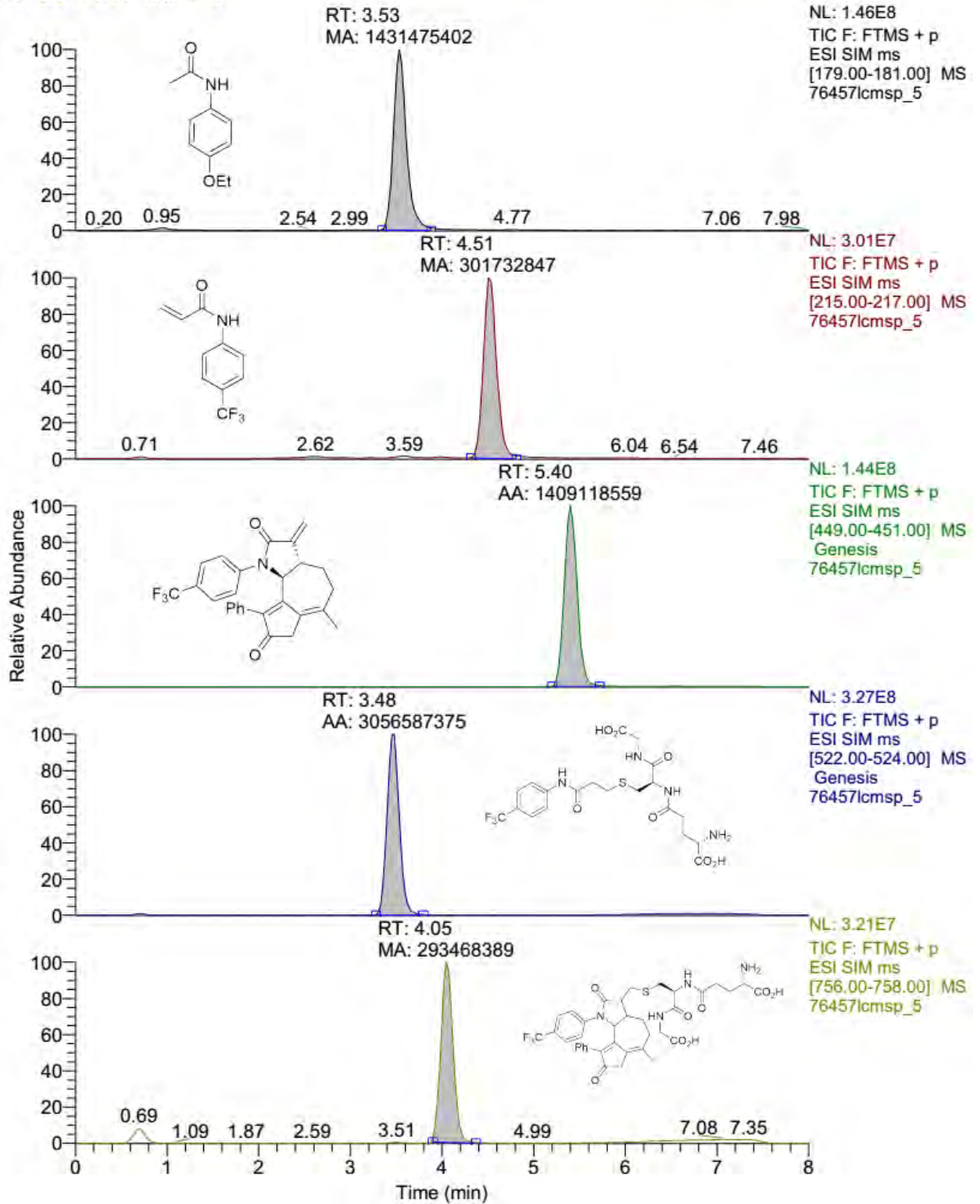
45 min

RT: 0.00 - 8.00 SM: 11G



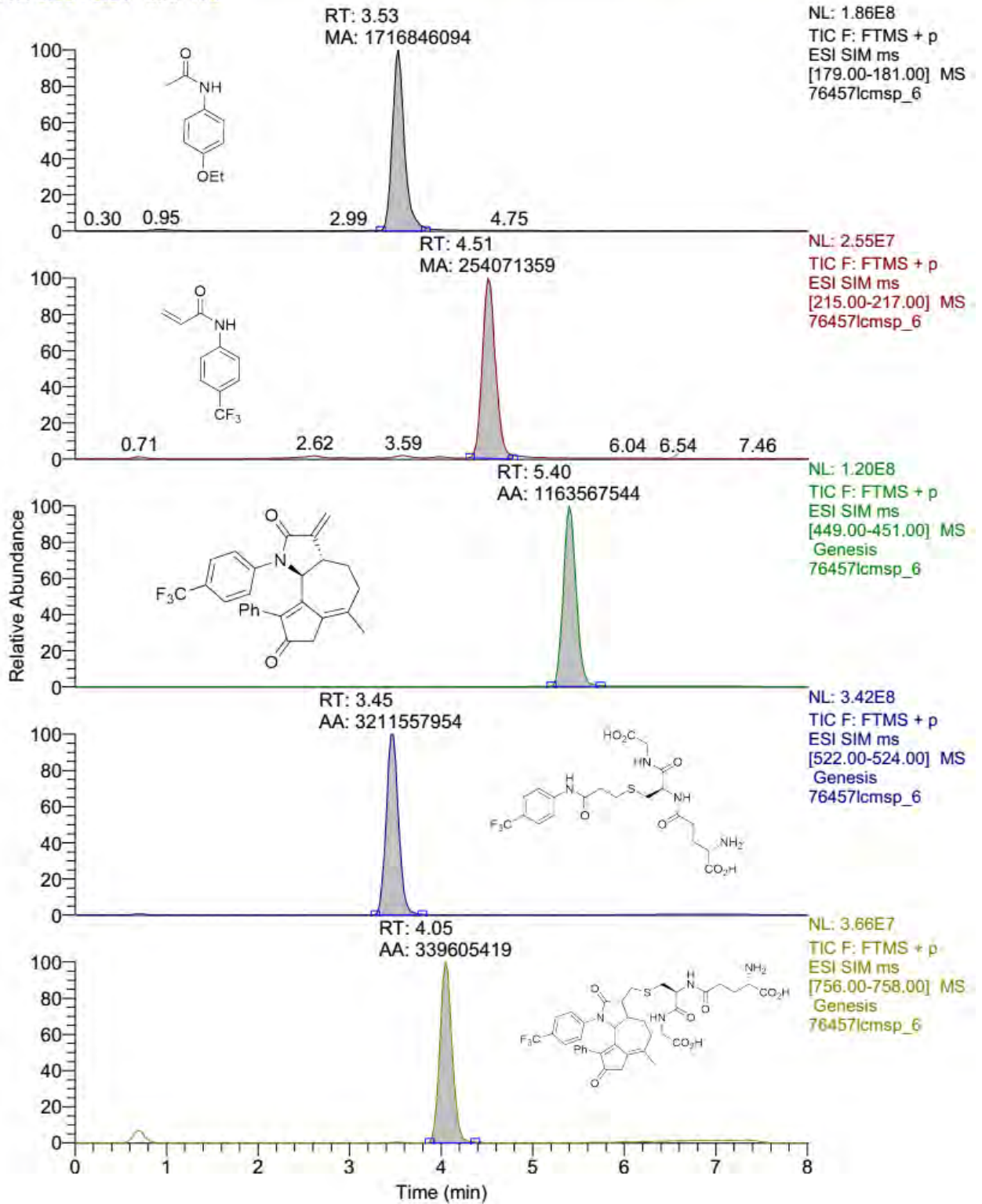
60 min

RT: 0.00 - 8.01 SM: 11G



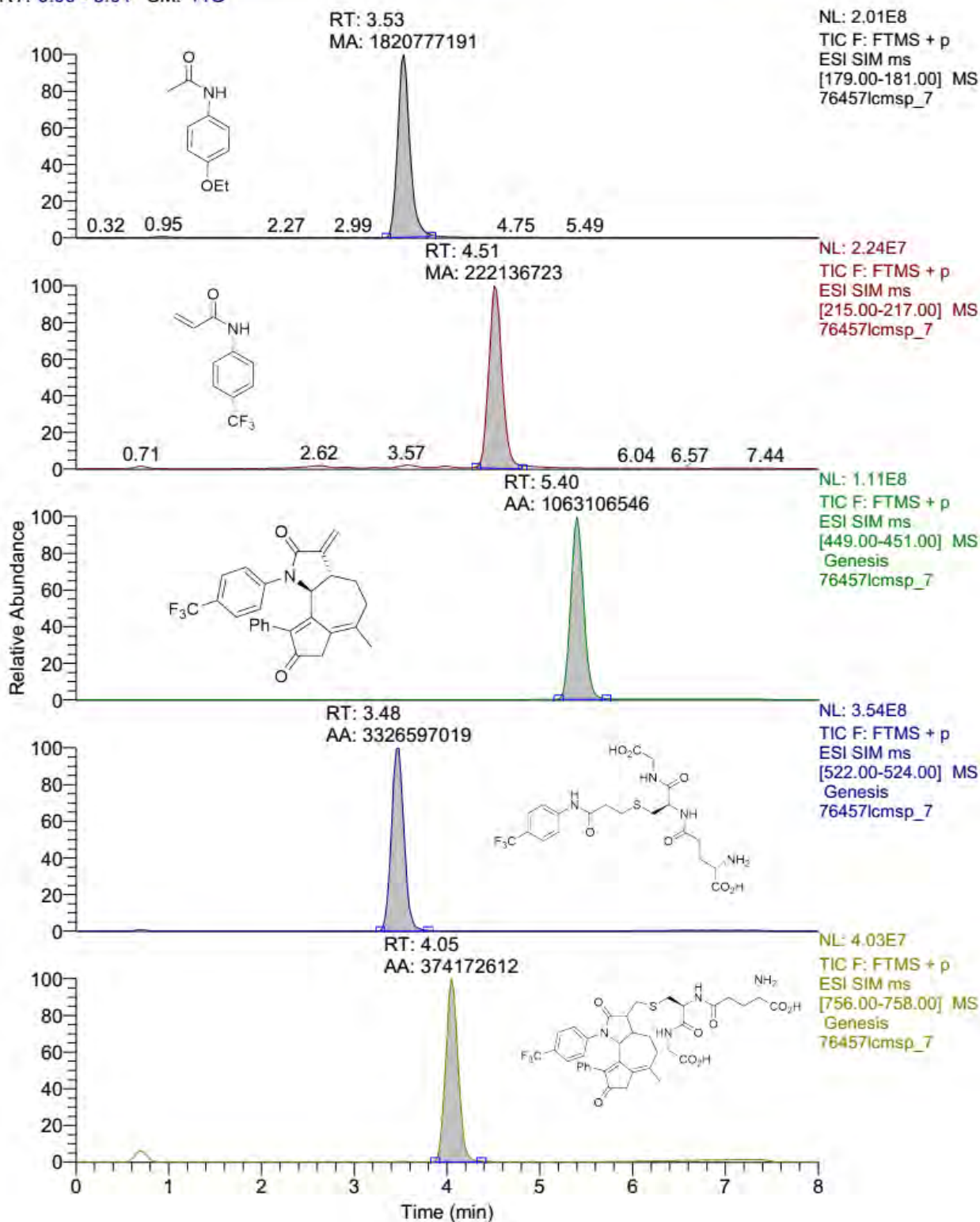
75 min

RT: 0.00 - 8.01 SM: 11G



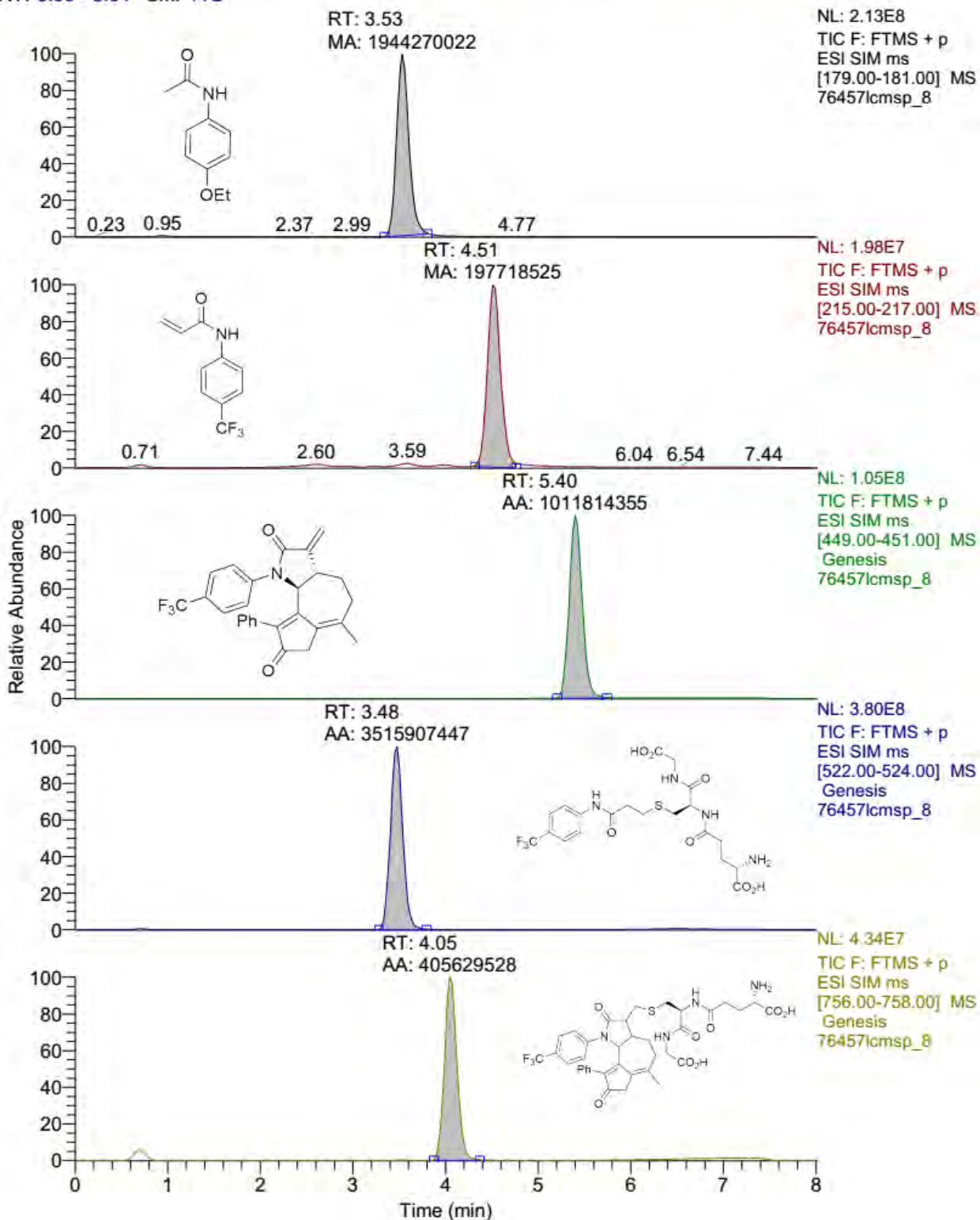
90 min

RT: 0.00 - 8.01 SM: 11G



105 min

RT: 0.00 - 8.01 SM: 11G



120 min

BIBLIOGRAPHY

1. Afatanib.
<http://www.fda.gov/Drugs/InformationOnDrugs/ApprovedDrugs/ucm360574.htm>
(accessed 8/8/16).
2. FDA Approves New Pill to Treat Certain Patients with Non-Small Cell Lung Cancer.
<http://www.fda.gov/NewsEvents/Newsroom/PressAnnouncements/ucm472525.htm>
(accessed 8/8/2016).
3. FDA Approves Imbruvica to Treat Chronic Lymphocytic Leukemia.
<http://www.fda.gov/NewsEvents/Newsroom/PressAnnouncements/ucm385764.htm>
(accessed 8/8/16).
4. FDA Approves Imbruvica for Rare Blood Cancer.
<http://www.fda.gov/NewsEvents/Newsroom/PressAnnouncements/ucm374761.htm>
(accessed 8/8/16).
5. Kwak, E. L.; Sordella, R.; Bell, D. W.; Godin-Heymann, N.; Okimoto, R. A.; Brannigan, B. W.; Harris, P. L.; Driscoll, D. R.; Fidias, P.; Lynch, T. J.; Rabindran, S. K.; McGinnis, J. P.; Wissner, A.; Sharma, S. V.; Isselbacher, K. J.; Settleman, J.; Haber, D. A., Irreversible Inhibitors of the EGF Receptor May Circumvent Acquired Resistance to Gefitinib. *PNAS* **2005**, *102*, 7665-7670.
6. Kohler, J.; Schuler, M., Afatinib, Erlotinib and Gefitinib in the First-Line Therapy of EGFR Mutation-Positive Lung Adenocarcinoma: A Review. *Onkologie* **2013**, *36*, 510-518.
7. Lou, Y.; Owens, T. D.; Kuglstatter, A.; Kondru, R. K.; Goldstein, D. M., Bruton's Tyrosine Kinase Inhibitors: Approaches to Potent and Selective Inhibition, Preclinical and Clinical Evaluation for Inflammatory Diseases and B Cell Malignancies. *J. Med. Chem.* **2012**, *55*, 4539-4550.
8. Cross, D. A. E.; Ashton, S. E.; Ghiorghiu, S.; Eberlein, C.; Nebhan, C. A.; Spitzler, P. J.; Orme, J. P.; Finlay, M. R. V.; Ward, R. A.; Mellor, M. J.; Jin, H.; Ballard, P.; Al-Kadhimi, K.; Rowlinson, R.; Klinowska, T.; Richmond, G. H. P.; Cantarini, M.; Kim, D.-W.; Ranson, M. R.; Pao, W., AZD9291, an Irreversible EGFR TKI, Overcomes T790M-Mediated Resistance to EGFR Inhibitors in Lung Cancer. *Cancer Discov.* **2014**, *4*, 1046-1061.
9. Hagel, M.; Niu, D.; Martin, T. S.; Sheets, M. P.; Qiao, L.; Bernard, H.; Karp, R. M.; Zhu, Z.; Labenski, M. T.; Chaturvedi, P.; Nacht, M.; Westlin, W. F.; Petter, R. C.; Singh, J.,

- Selective Irreversible Inhibition of a Protease by Targeting a Noncatalytic Cysteine. *Nat. Chem. Biol.* **2011**, *7*, 22-24.
10. Solca, F.; Dahl, G.; Zoephel, A.; Bader, G.; Sanderson, M.; Klein, C.; Kraemer, O.; Himmelsbach, F.; Haaksmma, E.; Adolf, G. R., Target Binding Properties and Cellular Activity of Afatinib (BIBW 2992), an Irreversible ErbB Family Blocker. *J. Pharmacol. Exp. Ther.* **2012**, *343*, 342-50.
 11. Zhou, W.; Hur, W.; McDermott, U.; Dutt, A.; Xian, W.; Ficarro, S. B.; Zhang, H.; Sharma, S. V.; Brugge, J.; Meyerson, M.; Settleman, J.; Gray, N. S., A Structure Guided Approach to Creating Covalent FGFR Inhibitors. *Chem. Biol.* **2010**, *17*, 285-295.
 12. Pan, Z.; Scheerens, H.; Li, S.-J.; Schultz, B. E.; Sprengeler, P. A.; Burrill, L. C.; Mendonca, R. V.; Sweeney, M. D.; Scott, K. C. K.; Grothaus, P. G.; Jeffery, D. A.; Spoerke, J. M.; Honigberg, L. A.; Young, P. R.; Dalrymple, S. A.; Palmer, J. T., Discovery of Selective Irreversible Inhibitors for Bruton's Tyrosine Kinase. *ChemMedChem* **2007**, *2*, 58-61.
 13. Zhang, T.; Inesta-Vaquera, F.; Niepel, M.; Zhang, J.; Ficarro, S. B.; Machleidt, T.; Xie, T.; Marto, J. A.; Kim, N.; Sim, T.; Laughlin, J. D.; Park, H.; LoGrasso, P. V.; Patricelli, M.; Nomanbhoy, T. K.; Sorger, P. K.; Alessi, D. R.; Gray, N. S., Discovery of Potent and Selective Covalent Inhibitors of JNK. *Chem. Biol.* **2012**, *19*, 140-154.
 14. Nacht, M.; Qiao, L.; Sheets, M. P.; Martin, T. S.; Labenski, M.; Mazdiyasni, H.; Karp, R.; Zhu, Z.; Chaturvedi, P.; Bhavsar, D.; Niu, D.; Westlin, W.; Petter, R. C.; Medikonda, A. P.; Singh, J., Discovery of a Potent and Isoform-Selective Targeted Covalent Inhibitor of the Lipid Kinase PI3K α . *J. Med. Chem.* **2013**, *56*, 712-721.
 15. Potashman, M. H.; Duggan, M. E., Covalent Modifiers: An Orthogonal Approach to Drug Design. *J. Med. Chem.* **2009**, *52*, 1231-1246.
 16. Singh, J.; Petter, R. C.; Baillie, T. A.; Whitty, A., The Resurgence of Covalent Drugs. *Nat. Rev. Drug Disc.* **2011**, *10*, 307-317.
 17. Barf, T.; Kaptein, A., Irreversible Protein Kinase Inhibitors: Balancing the Benefits and the Risks. *J. Med. Chem.* **2012**, *55*, 6243-6262.
 18. Wissner, A.; Overbeek, E.; Reich, M. F.; Floyd, M. B.; Johnson, B. D.; Mamuya, N.; Rosfjord, E. C.; Dicaiani, C.; Davis, R.; Shi, X.; Rabindran, S. K.; Gruber, B. C.; Ye, F.; Hallett, W. A.; Nilakantan, R.; Shen, R.; Wang, Y.-F.; Greenberger, L. M.; Tsou, H.-R., Synthesis and Structure-Activity Relationships of 6,7-Disubstituted 4-Anilinoquinoline-3-carbonitriles. The Design of an Orally Active, Irreversible Inhibitor of the Tyrosine Kinase Activity of the Epidermal Growth Factor Receptor (EGFR) and the Human Epidermal Growth Factor Receptor-2 (HER-2). *J. Med. Chem.* **2003**, *46*, 49-63.
 19. Tsou, H.-R.; Mamuya, N.; Johnson, B. D.; Reich, M. F.; Gruber, B. C.; Ye, F.; Nilakantan, R.; Shen, R.; Dicaiani, C.; DeBlanc, R.; Davis, R.; Koehn, F. E.; Greenberger, L. M.;

- Wang, Y.-F.; Wissner, A., 6-Substituted-4-(3-bromophenylamino)quinazolines as Putative Irreversible Inhibitors of the Epidermal Growth Factor Receptor (EGFR) and Human Epidermal Growth Factor Receptor (HER-2) with Enhanced Antitumor Activity. *J. Med. Chem.* **2001**, *44*, 2719-2734.
20. Drew, D. P.; Krichau, N.; Reichwald, K.; Simonsen, H. T., Guaianolides in Apiaceae: Perspectives on Pharmacology and Biosynthesis. *Phytochemistry Reviews* **2009**, *8*, 581-599.
 21. Simonsen, H.; Weitzel, C.; Christensen, S., Guaianolide Sesquiterpenoids: Pharmacology and Biosynthesis. In *Natural Products*, Ramawat, K. G.; Mérillon, J.-M., Eds. Springer Berlin Heidelberg: 2013; pp 3069-3098.
 22. Kitson, R. R.; Millemaggi, A.; Taylor, R. J., The Renaissance of alpha-Methylene-gamma-Butyrolactones: New Synthetic Approaches. *Angew. Chem. Int. Ed.* **2009**, *48*, 9426-9451.
 23. Beekman, A. C.; Woerdenbag, H. J.; Uden, W.; Pras, N.; Konings, A. W.; Wikstrom, H. V.; Schmidt, T. J., Structure-Cytotoxicity Relationships of Some Helenanolide-Type Sesquiterpene Lactones. *J. Nat. Prod.* **1997**, *60*, 252-257.
 24. Csuk, R.; Heinold, A.; Siewert, B.; Schwarz, S.; Barthel, A.; Kluge, R.; Strohl, D., Synthesis and Biological Evaluation of Antitumor-Active Arglabin Derivatives. *Arch Pharm (Weinheim)* **2012**, *345*, 215-222.
 25. Siedle, B.; García-Piñeres, A. J.; Murillo, R.; Schulte-Mönting, J.; Castro, V.; Rüngeler, P.; Klaas, C. A.; Da Costa, F. B.; Kisiel, W.; Merfort, I., Quantitative Structure–Activity Relationship of Sesquiterpene Lactones as Inhibitors of the Transcription Factor NF- κ B. *J. Med. Chem.* **2004**, *47*, 6042-6054.
 26. Dey, A.; Tergaonkar, V.; Lane, D. P., Double-edged swords as cancer therapeutics: simultaneously targeting p53 and NF-[kappa]B pathways. *Nat Rev Drug Discov* **2008**, *7*, 1031-1040.
 27. Gilmore, T. D.; Herscovitch, M., Inhibitors of NF-[kappa]B signaling: 785 and counting. *Oncogene* **2006**, *25*, 6887-6899.
 28. Guterman, L., Covalent Drugs Form Long-Lived Ties. *Chem. Eng. News* **2011**, *89*, 19-26.
 29. Grillot, A. L.; Farmer, L. J.; Rao, B. G.; Taylor, W. P.; Weisberg, I. S.; Jacobson, I. M.; Perni, R. B.; Kwong, A. D., Discovery and Development of Telaprevir. In *Antiviral Drugs: From Basic Discovery through Clinical Trials*, Kazmierski, W. M., Ed. Wiley: Hoboken, NJ, 2011; pp 207-224.
 30. Blazer, L. L.; Neubig, R. R., Small Molecule Protein-Protein Interaction Inhibitors as CNS Therapeutic Agents: Current Progress and Future Hurdles. *Neuropsychopharmacology* **2009**, *34*, 126-141.

31. Way, J. C., Covalent Modification as a Strategy to Block Protein-Protein Interactions with Small-Molecule Drugs. *Curr. Opin. Chem. Biol.* **2000**, *4*, 40-46.
32. Arkin, M. R.; Wells, J. A., Small-Molecule Inhibitors of Protein-Protein Interactions: Progressing Towards the Dream. *Nature Reviews: Drug Discovery* **2004**, *3*, 301-317.
33. Kimple, A. J.; Willard, F. S.; Giguère, P. M.; Johnston, C. A.; Mocanu, V.; Siderovski, D. P., The RGS Protein Inhibitor CCG-4986 is a Covalent Modifier of the RGS4 Gα-Interaction Face. *Biochim. Biophys. Acta* **2007**, *1774*, 1213-1220.
34. Leproult, E.; Barluenga, S.; Moras, D.; Wurtz, J.-M.; Winssinger, N., Cysteine Mapping in Conformationally Distinct Kinase Nucleotide Binding Sites: Application to the Design of Selective Covalent Inhibitors. *J. Med. Chem.* **2011**, *54*, 1347-1355.
35. Parsons, Z. D.; Gates, K. S., Redox Regulation of Protein Tyrosine Phosphatases: Methods for Kinetic Analysis of Covalent Enzyme Inactivation. In *Methods in Enzymology Volume 528: Hydrogen Peroxide and Cell Signaling Part C*, Cadenas, E.; Packer, L., Eds. Elsevier Science Publishing Co Inc: San Diego, 2013; Vol. 528, pp 130-154.
36. Kitz, R.; Wilson, I. B., Esters of Methanesulfonic Acid as Irreversible Inhibitors of Acetylcholinesterase. *J. Biol. Chem.* **1962**, *237*, 3245-3249.
37. Nagahara, N.; Sawada, N.; Nakagawa, T., Affinity Labeling of a Catalytic Site, Cysteine 247, in Rat Mercaptopyruvate Sulfurtransferase by Chloropyruvate as an Analog of a Substrate. *Biochimie* **2004**, *86*, 723-729.
38. Michalczyk, A.; Klüter, S.; Rode, H. B.; Simard, J. R.; Grütter, C.; Rabiller, M.; Rauh, D., Structural Insights into How Irreversible Inhibitors Can Overcome Drug Resistance in EGFR. *Bioorg. Med. Chem.* **2008**, *16*, 3482-3488.
39. Engel, J.; Lategahn, J.; Rauh, D., Hope and Disappointment: Covalent Inhibitors to Overcome Drug Resistance in Non-Small Cell Lung Cancer. *ACS Med. Chem. Lett.* **2016**, *7*, 2-5.
40. Sequist, L. V.; Soria, J. C.; Goldman, J. W.; Wakelee, H. A.; Gadgeel, S. M.; Varga, A.; Papadimitrakopoulou, V.; Solomon, B. J.; Oxnard, G. R.; Dziadziuszko, R.; Aisner, D. L.; Doebele, R. C.; Galasso, C.; Garon, E. B.; Heist, R. S.; Logan, J.; Neal, J. W.; Mendenhall, M. A.; Nichols, S.; Piotrowska, Z.; Wozniak, A. J.; Raponi, M.; Karlovich, C. A.; Jaw-Tsai, S.; Isaacson, J.; Despain, D.; Matheny, S. L.; Rolfe, L.; Allen, A. R.; Camidge, D. R., Rociletinib in EGFR-Mutated Non-Small-Cell Lung Cancer. *N. Engl. J. Med.* **2015**, *372*, 1700-1709.
41. Walter, A. O.; Sjin, R. T. T.; Haringsma, H. J.; Ohashi, K.; Sun, J.; Lee, K.; Dubrovskiy, A.; Labenski, M.; Zhu, Z.; Wang, Z.; Sheets, M.; Martin, T. S.; Karp, R.; Kalken, D.; Chaturvedi, P.; Niu, D.; Nacht, M.; Petter, R. C.; Westlin, W.; Lin, K.; Jaw-Tsai, S.;

- Raponi, M.; Dyke, T. V.; Etter, J.; Weaver, Z.; Pao, W.; Singh, J.; Simmons, A. D.; Harding, T. C.; Allen, A., Discovery of a Mutant-Selective Covalent Inhibitor of EGFR that Overcomes T790M-Mediated Resistance in NSCLC. *Cancer Discov.* **2013**, *3*, 1404-1415.
42. Thress, K. S.; Paweletz, C. P.; Felip, E.; Cho, B. C.; Stetson, D.; Dougherty, B.; Lai, Z.; Markovets, A.; Vivancos, A.; Kuang, Y.; Ercan, D.; Matthews, S. E.; Cantarini, M.; Barrett, J. C.; Janne, P. A.; Oxnard, G. R., Acquired EGFR C797S Mutation Mediates Resistance to AZD9291 in Non-small Cell Lung Cancer Harboring EGFR T790M. *Nat. Med.* **2015**, *21*, 560-562.
43. Rockoff, J. D.; Loftus, P. AbbVie to Buy Pharmacyclics in \$21 Billion Deal. <http://www.wsj.com/articles/abbvie-to-buy-pharmacyclics-in-21-billion-deal-1425528086> (accessed 9/8/16).
44. D'Cruz, O. J.; Uckun, F. M., Novel Bruton's Tyrosine Kinase Inhibitors Currently in Development. *Onco Targets Ther.* **2013**, *6*, 161-176.
45. Eda, H.; Santo, L.; Cirstea, D. D.; Yee, A. J.; Scullen, T. A.; Nemani, N.; Mishima, Y.; Waterman, P. R.; Arastu-Kapur, S.; Evans, E.; Singh, J.; Kirk, C. J.; Westlin, W. F.; Raje, N. S., A Novel Bruton's Tyrosine Kinase Inhibitor CC-292 in Combination with the Proteasome Inhibitor Carfilzomib Impacts the Bone Microenvironment in a Multiple Myeloma Model with Resultant Antimyeloma Activity. *Leukemia* **2014**, *28*, 1892-1901.
46. Liu, Q.; Sabnis, Y.; Zhao, Z.; Zhang, T.; Buhrlage, S. J.; Jones, L. H.; Gray, N. S., Developing Irreversible Inhibitors of the Protein Kinase Cysteine. *Chem. Biol.* **2013**, *20*, 146-159.
47. Jones, D. P.; Go, Y.-M., Mapping the Cysteine Proteome: Analysis of Redox-sensing Thiols. *Curr. Opin. Chem. Biol.* **2011**, *15*, 103-112.
48. Liu, F.; Zhang, X.; Weisberg, E.; Chen, S.; Hur, W.; Wu, H.; Zhao, Z.; Wang, W.; Mao, M.; Cai, C.; Simon, N. I.; Sanda, T.; Wang, J.; Look, A. T.; Griffin, J. D.; Balk, S. P.; Liu, Q.; Gray, N. S., Discovery of a Selective Irreversible BMX Inhibitor for Prostate Cancer. *ACS Chem. Biol.* **2013**, *8*, 1423-1428.
49. Kwiatkowski, N.; Zhang, T.; Rahl, P. B.; Abraham, B. J.; Reddy, J.; Ficarro, S. B.; Dastur, A.; Amzallag, A.; Ramaswamy, S.; Tesar, B.; Jenkins, C. E.; Hannett, N. M.; McMillin, D.; Sanda, T.; Sim, T.; Kim, N. D.; Look, T.; Mitsiades, C. S.; Weng, A. P.; Brown, J. R.; Benes, C. H.; Marto, J. A.; Young, R. A.; Gray, N. S., Targeting Transcription Regulation in Cancer with a Covalent CDK7 Inhibitor. *Nature* **2014**, *511*, 616-620.
50. Serafimova, I. M.; Pufall, M. A.; Krishnan, S.; Duda, K.; Cohen, M. S.; Maglathlin, R. L.; McFarland, J. M.; Miller, R. M.; Frodin, M.; Taunton, J., Reversible Targeting of Noncatalytic Cysteines with Chemically Tuned Electrophiles. *Nat. Chem. Biol.* **2012**, *8*, 471-476.

51. Miller, R. M.; Paavilainen, V. O.; Krishnan, S.; Serafimova, I.; Taunton, J., Electrophilic Fragment-Based Design of Reversible Covalent Kinase Inhibitors. *J. Am. Chem. Soc.* **2013**, *135*, 5298-5301.
52. Garuti, L.; Roberti, M.; Bottegoni, G., Irreversible Protein Kinase Inhibitors *Curr. Med. Chem.* **2011**, *18*, 2981-2994.
53. Mah, R.; Thomas, J. R.; Shafer, C. M., Drug Discovery Considerations in the Development of Covalent Inhibitors. *Bioorg. Med. Chem. Lett.* **2014**, *24*, 33-39.
54. Bauer, R. A., Covalent Inhibitors in Drug Discovery: From Accidental Discoveries to Avoided Liabilities and Designed Therapies. *Drug Discov. Today* **2015**, *20*, 1061-1073.
55. Johnson, D. S.; Weerapana, E.; Cravatt, B. F., Strategies for Discovering and Derisking Covalent, Irreversible Enzyme Inhibitors. *Future Med. Chem* **2010**, *2*, 949-964.
56. Woods, J. R.; Mo, H. P.; Bieberich, A. A.; Alavanja, T.; Colby, D. A., Amino-Derivatives of the Sesquiterpene Lactone Class of Natural Products as Prodrugs. *MedChemComm* **2013**, *4*, 27-33.
57. Amslinger, S., The Tunable Functionality of alpha,beta-Unsaturated Carbonyl Compounds Enables Their Differential Application in Biological Systems. *ChemMedChem* **2010**, *5*, 351-356.
58. Ghantous, A.; Gali-Muhtasib, H.; Vuorela, H.; Saliba, N. A.; Darwiche, N., What Made Sesquiterpene Lactones Reach Cancer Clinical Trials? *Drug Discov. Today* **2010**, *15*, 668-678.
59. Kupchan, S. M.; Fessler, D. C.; Eakin, M. A.; Giacobbe, T. J., Reactions of alpha Methylene Lactone Tumor Inhibitors with Model Biological Nucleophiles. *Science* **1970**, *168*, 376-378.
60. Hall, I. H.; Lee, K.-H.; Mar, E. C.; Starnes, C. O.; Waddell, T. G., Antitumor Agents 21. A Proposed Mechanism for Inhibition of Cancer Growth by Tenulin and Helenalin and Related Cyclopentenones. *J. Med. Chem.* **1977**, *20*, 333-337.
61. Schmidt, T. J., Helenanolide-Type Sesquiterpene Lactones-III. Rates and Stereochemistry in the Reaction of Helenalin and Related Helenanolides with Sulfhydryl Containing Biomolecules. *Bioorg. Med. Chem.* **1997**, *5*, 645-653.
62. Schmidt, T. J.; LyB, G.; Pahl, H. L.; Merfort, I., Helenanolide Type Sesquiterpene Lactones. Part 5. The Role of Glutathione Addition Under Physiological Conditions. *Bioorg. Med. Chem.* **1999**, *7*, 2849-2855.
63. Pei, S. S.; Minhajuddin, M.; Callahan, K. P.; Balys, M.; Ashton, J. M.; Neering, S. J.; Lagadinou, E. D.; Corbett, C.; Ye, H. B.; Liesveld, J. L.; O'Dwyer, K. M.; Li, Z.; Shi, L.; Greninger, P.; Settleman, J.; Benes, C.; Hagen, F. K.; Munger, J.; Crooks, P. A.; Becker,

- M. W.; Jordan, C. T., Targeting Aberrant Glutathione Metabolism to Eradicate Human Acute Myelogenous Leukemia Cells. *J. Biol. Chem.* **2013**, *288*, 33542-33558.
64. Nasim, S.; Pei, S. S.; Hagen, F. K.; Jordan, C. T.; Crooks, P. A., Melampomagnolide B: A New Antileukemic Sesquiterpene. *Biorg. Med. Chem.* **2011**, *19*, 1515-1519.
65. Kwok, B. H.; Koh, B.; Ndubuisi, M. I.; Elofsson, M.; Crews, C. M., The Anti-Inflammatory Natural Product Parthenolide from the Medicinal Herb Feverfew Directly Binds to and Inhibits IkappaB Kinase. *Chem Biol* **2001**, *8*, 759-766.
66. Kunzmann, M. H.; Bach, N. C.; Bauer, B.; Sieber, S. A., alpha-Methylene-gamma-Butyrolactones Attenuate Staphylococcus Aureus Virulence by Inhibition of Transcriptional Regulation. *Chem. Sci.* **2014**, *5*, 1158-1167.
67. Kunzmann, M. H.; Sieber, S. A., Target Analysis of α -Alkylidene- γ -Butyrolactones in Uropathogenic *E. Coli*. *Mol. BioSyst.* **2012**, *8*, 3061-3067.
68. Polo, L. M.; Castro, C. M.; Cruzado, M. C.; Collino, C. J. G.; Cuello-Carrión, F. D.; Ciocca, D. R.; Giordano, O. S.; Ferrari, M.; López, L. A., 11,13-Dihydro-dehydroleucodine, a Derivative of Dehydroleucodine with an Inactivated Alkylating Function Conserves the Anti-proliferative Activity in G2 but does not Cause Cytotoxicity. *Eur. J. Pharmacol.* **2007**, *556*, 19-26.
69. Albrecht, A.; Albrecht, L.; Janecki, T., Recent Advances in the Synthesis of α -Alkylidene-substituted δ -Lactones, γ -Lactams and δ -Lactams. *Eur. J. Org. Chem.* **2011**, 2747-2766.
70. Di Maso, M. J.; Nepomuceno, G. M.; St. Peter, M. A.; Gitre, H. H.; Martin, K. S.; Shaw, J. T., Synthesis of (\pm)-Bisavenanthramide B-6 by an Anionic Anhydride Mannich Reaction. *Org. Lett.* **2016**, *18*, 1740-1743.
71. Janecka, A.; Wyrębska, A.; Gach, K.; Fichna, J.; Janecki, T., Natural and Synthetic α -Methylenelactones and α -Methylenelactams with Anticancer Potential. *Drug Discov. Today* **2012**, *17*, 561-572.
72. Janecki, T.; Blaszczyk, E.; Studzian, K.; Janecka, A.; Krajewska, U.; Róžalski, M., Novel Synthesis, Cytotoxic Evaluation, and Structure-Activity Relationship Studies of a Series of alpha-Alkylidene-gamma-Lactones and Lactams. *J. Med. Chem.* **2005**, *48*, 3516-3521.
73. Albrecht, A.; Koszuc, J. F.; Modranka, J.; Róžalski, M.; Krajewska, U.; Janecka, A.; Studzian, K.; Janecki, T., Synthesis and Cytotoxic Activity of γ -Aryl Substituted α -Alkylidene- γ -lactones and α -Alkylidene- γ -lactams. *Biorg. Med. Chem.* **2008**, *16*, 4872-4882.
74. Krawczyk, H.; Albrecht, Ł.; Wojciechowski, J.; Wolf, W. M.; Krajewska, U.; Róžalski, M., A Convenient Synthesis and Cytotoxic Evaluation of *N*-Unsubstituted α -Methylene- γ -lactams. *Tetrahedron* **2008**, *64*, 6307-6314.

75. Janecki, T.; Wąsek, T.; Różalski, M.; Krajewska, U.; Studzian, K.; Janecka, A., 4-Methylideneisoxazolidin-5-ones--A New Class of α -Methylidene- γ -lactones with High Cytostatic Activity. *Bioorg. Med. Chem. Lett.* **2006**, *16*, 1430-1433.
76. Albrecht, A.; Albrecht, Ł.; Różalski, M.; Krajewska, U.; Janecka, A.; Studzian, K.; Janecki, T., A Convenient Synthesis and Cytotoxic Evaluation of β -Aryl- α -methylidene- γ -lactones and β -Aryl- α -methylidene- γ -lactams. *New J. Chem.* **2010**, *34*, 750-761.
77. Elford, T. G.; Ulaczyk-Lesanko, A.; Pascale, G. D.; Wright, G. D.; Hall, D. G., Diversity-Oriented Synthesis and Preliminary Biological Screening of Highly Substituted Five-Membered Lactones and Lactams Originating From an Allylboration of Aldehydes and Imines. *J. Comb. Chem.* **2009**, *11*, 155-168.
78. Avonto, C.; Tagliatela-Scafati, O.; Pollastro, F.; Minassi, A.; Marzo, V. D.; Petrocellis, L. D.; Appendino, G., An NMR Spectroscopic Method to Identify and Classify Thiol-Trapping Agents: Revival of Michael Acceptors for Drug Discovery. *Angew. Chem. Int. Ed.* **2011**, *50*, 467-471.
79. Hanson, R. L.; Lardy, H. A.; Kupchan, S. M., Inhibition of Phosphofructokinase by Quinone Methide and α -Methylene Lactone Tumor Inhibitors. *Science* **1970**, *168*, 378-80.
80. Fukuda, K.; Akao, S.; Ohno, Y.; Yamashita, K.; Fujiwara, H., Inhibition by Costunolide of Phorbol Ester-induced Transcriptional Activation of Inducible Nitric Oxide Synthase Gene in a Human Monocyte Cell Line THP-1. *Cancer Lett.* **2001**, *164*, 7-13.
81. Arumugam, V.; Routledge, A.; Abell, C.; Balasubramanian, S., Synthesis of 2-Oxindole Derivatives *via* the Intramolecular Heck Reaction on Solid Support. *Tet. Lett.* **1997**, *38*, 6473-6476.
82. Kornet, M. J., Synthesis and Anticonvulsant Activity of 1-Aryl-3-Methylene-2-Pyrrolidinone Adducts. *J. Heterocycl. Chem.* **1985**, *22*, 129-130.
83. Pettigrew, N. E.; Brush, E. J.; Colman, R. F., 3-Methyleneoxindole: An Affinity Label of Glutathione *S*-Transferase pi Which Targets Tryptophan 38. *Biochem.* **2001**, *40*, 7549-7558.
84. Wieland, T.; Unger, O., Synthese Einiger Methoxy-oxindole Und-indoline. *Chem. Ber.* **1963**, *96*, 253-259.
85. Klutchko, S.; Hoefle, M. L.; Smith, R. D.; Essenburg, A. D.; Parker, R. B.; Nemeth, V. L.; Ryan, M. J.; Dugan, D. H.; Kaplan, H. R., Synthesis and Angiotensin-Converting Enzyme Inhibitory Activity of 3-(Mercaptomethyl)-2-Oxo-1-Pyrrolidineacetic Acids and 3-(Mercaptomethyl)-2-Oxo-1-Piperidineacetic Acids. *J. Med. Chem.* **1981**, *24*, 104-109.

86. Drahl, C.; Cravatt, B. F.; Sorenson, E. J., Protein-Reactive Natural Products. *Angew. Chem. Int. Ed.* **2005**, *44*, 5788-5809.
87. Kondo, F.; Ikai, Y.; Oka, H.; Okumura, M.; Ishikawa, N.; Harada, K.-I.; Matsuura, K.; Murata, H.; Suzuki, M., Formation, Characterization, and Toxicity of the Glutathione and Cysteine Conjugates of Toxic Heptapeptide Microcystins. *Chem. Res. Toxicol.* **1992**, *5*, 591-596.
88. Runnegar, M.; Berndt, N.; Kong, S.-M.; Lee, E. Y. C.; Zhang, L., *In Vivo* and *In Vitro* Binding of Microcystin to Protein Phosphatases 1 and 2A. *Biochem. Biophys. Res. Commun.* **1995**, *216*, 162-169.
89. Craig, M.; Luu, H. A.; McCready, T. L.; Holmes, C. F. B.; Williams, D.; Andersen, R. J., Molecular Mechanisms Underlying the Interaction of Motuporin and Microcystins with Type-1 and Type-2A Protein Phosphatases. *Biochem. Cell* **1996**, *74*, 569-578.
90. Clement, L. L.; Tsakos, M.; Schaffert, E. S.; Scavenius, C.; Enghild, J. J.; Poulsen, T. B., The Amido-Pentadienoate-Functionality of the Rakicidins is a Thiol Reactive Electrophile - Development of a General Synthetic Strategy. *Chem. Commun.* **2015**, *51*, 12427-12430.
91. Cee, V. J.; Volak, L. P.; Chen, Y.; Bartberger, M. D.; Tegley, C.; Arvedson, T.; McCarter, J.; Tasker, A. S.; Fotsch, C., Systematic Study of the Glutathione (GSH) Reactivity of *N*-Arylacrylamides: 1. Effects of Aryl Substitution. *J. Med. Chem.* **2015**, *58*, 9171-9178.
92. $\ln([\text{electrophile}]) = (-k_{\text{pseudofirst}})t + \ln([\text{electrophile}])$
93. Flanagan, M. E.; Abramite, J. A.; Anderson, D. P.; Aulabaugh, A.; Dahal, U. P.; Gilbert, A. M.; Li, C.; Montgomery, J.; Oppenheimer, S. R.; Ryder, T.; Schuff, B. P.; Uccello, D. P.; Walker, G. S.; Wu, Y.; Brown, M. F.; Chen, J. M.; Hayward, M. M.; Noe, M. C.; Obach, R. S.; Philippe, L.; Shanmugasundaram, V.; Shapiro, M. J.; Starr, J.; Stroh, J.; Che, Y., Chemical and Computational Methods for the Characterization of Covalent Reactive Groups for the Prospective Design of Irreversible Inhibitors. *J. Med. Chem.* **2014**, *57*, 10072-10079.
94. Krishnan, S.; Miller, R. M.; Tian, B.; Mullins, R. D.; Jacobson, M. P.; Taunton, J., Design of Reversible, Cysteine-Targeted Michael Acceptors Guided by Kinetic and Computational Analysis. *J. Am. Chem. Soc.* **2014**, *136*, 12624-12630.
95. Ray, A. K.; Nilsson, U.; Magnusson, G., Synthesis and Conformational Analysis of GM₃ Lactam, a Hydrolytically Stable Analogue of GM₃ Ganglioside Lactone. *J. Am. Chem. Soc.* **1992**, *114*, 2256-2257.
96. Nilsson, J.; Gidlöf, R.; Johansson, M.; Sterner, O., Lactam Analogues of Galiellalactone. *Tetrahedron* **2012**, *68*, 3336-3341.

97. Torok, D. S.; Ziffer, H.; Meshnick, S. R.; Pan, X.-Q.; Ager, A., Syntheses and Antimalarial Activities of N-Substituted 11-Azaartemisinins. *J. Med. Chem.* **1995**, *38*, 5045-5050.
98. Balan, D.; Burns, C. J.; Gisk, N. G.; Hugel, H.; Huang, D. C. S.; Segal, D.; White, C.; Wagler, J.; Rizzacasa, M. A., Synthesis and Biological Evaluation of a Potent Salicylilalamide A Lactam Analogue. *Org. Biomol. Chem.* **2012**, *10*, 8147-8153.
99. Borzilleri, R. M.; Zheng, X.; Schmidt, R. J.; Johnson, J. A.; Kim, S.-H.; DiMarco, J. D.; Fairchild, G. R.; Gougoatas, J. Z.; Lee, F. Y. F.; Long, B. H.; Vite, G. D., A Novel Application of a Pd(0)-Catalyzed Nucleophilic Substitution Reaction to the Regio- and Stereoselective Synthesis of Lactam Analogues of the Epothilone Natural Products. *J. Am. Chem. Soc.* **2000**, *122*, 8890-8897.
100. Hunt, J. T., Discovery of Ixabepilone. *Molecular Cancer Therapeutics* **2009**, *8*, 275-281.
101. Sayed, K. A. E.; Orabi, K. Y.; Dunbar, D. C.; Hamann, M. T.; Avery, M. A.; Sabnis, Y. A.; Mossa, J. S.; El-Feraly, F. S., Transformation of lactone to lactam in sarcophine and antimalarial activity of the resulting N-substituted azasarcophines. *Tetrahedron* **2002**, *58*, 3699-3708.
102. Matsuya, Y.; Kawaguchi, T.; Nemoto, H., New Strategy for the Total Synthesis of Macrophelides A and B Based on Ring-Closing Metathesis. *Org. Lett.* **2003**, *5*, 2939-2941.
103. Sugimoto, K.; Kobayashi, Y.; Hori, A.; Kondo, T.; Toyooka, N.; Nemoto, H.; Matsuya, Y., Syntheses of Aza-Analogues of Macrophelides via RCM Strategy and Their Biological Evaluation. *Tetrahedron* **2011**, *67*, 7681-7685.
104. Canova, S.; Lepine, R.; Thys, A.; Baron, A.; Roche, D., Synthesis and Biological Properties of Macrolactam Analogs of the Natural Product Macrolide (-)-A26771B. *Bioorg. Med. Chem. Lett.* **2011**, *21*, 4768-4772.
105. Wilstermann, M.; Kononov, L. O.; Nilsson, U.; Ray, A. K.; Magnusson, G., Synthesis of Ganglioside Lactams Corresponding to GM1-, GM2-, GM3-, and GM4-Ganglioside Lactones. *J. Am. Chem. Soc.* **1995**, *117*, 4742-4754.
106. Hossain, N.; Zapata, A.; Wilstermann, M.; Nilsson, U.; Magnusson, G., Synthesis of GD3-lactam: A Potential Ligand for the Development of an Anti-Melanoma Vaccine. *Carbohydr. Res.* **2002**, *337*, 569-580.
107. Brase, S.; Glaser, F.; Kramer, C. S.; Lindner, S.; Linsenmeier, A. M.; Masters, K.-S.; Meister, A. C.; Ruff, B. M.; Zhong, S., *The Chemistry of Mycotoxins*. 1 ed.; Springer-Verlag Wein: Heidelberg, New York, Dordrecht, London, 2013; Vol. 97, p 300.
108. Winssinger, N.; Barluenga, S., Chemistry and Biology of Resorcylic Acid Lactones. *Chem. Commun.* **2007**, 22-36.

109. Ayers, S.; Graf, T. N.; Adcock, A. F.; Kroll, D. J.; Matthew, S.; de Blanco, E. J. C.; Shen, Q.; Swanson, S. M.; Wani, M. C.; Pearce, C. J.; Oberlies, N. H., Resorcylic Acid Lactones with Cytotoxic and NF-kappa B Inhibitory Activities and Their Structure-Activity Relationships. *J. Nat. Prod.* **2011**, *74*, 1126-1131.
110. Wei, L.; Wu, J.; Li, G.; Shi, N., *Cis*-Enone Resorcylic Acid Lactones (RALs) as Irreversible Protein Kinase Inhibitors. *Curr. Pharm. Des.* **2012**, *18*, 1186-1198.
111. Schirmer, A.; Kennedy, J.; Murli, S.; Reid, R.; Santi, D. V., Targeted Covalent Inactivation of Protein Kinases by Resorcylic Acid Lactone Polyketides. *PNAS* **2006**, *103*, 4234-4239.
112. Jogireddy, R.; Barluenga, S.; Winssinger, N., Molecular Editing of Kinase-Targeting Resorcylic Acid Lactones (RAL): Fluoroenone RAL. *ChemMedChem* **2010**, *5*, 670-673.
113. Xu, J.; Chen, A.; Joy, J.; Xavier, V. J.; Ong, E. H. Q.; Hill, J.; Chai, C. L. L., Rational Design of Resorcylic Acid Lactone Analogues as Covalent MNK1/2 Kinase Inhibitors by Tuning the Reactivity of an Enamide Michael Acceptor. *ChemMedChem* **2013**, *8*, 1483-1494.
114. Long, J.; Ding, Y.-H.; Wang, P.-P.; Zhang, Q.; Chen, Y., Total Syntheses and Structure-Activity Relationship Study of Parthenolide Analogues. *Tet. Lett.* **2016**, *57*, 874-877.
115. Lachia, M.; Wolf, H. C.; Jung, P. J. M.; Screpanti, C.; De Mesmaeker, A., Strigolactam: New Potent Strigolactone Analogues for the Germination of *Orobanche Cumana*. *Bioorg. Med. Chem. Lett.* **2015**, *25*, 2184-2188.
116. Jackson, P. A.; Widen, J. C.; Harki, D. A.; Brummond, K. M., Covalent Modifiers: A Chemical Perspective on the Reactivity of α,β -Unsaturated Carbonyls with Thiols via Hetero-Michael Addition Reactions. *J. Med. Chem.* **2017**, *60*, 839-885.
117. Grillet, F.; Huang, C.; Brummond, K. M., An Allenic Pauson-Khand Approach to 6,12-Guaianolides. *Org. Lett.* **2011**, *13*, 6304-6307.
118. Wen, B.; Hexum, J. K.; Widen, J. C.; Harki, D. A.; Brummond, K. M., A Redox Economical Synthesis of Bioactive 6,12-Guaianolides. *Org. Lett.* **2013**, *15*, 2644-2647.
119. Xie, X.; Lu, X.; Liu, Y.; Xu, W., Palladium(II)-Catalyzed Synthesis of α -Alkylidene- γ -butyrolactams from N-Allylic 2-Alkynamides. Total Synthesis of (\pm)-Isocynodine and (\pm)-Isocynometrine. *The Journal of Organic Chemistry* **2001**, *66*, 6545-6550.
120. Reddy, L. R.; Saravanan, P.; Corey, E. J., A Simple Stereocontrolled Synthesis of Salinosporamide A. *J. Am. Chem. Soc.* **2004**, *126*, 6230-6231.
121. Thuong, M. B. T.; Sottocornola, S.; Prestat, G.; Broggin, G.; Madec, D.; Poli, G., New Access to Kainic Acid via Intramolecular Palladium-Catalyzed Allylic Alkylation. *Synlett* **2007**, *2007*, 1521-1524.

122. Pérard-Viret, J.; Souquet, F.; Manisse, M.-L.; Royer, J., An expeditious total synthesis of (\pm)-jamtine using condensation between imine and acid anhydride. *Tet. Lett.* **2010**, *51*, 96-98.
123. Wang, L.; Xu, C.; Chen, L.; Hao, X.; Wang, D. Z., Asymmetric Synthesis of the Tricyclic Core of *Calyciphylline* A-Type Alkaloids via Intramolecular [3 + 2] Cycloaddition. *Org. Lett.* **2014**, *16*, 1076-1079.
124. Basavaiah, D.; Reddy, G. C.; Bharadwaj, K. C., The Acrylamide Moiety as an Activated Alkene Component in the Intramolecular Baylis-Hillman Reaction: Facile Synthesis of Functionalized α -Methylene Lactam and Spirolactam Frameworks. *Eur. J. Org. Chem.* **2014**, 1157-1162.
125. Basavaiah, D.; Reddy, G. C.; Bharadwaj, K. C., Less Reactive Ketones as Electrophiles and Acrylamides as Activated Alkenes in Intramolecular Baylis-Hillman Reaction: Facile Synthesis of Functionalized γ -Lactam Frameworks. *Tetrahedron* **2014**, *70*, 7991-7995.
126. Lee, K. Y.; Lee, Y. J.; Kim, J. N., Synthesis of β,γ -Disubstituted α -Methylene- γ -butyrolactams Starting from the Baylis-Hillman Adducts. *Bull. Korean Chem. Soc.* **2007**, *28*, 143-146.
127. Sing, V.; Kanojiya, S.; Batra, S., Studies on the Reduction of the Nitro Group in 3-Aryl-2-methylene-4-nitro-alkanoates afforded by the Baylis-Hillman Adducts: Synthesis of 4-Aryl-3-methylene-2-pyrrolidinones and 3-(1-Alkoxy-carbonyl-vinyl)-1H-indole-2-carboxylates. *Tetrahedron* **2006**, *62*, 10100-10110.
128. Companyó, X.; Geant, P.-Y.; Mazzanti, A.; Moyano, A.; Rios, R., Catalytic Asymmetric One-Pot Synthesis of α -Methylene- γ -lactams. *Tetrahedron* **2014**, *70*, 75-82.
129. Pan, F.; Chen, J.-M.; Zhuang, Z.; Fang, Y.-Z.; Zhang, S. X.-A.; Liao, W.-W., Construction of Highly Functional α -Amino Nitriles via a Novel Multicomponent Tandem Organocatalytic Reaction: A Facile Access to α -Methylene- γ -lactams. *Org. Biomol. Chem.* **2012**, *10*, 2214-2217.
130. Dembélé, Y. A.; Belaud, C.; Hitchcock, P.; Villieras, J., Stereocontrolled Addition of Organozinc Reagents Derived from 2-(Bromomethyl)acrylates to Chiral Imines. *Tetrahedron: Asymmetry* **1992**, *3*, 351-354.
131. Dembélé, Y. A.; Belaud, C.; Villieras, J., Stereocontrolled Preparation of Chiral Secondary α -Methylene- γ -lactams by Addition of Organozinc Reagents derived from 2-(Bromomethyl)acrylates to Imines using β -Aminoalcohols as Chiral Auxiliaries. *Tetrahedron: Asymmetry* **1992**, *3*, 511-514.

132. Nyzam, V.; Belaud, C.; Zammatio, F.; Villieras, J., Stereocontrolled Synthesis of Chiral Secondary (α -Methylene- β -substituted)- γ -lactams by Addition of β -Functional Crotylzinc Reagents to Chiral Imines. *Tetrahedron: Asymmetry* **1996**, *7*, 1835-1843.
133. Choudhury, P. K.; Foubelo, F.; Yus, M., Indium-Promoted Preparation of α -Methylene- γ -butyrolactams from 2-(Bromomethyl)acrylic Acid and Aldimines. *J. Org. Chem.* **1999**, *64*, 3376-3378.
134. Shen, A.; Liu, M.; Jia, Z.-S.; Xu, M.-H.; Lin, G.-Q., One-Pot Synthesis of Chiral α -Methylene- γ -lactams with Excellent Diastereoselectivities and Enantioselectivities. *Org. Lett.* **2010**, *12*, 5154-5157.
135. Tan, Y.; Yang, X.-D.; Liu, W.-J.; Sun, X.-W., Novel One-Pot Asymmetric Cascade Approach Toward Densely Substituted Enantioenriched α -Methylene- γ -lactams. *Tet. Lett.* **2014**, *55*, 6105-6108.
136. Elford, T. G.; Hall, D. G., Imine Allylation Using 2-Alkoxy carbonyl Allylboronates as an Expedient Three-Component Reaction to Polysubstituted α -*exo*-Methylene- γ -Lactams. *Tet. Lett.* **2008**, *49*, 6995-6998.
137. Chataigner, I.; Zammatio, F.; Lebreton, J.; Villieras, J., Enantioselective Addition of β -Functionalized Allylboronates to Aldehydes and Aldimines. Stereocontrolled Synthesis of α -Methylene- γ -lactones and Lactams. *Tetrahedron* **2008**, *64*, 2441-2455.
138. Deredas, D.; Albrecht, Ł.; Krawczyk, H., An Efficient Synthesis of β,γ,γ -Trisubstituted- α -diethoxyphosphoryl- γ -lactams: A Convenient Approach to α -Methylene- γ -Lactams. *Tet. Lett.* **2013**, *54*, 3088-3090.
139. Riofski, M. V.; John, J. P.; Zheng, M. M.; Kirshner, J.; Colby, D. A., Exploiting the Facile Release of Trifluoroacetate for α -Methylenation of the Sterically Hindered Carbonyl groups on (+)-Sclareolide and (-)-Eburnamonine. *J. Org. Chem.* **2011**, *76*, 3676-3683.
140. Kürti, L.; Czakó, B., *Strategic Applications of Named Reactions in Organic Synthesis: Background and Detailed Mechanisms*. Elsevier: 2005; p 864.
141. Craven, P.; Aimon, A.; Dow, M.; Fleury-Bregeot, N.; Guilleux, R.; Morgentin, R.; Roche, D.; Kalliokoski, T.; Foster, R.; Marsden, S. P.; Nelson, A., Design, Synthesis and Decoration of Molecular Scaffolds for Exploitation in the Production of Alkaloid-like Libraries. *Biorg. Med. Chem.* **2015**, *23*, 2629-2635.
142. Neuhaus, K.; Ritter, H., Forgotten Monomers: Isotactic Polymers from N-Benzyl-3-methylenepyrrolidin-2-one via Free Radical Polymerization. *Polym. Int.* **2015**, *64*, 1690-1694.
143. Kornet, M. J., Synthesis of α -Methylenebutyrolactams as Potential Antitumor Agents. *J. Pharm. Sci.* **1979**, *68*, 350-353.

144. Ryu, I.; Miyazato, H.; Kuriyama, H.; Matsu, K.; Tojino, M.; Fukuyama, T.; Minakata, S.; Komatsu, M., Broad-Spectrum Radical Cyclizations Boosted by Polarity Matching. Carbonylative Access to α -Stannylmethylene Lactams from Azaenynes and CO. *J. Am. Chem. Soc.* **2003**, *125*, 5632-5633.
145. Denmark, S. E.; Baiazitov, R. Y., Tandem Double-Intramolecular [4 + 2]/[3 + 2] Cycloadditions of Nitroalkenes. Studies Toward a Total Synthesis of Daphnilactone B: Piperidine Ring Construction. *J. Org. Chem.* **2006**, *71*, 593-605.
146. He, W.; Yip, K.-T.; Zhu, N.-Y.; Yang, D., Pd(II)/tBu-quinolineoxazoline: An Air-Stable and Modular Chiral Catalyst System for Enantioselective Oxidative Cascade Cyclization. *Org. Lett.* **2009**, *11*, 5626-5628.
147. Förster, S.; Helmchen, G., Stereoselective Synthesis of a Lactam Analogue of Brefeldin C. *SYNLETT* **2008**, *6*, 831-836.
148. Baell, J.; Walters, M. A., Chemical Con Artists Foil Drug Discovery. *Nature* **2014**, *513*, 481-483.
149. Baell, J. B.; Holloway, G. A., New Substructure Filters for Removal of Pan Assay Interference Compounds (PAINS) from Screening Libraries and for Their Exclusion in Bioassays. *J. Med. Chem.* **2010**, *53*, 2719-2740.
150. Baell, J., Observations on Screening-based Research and Some Concerning Trends in the Literature. *Future Med. Chem* **2010**, *2*, 1529-1546.
151. Schall, A.; Reiser, O., Synthesis of Biologically Active Guaianolides with a *trans*-Annulated Lactone Moiety. *Eur. J. Org. Chem.* **2008**, 2353-2364.
152. Zhai, J.-D.; Li, D.; Long, J.; Zhang, H.-L.; Lin, J.-P.; Qiu, C.-J.; Zhang, Q.; Chen, Y., Biomimetic Semisynthesis of Arglabin from Parthenolide. *The Journal of Organic Chemistry* **2012**, *77*, 7103-7107.
153. Marx, J. N.; White, E. H., The stereochemistry and synthesis of Achillin. *Tetrahedron* **1969**, *25*, 2117-2120.
154. Edgar, M. T.; Greene, A. E.; Crabbe, P., Stereoselective synthesis of (-)-estafiatin. *The Journal of Organic Chemistry* **1979**, *44*, 159-160.
155. Barges, V.; Blay, G.; Cardona, L.; García, B.; Pedro, J. R., Stereoselective Synthesis of (+)-11 β H,13-Dihydroestafiatin, (+)-11 β H,13-Dihydroludartin, (-)-Compressanolide, and (-)-11 β H,13-Dihydromicheliolide from Santonin. *J. Nat. Prod.* **2002**, *65*, 1703-1706.

156. Lee, E.; Yoon, C. H., Stereoselective Favorskii rearrangement of carvone chlorohydrin; expedient synthesis of (+)-dihydronepetalactone and (+)-iridomyrmecin. *J. Chem. Soc., Chem. Commun.* **1994**, 479-481.
157. Andrews, S. P.; Ball, M.; Wierschem, F.; Cleator, E.; Oliver, S.; Högenauer, K.; Simic, O.; Antonello, A.; Hüniger, U.; Smith, M. D.; Ley, S. V., Total Synthesis of Five Thapsigargins: Guaianolide Natural Products Exhibiting Sub-Nanomolar SERCA Inhibition. *Chemistry – A European Journal* **2007**, *13*, 5688-5712.
158. Devreese, A. A.; Demuynck, M.; De Clercq, P. J.; Vandewalle, M., Guaianolides 1. Perhydroazulenenic Lactones as Intermediates for Total Synthesis. *Tetrahedron* **1983**, *39*, 3039-3048.
159. Carret, S.; Deprés, J.-P., Access to Guaianolides: Highly Efficient Stereocontrolled Total Synthesis of (±)-Geigerin. *Angew. Chem. Int. Ed.* **2007**, *46*, 6870-6873.
160. McKerrall, S. J.; Jørgensen, L.; Kuttruff, C. A.; Ungeheuer, F.; Baran, P. S., Development of a Concise Synthesis of (+)-Ingenol. *J. Am. Chem. Soc.* **2014**, *136*, 5799-5810.
161. Kawamura, S.; Chu, H.; Felding, J.; Baran, P. S., Nineteen-Step Total Synthesis of (+)-Phorbol. *Nature* **2016**, *532*, 90-93.
162. Jørgensen, L.; McKerrall, S. J.; Kuttruff, C. A.; Ungeheuer, F.; Felding, J.; Baran, P. S., 14-Step Synthesis of (+)-Ingenol from (+)-3-Carene. *Science* **2013**, *341*, 878-882.
163. Wells, S. M.; Brummond, K. M., Conditions for a Rh(I)-catalyzed [2+2+1] cycloaddition reaction with methyl substituted allenes and alkynes. *Tet. Lett.* **2015**, *56*, 3546-3549.
164. Kang, S. W.; Kim, Y. H.; Kim, J. J.; Lee, J. H.; Kim, S. H., A Convenient Synthesis of Polycyclic γ -Lactams via Pauson-Khand Reaction. *Bull. Korean Chem. Soc.* **2009**, *30*, 691-694.
165. Strübing, D.; Neumann, H.; Hübner, S.; Klaus, S.; Beller, M., Straightforward synthesis of di-, tri- and tetracyclic lactams via catalytic Pauson–Khand and Alder–Ene reactions of MCR products. *Tetrahedron* **2005**, *61*, 11345-11354.
166. Alcaide, B.; Almendros, P.; Aragoncillo, C., Additions of Allenyl/Propargyl Organometallic Reagents to 4-Oxoazetidene-2-carbaldehydes: Novel Palladium-Catalyzed Domino Reactions in Allenynes. *Chemistry – A European Journal* **2002**, *8*, 1719-1729.
167. Painter, T. O.; Wang, L.; Majumder, S.; Xie, X.-Q.; Brummond, K. M., Diverging DOS Strategy Using an Allene-Containing Tryptophan Scaffold and a Library Design that Maximizes Biologically Relevant Chemical Space While Minimizing the Number of Compounds. *ACS Combinatorial Science* **2011**, *13*, 166-174.

168. Grillet, F.; Brummond, K. M., Enantioselective Synthesis of 5,7-Bicyclic Ring Systems from Axially Chiral Allenes Using a Rh(I)-Catalyzed Cyclocarbonylation Reaction. *The Journal of Organic Chemistry* **2013**, *78*, 3737-3754.
169. Brummond, K. M.; Painter, T. O.; Probst, D. A.; Mitasev, B., Rhodium(I)-Catalyzed Allenic Carbocyclization Reaction Affording δ - and ϵ -Lactams. *Org. Lett.* **2007**, *9*, 347-349.
170. Brummond, K. M.; Lu, J., A Short Synthesis of the Potent Antitumor Agent (\pm)-Hydroxymethylacetylfulvene Using an Allenic Pauson-Khand Type Cycloaddition. *J. Am. Chem. Soc.* **1999**, *121*, 5087-5088.
171. Daeuble, J. F.; Stryker, J. M.; Chiu, P.; Ng, W. H., Hexa- μ -hydrohexakis(triphenylphosphine)hexacopper. In *Encyclopedia of Reagents for Organic Synthesis*, John Wiley & Sons, Ltd: 2001.
172. Elford, T. G.; Hall, D. G., Total Synthesis of (+)-Chinensiolide B via Tandem Allylboration/Lactonization. *J. Am. Chem. Soc.* **2010**, *132*, 1488-1489.
173. Klapars, A.; Huang, X.; Buchwald, S. L., A General and Efficient Copper Catalyst for the Amidation of Aryl Halides. *J. Am. Chem. Soc.* **2002**, *124*, 7421-7428.
174. Görl, C.; Alt, H. G., The combination of mononuclear metallocene and phenoxyimine complexes to give trinuclear catalysts for the polymerization of ethylene. *J. Organomet. Chem.* **2007**, *692*, 5727-5753.
175. Abidi, S. L., Direct conversion of terpenylalkanolamines to ethylidyne N-nitroso compounds. *J. Org. Chem.* **1986**, *51*, 2687-2694.
176. Balog, A.; Curran, D. P., Ring-Enlarging Annulations. A One-Step Conversion of Cyclic Silyl Acyloins and ω -Alkynyl Acetals to Polycyclic Enediones. *J. Org. Chem.* **1995**, *60*, 337-344.
177. Hoye, T. R.; Aspaas, A. W.; Eklov, B. M.; Ryba, T. D., Reaction Titration: A Convenient Method for Titering Reactive Hydride Agents (Red-Al, LiAlH₄, DIBALH, L-Selectride, NaH, KH, by No-D NMR Spectroscopy. *Org. Lett.* **2005**, *7*, 2205-2208.
178. Nyzam, V.; Belaud, C.; Villiéras, J., Preparation of (2-methoxycarbonyl)allylboronates from (α -methoxycarbonyl)vinylalenate. *Tet. Lett.* **1993**, *34*, 6899-6902.
179. Tsuda, T.; Yoshida, T.; Kawamoto, T.; Saegusa, T., Conjugate reduction of α,β -acetylenic ketones and esters by diisobutylaluminum hydride-hexamethylphosphoric triamide. *The Journal of Organic Chemistry* **1987**, *52*, 1624-1627.
180. Tsuda, T.; Hayashi, T.; Satomi, H.; Kawamoto, T.; Saegusa, T., Methylcopper(I)-catalyzed selective conjugate reduction of α,β -unsaturated carbonyl compounds by di-iso-

- butylaluminum hydride in the presence of hexamethylphosphoric triamide. *The Journal of Organic Chemistry* **1986**, *51*, 537-540.
181. Whiting, A., A Convenient Preparation of β -Boronate Carbonyl Derivatives. Evidence for the Intervention of Boronate "Ate"-Complexes in Enolate Alkylations. *Tet. Lett.* **1991**, *32*, 1503-1506.
 182. Cahiez, G.; Alami, M., Manganese Dioxide. In *Encyclopedia of Reagents for Organic Synthesis*, John Wiley & Sons, Ltd: 2001.
 183. Kern, N.; Hoffmann, M.; Blanc, A.; Weibel, J.-M.; Pale, P., Gold(I)-Catalyzed Rearrangement of N-Aryl 2-Alkynylazetidines to Pyrrolo[1,2-a]indoles. *Org. Lett.* **2013**, *15*, 836-839.
 184. Alam, R.; Das, A.; Huang, G.; Eriksson, L.; Himo, F.; Szabó, K. J., Stereoselective Allylboration of Imines and Indoles Under Mild Conditions. An *in situ* E/Z Isomerization of Imines by Allylboroxines. *Chem. Sci.* **2014**, *5*, 2732-2738.
 185. Hall, D. G., Lewis and Bronsted Acid Catalyzed Allylboration of Carbonyl Compounds: From Discovery to Mechanism and Applications. *Synlett* **2007**, *11*, 1644-1655.
 186. Brestensky, D. M.; Stryker, J. M., Regioselective Conjugate Reduction and Reductive Silylation of α,β -Unsaturated Ketones. *Tet. Lett.* **1989**, *30*, 5677-5680.
 187. Koenig, T. M.; Daeuble, J. F.; Brestensky, D. M.; Stryker, J. M., Conjugate Reduction of Polyfunctional α,β -Unsaturated Carbonyl Compounds using $[(\text{Ph}_3\text{P})\text{CuH}]_6$. Compatibility with Halogen, Sulfonate, and γ -Oxygen and Sulfur Substituents. *Tet. Lett.* **1990**, *31*, 3237-3240.
 188. Daeuble, J. F.; McGettigan, C.; Stryker, J. M., Selective Reduction of Alkynes to cis-Alkenes by Hydrometallation using $[(\text{Ph}_3\text{P})\text{CuH}]_6$. *Tet. Lett.* **1990**, *31*, 2397-2400.
 189. Lee, D.-w.; Yun, J., Direct Synthesis of Stryker's Reagent from a Cu(II) Salt. *Tet. Lett.* **2005**, *46*, 2037-2039.
 190. Sass, D. C.; Heleno, V. C. G.; Cavalcante, S.; da Silva Barbosa, J.; Soares, A. C. F.; Constantino, M. G., Solvent Effect in Reactions Using Stryker's Reagent. *The Journal of Organic Chemistry* **2012**, *77*, 9374-9378.
 191. Pelšs, A.; Kumpulainen, E. T. T.; Koskinen, A. M. P., Highly Chemoselective Copper-Catalyzed Conjugate Reduction of Stereochemically Labile α,β -Unsaturated Amino Ketones. *The Journal of Organic Chemistry* **2009**, *74*, 7598-7601.
 192. Zhong, C.; Sasaki, Y.; Ito, H.; Sawamura, M., The Synthesis of Allenes by Cu(I)-Catalyzed Regio- and Stereoselective Reduction of Propargylic Carbonates with Hydrosilanes. *Chem. Commun.* **2009**, 5850-5852.

193. Deutsch, C.; Lipshutz, B. H.; Krause, N., (NHC)CuH-Catalyzed Entry to Allenes via Propargylic Carbonate SN2'-Reductions. *Org. Lett.* **2009**, *11*, 5010-5012.
194. Urbach, A.; Muccioli, G. G.; Stern, E.; Lambert, D. M.; Marchand-Brynaert, J., 3-Alkenyl-2-azetidinones as Fatty Acid Amide Hydrolase Inhibitors. *Bioorg. Med. Chem. Lett.* **2008**, *18*, 4163-4167.
195. Reisman, S. E.; Ready, J. M.; Weiss, M. M.; Hasuoka, A.; Hirata, M.; Tamaki, K.; Ovaska, T. V.; Smith, C. J.; Wood, J. L., Evolution of a Synthetic Strategy: Total Synthesis of (±)-Welwitindolinone A Isonitrile. *J. Am. Chem. Soc.* **2008**, *130*, 2087-2100.
196. Myers, A. G.; Zheng, B., New and Stereospecific Synthesis of Allenes in a Single Step from Propargylic Alcohols. *J. Am. Chem. Soc.* **1996**, *118*, 4492-4493.
197. Liu, Z.; Liao, P.; Bi, X., Lewis and Bronsted Acid Cocatalyzed Reductive Deoxyallenylation of Propargylic Alcohols with 2-Nitrobenzenesulfonylhydrazide. *Chem. Eur. J.* **2014**, *20*, 17277-17281.
198. Petasis, N. A.; Hu, Y.-H., Allenation of Carbonyl Compounds with Alkenyltitanocene Derivatives. *The Journal of Organic Chemistry* **1997**, *62*, 782-783.
199. Tsuji, J.; Sugiura, T.; Yuhara, M.; Minami, I., Palladium-Catalyzed Preparation of 1,2-Dienes by Selective Hydrogenolysis of Alk-2-ynyl Carbonates with Ammonium Formate. *J. Chem. Soc., Chem. Commun.* **1986**, 922-924.
200. Mandai, T.; Matsumoto, T.; Tsujiguchi, Y.; Matsuoka, S.; Tsuji, J., Palladium-Catalyzed Hydrogenolysis of 2-Alkynyl Formates and Elimination of 2-Alkynyl Carbonates. 2-Alkynylpalladium Complex vs. Allenylpalladium Complex as Intermediates. *J. Organomet. Chem.* **1994**, *473*, 343-352.
201. Tsuji, J.; Sugiura, T.; Minami, I., Preparation of 1,2-Dienes by the Palladium-Catalyzed Hydrogenolysis of 3-Methoxycarbonyloxy-1-alkynes with Ammonium Formate. *Synthesis* **1987**, *1987*, 603-606.
202. unpublished results
203. Huang, M.-Y.; Chen, L.; Li, R.; Jia, X.; Hong, R., Synthesis of (±)-Bakuchiol via a Pot-Economy Approach. *Chin. J. Chem.* **2014**, *32*, 715-720.
204. Ohmiya, H.; Yang, M.; Yamauchi, Y.; Ohtsuka, Y.; Sawamura, M., Selective Synthesis of Allenes and Alkynes through Ligand-Controlled, Palladium-Catalyzed Decarboxylative Hydrogenolysis of Propargylic Formates. *Org. Lett.* **2010**, *12*, 1796-1799.
205. Doyle, M. P.; Hu, W.; Wee, A. G. H.; Wang, Z.; Duncan, S. C., Influences of Catalyst Configuration and Catalyst Loading on Selectivities in Reactions of Diazoacetamides.

- Barrier to Equilibrium between Diastereomeric Conformations. *Org. Lett.* **2003**, *5*, 407-410.
206. Trost, B. M.; Zhang, Y.; Zhang, T., Direct N-Carbamoylation of 3-Monosubstituted Oxindoles with Alkyl Imidazole Carboxylates. *The Journal of Organic Chemistry* **2009**, *74*, 5115-5117.
207. Amin, R.; Ardeshir, K.; Heidar Ali, A.-N.; Zahra, T.-R., Formylation of Alcohol with Formic Acid under Solvent-Free and Neutral Conditions Catalyzed by Free I₂ or I₂ Generated in situ from Fe(NO₃)₃·9H₂O/NaI. *Chinese Journal of Catalysis* **2011**, *32*, 60-64.
208. Schor, L.; Seldes, A. M.; Gros, E. G., Zinc(II)-promoted stereospecific rearrangement of 17-hydroxy-20-oxopregnane derivatives. *J. Chem. Soc., Perkin Trans. 1* **1990**, 163-166.
209. Zalesskiy, S. S.; Ananikov, V. P., Pd₂(dba)₃ as a Precursor of Soluble Metal Complexes and Nanoparticles: Determination of Palladium Active Species for Catalysis and Synthesis. *Organometallics* **2012**, *31*, 2302-2309.
210. Effenberger, F.; Keil, M.; Bessey, E., Darstellung von N-Formylpyridonen — Selektive Veresterung primärer, sekundärer und tertiärer Alkohole mit N-Acylpyridonen. *Chem. Ber.* **1980**, *113*, 2110-2119.
211. Yin, J.; Buchwald, S. L., Pd-Catalyzed Intermolecular Amidation of Aryl Halides: The Discovery that Xantphos Can Be Trans-Chelating in a Palladium Complex. *J. Am. Chem. Soc.* **2002**, *124*, 6043-6048.
212. Strieter, E. R.; Bhayana, B.; Buchwald, S. L., Mechanistic Studies on the Copper-Catalyzed N-Arylation of Amides. *J. Am. Chem. Soc.* **2009**, *131*, 78-88.
213. Yoshioka, S.; Nagatomo, M.; Inoue, M., Application of Two Direct C(sp³)-H Functionalizations for Total Synthesis of (+)-Lactacystin. *Org. Lett.* **2015**, *17*, 90-93.
214. Kallepalli, V. A.; Shi, F.; Paul, S.; Onyeozili, E. N.; Maleczka, R. E.; Smith, M. R., Boc Groups as Protectors and Directors for Ir-Catalyzed C-H Borylation of Heterocycles. *The Journal of Organic Chemistry* **2009**, *74*, 9199-9201.
215. García-Piñeres, A. J.; Castro, V. c.; Mora, G.; Schmidt, T. J.; Strunck, E.; Pahl, H. L.; Merfort, I., Cysteine 38 in p65/NF-κB Plays a Crucial Role in DNA Binding Inhibition by Sesquiterpene Lactones. *J. Biol. Chem.* **2001**, *276*, 39713-39720.
216. Lyß, G.; Knorre, A.; Schmidt, T. J.; Pahl, H. L.; Merfort, I., The Anti-inflammatory Sesquiterpene Lactone Helenalin Inhibits the Transcription Factor NF-κB by Directly Targeting p65. *J. Biol. Chem.* **1998**, *273*, 33508-33516.

217. Widen, J. C.; Kempema, A. M.; Villalta, P. W.; Harki, D. A., Targeting NF- κ B p65 with a Helenalin Inspired Bis-electrophile. *ACS Chem. Biol.* **2017**, *12*, 102-113.
218. Hexum, J. K.; Tello-Aburto, R.; Struntz, N. B.; Harned, A. M.; Harki, D., Bicyclic Cyclohexenones as Inhibitors of NF- κ B Signaling. *ACS Med. Chem. Lett.* **2012**, *3*, 459-464.
219. Chen, J.; Ng, M. M.-L.; Chu, J. J. H., Activation of TLR2 and TLR6 by Dengue NS1 Protein and Its Implications in the Immunopathogenesis of Dengue Virus Infection. *PLOS Pathogens* **2015**, *11*, e1005053.
220. Chu, H.; Smith, J. M.; Felding, J.; Baran, P. S., Scalable Synthesis of (-)-Thapsigargin. *ACS Central Science* **2017**, *3*, 47-51.
221. Burns, N. Z.; Baran, P. S.; Hoffmann, R. W., Redox Economy in Organic Synthesis. *Angew. Chem. Int. Ed.* **2009**, *48*, 2854-2867.
222. Brummond, K. M.; Davis, M. M.; Huang, C., Rh(I)-Catalyzed Cyclocarbonylation of Allenol Esters To Prepare Acetoxy 4-Alkylidenecyclopent-3-en-2-ones. *The Journal of Organic Chemistry* **2009**, *74*, 8314-8320.
223. Dr. Francois Grillet, unpublished results
224. Alcaide, B.; Almendros, P.; Aragoncillo, C., Exploiting [2+2] Cycloaddition Chemistry: Achievements with Allenes. *Chem. Soc. Rev.* **2010**, *39*, 783-816.
225. Carreira, E. M.; Hastings, C. A.; Shepard, M. S.; Yerkey, L. A.; Millward, D. B., Asymmetric Induction in Intramolecular [2 + 2]-Photocycloadditions of 1,3-Disubstituted Allenes with Enones and Enoates. *J. Am. Chem. Soc.* **1994**, *116*, 6622-6630.
226. Becker, D.; Nagler, M.; Sahali, Y.; Haddad, N., Regiochemistry and stereochemistry of intramolecular [2+2] photocycloaddition of carbon-carbon double bonds to cyclohexenones. *The Journal of Organic Chemistry* **1991**, *56*, 4537-4543.
227. Schuster, H. F.; Coppola, G. M., *Allenenes in Organic Synthesis*. John Wiley & Sons: 1984.
228. Padwa, A.; Meske, M.; Murphree, S. S.; Watterson, S. H.; Ni, Z., (Phenylsulfonyl)allenenes as Substrates for Cycloaddition Reactions: Intramolecular Cyclizations onto Unactivated Alkenes. *J. Am. Chem. Soc.* **1995**, *117*, 7071-7080.
229. Xu, Y.; Conner, M. L.; Brown, M. K., Cyclobutane and Cyclobutene Synthesis: Catalytic Enantioselective [2+2] Cycloadditions. *Angew. Chem. Int. Ed.* **2015**, *54*, 11918-11928.
230. Conner, M. L.; Brown, M. K., Synthesis of 1,3-Substituted Cyclobutanes by Allenolate-Alkene [2 + 2] Cycloaddition. *The Journal of Organic Chemistry* **2016**, *81*, 8050-8060.

231. Conner, M. L.; Xu, Y.; Brown, M. K., Catalytic Enantioselective Allenolate–Alkene [2 + 2] Cycloadditions. *J. Am. Chem. Soc.* **2015**, *137*, 3482-3485.
232. Luzung, M. R.; Mauleón, P.; Toste, F. D., Gold(I)-Catalyzed [2 + 2]-Cycloaddition of Allenenes. *J. Am. Chem. Soc.* **2007**, *129*, 12402-12403.
233. González, A. Z.; Benitez, D.; Tkatchouk, E.; Goddard, W. A.; Toste, F. D., Phosphoramidite Gold(I)-Catalyzed Diastereo- and Enantioselective Synthesis of 3,4-Substituted Pyrrolidines. *J. Am. Chem. Soc.* **2011**, *133*, 5500-5507.
234. Jia, M.; Monari, M.; Yang, Q.-Q.; Bandini, M., Enantioselective gold catalyzed dearomative [2+2]-cycloaddition between indoles and allenamides. *Chem. Commun.* **2015**, *51*, 2320-2323.
235. Serra, S.; Fuganti, C., Benzannulation of Substituted 3-Alkoxyhex-3-en-5-ynoic Acids: A New Route to 4-Substituted 3,5-Dihydroxybenzoic Acids Derivatives. *Synlett* **2002**, *2002*, 1661-1664.
236. Fatiadi, A. J., Active Manganese Dioxide Oxidation in Organic Chemistry. *Synthesis* **1976**, 65-167.